Methods in Molecular Biology 1046

Springer Protocols

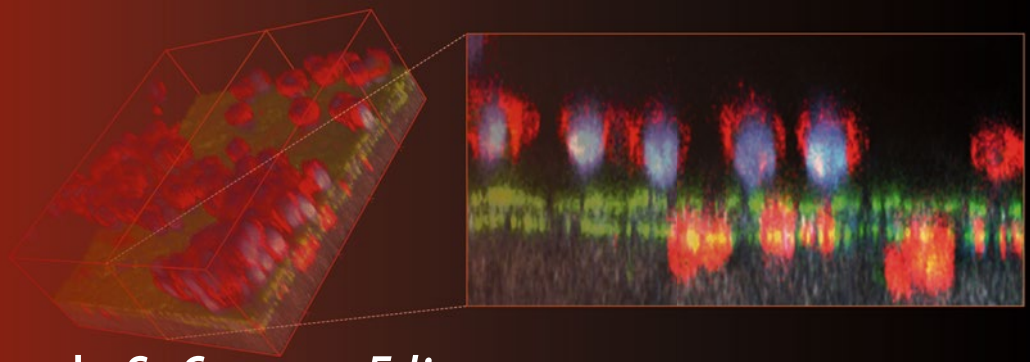

Amanda S. Coutts *Editor*

Adhesion Protein Protocols

Third Edition

Humana Press

METHODS IN MOLECULAR BIOLOGY™

Series Editor
John M. Walker
School of Life Sciences
University of Hertfordshire
Hatfield, Hertfordshire, AL10 9AB, UK

For further volumes:
http://www.springer.com/series/7651

Adhesion Protein Protocols

Third Edition

Edited by

Amanda S. Coutts

Department of Oncology, University of Oxford, Oxford, UK

Humana Press

Editor
Amanda S. Coutts
Department of Oncology
University of Oxford
Oxford, UK

ISSN 1064-3745 ISSN 1940-6029 (electronic)
ISBN 978-1-62703-537-8 ISBN 978-1-62703-538-5 (eBook)
DOI 10.1007/978-1-62703-538-5
Springer New York Heidelberg Dordrecht London

Library of Congress Control Number: 2013942870

Printed on acid-free paper

Humana Press is a brand of Springer
Springer is part of Springer Science+Business Media (www.springer.com)

Preface

Cellular adhesion is a fundamental process that influences numerous biological activities such as morphogenesis, cell motility and division, as well as signalling. In addition, adhesion is a process important not only in normal physiology and development but also in disease states such as tumorigenesis, cardiovascular disease, inflammation, and infection. There are a plethora of proteins involved in adhesion-related events with a huge diversity in function. As a result, a wide variety of techniques exist to study adhesion-related proteins and processes and choosing which to include was a difficult task, but I hope the end result will provide a diverse collection of useful techniques.

Many of the microscopy techniques will be of use to a broad range of disciplines and this text provides excellent chapters on total internal reflection fluorescence microscopy, localization-based super-resolution imaging, and atomic force microscopy (Chapters 2–4, 9). In addition, the use of fixed and live cell imaging to study podosome formation is outlined in Chapter 6, while Chapter 21 details a custom-built high-resolution fluorescence microscope to enable high-resolution live-cell imaging and time-lapse microscopy of invadopodium dynamics.

As well, the use of microarrays and proteomics, more commonly used in various disciplines, is outlined in Chapters 5 and 12 and will be applicable to many areas of study.

Novel platforms to analyze cell adhesion using micropatterning are described in Chapters 7 and 13, while in Chapter 23 McLane et al. describe how to generate biomimetic nanofibers to evaluate the effects of specific extracellular matrix features on cell adhesion. Cell invasion is expertly dealt with in Chapters 8 and 10 using both synthetic and tissue-derived substrates and the measurement of cell motility and invasion in real time is outlined by Scrace et al. in Chapter 17. In Chapter 18, the Insall lab describes their novel direct visualization chemotaxis chamber for studying cell migration.

Various chapters describe protocols for the study of specific adhesion molecules including Chapter 1 where the Ginsberg lab explain how to reconstruct integrin activation in vitro using phospholipid nanodiscs, Chapter 11 describes how to perform biochemical Rho GTPase assays, and Chapter 22 provides procedures for imaging Rho GTPase biosensors in tumor cells.

In Chapter 20 Monaghan-Benson and Burridge describe how to use cadherin status of microvascular endothelial cells as a measure of permeability. In Chapter 24 the Ostap lab details a single-molecule, optical-trapping method for the measurement of protein–membrane adhesion forces. The microtubule cytoskeleton undergoes constant and dynamic remodelling and in Chapter 19 Ziółkowska and Roll-Mecak describe how to set up in vitro microtubule severing assays in order to explore this poorly understood process.

Several detailed protocols (Chapters 9, 14–16) deal with purification of the fundamental adhesion proteins actin and the Arp2/3 complex from a variety of sources and their subsequent use in polymerization assays. These techniques are commonly employed to investigate the roles of actin-binding proteins in the kinetics and morphology of actin assembly and will thus be of wide use.

I hope you will agree that this third edition of Adhesion Protein Protocols brings together a unique collection of protocols that covers standard, as well as novel and more specialized, techniques. Because of this range, the protocols will be useful for those new to the field of adhesion protein research as well as the more experienced scientist. Importantly, I hope these techniques will be used to gain further insight into the complex and incompletely understood processes that are involved in cellular adhesion.

Lastly, I would also like to thank all the authors for their excellent contributions, John Walker for his expert advice and assistance, and Springer/Humana Press for all their efforts.

Oxford, UK *Amanda S. Coutts*

Contents

Contributors

Mirjam Andreasson-Ochsner • *Department of Materials, Laboratory for Surface Science and Technology, ETH Zurich, Zurich, Switzerland*

Jose Javier Bravo-Cordero • *Department of Anatomy and Structural Biology and Gruss Lipper Biophotonics Center, Albert Einstein College of Medicine of Yeshiva University, Bronx, NY, USA*

Keith Burridge • *Department of Cell and Developmental Biology, Lineberger Comprehensive Cancer Center, University of North Carolina at Chapel Hill, Chapel Hill, NC, USA*

Pasquale Cervero • *Institut für medizinische Mikrobiologie, Virologie und Hygiene, Universitätsklinikum Eppendorf, Hamburg, Germany*

Sunkyu Choi • *Department of Pathology and Moores Cancer Center, University of California, San Diego, La Jolla, CA, USA*

John Condeelis • *Department of Anatomy and Structural Biology and Gruss Lipper Biophotonics Center, Albert Einstein College of Medicine, Bronx, NY, USA*

Lynda K. Doolittle • *Department of Biophysics, UT Southwestern Medical Center and Howard Hughes Medical Institute, Dallas, TX, USA*

David Entenberg • *Department of Anatomy and Structural Biology and Gruss Lipper Biophotonics Center, Albert Einstein College of Medicine, Bronx, NY, USA*

Jens Friedrichs • *Leibniz Institute of Polymer Research Dresden, Institute for Biofunctional Polymer Materials, Dresden, Germany*

Ryan J. Gilbert • *Center for Biotechnology and Interdisciplinary studies, Rensselaer Polytechnic Institute, Troy, NY, USA; Department of Biomedical Engineering, Rensselaer Polytechnic Institute, Troy, NY, USA*

Alexandre R. Gingras • *Department of Medicine, University of California, San Diego, La Jolla, CA, USA*

Mark H. Ginsberg • *Department of Medicine, University of California, San Diego, La Jolla, CA, USA*

Alexandros Glentis • *Institut Curie/UMR144 CNRS, Paris, France*

Scott A. Guelcher • *Department of Chemical and Biomolecular Engineering, Vanderbilt University, Nashville, TN, USA*

Vasily V. Gurchenkov • *Institut Curie/UMR144 CNRS, Paris, France*

Ester M. Hammond • *Department of Oncology, Gray Institute for Radiation Oncology and Biology, University of Oxford, Oxford, UK*

Scott D. Hansen • *Department of Cellular and Molecular Pharmacology, University of California, San Francisco, CA, USA*

Ian S. Harper • *Monash Microimaging, Monash University, Melbourne, VIC, Australia*

David J. Harrison • *School of Medicine, University of St Andrews, St Andrews, UK*

Louis Hodgson • *Department of Anatomy and Structural Biology and Gruss Lipper Biophotonics Center, Albert Einstein College of Medicine of Yeshiva University, Bronx, NY, USA*

Robert H. Insall • *CRUK Beatson Institute for Cancer Research, Glasgow, UK*

Shaun P. Jackson • *The Australian Centre for Blood Diseases, Alfred Medical Research and Educational Precinct, Monash University, Melbourne, VIC, Australia*
Xinning Jiang • *Department of Pathology and Moores Cancer Center, University of California, San Diego, La Jolla, CA, USA*
Gabriela Kalna • *CRUK Beatson Institute for Cancer Research, Glasgow, UK*
Pakorn Kanchanawong • *Department of Bioengineering, Mechanobiology Institute, National University of Singapore, Singapore, Singapore*
Elad Katz • *AMS Biotechnology, Abingdon, UK*
Jonathan A. Kelber • *Department of Biology, California State University, Northridge, Northridge, CA, USA*
Richard L. Klemke • *Department of Pathology and Moores Cancer Center, University of California, San Diego, La Jolla, CA, USA*
David A. Knecht • *Department of Molecular and Cell Biology, University of Connecticut, Storrs, CT, USA*
Alexey A. Larionov • *Breakthrough Breast Cancer Research Unit, Western General Hospital, Edinburgh, UK*
Lee A. Ligon • *Department of Biology, Rensselaer Polytechnic Institute, Troy, NY, USA; Center for Biotechnology and Interdisciplinary studies, Rensselaer Polytechnic Institute, Troy, NY, USA*
Stefan Linder • *Institut für medizinische Mikrobiologie, Virologie und Hygiene, Universitätsklinikum Eppendorf, Hamburg, Germany*
Molly Lowndes • *Cancer Biology Program, Stanford University, Stanford, CA, USA*
Joshua S. McLane • *Department of Biology, Rensselaer Polytechnic Institute, Troy, NY, USA; Center for Biotechnology and Interdisciplinary studies, Rensselaer Polytechnic Institute, Troy, NY, USA*
Elizabeth Monaghan-Benson • *Department of Cell and Developmental Biology, Lineberger Comprehensive Cancer Center, University of North Carolina at Chapel Hill, Chapel Hill, NC, USA*
Yasmin Moshfegh • *Department of Anatomy and Structural Biology and Gruss Lipper Biophotonics Center, Albert Einstein College of Medicine of Yeshiva University, Bronx, NY, USA*
Andrew J. Muinonen-Martin • *CRUK Beatson Institute for Cancer Research, Glasgow, UK*
Daniel J. Müller • *Department of Biosystems Science and Engineering, ETH Zürich, Basel, Switzerland*
R. Dyche Mullins • *Department of Cellular and Molecular Pharmacology, University of California, San Francisco, CA, USA*
W. James Nelson • *Department of Biology, Stanford University, Stanford, CA, USA; Department of Molecular and Cellular Physiology Stanford University, Stanford, CA, USA*
Warwick S. Nesbitt • *The Bionics Institute, St Vincent's Hospital, Melbourne, VIC, Australia*
Eric O'Neill • *Department of Oncology, Gray Institute for Radiation Oncology and Biology, University of Oxford, Oxford, UK*
E. Michael Ostap • *Department of Physiology, Pennsylvania Muscle Institute, Perelman School of Medicine at the University of Pennsylvania, Philadelphia, PA, USA*
Shae B. Padrick • *Department of Biophysics, UT Southwestern Medical Center and Howard Hughes Medical Institute, Dallas, TX, USA*

Jonathan M. Page • *Department of Chemical and Biomolecular Engineering, Vanderbilt University, Nashville, TN, USA*
Linda Panzer • *Institut für medizinische Mikrobiologie, Virologie und Hygiene, Universitätsklinikum Eppendorf, Hamburg, Germany*
Aron Parekh • *Department of Otolaryngology, Vanderbilt University Medical Center, Nashville, TN, USA*
Isabel M. Pires • *School of Biological, Biomedical and Environmental Sciences, University of Hull, Hull, UK*
Serapion Pyrpassopoulos • *Department of Physiology, Pennsylvania Muscle Institute, Perelman School of Medicine at the University of Pennsylvania, Philadelphia, PA, USA*
Erik Reimhult • *Department of Nanobiotechnology, Institute for Biologically inspired materials, University of Natural Resources and Life Sciences Vienna, Vienna, Austria*
Anne J. Ridley • *Randall Division of Cell and Molecular Biophysics, King's College London, London, UK*
Antonina Roll-Mecak • *Cell Biology and Biophysics Unit, Center for Biophysics, National Institute of Neurological Disorders and Stroke, National Heart, Lung and Blood Institute, Bethesda, MD, USA*
Michael K. Rosen • *Department of Biophysics, UT Southwestern Medical Center and Howard Hughes Medical Institute, Dallas, TX, USA*
Nicholas J. Schaub • *Center for Biotechnology and Interdisciplinary studies, Rensselaer Polytechnic Institute, Troy, NY, USA; Department of Biomedical Engineering, Rensselaer Polytechnic Institute, Troy, NY, USA*
Marie Schoumacher • *Institut Curie/UMR144 CNRS, Paris, France; Novartis Institute of Biomedical Research, Cambridge, MA, USA*
Simon Scrace • *Department of Oncology, Gray Institute for Radiation Oncology and Biology, University of Oxford, Oxford, UK*
Ved P. Sharma • *Department of Anatomy and Structural Biology and Gruss Lipper Biophotonics Center, Albert Einstein College of Medicine, Bronx, NY, USA*
Henry Shuman • *Department of Physiology, Pennsylvania Muscle Institute, Perelman School of Medicine at the University of Pennsylvania, Philadelphia, PA, USA*
Andrew H. Sims • *Breakthrough Breast Cancer Research Unit, Western General Hospital, Edinburgh, UK*
Narendra Suryavanshi • *Randall Division of Cell and Molecular Biophysics, King's College London, London, UK*
Peter A. Thomason • *CRUK Beatson Institute for Cancer Research, Glasgow, UK*
Francisco J. Tovar-Lopez • *Microplatforms Research Group, Melbourne, VIC, Australia*
Douwe M. Veltman • *CRUK Beatson Institute for Cancer Research, Glasgow, UK*
Danijela M. Vignjevic • *Institut Curie/UMR144 CNRS, Paris, France*
Clare M. Waterman • *Cell Biology and Physiology Center, National Heart Lung and Blood Institute, National Institutes of Health, Bethesda, MD, USA*
Alissa M. Weaver • *Department of Cancer Biology, Vanderbilt University Medical Center, Nashville, TN, USA; Department of Pathology,Vanderbilt University Medical Center, Nashville, TN, USA*
Carsten Werner • *Leibniz Institute of Polymer Research Dresden, Institute for Biofunctional Polymer Materials, Dresden, Germany*

Erik Westein • *Baker IDI Heart and Diabetes Institute, Alfred Medical Research and Educational Precinct, Melbourne, VIC, Australia*
Feng Ye • *Department of Medicine, University of California, San Diego, La Jolla, CA, USA*
Natasza E. Ziółkowska • *Cell Biology and Biophysics Unit, National Institute of Neurological Disorders and Stroke, Bethesda, MD, USA*
J. Bradley Zuchero • *Department of Neurobiology, Stanford University, Stanford, CA, USA*

Chapter 1

Reconstructing Integrin Activation In Vitro

Alexandre R. Gingras, Feng Ye, and Mark H. Ginsberg

Abstract

Integrin activation leads to an increased affinity for the extracellular matrix and regulates many cellular processes such as cell adhesion and migration. To capture the process of integrin inside-out activation in a purified system, we describe here methods to isolate platelet αIIbβ3 integrins in the inactive state and to incorporate them into phospholipid nanodiscs each bearing a single lipid-embedded αIIbβ3 integrin. We delineate a simple enzyme-linked immunosorbent assay that can be used in conjunction with binding of an activation specific monoclonal antibody, PAC1, to monitor the affinity of the integrin before and after the addition of activators such as the Talin Head Domain (THD). The system has been used to show that binding of the THD to both the integrin and the phospholipid bilayer is necessary and sufficient to activate and promote molecular extension of unclustered integrins in the absence of force. This method can be used to test various integrin-binding proteins, membrane phospholipid compositions and different types of integrins. It can also serve as the nidus for synthetic assembly of adhesion plaque like complexes from purified proteins.

Key words Integrin, Talin, Nanodiscs, Activation, Platelets, Membrane scaffold protein (MSP)

1 Introduction

Increased ligand binding affinity of integrins, or activation, is central to many cellular processes such as cell migration, extracellular matrix assembly, hemostasis, and immune response [1]. Integrins are non-covalent heterodimers of transmembrane α- and β-subunits, each with a single transmembrane and cytoplasmic domain. Their activation involves a series of transitions from bent low-affinity states to extended high-affinity states with an open head piece [2]. This extensive conformational change is initiated through interactions at the integrin cytoplasmic domain to regulate their affinity for extracellular ligands, a process referred to as "inside-out" signaling [3–5].

Integrin activation has been analyzed by forward and reverse genetics; however, the many unknowns present in cells and the possible complex effects of over-expression or deletion make it mandatory to complement these cell-based studies with analyses in

Amanda S. Coutts (ed.), *Adhesion Protein Protocols*, Methods in Molecular Biology, vol. 1046,
DOI 10.1007/978-1-62703-538-5_1,

purified systems. Previous in vitro methods analyzed the interaction of cytoplasmic proteins with the α and β integrin tails and measured activation induced by non-physiological agents such as divalent cations or monoclonal antibodies. Although these methodologies reveal valuable information about integrin activation, they fail to capture the entire process of physiological inside-out signaling. Moreover, it is now clear that physiological activation is regulated through interactions of the α- and β-transmembrane and cytoplasmic domains and some of these interactions require embedding in a phospholipid bilayer.

Here we describe methods to purify the inactive αIIbβ3 integrin from platelets, to synthesize phospholipid bilayer nanodiscs, to generate integrin nanodiscs each bearing a single lipid-embedded integrin, and how to use these to study physiologically relevant activation of unclustered integrins.

2 Materials

2.1 KYGRGDS Column Preparation

1. Coupling buffer: 0.1 M $NaHCO_3$, 0.5 M NaCl, pH 8.3.
2. Cyanogen bromide (CNBr) Sepharose: 15 mL of resin (GE Healthcare).
3. KYGRGDS peptide: 50 mg.

2.2 Integrin αIIbβ3 Preparation

1. Calpeptin: 2.76 mM solubilized in DMSO.
2. Leupeptin: 11.7 mM solubilized in dH_2O.
3. PMSF: 200 mM solubilized in ethanol.
4. Protease inhibitor E64 (Sigma-Aldrich) [10 mM].
5. Wash buffer: 20 mM Tris, 150 mM NaCl, pH 7.4.
6. Lysis buffer: 200 mL of 20 mM Tris, 150 mM NaCl, pH 7.4, 1 % Triton X-100, 0.5 mM $CaCl_2$, 5 mM PMSF, 10 μM Leupeptin, 10 μM protease inhibitor E64, 2.76 μM Calpeptin.
7. Platelet-rich plasma, 100 U (~5 L total) (*see* **Note 1**).
8. Centrifuge pots, ideally 500 mL disposable.
9. Integrin buffer: 20 mM Tris, 150 mM NaCl, pH 7.4, 1 mM $CaCl_2$, 1 mM $MgCl_2$, 0.1 % Triton X-100.
10. Con A elution buffer: 20 mM Tris, 150 mM NaCl, pH 7.4, 1 mM $CaCl_2$, 1 mM $MgCl_2$, 0.1 % Triton X-100, 5 mM Leupeptin, 200 mM methyl α-D-mannopyranoside.
11. Concanavalin A Sepharose (Con A) column containing 25 mL of resin (GE Healthcare).
12. Heparin Sepharose: 10 mL of resin (GE Healthcare).
13. A 15 mL KYGRGDS column.

14. Aquacide II (Calbiochem).
15. Dialysis bag of MWCO 25,000 (Spectra/Por).
16. Sephacryl S-300 column 16/60 (GE Healthcare).
17. High pH buffer: 20 mM Tris, 0.5 M NaCl, pH 8.5.
18. Low pH buffer: 20 mM Acetate, 0.5 M NaCl, pH 4.5.
19. Competitive small molecule inhibitor eptifibatide.

2.3 Integrin Activity ELISA (Enzyme-Linked Immunosorbent Assay)

This ELISA is used to assay (a) the purified integrin activity (Subheading 3.2), (b) integrin nanodiscs activity (Subheading 3.6), and (c) the integrin nanodisc activation (Subheading 3.7). The only difference between the assays is the presence of 0.1 % Triton X-100 in the buffer with purified integrins (Subheading 3.2), which is not present in the buffer for the nanodisc assays (Subheadings 3.6 and 3.7) (*see* **Note 2**).

1. Anti-β3 mouse monoclonal AP3 antibody (ATCC).
2. Anti-β3 polyclonal antibody Rb8053, rabbit sera (Ginsberg lab and many others).
3. Purified Mouse IgM anti-human αIIbβ3 integrin PAC1 antibody (for active integrin) (Becton Dickinson).
4. Anti-LIBS mouse monoclonal antibody: anti-LIBS2 or anti-LIBS6 (integrin activating antibodies) (Millipore).
5. Competitive small molecule inhibitor eptifibatide.
6. HRP-anti-mouse IgM.
7. HRP-anti-rabbit IgG.
8. Plate reader for chemi-luminescence.
9. Microfluor2 plates.
10. Purified integrins as prepared in Subheading 3.1.
11. HBS-T buffer: 20 mM HEPES, 150 mM NaCl, pH 7.4, 0.5 mM $CaCl_2$, 0.5 mM $MgCl_2$, 0.1 % Triton X-100.
12. Blocking buffer: HBS-T with 10 % BSA.
13. ECL Western Blotting Substrate (Pierce).

2.4 Purification of Recombinant MSP1

1. Luria Bertani medium (LB).
2. 100 mM Isopropyl-beta-D-thiogalactopyranoside (IPTG), dioxane free in ddH_2O.
3. MSP1 lysis buffer: 40 mM Tris, 0.3 M NaCl, pH 8.0, 1 % Triton X-100, 1 mM PMSF.
4. Nickel column containing 5 mL of resin charged with Ni^{2+} according to manufacturer's instructions.
5. His-MSP1 cloned into your vector of choice, we used pET-28a (Novagen).

6. *E. coli* BL21 (DE3) strain.
7. MSP1 wash buffer 1: 40 mM Tris, 0.3 M NaCl, pH 8.0, 1 % Triton X-100.
8. MSP1 wash buffer 2: 40 mM Tris, 0.3 M NaCl, pH 8.0, 50 mM cholate.
9. MSP1 wash buffer 3: 40 mM Tris, 0.3 M NaCl, pH 8.0.
10. MSP1 wash buffer 4: 40 mM Tris, 0.3 M NaCl, 50 mM imidazole, pH 8.0.
11. MSP1 elution buffer: 40 mM Tris, 0.3 M NaCl, 0.3 M imidazole, pH 8.0.
12. MSP1 buffer: 10 mM Tris, 0.1 M NaCl, pH 7.4, 1 mM EDTA.
13. Sonicator or French pressure cell press (French press).

2.5 Purification of Recombinant Talin Head Domain (THD)

1. Luria Bertani medium (LB).
2. 100 mM Isopropyl-beta-D-thiogalactopyranoside (IPTG), dioxane free in ddH_2O.
3. Nickel column containing 5 mL of resin charged with Ni^{2+} according to the manufacturer's instructions.
4. Sonicator or French pressure cell press (French press).
5. Recombinant human talin head. We used residues 1–433 cloned in pET-30a (Novagen) with a C-terminus hexahistidine tag (*see* **Note 3**).
6. *E. coli* BL21 (DE3) pLysS.
7. Nickel buffer A: 20 mM Tris, 0.5 M NaCl, 20 mM imidazole, pH 8.0.
8. Nickel buffer B: 20 mM Tris, 0.5 M NaCl, 0.5 M imidazole, pH 8.0.
9. Tris-buffered saline (TBS): 20 mM Tris, 150 mM NaCl, pH 7.4.

2.6 Integrin Nanodiscs

1. Purified integrin αIIbβ3 in integrin buffer (at least 5 μM). Use a fresh tube from the −80 °C.
2. Purified membrane scaffold protein (MSP) MSP1D1 as prepared in Subheading 3.3.
3. Synthetic lipids: 1,2-dimyristoyl-*sn*-glycero-3-phosphocholine (DMPC), 1,2-dimyristoyl-*sn*-glycero-3-phospho-(1′-rac-glycerol) (DMPG) from Avanti Polar Lipids. They are solubilized in 2.5 mL chloroform (DMPC) or chloroform/methanol mixture (2:1 volume ratio) (DMPG) at a concentration of 10 mg/mL. All lipids should be freshly made.
4. SM-2 Biobeads from Bio-Rad.
5. Tris-buffered saline (TBS): 20 mM Tris, 150 mM NaCl, pH 7.4.

6. Lipid resuspension buffer: 10 mM Tris, 100 mM NaCl, pH 7.4, 100 mM cholate.
7. Superdex 200 (16/300) size exclusion column (GE Healthcare).
8. TBS + 0.5 mM $CaCl_2$.

2.7 Integrin Nanodisc Activation ELISA

Use the same material as described in Subheading 2.3 with the exception of the HBS-T buffer which is now replaced with HBS buffer.

1. HBS buffer: 20 mM HEPES, 150 mM NaCl, pH 7.4, 0.5 mM $CaCl_2$, and 0.5 mM $MgCl_2$.
2. Integrin nanodiscs as prepared in Subheading 3.5.
3. Blocking buffer: HBS with 10 % BSA.

2.8 Integrin Nanodiscs Activation by THD

Use the same material as described in Subheading 2.7.

1. Recombinant Talin Head Domain (THD) as prepared in Subheading 3.4.

3 Methods

Here we describe how to purify the inactive αIIbβ3 integrin from platelets, to synthesize phospholipid bilayer nanodiscs, to generate integrin nanodiscs each bearing a single lipid-embedded integrin, and how to use them to study inside-out regulation of unclustered integrins leading to molecular extension in the absence of force or other membrane proteins. The overall procedure is outlined in Fig. 1.

3.1 Purification of Integrin αIIbβ3 (GP IIb–IIIa) from Platelets

Many methods have been described for purification of the platelet fibrinogen receptor [6] integrin αIIbβ3 or Glycoprotein IIb–IIIa. However, for the experiment described here, it is critical to isolate the inactive integrin fraction. The procedure involves lectin affinity chromatography on concanavalin A Sepharose followed by Heparin Sepharose. The inactive integrin is further purified by separating it from the active integrin by the use of a KYGRGDS affinity purification column, which binds the active integrin fraction [7]. The flow through containing the inactive integrin is further purified by gel filtration chromatography on a Sephacryl S-300 column.

3.1.1 Preparation of a KYGRGDS Column

1. Dissolve 50 mg of KYGRGDS peptide in 1 mL of ddH_2O and dilute in 15 mL coupling buffer. Determine the peptide concentration by A_{280} (we use 1.637 as extinction coefficient).
2. Prepare 15 mL CNBr sepharose as per the manufacturer's instructions and combine the sucked dry slurry with the peptide solution. Incubate at 4 °C overnight with rocking.

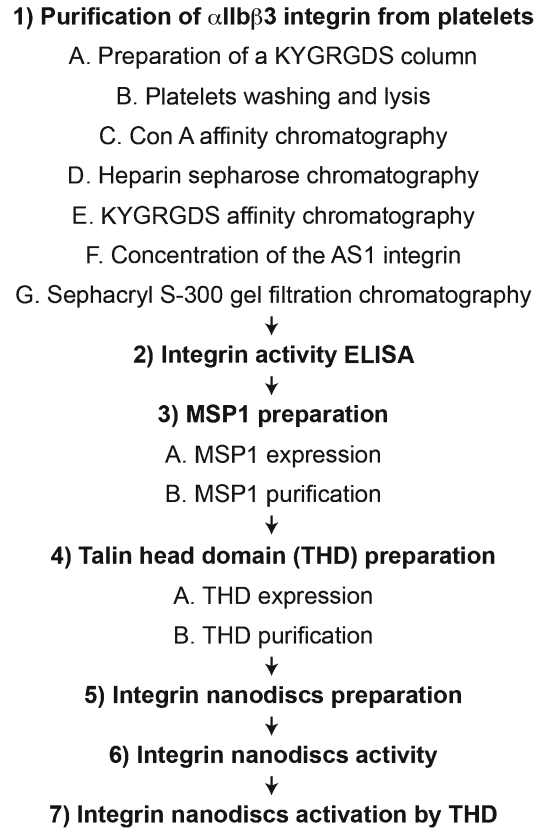

Fig. 1 Diagram of the major steps for isolation of the integrin αIIbβ3 from platelets, followed by an integrin activity ELISA, purification of the MSP1 protein, purification of the talin head domain (THD), preparation of the integrin nanodiscs, testing for the integrin nanodiscs activity, and measurement of the integrin activation within a nanodisc by THD

3. Determine the A_{280} of the supernatant in order to determine if the coupling was efficient (*see* **Note 4**).
4. Pack the KYGRGDS resin in a column.
5. If the column is to be used later, store in 20 % ethanol.

3.1.2 Platelet Washing and Lysis

1. Collect the platelet enriched plasma in 500 mL centrifuge pots (*see* **Note 5**) and centrifuge once at 300 × *g* for 10 min at room temperature (RT) to remove red blood cells (*see* **Note 6**).
2. Transfer the supernatants to new centrifuge pots taking extra care not to disturb the loose pellet of red blood cells and centrifuge at 1,800 × *g* for 30 min at RT to pellet the platelets (*see* **Note 6**).
3. Discard the supernatants and gently resuspend each pellet in 200 mL wash buffer and centrifuge at 1,800 × *g* for 60 min at RT. Repeat to remove the majority of plasma proteins (*see* **Note 6**).

4. Solubilize all the platelet pellets in 200 mL lysis buffer and leave rocking at 4 °C overnight.
5. Centrifuge the lysate at 30,000 × *g* for 60 min at 4 °C.
6. Collect the supernatant and discard the Triton X-100 insoluble pellet (*see* **Note 7**).

3.1.3 Con A Affinity Chromatography

The concanavalin A binds specifically to mannosyl and glucosyl residues of polysaccharides and glycoproteins. Here it is used to concentrate the platelet glycoproteins such as thrombospondin, the αIIbβ3 integrin, and fibrinogen.

1. Equilibrate the Con A Sepharose column with integrin buffer at 4 °C.
2. Load the platelet lysate over a 25 mL Con A Sepharose column using a flow rate of 1 mL/min and recirculate overnight at 4 °C (*see* **Note 8**).
3. Wash at 4 °C the Con A Sepharose column with integrin buffer until the A_{280} goes down to 0.02.
4. Elute the bound material with 200 mL of Con A elution buffer and collect 4 mL fractions at 4 °C.
5. Run the eluted fractions on SDS-PAGE for analysis (*see* **Note 9**). Pool the fractions containing the integrins and keep them at 4 °C (*see* **Note 10**).

3.1.4 Heparin Sepharose Chromatography

Heparin is a highly sulphated glycosaminoglycan which serves as an anticoagulant by selectively binding antithrombin III. This column here is primarily used to remove the thrombospondin which is a major contaminant of the Con A eluate.

1. Prepare 10 mL of Heparin Sepharose resin (~20 mL slurry) in a 50 mL plastic tube. Fill the tube with ddH_2O and centrifuge at 3,500 × *g* for 30 min at 4 °C.
2. Discard the supernatant and fill the tube with integrin buffer to equilibrate the resin. Resuspend the resin and centrifuge at 3,500 × *g* for 30 min at 4 °C. Repeat this step to wash the resin properly.
3. Add the Heparin Sepharose to the pooled fractions eluted from the Con A column and leave rocking overnight at 4 °C.
4. Spin the Heparin beads at 3,500 × *g* for 30 min at 4 °C and collect the supernatant. Repeat this step if necessary until the supernatant is clear.

3.1.5 KYGRGDS Affinity Chromatography

Active integrins recognize the RGD sequence, therefore the active integrin will bind to the immobilized KYGRGDS peptide on the column and get separated from the inactive integrins in the flow through.

1. Wash the KYGRGDS column with three changes of high and low pH buffer and then equilibrate with two column volumes of integrin buffer.
2. Apply the Heparin Sepharose supernatant to the KYGRGDS using a flow rate of 1 mL/min and recirculate overnight at 4 °C.
3. Collect the flow through containing the inactive integrins. Generally, >90 % of the integrins are inactive and found in the flow through.
4. To recover the active integrin bound to the KYGRGDS column, wash the column with integrin buffer and elute the active integrin with 20 μM eptifibatide compound in integrin buffer. This active integrin fraction can be used for other types of experiments.

3.1.6 Concentration of the Inactive Integrins

1. Load the KYGRGDS flow through, inactive integrin, into a dialysis bag of MWCO 25,000.
2. Cover a flat container with Aquacide II, place the dialysis bag into the bed of Aquacide II and cover with more Aquacide II (*see* **Note 11**). Place at 4 °C.
3. Constantly monitor the remaining volume until it is <10 mL. Approximately every hour, peel off the Aquacide II from the dialysis bag and cover again. According to the manufacturer's instructions, 1 g of Aquacide will absorb 5 mL of water in 1 h.

3.1.7 Sephacryl S-300 Gel Filtration Chromatography

Fibrinogen is the major contaminant left from the preparation (MW under non-reducing conditions = 340,000 kDa) and can be separated from the αIIbβ3 integrin using gel filtration.

1. Pre-equilibrate the Sephacryl S-300 16/60 column with integrin buffer.
2. Load the concentrated inactive integrin onto the Sephacryl S-300 at RT using a flow rate of 1 mL/min. Collect 4 mL fractions.
3. Run the fractions on SDS-PAGE for analysis (*see* **Note 9**).
4. Keep the integrin fractions, taking extra care to discard the fractions containing fibrinogen.
5. Determine the integrin concentration using a BCA assay.
6. Freeze the samples at −80 °C in small aliquots.

3.2 Integrin Activity ELISA

Here we describe an ELISA method to measure integrin activation in vitro. Our ELISA assay relies on the selective binding of integrin ligands and ligand-mimetic antibodies to activated integrins as shown in Fig. 2. The basis of the integrin αIIbβ3 activation assay is the mouse monoclonal antibody PAC1, as it is a ligand-mimetic

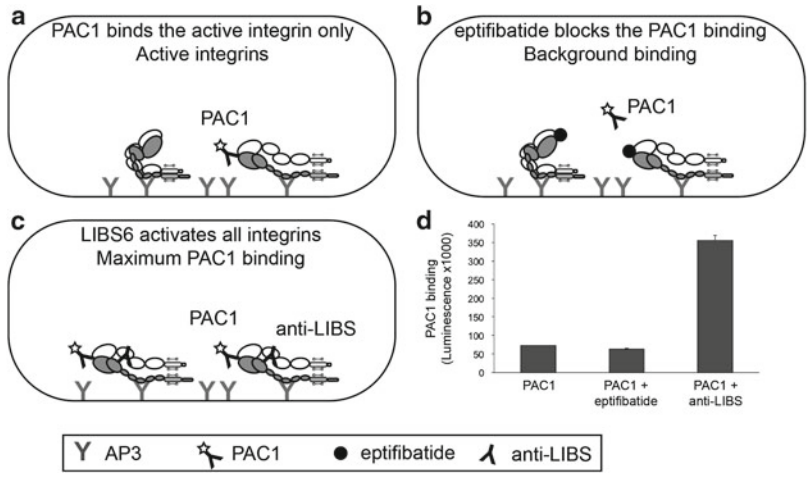

Fig. 2 Schematic of assays for measuring activation of detergent solubilized αIIbβ3. (**a**) The integrins are immobilized using the AP3 antibody and the PAC1 antibody is used to measure the integrins in their active conformation. (**b**) To measure the background signal, eptifibatide is used to block the PAC1 antibody binding site. (**c**) To measure the maximum PAC1 binding to the integrins, the anti-LIBS antibody is used to activate the integrins. Anti-LIBS2 or -LIBS6 are IgG and PAC1 is an IgM, therefore the secondary antibody which is an anti-IgM will only detect PAC1 binding. (**d**) Measurement of the fraction of active integrins in the detergent solubilized preparation

antibody that binds to the ligand-binding site in the integrin. The PAC1 antibody binds only the active form of the integrin, so here it is used to measure the fraction of active integrins in our preparation as shown in Fig. 2a.

To accurately measure the background of the assay, we use eptifibatide to block PAC1 binding to the integrins as shown in Fig. 2b. Eptifibatide, also known as integrilin, is a cyclic heptapeptide that behaves as an RGD-mimetic and therefore competes for binding with PAC1.

To measure the maximum integrin activation, we measure PAC1 binding in the presence of an activating antibody (anti-LIBS) that binds the extracellular domain of β3 [8] as shown in Fig. 2c. As a supplementary control, one can use the rabbit anti-αIIbβ3 (Rb8053) to measure the total integrin loading.

1. Coat each well of the plate with 100 μL of 5 μg/mL AP3 antibody. Cover the plate and incubate at 4 °C overnight. Make sure that the solution covers the entire well and that there are no air bubbles.
2. Remove the coating solutions and block with 150 μL of blocking buffer at 37 °C for 1 h.
3. Remove the blocking buffer and wash three times with 150 μL HBS-T buffer.

Table 1
Plate layout for integrin activity assay (*see* Note 12)

Integrin	Integrin + eptifibatide	Integrin + anti-LIBS	Integrin
PAC1 detection	PAC1 detection	PAC1 detection	Rb8053 detection

4. Add 75 µL of purified integrin solution (6 µg/mL) according to the layout in Table 1. Incubate at RT for 3 h.
5. Remove the binding mixture and wash three times with 150 µL HBS-T buffer.
6. PAC1 detection: Add 75 µL of the antibody PAC1 (1:4,000), with the appropriate controls as described in Table 1: (a) 20 µM eptifibatide as negative control, and (b) anti-LIBS as positive control (1:100).
   Rb8053 detection: Add 75 µL of the detection antibody Rb8053 to measure the amount of integrin capturing (1:1,000).
7. Incubate at RT for 1.5 h.
8. Wash three times with 150 µL HBS-T buffer.
9. Add 75 µL of secondary antibody: (a) HRP-anti-mouse IgM for PAC1 (1:1,000), or (b) HRP-anti-rabbit IgG for Rb8053 (1:1,000). Incubate at RT for 1.5 h.
10. Wash three times with 150 µL HBS-T buffer.
11. Add 75 µL of ECL to each well. Incubate for 5–10 min at RT.
12. Read the luminescence using a plate reader.
13. Analyze the data as shown in Fig. 2. The activation indices are calculated as $100 \times (L - L_0)/(L_{max} - L_0)$, where L = luminescence in the presence of 20 µM eptifibatide, and L_{max} = luminescence in presence of anti-LIBS antibody.

In this experiment, 3 % of the integrins are active so the major portion of our integrin preparation (97 %) is in the inactive conformation.

3.3 Membrane Scaffold Protein (MSP) Preparation

Nanoparticulate phospholipid bilayer disks, termed nanodiscs, can be assembled using a class of amphipathic helical proteins termed membrane scaffold proteins (MSP). Here we used MSP1 that forms nanodiscs of approximately 10 nm in diameter and 5.5 nm thickness [9].

3.3.1 MSP1 Expression

1. Inoculate 100 mL of LB containing the appropriate antibiotic with *E. coli* BL21 (DE3) culture containing His-MSP1 fusion protein expression construct. Grow overnight at 37 °C in a rotary shaker incubator with agitation at 225 rpm.
2. Use 1 mL of the overnight culture to inoculate 1 L of LB with the appropriate antibiotic and grow the culture to an approximate OD_{600} of 0.6.

3. Induce the protein expression by adding 1 mM IPTG to the culture and grow for 3 h.
4. Harvest the bacteria by centrifugation at 3,600 × *g* for 20 min and store the pellet at −20 °C until use.

3.3.2 Purification of MSP1

1. Resuspend the cell pellet in 50 mL of ice cold MSP1 lysis buffer.
2. Lyse the cells using sonication or a French press while keeping the sample on ice.
3. Clear the lysate by centrifugation at 30,000 × *g* for 30 min at 4 °C.
4. Load the supernatant onto the nickel column.
5. Wash the column with four bed volumes of each of the following: (a) MSP1 wash buffer 1, (b) MSP1 wash buffer 2, (c) MSP1 wash buffer 3, (d) MSP1 wash buffer 4.
6. Elute the MSP1 with the MSP1 elution buffer and collect 4 mL fractions.
7. Check for purity by SDS-PAGE (MW = 24.66 kDa).
8. Pool the fractions containing MSP1 and dialyze against MSP1 buffer at 4 °C.
9. Determine the protein concentration using a BCA assay or using the absorbance at 280 nM (extinction coefficient of 0.869).
10. Freeze the protein in small aliquots and store at −80 °C.

3.4 Talin Head Domain Preparation

Here we describe how to purify the recombinant THD as a hexahistidine tagged protein for easy purification.

3.4.1 Talin Head Domain Expression

1. Inoculate 100 mL of LB containing the appropriate antibiotic with *E. coli* BL21 (DE3) pLysS culture containing THD-His fusion protein expression construct. Grow overnight at 37 °C in a rotary shaker incubator with agitation at 225 rpm.
2. Use 1 mL of the overnight culture to inoculate 1 L of LB with appropriate antibiotic and grow the culture to an approximate OD_{600} of 0.5.
3. Transfer the culture to a 20 °C shaker for 1 h.
4. Induce the protein expression by adding 0.5 mM IPTG to the culture and grow for 10 h or overnight at 20 °C.
5. Harvest the bacteria by centrifugation at 3,600 × *g* for 20 min and store the pellet at −20 °C until use.

3.4.2 Purification of TALIN HEAD DOMAIN

1. Resuspend the cell pellet in 50 mL of ice cold Nickel buffer A.
2. Lyse the cells using sonication or a French press while keeping the sample on ice.
3. Clear the lysate by centrifugation at 30,000 × *g* for 30 min at 4 °C.

4. Load the supernatant onto the nickel column.
5. Wash the column with five bed volumes of Nickel buffer A.
6. Elute the THD with a gradient of Nickel buffer B and collect 3 mL fractions.
7. Check for purity by SDS-PAGE (MW = 53 kDa).
8. Pool the fractions containing THD and dialyze twice for 1 h against 1 L TBS containing 2 mM EDTA at 4 °C (*see* **Note 13**).
9. Dialyze twice for 1 h against 1 L TBS at 4 °C.
10. Determine the protein concentration using a BCA assay.
11. Freeze the protein in small aliquots and store at −80 °C.

3.5 Integrin Nanodiscs Preparation

Many membrane proteins have been successfully embedded into nanodiscs [10–12], including integrins [13]. The self-assembly process begins with a mixture of the purified integrin αIIbβ3 and MSP1 in the presence of a detergent, the phospholipids are then added and the detergent removed (*see* **Note 14**).

1. Mix 339 µL of DMPC (3.39 mg) with 344 µL of DMPG (3.44 mg) (1:1 ratio) into a glass tube and mix thoroughly.
2. Dry the lipids into a glass tube with a steady flow of nitrogen air and leave in the fume hood overnight.
3. Solubilize the MSP1 in ddH_2O such that the final concentration is 200 µM.
4. Solubilize the dried lipids in 200 µL of lipid resuspension buffer, giving a lipid concentration of 50 mM. Vortex until the lipids are fully solubilized. This may take several hours.
5. Mix 72 µL of lipid solution with 200 µL of 200 µM MSP1 in dH_2O and 200 µl of 5 µM purified inactive integrin. The final ratio of lipids:MSP:protein is 90:1:0:025 in a total volume of 472 µL.
6. Add some $CaCl_2$ to the mixture to reach a 0.5 mM final concentration as the lipid and MSP1 solutions do not have calcium in them (*see* **Note 15**).
7. Prewash 1 mL of SM-2 Biobeads with methanol (three times), water (seven times) and TBS (twice) by centrifugation at 3,500 × *g* for 5 min at RT.
8. Add 1 mL of SM-2 Biobeads to the nanodiscs tube to remove the detergent (*see* **Note 16**). Incubate overnight with gentle agitation at RT.
9. Remove the supernatant containing the integrin nanodiscs from the Biobeads.
10. Equilibrate a Superdex 200 (16/300) size exclusion column with TBS + 0.5 mM $CaCl_2$.

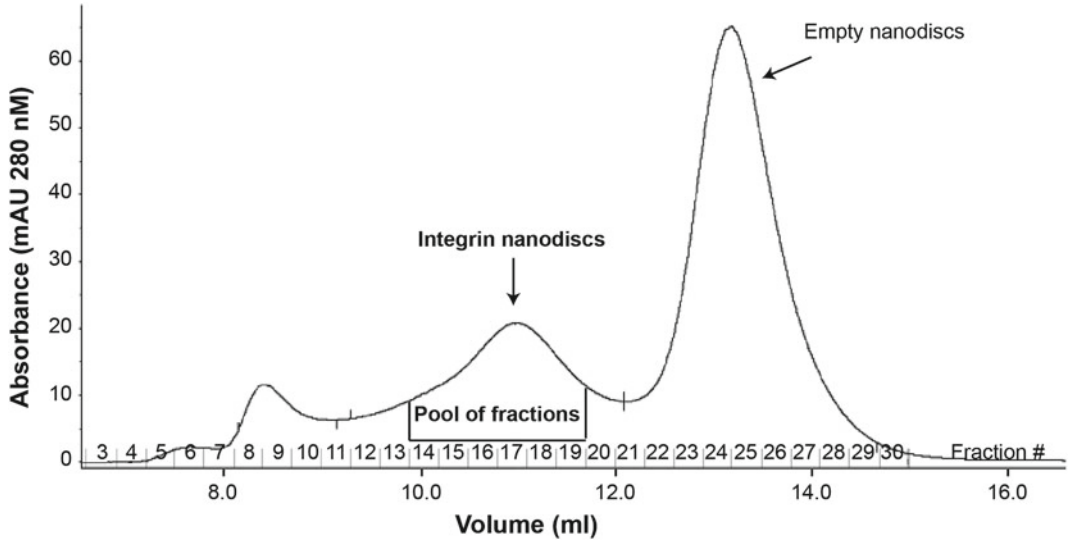

Fig. 3 Profile of the Superdex 200 (16/300) gel filtration chromatography. The fractions which contain the integrin nanodiscs and empty nanodiscs are shown. The column was run in TBS + 0.5 mM $CaCl_2$ at a flow rate of 0.5 mL/min and fractions of 0.3 mL were collected

11. Load 0.25 mL of the integrin nanodiscs solution onto the Superdex 200 size exclusion column. Use a flow rate of 0.5 mL/min and collect fractions of 0.3 mL. Two runs are necessary to purify ~0.5 mL of integrin nanodiscs mixture.
12. Run an SDS-PAGE to identify the fractions containing both integrins and nanodiscs.
13. Pool the fractions containing the integrin nanodiscs as shown in Fig. 3. The integrin nanodiscs and empty nanodiscs should be separated.

3.6 Integrin Nanodisc Activity

This section describes how to test the activity of the integrins within the nanodiscs using a method almost identical to that described in Subheading 3.2. It is critical to know which portion of the integrin nanodiscs is active: the less, the better. Measuring integrin activation with talin for example with a preparation that is largely active could be difficult.

1. Follow the method outlined for the integrin activity ELISA, *see* Subheading 3.2, but throughout use HBS buffer instead of HBS-T buffer.
2. Instead of adding 75 μL of purified integrin, add 75 μL of purified integrin nanodiscs.
3. Analyze the data as shown in Fig. 4.

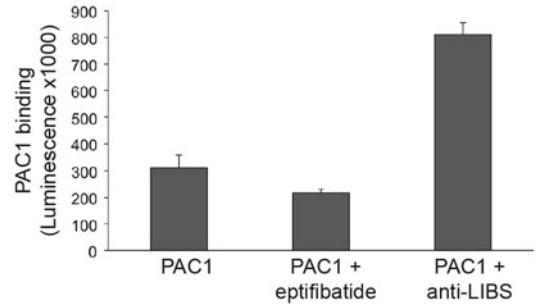

Fig. 4 Measurement of the fraction of active integrin within the integrin nanodiscs preparation

Table 2
Plate layout for integrin nanodisc activation assay (*see* Note 12)

Nanodisc	Nanodisc +eptifibatide	Nanodisc + anti-LIBS	Nanodisc
PAC1 detection	PAC1 detection	PAC1 detection	Rb8053 detection
Nanodisc + THD	*Nanodisc + THD + eptifibatide*	*Nanodisc + THD + anti-LIBS*	*Nanodisc + THD*
PAC1 detection	PAC1 detection	PAC1 detection	Rb8053 detection

In our experiment, 16 % of the integrin nanodiscs were active as determined by PAC1 binding. Therefore, the major portion of the integrin nanodiscs (84 %) can, in theory, be activated by adding other components to the experimental setup as described in Subheading 3.7.

3.7 Integrin Nanodisc Activation

This method provides a powerful tool in screening for players in integrin signaling and discovering new regulators of talin mediated integrin activation. Obviously this method does not only apply to talin, other regulators, such as kindlins, can be added to the system [14, 15].

Again, it is the same experiment as for the integrin nanodiscs activity ELISA, *see* Subheading 3.6, except that the plate layout is slightly more complex because here we will add THD to activate the integrins.

1. PAC1 detection: Add 75 μL of the antibody PAC1 (1:4,000), with the appropriate controls as described in Table 2: (a) 2.5 μM of THD for activation, (b) 20 μM eptifibatide as negative control, and (c) anti-LIBS as positive control (1:100).

   Rb8053 detection: Add 75 μL of the detection antibody Rb8053 to measure the amount of integrin capturing (1:1,000).
2. Analyze the data as shown in Fig. 5a. Calculate the activation indices as described in Subheading 3.2 and as show in Fig. 5b. In our experiment 21 % of the integrin nanodiscs alone are active and 62 % in the presence of 2.5 μM THD.

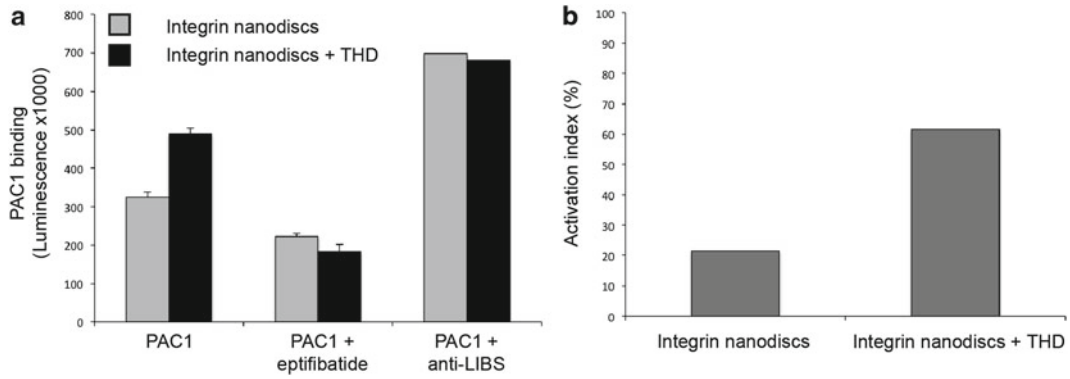

Fig. 5 Measurement of the integrin activation by THD. (**a**) Measurement of the active integrin nanodiscs in the absence and presence of THD. (**b**) Integrin nanodiscs activation index in the absence and presence of THD. There is a 40 % increase in active integrins in the presence of 2.5 μM THD

3. Calculate the increase in activation using $AI_{with\text{-}THD} - AI_{integrin\text{-}alone}$, where AI stands for activation indices. In our experiment, adding 2.5 μM of THD produced a 40 % increase in integrin nanodiscs activation.

4 Notes

1. It is important to have the platelet-rich plasma delivered at room temperature. Cold can lead to platelet activation and aggregation.
2. The Triton X-100 in the buffer is used to keep the purified integrin soluble in solution. Within a nanodisc, the integrins are inserted into a phospholipid bilayer and adding detergent in those experiments would disrupt that phospholipid bilayer and therefore affect the integrins.
3. The THD has been extensively studied and smaller subdomains, such as the F2–F3 region could work just as well for integrin activation [16–19].
4. In our experiment more than 60 % of the peptide was coupled to the resin, but we did not perform any test to verify if the efficiency can be improved by using more resin or less peptide.
5. The handling and disposal of human blood products should be performed with biohazard precautions.
6. It is important to keep the centrifuge temperature around 20 °C to prevent platelet aggregation and activation.
7. If necessary, the supernatant can be frozen at −80 °C until further use. This crude lysate can then be thawed rapidly and centrifuged at 30,000 × *g* for 60 min at 4 °C to remove residual cytoskeleton.

8. This can be performed using a peristaltic pump or an FPLC.
9. Under reducing conditions, αIIb has a MW of ~120 kDa and β3 has a MW of ~95 kDa. Thrombospondin has a MW of 160 kDa and fibrinogen alpha, beta and gamma chains of ~95, ~55 and ~51.5 kDa respectively.
10. If necessary, the eluate can be frozen at −80 °C until further use.
11. There are several simple and relatively inexpensive methods for concentrating protein solutions. Dialysis against Aquacide II (Calbiochem), which removes water through the dialysis tubing, is what we use. Alternatively, centrifugal concentrators or ultrafiltration membranes may be used.
12. For the ELISA each experiment has to be performed in triplicate.
13. It is important to dialyze all traces of nickel from the THD preparation because residual Ni^{2+} on the hexahistidine tag can cause lipid precipitation problems.
14. The preparation has been described by Ye et al. [13] and it was shown that each nanodisc contained a single αIIbβ3 integrin.
15. It is important to keep a divalent cation present with integrins as the α and β subunits could separate.
16. Use a 1.5 mL Eppendorf as the integrin nanodiscs mixture is about 0.5 mL and filling the tube with SM-2 Biobeads will result in approximately 1 mL of beads added.

Acknowledgments

This work was supported by the American Heart Association 12SDG11610043 (A.R. Gingras) and NIH (M.H. Ginsberg).

References

1. Calderwood DA (2004) Integrin activation. J Cell Sci 117:657–666
2. Shattil SJ, Hoxie JA, Cunningham M et al (1985) Changes in the platelet membrane glycoprotein IIb.IIIa complex during platelet activation. J Biol Chem 260:11107–11114
3. Kim C, Ye F, Ginsberg MH (2011) Regulation of integrin activation. Annu Rev Cell Dev Biol 27:321–345
4. Anthis NJ, Wegener KL, Ye F et al (2009) The structure of an integrin/talin complex reveals the basis of inside-out signal transduction. EMBO J 28:3623–3632
5. Travis MA, Humphries JD, Humphries MJ (2003) An unraveling tale of how integrins are activated from within. Trends Pharmacol Sci 24:192–197
6. Fitzgerald LA, Leung B, Phillips DR (1985) A method for purifying the platelet membrane glycoprotein IIb–IIIa complex. Anal Biochem 151:169–177
7. Kouns WC, Hadvary P, Haering P et al (1992) Conformational modulation of purified glycoprotein (GP) IIb–IIIa allows proteolytic generation of active fragments from either active or inactive GPIIb–IIIa. J Biol Chem 267:18844–18851

8. Frelinger AL 3rd, Du XP, Plow EF et al (1991) Monoclonal antibodies to ligand-occupied conformers of integrin alpha IIb beta 3 (glycoprotein IIb–IIIa) alter receptor affinity, specificity, and function. J Biol Chem 266: 17106–17111
9. Denisov IG, Grinkova YV, Lazarides AA et al (2004) Directed self-assembly of monodisperse phospholipid bilayer nanodiscs with controlled size. J Am Chem Soc 126:3477–3487
10. Katayama H, Wang J, Tama F et al (2010) Three-dimensional structure of the anthrax toxin pore inserted into lipid nanodiscs and lipid vesicles. Proc Natl Acad Sci U S A 107: 3453–3457
11. Denisov IG, Sligar SG (2011) Cytochromes P450 in nanodiscs. Biochim Biophys Acta 1814:223–229
12. Raschle T, Hiller S, Yu TY et al (2009) Structural and functional characterization of the integral membrane protein VDAC-1 in lipid bilayer nanodiscs. J Am Chem Soc 131: 17777–17779
13. Ye F, Hu G, Taylor D et al (2010) Recreation of the terminal events in physiological integrin activation. J Cell Biol 188:157–173
14. Moser M, Legate KR, Zent R et al (2009) The tail of integrins, talin, and kindlins. Science 324:895–899
15. Ye F, Kim C, Ginsberg MH (2011) Molecular mechanism of inside-out integrin regulation. J Thromb Haemost 9(Suppl 1):20–25
16. Bouaouina M, Harburger DS, Calderwood DA (2012) Talin and signaling through integrins. Methods Mol Biol 757:325–347
17. Elliott PR, Goult BT, Kopp PM et al (2010) The Structure of the talin head reveals a novel extended conformation of the FERM domain. Structure 18:1289–1299
18. Garcia-Alvarez B, de Pereda JM, Calderwood DA et al (2003) Structural determinants of integrin recognition by talin. Mol Cell 11: 49–58
19. Anthis NJ, Wegener KL, Critchley DR et al (2010) Structural diversity in integrin/talin interactions. Structure 18:1654–1666

Chapter 2

Quantifying Cellular Adhesion to Covalently Immobilized Extracellular Matrix Proteins by Single-Cell Force Spectroscopy

Jens Friedrichs, Carsten Werner, and Daniel J. Müller

Abstract

Atomic force microscopy (AFM)-based single-cell force spectroscopy (SCFS) enables the quantitative study of cell adhesion under physiological conditions. SCFS probes adhesive interactions of single living cells with substrates such as extracellular matrix (ECM) proteins and other cells. Here, we present a protocol to quantitatively study the adhesion of HeLa cells to covalently immobilized fibronectin and Matrigel™ using SCFS. We describe procedures for (a) functionalization of AFM cantilevers, (b) preparation of maleic anhydride copolymer thin films, (c) covalent immobilization of ECM proteins on the thin films, (d) cell handling and attachment to the AFM cantilever, and (e) measurement of adhesion forces. The protocol can be easily modified for other cell types and substrate proteins.

Key words AFM, Atomic force microscopy, Extracellular matrix, Cell adhesion, SCFS, Single-cell force spectroscopy

1 Introduction

Crucial to multicellular organisms is the physical interaction of cells with the extracellular matrix (ECM) [1, 2]. These interactions regulate growth, differentiation, migration as well as the survival of cells. Consequently, elucidating the interactions between cells and ECM is of particular interest. To quantify the adhesive interaction of cells with ECM proteins, force spectroscopy assays are particularly useful. Atomic force microscopy (AFM)-based single-cell force spectroscopy (SCFS) has proven to be very versatile since it allows a wide range of forces, from ≈5 pN to ≈100 nN, to be measured [3]. Due to this wide force detection range the adhesive strength of entire cells [4–7] as well as the forces required to separate single ligand–receptor pairs [8] can be measured. Thereby a broad range of biological questions can be addressed.

Amanda S. Coutts (ed.), *Adhesion Protein Protocols*, Methods in Molecular Biology, vol. 1046,
DOI 10.1007/978-1-62703-538-5_2,

AFM-based SCFS can be performed in two ways. Either, the adhesion of a cantilever-attached cell to a given substrate is probed [9] or the adhesion of a cell, immobilized onto a substrate, to a functionalized cantilever is probed [10]. In this chapter, we explain the use of the former approach whose principle is schematically illustrated in Fig. 1a. A living cell, attached to an AFM cantilever is positioned above a substrate of ECM proteins covalently attached to a glass support. The cell is lowered onto the substrate at constant speed until a preset contact force is reached. The contact force is kept stationary for a defined contact time. This allows the formation of bonds between cell adhesion molecules (CAMs) and ligand molecules on the substrate. Subsequently, the cell is retracted from the substrate at constant speed. Bonds between CAMs and ligand molecules sequentially break until cell and substrate are completely separated. During approach and retraction of the cell, the force acting on the cantilever, which is proportional to the cantilever deflection, is recorded in a force–distance (F-D) curve (Fig. 1b). Several cell adhesion-related parameters can be extracted from F-D curves:

- *Detachment force,* F_D: The detachment force is the maximal force required to separate the cell from the substrate (Figs. 1b and 2). During the initial detachment phase, bonds in the outer radial area of the contact zone formed between cell and substrate are predominantly stressed. Upon proceeding retraction of the cantilever, the cell is stretched until a maximal force is reached. As soon as the bonds that formed between CAMs and ligand molecules rupture, the contact zone shrinks. Assuming a homogenous distribution of CAMs over the contact zone, more bonds per radial area will have formed at the periphery of the contact zone than in the inner regions. Consequently, a maximal force is detected before the bonds at the periphery of the contact zone begin to rupture. As soon as these bonds rupture the adhesive force decreases quickly since the applied force load is shared by fewer CAMs in the inner contact zones and the probability that these smaller zones can resist large rupture forces decreases.
- *Detachment work,* W_D: Another type of quantitative data extracted from adhesion experiments is the work needed to separate a cell from the substrate. The work is defined as the integral of the adhesive force that has been detected over the pulling distance until the cell is completely separated from the substrate. Accordingly, W_D can be calculated by integrating the adhesive (negative) force of the retraction F-D curve (Fig. 1b). The number of receptor–ligand bonds, the stretching of cell body during retraction (deformation) and the number and length of membrane tethers (see below) contribute to the total amount of detachment work.

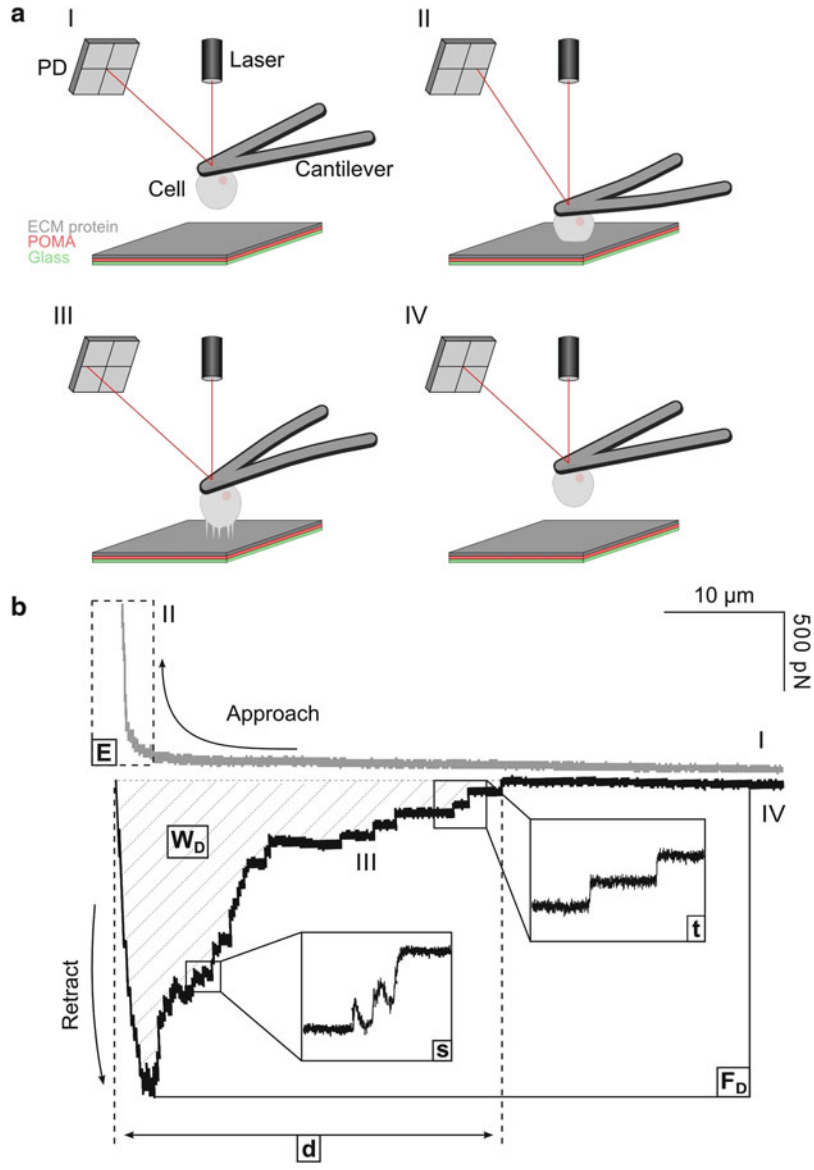

Fig. 1 SCFS setup. (**a**) SCFS—(I) A cell is attached to a coated cantilever. To measure the force acting on the cantilever, the cantilever deflection is determined using a laser beam reflected by the back of the cantilever onto a multi-segment photodiode (PD). (II) The cantilever-bound cell is lowered towards the covalently bound ECM proteins on the polymer-coated supports until a preset force is reached. (III) After a given contact time, the cantilever is retracted until cell and substrate are completely separated (IV). (**b**) F-D curve showing steps (I), (II), (III), and (IV) corresponding to those outlined in (**a**). Several parameters can be extracted; F_D, detachment force; W_D, detachment work; *s*, force steps; *t*, unbinding of membrane tethers; *d*, separation distance and *E*, elastic properties of the cell. The approach and retraction F-D curves are colored *grey* and *black*, respectively

- *Discrete unbinding events*: Retraction F-D curves usually display discrete unbinding events (Fig. 1b) that can be distinguished into steps and tethers. A nonlinear force loading typically

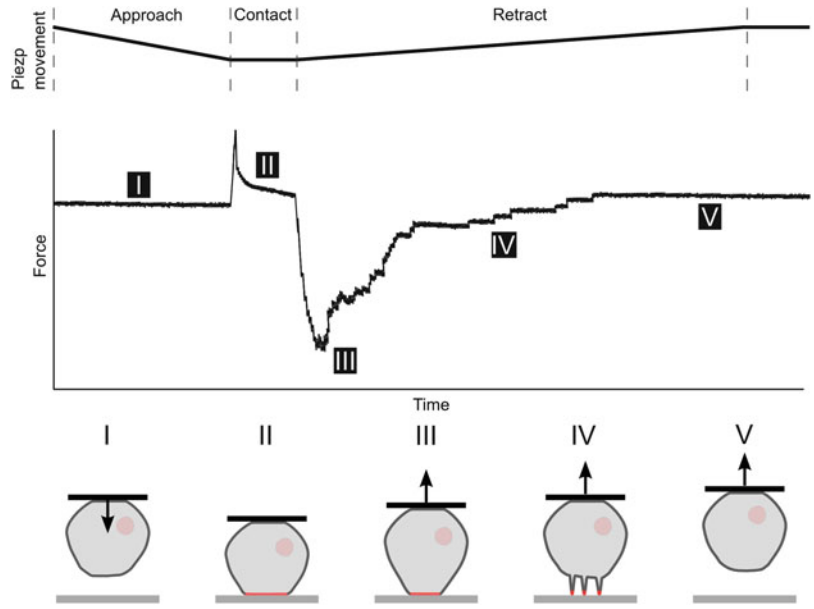

Fig. 2 Schematic representation of the cell attachment and detachment process. The process is separated into different phases. (I) The cantilever-bound cell is moved towards the substrate and pressed onto the substrate until a preset force is reached. (II) In constant height-mode, the cantilever position is maintained constant during contact. Due to its viscous properties, the cell relaxes and the force exerted on the cantilever decays during the first seconds of contact. In the contact zone of the cell with the substrate (*bottom area*) adhesive interactions occur. (III) During cell detachment, bonds formed between CAMs and ligand molecules on the substrate rupture and the contact zone shrinks. (IV) When the cell body is separated from the substrate, only membrane nanotubes link cell and substrate until the cell fully detaches (V) (Color figure online)

precedes step-events, whereas a force plateau is detected prior to tether-events. Separating step- and tether-events is necessary, since they contribute to different detachment scenarios. Step-events can be interpreted as the unbinding of single or few CAMs from the substrate. The nonlinear force loading prior to rupture suggests that the probed receptors are connected to the actin cytoskeleton [11]. The magnitude of the force step reflects the stochastic survival of receptor–ligand bonds under an increasing force load [11, 12]. The ensemble of step-events can provide information on the affinity and avidity of receptors. Tether-events can be found at pulling distances up to several tens of micrometers after the major rupture peak of the retraction F-D curve. The force plateau preceding these unbinding events originates from the extraction of membrane tethers (membrane nanotubes) from the cell membrane. Membrane tethers are formed when CAMs that are not, or weakly, connected to the cytoskeleton, are pulled from the cell membrane [11]. The force plateau measured upon extraction of a membrane tether shows that the force required to extract the tether

is constant over long extraction lengths. Extracting membrane tethers by AFM can be used to characterize cell membrane properties such as anchoring to the cytoskeleton or viscosity [13, 14]. Since membrane tethers apply a constant force (force clamp) to CAMs that anchor the tether end, tether length and pulling velocity can be used to determine the lifetime of receptor–ligand bonds [15].

- *Separation distance, d*: The separation distance characterizes the distance at which all linkages between cell and substrate have been ruptured. This length is highly influenced by membrane tethers.
- *Elastic properties of the cell, E*: The slope of the approach F-D curve in the contact region is influenced by the elastic properties of the cell (Fig. 1b). Organized actin filaments of the cell cortex can substantially influence the elastic properties of most cell types.

The purpose of this protocol is to describe a method by which the adhesive strength and dynamics of virtually every cell type to various ECM components can be quantified. To simplify matters, we describe the experimental setup and procedure for SCFS measurements of HeLa cells to fibronectin- and Matrigel™-coated surfaces. To covalently attach fibronectin and Matrigel™ to glass substrates we describe the application of maleic anhydride co-polymer thin films. Specifically, we describe the immobilization and application of poly(octadecene-*alt*-maleic anhydride) (POMA) thin films. Thin films of alternating maleic anhydride co-polymers with different co-monomers offer a versatile platform for bioactive coatings on solid supports.

2 Materials

2.1 Preparation of Co-polymer Solutions

1. Poly(octadecene-*alt*-maleic anhydride) (POMA) (MW 30,000–50,000) (Polysciences, Inc.).
2. Tetrahydrofuran (THF).
3. η-Hexane.
4. Acetone.
5. Ultrapure water (18 MOhm/cm).
6. PTFE syringe filters, 0.22 μm pore size.

2.2 Thin Film Preparation

1. Glass coverslips (∅ 12 mm) (*see* **Note 1**).
2. Isopropanol.
3. Hydrogen peroxide (35 % w/w), not stabilized (*see* **Note 2**).
4. Ammonium hydroxide solution (29 % w/w).

5. APTES (3-Aminopropyltriethoxysilane) solution: 20 mM in 90 % isopropanol (*see* **Note 3**).
6. Ultrapure water (18 MOhm/cm).
7. Teflon wafer basket (Entegris, Inc.).
8. Glass petri dishes.
9. Quartz-glass beaker.
10. Spin coater (up to 5,000 rpm).

2.3 Immobilization of ECM Proteins to Polymer Supports

1. Phosphate-buffered saline (PBS).
2. Fibronectin solution: Dilute a fibronectin stock solution to 50 mg/mL in PBS (*see* **Note 4**).
3. Matrigel™ solution: Dilute a Matrigel™ stock solution to 50 mg/mL in PBS (*see* **Note 5**).

2.4 AFM Cantilever Cleaning

1. 1 M sulfuric acid.
2. Plasma cleaner/sterilizer.

2.5 AFM Cantilever Functionalization

1. Tip-less AFM cantilevers, nominal spring constant between 0.03 and 0.2 N/m (*e.g.*, NP-O, Bruker AFM Probes).
2. Con A stock solution: Dissolve Concanavalin A (Con A; Type IV) to 2 mg/mL in PBS (*see* **Note 6**).
3. 0.1 M $NaHCO_3$ buffer solution: Dissolve an appropriate amount of $NaHCO_3$ in ultrapure water. Adjust to pH 8.0 with NaOH solution. The buffer can be stored for several weeks at room temperature (25 °C).
4. Biotin-conjugated Con A stock solution (Biotin-Con A; Type IV): 0.4 mg/mL in PBS (*see* **Note 6**).
5. Biotinamidocaproyl-labeled bovine serum albumin (Biotin-BSA; Sigma-Aldrich) stock solution: 0.5 mg/mL in 0.1 M $NaHCO_3$ buffer solution (*see* **Note 6**).
6. Streptavidin stock solution: 0.5 mg/mL in PBS (*see* **Note 6**).
7. Cell-Tak (BD Bioscience).
8. PBS without Ca^{2+}, Mg^{2+}.
9. NaOH solution: 1 M in ultrapure water.

2.6 Cell Culture

1. Accutase.
2. Penicillin.
3. Streptomycin.
4. PBS.
5. 4-(2-hydroxyethyl)-1-piperazineethanesulfonic acid (HEPES).
6. HeLa cells (ATCC).

7. Fetal bovine serum (FBS).
8. DMEM (containing GlutaMAX™, 4,500 mg/L D-glucose, sodium pyruvate, $NaHCO_3$):
   Mix DMEM with 10 % FBS, 100 U/mL penicillin and 100 µg/mL streptomycin. Sterile filter the medium using a 0.22 µm filter (*see* **Note 7**).
9. CO_2-independent AFM medium: Dissolve DMEM powder (containing glutamine, 4,500 mg/L D-glucose, sodium pyruvate, no $NaHCO_3$) in the appropriate amount of ultrapure water. Add 20 mM HEPES, 4 mM $NaHCO_3$, 100 U/mL penicillin and 100 µg/mL streptomycin. Adjust pH to 7.2 with 1 M NaOH. Sterile filter the medium using a 0.22 µm filter (*see* **Notes 7** and **8**).
10. T25 and T75 tissue culture flasks.

2.7 SCFS Measurements

1. Active damping table on a stable support frame.
2. PetriDishHeater™ temperature controlled sample chamber (JPK Instruments) (*see* **Note 9**).
3. Tissue-culture dish (35 mm × 10 mm) (*see* **Note 10**).
4. CellHesion™ 100 µm vertical pulling module (JPK Instruments) (*see* **Note 11**).
5. Data processing software (JPK Instruments) (*see* **Note 12**).
6. NanoWizard® AFM system (JPK Instruments) (*see* **Note 13**).
7. AFM cantilever holder (Supercut extended version, JPK Instruments).
8. BSA solution: 1 mg/mL in PBS (*see* **Note 14**).
9. Prior to SCFS experiments, prepare a non-adhesive spot within a petri dish by applying 50 µL of the 1 mg/mL BSA solution to a defined area of the petri dish (Fig. 4a) (*see* **Note 15**). Incubate the petri dish at 37 °C for 90 min. Remove unbound BSA by a washing step with PBS. Aspirate the PBS.
10. Ethanol p.a. quality.

3 Methods

3.1 Preparation of Maleic Anhydride Polymer Thin Films

The mechanism and procedure for surface immobilization of the reactive co-polymers and their subsequent conversion with layered bioactive molecules has been described in detail [16–19]. Here, we present the immobilization and application of poly(octadecene-*alt*-maleic anhydride) (POMA) with a molecular weight of 40,000 g/mol (Fig. 3). POMA thin films of about 5 nm, obtained by spin coating, are very hydrophobic (water contact angles of about 100°). In Fig, 3a, b the co-polymer platform and its functionality is schematically shown. Covalent attachment of the

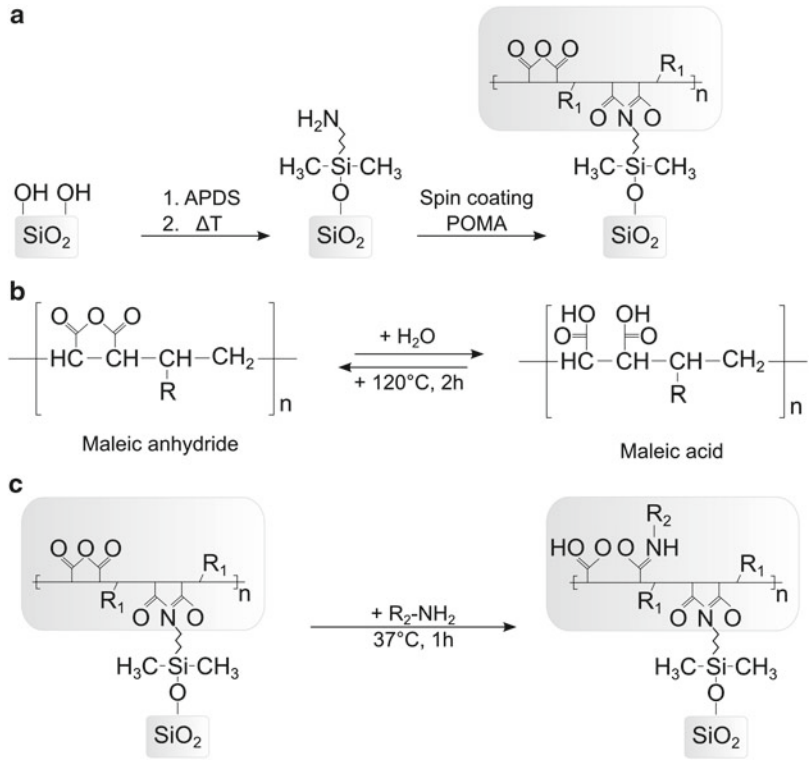

Fig. 3 (**a**) Schematic representation of the maleic acid co-polymer platform, covalently immobilized on a silicon dioxide surface via an aminosilane functionality. (**b**) Maleic anhydride repeating unit and its hydrolysis in water and the reversible annealing at 120 °C for 2 h. (**c**) Binding of ECM molecules to POMA-functionalized silicon dioxide surfaces

co-polymer to a glass substrate is achieved via aminosilane chemistry (Fig. 3a). The switchable reactivity of the maleic anhydride co-polymers allows for controlled covalent binding of proteins and other bioactive compounds to polymer pre-coated surfaces. Proteins spontaneously react with the anhydride moieties of the co-polymer via free amino groups, as occurring on lysine residues (Fig. 3c).

3.1.1 Co-polymer Solutions

1. To remove olefin impurities, mix POMA and ultrapure water at a ratio of 1:10 (w/v) and stir the suspension at room temperature overnight. Remove the water by suction filtration and dry the residual polymer at 50 °C for 24 h under vacuum. Mix the dried POMA with η-hexane at a ratio of 1:10 (w/v) and agitate the solution for 3 h. Filter off the polymer and wash with η-hexane. Dry the purified POMA in a two-step process; first at 50 °C for 2 h then at 120 °C for 20 h under vacuum. Store the purified polymer at room temperature.
2. Prepare a 0.16 % (w/w) solution of POMA in THF and filter using a 0.22 μm syringe filter. Sealed solutions can be stored at room temperature in the dark for 2 weeks.

3.1.2 Thin Film Preparation

1. Distribute the coverslip substrates into a Teflon wafer basket. Immerse the basket into a beaker containing ultrapure water, and expose it to ultrasound for 30 min. Rinse the substrates at least three times in fresh ultrapure water (*see* **Note 16**).
2. Repeat the ultrasonic cleaning step in ethanol.
3. Rinse the coverslip substrates three times using ultrapure water as described above.
4. Transfer the coverslips in the Teflon wafer basket into a quartz-glass beaker filled with a mixture of hydrogen peroxide, aqueous ammonium hydroxide solution, and ultrapure water at a volume ratio of 1:1:5. Heat the mixture to 70 °C and maintain at this temperature for 10 min. Perform this step in a fume hood.
5. Rinse the coverslips at least twice in a minimum volume of 500 mL of ultrapure water. Dry the coverslips in a stream of nitrogen (*see* **Note 17**).
6. Immediately transfer the substrates into APTES solution for 2 h. Rinse the coverslips in isopropanol and dry them in a stream of nitrogen.
7. Anneal the coverslips at 120 °C for 1 h (*see* **Note 18**).
8. Attach a coverslip to the spin coater and apply the POMA solution onto the glass substrates such that liquid covers the entire surface. Immediately (<3 s) turn the spin coater on (settings: acceleration = 1,500 rpm/s, speed = 4,000 rpm, duration = 30 s).
9. Cure the glass substrates at 120 °C for 2 h.
10. Let the substrates cool down to room temperature.
11. Immerse the substrates in acetone for 10 min. Rinse three times with fresh acetone and immediately dry in a stream of nitrogen (*see* **Note 19**). Samples can be stored in sealed containers at room temperature in the dark for ≈3 months. If the samples are not immediately used, a heat treatment (2 h, 120 °C) is required prior to use (*see* **Note 20**).

3.2 Immobilization of ECM Proteins to Polymer Supports

1. Add 30 μL each of fibronectin- and Matrigel™-solution onto separate POMA-coated coverslips.
2. Put another two POMA-coated coverslips, upside down, onto the first coverslips, to simultaneously coat two surfaces (*see* **Note 21**).
3. Incubate the coverslip sandwiches at 37 °C for 1 h.
4. Separate the coverslips by immersing the sandwich in PBS (*see* **Note 22**).
5. Remove unbound protein with an additional washing step in fresh PBS.
6. If the samples are not immediately used, they can be stored in PBS at 4 °C for up to 48 h.

3.3 Cantilever Cleaning

1. Clean tip-less AFM cantilevers in sulfuric acid for 1 h and thoroughly rinse them with ultrapure water (*see* **Note 23**).
2. Place cantilevers on a glass slide and insert them into a plasma cleaner. Operate the plasma cleaner at maximum power for 3 min (*see* **Note 24**).

3.4 Cantilever Functionalisation

Here we describe three different types of cantilever functionalization. For applications where only moderate detachment forces (<5 nN) are expected it is usually sufficient to functionalize the AFM cantilever by simple Con A physisorption (*see* Subheading 3.4.1). When this means of cantilever functionalization is used for SCFS measurements, cells occasionally detach from the cantilever during cantilever retraction. The probability of detachment from the cantilever increases with the contact time between the cell and the substrate. However, when studying short contact times (<2 min) this protocol is an economical alternative to the more time- and cost-intensive chemical functionalization described below.

For longer contact times between cell and substrate or applications where high detachment forces are expected, we advise to use the protocol described in Subheading 3.4.2. Here, the cantilevers are first functionalized with biotin-BSA, followed by the binding of streptavidin. Finally, biotinylated proteins can be bound to the cantilevers. In Subheading 3.4.2 we describe the use of biotin-Con A; however, the users may choose other biotinylated proteins that are more suitable for their experiments of choice (other lectins [*e.g.*, WGA], ECM proteins [e.g., collagen, fibronectin], etc.).

Another elegant type of adhesive cantilever coating is Cell-Tak. Cell-Tak is a formulation of the "polyphenolic proteins" extracted from the marine mussel, *Mytilus edulis*. This family of related proteins is the key component of the glue secreted by the mussel to anchor itself to solid structures in its natural environment. The Cell-Tak coating usually resists high detachment forces; however, users have to test the suitability of the coating for their individual experimental setup.

3.4.1 Physisorption

1. Place cantilevers in 50 µL droplets of the 2 mg/mL Con A stock solution. Incubate in a humidified atmosphere overnight at 37 °C.
2. Wash the cantilevers in PBS. Repeat this step 2–3 times using fresh PBS. Store cantilevers submerged in a petri dish containing 10 mL PBS (*see* **Note 25**).

3.4.2 Biotinylated Protein

1. Place cantilevers in 50 µL droplets of the 0.5 mg/mL biotin-BSA stock solution. Incubate in a humidified atmosphere overnight at 37 °C.
2. Wash the cantilevers in PBS. Repeat this step 2–3 times using fresh PBS.

3. Place cantilevers in 50 µL droplets of the streptavidin stock solution. Incubate for 30 min in a humidified atmosphere at room temperature.
4. Wash cantilevers as described in **step 2**.
5. Place cantilevers in 50 µL droplets of the biotin-Con A stock solution. Incubate for 30 min in a humidified atmosphere at room temperature.
6. Wash cantilevers as described in **step 2** and store them submerged in a petri dish containing 10 mL PBS (*see* **Note 25**).

3.4.3 Cell-Tak

1. Mix 0.1 M $NaHCO_3$ buffer solution with the Cell-Tak solution and NaOH solution at a volume ratio of 57:2:1.
2. Immediately, place cantilevers in 50 µL droplets of the solution. Incubate for 30 min in a humidified atmosphere at room temperature (*see* **Note 26**).
3. Wash the cantilevers in PBS. Repeat this step 2–3 times using fresh PBS. Store them submerged in a petri dish containing 10 mL PBS (*see* **Note 25**).

3.5 Cell Culture

1. Culture HeLa cells in DMEM in T75 tissue culture flasks.
2. Passage cells 1:10 every third day before they reach confluence.
3. For SCFS experiments, inoculate 2×10^5 cells into T25 tissue culture flasks 24 h prior to SCFS experiments (*see* **Note 27**).
4. One hour prior to SCFS experiments, aspirate the DMEM from the T25 tissue culture flask. Wash the cells with 5 mL PBS, aspirate and equilibrate cells in 5 mL CO_2-independent AFM medium (*see* **Note 28**).
5. Aspirate CO_2-independent AFM medium. Wash cells with 5 mL PBS and remove the PBS after the washing step.
6. Harvest the cells by incubation with 1.5 mL Accutase for ≈3 min.
7. Add 4.5 mL CO_2-independent AFM medium and transfer the cells into a 15 mL conical tube.
8. Spin down the cells by centrifugation at $400 \times g$ for 2 min at room temperature.
9. Carefully remove the supernatant and resuspend the cells in CO_2-independent AFM medium to a concentration of $\approx 1 \times 10^5$ cells/mL (*see* **Note 29**).

3.6 Single-Cell Force Spectroscopy

3.6.1 Equipment Setup

1. Start up all components of the AFM setup (AFM controller, CellHesion™ controller, and PetriDishHeater™ controller (*see* **Note 30**)) 24 h prior to SCFS experiments to ensure thermal equilibration and reduce drift during experiments (*see* **Note 31**).
2. Add a BSA-functionalized petri dish into the PetriDishHeater™ and add approximately 3 mL CO_2-independent AFM medium into the petri dish.

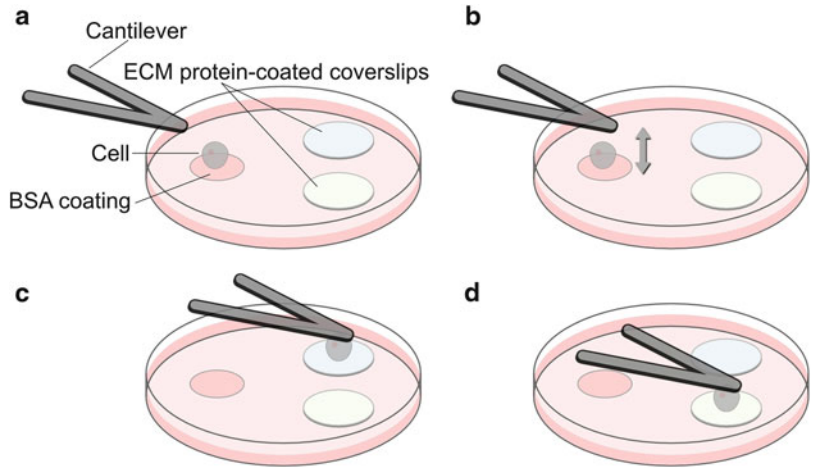

Fig. 4 Schematic representation of the experimental SCFS procedure. (**a**) Two (or more) ECM protein-coated coverslips are placed in a cell culture medium-filled petri dish. Suspended cells are placed on a BSA-coated spot. (**b**) A functionalized AFM cantilever is positioned above a single cell. The cantilever is gently pushed onto the cell. Thereby the cell attaches to the cantilever. Withdrawal of the cantilever separates the cantilever-bound cell from the support. Resting the cell in this retracted position allows the cell to establish firm adhesion to the cantilever. (**c**) The cantilever-bound cell is positioned above an ECM protein-coated coverslip and F-D curves are recorded to determine the adhesive strength between the cell and the ECM protein. (**d**) F-D curves are recorded on the second ECM protein-coated coverslip

3. Place a fibronectin- and a Matrigel™-functionalized coverslip into the petri dish (Fig. 4a).
4. Clean the AFM cantilever holder and all removable components of the PetriDishHeater™ with detergent. Repeatedly, rinse all parts with ultrapure water and ethanol. Gently dry all parts in a stream of nitrogen.
5. Mount a functionalized cantilever into the AFM cantilever holder. Insert the cantilever holder into the AFM head and position the head onto the CellHesion™ stage (*see* **Note 32**).
6. Wait at least 10 min for thermal equilibration.
7. Focus the laser onto the back of the cantilever and adjust the photodiode signal according to the guidelines of the AFM manufacturer.
8. Approach the cantilever to the surface of the petri dish.

3.6.2 Cantilever Calibration

1. Maneuver the cantilever to a position outside of the BSA-coated spot.
2. To measure the sensitivity of the cantilever, record an F-D curve with a vertical movement of 2 μm and an approach and retract speed of 10 μm. Determine cantilever sensitivity using the routines incorporated in the AFM control software (*see* **Note 33**).

3. Retract the cantilever ≈80 μm to exclude negative impacts of long-range interactions from the surface on the subsequent cantilever spring constant calibration.
4. Determine the cantilever spring constant using the routines incorporated into the AFM control software (*see* **Note 34**).

3.6.3 Attaching a Cell to Cantilever

1. Lift the AFM head and inject $\approx 1 \times 10^3$ cells into the PetriDishHeater™ right on top of the BSA-coated spot.
2. Immediately place the AFM head on the CellHesion™ stage and manually position the apex of the cantilever above a suitable cell (Fig. 4b).
3. Attach the cell to the cantilever by performing an approach-retract cycle. During approach, manually adjust the cantilever position to attach the cell to the apex of the cantilever. Suitable parameters for cell attachment are a contact force between 1 and 2 nN, a contact time between 2 and 6 s and an approach and retract rate between 5 and 10 μm/s (Fig. 4b).
4. After attaching the cell to the cantilever, allow the cell to recover for at least 10 min. During this time the cell will form firm contacts with the cantilever surface (*see* **Note 35**).

3.6.4 Force–Distance Curve Acquisition

1. Retract the cantilever approximately 300 μm from the surface (*see* **Note 36**).
2. Maneuver the cell-cantilever couple on top of an ECM protein-coated coverslip (*see* **Note 37**) (Fig. 4c).
3. Using the AFM stepper motors, adjust the vertical distance between cell and ECM protein-coated support. Depending on contact time and force, between 30 and 100 μm are needed to fully separate the cell from the ECM protein-coated supports.
4. Adjust the contact force between 0.5 and 1.5 nN and record F-D curves for different contact times (1–600 s) at different locations on the ECM protein-coated supports. Depending on the type of experiment, the user may record a set of F-D curves on one support and then move to the next one, or may cycle between supports in successive F-D curves (*see* **Note 38**) (Fig. 4d).
5. Lift the AFM head, remove cantilever and petri dish and restart the procedure by mounting a fresh cantilever and a new petri dish with fresh ECM-coated coverslips.

3.7 Data Analysis

1. The acquired F-D curves are analyzed using the JPK data processing software (*see* **Note 12**). With the help of this software, several parameters can be extracted (*see* **Note 39**).

4 Notes

1. Glass coverslips of other dimensions may be used.
2. Do not use stabilized hydrogen peroxide, since it may contain nonvolatile stabilizers.
3. APTES must be opened under nitrogen (or argon) to avoid contamination with moisture.
4. The stock solution can be stored at –20 °C for several months. Do not agitate the protein solution during and after thawing. Carefully pipette the solution. Harsh treatments will cause fibril formation.
5. Matrigel™ will rapidly form a gel at 22–35 °C. Thaw the Matrigel™ stock solution overnight at 4 °C on ice. Keep the protein solution on ice before use. Use precooled pipette tips, tubes and ice-cold PBS when diluting the stock solution for use.
6. The stock solution can be stored for several months at –20 °C.
7. The medium can be stored for several months at 4 °C.
8. CO_2-independent AFM medium is DMEM buffered with HEPES instead of carbonate. This ensures a constant pH during the SCFS measurements. The medium can be stored for several months at 4 °C.
9. To claim that experiments are performed in a near-physiological environment, it is indispensable to maintain the cells at 37 °C. As an alternative to the PetriDishHeater™, several manufacturer (e.g., Zeiss, Life Imaging Services) offer solutions where the entire AFM-setup is housed in a temperature-controlled chamber.
10. The PetriDishHeater™ supports a large range of different culture dishes. However, petri dishes from some manufacturers are too high. For standard SCFS measurements we suggest plastic-bottom tissue-culture dishes (TPP, #93040). For applications where the SCFS measurements are combined with fluorescence techniques, glass-bottom tissue-culture dishes (WPI, #FD35) are recommended.
11. The maximal vertical pulling ranges provided by other AFM systems are ≈20 μm (BioScope™ Catalyst™ AFM, Bruker AXS), ≈25 μm (XE-Bio AFM, Park Systems), and ≈40 μm (MFP-3D-BIO AFM, Asylum Research). These AFM systems can be employed for cell types that show low adhesion and for stronger adhering cell types at short contact times and low contact forces. However, for most cell types and for long contact times and high contact forces a vertical pulling range exceeding 40 μm is needed to fully separate the cell from the ECM-coated support during retraction.

12. To extract cell adhesion parameters from the numerical data recorded analysis software is required. We use the data processing software provided by the AFM manufacturer (JPK Instruments), but in-house algorithms in scientific data analysis software (e.g., IGOR Pro or MATLAB) might be equally used. On the one hand, in-house algorithms take time to develop and are more complicated to use but allow, on the other hand, full control of the data processing. However, for most SCFS users the manufacturer's software may be sufficient since it is easy to use and provides some control of how the data is processed.
13. Currently the NanoWizard® AFM system is not available in the USA. Researchers in the USA can alternatively use the CellHesion® 200 system from JPK Instruments.
14. The BSA solution is used to create a non-adhesive area within the petri dish to facilitate smooth binding of single cells to the AFM cantilever.
15. Mark the area on the back of the petri dish using a lab marker.
16. During all cleaning and rinsing steps, make sure that the glass coverslips are fully covered by the surrounding solution.
17. It is essential to process the glass substrates immediately after cleaning to avoid recontaminating the glass surface.
18. The polymer coating should be performed directly subsequent to aminosilanization due to the susceptibility of the generated surface amino groups to oxidizing substances.
19. Samples must be quickly dried after their removal from the acetone solution.
20. The maleic anhydride moiety of the co-polymer converts into carboxylic acid groups via hydrolysis in aqueous solution or during long-term storage at ambient conditions (Fig. 2b). Repeated heat treatment (2 h, 120 °C) is required to activate the anhydride moieties if the coated glass coverslips are either stored for a long period of time or autoclaved.
21. POMA-coated surfaces are very hydrophobic. The sandwich technique is utilized to minimize the amount of applied protein solution.
22. Do not forget to invert the upper coverslip.
23. Incubation in sulfuric acid for significantly longer than 1 h can damage the reflective gold coating of the cantilever. New cantilever does not have to be cleaned.
24. Plasma cleaning removes residual contaminants and hydrophilizes the cantilever surfaces.
25. The functionalized cantilever can be stored at 4 °C for several days.

26. Adsorption begins immediately after mixing of the constituents. Therefore, dispense the solution within 10 min.
27. Several T25 tissue culture flasks may be prepared for each experiment since it is advised that a fresh cell suspension is used for each cantilever-cell pair.
28. In this step cells adapt to the changed medium conditions (presence of HEPES and lack of FCS). SCFS experiments are performed in serum-free medium to prevent adhesion-related serum constituents (e.g., fibronectin) from interfering with the adhesion measurements.
29. Before starting SCFS experiments, cells should recover from the harvesting procedure for approximately 15 min at 37 °C under agitation.
30. For a temperature of ≈37 °C in the center of the culture dish the nominal temperature setpoint of the PetriDishHeater™ controller should be set to 39.5 °C (at a room temperature of ≈25 °C). The temperature offset is dependent on the type of culture dish, liquid volume, room temperature and the use of immersion objectives, optical microscope, vibration isolation table, and AFM control software.
31. AFMs, and especially AFMs mounted on an optical microscope, suffer from thermal drift due to the numerous heat-generating sources within the AFM and the microscope. Therefore, the relatively long equilibration time is recommended.
32. Be careful to not touch the side of the petri dish with the glass cantilever holder while mounting the AFM head onto the CellHesion™ stage, as this can damage the cantilever holder and the cantilever. Before mounting the AFM head, it is advised to adjust the PetriDishHeater™ stage position until the microscope objective is in the center of the petri dish.
33. The factor used to convert the volts measured to nanometers of cantilever deflection is usually called sensitivity. The sensitivity depends on many parameters including the type of cantilever and how the cantilever is mounted. Thus, the sensitivity must be determined each time a cantilever is mounted or remounted. To determine the sensitivity, an F-D curve is recorded on a stiff surface, and the deflection signal is analyzed when cantilever and surface are in contact. In the contact region of the F-D curve, the deflection of the cantilever is equal to the vertical movement of the AFM piezo element.
34. Most manufacturers specify a nominal spring constant for a given cantilever. Usually, the spring constant has been calculated using the cantilever shape (length, width, thickness). However, frequently the true spring constants of cantilevers differ from the nominal values by a factor of up to 3. Most AFM control software provides an option to measure the

spring constant of cantilevers using the thermal noise method. The thermal noise method uses the thermal fluctuations of the cantilever and the equipartition theorem to calculate the cantilever spring constant [20]. Essentially, the theorem equates the thermal energy at a given temperature with the energy within the oscillation of the cantilever. The thermal noise method is the most versatile and implementable method of cantilever calibration [21]. A high estimate of the method's error is 20 % [21]. It can be argued that other calibration methods are more accurate but the extra efforts required with the numerous cantilevers used for SCFS measurements make them unfeasible.

35. Firm attachment of the cell to the AFM cantilever is vital to prevent detachment of the cell from the cantilever during SCFS measurements. To ensure firm attachment of the cell after the incubation time, gently tap onto the side of the microscope while simultaneously observing the cell. If the cell is markedly moving on the cantilever, lift the AFM head to completely detach the cell from the cantilever and restart the procedure from **step 2** of this section. If the next cell is also not firmly attached, exchange the cantilever for a fresh one and restart from Subheading 3.6.2.
36. The retraction ensures that the cantilever does not crash into the ECM protein-coated coverslips when moving the cantilever on top of the substrates. Coverslips are widely available in several standard thicknesses ranging from 100 to 600 μm. Depending on the type of coverslip, the user may adjust the retraction distance accordingly.
37. Do not touch the side of petri dish with the AFM cantilever holder during movement. Otherwise, the laser alignment of the AFM system and therefore the cantilever calibration will be altered. In such a case, a fresh cantilever has to be mounted and calibrated.
38. The number of F-D curves that can be recorded with a single cell critically depends on contact time. For short contact times (<40 s), up to 50 F-D curves may be recorded per cell. With excessive number of contacts, the cell will start to deform and F-D curves may show abnormal de-adhesion patterns. For longer contact times, the number of recorded F-D curves should be reduced. Between single F-D curve cycles, the cell should be allowed to recover. This cell recovery time should not be shorter than the cell-substrate contact time. For very long contact times (>10 min) the adhesion established between cell and substrate may become very strong, and the cell may detach from the cantilever. In this case, discard the corresponding F-D curve and restart the procedure by mounting a fresh cantilever. Continuously monitor the cantilever-attached

cell by light microscopy. Changes in cell morphology may indicate loss of cell viability. Cells occasionally start to divide on the cantilever or migrate away from the cantilever apex. In either case discontinue measurements and restart the procedure by mounting a fresh cantilever.

39. The automated detection and analysis of the small force steps following the major rupture peak is still not fully developed. The JPK data processing software provides a routine that detects steps in the F-D curve by fitting a model that combines sharp steps with slowly varying background [22]. This model is only appropriate for regions of F-D curves that have tether rupture events. The initial part of the retraction F-D curve records the mechanical deformation of the cell, as well as many complex detachment rupture events. A different kind of model is required to analyze this process of cell detachment. The transition from the initial phase to the tether phase is not clear. In fact, some tethers are likely already unbinding in the initial phase. We refer the reader to the excellent JPK data processing manual for further information.

Acknowledgments

This work was supported by the Swiss National Science Foundation, the Leibniz Association, and the German Federation of Industrial Research Association.

References

1. Adams JC (2002) Regulation of protrusive and contractile cell-matrix contacts. J Cell Sci 115:257–265
2. Lauffenburger DA, Wells A (2001) Getting a grip: new insights for cell adhesion and traction. Nat Cell Biol 3:110–112
3. Helenius J, Heisenberg CP, Gaub H et al (2008) Single-cell force spectroscopy. J Cell Sci 121:1785–1791
4. Benoit M, Gabriel D, Gerisch G et al (2000) Discrete interactions in cell adhesion measured by single-molecule force spectroscopy. Nat Cell Biol 2:313–317
5. Taubenberger A, Cisneros DA, Friedrichs J et al (2007) Revealing early steps of alpha-2beta1 integrin-mediated adhesion to collagen type I by using single-cell force spectroscopy. Mol Biol Cell 18:1634–1644
6. Friedrichs J, Torkko JM, Helenius J et al (2007) Contributions of galectin-3 and -9 to epithelial cell adhesion analyzed by single cell force spectroscopy. J Biol Chem 282: 29375–29383
7. Friedrichs J, Manninen A, Müller DJ et al (2008) Galectin-3 regulates integrin alpha2beta1-mediated adhesion to collagen-I and -IV. J Biol Chem 283:32264–32272
8. Florin EL, Moy VT, Gaub HE (1994) Adhesion forces between individual ligand-receptor pairs. Science 264:415–417
9. Zhang X, Wojcikiewicz E, Moy VT (2002) Force spectroscopy of the leukocyte function-associated antigen-1/intercellular adhesion molecule-1 interaction. Biophys J 83: 2270–2279
10. Lehenkari PP, Horton MA (1999) Single integrin molecule adhesion forces in intact cells measured by atomic force microscopy. Biochem Biophys Res Commun 259:645–650
11. Evans EA, Calderwood DA (2007) Forces and bond dynamics in cell adhesion. Science 316:1148–1153
12. Evans E, Ritchie K (1997) Dynamic strength of molecular adhesion bonds. Biophys J 72: 1541–1555

13. Sun M, Northup N, Marga F et al (2007) The effect of cellular cholesterol on membrane-cytoskeleton adhesion. J Cell Sci 120:2223–2231
14. Sun M, Graham JS, Hegedüs B et al (2005) Multiple membrane tethers probed by atomic force microscopy. Biophys J 89:4320–4329
15. Krieg M, Helenius J, Heisenberg CP et al (2008) A bond for a lifetime: employing membrane nanotubes from living cells to determine receptor–ligand kinetics. Angew Chem Int Ed Engl 47:9775–9777
16. Salchert K, Pompe T, Sperling C et al (2003) Quantitative analysis of immobilized proteins and protein mixtures by amino acid analysis. J Chromatogr A 1005:113–122
17. Pompe T, Zschoche S, Herold N et al (2003) Maleic anhydride copolymers-a versatile platform for molecular biosurface engineering. Biomacromolecules 4:1072–1079
18. Salchert K, Streller U, Pompe T et al (2004) In vitro reconstitution of fibrillar collagen type I assemblies at reactive polymer surfaces. Biomacromolecules 5:1340–1350
19. Salchert K, Oswald J, Streller U et al (2005) Fibrillar collagen assembled in the presence of glycosaminoglycans to constitute bioartificial stem cell niches in vitro. J Mater Sci Mater Med 16:581–585
20. Hutter J, Bechhoefer J (1993) Calibration of atomic-force microscope tips. Rev Sci Instrum 64:1868–1873
21. Burnham N, Chen X, Hodges C et al (2003) Comparison of calibration methods for atomic-force microscopy cantilevers. Nanotechnology 14:1–6
22. Kerssemakers JWJ, Munteanu EL, Laan L et al (2006) Assembly dynamics of microtubules at molecular resolution. Nature 442:709–712

Chapter 3

A Multimode-TIRFM and Microfluidic Technique to Examine Platelet Adhesion Dynamics

Warwick S. Nesbitt, Francisco J. Tovar-Lopez, Erik Westein, Ian S. Harper, and Shaun P. Jackson

Abstract

Fluorescence microscopy techniques have provided important insights into the structural and signalling events occurring during platelet adhesion under both static and blood flow conditions. However, due to limitations in sectioning ability and sensitivity these techniques are restricted in their capacity to precisely image the adhesion footprint of spreading platelets. In particular, investigation of platelet adhesion under hemodynamic shear stress requires an imaging platform with high spatial discrimination and sensitivity and rapid temporal resolution. This chapter describes in detail a multimode imaging approach combining total internal reflection fluorescence microscopy (TIRFM) with high speed epifluorescence and differential interference contrast (DIC) microscopy along with a novel microfluidic perfusion system developed in our laboratory to examine platelet membrane adhesion dynamics under static and flow conditions.

Key words Platelets, TIRFM, Microscopy, Adhesion, Hemodynamics

1 Introduction

The ability of cells to form stable adhesive interactions under static and hemodynamic shear stress conditions is essential for a broad range of biological processes, including leukocyte recruitment to the vascular endothelium, lymphocyte homing, cancer metastasis, and platelet thrombus formation. Circulating blood platelets have evolved specialized adhesive and mechanotransduction mechanisms to promote efficient adhesion under hemodynamic shear [1–9]. Flowing blood imposes significant shear and drag forces on adhesive bonds, undermining the formation and stability of adhesion contacts. Platelet adhesion must occur over a broad range of shear conditions, e.g., <300 s^{-1} in post-capillary venules and approaching 50,000–200,000 s^{-1} within regions of severe stenosis [5, 10, 11]. To facilitate adhesion in a shear field, platelets utilize an initial capturing step mediated by the binding of platelet GPIb to the vascular

Amanda S. Coutts (ed.), *Adhesion Protein Protocols*, Methods in Molecular Biology, vol. 1046,
DOI 10.1007/978-1-62703-538-5_3,

adhesive protein, von Willebrand Factor (VWF) followed by a firm adhesion step, mediated by one or more platelet integrins [6].

As a result of surface adhesion under blood flow and in response to applied compressive and elongation stresses, platelets exhibit marked changes in their plasma membranes and underlying cytoskeletal networks, leading to a series of morphological changes [12, 13]. A characteristic feature of initial platelet adhesion is the development of membrane tethers; defined as locally extended regions of lipid bilayer that are extruded from the cell surface under the influence of drag forces [11, 12, 14, 15]. Platelet tether formation is a dynamic process involving differential phases of initial formation, elongation and contractile restructuring. Recent evidence suggests that tether formation and restructuring plays a major role in the initial recruitment and aggregation of discoid platelets during the earliest phases of thrombus formation [11]. This discoid platelet aggregation mechanism is highly dynamic in nature and is driven principally by the formation of small-scale shear gradients generated at sites of vessel stenosis [11]. In vitro analysis has demonstrated that platelet tethers undergo a series of structural transitions intimately linked to the applied shear stress conditions and concomitant platelet calcium signal transduction [11]. Specifically, platelet tethers have been observed to transition through an initial filamentous elongation phase, through to a low shear-dependent restructuring phase that is closely associated with contractile consolidation of platelet aggregates. These nanometer to micrometer scale changes in platelet membrane structure appear to play a key role in initiating platelet adhesion formation.

Examining the relationship between the earliest phases of platelet adhesion with subsequent morphological and cytoskeletal remodelling events at the heart of thrombus formation represents a challenging technical problem. Transmitted light imaging techniques in combination with epifluorescence wide-field microscopy (WFM) have provided important insights into the temporal sequence of events initiating signalling and early morphological changes during platelet adhesion under static and flow conditions [11, 14–18]. However, due to inherent limitations in axial resolution, these techniques are limited in their ability to resolve membrane adhesion contacts at the sub-platelet level and correlate these with overall signalling and platelet morphology. The recent development and application of internal reflection microscopy (IRM) techniques to monitor platelet to VWF adhesion has provided new insights into the discrete membrane adhesion point contacts (DAP's) and tethering mechanisms that underlie platelet capture to thrombogenic surfaces [19]. This chapter describes in detail a novel multimode total internal reflection fluorescence microscopy (TIRFM) based imaging and microfluidic perfusion system, along with relevant troubleshooting procedures, developed in our laboratory to examine platelet adhesion dynamics under static and

shear flow conditions. This methodology enables the correlation of these membrane adhesion events with specific alterations in overall platelet morphology and signalling.

2 Materials

2.1 Blood Platelet Preparation

1. 7× Acid citrate dextrose containing theophylline (ACD): sodium citrate (2.5 g/100 mL), 85 mM citric acid (anhydrous), 72.9 mM D-glucose, 110 mM theophylline (*see* **Note 1**).
2. 10× Platelet Wash Buffer (PWB): 43 mM K_2HPO_4, 43 mM Na_2HPO_4, 243 mM NaH_2PO_4, 1.13 M NaCl, 55 mM D-glucose, 100 mM theophylline.
3. 1× PWB (pH 6.5, prepared in ultrapure water; final conductivity 13–15 mS/cm): 10× PWB (5 mL), 10 % w/v BSA (2.5 mL), ddH_2O 42.5 mL.
4. 10× Tyrode's Buffer, pH 7.2: 120 mM $NaHCO_3$, 100 mM (final concentration) Hepes, 1.37 M NaCl, 27 mM KCl, 55 mM D-glucose.
5. 1× Tyrode's Buffer pH 7.2: Prepared in ultrapure water; final conductivity 13–15 mS/cm.
6. Apyrase purified from potatoes according to the method of Molnar and Lorand [20]. (This can also be purchased commercially, e.g., Sigma-Aldrich.)

2.2 TIRFM

1. $DiIC_{12}$ at a concentration of 1 mg/mL in DMSO (Molecular Probes).
2. 25 mm round SF11 coverslips (V-A Optical Co) (*see* **Note 2**).
3. Series M, 1.75 refractive index liquid (methylene iodide formulation) (Cargille Laboratories).
4. Extran® solution 10 % v/v with ddH_20 (Merck Chemicals).
5. 1,1,1,3,3,3-hexamethyldisilazane (HMDS; Sigma-Aldrich).
6. Fibrinogen 100 mg (Sigma-Aldrich).
7. 0.21 μm FITC labeled polymer microspheres (FS02F/4677) (Bangs Laboratories Inc).

2.3 Microfabrication

1. Isopropanol.
2. Acetone.
3. Methanol.
4. 1,1,1,3,3,3-hexamethyldisilazane (HMDS; Sigma-Aldrich).
5. Edge bead removal solvent (MicroChem Corp).
6. KMPR 1025 (high contrast, epoxy-based) photoresist (MicroChem Corp).

7. Photoresist Developer for KMPR (MicroChem Corp).
8. Chrome mask on soda lime glass 0.5 μm resolution.
9. MJB3 contact mask aligner (SUSS Microtech).
10. SU-8 Developer (MicroChem Corp).
11. Sylgard® 184 Silicone Elastomer (polydimethyl siloxane; PDMS). Supplied as two-part liquid component kits comprised of Base/Curing Agent to be mixed in a 10:1 ratio by weight or volume; manual mixing.
12. Circular polymethyl methacrylate (PMMA) shim.
13. 1 and 8 mm Biopsy punch.

2.4 Microfluidic Flow System

1. Harvard syringe pump: We use the Harvard Apparatus PHD2000 Infusion/Withdraw Programmable Pump to control flow rates in our microfluidic perfusion system.
2. Tubing: To connect the microfluidic cell to the Harvard syringe pump (Fig. 4), 10 cm of medical grade Tygon tubing of 0.8 mm ID and 1.6 mm OD (Watson-Marlow) is used. This tubing is strong, durable, and easy to clean and does not support the nonspecific adhesion of platelets in reconstituted blood.

2.5 TIRFM Imaging Setup

1. TIRFM: In order to achieve the combination of imaging modalities necessary for investigating platelet signalling and adhesion dynamics under shear flow at high speed and high magnification, we routinely use a modified Olympus IX81 microscope fitted with differential interference contrast (DIC) optics and high magnification, high numerical aperture, plan apochromatic (PlanApo) objectives along with a modified TIRFM optical setup, to allow rapid switching between widefield fluorescence microscopy (WFM), DIC and TIRFM. To achieve this we use a modified Olympus TIRFM optical coupling in which the standard TIRF illumination (IX2-RFAEVA2) beam splitter is replaced with a 60/40 splitter to allow rapid switching between an arc lamp light source for WFM and a laser source for TIRFM (Fig. 1).
2. Typically we utilize a Uniblitz 35 mm shutter mounted on the microscope illumination pillar (for DIC), the internal DG4 shutter and a set of high speed Uniblitz LS3T2 shutters mounted in the laser combiner, respectively to shutter illumination for DIC, WFM and TIRFM (Fig. 1).
3. For control of emission wavelength we routinely use either a Sutter Lambda 10-2 (λ10-2) filter changer (517/30, 605/40 and 660/40 m emission filters) or a Quadview (QV-Photometrics) emission splitter (520/40, 605/55 m emission filters), behind which is coupled a sensitive CCD camera (Fig. 1).

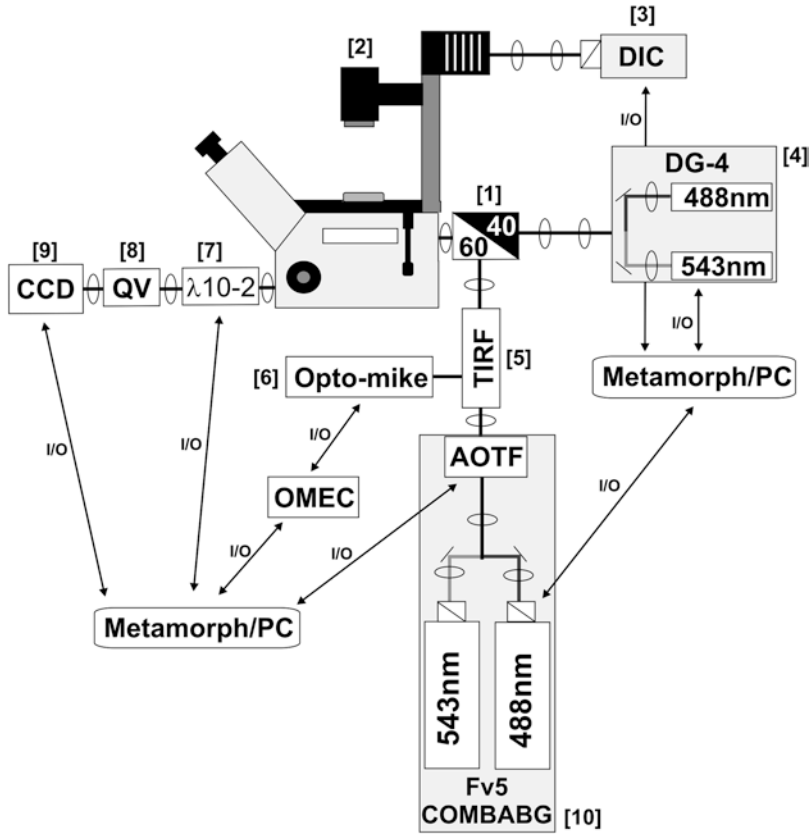

Fig. 1 Schematic of Multimode-TIRF Microscope System. [*1*] 60/40 beam splitter coupling TIRF laser optics to IX81 microscope. [*2*] Uniblitz shuttered condenser. [*3*] DIC/Transmitted light source. [*4*] Sutter DG4 Exon arc lamp light source with 488 and 543 nm excitation filters. [*5*] TIRF optical train. [*6*] Opto-mike micrometer and OMEC controller interfaced with TIRF optical train. [*7*] Sutter λ 10-2 filter wheel with 517/30, 605/40 and 660/40 m emission filters. [*8*] Photometrics Quadview coupled to λ 10-2 filter wheel with 520/40, 605/55 m emission filters. [*9*] Hamamatsu Orca-ER monochromatic CCD. [*10*] Olympus Fv5 COMBABG laser combiner housing He/Ne 543 nm (1 mW) and Ar 488 nm (9 mW) lasers and a FV5-AOTF unit, fully tuneable via PC (FVKC004) interface. All hardware controlled through Metamorph 6.3 and custom Journals

4. Objectives: The APO100X OHR/1.65 (1.75 immersion liquid, Cargille) objective has been used routinely in the course of our TIRFM and epifluorescence platelet imaging experiments with exceptional results. This objective although specialized for TIRFM applications can also be used for in vitro platelet flow experiments where dye loading concentrations have to be minimized and the associated fluorescence emission is low and where high resolution images are a prerequisite.
5. Excitation Source: We use a Lambda DG-4 Ultra High Speed Wavelength Switcher fitted with a 175 W, pre-aligned, Xenon arc lamp with integrated shutter (Sutter Instruments) connected via a LG-Y50 liquid light guide (Fig. 1) as the WFM

light source. TIRF illumination is provided by 9 mW krypton/argon (488 nm) and 1 mW helium/neon (543 nm) lasers housed in a FV5-COMBABG combiner incorporating a customized FV5-AOTF unit, fully tuneable via PC (FVKC004) interface (Fig. 1).

6. TIRF laser control: Typically we have replaced the standard micrometer control for TIRFM with a motorized micrometer driver (OptoMike, OptoSigma) controlled via a PC (OMEC) interface, allowing automated rapid and accurate control of the laser incidence angle [θ_i] (Fig. 1). OptoMike positioning is controlled through a custom Metamorph 6.3 (MM-6.3) journal that records micrometer position for each imaging frame.
7. Dichroics: For multimode imaging applications such as combined ratiometric Ca^{2+} imaging and TIRFM or FITC/TRITC epifluorescence + TIRFM combinations, we utilize a Chroma 86013bs (trichroic) mounted in the IX81 filter turret. For DIC imaging applications we utilize a secondary DIC filter block mounted next to the 86013bs to minimize the interval between fluorescence and transmitted light imaging.
8. Emission Filters: In the case of low shear and/or static platelet imaging experiments we utilize a Sutter λ10-2 filter wheel housing 517/30, 605/40 and 660/40 m emission filters (Chroma). In the case of high speed imaging, such as that associated with high shear rate (≥1,800 s^{-1}) platelet flow experiments, it is advisable to utilize an image field splitting system that divides the emission output onto the same camera CCD rather than the filter wheel assembly. We utilize the Quadview (Optical Insights) simultaneous imaging system fitted with both 517/30 m and D605/40 m (Chroma Technology) emission filters coupled between the filter wheel unit and the CCD for greater experimental flexibility.
9. CCD Camera: Although most microscopy grade cooled CCD cameras are acceptable, we have opted for the Orca-ER CCD (Hamamatsu Photonics) operating in low light mode for $DiIC_{12}$ labeling TIRFM experiments. The low dark current and high sensitivity of this CCD have proven to be particularly useful for TIRFM involving platelets (*see* **Note 3**).

3 Methods

3.1 Collection of Whole Blood

1. Blood is collected into acid citrate dextrose (at a ratio of 6/1, blood/ACD) via venisection of the antecubital vein of consenting healthy volunteers who have not ingested any antiplatelet medication (e.g., aspirin or ibuprofen) in the 2 weeks preceding the procedure (*see* **Note 4**). Use of butterfly needles smaller than 19-G is not recommended, as high shear forces are generated when drawing through smaller-sized needles.

Table 1
Blood volume to centrifugation speed (× *g*)

	Vol. of blood (mL)			
	10 mL tubes	50 mL tubes	Speed (× *g*)	Time (min)
Blood	15	50	300	16
	10	40	300	15
	6	25	300	13

Blood is withdrawn at a reasonably slow and steady rate, taking care to avoid frothing, and is immediately mixed by gentle inversions of the syringe.

2. To avoid the effects of trace amounts of thrombin generated during venipuncture, the first 5 mL of blood taken is discarded.
3. Following collection the blood sample is placed in a Falcon tube containing hirudin (lepirudin) to a final concentration of 800 U/ml and 0.005 U/mL apyrase and incubated at 37 °C for 15 min to equilibrate prior to further processing.

3.2 Preparation of Washed Human Platelets

1. The equilibrated blood sample is centrifuged at 300 × *g* for a time dependent on the volume of blood taken (Table 1). The braking phase of the centrifugation step should be set to the slowest rate of deceleration to prevent mixing of the erythrocyte suspension with the platelet rich plasma (PRP) phase.
2. The PRP is transferred to a fresh Falcon tube (use of a syringe with slow suction to avoid shearing for this step is recommended), and allowed to rest for 10 min at 37 °C in a water bath.
3. The PRP is subsequently centrifuged at 1,700 × *g* for 7 min to separate the platelet pellet from the platelet poor plasma (PPP) fraction.
4. All of the PPP is gently aspirated as quickly as possible without disturbance of the platelet pellet.
5. The resulting platelet pellet is resuspended via gentle aspiration with 1× PWB + hirudin (800 U/mL final) and apyrase (0.01 U/mL) to a volume equal to the original volume of PRP.
6. The platelet count and level of erythrocyte contamination is assessed via an automated blood analyzer (Sysmex) and the count corrected to 3×10^8/mL via removal or addition of 1× PWB (*see* **Note 5**).
7. The platelet suspension, in the presence of apyrase (0.01 U/mL), is allowed to equilibrate at 37 °C for 10 min prior to $DiIC_{12}$ dye loading.

3.3 Membrane ($DiIC_{12}$) Dye Loading of Washed Platelet Suspensions for TIRFM

A range of fluorescent membrane probes can, and have been, utilized in the context of platelet adhesion experiments. However, caution must be exercised as many of these probes can cause direct and/or indirect activation/photo-activation of isolated platelet preparations. Furthermore commonly used membrane dyes such as $DiOC_6$ rapidly leach out of platelet membranes and are therefore unsuitable for TIRFM based imaging due to direct binding with microscope coverslips and thus uncontrolled fluorescence background. $DiIC_{12}$ (1 μg/mL) loads readily into platelet membranes and is efficiently retained.

1. 1 mL aliquots of isolated platelet suspension (3×10^8/mL in 1× PWB) are incubated for 10 min at 37 °C with $DiIC_{12}$ (1 μg/mL) (*see* **Note 6**).
2. The dye loaded platelet suspension is subsequently centrifuged in a bench-top Eppendorf centrifuge at 2,000 × *g* for 1 min and the supernatant gently aspirated (*see* **Notes 5** and **6**).
3. The platelet pellet is immediately resuspended at a concentration of 3×10^8/mL in 1× PWB containing apyrase (0.01 U/mL) (*see* **Notes 7–11**).

3.4 Preparation of Reconstituted Blood

The $DiIC_{12}$ dye loading method described in Subheading 3.3 requires the use of isolated platelet preparations. Because of this restriction flow based experiments must be carried out using reconstituted blood preparations in which autologous erythrocytes and plasma are recombined with the dye loaded platelet suspension.

In reconstitution experiments, platelets prepared as per Subheading 3.3 are resuspended with isolated erythrocytes in either modified Tyrode's buffer or alternatively, platelets can be reconstituted with platelet poor plasma (PPP) at a final concentration of $50–300 \times 10^9$/L no more than 10 min prior to experimentation.

3.4.1 Preparation of Autologous Platelet Poor Plasma (PPP)

1. 50 mL hirudin anticoagulated blood is collected in acid citrate dextrose (ACD).
2. Platelet rich plasma (PRP) is separated from the erythrocyte pellet by centrifugation at 300 × *g* for 16 min.
3. Carefully remove the PRP phase being careful not to disturb the buffy coat or erythrocyte phases.
4. Centrifuge the PRP at 2,000 × *g* for 7 min (50 mL) and carefully remove the PPP phase without disturbing the platelet pellet.
5. Supplement the PPP with 800 U/mL hirudin and 0.01 U/mL apyrase and incubate for 30 min at 37 °C prior to use.

3.4.2 Preparation of Washed Erythrocytes

1. 50 mL hirudin anticoagulated blood is collected in ACD.
2. PRP is separated from the erythrocyte pellet by centrifugation at 300 × *g* for 16 min.

3. Carefully remove the PRP phase along with the buffy coat from the top of the erythrocyte phase.
4. Wash the erythrocyte phase with an equal volume of 1× Tyrode's buffer (no BSA) and mix by gentle inversion.
5. Centrifuge at 2,000 × *g* for 6 min (50 mL) to pack the erythrocyte phase.
6. Remove the supernatant and any remaining buffy coat.
7. Repeat **steps 4–6**.
8. Resuspend the erythrocyte pellet from **step 7** in an equal volume of supplemented 1× Tyrode's buffer (+1 mM $CaCl_2$ + 0.5 % BSA).
9. Repeat **steps 5** and **6**.
10. Supplement the packed erythrocyte suspension with 800 U/mL hirudin and 0.02 U/mL apyrase and incubate for 30 min at 37 °C.
11. Immediately prior to reconstitution with the platelet suspension, supplement the erythrocyte suspension with a further 0.02 U/mL apyrase to prevent erythrocyte derived ADP from activating the isolated platelet suspension.
12. Allow the reconstituted blood suspension to equilibrate for 10 min at 37 °C prior to use (*see* **Note 12**).

3.5 Microfluidic Sample Perfusion System

A critical requirement for TIRFM based platelet imaging is the minimization of imaging artifacts introduced by focal drift and sample movement during time-lapse experiments. We have found that under conditions of high shear rate, pressure differentials caused by small volume high resistance, high velocity sample flow can create serious distortions of the optical window or coverslip, limiting the use of standard parallel plate flow chambers. To overcome this problem we have developed a microfluidic perfusion system that allows for the unique combination of high shear, low flow rate sample perfusion, thereby minimizing focal aberrations. Figure 2 illustrates the overall design of the microfluidic perfusion system, comprising a top polydimethylsiloxane (PDMS) chip consisting of; [1] an inlet reservoir of 200 μL volume (8 mm diameter) for sample delivery, [2] a single high resolution straight microchannel of either 100 or 300 μm diameter and 42 μm in height, [3] a small bore (1.5 mm) exhaust channel that connects to a stainless steel outlet connection attached to 10 cm of medical grade Tygon tubing (0.8 mm ID/1.6 mm OD) and a Harvard PHD-2000 syringe driver. The PDMS chip is surface adhered to a 25 mm diameter SF11 coverslip that forms the 0.1 mm thick floor of the micro-channel and allows for transmitted light, epifluorescence, and TIRFM imaging.

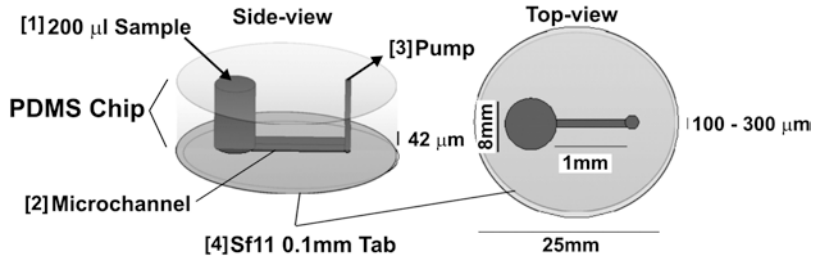

Fig. 2 Microfabricated flow cell schematic. Schematic showing the overall PDMS microfluidic cell architecture comprising a top PDMS chip consisting of; [*1*] a sample reservoir of 200 µL volume, [*2*] a high resolution micro-channel with the overall geometry (100 or 300 µm width × 42 µm height), [*3*] a small bore (1.5 mm) exhaust channel and a stainless steel outlet connection attached to 10 cm of medical grade Tygon tubing (0.8 mm ID/1.6 mm OD) and a Harvard PHD-2000 syringe driver, [*4*] the micro-channel chip is surface adhered to a 25 mm diameter SF11 glass tab that forms the 0.1 mm thick bottom wall of the micro-channel and allows for both DIC, epi-F and high magnification (×100 using a APO100XOHR objective lens) TIRFM imaging within the micro-channels

3.5.1 Flow Cell Fabrication

The microfluidic flow cells can be fabricated in polydimethyl siloxane (PDMS Sylgard 184) using standard photo-lithography as previously described [11, 21].

1. A 4 in. silicon wafer was spin coated with KMPR 1025 (high contrast, epoxy-based) photoresist using a spread cycle of 300 and 100 rpm/s for 10 s and a development cycle of 1,000 and 300 rpm/s for 30 s in order to achieve a film thickness of 42 µm which defines the channel height.
2. A cycle of edge bead removal is conducted for 30 s using edge bead removal solvent.
3. The KMPR coated wafer was soft-baked by ramping the temperature at 6 °C/min starting at 23 °C and holding at 100 °C for 25 min to dry out the solvents.
4. The KMPR film is exposed, with a patterned high resolution (250 nm) chrome mask on soda lime glass, defining the working channel geometry, to UV (360 nm; 8 mW/cm^2) on a MJB3 contact mask aligner using two exposures of 1 min each, in order to avoid overheating of the substrate.
5. Following UV exposure the channel pattern was cross linked by baking on a hotplate for 4 min at 100 °C ramping the temperature at 6 °C/min starting at 23 °C.
6. The cross linked film is cooled down slowly to room temperature (RT) with the sample on the hotplate to avoid thermal stress.
7. Unexposed KMPR photoresist is subsequently developed using SU-8 Developer for 12 min with periodic agitation to remove unexposed resist.

8. Following development the KMPR pattern is cleaned with isopropanol and ddH_2O.
9. A final hard bake is carried out by heating the pattern to 95 °C for 3 h, in order to strengthen the KMPR and extend the service life of the mold.
10. Once the photoresist mold is fabricated, Sylgard 184 polydimethylsiloxane (PDMS) is mixed with cross linker (ratio 10:1) for 5 min manually using a stirrer and degassed for 30 min under vacuum.
11. The mixture is poured onto the KMPR mold housed within a polymethyl methacrylate (PMMA) shim.
12. The PDMS is then cured in an oven at 75 °C for 40 min.
13. The PDMS channel replicas are peeled from the KMPR mold.
14. An inlet reservoir hole is made using a 6 mm biopsy punch.
15. For the outlet connection to the syringe pump, a 1 mm biopsy punch is used.
16. The PDMS channels are placed directly onto 25 mm SF11 circular coverslips prepared as outlined in Subheading 3.5.2. Adhesion is achieved due to the low surface energy of the PDMS.

3.5.2 SF11 Coverslip Preparation

1. 25 mm round SF11 coverslips are sonicated at 50 Hz in a sonication bath for 15 min in a 10 % Extran solution.
2. Rinse coverslips thoroughly 2× in ddH_2O in a sonication bath (50 Hz) for 15 min.
3. Cleaned coverslips are dipped in methanol and dried under a nitrogen stream.
4. Dried coverslips are subsequently derivatized by submersion in 1,1,1,3,3,3-hexamethyldisilazane (HMDS) for 15 min.
5. Rinse coverslips thoroughly 2× in ddH_2O under sonication for 15 min.
6. Derivatized coverslips are dipped in methanol and dried under nitrogen stream.
7. Dried HMDS derivatized coverslips are coated with (100 μg/mL fibrinogen (w/v)) for 1 h at RT.
8. Wash coverslips once with 1× Tyrode's buffer (pH 7.2).
9. Coverslips are subsequently dried under a nitrogen stream and annealed to prefabricated PDMS channels (*see* Subheading 3.5.1).
10. Perfuse the micro-channels with 2 % BSA (w/v) for 30 min to block any naïve glass.
11. Perfuse with 1× Tyrode's buffer to clear excess BSA ready for sample introduction (*see* **Notes 12** and **13**).

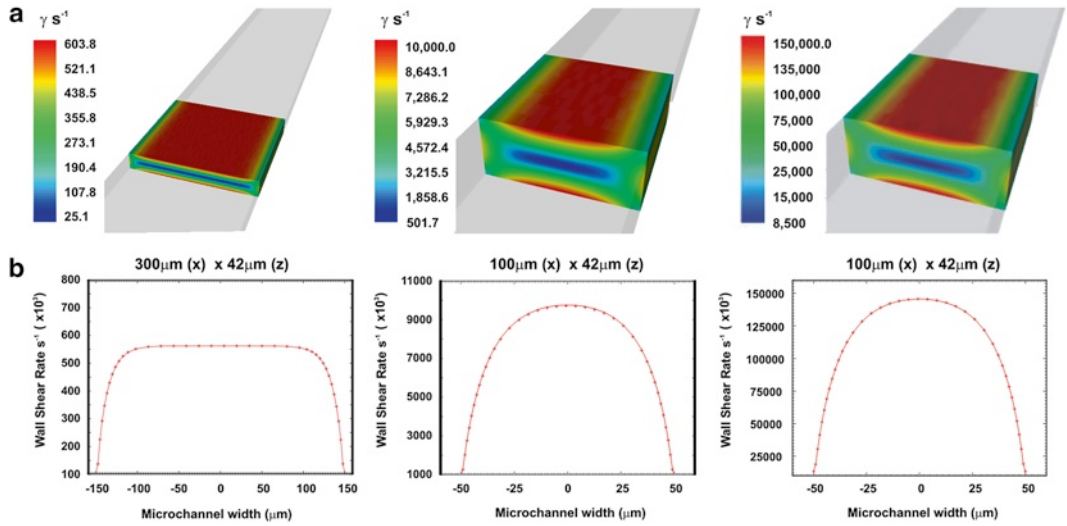

Fig. 3 Hydrodynamic characterization of microfluidic perfusion system. (**a**) 3-Dimensional shear rate distribution in 100 and 300 μm micro-channel variants at constant input flow rates of 3.09 μL/min (600 s^{-1}), 14.39 and 215.85 μL/min (10,000 and 150,000 s^{-1}). (**b**) Wall shear rate distribution 1 μm from the SF11 coverslip floor of the micro-channels for peak shear rates of 600, 10,000 and 150,000 s^{-1}

3.5.3 Setting the Pump Perfusion Rates for the Microfluidic Channels

In order to establish the correct flow (pump) rate for a given nominal shear rate in the microfluidic cell we utilize the analytical solution of the velocity profile for a Newtonian fluid in rectangular geometries [21].

$$V_{(y,z)} = \frac{12Q}{ab\pi^3} \frac{\sum_{t=1,3,\ldots} \frac{-1\frac{i-1}{2}}{i^3} \cos\left(\frac{i\pi y}{2a}\right)\left(1 - \frac{\cosh\frac{i\pi z}{2a}}{\cosh\left(\frac{i\pi b}{2a}\right)}\right)}{1 - \frac{192a}{\pi^5 b}\sum_{t=1,3\ldots} \frac{\tan\frac{i\pi b}{2a}}{i^5}}. \quad (1)$$

Q is the flow rate, a is half the channel height (300 or 100 μm), and b is the half channel width (42 μm), given by the thickness of the photoresist.

1. The laminar shear-rate for a given flow rate is obtained once the velocity is calculated by taking a discrete derivative near the wall according to Eq. 1.
2. This shear-rate calculation is then verified once the three-dimensional view of the shear-rate distribution (Fig. 3) is generated by performing a fluid-flow simulation solving the Navier–Stokes Equations, using commercial software

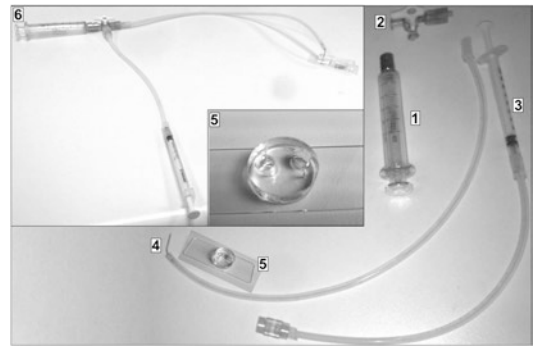

Fig. 4 Microfluidic flow setup. [*1*] 5 mL Becton Dickinson glass syringe. [*2*] Three way tap. [*3*] 1 mL Terumo plastic syringe and attached tubing with Luer lock fitting. [*4*] 1 mm diameter stainless steel tubing and attached Tygon tubing. [*5*] Microfluidic flow cell. [*6*] Tubing and flow cell configuration ready for perfusion

(FLUENT 6.0). For the three-dimensional simulations, the fluid medium simulating the washing buffer is considered with a constant density $\rho = 998.2$ kg/m^3 and constant viscosity of $\nu = 0.001$ Pa s (*see* **Notes 14** and **15**).

3.5.4 Microfluidic Flow Cell Setup

1. Assemble the 5 mL glass syringe and prime by filling with approximately 1 mL ddH_2O (Fig. 4[1]).
2. The plunger of the glass syringe is lightly greased to ensure smooth movement during flow.
3. The nozzle of the syringe is attached to a three-way tap (Fig. 4[2]).
4. This in turn is connected to a long length (~10 cm) of tubing attached to a 1 cm (1 mm ID) metal connector (Fig. 4[4]).
5. The plastic 1 mL syringe is attached to a length of tubing with a luer lock fitting (Fig. 4[3]). This plastic syringe assembly is used to purge the microfluidic chip of air bubbles prior to pump perfusion.
6. The assembled tubing (Fig. 4—inset [5]) is connected to the microfluidic flow cell (Fig. 4[5]) via the metal connector (*see* **Note 16**).
7. Clamp the flow cell firmly in place on the microscope stage plate (*see* **Note 17**).

3.6 TIRFM Imaging Setup

To extract semiquantitative measurements of platelet membrane-surface distance from raw TIRFM imaging sequences, we have adapted the simplified model of TIRFM optics described by Truskey et al., to extract relative platelet membrane/substratum separation distances from the spatial pattern of TIRF image intensity [23] (*see* **Note 18**).

3.6.1 Calibration of TIRFM Laser Position

1. To initially calibrate the TIRF microscope, set up the microfluidic flow cell on the microscope stage and clamp in place making sure it is flat.
2. Prepare a suspension of $DiIC_{12}$ labeled platelets in 1× Tyrode's supplemented with 1 mM $CaCl_2$ to a final density of 3×10^8/mL and flow the sample into the flow cell at a rate of 100 μL/min. The objective should already be positioned close to the sample focal plane. Monitor the inflow of platelets using transmitted (DIC) illumination. When platelets are detected, by slightly focusing through the sample, stop the flow and turn off the pump and close the tap on the inflow tubing.
3. Allow the platelet suspension to settle onto the glass coverslip for 10–15 min, monitoring periodically.
4. When a number of adherent platelets are visible switch to TIRFM illumination.
5. Center the TIRF laser so that a clear epifluorescence image is achieved. This will be apparent when non-adherent (floating) platelets appear clearly in the field of view.
6. While imaging, progressively reposition the TIRF laser to the point where the suspended platelets disappear from view and a homogenous (top to bottom) TIRF image of the adherent platelets is achieved. This point will be preceded by a rapid increase and then drop-off in fluorescence intensity. This position represents the TIRF critical angle (θ_c) and should be logged (*see* **Note 19**).
7. Keeping the sample in sharp focus slowly reposition the TIRF laser until the adherent platelets are no longer visible. This laser position represents the extinction angle (θ_e) and should be logged.

3.6.2 Defining the Appropriate θ_i for TIRFM of Spreading Platelets

A critical technical challenge associated with the use of TIRFM to analyze platelet adhesion dynamics is the relatively thin cross-sectional height of spread(ing) platelets, which typically exhibit lamellipodial (hyalomere) thicknesses of ≤100 nm (aspect ratio of ~1:100 for fully spread platelets) [24]. It is therefore essential to determine the angle of incidence (θ_i) cutoffs for the microscope system such that accurate discrimination can be made between the basal platelet membrane surface (at or proximal to the adhesive surface), and a full platelet thickness image.

1. To establish the angle of incidence (θ_i), cutoffs at which TIRFM is capable of accurately discriminating between the basal platelet membrane and a full thickness image, experiments are carried out in which isolated platelets suspended in 1× Tyrode's buffer supplemented with 1 mM $CaCl_2$ are allowed to spread on SF11 glass coverslips for 30 min in the presence of 1 U/mL thrombin.

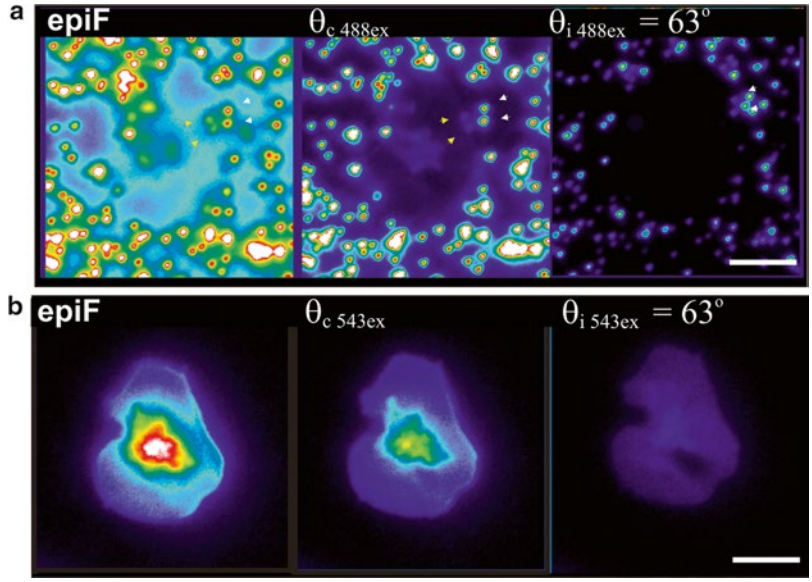

Fig. 5 Defining θ_l for spread platelets. (**a**) Representative epifluorescence and TIRF imaging of 0.2 μm FITC polymer microspheres settling under gravity on a fully spread human platelet. Note that at the critical angle ($\theta_{c\ 488ex}$) significant fluorescence bleed-through from the apical platelet surface is observable. *Yellow arrow heads* highlight two fluorescent beads sitting on the apical platelet surface that are visible at $\theta_{c\ 488ex}$. At an angle of incidence ($\theta_{l\ 488ex}$) of 63° fluorescence bleed-through is eliminated. (**b**) Representative TIRF imaging of the $DiIC_{12}$ labeled platelet. Note that at the $\theta_{c\ 543ex}$ a large proportion of fluorescence bleed-through from the apical platelet membrane is evident. In contrast at or above a $\theta_{l\ 543ex}$ of 63° the image substantially changes and only the adherent footprint of the platelet (in contact with the coverslip) is visible. Scale bars = 4 μm

2. Following platelet spreading, 0.21 μm FITC labeled polymer microspheres are added to the buffer medium. Beads are allowed to sediment onto the adherent platelets for 10 min and TIRFM images (488_{ex}) taken at varying θ_i covering the range 62–75° (Fig. 5).
3. The θ_i at or below the critical angle at which beads settled on the apical surface of the spread platelets are no longer visible should be used for all subsequent imaging experiments. Based on our analysis a θ_i cutoff of ~63° has been established using the APO100X OHR/1.65 objective for all platelet adhesion experiments regardless of excitation wavelength using our specific imaging setup.

3.6.3 Semiquantitative Measurement of Membrane to Surface Distance

1. In order to calibrate the depth of penetration (dp) of the TIRF evanescent field against the micrometer position of the Olympus TIRF microscope, we have developed a user program within the software package Metamorph 6.3 (MM-6.3). This "Run User" program and collection of Journals sends and receives serial RS-232 data to and from the OMEC controller, which in turn

drives the TIRFM laser angle along with a number of tools to carry out the experiments (*see* **Notes 20** and **21**).

$$\mathrm{dp}(\theta_i) = \frac{\lambda \eta_{ex}}{4\pi\sqrt{\sin^2\theta_i - \left(\eta_{platelet} / \eta_g\right)^2}}. \quad (2)$$

$$\Delta_{(x,y)} = \Delta_0 + \mathrm{dpln}\left[F_0 / F_{(x,y)}\right]. \quad (3)$$

dp = depth of penetration; λ_{ex} = excitation wavelength; θ_i = derived TIRFM laser angle of incidence; $\eta_{platelet}$ = refractive index of platelet cytosol; η_g = refractive index of SF11 glass; $\Delta_{(x,y)}$ = separation distance for each pixel in the image; Δ_0 = minimum separation distance preset to 15 nm; F_0 = the pixel of maximal intensity following thrombin treatment; $F_{(x,y)}$ = the fluorescence intensity of each pixel in the image.

By recording the outputted micrometer travel between the critical angle and the angle of extinction ($\theta_c - \theta_c$ corresponding to ~17° of angular displacement for the Olympus APO100XO HR objective) for each imaging frame the depth of penetration of the TIRF evanescent field (dp) can be calculated based on the refractive index of the immersion media in use and the excitation wavelength according to Eq. 2.

2. To derive relative membrane-substrate separation distances ($\Delta_{(x,y)}$) from the raw imaging data, a second set of Journals are used to interrogate every pixel comprising an adherent platelet (defined as a thresholded region of interest, ROI) over all image frames in a time series (*see* **Note 21**).
3. For each defined thresholded pixel in the defined ROI in the image a scaling operation is carried out according to Eq. 3. This analysis is based on the assumption that the pixel of highest intensity over the adhesion/spreading time course represents the point of closest contact with the surface, with this pixel set as the relative point of minimum separation distance (Δ_0), set as 15 nm based on EM studies of adhesion contact distances.
4. The spreading platelet surface over the entire image series is subsequently re-scaled according to Δ_0 in accord with Eq. 3, using the excitation wavelength (λ_{ex}) and refractive indices of SF11 glass ($\eta_g = 1.78$) and the platelet cytosol ($\eta_{platelet} = 1.38$), respectively. Figure 6a displays raw and calibrated TIRFM imaging panels of a single thrombin-stimulated platelet spreading at the surface of 100 μg/mL fibrinogen (*see* **Note 22**).
5. Semiquantitative flow based experiments are performed in a similar manner to static experiments. Following blood platelet perfusion over the adhesive substrate of choice the blood sample is chased with a bolus of thrombin (1 U/mL) in 1× Tyrode's buffer to trigger irreversible platelet adhesion and spreading.

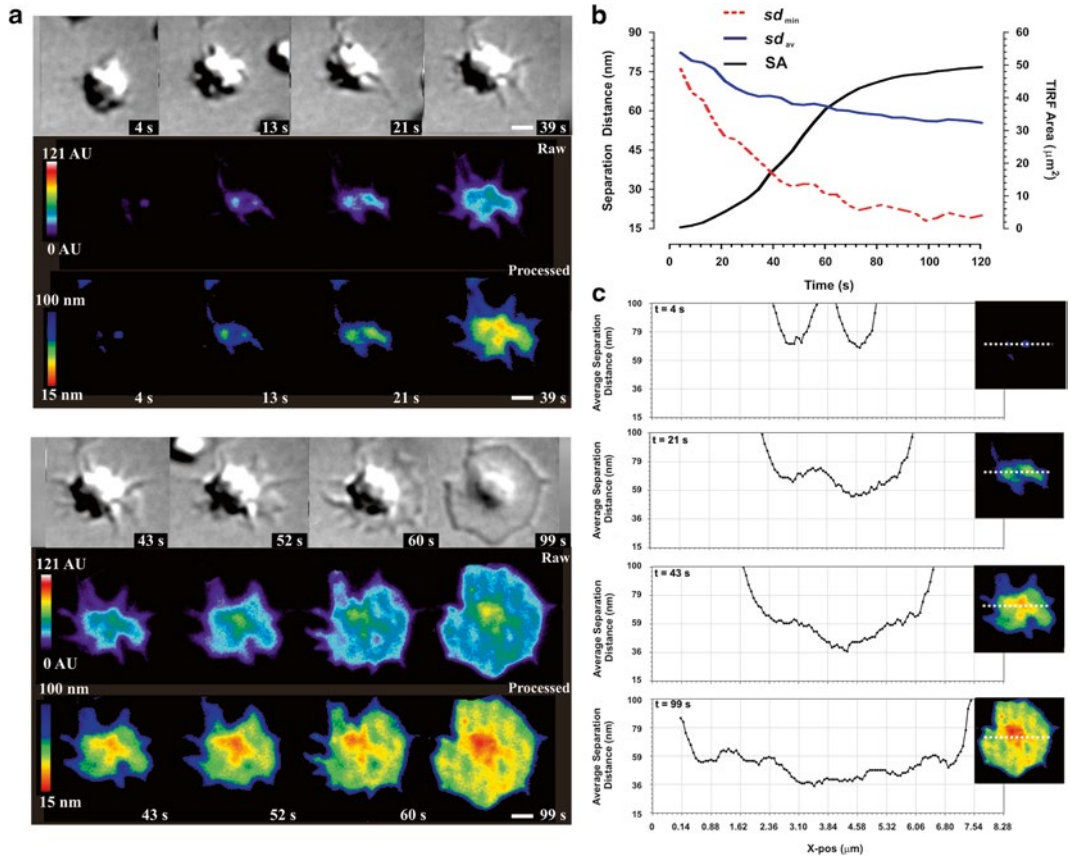

Fig. 6 TIRFM calibration method. (**a**) DIC, unprocessed and processed TIRFM ($\theta_{i\,543ex} = 63.71°$) imaging of a thrombin (1 U/mL) stimulated platelet spreading at the surface of immobilized fibrinogen (100 μg/mL). The raw TIRFM imaging data (*Raw*) were processed offline to generate the rescaled images (*Processed*). Intensity values in the unprocessed image are in arbitrary fluorescence units (AU). Intensity values in the processed image are a measure of relative cell-substrate separation distance in nm. Scale bars = 4 μm. (**b**) Whole platelet TIRFM measurements derived from the calibrated TIRFM imaging in (**a**). sd_{min} minimum separation distance within the TIRFM visible platelet footprint, sd_{av} average separation distance for the TIRFM visible footprint, *SA* surface area of the TIRFM visible footprint. Note the close correlation between surface area increase and reduction in sd_{min}. (**c**) Line scan interrogation of the initial contact adhesion points in (**b**). *Insets* show the line scan position for each frame

The flow is stopped and the adherent platelets allowed to fully spread for 10 min. Image calibration is carried out as above (*see* **Note 23**).

4 Notes

1. Theophylline is insoluble at RT and the solution must be heated to ≥70 °C to dissolve it prior to use.
2. We utilize SF11 coverslips in place of more expensive SF12 coverslips. It should be noted that some chromatic error is introduced when using SF11 glass and care must be taken to

recalibrate TIRFM imaging when using multiple emission excitation sources.

3. Newer EM-CCD cameras would also be suitable and should give excellent results.
4. Be careful to avoid bubbles during the blood collection process.
5. The platelet count should not exceed 1×10^9/mL to avoid undue platelet activation.
6. It is important to not load the platelets with more than 1 μg/mL (final concentration) of $DiIC_{12}$, as higher solution concentrations have been observed to severely disrupt platelet function.
7. There should be no free dye visible by eye in the supernatant at this point.
8. The use of heparin as an anticoagulant significantly retards $DiIC_{12}$ labeling of isolated platelet preparations. We therefore recommend hirudin as anticoagulant (*see* Subheading 3.1) for TIRFM based imaging experiments.
9. $DiIC_{12}$ labeled platelets should be utilized no more than 30 min following dye loading for imaging experiments. We have found that at longer time points a significant proportion of the $DiIC_{12}$ is sequestered into the internal organelle membranes of human platelets.
10. Ideally we recommend that platelets are freshly labeled with $DiIC_{12}$ for each imaging experiment; the use of small platelet aliquots is therefore recommended. It is advisable to retain the remainder of the platelet preparation in 1× PWB at 37 °C and suspend aliquots in modified 1× Tyrode's buffer when needed, rather than maintaining the platelet sample in 1× Tyrode's buffer for the duration of the experiment.
11. Care needs to be taken when using any membrane probe in the context of live platelet studies due to the potential to alter membrane biochemistry and impair platelet function. It is recommended that platelet functional studies such as low dose ADP (2.5 μM) aggregometry and FACS analysis of integrin $\alpha_{IIb}\beta_3$ dependent fibrinogen and/or PAC-1 binding, and P-selectin expression be undertaken as a function of $DiIC_{12}$ concentration during the initial work-up phase, to rule out loading or phototoxic artifacts. Where appropriate and dependent on the sensitivity of the chosen micro-imaging apparatus, dye concentration can be lowered to minimize buffering effects.
12. Platelet interactions with thrombogenic surfaces under conditions of blood flow in vitro are influenced significantly by the presence and density of erythrocytes (hematocrit) in the bulk flow. In the case of reconstituted blood flow experiments the percent hematocrit directly impacts on the number and frequency of platelet–surface interactions and resulting adhesion.

We generally use a hematocrit of 40 % for all reconstituted blood flow experiments.

13. Channels with annealed coverslips may be stored in this state at 4 °C for several weeks prior to use.
14. The pressure discretization scheme is set as standard and the second order upwind momentum option was enabled. The boundary condition at the walls is set as zero velocity to enforce the no slip condition.
15. Based on the calculated wall shear rate profiles (Fig. 3b) flow based TIRFM imaging should be performed at the center of the micro-channel, while avoiding the channel side walls where flow characteristics may deviate significantly from laminar flow.
16. All tubing needs to be primed with 1× Tyrode's buffer prior to the perfusion of blood, ensuring that there are no air bubbles present throughout the system.
17. It is critical that the perfusion system is clamped completely flat on the stage plate to ensure consistent and accurate TIRFM imaging.
18. Semiquantitative calibrations can only be carried out under conditions in which the platelet(s) under study are capable of full spreading in response to thrombin activation. This is based on the assumption that the point of closest apposition of the platelet to the adherent surface only occurs once the maximum extent of spreading has been achieved.
19. Make sure active gain is operating. This point of extinction will be marked by the almost complete loss of fluorescence signal and a very noisy pixelated background image.
20. The scaling is such that that each pixel intensity unit represents 0.1 nm, i.e., a pixel value of, for example, 90 represents a calculated distance of 9.0 nm. Pixels which have zero intensity in the original raw image data receive a value of 32,767, representing an infinite distance.
21. Copies of the Journals and TIRFM control software can be obtained by contacting the authors.
22. The recalibrated image stack allows for the interrogation of whole platelet average and minimum relative separation distance along with adhesive surface area at defined separation distances at each time point in the spreading process. Analysis can also be carried out on the whole platelet, as well as subregions within the platelet in question, down to the single pixel level (Fig. 6b, c).
23. Calibration of TIRFM images under flow requires that the platelet(s) under examination can be imaged following the thrombin (1 U/mL) infusion and are capable of undergoing full spreading. The entire image sequence in a time series can then be calibrated based on this reference image.

References

1. Dosquet C, Weill D, Wautier JL (1992) Molecular mechanism of blood monocyte adhesion to vascular endothelial cells. Nouv Rev Fr Hematol 34(Suppl):S55–S59
2. Zarbock A, Ley K (2009) Neutrophil adhesion and activation under flow. Microcirculation 16:31–42
3. Simon SI, Sarantos MR, Green CE et al (2009) Leucocyte recruitment under fluid shear: mechanical and molecular regulation within the inflammatory synapse. Clin Exp Pharmacol Physiol 36:217–224
4. Simon SI, Goldsmith HL (2002) Leukocyte adhesion dynamics in shear flow. Ann Biomed Eng 30:315–332
5. Jackson SP, Nesbitt WS, Westein E (2009) Dynamics of platelet thrombus formation. J Thromb Haemost 7(Suppl 1):17–20
6. Ruggeri ZM (2009) Platelet adhesion under flow. Microcirculation 16:58–83
7. Makino A, Shin HY, Komai Y et al (2007) Mechanotransduction in leukocyte activation: a review. Biorheology 44:221–249
8. Sriramarao P, Broide DH (1996) Differential regulation of eosinophil adhesion under conditions of flow in vivo. Ann N Y Acad Sci 796:218–225
9. Jones DA, Smith CW, McIntire LV (1996) Leucocyte adhesion under flow conditions: principles important in tissue engineering. Biomaterials 17:337–347
10. Nesbitt WS, Mangin P, Salem HH et al (2006) The impact of blood rheology on the molecular and cellular events underlying arterial thrombosis. J Mol Med 84:989–995
11. Nesbitt WS, Westein E, Tovar-Lopez FJ et al (2009) A shear gradient-dependent platelet aggregation mechanism drives thrombus formation. Nat Med 15:665–673
12. Dopheide SM, Maxwell MJ, Jackson SP (2002) Shear-dependent tether formation during platelet translocation on von Willebrand factor. Blood 99:159–167
13. Maxwell MJ, Dopheide SM, Turner SJ et al (2006) Shear induces a unique series of morphological changes in translocating platelets: effects of morphology on translocation dynamics. Arterioscler Thromb Vasc Biol 26:663–669
14. Maxwell MJ, Westein E, Nesbitt WS et al (2007) Identification of a 2-stage platelet aggregation process mediating shear-dependent thrombus formation. Blood 109:566–576
15. Nesbitt WS, Kulkarni S, Giuliano S et al (2002) Distinct glycoprotein Ib/V/IX and integrin alpha IIbbeta 3-dependent calcium signals cooperatively regulate platelet adhesion under flow. J Biol Chem 277:2965–2972
16. Nesbitt WS, Giuliano S, Kulkarni S et al (2003) Intercellular calcium communication regulates platelet aggregation and thrombus growth. J Cell Biol 160:1151–1161
17. Goncalves I, Nesbitt WS, Yuan Y et al (2005) Importance of temporal flow gradients and integrin alphaIIbbeta3 mechanotransduction for shear activation of platelets. J Biol Chem 280:15430–15437
18. Nesbitt WS, Jackson SP (2006) Imaging signaling processes in platelets. Blood Cells Mol Dis 36:139–144
19. Reininger AJ, Heijnen HF, Schumann H et al (2006) Mechanism of platelet adhesion to von Willebrand factor and microparticle formation under high shear stress. Blood 107:3537–3545
20. Molnar J, Lorand L (1961) Studies on apyrases. Arch Biochem Biophys 93:353–363
21. Tovar-Lopez FJ, Rosengarten G, Westein E et al (2010) A microfluidics device to monitor platelet aggregation dynamics in response to strain rate micro-gradients in flowing blood. Lab Chip 10:291–302
22. White F (1991) Viscous fluid flow. McGraw-Hill, New York
23. Truskey GA, Burmeister JS, Grapa E et al (1992) Total internal reflection fluorescence microscopy (TIRFM). II. Topographical mapping of relative cell/substratum separation distances. J Cell Sci 103:491–499
24. Allen RD, Zacharski LR, Widirstky ST et al (1979) Transformation and motility of human platelets: details of the shape change and release reaction observed by optical and electron microscopy. J Cell Biol 83:126–142

Chapter 4

Localization-Based Super-Resolution Imaging of Cellular Structures

Pakorn Kanchanawong and Clare M. Waterman

Abstract

Fluorescence microscopy allows direct visualization of fluorescently tagged proteins within cells. However, the spatial resolution of conventional fluorescence microscopes is limited by diffraction to ~250 nm, prompting the development of super-resolution microscopy which offers resolution approaching the scale of single proteins, i.e., ~20 nm. Here, we describe protocols for single molecule localization-based super-resolution imaging, using focal adhesion proteins as an example and employing either photoswitchable fluorophores or photoactivatable fluorescent proteins. These protocols should also be easily adaptable to imaging a broad array of macromolecular assemblies in cells whose components can be fluorescently tagged and assemble into high density structures.

Key words Super-resolution microscopy, Focal adhesions, Localization microscopy, TIRF, PALM, Single molecules, Photoswitchable fluorophores, Photoactivatable fluorescent proteins

1 Introduction

Fluorescence microscopy has proven an indispensable tool in modern cell biology, offering unparalleled abilities to interrogate the presence and spatial distribution of specific biomolecules within cells or tissues, as well as determine how they change during the course of biological functions or in response to perturbations. These days, researchers can visualize most classes of biomolecules by tapping into a wide array of fluorescent labelling strategies, ranging from antibodies conjugated to fluorescent dyes, to proteins fused to green fluorescent protein (GFP) or spectral variants, to oligonucleotides tagged with fluorophores (fluorescent in situ hybridization: FISH), to genetically encoded protein linkers that allow covalent linkage of synthetic fluorophores (SNAP$^{(C)}$ and HALO$^{(C)}$ tags). These methods are capable of exquisite sensitivity, in many cases to single or few copies of molecules. Furthermore, they are generally widely available (commercially in many cases), well-developed, and well-documented.

Amanda S. Coutts (ed.), *Adhesion Protein Protocols*, Methods in Molecular Biology, vol. 1046,
DOI 10.1007/978-1-62703-538-5_4,

Nevertheless, despite these strengths, conventional fluorescence microscopy is still limited in one important aspect, that is, in its diffraction-limited spatial resolution. Even though a fluorescent source can be reliably detected at the single molecule level by modern detectors such as the EMCCD (Electron Multiplying Charge Coupled Device) cameras, due to the fundamental properties of light, their images appear as diffraction-limited spots, i.e., the so-called point spread function (PSF). For light microscopes operating in the visible spectral range, the PSF dimension is more than an order of magnitude larger than the size of typical protein molecules, at ~250 nm laterally (x, y) and >500 nm axially (z). The PSF dimension determines the microscope's resolving power; spatial features within the cells finer than ~250 nm are essentially unresolvable.

In the past decade or so, physicists have exploited several optical and photophysical phenomena to circumvent the diffraction limit, giving rise to a range of new Super-Resolution Microscopy (SRM) techniques. These techniques and their applications in cell biology have gained rapidly in recognition in recent years [1–5]. The three most well-known SRM approaches include STED (STimulated Emission Depletion) microscopy [6, 7], SIM (Structured Illumination Microscopy) [8], and single molecule-based Localization Microscopy [9–11]. In this chapter, we focus on Localization Microscopy, which encompasses techniques known by acronyms such as PALM (PhotoActivated Localization Microscopy) [9] and STORM (STochastic Optical Reconstruction Microscopy) [11], as well as several others [10, 12]. These are particularly attractive and practical for many cell biology labs, in no small part due to their comparatively simple hardware requirements similar to that of Total Internal Reflection Fluorescence (TIRF) microscopy. Indeed such accessibility is likely one major factor in the wide adoption of Localization Microscopy compared to other SRM modalities.

The protocols described in this chapter are geared toward setting up and performing Localization Microscopy for visualizing proteins in Focal Adhesions (FAs). These are dense plaques of proteins associated with plasma membrane sites where cells adhere to the extracellular matrix (ECM) and form linkages between the ECM and the actin cytoskeleton. While the molecular complexity and high protein density in FAs have long impeded protein-specific ultrastructural analysis by immuno-EM approaches, FAs are quite suitable for Localization Microscopy [13–16]. This is due to the high molecular specificity of fluorescent labelling as well as the proximity of the FAs to an ECM-coated cover glass surface, which allows high signal-to-noise, low background single molecule detection. Note that although the FA is the example used in this chapter, the protocols described herein should also be easily applied to imaging any cellular macromolecular assembly whose components can be fluorescently tagged and assemble into high density structures.

In the following sections of the introduction, we further discuss the fundamentals and experimental considerations important for

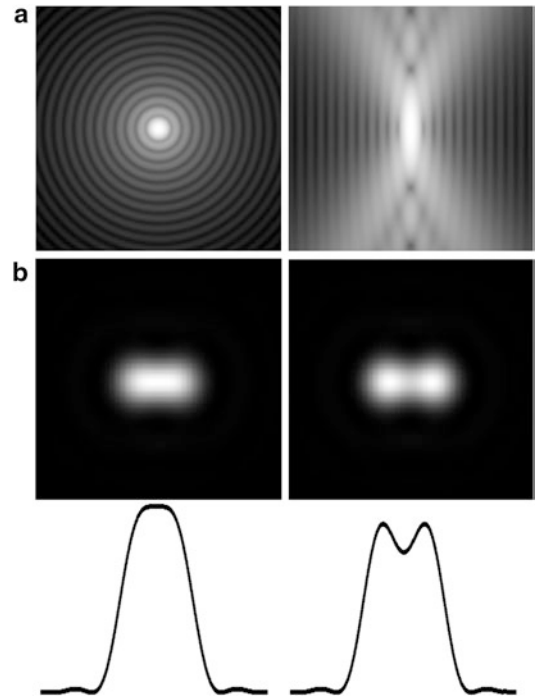

Fig. 1 Microscope point spread function and Rayleigh resolution criterion. The dimension of the microscope point spread function (PSF) (**a**, *left*: lateral or *x*,*y*; *vertical x*,*z* view) limits the resolution of the conventional light microscope. Two fluorophores in close proximity below the size scale of the central PSF intensity peak will appear to merge (**b** *left*) and thus cannot be resolved as distinct fluorophores. The limit at which the molecules appear separate as judged by the intensity cross-section (*bottom*) is called the Rayleigh criterion. (**a**) is in log scale to show the structure of the PSF, whereas in (**b**), linear intensity scale is used

designing a Localization Microscopy experiment. This background is particularly pertinent for new practitioners since Localization Microscopy is a recent and highly interdisciplinary technique, and some of the key concepts are borrowed from physical chemistry and thus may be unfamiliar to cell biology-oriented researchers. In Subheading 2, we describe a procedure for setting up a customized microscope system for Localization Microscopy imaging, as well as protocols for preparing ultraclean fiducialed substrates for culturing cells for Localization Microscopy. Finally, in the Subheading 3 we present a protocol for the acquisition and processing of Localization Microscopy data. Where necessary, expanded discussions are included as Notes at the end of the chapter.

1.1 Basic Principles and Considerations for Localization Microscopy

The diffraction limit of the conventional light microscope can be illustrated by the well-known Rayleigh criterion (Fig. 1) which posits that two fluorescent molecules situated closer than the PSF dimension cannot be resolved (Fig. 1b). However, this holds true only if both fluorescent molecules are observed simultaneously.

While this applies for most situations in conventional fluorescence microscopy, single molecule studies in the 1990s revealed that many fluorophores ranging from GFP to synthetic dyes exhibit more complicated photophysics such as blinking or photoswitching [17, 18]. Although this phenomenon was initially considered a nuisance in single molecule enzymology experiments, it was soon recognized that this effect can be exploited for super-resolution imaging [19]—closely spaced molecules that would otherwise overlap can be detected separately in time, due to their stochastic blinking/switching. Three key requirements necessary for Localization Microscopy are: (1) *single molecule contrast*: the brightness of the fluorophore (characterized as photon numbers) relative to background noise is critical for accurate determination of the position of each fluorophore; (2) *sparsity*: to detect molecules individually, they must be sufficiently isolated spatially from one another; (3) *high total spatial density:* high density of labelling is needed to sample the spatial profile of the underlying structure (known as Nyquist–Shannon sampling criterion [20]).

To meet these requirements, photoswitchable (or photoactivatable) fluorophores are needed for Localization Microscopy. A well-known example in cell biology of such photoswitchable fluorophores is PA-GFP (photoactivatable-GFP), which was originally developed as an optical highlighter for tracking subcellular organelles [21], but has since been used successfully for Localization Microscopy [9, 22, 23]. PA-GFP is a photoswitchable variant of GFP, whereby, prior to photoactivation, it exists in the non-activated state, with negligible emission in the GFP channel (520 nm). Upon illumination by photoactivating blue light at 405 nm, PA-GFP turns into a photoactivated form which now absorbs and fluoresces in the GFP channel. In order to fulfil the sparsity requirement above, researchers can control the amount of photoactivating blue light (405 nm), i.e., by controlling the duration or the intensity, so that only a sparse subset of PA-GFP is photoactivated at a given instance. With proper excitation intensity and a sensitive EMCCD camera, a random subset of isolated PA-GFP molecules can be readily observed as spatially segregated diffraction-limited spots. These activated PA-GFPs typically appear for a brief period of a few seconds while being imaged before disappearing. Such so-called "photobleaching" serves to clear out the molecules that have been imaged, maintaining sparsity, while newly activated molecules become visible. Note that the appearance and disappearance of the fluorophores is a stochastic process, such that the molecules appear to blink randomly and there is a spread in how long they remain fluorescent during their activated state, and likewise in their brightness. By collecting a series of images of such blinking over a sufficiently long time, the cellular structures labelled by PA-GFP are spatially and cumulatively sampled, fulfilling the high spatial density requirement.

1.2 Localization Analysis of Single Molecule Fluorescence

The imaging protocols for Localization Microscopy consist of the acquisition of raw data and subsequent image processing and reconstruction steps. Upon the acquisition of high quality single molecule datasets, peak detection and localization analysis algorithms are employed to extract the molecular coordinate of each observed fluorophore. Although an individual fluorescent molecule is detected as a diffraction-limited spot spread over several pixels on the detector (Fig. 2a), the centroid position of such a spot can be "localized" by fitting to a model of point-spread function, and assumed to be the position of the emitting molecules. A 2-dimensional Gaussian function is commonly used as it provides a close approximation while being fast to compute [24]. The Gaussian approximation usually suffices for most applications of Localization Microscopy, providing that the fluorophores are freely rotating during the imaging time scale. However, it should be noted that there are special cases, for example where the fluorophores are directionally constrained and the emission dipole is not well averaged, such as when the dye is embedded in the membrane. In these cases, a more advanced (and computationally demanding) model is required [25]. The precision at which the lateral molecular coordinate (i.e., the *xy*-centroid) can be localized is dependent upon the brightness of the molecule relative to the background signals. Localization uncertainty (σ_{xy}) is commonly computed [24] based on the following equation (further derivation and refinement in ref. 34): $\sigma_{xy} = ((s^2 + a^2/12)/N + (8\pi s^4 b^2/(a^2 N^2)))^{1/2}$ (N: detected photons; s: width of the PSF; a: pixel size; b: background noise). Thus, the brighter the fluorophore, the more precise the localization. Likewise, lower background is also desirable for high localization precision. On average, PA-FP (photoactivatable-fluorescent proteins) typically emit 500 or more detected photons before undergoing photobleaching, allowing localization precision of ~20 nm. Some organic fluorophores such as Cy5 or AlexaFluor 647 are brighter, thus giving rise to higher localization precision [26]. Note that since the photoswitching of fluorophores is a stochastic process influenced by both the intrinsic fluorophore properties and other environmental factors (such as redox potential [27] and oxygen level [28]), the brightness and hence localization precision could vary between preparations. Also, since the molecules in the sample exhibit varying brightness, this results in a distribution of their localization uncertainties (σ_{xy}). Thus, rather than a uniform single resolution number for the entire image, the spatial resolution of Localization Microscopy varies depending on local density, fluorophore brightness, and background noise.

Due to the large volume of raw data sets (gigabytes), and the numbers of iterations needed for localizing each molecule, it is highly recommended that a sufficiently powerful computer is used for image processing. Thanks to the increasingly wide adoption of

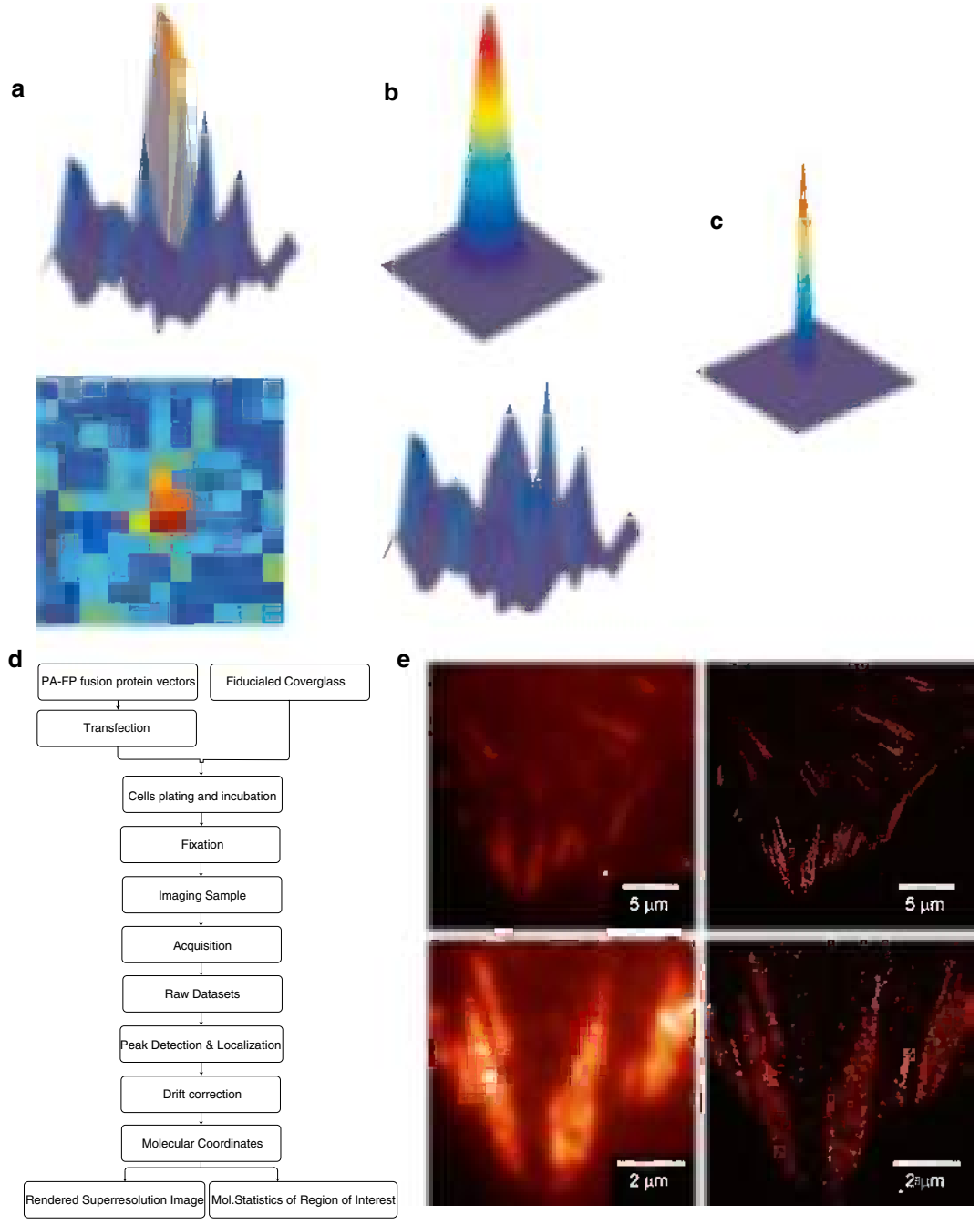

Fig. 2 Schematic diagram of single molecule localization analysis and localization microscopy. Isolated single fluorophores such as EosFP can be detected as diffraction limited spots by an EMCCD camera (**a**, *top*: 3-D plot of pixel intensity, *bottom*: 2-D view). These can be fitted by a model of the point-spread function (PSF) such as a 2-dimensional Gaussian (**b**, *top*). Localization analysis computationally minimizes the residual (**b**, *bottom*), by determining the centroid position as well as the width of the observed PSF. The resulting centroid coordinate represents the position of the molecule with much better precision than the PSF. The position of the molecule can be rendered as a 2-D Gaussian with the width corresponding to the localization uncertainty (**c**). Flowchart for Localization Microscopy is shown in (**d**), whereas in (**e**) the super-resolved image (*right*) of Paxillin-tdEos is shown next to diffraction-limited TIRF image (*left*), demonstrating the significant gain in resolution due to Localization Microscopy. *Bottom panels* show zoomed-in views. *Bright spots* in the *top left panel* are due to the gold nanoparticle fiducials

Localization Microscopy, several software packages for performing single molecule detection and localization analyses have been published and are freely distributed [29–31].

1.3 Labelling Proteins for Localization Microscopy

The requirement for high spatial sampling density and localization also has implications for the nature of the fluorescent probes used for labelling the molecules of interest. While in conventional fluorescence microscopy, the size of the probe molecule itself is rarely an issue since the spatial resolution is an order of magnitude coarser than the molecular length scale, in Localization Microscopy, the resolution of the imaging method approaches the molecular length scale, and thus judicious selection of the labelling strategy is important.

For imaging of proteins, two common labelling approaches are protein fusion with PA-FP and antibodies conjugated with synthetic fluorophores. These two approaches offer different advantages and disadvantages. PA-FP fusion is genetically encoded and is inherently compatible with live cells. Furthermore, many PA-FP are also useful for other cell biology experiments. Similar to GFP, the PA-FP tag is a highly compacted globular domain of <300 amino acids, with a diameter of <5 nm across. Thus, in principle a large number of fusion proteins can be packed together into a small volume, providing higher sampling density. However, in practice typical cells also express unlabelled endogenous protein which effectively dilutes the labelling density of the expressed fusion protein. Thus, where necessary, this should be addressed by using genetic knock-out or RNAi-mediated knockdown in cells to gain a more complete replacement of the endogenous protein by the fusion construct. Of note, recent gene editing technologies such as TALEN (Transcription-Activator-Like Effector Nuclease) [32] may also offer a promising solution for a complete replacement of endogenous protein with labelled proteins. Finally, the main disadvantage of PA-FP is that their photophysical properties are not as good as the best of the synthetic fluorophores.

The major strength of the antibody-based synthetic fluorophore approach is the high brightness of such fluorophores. Additionally, where available, antibodies allow detection of diverse post-translationally modified forms of proteins, such as phosphorylation. However, in practice, where the antibodies are not commercially available for the target proteins, a greater amount of resources and effort is required to produce such antibodies. Furthermore, the antibodies are multi-domain proteins much larger than FPs (>10 nm for an IgG). This size is compounded by the fact that common immunofluorescence (IF) protocols use unlabelled primary antibodies to detect the proteins and fluorescent-tagged secondary antibodies as probes for the primary antibodies. The large combined size of the probes (on the order of ~20 nm) therefore limits how densely these probes can be packed into a given volume, as well as how well the probes can access

tightly packed structures. Also, the labelling of cells with antibodies generally requires fixation and permeabilization and thus is not compatible with live cells.

1.4 Visual Representation of Localization Microscopy Datasets

Unlike most other imaging modalities, the so-called "finished product" for Localization Microscopy is not the super resolved image per se. Rather, the result is essentially a long list of single molecule attributes, containing entries such as the spatial coordinates: x, y, and/or z; uncertainty of the spatial coordinates: σ_x, σ_y, σ_z; amplitudes; brightness; fit quality and so on. A standard convention for Localization Microscopy is to represent each molecule with a normalized 2-dimension Gaussian function, with the width corresponding to the coordinate uncertainty (σ). In other words, the intensity shown in the super-resolution reconstructed image is proportional to the probability of finding a molecule at a particular coordinate. Thus, a bright and well localized molecule will be portrayed as a sharp and narrow point with a relatively high peak intensity, whereas a dimmer and less well localized molecule will be shown as being less distinct with a smaller peak intensity.

2 Materials

Localization Microscopy requires a research-grade TIRF microscope capable of detecting single molecule fluorescence. Instructions below describe a custom-built open-beam microscope system equipped with moderately high-powered lasers (~100 mW) and coupled with an EMCCD camera and appropriate filter sets (Fig. 3). Custom-built systems offer more flexibility and savings on equipment cost, although familiarity with optical instrumentation will be required. As a guideline, examples of manufacturers and parts numbers are given below for each component. We found that commercial TIRF microscopes are also usually adequate (available from most major manufacturers: Nikon, Olympus, Zeiss, Leica). These typically offer fiber-coupled lasers, which simplify much of the alignment work, albeit with reduced power output and higher cost. In addition to the microscope, appropriate sample preparation is essential for successful imaging. Protocols later on in this section describe the preparation of fiducialed cover glasses, pretreatment of these cover glasses for cell culture, as well as the preparation of fixed cell samples for Localization Microscopy.

2.1 Instrumentation for Localization Microscopy

1. Suggested components:
   - Research grade inverted microscope (e.g., Nikon Eclipse Ti).
   - 100× High numerical aperture (NA) objective lens (Nikon, 100× Apo TIRF NA 1.49).
   - Piezoelectric Z-translation stage (optional) (Mad City Labs, #Nano-Bio100).

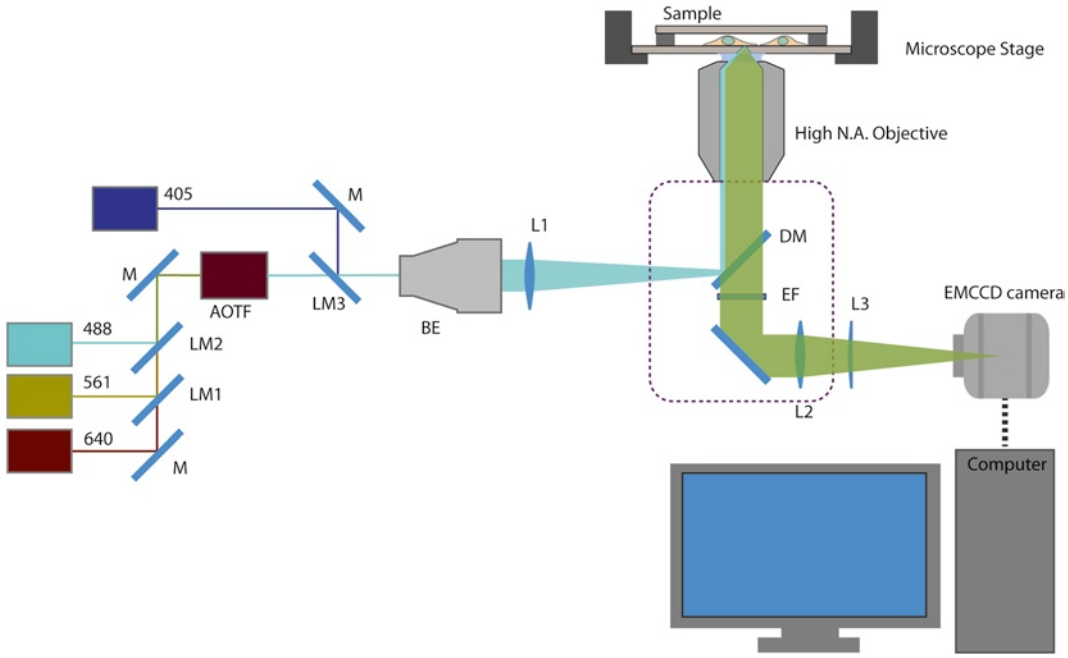

Fig. 3 Schematic diagram of a microscope configured for Localization Microscopy. Laser beams (wavelength of 488, 561, 640 nm) are directed by mirror (M) and combined by laser merging dichroic mirror (LM) and coupled into an AOTF (Acousto-Optical Tunable Filter). The 405 nm laser is combined separately due to AOTF bandwidth limitation. The combined laser beam is expanded by a beam expander (BE) and focused onto the back focal plane of the high NA objective via a lens ($f \sim 300$ mm), mounted on a translatable platform. The illumination laser is reflected toward the sample by a dichroic mirror (DM). The fluorescence emission passes through the dichroic mirror and is filtered by the emission filter (EF), before being focused by the tube lens and/or magnification changer lens (L2). For 3-D Localization Microscopy, a weak cylindrical lens (L3) could be mounted on a translatable platform in front of the EMCCD camera. The microscope body is denoted by the *dashed line*. The sample is mounted on a microscope stage (optional: Z-piezo for 3-D Localization Microscopy). For examples of manufacturers and part numbers, *see* Subheading 2

- Vibration-damped optical table (at least 3 ft×6 ft, e.g., Newport Corp. #RS-2000-36-8).
- Lasers with the following wavelengths and power: 405 nm (100 mW, Coherent, #1142279), 488 nm (200 mW, Coherent, #1137964), 561 nm (200 mW, Coherent, #1137977), 640 nm (100 mW, Coherent, #1185055).
- Acousto-Optic Tunable Filter (A-A Optoelectronic, #AOTFnCVis).
- Heatsink mounts for lasers and AOTF, custom-machined from Aluminum.
- Dichroic mirror (for filter cube, DM in Fig. 3: Semrock, #Di01-R405/488/561/635-25x36; for combining laser beams: #LM01-613-25, #LM01-503-25, and #LM0-427-25; LM1, LM2, LM3 in Fig. 3, respectively).

- Emission filter (Semrock, green, #FF01-525/50-25; red, #FF01-609/57-25; far-red, #FF01-676/37-25; EF in Fig. 3).
- Steerable mirror mounts (ThorLabs, #KS1).
- Neutral density filter wheel (ThorLabs, #NDC-25-C).
- First surface mirrors (New Focus, #5101; M in Fig. 3).
- 10× beam expander (ThorLabs, # BE10M; BE in Fig. 3).
- Achromatic doublet lens (f = 300 mm, CVI MellesGriot, #LAO-300.0-25.0; L1 in Fig. 3).
- Cylindrical lens (optional, f = 1,000 mm, CVI MellesGriot, #SCC-25.4-508.6-C; L3 in Fig. 3).
- Translational stage (ThorLabs, #PT1).
- EMCCD camera (Andor, #DU-897U-CS0#BV).
- Desktop Workstation PC.

2. Secure an inverted microscope on a research-grade optical table with good vibration damping. Ensure that the room housing the microscope has good temperature stability. (Note the position of the air vent, and if necessary install a deflector or put the microscope in an enclosure to minimize mechanical instability.)
3. On the optical table, set up continuous wave (CW) solid state lasers with the following wavelengths and power (see above for specific model suggestions): 405 nm (50–100 mW, for photoactivation), 488 nm (~100 mW or greater, for imaging of PA-GFP [21] or Dronpa [33]), 561 nm (~100 mW or greater, for imaging EosFP [34], Dendra2 [35], or PAmCherry [22]), and 640 nm (~100 mW or greater, for imaging of Cy5 or AlexaFluor 647 [11]). To simplify alignment, obtain custom-machined heatsink (these can be machined from standard aluminum block by any local machine shop) with the appropriate height so that all the lasers beams are at the same heights above the optical table (*see* **Notes 1** and **2**).
4. Combine laser beams using appropriate dichroic mirrors in suitable steerable mounts. The longest wavelength line in the system, such as 640 nm, should be used as the primary beam against which all other lasers are aligned. It is generally useful to install a filter wheel with neutral density (ND) filters in front of the laser heads, for an added degree of intensity control. Align the mirrors and dichroic so that the laser beams are colinear. Depending on laser regulations at different institutions, it may be advisable to build an opaque enclosure to contain stray light.
5. Position an Acousto-Optic Tunable Filter (AOTF) on the optical table. Make sure that the AOTF optical opening is well matched to the laser beam height. If needed, obtain a

custom-machined aluminum pedestal of appropriate height. Position a mirror to direct the filtered beam into a 5–10× beam expander (*see* **Note 3**).

6. Install a 100× high NA oil-immersion objective lens (NA > 1.45) on the microscope objective turret (*see* **Note 4**).
7. To illuminate the sample in epifluorescence geometry, focus the expanded laser beam onto the back focal plane of the microscope objective. This can be achieved by mounting a 300 mm achromatic doublet lens on a 2-axis translational stage near the illumination port of the microscope (*see* **Note 5**).
8. Select the appropriate dichroic mirror and emission filters and install them in the appropriate filter cubes of the microscope (*see* **Note 6**).
9. Install an EMCCD camera (*see* **Note 7**) at the microscope emission port. Securely fasten the camera to the optical table to minimize vibration.
10. (Optional) For 3-D Localization Microscopy using astigmatism [36], install a piezoelectric Z-translation stage (e.g., Nano-Bio100 from Mad City Labs, Madison, WI). Place a defocusing lens (a weak cylindrical lens with long focal length of 1,000 mm or more) before the camera. Mount the lens on a translation stage with good repeatability. Make sure to build a light-tight enclosure for this assembly to protect the EMCCD from stray light. The distance between the cylindrical and the EMCCD chip can be calculated from the formula for calculating back focal length of a compound lens system: $S = (f_2(d - f_1))/(d - f_1 - f_2)$, where S is the back focal length, f_1 and f_2 the focal length of the first (in this case, the microscope tube lens) and the second lens (cylindrical lens), respectively, and d the distance between the two lenses. As an example, for a relative defocused difference of 400 nm, the cylindrical lens ($f = 1{,}000$ mm), should be placed at $d \sim 179.8$ mm behind the tube lens ($f = 200$ mm for Nikon microscope).
11. Set up a desktop computer for controlling the microscope. Configure the microscope and peripheral control software. Commercial software such as Metamorph (Molecular Devices, Sunnyvale, CA) can be used. Alternatively, if cost is an important consideration, MicroManager, a freely available microscope control software should be considered [37] (*see* **Note 8**).
12. Configure the image processing computer. A desktop computer with multiple-core CPU and a 64-bit operating system is recommended in order to take advantage of large memory—16 GB or more may be required for large datasets. Alternatively, the data can be processed in smaller chunks on a more modest machine and pieced together afterward. Typically, several hours of processing on a workstation level

machine are needed for a single data set. Alternatively, many academic institutions have a centralized high performance computing cluster which can speed up the processing steps significantly. While initial setup work may be needed to configure the software for distributed computing, this may be a more efficient solution in the long run.

2.2 Preparation of Cover glasses for Cell Culture

Stringent cleaning of the cover glasses is mandatory for Localization Microscopy since any background fluorescent signal will interfere with the fluorescence from labelled molecules. Of equal importance, since acquisition time is on the order of several minutes or more, mechanical drift is inevitable and must be corrected for. We recommend using fluorescent beads or fluorescent nanoparticles affixed to the coverslip as fiducial marks. Since the dynamic range of the EMCCD camera is limited in the EM-gain mode, an important consideration is to ensure that the fiducials are not so excessively bright as to become saturated. Our choices for the fiducials are gold or bimetallic gold–silver nanoparticles whose plasmonic emissions are within similar spectral ranges to PA-FPs. These also exhibit appropriate brightness and are resistant to photobleaching. In the simplest preparation, these nanoparticles can be added into the sample prior to imaging and allowed to adsorb to the cover glass via non-specific adhesion. However, fiducials affixed this way typically still exhibit thermal fluctuations and can be dislodged over time. In the protocol below, we describe a method for immobilizing pre-attached fiducials with a thin layer of SiO_2 which allows for much more stable fiducials and reliable drift correction. Note that fiducialed cover glasses have recently become commercially available (www.hestzig.com) which provide an alternative for cases where access to a sputter coating instrument is difficult.

1. Suggested equipment and materials:
    - Plasma cleaner (e.g., Harricks, #PDC/32-G).
    - Laminar flow hood with UV lamp.
    - Hotplate/Stirrer.
    - Shaker/Rotator.
    - Ultrasonic Bath.
    - Sputter coater (Denton Vacuum Technologies).
    - Cover glass (#1.5, 22 mm square, Fisher Scientific, #12-541B).
    - Porcelain staining rack (Thomas Scientific, #8542E40).
    - Adhesive spacer (BioscienceTools, #UTIC-21).
    - Dry N_2 gas.
    - Ethanol.
    - Acetone.

2. Dulbecco's Phosphate Buffered Saline (DPBS): 2.7 mM KCl, 1.5 mM KH_2PO_4, 136.9 mM NaCl, 8.9 mM $Na_2HPO_4 \cdot 7H_2O$.
3. Poly-L-lysine solution: 0.1 % w/v solution of poly-L-lysine (m.w. 150,000–300,000) in double deionized water (ddH_2O). Alternatively, ready-made solution is also commercially available (e.g., Sigma, #P8920).
4. 100 nm gold nanoparticle solution: Resuspend gold nanoparticles solution (Corpuscular Inc., #790122), then dilute 1:1,000 in DPBS.
5. Fibronectin solution: Dilute 1 mg/mL fibronectin stock solution (Millipore, #FC010) in sterile DPBS to 2–10 μg/mL. Perform the dilution in sterile laminar flow hood.
6. 1 M HNO_3: Add 63.3 mL of concentrated nitric acid (15.8 M) into approximately 500 mL of ddH_2O. Adjust volume to 1 L. Make sure to perform dilution in a chemical fume hood, with appropriate protection equipment.
7. Select #1.5 cover glasses individually and arrange them on an acid-resistant porcelain rack. Sonicate for 15–30 min in the following solutions in the following order: ddH_2O, acetone, 100 % ethanol. Rinse in ddH_2O and immerse in 1 M HNO_3 (in chemical fume hood). Heat the nitric acid to a boil and let cool overnight. Rinse the cover glasses in ddH_2O multiple times and then dry by compressed air or N_2. Clean the cover glasses for 5 min in a plasma cleaner or a UV–ozone cleaner. If either of these pieces of equipment are not available, RCA etch can be used (*see* **Note 9**).
8. Incubate cleaned cover glass with the poly-L-lysine solution for 10–20 min to aid in the adsorption of fiducials. Rinse thoroughly with ddH_2O and let dry. Dilute nanoparticle fiducials to approximately 1:1,000 (the concentration should be empirically adjusted to obtain appropriate density of several fiducials per a field of view of ~5,000 μm^2). Incubate individual poly-L-lysine-coated cover glass with 2 mL of the fiducial solution for ~30 min. Rinse away excess fiducials by ddH_2O and dry by compressed air or nitrogen gas. Using a sputter coater, deposit 30–50 nm of SiO_2 onto the fiducial-affixed side of the cover glass. Plasma clean the cover glass upon finishing.
9. Place each cleaned cover glass into a 6-well tissue culture plate. Sterilize by UV radiation in a laminar flow hood for 15 min.
10. Rinse three times with DPBS. Incubate each well with 2 mL of fibronectin solution at desired concentration (typically 2–10 μg/mL). Let the cover glasses incubate overnight at 4 °C, or with gentle rocking at 37 °C for a few hours. Aspirate out the fibronectin solution. Replace with DPBS. The cover glasses can be stored at 4 °C for up to 7–10 days until needed for cell plating.

2.3 Cell Culture and Preparation of Fixed Cells for Imaging

High quality single molecule raw image data is the most important ingredient for successful Localization Microscopy. This is strongly influenced by the properties of the fluorophores. In particular, EosFP (tdEos [34] and mEos2 [38]) and AlexaFluor647 are among the best performing PA-FPs and synthetic fluorophores, respectively. Thus, we recommend that novice users start imaging with these fluorophores. The preparation of cell cultures for imaging, for the most part, is similar to that of standard imaging protocols. Since Localization Microscopy depends on single molecule imaging, it is important to make sure that the expression level is appropriate—due to background auto-activation of PA-FPs in highly expressing cells, the single molecule signals can be too dense even before any photoactivation light is applied. It is highly recommended to compare expression and localization of multiple FP fusions of the same protein, to ascertain that the constructs are minimally perturbative (*see* **Note 10**). Potential artifacts include protein aggregation, incorrect localization, and altered cellular morphology. Where possible, test the biological function of the fusion construct and compare the localization with known immunofluorescence staining.

1. Suggested equipment and materials:
   - Tissue culture incubator (37 °C, 5 % CO_2).
   - Sterile laminar flow biosafety hood.
   - Transfection reagents and apparatus (e.g., Life Technologies, Neon).
   - U2OS cell line (ATCC).
   - McCoy5A media (Life Technologies).
   - Fetal Bovine Serum (Life Technologies).
   - Penicillin/Streptomycin (Life Technologies).
   - Trypsin/EDTA (Life Technologies).
   - Endofree Plasmid Maxi kit (Qiagen).
   - DPBS.
   - Phalloidin-AlexaFluor647 (Life Technologies).
2. KOH solution (10 M): 74.55 g of KOH added to 100 mL ddH_2O (care should be taken as KOH is highly corrosive).
3. PHEM buffer (2× stock solution): 120 mM PIPES, 50 mM HEPES, 20 mM EGTA, 4 mM $MgCl_2$, pH 7.0 with KOH. Dissolve 6.5 g of HEPES, 3.8 g of EGTA, and 190 mg of $MgCl_2$ in ~300 mL of ddH_2O. With vigorous stirring, monitor the pH (should be acidic), and start adding concentrated KOH solution dropwise to bring the pH to approximately 6. Start adding 18.14 g of PIPES in small batches. PIPES will start to dissolve at pH > 6. Adjust the pH to 7.0 with KOH

solution, and bring the volume to 500 mL by adding ddH_2O. Filter-sterilize and store at 4 °C. Dilute PHEM 2× stock 1:1 with ddH_2O before use.

4. Permeabilization buffer (0.1 % Triton): Dilute 1 mL of Triton X-100 in 1 L of PHEM 1× buffer. Fresh preparation of Triton solution on the day of the experiment is recommended for effective permeabilization and antibody penetration into the cells.
5. Quenching buffer (50 mM NH_4Cl): 2.68 g of NH_4Cl in 1 L of PHEM 1× buffer.
6. Oxygen-depleted Imaging buffers: (a) 1 M of glucose solution: Add 18 g of glucose to 100 mL of PHEM 1× buffer. (b) 1 M (10×) cysteamine solution: Add 770 mg cysteamine to 10 mL of PHEM 1× buffer. (c) 100× stock enzyme mixture: Add 4 mg of catalase and 10 mg of glucose oxidase to 100 µL of PHEM 1× buffer. Mix well by vortexing. Centrifuge for 2–3 min and aliquot supernatant for storage at 4 °C. (d) Right before imaging, mix 75 µL of 1 M glucose solution, 30 µL of 1 M cysteamine solution, 3 µL of 100× stock enzyme mixture, and adjust the volume to 300 µL with PHEM 1× buffer and use immediately after mixing to mount the sample.
7. VALAP: Melt 100 g each of vaseline, lanolin, and paraffin in a beaker on a hotplate. Use a low heat level for melting (below 100 °C) to prevent ignition of the mixture. Stir until well mixed.
8. Culture the desired cell type in the appropriate medium and environmental conditions. For example, we culture the U2OS (human osteosarcoma) cell line in McCoy5A media supplemented with 10 % fetal bovine serum and penicillin/streptomycin under 5 % CO_2 at 37 °C.
9. For fluorescent protein labelling, a fusion construct of the protein of interest can be constructed from cDNA of the target protein and a photoactivatable fluorescent protein vector (several cloning vectors can be obtained from the AddGene repository (www.addgene.org)). We highly recommend that standard FP fusions such as GFP or mCherry be made in parallel to the PA-FP constructs (*see* **Note 10**).
10. Verify the sequence of the fusion construct and prepare high-purity endotoxin-free vectors for transfection.
11. Transfect cells with the fusion protein cDNA. We obtain good results using electroporators such as Amaxa nucleofector (Lonza, Basel, Switzerland) or Neon (Life Technologies, Carlsbad, CA). Alternatively, lipid-mediated approaches (Lipofectamine from Life Technologies or Fugene from Roche) can also be used.

12. Incubate transfected cells for 6 or more hours or until the desired expression level is attained (determined empirically). Rinse the cells with warm DPBS. Dislodge the cells by incubating with 1–2 mL warm trypsin for 1–2 min. Stop the trypsinization by adding complete (serum containing) media. Count the cells and replate the desired number of cells onto the prepared cover glass (Subheading 2.2). Incubate replated cells in a 37 °C, 5 % CO_2 incubator. For typical FA imaging, cells can be fixed 12–24 h after replating.
13. Fixative: Prepare the fixatives fresh before use. We use prepackaged methanol-free paraformaldehyde in ampoule format (16 % solution) diluted to 4 % in a cytoskeleton-stabilizing buffer (such as PHEM buffer, warmed to 37 °C).
14. Start the fixation by aspirating out the media and replace with warm fixative. Incubate in the dark for 12–15 min at 37 °C. Aspirate out the fixative. Rinse with PHEM buffer. If permeabilization is needed, incubate with permeabilization buffer for 15 min after fixation. Quench for 10 min with the quenching buffer.
15. (Optional) To visualize actin filaments, incubate the samples with phalloidin labelled with AlexaFluor647 (20–30 nM in PHEM buffer) for 30 min to 1 h.
16. Wash by incubating with PHEM buffer for 5 min and then exchange with fresh buffer. Repeat three times.
17. Following fixation, fiducial beads or gold nanoparticles can be added if fiducialed cover glasses are not being used. We obtain good results with a starting concentration of 1:1,000 dilution and 20–30 min incubation.
18. Wash with PHEM buffer to remove excess unbound fiducials.
19. Throughout the fixation steps, samples should be assessed by light microscopy for the integrity of cell morphology, and/or fluorescence of the target proteins. Make sure to dispense the solutions gently and to the edge of the well and never on top of the cells directly. Perform the change of solutions quickly and never let the cells dry out.
20. The sample should be imaged preferably as soon as the fixation is concluded. Alternatively, samples can be stored for a day or so at 4 °C. Be aware that the fluorescence of some PA-FPs degrades over time.
21. For PA-FPs, imaging can be done in PBS or PHEM buffer without additional components. However, in our experience a careful preparation of imaging buffer appears to improve the quality of the image. We typically use PHEM buffer, filtered by 0.22 μm filter. For vacuum-driven filtration, the filtering process will also help to partially degas the buffer. This can be

done by tapping the evacuated tube repeatedly to dislodge the bubbles. Additives such catalase (0.04 μg/mL) helps to remove peroxide and radicals that could be generated by the reaction of dissolved oxygen and excited fluorophores.

22. For imaging synthetic fluorophores such as AlexaFluor647, a reducing and oxygen-depleted imaging buffer is recommended. Prepare fresh imaging buffer just before mounting as above, and ensure that the sample is sealed completely as described below.
23. Mount the cover glass on a glass slide (3"×1") or another piece of large cover glass. We use double-sided adhesive spacer (Bioscience Tools) to aid in the assembly. The sample is rinsed once with the imaging buffer and then assembled into an enclosed cell. Make sure to perform this step gently to avoid any air bubbles. Afterward, gently blot away excess buffers. Seal the sample by melted VALAP. Clean the surface of the sealed imaging chamber by rinsing with deionized H_2O and blow dry with compressed air. The sample can then be mounted onto the microscope for imaging.

3 Methods

Since multiple parameters must be optimized for proper imaging, researchers are encouraged to become familiarized with the acquisition and analysis workflow using easy-to-prepare test samples (such as bare fiducialed cover glass) before embarking on imaging their research samples. Procedures detailed below include the initial optimization needed to ensure proper and stable microscope operation, followed by guidelines for the acquisition of raw datasets from cellular samples and, finally, the image processing required to obtain super-resolved images.

3.1 Initial Characterization of Microscope Stability

Since mechanical stability is important for Localization Microscopy, prior to imaging fixed cell samples, users should take great care in characterizing and optimizing the stability of the microscopy system. This can be carried out by imaging a simple test sample as described below.

1. A fiducialed cover glass prepared earlier can be used directly as a test sample. Alternatively, the test samples can be prepared by incubating fluorescent beads on poly-lysine coated cover glasses for 30 min, followed by sample assembly as described earlier.
2. Mount the sample onto the microscope stage, and bring into focus. Make sure the proper filters are in place, and then switch the emission path to the camera, and the excitation path for the lasers.

3. Configure the camera with moderate EM-gain settings according to the manufacturer's recommendation. Set the readout mode to the highest bit depth available. Set the exposure time to 50 ms for the frame rate of 20 frames per second in frame transfer mode.
4. Adjust the illumination lens until total internal reflection (TIR) condition is achieved. Adjust the laser intensity so that the fluorescent bead is not saturating the camera (relatively low power is needed for very bright fiducials). Locate an area with sufficient number of fiducials for imaging.
5. Collect a stream of images of between 1,000 and 10,000 frames, or longer if necessary. In cases where the microscope is not equipped with focus correction, it is recommended to monitor the focal drift and apply gentle and gradual manual adjustment as needed.
6. Perform localization analysis on the test data sets (see below). Evaluate and apply drift correction. The fiducials should be brought into registration with an uncertainty of <20 nm or so, such that the uncertainty in the drift correction is smaller than the uncertainty of fluorophore localization.
7. If the magnitude of the drift is larger than a few microns over the acquisition time scale, monitor temperature fluctuation as well as other mechanical disturbances, particularly the air circulation (many electronic equipment and computers contain fans which may inadvertently blow directly onto the microscope), and take remedial action as needed. Also, mechanical drifts tend to be greatest soon after sample mounting. Thus, a period of waiting may lessen the magnitude of the drift.

3.2 Imaging Cells Expressing PA-FP by Localization Microscopy

Upon ensuring the microscope is capable of stable operation, fixed cell samples can be imaged. Typically, higher excitation intensity is needed to visualize single molecule signals. However, too high intensity excitation could lead to saturation in the signal of the fluorescent fiducials, especially due to the limited dynamic range of the EMCCD camera. Thus, laser intensity must be carefully optimized to capture signals from both the labelled molecules and the fiducials without saturation.

1. Mount the sample, focus, and locate candidate cells for imaging by transmitted light or epifluorescence mode. In the case of photoconvertible proteins such as tdEos or mEos2, the cells can be located in the green fluorescence channel. Record images in the standard epifluorescence and/or transmitted light modes for reference.
2. Many PA-FPs are highly sensitive to photoactivation. Thus, it is recommended to prevent illumination by 405 nm prior to imaging.

3. Switch to TIRF mode and make sure that the desired imaging area contains multiple fiducials for the assessment and correction of drift.
4. For EosFP imaging, excite with the 561 nm laser and observe in the red emission channel. Adjust the laser intensity so that bright single molecules are observable. There should be sparse blinking of molecules that last for a few image frames.
5. Make sure that the 405 nm photoactivation line is strongly attenuated. Illuminate the sample with 405 nm, starting at the lowest intensity. A rapid increase of single molecule fluorescence in the red emission channel should be observed.
6. Adjust 561 and 405 nm intensity so that on balance, there are sparse but sufficiently large numbers of molecules appearing in each frame. Make sure that the fiducials are not saturated.
7. The intensity control of the 405 nm laser should be set up so that it can be controlled independently of the acquisition process. This is recommended since molecules are continually depleted during long acquisitions, and the 405 nm intensity needs to be increased progressively. Note that some models of 405 nm lasers (such as Coherent Cube) are supplied with a USB-based control software that can be used to adjust the laser intensity on-the-fly during the acquisition.
8. Once proper acquisition conditions are set, start the acquisition stream. An initial number of frames of 20,000 is suggested. For high quality images, obtain as many frames as practical (50,000 frames or more is not uncommon).
9. Transfer data to the image processing computer.

3.3 Processing and Analysis of Localization Microscopy Data Sets

Localization Microscopy requires intensive computation on a large volume of image data sets, with the results being a list of the coordinates for each single molecule. A typical raw image data set can range from 20,000 to 100,000 or more frames, depending on the labelling density and fluorophore blinking characteristics. Thus, the localization coordinates usually contain a few to several millions of molecular entries. These can be rendered to reconstruct a super-resolved image to be used in subsequent analyses in standard image processing software. Advanced applications and statistical analyses are also possible with the use of a programming language such as MATLAB but is beyond the scope of this protocol (for an example of advanced analysis, *see* ref. 39). The instructions below describe the processing and analysis of Localization Microscopy data using QuickPALM software, freely available as a plug-in in ImageJ.

1. Install QuickPALM plug-in in ImageJ (already included on FIJI distribution of ImageJ, www.fiji.sc).
2. Open single molecule time-series data in ImageJ (or FIJI). Make sure that the data have been saved with the full bit-depth, for example using 16-bit TIFF format.

3. Open the QuickPALM plug-ins (under Analyze/QuickPALM/Analyze Particles in FIJI).
4. Enter the three key parameters necessary for particle detection: minimum SNR (signal-to-noise ratio), maximum FWHM (full-width-half-maximum), and Image plane pixel size (nm).
5. Of these, SNR corresponds to the brightness of the fluorophores relative to the background (which is in turn proportional to the localization precision [24]). Only single molecules with SNR above the minimum threshold are accepted. Depending on the type of fluorophores, and experimental conditions, the minimum SNR can be adjusted for proper balance between sufficient density and rejection of noise (typical starting values of 4–10 can be used). Higher minimum SNR results in sparse detection, while lower SNR gives more localization points but also with increased spurious noise.
6. The image plane pixel size parameters can be calculated from the camera pixel size and the magnification of the microscope. As an example, for Andor Ixon-Ultra EMCCD camera, the camera pixel size is 16 μm. If a magnification of 150× is used (100× and 1.5× Optovar), the image plane pixel size is then: 16 μm/150 or 106.7 nm.
7. Since single molecules appear as diffraction limited spots, their ideal sizes can be estimated from the emission wavelength (λ) and the objective NA according to the formula: FWHM = 0.52λ/NA. For 600 nm emission and with a NA 1.49 objective, the ideal FWHM is ~205 nm or approximately 2 pixels (assuming an image plane pixel size of 106.7 nm). Thus, a maximum FWHM parameter of 4 pixels can be used as the initial value for rejecting peaks that appear too broad (this could arise when adjacent molecules are activated at the same time).
8. We recommend an iterative parameter refinement step using a subset of data, for example, just the first 100 frames, in order to arrive at the appropriate parameters in a reasonable amount of time. Subsequently, these parameters can be used to analyze the full datasets. Upon completion, the results of the analysis are shown in a Particle Table window.
9. To render a super-resolved image, make sure that the Particle Table window is open. Select "Reconstruct Dataset" option (under Analyze/QuickPALM in FIJI), select the appropriate pixel size for the rendered image (5–10 nm is useful as the starting point).
10. To assess and correct for sample drift, make ROI (Region-of-Interest) selections around selected fiducial regions in the rendered image, and add each ROI to the ROI manager window in ImageJ. Fiducials close to the image center are preferred as optical aberrations can be more pronounced near the edge.

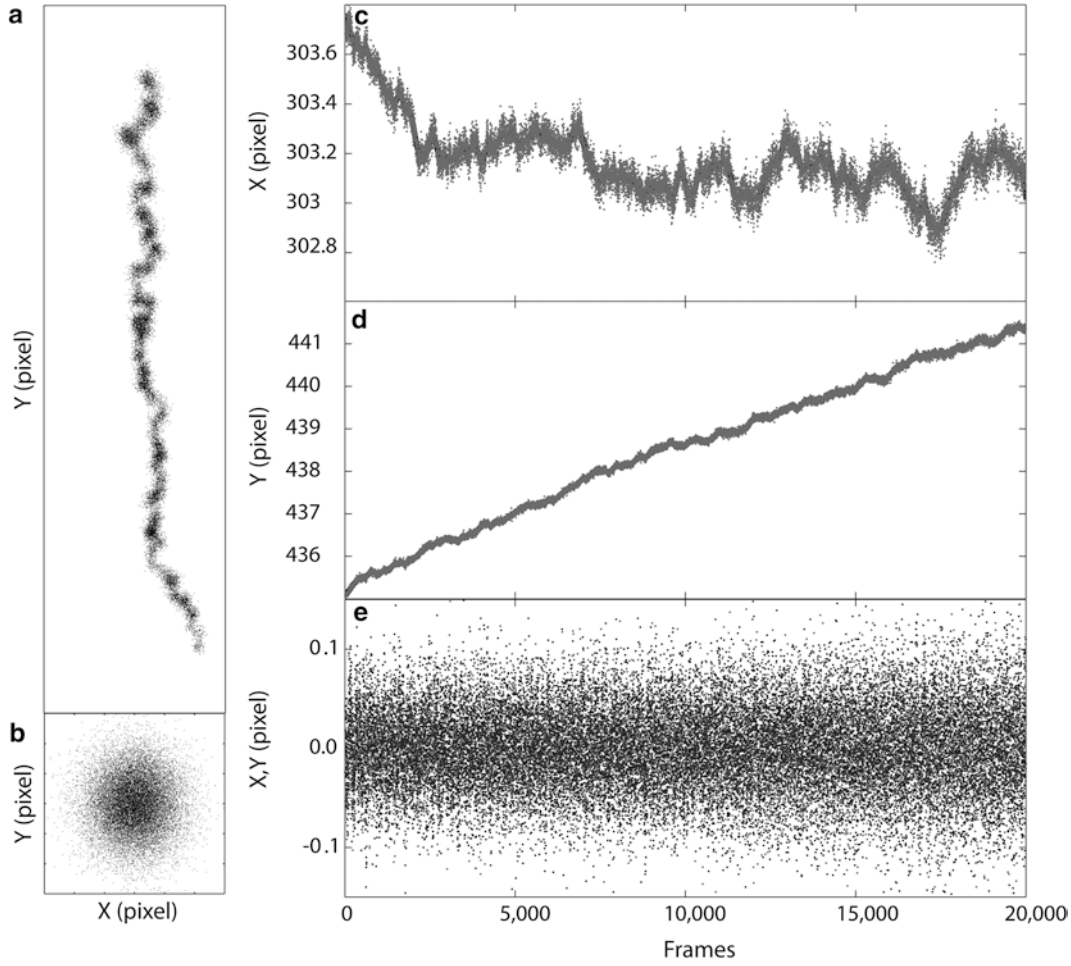

Fig. 4 Drift Correction by registration of fluorescent fiducial markers. The localized coordinate of fiducial (e.g., Fig. 2e) allows the measurement of mechanical drift of the sample during the acquisition period. An example of a rather high drift is shown for an acquisition of 20,000 frames (**a**, position of the fiducial; **c**, fluctuation of the *X* coordinate of the fiducial; **d**, fluctuation of the *Y* coordinate of the fiducial). The sample exhibits large drift along the Y-direction of more than 5 pixels or almost a micron. Such drift will smear the super-resolution image if not corrected for. Drift correction can be calculated by subtracting the moving averaged *X* and *Y* trajectories, resulting in a well-registered fiducial (**b**, using 200 frame moving average correction), and small residuals (**e**)

Subsequently, perform drift correction (Analyze/QuickPALM/Correct Particle Drift in FIJI). As shown in Fig. 4, typical drift can be more than several tens of nanometers.

11. The particle table will be updated with the drift-corrected coordinates and can be saved or exported for further analysis. Reconstruct a drift-corrected super-resolved image using the "Reconstruct Dataset" option as described earlier (*see* **Note 11**). The resulting super-resolved image reveals significant details within the FAs relative to the diffraction-limited image (Fig. 2c).

4 Notes

1. Localization Microscopy requires sufficiently high excitation intensity for single molecule imaging, and thus lasers are generally used as light sources. The wavelengths 405, 488, 561, and 640 nm are typically adequate for photoactivation and imaging of most fluorophores. Common manufacturers include Coherent, Spectra-Physics, MellesGriot, and Crystalaser. For convenience and versatility, a pre-aligned multi-laser fiber-coupled source can be used. These are typically available from the microscope manufacturer as part of the total internal reflection fluorescence (TIRF) or confocal system. The power output is typically attenuated by the fiber, however, which may result in longer exposure and acquisition times.
2. Since the acquisition of raw data sets takes at least several minutes, focal drift can be substantial and must be corrected for. Most manufacturers offer automatic focus tracking and correction options. These are based on the detection and tracking of infrared beams reflected off the cover glass surface. Among commercial options, hardware-based models such as the Perfect Focus System from Nikon (Melville, NY) or the CRISP add-on module from Applied Scientific Instrumentation (Eugene, OR) are the most suitable for Localization Microscopy, as it is fully independent of the acquisition software, allowing continuous maintenance of focus during PALM acquisition. Other designs that depend on image processing of the acquisition computer may be usable but will need further modification in the data acquisition control software.
3. An Acousto-Optic Tunable Filter (AOTF) allows the control of the intensity and the selection of the laser wavelengths. Note that since a typical AOTF has a limited spectral range (e.g., 450–700 nm for model AOTFnCVis from A-A Optoelectronic, Orsay, France), some laser lines outside of this range, such as 405 nm, may need to be modulated, expanded, and combined with the rest of the beams separately after the AOTF. Lasers from some manufacturers (e.g., from Crystalaser, or Cube and Obis models from Coherent) include the option of modulation by TTL pulse (0–5 V) or USB/Serial input, thus an AOTF is not required.
4. Since the localization precision depends on the brightness of the detected single molecule images, a high NA oil-immersion objective lens is advantageous due to its large light gathering cone. In particular for TIRF, an objective lens with NA > 1.45 is needed. The magnification of the objective lens must also be chosen to match the pixel size of the camera. For a 16 μm pixel, a 100× objective lens used in combination with either a 1× or 1.5× magnification changer lens is commonly used.

5. Since focal adhesions form via attachment to the extracellular matrix adhered to the cover glass, TIRF excitation is most suitable. This mode of illumination provides high signal to noise ratio, since the remainder of the cell beyond the evanescent field is not excited. Note, however, that certain structures linking up with the focal adhesions, such as actin stress fibers, could extend beyond the TIRF field. Localization Microscopy can also be applied in the wide-field or oblique illumination geometry, although the increased background will degrade the localization precision to some extent.
6. Altogether, dichroic mirror and emission filters are particularly important, as they serve to reject excitation light and permit the fluorescence emission to reach the camera. High quality multiband dichroic mirrors are available from several manufacturers such as Semrock and Chroma. This allows a single filter cube to be used for multichannel imaging. The dichroic spectral profile should be compared against the laser lines used, as well as the emission spectra of the fluorophores. Another important consideration is the flatness of the dichroic. Depending on how it is mounted, the dichroic could be slightly warped, resulting in unintended astigmatism in the excitation light. For emission filters, if a peripheral emission filter wheel is available, it may be more advantageous to mount only the dichroic in the cube, and place single band emission filters in the filter wheel. A single band filter is generally more economical and better matched to the spectral profile of the fluorophore emission. However, if the emission filter wheel is not available, a multiple band-pass emission filter can be mounted in the filter cube. In this case, users should be aware of the possibility for fluorophore cross-talk. Examples of the filters we use are (all from Semrock, Rochester, NY): green, FF01-525/50-25; red, FF01-609/57-25; far-red, FF01-676/37-25; dichroic mirror, Di01-R405/488/561/635-25×36; Laser Combiners, LM01-503-25, LM0-427-25, and LM01-613-25.
7. A common hardware for detecting single molecule fluorescence is the electron-multiplying charge coupled device (EMCCD) camera. Models with a back-illuminated sensor (such as the Ixon-Ultra model from Andor or the Evolve model from Photometrics) are capable of peak quantum efficiency of >90 %. Before further processing, the signal readouts from the camera should be converted into the unit of detected photons, using the appropriate calibration factors. The possible value of a 16-bit pixel is between 0 and 65,535. However, the actual signal is offset from zero by a certain amount (such as 200–1,000), depending on the manufacturer. Likewise, the digital value of the pixel is related to the actual photoelectron by a multiplication factor. A number of methods have been published for the calibration of the offset and conversion factor [40].

8. Because Localization Microscopy outputs large data sets, a computer with a sufficiently large memory bank and storage is recommended. As an example, at a typical frame rate of 20 frames per second, 15 min of acquisition yields 12,000 frames, or more than 6 GB of file size. For ease of configuration and future expansion, 64-bit Windows OS is recommended. The computer used for microscope control should also have sufficient peripheral ports to control camera, AOTF, and laser firing, during the acquisition. This computer should be dedicated for acquisition with a minimum of other software installed, and should have a sufficient amount of memory (4 GB or more) and a sufficiently large hard disk (>1 TB). For rapid boot-up and read/write rate, a solid state hard drive is recommended. The computer should also be connected to the local area network for ease of data transfer.
9. The cover glasses are first cleaned in ddH_2O, followed by 10 min heating in 1:1:5 mixture of NH_4OH, H_2O_2, and ddH_2O at 80 °C. Subsequently, the cover glasses are immersed briefly in 2 % hydrofluoric acid solution (1:50 HF in ddH_2O) at room temperature, followed by heating in a 1:1:6 mixture of HCl, H_2O_2, and ddH_2O at 80 °C for 15 min. Finally, the cover glasses are rinsed in ddH_2O and blown dry with nitrogen gas. Due to the highly corrosive nature of the chemicals used, these steps must be performed in a chemical fume hood. Appropriate safety precaution must also be strictly followed.
10. We recommend that researchers pay particular attention to the design of PA-FP fusion constructs. Many FA proteins are multidomain and the function of different parts of the proteins should be taken into consideration when designing the probe, since the location (i.e., amino (N) versus carboxy (C) terminus) of the PA-FP probe can have a strong effect on whether the fusion will localize properly and be functional, or not. Also, in addition to physiological expression levels, in certain cases co-expression of binding partners may be important for proper localization. As an example, integrin is a heterodimeric transmembrane protein. In our experience, we obtain good results by conjugating the PA-FP probe to the C-terminal cytoplasmic tail of the α subunit. We found that N-terminal PA-FP position is problematic since this region contains signal sequence for membrane insertion and transport. Also, we chose the α subunit for tagging since the cytoplasmic tail of the β subunit is well documented to participate in many essential binding interactions, whereas much fewer binding partners have been identified for the α tail. Finally, since αβ heterodimerization is required for export to the plasma membrane, we found that co-transfection with untagged β integrin is often required for proper localization in many cell types—without which a significant fraction of integrin appears to remain in the endoplasmic reticulum.

11. Because Localization Microscopy data sets essentially are comprised of a list of molecular positions, instead of conventional images, region analysis is not straightforward. To apply conventional image analysis techniques, the super-resolved image should be reconstructed first. Alternatively, advanced users may choose to develop custom programs for analyzing molecular positions data. For instance, to selectively analyze a region of interest such as the FAs, an image map of the dataset can be created from the rendered image, and thresholded to create a binary mask corresponding to FA regions. From the binary mask, morphological properties of the region such as area, aspect ratio, and ellipticity can be calculated. Molecular coordinates that belong to FAs (i.e., fall within the mask region) can then be selected, for example by using the command "ismember" in MATLAB to compare the molecule list against the coordinates of the mask regions.

Acknowledgments

PK is supported by the Singapore National Research Foundation under the NRF Fellowship (NRFF-2011-04). CMW is supported by the Division of Intramural Research, National Heart, Lung, and Blood Institute, National Institutes of Health. We thank Harald Hess and Gleb Shtengel (Howard Hughes Medical Institute, Janelia Farm Research Campus), and Michael Davidson (The Florida State University) for advice, equipment, reagents, and collaboration related to this work.

References

1. Patterson G, Davidson M, Manley S, Lippincott-Schwartz J (2010) Superresolution imaging using single-molecule localization. Annu Rev Phys Chem 61:345–367
2. Galbraith CG, Galbraith JA (2011) Super-resolution microscopy at a glance. J Cell Sci 124:1607–1611
3. Fernández-Suárez M, Ting AY (2008) Fluorescent probes for super-resolution imaging in living cells. Nat Rev Mol Cell Biol 9:929–943
4. Heintzmann R, Gustafsson MGL (2009) Subdiffraction resolution in continuous samples. Nat Photonics 3:362–364
5. Huang B, Bates M, Zhuang (2009) Super-resolution fluorescence microscopy. Annu Rev Biochem 78:993–1016
6. Willig KI, Rizzoli SO, Westphal V, Jahn R, Hell SW (2006) STED microscopy reveals that synaptotagmin remains clustered after synaptic vesicle exocytosis. Nature 440:935–939
7. Klar TA, Jakobs S, Dyba M, Egner A, Hell SW (2000) Fluorescence microscopy with diffraction resolution barrier broken by stimulated emission. Proc Natl Acad Sci USA 97: 8206–8210
8. Gustafsson MG (2000) Surpassing the lateral resolution limit by a factor of two using structured illumination microscopy. J Microsc 198:82–87
9. Betzig E, Patterson GH, Sougrat R et al (2006) Imaging intracellular fluorescent proteins at nanometer resolution. Science 313: 1642–1645
10. Hess ST, Girirajan TP, Mason MD (2006) Ultra-high resolution imaging by fluorescence photoactivation localization microscopy. Biophys J 91:4258–4272
11. Rust MJ, Bates M, Zhuang X (2006) Sub-diffraction-limit imaging by stochastic optical reconstruction microscopy (STORM). Nat Methods 3:793–795

12. Fölling J, Bossi M, Bock H et al (2008) Fluorescence nanoscopy by ground-state depletion and single-molecule return. Nat Methods 5:943–945
13. Shtengel G, Galbraith JA, Galbraith CG et al (2009) Interferometric fluorescent super-resolution microscopy resolves 3D cellular ultrastructure. Proc Natl Acad Sci USA 106:3125–3130
14. Shroff H, Galbraith CG, Galbraith JA, Betzig E (2008) Live-cell photoactivated localization microscopy of nanoscale adhesion dynamics. Nat Methods 5:417–423
15. Shroff H, Galbraith CG, Galbraith JA et al (2007) Dual-color superresolution imaging of genetically expressed probes within individual adhesion complexes. Proc Natl Acad Sci USA 104:20308–20313
16. Kanchanawong P, Shtengel G, Pasapera AM et al (2010) Nanoscale architecture of integrin-based cell adhesions. Nature 468:580–584
17. Dickson RM, Cubitt AB, Tsien RY, Moerner WE (1997) On/off blinking and switching behaviour of single molecules of green fluorescent protein. Nature 388:355–358
18. Levitus M, Ranjit S (2011) Cyanine dyes in biophysical research: the photophysics of polymethine fluorescent dyes in biomolecular environments. Q Rev Biophys 44:123–151
19. Moerner WE (2007) New directions in single-molecule imaging and analysis. Proc Natl Acad Sci USA 104:12596–12602
20. Shannon C (1949) Communication in the presence of noise. Proc IRE 37:10–21
21. Patterson GH, Lippincott-Schwartz J (2002) A photoactivatable GFP for selective photolabeling of proteins and cells. Science 297: 1873–1877
22. Subach FV, Patterson GH, Manley S, Gillette JM, Lippincott-Schwartz J, Verkhusha VV (2009) Photoactivatable mCherry for high-resolution two-color fluorescence microscopy. Nat Methods 6:153–159
23. Lippincott-Schwartz J, Patterson GH (2009) Photoactivatable fluorescent proteins for diffraction-limited and super-resolution imaging. Trends Cell Biol 19:555–565
24. Thompson RE, Larson DR, Webb WW (2002) Precise nanometer localization analysis for individual fluorescent probes. Biophys J 82:2775–2783
25. Mortensen KI, Churchman LS, Spudich JA, Flyvbjerg H (2010) Optimized localization analysis for single-molecule tracking and super-resolution microscopy. Nat Methods 7: 377–381
26. Dempsey GT, Vaughan JC, Chen KH, Bates M, Zhuang X (2011) Evaluation of fluorophores for optimal performance in localization-based super-resolution imaging. Nat Methods 8:1027–1036
27. Vogelsang J, Kasper R, Steinhauer C et al (2008) A reducing and oxidizing system minimizes photobleaching and blinking of fluorescent dyes. Angew Chem Int Ed Engl 47: 5465–5469
28. Aitken CE, Marshall RA, Puglisi JD (2008) An oxygen scavenging system for improvement of dye stability in single-molecule fluorescence experiments. Biophys J 94:1826–1835
29. Henriques R, Lelek M, Fornasiero EF, Valtorta F, Zimmer C, Mhlanga MM (2010) QuickPALM: 3D real-time photoactivation nanoscopy image processing in ImageJ. Nat Methods 7:339–340
30. Wolter S, Endesfelder U, van de Linde S, Heilemann M, Sauer M (2011) Measuring localization performance of super-resolution algorithms on very active samples. Opt Express 19:7020–7033
31. Schindelin J, Arganda-Carreras I, Frise E et al (2012) Fiji: an open-source platform for biological-image analysis. Nat Methods 9:676–682
32. Miller JC, Tan S, Qiao G et al (2011) A TALE nuclease architecture for efficient genome editing. Nat Biotechnol 29:143–148
33. Ando R, Mizuno H, Miyawaki A (2004) Regulated fast nucleocytoplasmic shuttling observed by reversible protein highlighting. Science 306:1370–1373
34. Wiedenmann J, Ivanchenko S, Oswald F et al (2004) EosFP, a fluorescent marker protein with UV-inducible green-to-red fluorescence conversion. Proc Natl Acad Sci USA 101: 15905–15910
35. Gurskaya NG, Verkhusha VV, Shcheglov AS et al (2006) Engineering of a monomeric green-to-red photoactivatable fluorescent protein induced by blue light. Nat Biotechnol 24:461–465
36. Huang B, Wang W, Bates M, Zhuang X (2008) Three-dimensional super-resolution imaging by stochastic optical reconstruction microscopy. Science 319:810–813
37. Edelstein A, Amodaj N, Hoover K, Vale R, Stuurman N (2010) Computer control of microscopes using microManager. Curr Protoc Mol Biol 14:14.20.1–14.20.17
38. McKinney SA, Murphy CS, Hazelwood KL, Davidson MW, Looger LL (2009) A bright and photostable photoconvertible fluorescent protein. Nat Methods 6:131–133
39. Sengupta P, Jovanovic-Talisman T, Skoko D, Renz M, Veatch SL, Lippincott-Schwartz J (2011) Probing protein heterogeneity in the plasma membrane using PALM and pair correlation analysis. Nat Methods 8:969–975
40. Murray JM, Appleton PL, Swedlow JR, Waters JC (2007) Evaluating performance in three-dimensional fluorescence microscopy. J Microsc 228:390–405

Chapter 5

Use of Microarray Analysis to Investigate EMT Gene Signatures

Andrew H. Sims, Alexey A. Larionov, David J. Harrison, and Elad Katz

Abstract

The epithelial-to-mesenchymal transition (EMT) is a widely studied program of development of cells characterized by loss of cell adhesion, repression of E-cadherin expression, and increased cell mobility. Microarrays have become a well-established technique for simultaneously measuring the expression of thousands of transcripts encoded by the genome. In this chapter, we demonstrate how microarray analysis can be used to assess the role of EMT-genes associated with a collagen invading phenotype by generating a gene expression signature and relating this to cell line and tumor datasets from published microarray studies.

Key words Epithelium, Mesenchyme, Microarrays, Gene expression signature, Transcriptomic profiles

1 Introduction

The epithelial-to-mesenchymal transition (EMT) is a developmental program in which epithelial cells down-regulate their cell–cell junctions, acquire spindle cell morphology, and exhibit cellular motility [1]. In human breast cancer, invasion into surrounding tissue is the first step in metastatic progression. The transformation of normal breast epithelial cells to metastatic cancer is the result of multiple epigenetic and genetic changes, leading to deregulated interactions with the microenvironment [2]. During this process, the cells ability to inhibit proliferation, cell survival, migration, and differentiation is lost, leading to the acquisition of an invasive phenotype. The ability to breach the basement membrane (BM) is a critical event in cancer progression and a prerequisite for metastasis. Having breached the BM, cells may then enter the lymphatic system, spread, and attempt to establish themselves as distant tumor foci [3].

Amanda S. Coutts (ed.), *Adhesion Protein Protocols*, Methods in Molecular Biology, vol. 1046,
DOI 10.1007/978-1-62703-538-5_5,

The trans-differentiation of cells from an epithelial to a mesenchymal phenotype is an essential part of normal embryogenesis and development [4]. Increasing evidence also supports a role for EMT in the progression of many cancer types including breast, with critical roles in invasion and metastatic dissemination [5, 6]. EMT involves loss of cell–cell junctions and reorganization of the actin cytoskeleton, resulting in loss of apical–basal polarity and acquisition of a spindle-like mesenchymal morphology [7]. At the same time, there is also decreased expression of epithelial-specific proteins, including E-cadherin, which may account at least in part for the altered properties of migrating tumor cells [8, 9]. An important event in EMT is switching in expression from E-cadherin to N-cadherin [10], in most cases this is associated with transcriptional repression of E-cadherin [9]. Several specific repressor factors have been identified including Snail, Slug, Zeb1, Zeb2 and Twist [11], all of which are zinc finger containing proteins that can bind with so called E-boxes within the *CDH1* (E-cadherin) gene promoter. N-cadherin is believed to promote cellular invasion by binding to and enhancing signalling by growth factors and is overexpressed in many invasive and metastatic human breast cancer cell lines and tumors [10, 12, 13].

Microarray analysis of mouse mammary carcinoma models and human breast tumors together identified a novel human molecular subtype of breast cancer, termed "claudin-low" [14]. These tumors are characterized by a lack of luminal differentiation markers, a high enrichment for EMT markers, immune response genes and cancer stem cell-like features [15–17]. These moderate-high grade invasive ductal carcinomas are morphologically distinct from lobular carcinomas despite their low expression of E-cadherin [14].

In this chapter, we describe how a gene expression signature can be derived from transformed cells with an EMT phenotype and consider approaches to compare microarray data generated with that of previous studies and illustrate how published microarray datasets can be mined to investigate the expression patterns of genes of interest.

2 Materials

2.1 Culture Materials in Studying Invasion in Three Dimensions (3D)

The methods described in this chapter draw on our experience of studying the MIEN1 (C35, C17orf37) protein [1, 18], but this approach could easily be adapted to the study of other genes that are potentially involved with EMT and their relevance to breast cancer subtypes. We have recently used a similar approach to studying the collective invasion of cancers with intact human tumor material, thereby using these experimental methods to more accurately replicate the in vivo processes of cancer growth and enable us to assess the efficacy of existing and novel treatments [19, 20].

Materials from experiments using the above approaches and other 3D culture formats (e.g., basement membrane extract-based cultures) can be used as a starting point to study EMT.

2.2 RNA Extraction, Labelling, and Hybridization

1. Take 50–100 mg of cell-containing gel to a weight-boat, cut to approximately 1 mm^3 pieces.
2. Homogenize in 1.5 mL RLT buffer (component of Qiagen RNEasy kit) using TissueRuptor (Qiagen), for 30 s on maximum speed, spin down debris by a brief centrifugation on a benchtop microcentrifuge at max speed for 3 min at room temperature.
3. Collect 1.5 mL of supernatant and complete RNA extraction according to the RNEasy kit manual, elute RNA in 30 μL of RNAse-free water, check the quality and quantity of RNA using Agilent 2100 BioAnalyser and NanoDrop spectrophotometer.
4. The RNA amplification and labelling method will depend upon the microarray platform to be used. In this example, the Illumina TotalPrep RNA Amplification Kit was used according to the kit manual.
5. Hybridization to microarrays and scanning is best performed by the dedicated personnel of a local microarray core facility or company, following the manufacturer's protocols.

2.3 Installation of R and BioConductor Packages for Analysis of the Microarray Data

1. Download R from the Website http://www.r-project.org/.
2. The core BioConductor packages (www.bioconductor.org/) can be installed by typing or copying and pasting the following text into the R command window.

```
source("http://bioconductor.org/biocLite.R")
biocLite()
```

specific packages, e.g., siggenes is installed with:

```
biocLite("siggenes")
```

2.4 Public Microarray Data Repositories and Annotation/ Visualization Resources

1. ArrayExpress (http://www.ebi.ac.uk/arrayexpress/) [21].
2. NCBI GEO (http://www.ncbi.nlm.nih.gov/geo/) [22].
3. caArray (https://array.nci.nih.gov/caarray/home.action).
4. University of North Carolina Microarray Database (https://genome.unc.edu/).
5. The Database for Annotation, Visualization, and Integrated Discovery (DAVID [23] http://david.abcc.ncifcrf.gov/) is a useful collection of tools to explore generated gene lists from high throughput analysis and to convert gene or protein identifiers and accession numbers.
6. Cluster and TreeView (http://rana.lbl.gov/EisenSoftware.htm), for generating heatmaps.

3 Methods

Preprocessing and analysis of microarrays is now routinely performed within the statistical programming environment "R." R is a freely available software program for statistics and graphics which runs on UNIX, Windows and MacOS platforms. BioConductor [24] is an open source community initiative to provide tools for the analysis and comprehension of high-throughput genomic data. Specific *packages* written and maintained by bioinformaticians enable complex analysis methods to be employed by simple commands that are explained in each accompanying *vignette* giving detailed easy to follow, specific instructions (*see* **Note 1**). What follows is a typical example with the Illumina Beadchip data, the required R commands are given in the alternative font.

3.1 Generate an EMT Gene List/Signature Based Upon the Recombinant and Parental Microarray Data

1. Grow cells with EMT and control phenotypes.
2. Extract RNA, label, hybridize, and scan microarrays to obtain raw data.

3.1.1 Derive Data by Growing Cells, Extracting RNA, and Hybridizing to Microarrays

3.1.2 Acquire and Preprocess the Data

1. Open the appropriate BioConductor package in R and read in the data (*see* **Note 2**), in this case "*lumi*"

```
library(lumi)
raw.data = lumiR("SampleProbeProfile.txt",
convertNuID = FALSE)
```

2. Examine the raw data in a variety of plots. Quality assessment of microarray data is necessary to identify poor-quality arrays and check for systematic biases. Boxplots and distributions for each sample should be compared to assess if there are any clearly unusual results or potential outliers. Samples with noticeably different dynamic ranges, reduced signal levels, or low numbers of detected probes may reflect poor hybridization.

```
plot(raw.data, what = 'boxplot')
plot(raw.data, what = 'density')
plot(raw.data, what = 'MAplot')
```

3. Normalize the data; by default the quantile method is used. "Robust spline", "Rank Invariant", "Variance stabilising", "Lowess" (locally weighted scatterplot smoothing) and "simple scaling" normalization are alternatives.

```
data.N = lumiN(raw.data)
```

4. Examine summary quality control information and plot as before to compare with raw data.

```
data.N.Q = lumiQ(data.N)
summary(data.N.Q, 'QC')
```

```
plot(data.N.Q, what='boxplot')
plot(data.N.Q, what='density')
plot(data.N.Q, what='MAplot')
```

5. The expression values are held in the exprs slot of the normalised data object.

```
dataMatrix=exprs(lumi.N.Q)
```

3.1.3 Identify Genes Differentially Expressed Between the Recombinant and Parental Samples

1. Open the analysis package (*see* **Note 3**), e.g., Significance analysis of microarrays (SAM) [25].

```
library(siggenes)
```

2. Assign binary classes to the triplicate recombinant (1) and parental cells (0) in the column order or the data matrix created. For paired analysis use positive/negative values (1,2,3… and –1,–2,–3…).

```
class=c(1,1,1,0,0,0)
```

3. Perform the analysis and generate a summary of the numbers of differentially expressed genes for a given false discovery rate (fdr) at a particular threshold of "delta," the distance between the observed and the expected (ordered) test scores.

```
sam.out=sam(dataMatrix, class, rand=123,
gene.names=rownames(dataMatrix))
summary(sam.out)
plot(sam.out)
```

4. Choose an appropriate number of genes or false discovery rate as the cut-off.

```
findDelta(sam.out, genes=500) list.siggenes
(sam.out, 3.3)
findDelta(sam.out, fdr=0.05)
```

5. Get a list of the genes meeting the criteria (e.g., where delta = 3.3).

```
list.siggenes(sam.out, 3.3)
```

3.2 Uncover the Functions of Genes or Pathways That are Overrepresented by the Signature

1. Go to the homepage of the Database for Annotation, Visualization, and Integrated Discovery (DAVID [23] http://david.abcc.ncifcrf.gov/), click on "start analysis" and "upload" by copying and pasting a list of gene symbols, microarray probe names or database accession numbers (*see* **Note 4**).
2. After successfully submitting, choose one of the analysis tools, such as functional annotation to identify terms (e.g., Gene Ontology) or pathways (e.g., KEGG pathways) which are significantly associated with your gene list.
3. DAVID can also be used to convert Gene IDs; e.g., copy and paste in a list of microarray probe names and click the options to get the corresponding list of gene symbols or particular database accession numbers.

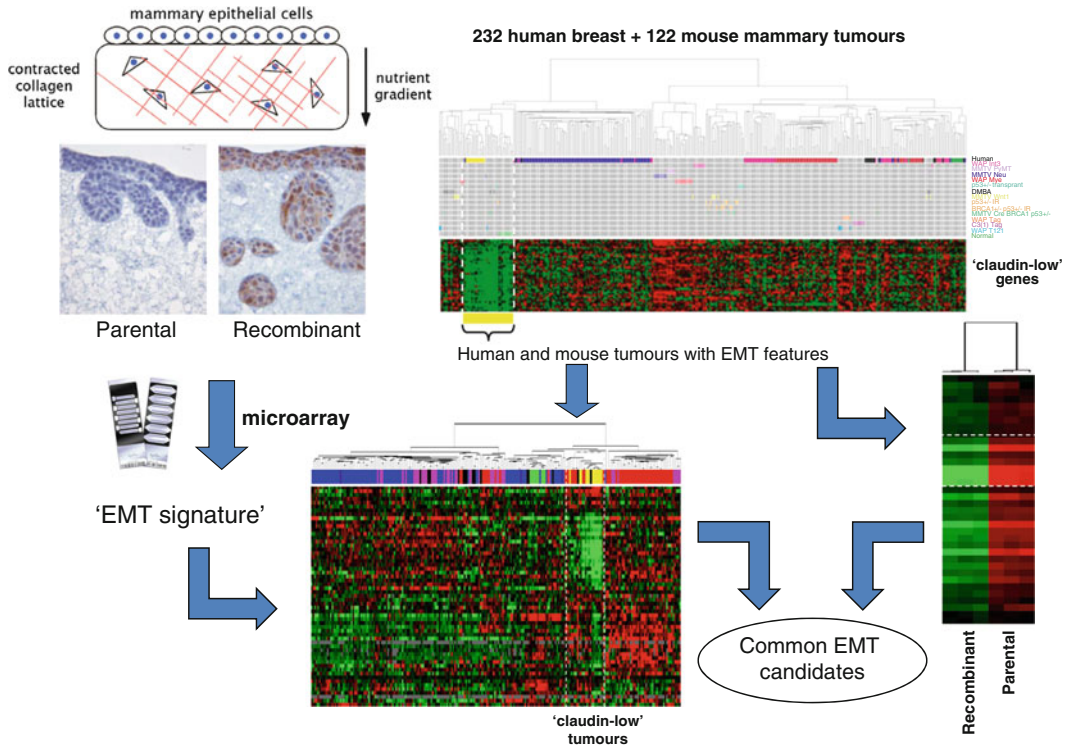

Fig. 1 Comparison of genes correlating with an EMT signature and those identifying the claudin-low breast cancer phenotype. The 100 Illumina probes most significantly differentially expressed using SAM analysis [25] between collagen-invading (recombinant MIEN1) and parental cells represented 57 genes that were able to cluster together the claudin-low tumors identified by Herschkowitz et al. [14] (*left panels*). A complementary approach found that the set of 34 claudin-low genes from the Herschkowitz et al. [14] study were all significantly down-regulated in the collagen-invading (MIEN1-expressing) cells compared to parental cells (*right panels*). A common signature of EMT-related genes is shared between the collagen-invading and claudin-low gene lists

3.3 Comparing Your Own Gene Expression Signature with that of a Previously Published Approach

1. Download data from a public microarray data repository (NCBI GEO or ArrayExpress, *see* Subheading 2.4) or in this example from a particular institution Website (murine mammary carcinomas and human breast tumors [14], University of North Carolina Microarray Database https://genome.unc.edu/).
2. Extract the data for the genes of interest you have identified in your own study from the downloaded file. Preprocessed data files are normally available (*see* **Note 5**). It may be necessary to convert the Gene IDs used in the published study to those of your own study (*see* notes above on DAVID in Subheading 3.2).
3. An alternative or complementary approach is to assess whether the genes identified in the published study are significantly up- or down-regulated between the recombinant and wild type cells (Fig. 1). In our example, nine genes (*CDH1*, *CLDN7*,

CRB3, *KRT8*, *TACSTD1*, *IRF6*, *SPINT2*, *MAL2*, and *MARVELD3*) were common between the "MIEN1 signature genes" and "claudin-low genes" signatures (Fig. 1).

3.4 Examining Expression of EMT-Related Genes in Published Cell Line and Tumor Microarray Datasets

1. Download raw Affymetrix U133A/plus 2 .cel files from appropriate primary breast tumor or cell line gene expression datasets from NCBI GEO, ArrayExpress or the caBIG repositories (*see* **Note 6**). In this example 17 tumor (GSE12276, GSE21653, GSE3744, GSE5460, GSE2109, GSE1561, GSE17907, GSE2990, GSE7390, GSE11121, GSE16716, GSE2034, GSE1456, GSE6532, GSE3494, geral-00143) and 3 cell line datasets Affymetrix U133A/plus 2 (GSE10890, GSE12777, E-TABM-194) were utilized.
2. Summarize the expression values of each dataset separately using the Ensembl alternative CDF [26] to generate single expression values for each gene and normalize the data with RMA [27] using R and BioConductor packages [24].

```
library(affy)
library(hgu133ahsensgcdf)
raw.data=ReadAffy(cdfname="hgu133ahsensgcdf")
normalised.dataset1=rma(raw.data)
```

3. Integrate the normalised expression values using the ComBat [28] script to remove dataset-specific bias as described previously [29, 30]. The inputs are a combined text file of all the normalised expression values for the datasets together and a sample information file. The first column of the sample information column must contain the names of the samples (exactly as in the normalised expression file), subsequent columns give the "batch" (dataset) number and any covariates. The batch column must be named "Batch". The output is an Excel file or an R data frame with batch-corrected values.

```
source('ComBat.R')
normalised.combat.data=ComBat("normalised.
txt", "sample.info.txt", skip=1)
```

4. Assign the intrinsic molecular subtypes using the highest correlation to the Prat et al. centroids [17] to each dataset separately.
5. Identify the 500 genes with the greatest variance across the integrated, batch corrected dataset.

```
variance=apply(normalised.combat.data,
1, var)
sorted.variance=sort(variance)
v500=sorted.variance[54176:54675]
write.table(normalised.data[names(v500),],
"NCdataV500.txt", sep="\t", quote=F)
```

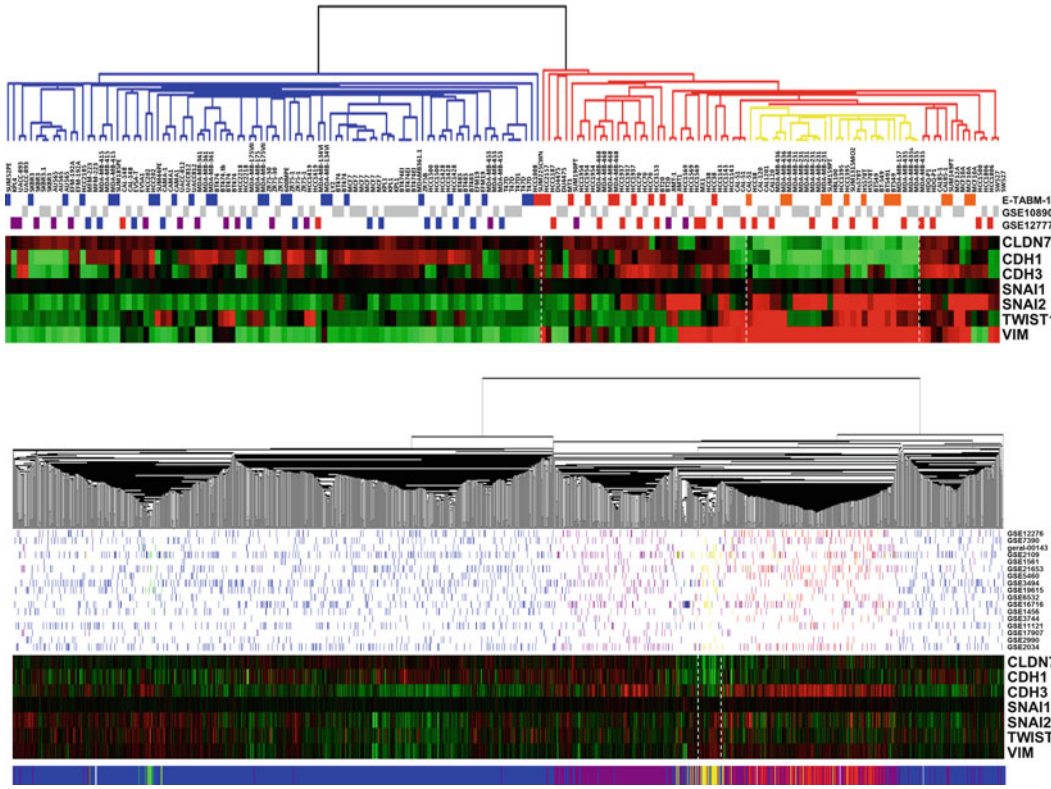

Fig. 2 Expression of EMT markers in integrated breast cancer cell line and primary tumor datasets. *Top*: Gene expression analysis data from three combined Affymetrix datasets using unsupervised clustering (average linkage, centered correlation) of the 500 most variable genes. The *lines* under the cell line names indicate the dataset from which each sample came and the *colors* indicate the type assigned in the original study (*Red* = Basal/Basal A, *Orange* = Basal B, *Purple* = HER2 amplified, *Blue* = Luminal). *Bottom*: Gene expression analysis data from 17 integrated Affymetrix datasets of primary breast tumors ($n = 2{,}999$) using unsupervised hierarchical clustering (average linkage, centered correlation) of the 500 most variable genes. The *lines* under the tree indicate the dataset (shown on *right*) from which each sample came and the *colors* indicate the intrinsic subtype assigned by highest correlation to the Prat et al. [17] centroids (*Red* = Basal, *Purple* = HER2, *Blue* = Luminal, *Green* = Normal-like, *Yellow* = Claudin-low)

6. Using the Cluster [31] program, read in the text file generated above and click to mean-center and cluster the data. The .cdt file output can be opened with the TreeView program, where the data can be visualized as a heatmap (Fig. 2).
7. Extract the genes of interest (such as those identified above or classic/possible markers of EMT) from the integrated datasets using the Ensembl gene accession numbers.

   ```
   GoI=normalised.combat.data[c("ENSG00000039068",
   "ENSG00000124216"),]
   ```

8. The assigned subtypes can be reconciled with the output of the clustering by using the ordering of the samples within the .cdt file.

4 Notes

1. The package used for preprocessing will depend upon the type of arrays used, a*ffy* [32] for Affymetrix GeneChips, *limma* [33] for Agilent arrays and *BeadArray* [34] or *lumi* [35] for Illumina BeadChips. It is recommended that users read the appropriate *vignette* (instruction manual) for each BioConductor package.
2. Identifying differentially expressed genes from microarray data is inherently challenging particularly with small numbers of samples and issues of multiple testing must be considered in order to minimize false positives [36]. In this example, the Significance Analysis of Microarrays (SAM) [25] method is implemented within the siggenes package. Alternatives include Rank Products analysis, *Rankprod* [37] or *limma* [33].
3. There are many similar, widely used alternative tools to DAVID including, but not limited to, GoMiner [38] and Gene Set Enrichment Analysis [39].
4. The association between EMT and the claudin-low breast cancer subtype is now well established [14, 17, 40]. However, many EMT signatures are possible and induction of EMT may result from a combination of factors, resulting in repression of common downstream molecules. From a functional point of view, this is consistent with loss of cell–cell contact as a prerequisite for the detachment of invading cells from the tumor mass and their penetration of surrounding stroma [41].
5. It is important to carefully consider whether it is appropriate to compare microarray signatures derived from functional experiments with those generated from primary clinical materials. Similarly, although batch-correction methods are effective at removing dataset-specific bias, it has been shown that combining datasets with significantly different compositions can lead to misleading results [29, 42].
6. Unsupervised clustering of the 500 most variable genes across the three integrated cell line datasets clearly identifies a subgroup of cell lines with an expression pattern consistent with an EMT phenotype or might be considered to represent "claudin-low" tumors (highlighted in yellow). Similarly, unsupervised clustering of the integrated primary tumor dataset suggested that there was a relatively small, but distinct subgroup of tumors with EMT features representing approximately 3 % of primary invasive breast cancer of no special type.

Acknowledgments

This work was supported by Breakthrough Breast Cancer and the Scottish Funding Council.

References

1. Katz E, Dubois-Marshall S, Sims AH, Gautier P, Caldwell H, Meehan RR, Harrison DJ (2011) An in vitro model that recapitulates the Epithelial to Mesenchymal Transition (EMT) in human breast cancer. PLoS One 6:e17083
2. Arendt LM, Rudnick JA, Keller PJ, Kuperwasser C (2010) Stroma in breast development and disease. Semin Cell Dev Biol 21:11–18
3. Weigelt B, Peterse JL, van't Veer LJ (2005) Breast cancer metastasis: markers and models. Nat Rev Cancer 5:591–602
4. Thiery JP (2003) Epithelial-mesenchymal transitions in development and pathologies. Curr Opin Cell Biol 15:740–746
5. Thiery JP, Sleeman JP (2006) Complex networks orchestrate epithelial-mesenchymal transitions. Nat Rev Mol Cell Biol 7:131–142
6. Polyak K, Weinberg RA (2009) Transitions between epithelial and mesenchymal states: acquisition of malignant and stem cell traits. Nat Rev Cancer 9:265–273
7. Huber MA, Kraut N, Beug H (2005) Molecular requirements for epithelial-mesenchymal transition during tumor progression. Curr Opin Cell Biol 17:548–558
8. Gupta PB, Onder TT, Jiang G, Tao K, Kuperwasser C, Weinberg RA, Lander ES (2009) Identification of selective inhibitors of cancer stem cells by high-throughput screening. Cell 138:645–659
9. Schmalhofer O, Brabletz S, Brabletz T (2009) E-cadherin, beta-catenin, and ZEB1 in malignant progression of cancer. Cancer Metastasis Rev 28:151–166
10. Hazan RB, Qiao R, Keren R, Badano I, Suyama K (2004) Cadherin switch in tumor progression. Ann N Y Acad Sci 1014: 155–163
11. Peinado H, Olmeda D, Cano A (2007) Snail, Zeb and bHLH factors in tumour progression: an alliance against the epithelial phenotype? Nat Rev Cancer 7:415–428
12. Hazan RB, Phillips GR, Qiao RF, Norton L, Aaronson SA (2000) Exogenous expression of N-cadherin in breast cancer cells induces cell migration, invasion, and metastasis. J Cell Biol 148:779–790
13. Nieman MT, Prudoff RS, Johnson KR, Wheelock MJ (1999) N-cadherin promotes motility in human breast cancer cells regardless of their E-cadherin expression. J Cell Biol 147:631–644
14. Herschkowitz JI, Simin K, Weigman VJ, Mikaelian I, Usary J, Hu Z, Rasmussen KE, Jones LP et al (2007) Identification of conserved gene expression features between murine mammary carcinoma models and human breast tumors. Genome Biol 8:R76
15. Creighton CJ, Li X, Landis M, Dixon JM, Neumeister VM, Sjolund A, Rimm DL, Wong H et al (2009) Residual breast cancers after conventional therapy display mesenchymal as well as tumor-initiating features. Proc Natl Acad Sci USA 106:13820–13825
16. Hennessy BT, Gonzalez-Angulo AM, Stemke-Hale K, Gilcrease MZ, Krishnamurthy S, Lee JS, Fridlyand J, Sahin A et al (2009) Characterization of a naturally occurring breast cancer subset enriched in epithelial-to-mesenchymal transition and stem cell characteristics. Cancer Res 69:4116–4124
17. Prat A, Parker JS, Karginova O, Fan C, Livasy C, Herschkowitz JI, He X, Perou CM (2010) Phenotypic and molecular characterization of the claudin-low intrinsic subtype of breast cancer. Breast Cancer Res 12:R68
18. Katz E, Dubois-Marshall S, Sims AH, Faratian D, Li J, Smith ES, Quinn JA, Edward M et al (2010) A gene on the HER2 amplicon, C35, is an oncogene in breast cancer whose actions are prevented by inhibition of Syk. Br J Cancer 103:401–410
19. Katz E, Sims AH, Sproul D, Caldwell H, Dixon MJ, Meehan RR, Harrison DJ (2012) Targeting of Rac GTPases blocks the spread of intact human breast cancer. Oncotarget 3: 608–619
20. Leeper AD, Farrell J, Williams LJ, Thomas JS, Dixon JM, Wedden SE, Harrison DJ, Katz E (2012) Determining tamoxifen sensitivity using primary breast cancer tissue in collagen-based three-dimensional culture. Biomaterials 33:907–915
21. Brazma A, Kapushesky M, Parkinson H, Sarkans U, Shojatalab M (2006) Data storage and analysis in ArrayExpress. Methods Enzymol 411:370–386
22. Barrett T, Suzek TO, Troup DB, Wilhite SE, Ngau WC, Ledoux P, Rudnev D, Lash AE et al

(2005) NCBI GEO: mining millions of expression profiles–database and tools. Nucleic Acids Res 33:D562–D566
23. da Huang W, Sherman BT, Lempicki RA (2009) Systematic and integrative analysis of large gene lists using DAVID bioinformatics resources. Nat Protoc 4:44–57
24. Gentleman RC, Carey VJ, Bates DM, Bolstad B, Dettling M, Dudoit S, Ellis B, Gautier L et al (2004) Bioconductor: open software development for computational biology and bioinformatics. Genome Biol 5:R80
25. Tusher VG, Tibshirani R, Chu G (2001) Significance analysis of microarrays applied to the ionizing radiation response. Proc Natl Acad Sci USA 98:5116–5121
26. Dai M, Wang P, Boyd AD, Kostov G, Athey B, Jones EG, Bunney WE, Myers RM et al (2005) Evolving gene/transcript definitions significantly alter the interpretation of GeneChip data. Nucleic Acids Res 33:e175
27. Irizarry RA, Hobbs B, Collin F, Beazer-Barclay YD, Antonellis KJ, Scherf U, Speed TP (2003) Exploration, normalization, and summaries of high density oligonucleotide array probe level data. Biostatistics 4:249–264
28. Johnson WE, Li C, Rabinovic A (2007) Adjusting batch effects in microarray expression data using empirical Bayes methods. Biostatistics 8:118–127
29. Sims AH, Smethurst GJ, Hey Y, Okoniewski MJ, Pepper SD, Howell A, Miller CJ, Clarke RB (2008) The removal of multiplicative, systematic bias allows integration of breast cancer gene expression datasets - improving meta-analysis and prediction of prognosis. BMC Med Genomics 1:42
30. Kitchen RR, Sabine VS, Simen AA, Dixon JM, Bartlett JM, Sims AH (2011) Relative impact of key sources of systematic noise in Affymetrix and Illumina gene-expression microarray experiments. BMC Genomics 12:589
31. Eisen MB, Spellman PT, Brown PO, Botstein D (1998) Cluster analysis and display of genome-wide expression patterns. Proc Natl Acad Sci USA 95:14863–14868
32. Gautier L, Cope L, Bolstad BM, Irizarry RA (2004) affy–analysis of Affymetrix GeneChip data at the probe level. Bioinformatics 20: 307–315
33. Smyth GK, Michaud J, Scott HS (2005) Use of within-array replicate spots for assessing differential expression in microarray experiments. Bioinformatics 21:2067–2075
34. Dunning MJ, Smith ML, Ritchie ME, Tavare S (2007) beadarray: R classes and methods for Illumina bead-based data. Bioinformatics 23:2183–2184
35. Du P, Kibbe WA, Lin SM (2008) Lumi: a pipeline for processing Illumina microarray. Bioinformatics 24:1547–1548
36. Clarke R, Ressom HW, Wang A, Xuan J, Liu MC, Gehan EA, Wang Y (2008) The properties of high-dimensional data spaces: implications for exploring gene and protein expression data. Nat Rev Cancer 8:37–49
37. Breitling R, Armengaud P, Amtmann A, Herzyk P (2004) Rank products: a simple, yet powerful, new method to detect differentially regulated genes in replicated microarray experiments. FEBS Lett 573:83–92
38. Zeeberg BR, Qin H, Narasimhan S, Sunshine M, Cao H, Kane DW, Reimers M, Stephens RM et al (2005) High-Throughput GoMiner, an 'industrial-strength' integrative gene ontology tool for interpretation of multiple-microarray experiments, with application to studies of Common Variable Immune Deficiency (CVID). BMC Bioinformatics 6:168
39. Subramanian A, Tamayo P, Mootha VK, Mukherjee S, Ebert BL, Gillette MA, Paulovich A, Pomeroy SL et al (2005) Gene set enrichment analysis: a knowledge-based approach for interpreting genome-wide expression profiles. Proc Natl Acad Sci USA 102:15545–15550
40. Taube JH, Herschkowitz JI, Komurov K, Zhou AY, Gupta S, Yang J, Hartwell K, Onder TT et al (2010) Core epithelial-to-mesenchymal transition interactome gene-expression signature is associated with claudin-low and metaplastic breast cancer subtypes. Proc Natl Acad Sci USA 107: 15449–15454
41. Yilmaz M, Christofori G (2010) Mechanisms of motility in metastasizing cells. Mol Cancer Res 8:629–642
42. Sims AH (2009) Bioinformatics and breast cancer: what can high-throughput genomic approaches actually tell us? J Clin Pathol 62:879–885

Chapter 6

Podosome Reformation in Macrophages: Assays and Analysis

Pasquale Cervero, Linda Panzer, and Stefan Linder

Abstract

Podosomes are multifunctional organelles of invasive cells that combine several key abilities including cell–matrix adhesion, extracellular matrix degradation, and mechanosensing. In combination with their high turnover rates that allow quick adaptation to the pericellular environment, podosomes are likely to play important roles during invasive migration of cells. Primary human macrophages constitutively form numerous podosomes and are thus an ideal system for the quantitative study of podosome dynamics. This protocol describes assays for the study of podosome dynamics, namely, reformation of podosomes, in fixed and living cells, with subsequent software-based analyses allowing the extraction of quantitative parameters such as the number of podosomes per cell, podosome density, and half times for podosome disruption and reformation. Moreover, we describe the preparation of podosome-enriched cell fractions and their analysis by immunoblotting.

Key words Podosomes, Podosome reformation, Macrophages, F-actin, Lifeact, Actin dynamics, Live cell imaging, Image analysis, PP2

1 Introduction

Podosomes and invadopodia, collectively called "invadosomes" [1–3], are actin-rich cell–matrix contacts that are characterized by their ability to locally degrade components of the extracellular matrix [4]. Podosomes are mostly formed in a physiological context in cells comprising monocytic cells such as macrophages [5], dendritic cells [6], and osteoclasts [7], endothelial cells [8], or smooth muscle cells [9], while invadopodia are found in pathological contexts comprising cancer cells such as carcinoma [10] or melanoma cells [11].

Podosomes are multifunctional organelles that combine several key abilities of invasive cells including cell–matrix adhesion, localized matrix degradation, and mechanosensing [2, 12, 13]. They are thus thought to be of key importance for invasive cell

Amanda S. Coutts (ed.), *Adhesion Protein Protocols*, Methods in Molecular Biology, vol. 1046,
DOI 10.1007/978-1-62703-538-5_6,

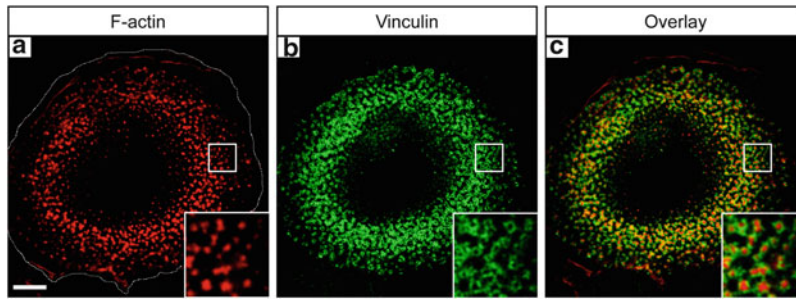

Fig. 1 Image of macrophage with podosomes, stained for F-actin and vinculin. Confocal micrograph of 7 day cultured primary human macrophage showing the typical bipartite architecture of podosomes, consisting of an F-actin-rich core (stained with Alexa568-labeled phalloidin) (**a**) and a ring structure of adhesion plaque proteins (stained for vinculin) (**b**). *Dotted line* shows the cell outline. White scale bar = 10 μm, with merge shown in (**c**)

migration. In fluorescence micrographs, podosomes present as dot-like structures with a diameter of ca. 0.5–1.0 μm and display a typical bipartite architecture consisting of an F-actin-rich core structure and a ring structure of adhesion plaque proteins such as talin or vinculin ([14]; Fig. 1). Recently, a cap-like structure on top of the actin core has also been described [2, 15, 16], while ultrastructural analysis has revealed that the "ring" structure is actually composed of individual clusters that surround the core [17].

Comparable to other adhesion structures, podosomes consist of a variety of structural and regulatory components, and recent mass spectrometric analysis revealed that the podosome proteome consists of at least 203 proteins [18], which is in the range of the proteome size for focal adhesions (ca. 150 components; [19]) and invadopodia (ca. 130 components; [20]). Key regulators of podosome formation and turnover include RhoGTPases [14, 21], actin-regulatory proteins [22], microtubule-dependent transport [2] and signalling by Src kinases [23, 24].

Podosomes are highly dynamic structures with a life time of 2–12 min [7, 25]. They display several levels of actin-based dynamics including de novo formation, fission and fusion, growth and dissolution [2]. Moreover, even in steady state podosomes show internal dynamics, as the actin-rich core (1) is turned over ca. three times within the life span of an individual podosome [7], and (2) shows internal cycles of stiffness, which are probably based on actomyosin contractility [26]. These multiple dynamics are probably key for quick adaptation of podosome formation and podosome-dependent function to a changing pericellular environment. At the same time, they implicate an intricate network of podosome components and regulators which ensures spatiotemporal fine-tuning of podosomes and their functions.

Analysis of podosome dynamics can yield important insights on the impact of novel podosome components or regulators. Primary human macrophages constitutively form numerous (>100)

podosomes per cell, and thus present as an excellent system for the study of podosome dynamics. Here, we describe assays that enable the measurement of podosome dynamics, namely, reformation of podosomes, in fixed and living cells. These assays are based on the key influence of Src kinases on podosome formation and turnover [14, 24] and use the general Src kinase inhibitor PP2 as a tool to disrupt podosomes, which enables the analysis of synchronized reformation of podosomes [27]. Subsequent software-based image analysis facilitates quantification of cells and podosomes and allows statistical analysis, yielding parameters such as the number of podosomes per cell, podosome density, and half times for podosome disruption and reformation. Moreover, we describe how these microscope-based assays can be coupled with a biochemical assay of podosome reformation, allowing one to monitor recruitment of proteins from the cell body fraction into the podosome fraction following PP2 treatment.

2 Materials

2.1 Isolation of Primary Human Monocytes

1. Buffy coats from human venous blood, incubated on a shaking plate at 4 °C overnight. You will get approximately 50–75 × 10^6 $CD14^+$ cells (i.e., monocytes) from 500 mL blood.
2. Lymphocyte Separation Medium LSM 1077 (LSM; PAA, J15-004), precooled at 4 °C (*see* **Note 1**).
3. RPMI-1640, precooled at 4 °C.
4. Monocyte isolation buffer: Dulbecco's phosphate buffered saline (DPBS; without Ca^{2+} or Mg^{2+}) plus 2 mM EDTA, pH 7.4 and 5 mg/mL human albumin with low endotoxin (Sigma-Aldrich, A5843); sterile-filtered and precooled at 4 °C. Always prepare fresh before use.
5. Anti-CD14 MicroBeads, human (Miltenyi, 130-050-201). CD14 is strongly expressed on most monocytes and thus useful as a marker molecule for purification.
6. Cell separator: QuadroMACS™ Separation Unit (Miltenyi, 130-090-976) with a MACS MultiStand (Miltenyi, 130-042-303) can be used.
7. Cell separation columns and pre-separation filters: LS Columns (Miltenyi, 130-042-401) and Pre-Separation Filters (Miltenyi, 130-041-407) can be used.
8. Counting chamber.
9. 6-well plates.
10. 50 mL tubes (Falcon).
11. 2 mL tubes (Eppendorf).

12. Macrophage culture medium: RPMI-1640 plus the following additional components: 20 % (v/v) human serum (HS), 100 units/mL penicillin, 100 μg/mL streptomycin, 2 mM glutamine. The complete medium is sterile-filtered and pre-warmed at 37 °C.

2.2 Cell Culture and Media

1. Primary human macrophages are grown in 6-well plates to a density of approximately 1.5×10^6 cells/well.
2. Macrophage culture medium (*see* Subheading 2.1).
3. Starvation medium: macrophage culture medium without HS.
4. DPBS without Ca^{2+} or Mg^{2+}.
5. Alfazyme.
6. PP2 (Src tyrosine kinase inhibitor; Calbiochem): 10 mM in DMSO is used at a final concentration of 25 μM for 30 min [or prolonged up to 1 h in live cell imaging (*see* **Note 2**)], after approximately 2 h of serum starvation.

2.3 Preparation of Podosome-Enriched Cell Fractions

1. Lysis buffer A: 20 mM Tris–HCl, pH 7.4, 5 mM EDTA, 1 % Triton X-100, 1 mM sodium ortho-vanadate plus protease inhibitors (Complete Mini Protease Inhibitor, Roche Diagnostics) and phosphatase inhibitors (PhosSTOP Phosphatase Inhibitor Cocktail Tablets, Roche Diagnostics).
2. Lysis buffer B: 20 mM Tris–HCl, pH 7.4, 5 mM EDTA, 1 % SDS, 0.1 % sodium deoxycholate, 1 mM sodium ortho-vanadate plus protease and phosphatase inhibitors.
3. Laemmli sample buffer: 10 % glycerol, 2 % SDS, 60 mM Tris–HCl, pH 6.8, 5 % mercaptoethanol, 0.01 % bromophenol blue.
4. Phosphate buffered saline (PBS).
5. Cell scrapers.
6. Sonicator.
7. Pierce BCA protein assay kit from Thermo Scientific (*see* **Note 3**).
8. Primary antibody: phospho-Tyr mouse monoclonal antibody (PY99 from Santa Cruz) for specific detection of proteins containing phosphorylated tyrosine (Tyr) residues.
9. Secondary antibody: Horseradish peroxidase linked antibody (sheep anti-mouse from GE Healthcare).
10. SDS-PAGE/Western blot apparatus.
11. Whatman Protran nitrocellulose transfer membrane.
12. Pierce ECL Western blotting substrate from Thermo Scientific.

2.4 Immunofluorescence

1. Sharp-tipped forceps (*see* **Note 4**).
2. Autoclaved glass coverslips (12 mm diameter).
3. Phosphate buffered saline (PBS).

4. Fixation: 3.7 % (v/v) formaldehyde freshly diluted in PBS, from 37 % stock solution.
5. Permeabilization: 0.5 % Triton X-100 in PBS.
6. Washing solution: 0.05 % Triton X-100 in PBS.
7. Alexa Fluor488-labeled phalloidin to stain F-actin.
8. HCS CellMask Red stain (Invitrogen, #H32712) to stain cytoplasm and nuclei: 2 μg/mL, prepared according to manufacturer's instructions.
9. Fluorescent mounting medium: Mowiol (Calbiochem) containing DABCO (25 mg/mL; Sigma–Aldrich) as anti-fading reagent.
10. Nail polish to seal the coverslips on the microscope slides.
11. Microscope slides.
12. Microscope oil.
13. Microscopy: Images of fixed samples are acquired with a confocal laser scanning microscope with a 63× objective. We use Leica DM IRE2 with a Leica TCS SP2 AOBS confocal point scanner, equipped with an oil-immersion HCX PL Apo 63× NA 1.4 lambda blue objective.
14. Acquisition of images is performed with appropriate software. We use Leica Confocal Software.
15. Image processing and analysis are performed using ImageJ ver. 1.47b (http://rsbweb.nih.gov/ij/) [28] and two lab-developed macros described in detail later (*see* Subheading 3.5).
16. Obtained data are collected in Excel, and statistical analysis is performed with GraphPad Prism (*see* Subheading 2.7).

2.5 Transfection of Primary Human Macrophages by Electroporation

1. Neon® Transfection system (Life Technologies) (*see* **Note 5**). Supplied R-Buffer is used for resuspension of cells prior to transfection.
2. 1 μL of Lifeact-GFP at a concentration of 0.5 μg/μL in TE-buffer (10 mM Tris–HCl, pH 8.5, 0.1 mM EDTA).
3. Glass-bottom dishes (*see* **Note 6**).

2.6 Live Cell Imaging

1. Microscopy: Time lapse movies are acquired with a spinning disk confocal microscope. We use Nikon Eclipse Ti with the Ultra*VIEW* VoX system, Perkin Elmer, equipped with a Yokogawa CSU X1 spinning disk, an oil-immersion 60× Apo TIRF (corr.) objective, a 527 nm (W55) emission filter and a Hamamatsu EM-CCD C9100-50 camera. The microscope should be equipped with an environmental chamber to allow temperature, humidity and CO_2 control. Experiments are performed at 37 °C, 5 % CO_2, and a humid atmosphere (*see* **Notes 7** and **8**). Microscope control and image acquisition are

performed with appropriate software. We use Volocity 6.1.1 software (Perkin Elmer).

2. Microscope oil.
3. Movie processing and analysis are performed using ImageJ ver. 1.47b [28] and a lab-developed macro described in detail later (*see* Subheading 3.8) in combination with another, already available, macro called "Find Stack Maxima" (http://rsbweb.nih.gov/ij/macros/FindStackMaxima.txt).
4. Obtained data are finally analyzed using statistical software. We use Excel and GraphPad Prism.

2.7 Statistical Analysis

Data obtained from image analysis are collected in Microsoft Excel and analyzed in GraphPad Prism, using an unpaired nonparametric Kruskal–Wallis test followed by Dunn's Multiple Comparison test. $P < 0.05$ was considered as statistically significant (single asterisk), $P < 0.01$ as highly statistically significant (double asterisks).

3 Methods

3.1 Isolation of Primary Human Monocytes

Isolation and differentiation of primary monocytes is time- and cost-consuming. However, immortalized monocytic cell lines mostly form only a few, irregularly shaped podosomes, compared to the mostly uniform and numerous podosomes formed in primary human macrophages and are thus not ideal for subsequent statistical analysis.

Primary human monocytes can be isolated as $CD14^+$ cells from buffy coats of peripheral venous blood using a Ficoll gradient to separate monocytic cells from erythrocytes and plasma. In the presence of human serum or cytokines such as M-CSF, the isolated monocytes are then differentiated into macrophages over 6–7 days.

All steps should be performed in a laminar flow hood to avoid contamination. Make sure that all necessary reagents are cold and kept on ice during the whole procedure.

1. Precool a centrifuge with a rotor able to spin down solutions in 50 mL tubes at 4 °C. All the following centrifugation steps have to be performed at 4 °C and 450 × *g* without brake.
2. Transfer the soluble part of the buffy coats from 500 mL human venous blood (ca. 60 mL) into 50 mL tubes.
3. Take three new 50 mL tubes and fill them each with 15 mL ice-cold LSM. Then carefully overlay the LSM with approximately 20 mL of the buffy coats. Try to avoid mixing of the two layers.
4. Spin for 30 min to separate lymphocytes from erythrocytes and plasma.

5. Tubes will now contain a gradient consisting of four layers. The bottom-most (red) fraction contains erythrocytes, followed by a clear LSM fraction. A white interphase containing the desired mononuclear cells separates the LSM fraction from the upper-most (yellow) blood plasma fraction.
6. Fill three new 50 mL tubes with 10 mL ice-cold RPMI-1640. (Use ice-cold RPMI-1640 for all subsequent steps.)
7. Aspirate the white interphases from the centrifuged tubes with serological pipettes and transfer them into the tubes containing the cold RPMI-1640. Fill up the tubes to 50 mL with RPMI-1640 to start a sequential washing process of the monocytes by gently resuspending the cell pellet each time (*see* **Note 9**).
8. Spin for 10 min.
9. Carefully discard the supernatants by aspiration with a serological pipette. Care must be taken because the cell pellets are not sticky and may slip along the tube wall.
10. Resuspend each pellet in 10 mL RPMI-1640 (*see* **Note 9**), combine all resuspended cells and split the solution into two 50 mL tubes. Fill up both tubes to 50 mL with RPMI-1640.
11. Spin for 10 min.
12. Discard the supernatants and resuspend each pellet in 10 mL RPMI-1640. Combine both solutions in a single 50 mL tube and fill it up to 50 mL with RPMI-1640.
13. Spin for 10 min.
14. Resuspend the pellet in 1.5 mL ice-cold monocyte isolation buffer. Transfer into a 2 mL tube and add 250 μL of anti-CD14 MicroBeads. Close the tube and mix gently by inverting three times. Incubate for 15 min on ice, to allow binding of the antibody-coupled beads to monocytes via the CD14 cell surface marker.
15. During this time, assemble the separation equipment consisting of holder, separation unit, separation column and pre-separation filter. Equilibrate the column and the pre-separation filter with 1 mL ice-cold monocyte isolation buffer.
16. Add the cell suspension to the column and let it run through completely.
17. Prepare a 50 mL tube with 10 mL RPMI-1640.
18. Add 3 mL monocyte isolation buffer to the column, remove the column from the separation unit and place it over the prepared 50 mL tube. Elute CD14-positive cells from the column by using the stamp provided in the kit.
19. Fill the tube to the 30 mL mark with RPMI-1640 and gently suspend the cells.

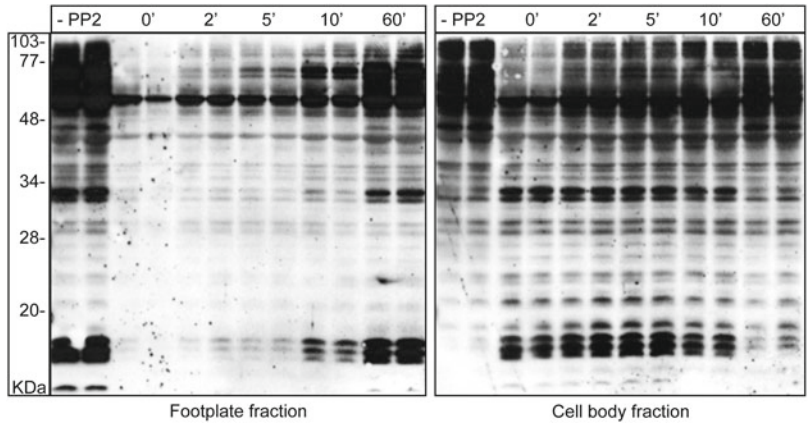

Fig. 2 Western blot analysis of podosome reformation. Western blots of macrophage lysates, developed using an anti-phosphotyrosine antibody (as proof of principle). *Left*: adhesive "footplate" fraction, *right*: cytosol and organelle fraction. Podosomes were disrupted by the use of the Src tyrosine kinase inhibitor PP2 (0 min), the inhibitor was subsequently washed out, and cells were differentially lysed at the indicated time points (0, 2, 5, 10, 60 min; two lanes for each condition). Note the successive recruitment of tyrosine-phosphorylated proteins from the cytoplasm into the podosome-containing footplate fraction. Molecular weight is indicated in kDa

20. Add an aliquot of the cell solution to a counting chamber, determine the cell number and seed the cells into 6-well plates at a density of 1.5×10^6 cells/well. If necessary, adjust the volume of the cell solution to approximately 1 mL/well with RPMI-1640.
21. Place the plates into a cell incubator at 37 °C and 5 % CO_2 for 2–4 h to allow the cells to settle and adhere. Then gently aspirate off the RPMI-1640 and add 1.5 mL of pre-warmed macrophage culture medium to each well.
22. Incubate the cells at 37 °C and 5 % CO_2 for at least 6 days to allow the development of monocytes into macrophages, which is induced by growth factors present in the human serum (*see* **Notes 10** and **11**).

3.2 Podosome Reformation Assay Using Podosome-Enriched Cell Fractions and Western Blotting

This section describes the biochemical analysis of podosome disruption and reformation, by preparation of podosome-enriched cell fractions, with subsequent Western blotting. This analysis requires the key step of differential cell lysis in order to "unroof" the cells, resulting in two different protein lysates: the "cell body" fraction, which contains cytoplasm, membranes, organelles, and cell debris, and the "footplate" fraction, which represents the adhesive membrane fraction and is enriched in podosomes [18].

This method, despite its apparent simplicity, allows one to monitor the recruitment of proteins to the footplate fraction during podosome reformation (here demonstrated for proteins enriched in phosphorylated tyrosine residues, Fig. 2).

1. 7 days cultured macrophages are grown in 6-well plates and starved for 2 h before PP2 treatment by exchanging macrophage culture medium with macrophage culture medium lacking HS (1 mL/well) (*see* **Note 12**).
2. During this period, pre-dilute the appropriate amount of PP2 in macrophage culture medium lacking HS (1 mL for each sample) to a final concentration of 25 μM; use the same procedure for control samples, but this time only with DMSO (as it is used as a dissolving agent for PP2).
3. Treatment of samples with PP2 to disrupt podosomes should start at different time points, to enable concomitant lysis of all samples. In this specific example (Fig. 2), chosen time points include 0, 2, 5, 10, and 60 min of reformation (*see* **Note 13**). The first sample to treat with PP2 is the 60 min reformation time point (30 min of PP2 treatment + 60 min of reformation = 90 min), then the reformation time point preceding it (10 min) and so on; the last time points are the control (with DMSO) and the 0 min reformation time point.
4. Podosome reformation is induced by carefully aspirating (*see* **Note 14**) the medium with PP2 and replacing it with macrophage culture medium for the intended reformation period.
5. Once all the samples are ready to be lysed differentially (to generate cell body and footplate fractions), carefully remove the medium from each well and wash the cells gently twice with PBS. After removal of PBS, add 600 μL of lysis buffer A/well to lyse cell bodies. After addition of lysis buffer A, place the plate immediately on ice to avoid protein degradation.
6. Gently shake the plate by hand for 30 s and rapidly check progression of cell lysis in phase contrast using a cell culture microscope. Onset of cell body lysis can be detected by the appearance of nuclei, cytoplasmic granules and cell debris in the lysis medium. Podosome-containing ventral membranes ("footplates") may be visible as opaque, light-scattering areas on the culture plate. Continue shaking on ice and periodically check the cells. Continue the treatment until all cell bodies are detached from the plate. Usually, after ca. 3 min, most of the cells are lysed.
7. At this point, the fraction containing cell bodies, cytoplasm, and nuclei can be removed and collected for consequent Western blotting. Remember to keep the plates on ice during all steps until the final sample collection. The remaining footplate fraction is now washed briefly twice with lysis buffer A to remove remaining cell debris. Solubilization of footplates is achieved by addition of 100 μL/well of lysis buffer B and thorough detachment of footplates with a cell scraper. Footplate fractions are collected for subsequent Western blotting analysis.

8. Sonicate the protein samples on ice for up to 10 s and 30 % of amplitude, mix them with the appropriate amount of Laemmli sample buffer and perform SDS-PAGE on 10–12 % polyacrylamide gels, loading equal volumes for the footplate and the cell bodies (*see* **Note 3**). Keep in mind that the protein concentration of the cell bodies is significantly higher than the footplate fraction (*see* **Note 3**). For this reason, fractions are lysed in different volumes of buffer (600 μL of lysis buffer A for cell bodies, compared to 100 μL of lysis buffer B for footplates).
9. The primary antibody (pY99) used as proof-of-principle (Fig. 2) in this experiment is against Tyr-phosphorylated proteins (1:1,000), with the secondary antibody being an anti-mouse horseradish peroxidase linked whole antibody (1:2,000). This allows simultaneous detection of a variety of tyrosine-phosphorylated proteins and illustrates the fact that podosomes are enriched in phosphotyrosine residues [14]. Of course, depending on the research question, a variety of different primary and secondary antibodies may be used.

3.3 Cell Culture and Coverslip Preparation for Podosome Reformation Assay Using Fixed Cells

This section describes how cultured macrophages are detached from culture dishes and seeded in a sub-confluent layer on coverslips or glass-bottom dishes. These seeded cell layers are then used to perform podosome reformation assays for fixed samples or for live cell imaging, respectively.

1. Coverslips should be sterilized before use and placed in a 6-well (one coverslip/well) plate.
2. After at least 6 days of culture (*see* **Note 11**), remove the media, wash twice with DPBS and then add 0.5–1.0 mL of alfazyme for 30 min (max. 45 min) at 37 °C.
3. After alfazyme incubation, add 0.5–1.0 mL/well of macrophage culture medium and collect the cells in a 50 mL tube prior to centrifugation (450 × *g* for 10 min).
4. Count the cells and seed approximately 60–70,000 cells/coverslip (80–100 μL) to generate a sub-confluent layer of macrophages (*see* **Note 15**).
5. After 30 min of incubation (37 °C, 5 % CO_2) to allow for sedimentation of cells, add 2 mL of pre-warmed macrophage culture medium per well.

3.4 Podosome Reformation Assay Using Fixed Cells and Immunofluorescence

This technique is based on the same principle as the sample preparation for podosome fractions (*see* Subheading 3.2), namely, podosome disruption by PP2 treatment, with subsequent podosome reformation by washout of the drug. However, as samples are then processed for immunofluorescence imaging, cells are plated on coverslips that are cultured in 6-well plates.

The advantages of using fixed cell samples include (1) the high number of cells that can be analyzed, yielding statistically robust parameters, and (2) the lack of need for a microscope equipped for live cell analysis.

1. Detach the cells and seed them on coverslips as described in Subheading 3.3.
2. Plan the time points for podosome reformation (for example, 0, 30, and 60 min) and proceed with the experiment as described in Subheading 3.2. This time cells will be only fixed, and not lysed, so it is not as important to perform the last step (in this case fixation) at the same time for all the samples (*see* **Note 16**).
3. Cells are fixed by transferring coverslips into wells containing freshly prepared 3.7 % (v/v) formaldehyde for 15 min at room temperature or ideally 37 °C (human primary macrophages are very sensitive to temperature changes) (*see* **Note 17**). After fixation, samples are washed three times (5 min each time) with PBS. Cells are permeabilized with 0.5 % Triton X-100 for 10 min at room temperature and washed again three times with 0.05 % Triton X-100 (5 min each).
4. Stain F-actin (labeling podosome cores) with Alexa Fluor488-labeled phalloidin (1:50) and cytoplasm with HCS CellMask Red stain both diluted in 0.05 % Triton X-100, for 30 min.
5. Wash coverslips three times with PBS (5 min each), dry coverslips by gentle contact with tissue to remove remaining liquid, and mount them with Mowiol (4 μL for a coverslip of 12 mm diameter) on microscope slides (cell side facing the slide). Seal samples by adding a layer of nail polish along the circumference of the coverslip (*see* **Note 18**).
6. Acquire fluorescent micrographs of podosomes and cell bodies. Depending on the quality and brightness of the staining, the ideal "standard" sample needs to have the following features (settings used for generation of Fig. 3 are given in brackets).
    - high magnification and resolution (oil-immersion HCX PL Apo 63× NA 1.4 lambda blue objective, 1,024 × 1,024 resolution and 1.5× zoom).
    - Low cell density/field of view (*see* **Note 15**).
    - Good signal to noise ratio to visualize bright and defined podosomes on dark background (pinhole airy 1 and 7 % 488 laser power).
    - Uniform and bright signal to visualize cell bodies on dark background (*see* **Note 19**) (pinhole 600 μm and 12 % 543 laser power).

The given settings can be adapted depending on the microscope parameters, the user needs and the quality of the staining. However, it is strongly suggested to keep the same settings, once defined, for the whole experiment, in order to enable a robust and statistically reliable image analysis.

3.5 Image Processing and Data Analysis of Fixed Samples

This section describes step-by-step the actions performed with ImageJ, which are assembled into a single macro using the "Record…" tool (Plugins > Macros > Record…). This analysis is based on the processing of images acquired in two channels (in this case red = cell body; green = podosomes), followed by merging the respective regions of interest (ROI), as shown in Fig. 3, yielding three different values: (A) area covered by each single cell, (B) number of podosomes in each single cell, (C) density of podosomes (here defined as number of podosomes/100 μm² of cell covered area).

In the first step, images acquired in the "cell channel" (HCS CellMask Red stain) are processed in order to get a final mask corresponding to all whole cells present in the respective field of view. For this purpose, it is important to reduce the background noise as much as possible, to ease the subsequent segmentation step, which enables recognition of individual cells as objects by the software. All settings can be adapted depending on the user needs and the quality of the staining, with settings used for the generation of images in Fig. 3 in brackets.

1. Open the "cell channel" image and calibrate the correct scale depending on the microscope settings used (Image > Properties…; if the "Global" box is checked, the software will keep the settings for the whole session, until it is closed).
2. Convert the image to 8-bit (Image > Type > 8-bit).
3. Reduce background noise by using the following tools: (*see* **Note 20**).
   (a) Smooth (Process > Smooth).
   (b) Gamma (here: 0.4) (Process > Math > Gamma…).
   (c) Median (radius used here: 4) (Process > Filters > Median…).
   (d) Gaussian Blur (sigma used here: 4) (Process > Filters > Gaussian Blur…).
4. Convert the image to black and white (Process > Binary > Make Binary) and then invert it (Edit > Invert).
5. Segment potentially adjacent objects (Process > Binary > Watershed). If you are satisfied with the output, you can proceed to the actual object analysis. In case the output is not satisfactory, adapt the previous settings to yield optimal results.
6. Highlight objects you are interested in by setting the expected size (in μm²) and the circularity (0 = straight line, 1 = perfect circle) (Analyze > Analyze Particles…). In this step, you can

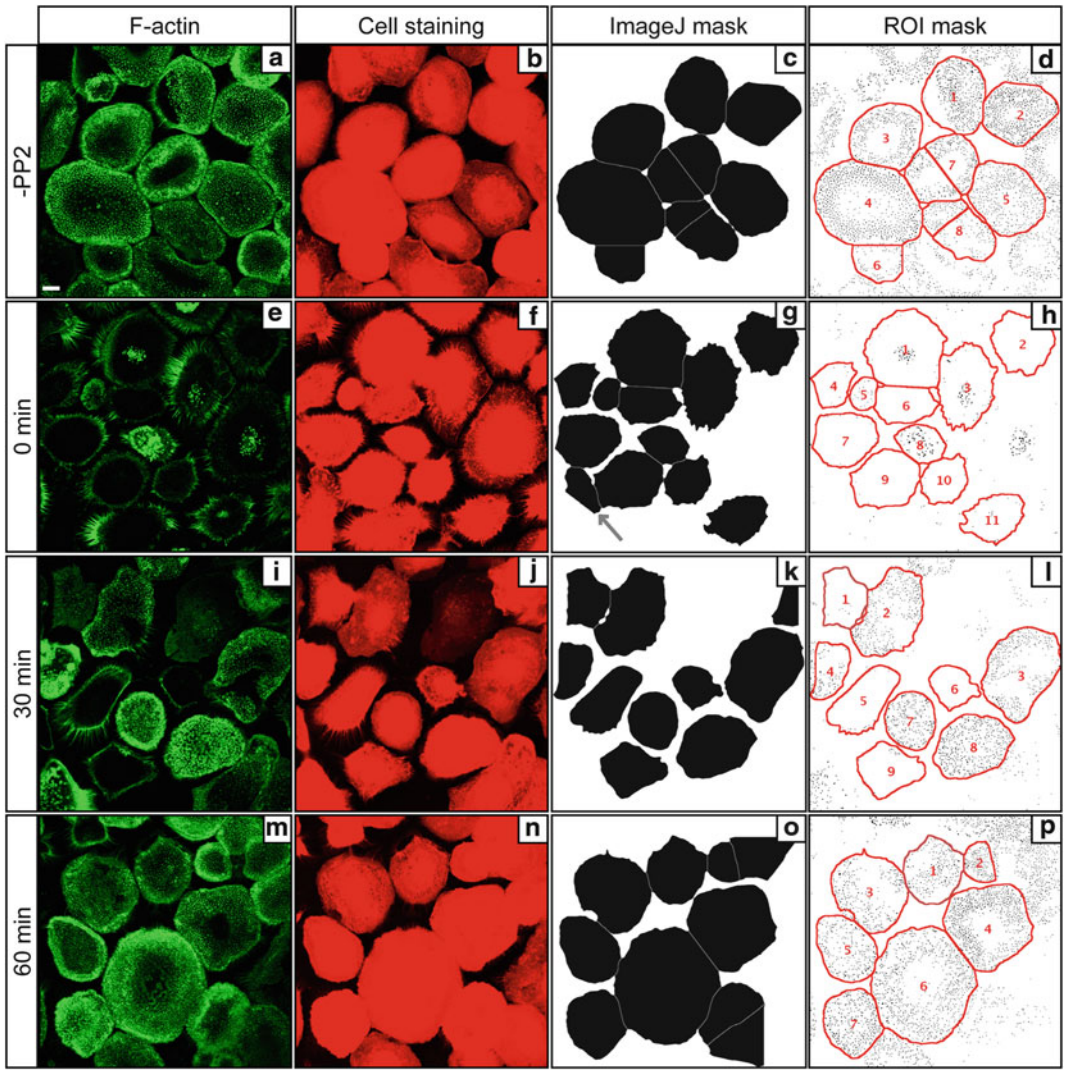

Fig. 3 Image analysis of podosome reformation using fixed samples. Gallery of confocal micrographs from macrophages stained for F-actin using Alexa488-labeled phalloidin to label podosomes (*green*; **a**, **e**, **i**, **m**), stained with CellMask to highlight individual cells (*red*; **b**, **f**, **j**, **n**), after application of the described ImageJ macro (*black*; **c**, **g**, **k**, **o**), and after using the ROI mask to correlate podosomes (*black dots*) with individual cells (*red outlines* and *numbers*; **d**, **h**, **l**, **p**). Images in *upper row* show untreated cells. *Lower rows* shows cells after 30 min treatment with PP2 to disrupt podosomes. Minutes after start of drug washout ($t = 0$ min) are indicated. Note that use of the ImageJ "ROI manager" tool allows the combination or deletion of ROI in case of oversegmentation (i.e., ROI 7 in **d** (*center*) is obtained by merging two segmented objects belonging to a single cell, while in **g**, a *grey arrow* indicates an object which was manually deleted, as it represents only a part of a cell not completely shown in the image. White scale bar = 10 μm

also check other options such as masks corresponding to the identified objects ("Show:Masks"), adding the obtained ROI to the ROI manager for further analysis ("Add to Manager"), and excluding incomplete objects identified on the edges of the image ("Exclude on edges").

7. Once the identified objects are recorded in the "ROI Manager", it is possible to modify them. This includes combining two segmented objects belonging to one single cell in case of oversegmentation (select the ROI that need to be merged, right-click and select the "OR (Combine)" function followed by "Add"; this will create a single new ROI that will include the previously selected ones, which have to be deleted individually) (*see* **Note 21**).
8. Set the values for calculation, for example cell area (Analyze > Set Measurements… > check only "Area"), then manually select all ROIs and click on "Measure". Save the obtained area values in a spreadsheet.
9. Recording all previous actions, including the settings used, will result in a macro that can be saved as a .txt file.

```
run("8-bit");
run("Smooth");
run("Gamma…", "value=0.40");
run("Median…", "radius=4");
run("Gaussian Blur…", "sigma=4");
run("Make Binary");
run("Invert");
run("Watershed");
run("Analyze Particles…", "size=150-Infinity circularity=0.30-1.00 show=Masks clear exclude add");
```

   Once the ROIs corresponding to the cell positions are recorded, open the "podosome channel" (phalloidin stain) of the same image and run a series of actions which will allow highlighting and better definition of podosomes as individual, countable objects (Fig. 4).
10. Convert the image to 8-bit and smooth it (*see* **steps 2** and **3**).
11. Subtract the background (rolling here: 5) (Process > Subtract Background…).
12. Perform a gamma correction to increase the contrast (here: 1.30) (Process > Math > Gamma…).
13. Carefully convolve to further increase the contrast (here, a 5×5 matrix is used in which all elements are −1 except the central one, which is 30; the "Normalize Kernel" box has to be checked).
14. Convert the picture to black and white (Process > Binary > Make Binary).
15. Repeat **steps 5–6**, but this time use the "Analyze Particles" filter with the appropriate settings, enabling a better definition of podosomes (i.e., size = 0.10–50 μm^2 and circularity = 0.80–1.0). Choose only the option showing the masks (Show:Masks), without adding the results to the "ROI Manager".

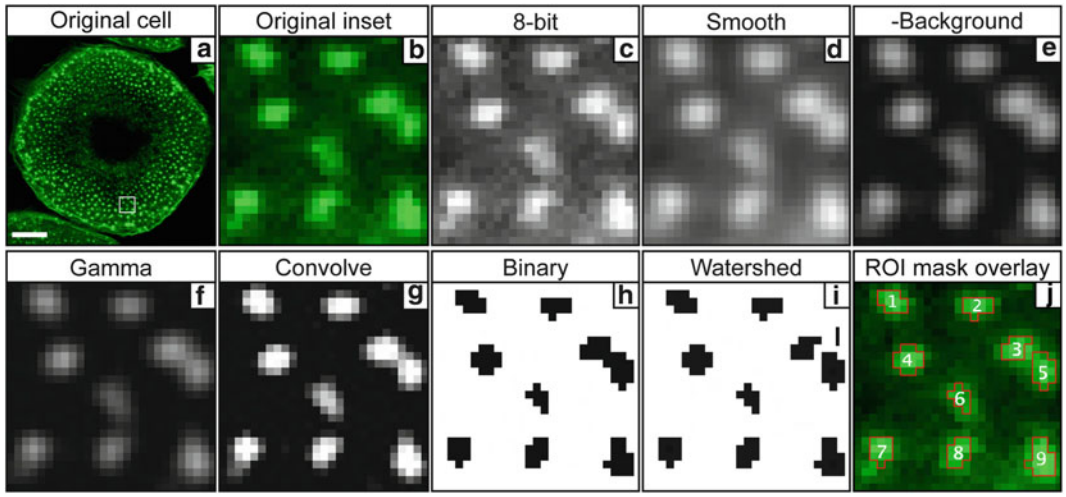

Fig. 4 Gallery of pictures showing the effects of the "podosome macro" step-by-step. The original picture (**b**; *inset* from image of complete cell in **a**) is first converted to an 8-bit image (**c**) and then smoothened (**d**). To allow for good detection of podosomes in the whole cell, it might be useful to increase the contrast by subtracting the background (**e**), performing the gamma correction (**f**) and the convolution (**g**). At the end of this process, podosomes are more easily detected by the software so that you can convert the picture to a binary image (**h**), ready to be watersheded (segmentation of touching objects; **i**). Note that the "watershed" step in (**i**) is able to separate a single detected object into two distinct podosomes (ROI *3* and *5*). The resulting ROI mask overlaying the original picture (**b**) is shown in (**j**). White scale bar = 10 μm; *White square inset* measures: 4.32 × 4.32 μm

16. Uncheck and recheck the "Show all" box in the "ROI Manager" to see the overlay of the cell ROI on the detected podosome mask.
17. Manually select a single cell ROI in the "ROI Manager" and use the "Find Maxima" tool (Process > Find Maxima…) to count the number of podosomes present in this ROI. Set "Noise tolerance" to 0 and "Output type" to "Count". The "Light background" box has to be checked.
18. **Step 17** can be fully automated for all of the cell ROI by adding respective instructions (here highlighted in bold) at the end of the "Podosomes" macro. The "Result" window will now show the number of podosomes detected in each cell ROI at the end of the list (keeping the same numbering order saved in the previous "Cell body" macro).

    Recording all previous actions, including the settings used, will result in the complete macro, which can be saved as a .txt file.

```
run("8-bit");
run("Smooth");
run("Subtract Background…", "rolling=5");
run("Gamma…", "value=1.30");
run("Convolve…", "text1=[-1 -1 -1 -1 -1\n-1 -1 -1 -1 -1\n-1 -1 30 -1 -1\n-1 -1 -1 -1 -1\n-1 -1 -1 -1 -1\n] normalize");
```

```
run("Make Binary");
run("Watershed");
run("Analyze Particles…", "size=0.10-50 circularity=0.80-1.00 show=Masks display");
roiManager("Show None");
roiManager("Show All");
n=roiManager("count");
for (i=0; i<n; i++) {
roiManager("select", i);
run("Find Maxima…", "noise=0 output=Count light");
}
```

19. It is now possible to save the number of podosomes detected in each identified cell. These values, in combination with the values for cell area, can be used to calculate the three parameters described in the introduction to this section (A, B, C) and perform statistical analysis as shown in Fig. 5.

3.6 Transfection of Primary Human Macrophages by Electroporation

Sufficiently effective transfection of primary macrophages is so far only possible by electroporation (*see* **Note 5**); a mechanical process, where an electrical pulse is used to create temporary pores in cell membranes through which substances like DNA or RNA can pass into cells.

All steps should be performed in a laminar flow hood to avoid contamination.

1. On the day before live cell imaging (*see* **Note 22**), detach macrophages from two wells of a 6-well plate (obtained as described in Subheading 3.3) (*see* **Note 11**).
2. Take 1×10^5 cells for one transfection with the Neon™ Transfection System 10 μL Kit and resuspend in 12 μL R-buffer (pre-warmed at room temperature), supplied in the Kit.
3. Add 0.5 μg Lifeact-GFP (1 μL of 0.5 μg/μL) and mix by pipetting up and down 5–10 times. (Make sure that the added DNA solution does not exceed 10 % of the total volume.)
4. Load the solution with a Neon™ Pipette into a Neon™ Tip, also supplied in the Neon™ Transfection System 10 μL Kit. Ensure that there are absolutely no air bubbles in the loaded solution, as they will interfere with the transmission of the electrical current!
5. Plug the Neon™ Pipette with Neon™ Tip into position in the Neon™ Pipette Station with Neon™ Tube, filled with 3 mL E-buffer at room temperature. Select your transfection protocol on the device and press Start. We have optimized a protocol for primary human macrophages with two pulses of 1,000 V and 40 ms each.

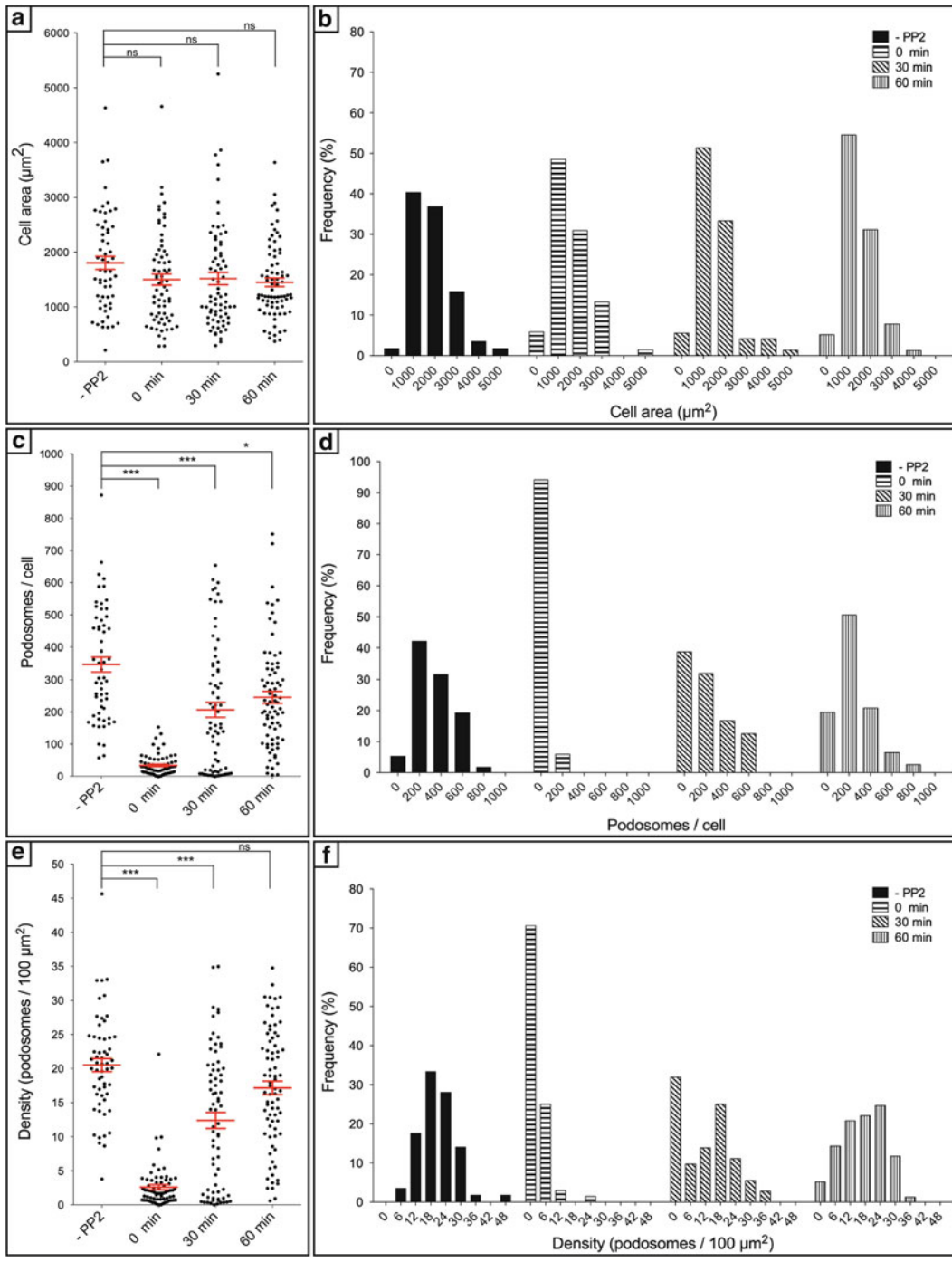

Fig. 5 Statistical analysis of podosome reformation using fixed samples. Measurements of (**a**, **b**) cell area, (**c**, **d**) number of podosomes per cell, and (**e**, **f**) density of podosomes. Each *dot* in (**a**, **c**, **e**) represents a value from a single cell, with mean values given ± SEM. (**b**, **d**, **f**) show respective frequency analyses of (**a**, **c**, **e**). Podosome density in (**e**, **f**) is given as (podosome number/100 µm²). Analyzed time points include 30 min before addition of Src tyrosine kinase inhibitor ("–PP2"), and 0, 30, and 60 min after the start of PP2 washout. Note that the high number of analyzed cells, coupled with frequency analysis of podosome numbers per cell reveals that the mean value for the 30 min time point in (**e**) is derived from a mixture of two cell subpopulations showing either numerous or almost no podosomes, as clearly visible in Fig. 3l (Color figure online)

6. Unplug the Neon™ Pipette and immediately transfer the transfected cells into a tube containing 100 µL macrophage culture medium pre-warmed to 37 °C. Mix the cells with the medium by gently pipetting up and down 5–10 times and transfer them to a glass-bottom dish for live cell imaging.
7. Place the dish in an incubator at 37 °C and 5 % CO_2 until you start the respective podosome reformation assay.

3.7 Podosome Reformation Assay Using Live Cell Imaging

Evaluating podosome reformation by live cell imaging enables the tracking of individual cells and their podosomes throughout the whole course of the experiment, yielding additional parameters including half times of podosome disruption and reformation, as well as the duration of the lag phase preceding podosome reformation (Fig. 6). Disadvantages include the need for a live cell microscope equipped with an environmental chamber, and the limited number of cells that can be analyzed. This assay thus displays different strengths and weaknesses compared to the analysis of fixed cell samples, and combining both setups is an ideal option.

1. Before the start of the experiment, equilibrate the environmental chamber in a humid atmosphere at 37 °C and 5 % CO_2 for at least 1 h (*see* **Note 8**).
2. Use cells transfected with Lifeact-GFP and seeded on glass-bottom dishes (as described in Subheading 3.6). Wash the cells two times with 1 mL of starvation medium (pre-warmed to 37 °C) and subsequently add 500 µL of starvation medium for 60–100 min to starve cells for a total period of at least 2 h. This starvation step makes the cells more susceptible to the PP2 treatment, allowing for lower doses of the drug and shorter incubation times (*see* **Note 2**). Place the cells into the equilibrated environmental chamber.
3. Prepare 1 mL of a 2× concentrated working solution of PP2 in starvation medium (= 50 µM) and at least 3 mL of washout medium (= macrophage culture medium). Place the solutions ready to use in not completely sealed vials (to allow pH-equilibration) in a nearby incubator, or even better in the environmental chamber.
4. Before imaging, place a drop of microscope oil on the (60×)-oil-immersion objective and the clean bottom of the live cell dish and fix the dish tightly on the stage. It is important that the dish does not move out of place during the imaging process, especially when solutions and media are added or removed.
5. Identify one or several cells (*see* **Note 23**) showing good expression of Lifeact-GFP and determine the optimal values for laser intensity, exposure time and camera settings for the time lapse imaging. While searching for appropriate cells, keep

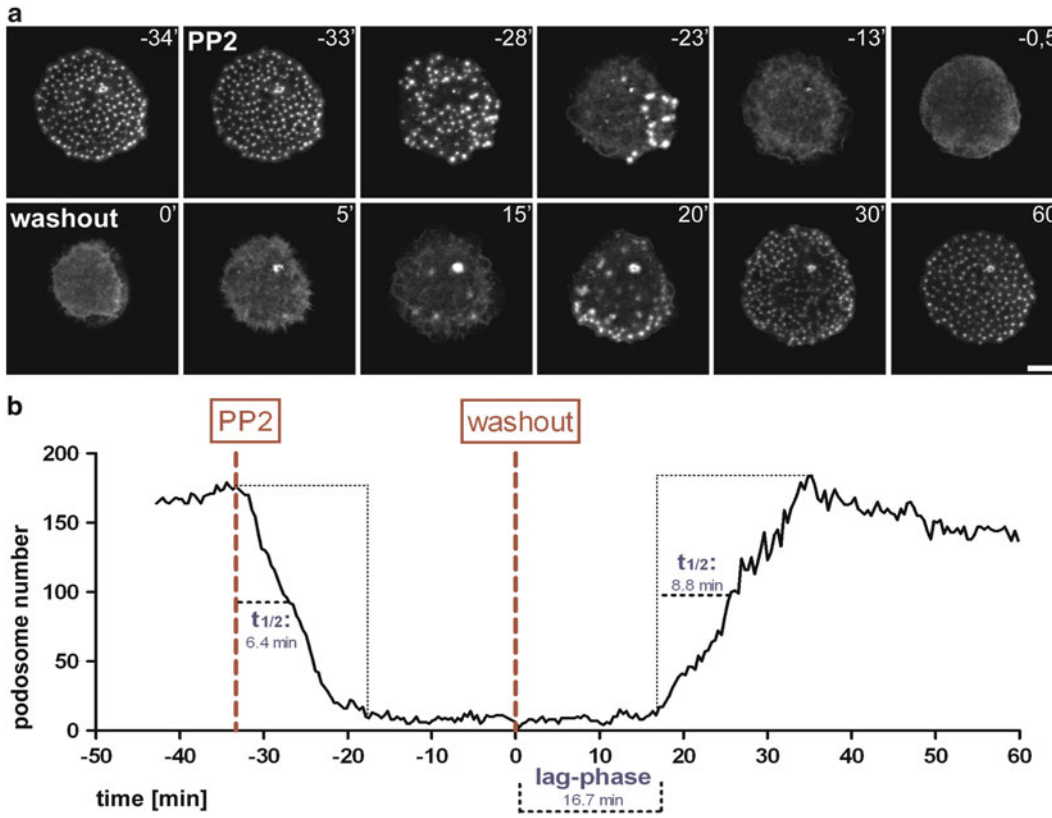

Fig. 6 Analysis of podosome reformation using live cell imaging. (**a**) Fluorescence micrographs of an 8 days cultured macrophage transfected with Lifeact-GFP. After transfection, cells were plated on a glass-bottom dish prior to serum starvation for 2 h. Time before and after washout of PP2 to start podosome reformation is given in minutes. Addition of PP2 to disrupt podosomes thus represents time point "−33′". Images were taken every 25 s. Scale bar: 10 μm. (**b**) Statistical evaluation of podosome disruption and reformation based on the live cell video of the cell shown in (**a**). Podosome number was measured by the described ImageJ macro and plotted over time using GraphPad Prism. Time points for addition of PP2 and washout of the inhibitor are indicated. Note that this analysis allows for the determination of several parameters, including the half times for podosome disruption and podosome reformation, as well as the duration of the lag phase until the start of podosome reformation, as indicated

in mind that high laser intensity and long exposure times lead to photobleaching and phototoxicity, resulting in a decrease in brightness and cell retraction (*see* **Note 24**).

6. Start the acquisition by taking an image every 15–30 s for 5–10 min. This acquisition rate is necessary because of the fast turnover and movement of podosomes. Keep in mind that podosomes have an average lifetime of about 2–12 min [7].
7. Stop the acquisition and add 500 μL of the 50 μM PP2 solution to the cells. Gently add and mix the PP2 solution with the starvation medium by carefully pipetting up and down three times. (timepoint 0 = start of PP2 treatment and of podosome disruption.)

8. Restart image acquisition immediately.
9. After 30 min, stop acquisition again for the washout of PP2. If not all of the podosomes have been disrupted, extend this period for up to 1 h (*see* **Note 2**). Carefully remove the starvation medium containing PP2 with a pipette tip from the edge of the live cell dish and gently add 1 mL of the washout medium also from this position. Repeat this step two times to ensure complete removal of the inhibitor-containing medium (=start of washout). Try to act fast to avoid loss of acquisition time, but treat cells gently, as the PP2 treatment makes them sensitive and prone to detachment.
10. Immediately resume image acquisition for 60 min.

3.8 Image Processing and Data Analysis of Live Cell Samples

This section describes the steps that enable the analysis of the recorded time-lapse videos, yielding parameters such as podosome numbers at each recorded time point, half times of podosome disruption and reformation, as well as duration of the lag phase preceding podosome reformation.

1. Open the sequence of recorded images as a TIFF-file stack in ImageJ.
2. As described in Subheading 3.5, it is necessary to initially enhance the image quality, which facilitates the subsequent analysis. The following ImageJ macro has been developed to optimize the contrast and the signal to noise ratio, also compensating for the unavoidable bleaching of specimens, to subtract the background and convert images to the required 8-bit format.

```
run("Enhance Contrast", "saturated=0 use");
run("Median…", "radius=1 stack");
run("Subtract Background…", "rolling=50 stack");
run("Gamma…", "value=1.50 stack");
run("8-bit");
```

   Run this macro.
3. Next, run an already available macro called "Find Stack Maxima" (http://rsbweb.nih.gov/ij/macros/FindStackMaxima.txt). This macro performs the Process > Binary > Find Maxima command on all images in a stack. The only parameter that you have to adapt is "Noise tolerance", according to the quality of your image stack. To find the respective optimal value, take the output sequence of the first macro and test different values for "Noise tolerance" on individual images of the stack using the "Find Maxima" command. Make sure that the "preview point selection" box is checked, to analyze only the chosen image. It is recommended to compare the respective results for a few images from different time points of the assay, which allows a better estimation of the optimal value for "Noise tolerance" for

best detection of the podosomes in all different states of the experiment (usually, this is in the range of 5–20).

4. Run the "Find Stack Maxima" macro using the appropriate value for "Noise tolerance" and "count" for output type. This results in a chart, listing the number of podosomes for every single image of the stack. For checking the reliability of your analysis, choose "single points" for the output type, which results in an image showing all structures that have been identified by the software as dots.
5. Use Excel or GraphPad Prism to draw a graph depicting the number of podosomes in a single cell over the course of the whole experiments (Fig. 6b). This graph also allows determination of the half times for podosome disruption after PP2 addition and for podosome reformation after PP2 washout, as well as the duration of the lag phase between washout of the drug and the actual onset of the podosome reformation.

4 Notes

1. LSM 1077 is a separation solution made with Ficoll™ density gradient media. It is used for the separation of cells and subcellular components, which sediment during centrifugation. Mononuclear cells are recovered from the white interface separating the uppermost two fractions (*see* Subheading 3.1).
2. This can depend on the individual properties of primary cells from different donors. However, the PP2 treatment should not exceed 1 h, as this will lead to pronounced cell contraction.
3. It is not strictly necessary to measure protein concentration, as the same amount of cells has been used for all samples. However, keep in mind that the adhesive (here: "footplate") fraction contains much less protein (five- to tenfold) than the cell body fraction [29], and it may be necessary to adjust the loaded amounts of both fractions in order to reach comparable protein levels for subsequent detection.
4. The choice of forceps to correctly handle glass coverslips is important. Very sharp-tipped forceps can help in carefully lifting coverslips from parafilm or the bottom of 6-well plates.
5. Both the Neon™ Transfection system (Invitrogen) and the Amaxa Nucleofector® II (Lonza) are suitable for electroporation-based transfection of human macrophages and give similar transfection efficiencies (ca. 10–15 % for vector-based constructs; ca. 90–100 % for siRNA). Advantages of the Neon™ system include (1) better viability of cells, (2) faster expression of fusion proteins (as early as 3 h post transfection), (3) the necessity of only one single kit for all cell types (available in

two sizes, according to the volume of the cell suspension to be used), (4) easy and transparent adjustment of all electroporation parameters by the researcher.

6. Glass-bottom dishes are strongly recommended when using high numerical Aperture coverslip corrected objectives. It is best to take a glass coverslip No. 1.5 (=0.17 mm thickness), because most microscope objectives are designed for their use. If your objective has a correction collar to compensate for coverslip thickness variations, set it to 0.17 mm. We are using No. 1.5 glass-bottom live cell dishes from WillCo (# GWSt-3512) with a diameter of 12 mm.
7. A humid atmosphere is achieved by passing the 0.5 % CO_2 containing air through an air outlet into a bottle of water and from there into the environmental chamber.
8. The minimal technical prerequisites for live cell imaging of podosome reformation are an inverted epifluorescence or confocal microscope with an at least 60× objective. In addition, you will need an excitation and emission filter for GFP (or another filter, if Lifeact coupled to a different fluorophore is used), a camera and a shutter, which should be computer-controlled. Finally, an environmental chamber is necessary, to maintain a constant temperature of 37 °C and a CO_2 level of 5 % (to maintain the correct pH of $NaHCO_3$ buffered media). Both are important for preservation of the normal cell physiology, and cells will respond with contraction to variations in these parameters. If you are not able to supply your environmental chamber with CO_2, you can make use of HEPES buffered media, which do not require a controlled atmosphere. A perfect focus system is very helpful for constantly keeping the focus of cells/podosomes during image acquisition. If your microscope is not equipped with such a tool, make sure that the environmental chamber as well as the objective are well equilibrated at 37 °C by both a stage warmer and an objective heater in case of an objective with high numerical aperture. This will stabilize the *Z*-positioning over time.
9. It is important to resuspend cells gently during this step, as vigorous mixing and the creation of air bubbles may lead to random activation of cells, resulting in enhanced migration during cell culture.
10. As an alternative to whole human serum, you can also add macrophage colony-stimulating factor MCSF at 5 ng/mL in addition to 20 % dialysed fetal bovine serum [18]. This cytokine induces the differentiation of the isolated monocytic cells into macrophages [30].
11. Minimal time of culture is 6 days post purification of monocytic cells. The optimal time for using differentiated macrophages for podosome reformation is 7–9 days. Transfection efficiency

decreases after 9 days, however, cells may be used for up to 2 weeks of culture.

12. Using a 6-well plate is important in order to have all the samples ready to be lysed at the same time.
13. Time points can be varied, but should cover at least a 60 min period to allow for full reformation of podosomes.
14. It is important to perform this washing step gently, as macrophages are less adherent after the PP2 treatment due to the loss of their main adhesion structures (podosomes and focal adhesions).
15. For the image analysis, it is recommendable to generate a layer of clearly recognizable individual cells in order to simplify the segmentation step ("Watershed"). However, don't decrease the density too much, as cells may then lose their spread morphology.
16. Cell adhesion on glass coverslips is usually weaker compared to plastic surfaces. Aspiration of media may thus result in a substantial loss of cells. A gentler alternative is to rapidly transfer the coverslips to new cell culture wells, or dishes pre-filled with warmed medium (with or without PP2, depending on the step in the experiment). Use a vacuum pump for aspiration only after fixation of cells.
17. Transfer the coverslips to the fixative-containing well manually and make sure that remaining drops of medium on the coverslips are dripped onto a tissue before placing them in the fixative to not dilute the solution.
18. Sealing serves two purposes: coverslips are immobilized on the slide, and drying-out of samples is prevented. If stored at 4 °C in the dark, samples may thus remain usable for several months.
19. Macrophages contain a high amount of granules, which appear as dark spots on the red background of the cytoplasm and may thus interfere with the image analysis.
20. If your sample is uniformly stained (i.e., no visible granules) and if cells are clearly separate, you can skip the points described in Subheading 3.5, **step 3** and use only the "Smooth" tool.
21. If you don't have any cell body staining available, you can still draw the cell ROI manually, add them to the "ROI Manager" and follow the next points of the paragraph.
22. If your construct of interest shows good expression early after transfection, this step is also possible on the day of use. However, for Lifeact-GFP expression in macrophages, overnight is optimal.

23. If your microscope is equipped with an automated stage and respective software, videos of several individual cells can be acquired at the same time.
24. It is important to find a good balance between optimal resolution and a minimal effect of photobleaching and phototoxicity in order to obtain the best results of cells showing a physiological morphology, combined with sufficient and constant image quality. Thus, you have to minimize the energy level of the excitation light and/or laser power and the duration of exposure with the goal to not damage the cells and the fluorophore, but to achieve an image of sufficiently good resolution at the same time.

Acknowledgments

We thank Andrea Mordhorst and Barbara Böhlig for excellent technical assistance, Mirko Himmel for help with live cell analysis of podosome reformation and discussions, Bernd Zobiak and Virgilio Failla (UKE microscope imaging facility) for help with ImageJ-based analysis of podosome reformation, and Martin Aepfelbacher for continuous support. This work is part of the doctoral theses of PC and LP. Work in the SL lab is supported by the European Union's Seventh Framework Programme (FP7/2007-2013) under grant agreement no FP7-237946 (T3Net), Deutsche Forschungsgemeinschaft (LI925/3-1) and Wilhelm Sander Stiftung (2012.026.01).

References

1. Gimona M, Buccione R, Courtneidge S, Linder S (2008) Assembly and biological role of podosomes and invadopodia. Curr Opin Cell Biol 20:235–241
2. Linder S, Wiesner C, Himmel M (2011) Degrading devices: invadosomes in proteolytic cell invasion. Annu Rev Cell Dev Biol 27:1 85–211
3. Saltel F, Daubon T, Juin A, Ganuza IE, Veillat V, Genot E (2011) Invadosomes: intriguing structures with promise. Eur J Cell Biol 90:100–107
4. Linder S (2007) The matrix corroded: podosomes and invadopodia in extracellular matrix degradation. Trends Cell Biol 17:107–117
5. Linder S, Nelson D, Weiss M, Aepfelbacher M (1999) Wiskott-Aldrich syndrome protein regulates podosomes in primary human macrophages. Proc Natl Acad Sci USA 96: 9648–9653
6. Burns S, Thrasher AJ, Blundell MP, Machesky L, Jones GE (2001) Configuration of human dendritic cell cytoskeleton by Rho GTPases, the WAS protein, and differentiation. Blood 98:1142–1149
7. Destaing O, Saltel F, Geminard J, Jurdic P, Bard F (2003) Podosomes display actin turnover and dynamic self-organization in osteoclasts expressing actin-green fluorescent protein. Mol Biol Cell 14:407–416
8. Moreau V, Tatin F, Varon C, Genot E (2003) Actin can reorganize into podosomes in aortic endothelial cells, a process controlled by Cdc42 and RhoA. Mol Cell Biol 23:6809–6822
9. Burgstaller G, Gimona M (2004) Actin cytoskeleton remodelling via local inhibition of contractility at discrete microdomains. J Cell Sci 117:223–231
10. Lorenz M, Yamaguchi H, Wang Y, Singer RH, Condeelis J (2004) Imaging sites of N-WASP

activity in lamellipodia and invadopodia of carcinoma cells. Curr Biol 14:697–703
11. Monsky WL, Lin C, Aoyama A (1994) A potential marker protease of invasiveness, separase, is localized on invadopodia of human malignant melanoma cells. Cancer Res 54:5702–5710
12. Gimona M, Buccione R (2006) Adhesions that mediate invasion. Int J Biochem Cell Biol 38:1875–1892
13. Murphy DA, Courtneidge SA (2011) The "ins" and "outs" of podosomes and invadopodia: characteristics, formation and function. Nat Rev Mol Cell Biol 12:413–426
14. Linder S, Aepfelbacher M (2003) Podosomes: adhesion hot-spots of invasive cells. Trends Cell Biol 13:376–385
15. Mersich AT, Miller MR, Chkourko H, Blystone SD (2010) The formin FRL1 (FMNL1) is an essential component of macrophage podosomes. Cytoskeleton 67:573–585
16. Bhuwania R, Cornfine S, Fang Z, Krüger M, Luna EJ, Linder S (2012) Supervillin couples myosin-dependent contractility to podosomes and enables their turnover. J Cell Sci 125:2300–2314
17. Cox S, Rosten E, Monypenny J, Jovanovic-Talisman T, Burnette DT, Lippincott-Schwartz J, Jones GE, Heintzmann R (2012) Bayesian localization microscopy reveals nanoscale podosome dynamics. Nat Methods 9:195–200
18. Cervero P, Himmel M, Krüger M, Linder S (2012) Proteomic analysis of podosome fractions from macrophages reveals similarities to spreading initiation centres. Eur J Cell Biol 91:908–922
19. Zaidel-Bar R, Itzkovitz S, Ma'ayan A, Iyengar R, Geiger B (2007) Functional atlas of the integrin adhesome. Nat Cell Biol 9:858–867
20. Attanasio F, Caldieri G, Giacchetti G, van Horssen R, Wieringa B, Buccione R (2010) Novel invadopodia components revealed by differential proteomic analysis. Eur J Cell Biol 90:115–127
21. Dovas A, Cox D (2011) Signaling networks regulating leukocyte podosome dynamics and function. Cell Signal 23:1225–1234
22. Albiges-Rizo C, Destaing O, Fourcade B, Planus E, Block MR (2009) Actin machinery and mechanosensitivity in invadopodia, podosomes and focal adhesions. J Cell Sci 122:3037–3049
23. Destaing O, Block MR, Planus E, Albiges-Rizo C (2011) Invadosome regulation by adhesion signaling. Curr Opin Cell Biol 23:597–606
24. Boateng LR, Huttenlocher A (2012) Spatiotemporal regulation of Src and its substrates at invadosomes. Eur J Cell Biol 91:878–898
25. Starnes TW, Cortesio CL, Huttenlocher A (2011) Imaging podosome dynamics and matrix degradation (Chapter 9). Methods Mol Biol 769:111–136
26. Labernadie A, Thibault C, Vieu C, Maridonneau-Parini I, Charrière GM (2010) Dynamics of podosome stiffness revealed by atomic force microscopy. Proc Natl Acad Sci USA 107:1–10
27. Linder S, Hüfner K, Wintergerst U, Aepfelbacher M (2000) Microtubule-dependent formation of podosomal adhesion structures in primary human macrophages. J Cell Sci 113:4165–4176
28. Schneider CA, Rasband WS, Eliceiri KW (2012) NIH Image to ImageJ: 25 years of image analysis. Nat Methods 9:671–675
29. Kuo J, Han X, Yates JR III, Waterman CM (2012) Isolation of focal adhesion proteins for biochemical and proteomic analysis. Methods Mol Biol 757:297–323
30. Stanley ER, Berg KL, Einstein DB, Lee PSW, Pixley FJ, Wang Y, Yeung Y (1997) Biology and action of colony-stimulating factor-1. Mol Reprod Dev 46:4–10

Chapter 7

Mobile and Three-Dimensional Presentation of Adhesion Proteins Within Microwells

Mirjam Andreasson-Ochsner and Erik Reimhult

Abstract

On traditional cell culture substrates cells adhere to a planar 2D surface where ligands are presented immobile. A more realistic presentation of cell adhesion ligands which can account for lateral mobility and a more tissue-like 3D presentation would allow studies addressing fundamental questions of significant importance for applications such as tissue engineering and implant intregration. To study the effect of lateral mobility of cell membrane interaction cues in three dimensions, we have developed and characterized a platform which generically enables patterning of single cells into microwells presenting a cell membrane mimetic interface pre-patterned to its walls. Here, we describe its application in presenting a soluble cell adhesive ligand coupled through streptavidin-antibody linkage to lipids in a supported lipid bilayer (SLB) coated microwell. The lateral mobility of the presented ligands was controlled through a small change in temperature. The SLB phospholipid composition was choosen such that below its melting transition at 30 °C the ligands are immobile, while above 30 °C they are laterally mobile. The platform thus enables the investigation of cell adhesion to either laterally immobile or mobile E-cadherin ligand presented on the same cell membrane mimetic surface.

Key words Supported lipid bilayer, Mobility, Dimensionality, Cell adhesion, Microwell

1 Introduction

Cell behavior and fate is influenced by the properties of the extracellular matrix (ECM). It is known that cells actively interact with the ECM. They do not only biochemically alter the ECM, but also rearrange the position and presentation of molecular motives within the ECM. The feedback loop from these changes to the ECM in turn dictates the cellular answer. Therefore the mobility of the adhesion molecules to which the cell is attached is likely to be one of the properties that affect cell behavior; for example, it allows for the aggregation of single cell–cell adhesive molecules within adhesion sites and force distribution over many adhesion molecules. The adhesion sites must be sufficiently strong to maintain tissue architecture but still be able to rapidly dissociate, in order to

Amanda S. Coutts (ed.), *Adhesion Protein Protocols*, Methods in Molecular Biology, vol. 1046,
DOI 10.1007/978-1-62703-538-5_7,

allow cells to move and divide [1, 2]. The spatial arrangement of both cell–cell and cell–ECM adhesive ligands can also influence cell signaling to instruct cellular behavior [3] and a variety of biological processes, such as immune synapse formation [4], cancer metastasis [5, 6], and lymphocyte migration [7]. Detailed, molecular level investigation of such events therefore requires reconstituted platforms which allow for ligand mobility and rearrangement.

Cadherins are a super-family of cell–cell adhesion molecules that are usually concentrated in adherens junctions in epithelial and neural cells. They act as mechanical hubs that connect the cortical actin cytoskeleton of adjacent cells. Multicellular tissue formation, cell association, and migration [8, 9] require cadherin mediated cell–cell interactions and cadherin dysfunction has been linked to diseases, such as cancer [10]. The adhesive strength of the cadherin and its cluster behavior is due to the attachment to the actin skeleton and consequently cadherin organization influences actin organization [11]. Its function is therefore a dynamic process involving both cadherin clustering and environmental cues, which regulate the cell response. In vitro platforms to investigate the influence of cadherin on cell growth and response should thus ideally capture cadherin mobility and variations in geometric presentation.

Functionalized supported lipid bilayers (SLBs) are suitable model systems to implement lateral mobility of cell adhesive ligands in a way that mimics a neighboring cell. SLBs as cell interaction partners were first introduced in the study of the adaptive immune system to model Fc receptor mediated adhesion and signaling between T-cells and antigen presenting cells [12]. More recently, SLBs functionalized with cell adhesive peptides [13–15] demonstrated the influence of ligand mobility through strengthening of cell adhesion [7], cluster formation [16], and differentiation levels [17], as well as its effect on cadherin recognition and cellular dynamics [14, 18].

We present an SLB platform for which the mobility of a wide range of attached ligands can be tuned by small temperature changes in a physiologically relevant range [19]. This surface modification has been combined with micropatterned, single-cell environments, which allow for culturing of cells with quasi-3D presentation of ligands by functionalizing exclusively all microwell walls [19–22]. By patterning an SLB to the microwell walls we can present mobile and immobile membrane cues from the same substrate to subsequently patterned single cells in each well (see schematic of the patterning and functionalization in Fig. 1), and to directly and easily investigate the respective or combined effects of ligand mobility and dimensionality of presentation. The platform is demonstrated through the culturing of Chinese hamster ovary (CHO) cells expressing GFP-cadherin in microwells functionalized with variably mobile and immobile E-cadherin.

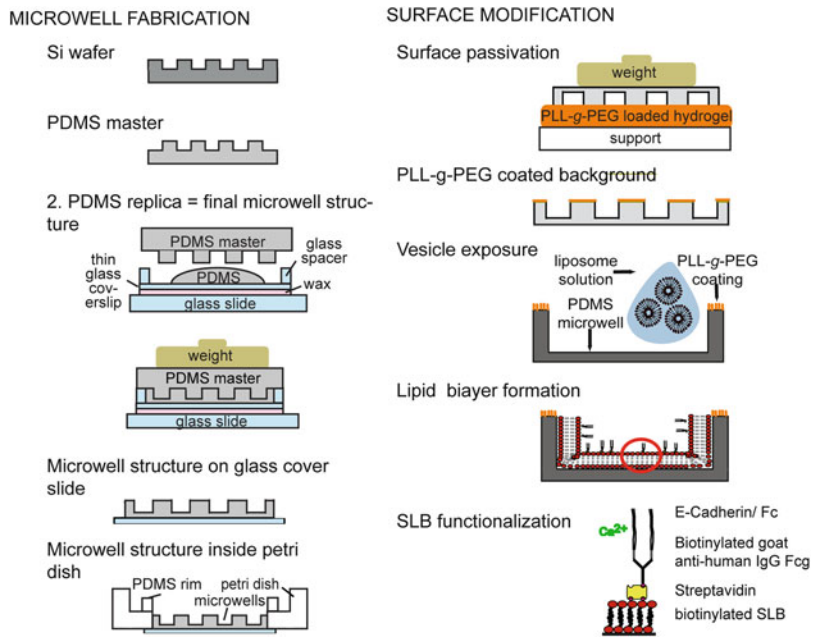

Fig. 1 Schematic of the fabrication of the microwell platform and subsequent chemical coating of the microwell. After fabrication of the microwell structure in silicon, the structure is replicated into PDMS. In order to transfer the microwell pattern from the silicon master into a thin film of PDMS, a thin glass coverslip is glued onto a glass specimen slide between which the PDMS is cast. This sandwich is pressed together with a weight while the PDMS is cured. The master and glass support are removed leaving behind a thin PDMS film bound to the coverslip which is then glued to the bottom of a Petri dish into which a hole has been drilled (*left*). The microwell plateau surface is passivated by inverted micro-contact printing of PLL-*g*-PEG using a PAAm stamp. After plateau passivation the sample is exposed to a solution containing liposomes. The liposomes can only adsorb inside the microwells. Subsequently the biotinylated SLB was functionalized with streptavidin, biotinylated IgG Fcg, and E-cadherin/Fc (*right*) (Figure adapted from [19, 21, 22])

2 Materials

Prepare all solutions using ultrapure water (prepared by purifying pre-filtered, UV-treated, and deionized water to attain a resistivity of 18.2 MΩ cm at 25 °C).

2.1 Buffer Solutions

1. PBS buffer: 137 mM NaCl, 10 mM Phosphate, 2.7 mM KCl, pH 7.4. Store at 4 °C. Filter the PBS buffer solution prior to use (0.22 μm syringe filter).
2. PBS calcium buffer: PBS buffer as described above with an additional 0.2 mM Ca^{2+}. Store at 4 °C.
3. HEPES Buffer: 10 nM 4(2-hydroxyethyl)piperazine-1-ethanesulfonic acid (HEPES), 150 mM NaCl. Adjust to pH 7.4 with 6 M NaOH. Store at 4 °C. Filter the HEPES buffer solution prior to use (0.22 μm syringe filter).

2.2 Microwell Fabrication

1. Produce a photolithographic mask with arrays of microwells with different geometries of choice (circles, squares, triangles, rectangles, spindles, etc.) and of dimensions matching the studied cell type (e.g., 81–900 μm² projected area) (*see* **Note 1**).
2. Silicon wafers (p type, <100>, polished, Si-Mat Silicon Materials, Germany).
3. SU-8 2010 (negative resist; MicroChem, USA).
4. SU-8 developer (MicroChem, USA).
5. Isopropanol.
6. Polydimethylsiloxane (PDMS) with curing agent.
7. 1H,1H,2H,2H-Perfluorooctyltrichlorosilane.
8. Air plasma cleaner.
9. Exsiccator.
10. Glass cover slides [round, $x = 10–24$ mm, thickness 0 (0.08–0.12 mm)].

2.3 Surface Modification

1. PAAm-pre-gel solution: Acrylamide 4K-Solution (30 %) Mix 37.5:1.
2. Ammonium persulfate (APS): 10 % w/v APS in PBS buffer.
3. *N*,*N*,*N*,*N*-tetramethyl ethylenediamine (TEMED).
4. PLL-*g*-PEG stock solution (PLL-*g*-PEG poly(L-lysine)-*graft*-*poly*(ethylene glycol) PLL(20 kDa)-*g*-[3.4]-PEG(2 kDa); SuSoS, Switzerland): 50 mg/mL in HEPES buffer. Store below −18 °C.
5. Glass slides (76 mm × 26 mm × 1 mm).

2.4 Liposome Preparation and SLB Functionalization

1. Liposome solution: Mix the lipids described below in the desired quantities. Vary the amount of PMMC in order to tune the mobility of the lipid system (*see* **Note 2**).
2. 1,2-Dioleoyl-*sn*-Glycero-3-Phosphoethanolamine-*N*-(Cap Biotinyl) Sodium salt (bDOPE): 25 mg/mL in chloroform. Store at −18 °C (*see* **Note 3**).
3. 1,2-Dioleoyl-*sn*-Glycero-3-Phosphocholine (DOPC): 25 mg/mL in chloroform. Store at −18 °C (*see* **Note 4**).
4. 1-myristoyl-2-palmitoyl-*sn*-glycero-3-phosphocholine (PMMC): 25 mg/mL in chloroform. Store at −18 °C (*see* **Note 5**).
5. LiposoFast extruder (Avestin, Canada).
6. Polycarbonate membrane, pore size 100 nm (Avestin, Canada).
7. Ultrasonicator.
8. Streptavidin (SA): 50 μg/mL in HEPES buffer, store at −18 °C.

9. Biotinylated goat anti-human IgG Fcg (bAB; eBioscience): 10 µg/mL in HEPES buffer, store at –18 °C.
10. E-cad/Fc: 10 µg/mL in PBS calcium buffer, store at –18 °C (*see* **Note 6**).

2.5 Cell Culture

1. Blocking solution: Bovine serum albumin (BSA) 4 wt.% in PBS buffer. Filter (0.22 µm syringe filter) and store at –18 °C.
2. Chinese hamster ovary (CHO) cells expressing GFP-cadherin were obtained from Deborah Leckband, University of Illinois, Urbana-Champagne (*see* **Note 7**).
3. Permeabilization solution: 0.1 % Triton X-100 and 1.5 % formalin in PBS buffer. Store at 4 °C.
4. Fixing solution: 3 % formalin in PBS buffer. Store at 4 °C.

3 Methods

3.1 Microwell Fabrication

This description corresponds to the schematic outlined in Fig. 1 left.

1. Place silicon wafers on a hot plate for 5 min at 190 °C for dehydration. Spin coat SU-8 2010 for 90 s at 2,000 rpm. To soft bake, heat the wafer for 2 min at 65 °C, followed by 2 min at 95 °C. Expose the photo resist on the sample for 15 s (12 mW/cm^2) to UV light using a mask aligner. In the following post-exposure bake, place the wafer onto a hot plate at 65 °C and at 95 °C for 2 min each. Develop the photoresist in SU-8 developer for 2 min, rinse thoroughly with isopropanol and dry with nitrogen. In the final hard baking step, place the sample onto a hot plate at 65 °C and heat up to 150 °C. Bake the sample at 150 °C for additional 5 min. These parameters lead to a resist thickness of 10 µm (*see* **Note 8**).
2. Mix polydimethylsiloxane 1:10 (weight ratio, w/w curing agent to pre-polymer), degas in an exsiccator until all air bubbles disappear. For silicon master replication, pour PDMS over the wafer to a thickness of about 5 mm. Cure the polymer at 80 °C for 4 h. Cut out the structure of interest.
3. Treat the structure of interest by air plasma for 30 s before exposing it to fluorosilanes in gas phase for 1 h.
4. Place the fluorosilanized master onto a drop of PDMS that is placed onto a thin glass coverslip. Apply a weight of 5 g to the sandwich structure to press it together while the PDMS is cured at 80 °C for 4 h. Remove the master and glass support leaving behind a thin PDMS film bound to the coverslip. Glue the coverslip with PDMS to the bottom of a Petri dish into which a hole has been drilled to accommodate the structure (*see* **Note 9** and Fig. 2 left).

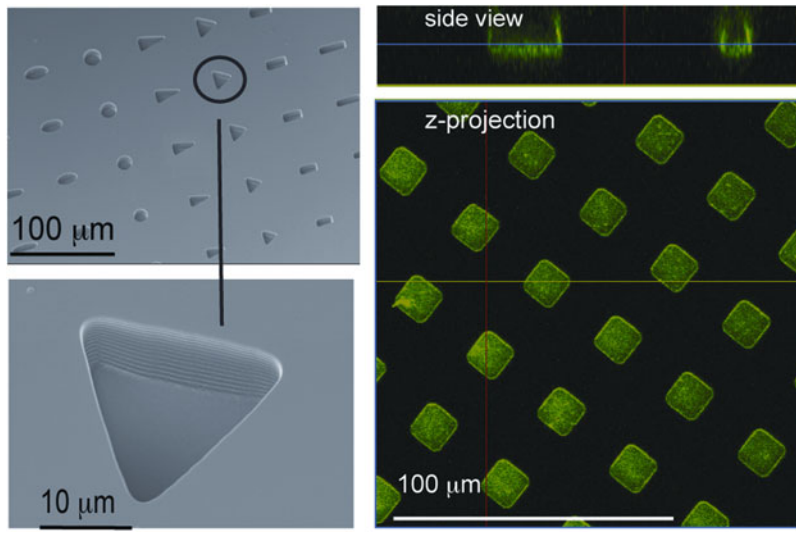

Fig. 2 Scanning electron micrographs of the microwell surface shows wells with different shapes and a zoom into a single triangular well (*left*). SLB coating inside microwells (*right*). The side view highlights SLB coverage of both the walls and the bottom of the microwells but not of the plateau. The bottom image shows a z-projection of a confocal image stack. The *green* signal is NBD-PC showing lipid presence only inside microwells (Figure adapted from [19]) (Color figure online)

3.2 Surface Modification

The following description corresponds to the schematic presented in Fig. 1 right.

1. PAAm hydrogel: Add 20 μL of the PLL-*g*-PEG stock solution to 1 mL of PAAm pre-gel solution, 10 μL of ammonium persulfate and 2 μL of TEMED. Mix gently.
2. Cast and cure the PAAm hydrogel containing the dissolved PLL-*g*-PEG between two 1 mm glass slide spacers resulting in a flat stamp. After 1 h remove the gel from the glass slide spacers, cut into smaller pieces (5 × 5 mm) and store in a humid environment (*see* **Note 10**).
3. Expose the microstructured PDMS surface (from Subheading 3.1) to air plasma (0.1 mbar, 30 s).
4. Place the flat hydrogel functionalized with PLL-*g*-PEG upside down onto the structured substrate. Apply a weight of 5 g during the 15 min stamping procedure (*see* **Note 11**).
5. Expose the microwells to the liposome solution for at least 15 min and rinse with HEPES buffer (*see* **Note 12**).

3.3 SLB Functionalization

1. Add streptavidin for 10 min to the sample. Rinse with HEPES buffer (*see* **Note 13** and Fig. 2 right).
2. Add biotinylated IgG for 30 min (bIgG). Rinse with HEPES buffer.

3. Add Fc tagged domain of human E-cadherin (E-cad/Fc) for 30 min. Rinse with HEPES buffer.
4. Store the final sample in PBS calcium buffer and continue immediately with cell culturing.

3.4 Cell Culture

1. Seed 50,000 cells/cm^2 onto the microwell surface and incubate for 2 h before gently rinsing with PBS calcium buffer (*see* **Notes 14–16**).
2. Permeabilize the cells with permeabilization solution for 5 min at room temperature. Rinse samples carefully.
3. Fix for 10 min at room temperature using fixing solution. Rinse samples carefully with PBS buffer.
4. Block the samples for 1 h at room temperature with blocking solution. Rinse samples carefully with PBS buffer.
5. Incubate with staining dye of interest (*see* **Note 17**).
6. Observe and image the stained sample under a regular fluorescence microscope or under a high resolution fluorescence scanning confocal microscope.

4 Notes

1. To provide the cell a 3D environment it is important that they fit perfectly into the microwell. If the microwell is too big, the cells will spread on the bottom; it is not possible for the cell to adhere to the walls and the higher dimensionality is lost. Depending on the cell type the size of the microwell has to be adjusted.
2. Depending on the requirements of your system the lipid composition melting temperature can be controlled by the lipid mixture. DOPC or MPPC are used as the main lipid fraction and mixed with bDOPE. If the cell adhesive ligands are desired in only the laterally mobile state, a DOPC/bDOPE mixture is sufficient. The melting transition temperature of the main lipid fraction will determine the temperature at which the ligand mobility can be switched on and off, and should be tuned to close to the preferred cell culture temperature.
3. Depending on the desired density of the presented ligand, the amount of bDOPE might be varied. In our studies 99.5 wt.% DOPC with 0.5 wt.% bDOPE for low density ligand presentation or 95 wt.% DOPC with 5 wt.% bDOPE for high density was used.
4. DOPC/bDOPE liposomes were extruded following a modified protocol from MacDonald et. al. [23]. Mix lipid solutions

in a clean glass flask. Dry the lipids for at least 30 min under a flow of nitrogen. Add 1 mL of HEPES buffer to hydrate the lipid film forming liposomes. Extrude the liposome suspension 31 times through a 100 nm polycarbonate membrane using a LiposoFast extruder (Avestin, Canada). Dilute the liposome solution with HEPES buffer to a final concentration of 0.5 mg/mL and store at 18 °C for up to 2 weeks.

5. Mix lipid solutions in a clean glass flask. Dry the lipids for at least 30 min under a flow of nitrogen. Add 1 mL of HEPES buffer to hydrate the lipid film forming liposomes. Sonicate 1 mL of a 5 mg/mL rehydrated lipid solution in a glass tube in a 40 °C warm water bath.
6. The cell type can be exchanged for any cell of interest under application of the appropriate culture conditions. In the presented protocol the cell type and conditions were developed as follows. The plasmid encoding the full length human E-cadherin cDNA was obtained from B. Gumbiner (University of Virginia) [24]. Human E-cadherin/Fc chimera (E-cad/Fc) was received from D. Leckband (University of Illinois) and engineered by Yuan Hung Chien as described in [25].
7. Chinese hamster ovary (CHO) cells expressing GFP-cadherin were obtained from Deborah Leckband (University of Illinois). The cells were stably transfected with plasmids encoding the Fc tagged extracellular domain of human E-cadherin as described in [26]. They were cultured in DMEM with 10 % serum plus 150 μg/mL G418 (Gibco). CHO cells expressing full-length human E-cadherin were transfected with the plasmid using Lipofectamine, and stable clones were selected with G418 (800 μg/mL). Surface expression was verified by fluorescence activated cell sorting [24, 26].
8. This is a standard photolithographic process and more details can be found in literature [27]. Alternatively, the microwell structure can be etched into a silicon wafer. The rest of the protocol can be used as described here.
9. You can prepare many microwell dishes in parallel and store them for up to 3 months at room temperature. When you take them from storage to perform experiments you should do the steps from the stamping (*see* Subheading 3.2) until the cell fixation (*see* Subheading 3.4) in one run.
10. The samples can be stored in a Petri dish; add a piece of tissue soaked in water and seal with parafilm. The sample can be stored at 4 °C for up to 1 week.
11. PLL-*g*-PEG can partially coat the walls of the microwell if the stamping step is not carefully performed. This prevents a homogenous SLB from forming in the subsequent step. It

helps to perform the stamping upside down so that the PLL-*g*-PEG cannot flow into the microwells.

12. The sample is never exposed to air after liposome exposure, as air exposure results in SLB delamination and aggregation.
13. 100 μL are normally needed to keep the sample well covered with solution. This volume can be applied for all the solutions in the functionalization steps.
14. It is very important to rinse the sample carefully but gently. In order to have a sample with cells only in the microwells all the non-attached cells on the substrate top surface have to be removed, but the adhering cells in the microwells should remain unperturbed. We succeeded in rinsing up to ten times very gently and slowly. It is also very important that the sample is not exposed to air, but a PBS film remains on the substrate at all times.
15. Depending on the cell type the incubation time has to be adjusted. If there are no cells adhering, it is worth trying to lengthen the incubation time. If cells are adhering everywhere, a shortening of the incubation time might give better results.
16. For a mobile ligand presentation a DOPC/bDOPE mixture of the lipid was used; regular cell culture conditions are applied (37 °C, 5 % CO_2). If working with a tunable mobility, the temperature has to be adjusted. With a pure MPPC/bDOPC mixture, a cell culture temperature of 30 °C results in immobile presentation of the cell adhesive ligands while the regular settings at 37 °C present them in their mobile state.
17. A dye directly detecting a specific protein can be used, e.g., Phalloidin-Alexa 488 labeling actin, alternatively an antibody of interest might be used and fluorescently labeled via a secondary antibody. The incubation times of the dye of interest might have to be slightly prolonged compared to labeling of a flat interface.

References

1. Kusumi A, Suzuki K, Koyasako K (1999) Mobility and cytoskeletal interactions of cell adhesion receptors. Curr Opin Cell Biol 11:582–590
2. Yap AS, Brieher WM, Gumbiner BM (1997) Molecular and functional analysis of cadherin-based adherens junctions. Annu Rev Cell Dev Biol 13:119–146
3. Cavallaro U, Christofori G (2004) Cell adhesion and signalling by cadherins and Ig-CAMs in cancer. Nat Rev Cancer 4:118–132
4. Mossman KD, Campi G, Groves JT, Dustin ML (2005) Altered TCR signaling from geometrically repatterned immunological synapses. Science 310:1191–1193
5. Takeichi M (1991) Cadherin cell-adhesion receptors as a morphogenetic regulator. Science 251:1451–1455
6. Salaita K, Nair PM, Petit R, Neve R, Das D, Grey J, Groves J (2010) Restriction of receptor movement alters cellular response: physical force sensing by EphA2. Science 327: 1380–1385
7. Tozeren A, Sung KL, Sung LA, Dustin ML, Chan PY, Springer TA, Chien S (1992) Micromanipulation of adhesion of a Jurkat cell to a planar bilayer membrane containing lymphocyte function-associated antigen 3 molecules. J Cell Biol 116: 997–1006

8. Gumbiner BM (1996) Cell adhesion: the molecular basis of tissue architecture and morphogenesis. Cell 84:345–357
9. Takeichi M (1995) Morphogenetic roles of classic cadherins. Curr Opin Cell Biol 7:619–627
10. Yap AS (1998) The morphogenetic role of cadherin cell adhesion molecules in human cancer: a thematic review. Cancer Invest 16: 252–261
11. Mege R-M, Gavard J, Lambert M (2006) Regulation of cell-cell junctions by the cytoskeleton. Curr Opin Cell Biol 18:541–548
12. Groves JT, Dustin ML (2003) Supported planar bilayers in studies on immune cell adhesion and communication. J Immunol Methods 278:19–32
13. Berat R, Remy-Zolghadry M, Gounou C, Manigand C, Tan S, Salto C, Arenas E, Bordenave L, Brisson AR (2007) Peptide-presenting two-dimensional protein matrix on supported lipid bilayers: an efficient platform for cell adhesion. Biointerphases 2:165–172
14. Perez TD, Nelson WJ, Boxer SG, Kam L (2005) E-Cadherin tethered to micropatterned supported lipid bilayers as a model for cell adhesion. Langmuir 21:11963–11968
15. Svedhem S, Dahlborg D, Ekeroth J, Kelly J, Hook F, Gold J (2003) In situ peptide-modified supported lipid bilayers for controlled cell attachment. Langmuir 19:6730–6736
16. Nam J-M, Nair PM, Neve RM, Gray JW, Groves JT (2006) A fluid membrane-based soluble ligand-display system for live-cell assays. Chembiochem 7:436–440
17. Thid D, Holm K, Eriksson PS, Ekeroth J, Kasemo B, Gold J (2008) Supported phospholipid bilayers as a platform for neural progenitor cell culture. J Biomed Mater Res A 84:940–953
18. Tsai J, Kam LC (2010) Lateral mobility of E-Cadherin enhances rac1 response in epithelial cells. Cell Mol Bioeng 3:84–90
19. Andreasson-Ochsner M, Romano G, Håkanson M, Smith ML, Reimhult E, Vogel V, Textor M (2011) Single cell 3-D platform to study ligand mobility in cell–cell contact. Lab Chip 11:2876–2883
20. Dusseiller M, Smith ML, Vogel V, Textor M (2006) Microfabricated three-dimensional environments for single cell studies. Biointerphases 1:P1–P4
21. Ochsner M, Dusseiller MR, Grandin HM, Luna-Morris S, Textor M, Vogel V, Smith ML (2007) Micro-well arrays for 3D shape control and high resolution analysis of single cells. Lab Chip 7:1074–1077
22. Ochsner M, Textor M, Vogel V, Smith ML (2010) Dimensionality controls cytoskeleton assembly and metabolism of fibroblast cells in response to rigidity and shape. PLoS One 5:e9445
23. MacDonald RC, MacDonald RI, Menco BPM, Takeshita K, Subbarao NK, Hu LR (1991) Small-volume extrusion apparatus for preparation of large, unilamellar vesicles. Biochim Biophys Acta 1061:297–303
24. Niessen CM, Gumbier BM (2002) Cadherin-mediated cell sorting not determined by binding or adhesion specificity. J Cell Biol 156: 389–399
25. Chien Y-H, Jiang N, Li F, Zhang F, Zhu C, Leckband D (2008) Two-stage cadherin kinetics require multiple extracellular domains but not the cytoplasmic region. J Biol Chem 283: 1848–1856
26. Zhu B, Chappuis-Flament S, Wong E, Jensen IE, Gumbiner BM, Leckband D (2003) Functional analysis of the structural basis of homophilic cadherin adhesion. Biophys J 84: 4033–4042
27. Sorribas H, Padeste C, Tiefenauer L (2002) Photolithographic generation of protein micropatterns for neuron culture applications. Biomaterials 23:893–900

Chapter 8

Basement Membrane Invasion Assays: Native Basement Membrane and Chemoinvasion Assay

Marie Schoumacher, Alexandros Glentis, Vasily V. Gurchenkov, and Danijela M. Vignjevic

Abstract

To escape the primary tumor and infiltrate stromal compartments, invasive cancer cells must traverse the basement membrane (BM). To break this dense matrix, cells develop finger-like protrusions, called invadopodia, at their ventral surface. Invadopodia secrete proteases to degrade the BM, and then elongate which allows the cell to invade the subjacent tissue. Here, we describe two complementary invasion assays. The native BM invasion assay, based on BM isolated from rat or mouse mesentery, is a physiologically significant approach for studying the stages of BM crossing at the cellular level. The Matrigel-based chemoinvasion assay is a powerful technique for studying invadopodia's molecular composition and organization at the subcellular level.

Key words Invasion, Basement membrane, Invadopodia, Chemoinvasion assay

1 Introduction

The formation of secondary tumors or metastases is the major cause of death by cancer. To form metastases, cancer cells must escape the primary tumor site, migrate into surrounding tissues, and colonize a distant organ. The first barrier faced by invasive cancer cells is the basement membrane (BM), a dense and rigid matrix, composed mainly of collagen IV and laminin [1]. Invasive cancer cells use a similar mechanism as leucocytes and the Anchor Cell in *Caenorhabditis Elegans* to cross this physiological obstacle [2–6]. First, they develop invasive feet (described as invadopodia for cancer cells) which perforate the BM. Later these protrusions elongate (up to 7 μm) into the degraded zone, and finally, the cell infiltrates the underlying stromal compartment [7].

Amanda S. Coutts (ed.), *Adhesion Protein Protocols*, Methods in Molecular Biology, vol. 1046,
DOI 10.1007/978-1-62703-538-5_8,

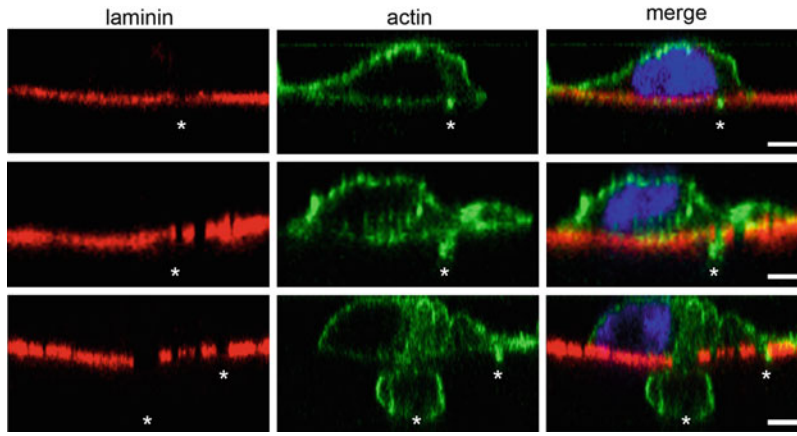

Fig. 1 Invasion of cancer cells—native basement membrane assay. Human colon carcinoma cells (HCT116) cultured atop of a mesothelial basement membrane. BM detected by laminin staining (*red*). Cells were visualized by staining the actin cytoskeleton using phalloidin-A488 (*green*) and the nucleus using DAPI (*blue*). *Top panels*: stage 1-early stage of invasion characterized by degradation of the BM and formation of short invasive protrusions (invadopodia). *Middle panels*: stage 2-intermediate stage of invasion and formation of long invasive protrusions (mature invadopodia). *Bottom panels*: stage 3-late stage of invasion and infiltration of the cell on the other side of the membrane. *Asterisks* indicate sites of degradation and localization of invasive protrusions. Scale bars 5 μm. Modified from [7] (Color figure online)

This BM transmigration program has been described using a native BM isolated from the rat mesentery, which is the best mimic for in vivo BM [5, 8] (Fig. 1). However, the isolation of this native BM does not allow high throughput experiments. Thus, in vitro studies on BM degradation and invadopodia routinely use commercially available artificial matrixes, mostly a 2 μm-thin layer of fluorescent gelatin [9] or a thick layer of Matrigel [10, 11]. Both have advantages and disadvantages [4]. While the use of fluorescent gelatin allows precise quantification of matrix degradation and the characterization of invadopodia formation, the advantage of using Matrigel, is that it has a similar molecular composition as the native BM. However, neither is adequate to study invadopodia elongation: the limited thickness (2 μm) of the gelatin layer and the absence of cell attraction for the thick layer of Matrigel prevent the elongation of invadopodia as it occurs on a physiological BM.

To overcome these issues, we have developed a new technique: the chemoinvasion assay [4, 7]. This assay is similar to the modified Boyden chamber in which cells are plated on filters containing 8 μm-diameter pores and chemo-attracted using growth factor-enriched medium in the lower chamber. In the chemoinvasion assay, cells are plated on membranes containing 1 μm-diameter pores and coated with a thin layer of fluorescently labeled Matrigel to mimic BM. The matrix closes the entry of the pores and fills them at least along the two first microns (Fig. 2). One micron corresponds to the average diameter of invadopodia and is smaller

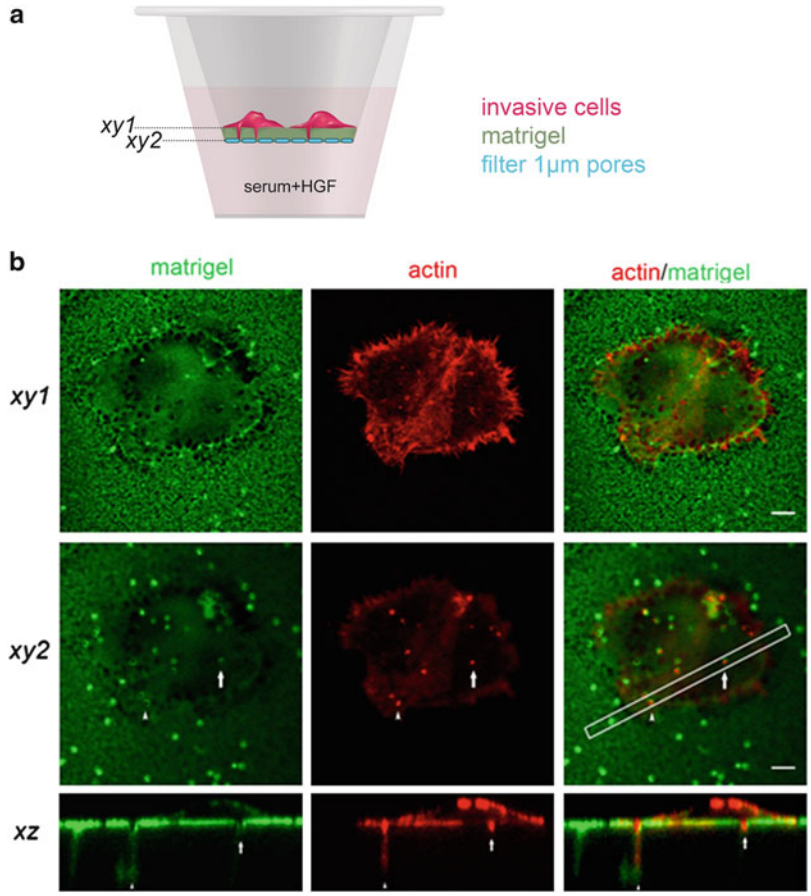

Fig. 2 Invasion of cancer cells—chemoinvasion assay. (**a**) Schematic diagram of the chemoinvasion assay. (**b**) Immunofluorescence of MDA-MB-231 cells in the chemoinvasion assay. Fluorescent Matrigel (*green*); actin stained with phalloidin-Cy3 (*red*). *Top panels*: *x–y* projections, representing the cells at the focal plane of the filter. *Arrows* indicate a protrusion. On the merge picture, the white rectangle highlights the transversal cut shown in the bottom panels. Scale bar 5 μm. *Bottom panels: x–z* projections showing transversal cut through the cell at the level of the protrusion. Scale bars 1 μm. Adapted from [7] (Color figure online)

than cell nuclei. As a consequence, cells are unable to traverse the membrane and invadopodia are captured within the pores. Moreover, the membrane is about 10 μm-thick, which allows the elongation of invadopodia. Therefore, the chemoinvasion assay provides a robust method to study the second step of BM crossing and to "capture" elongated invadopodia.

In the first part of this chapter, we describe an invasion assay based on native BM from rat or mouse mesentery initially developed by Steve Weiss' laboratory, and in the second part, how to assemble the chemoinvasion assay. In the third section we describe how to stain invasive cells by immunofluorescence for both assays and provide advice for the imaging of the invasive structures.

2 Materials

2.1 Native BM Invasion Assay

1. 9–12 months-old male Wistar rats (approximately 500 g) or C57/B6 mice (*see* **Note 1**).
2. Tails of 9–12 months-old male Wistar rats. Store tails at −80 °C.
3. Ketamine or any other drug to euthanize rats.
4. Non-coated cell culture inserts for 24-well plates of any pore size, transparent PET membrane, with their companion plate (BD Biosciences).
5. 15 cm petri dishes.
6. Silk sewing thread (Péters Surgical) (*see* **Note 2**) or Vetbond tissue adhesive (3M).
7. Ammonium hydroxide, 1 N in dH_2O. Store at 4 °C.
8. Acetic acid diluted 1:500 in dH_2O. Store at 4 °C.
9. *Optional*: Hank's balanced salt solution (HBSS) 1×: 1.26 mM $CaCl_2$, 0.49 mM $MgCl_2$, 0.4 mM $MgSO_4$, 5.33 mM KCl, 0.44 mM KH_2PO_4, 4.17 mM $NaHCO_3$, 137.93 mM NaCl, 0.338 mM Na_2PO_4, 5.56 mM D-Glucose.
10. Phosphate buffer saline (PBS): 137 mM NaCl, 2.7 mM KCl, 4.3 mM Na_2HPO_4, 1.47 mM KH_2PO_4.
11. Antimycotic amphotericin B solution (trade name Fungizone, Sigma-Aldrich).
12. Antibiotic gentamicin solution (Sigma-Aldrich).
13. Antibiotic–Antimycotic solution (100×, amphotericin B, penicillin, streptomycin; Invitrogen).
14. Complete medium: DMEM supplemented with 10 % FBS, 100 μg/mL gentamicin and 1 μg/mL Fungizone (*see* **Note 3**).
15. 70 % ethanol.

2.2 Chemoinvasion Assay

1. Laminin from Engelbreth-Holm-Swarm murine sarcoma basement membrane 1 mg/mL in Tris buffered NaCl, suitable for cell culture (Sigma-Aldrich).
2. Matrigel (BD Matrigel—BD Biosciences) (*see* **Note 4**): Upon reception, thaw on ice at 4 °C overnight. Aliquot and store at −20 °C.
3. Trypsin.
4. Complete medium.
5. Hepatocyte Growth Factor (HGF) (EMD Millipore): Upon reception, reconstitute the powder in water to a stock concentration of 0.5 mg/mL. Aliquot and store at −20 °C (*see* **Note 5**).
6. PBS.

7. Slide-A-Lyzer Dialysis Cassettes, 10K MWCO (Pierce, Thermo Fisher Scientific).
8. Protein labeling kit (Invitrogen) (*see* **Note 6**).
9. Non-coated cell culture inserts for 12-well plates (10.5 mm-diameter membrane), 1 μm pores, transparent PET membrane, with their companion plate (BD Biosciences) (*see* **Note 7**).

2.3 Immunofluorescence

1. Paraformaldehyde (PFA): 4 % in PBS.
2. PBS.
3. 1× PEM buffer: 100 mM PIPES pH 6.9, 1 mM $MgCl_2$, 1 mM EGTA.

   To make 100 mL of 2× stock solution, mix 70 mL of dH_2O and 6 g of PIPES. While stirring, add concentrated KOH to this turbid solution until it almost clears. Add 76 mg of EGTA and 200 μL of 1 M stock of $MgCl_2$, adjust pH to 6.9 with 1 N KOH, and complete with distilled water to 100 mL. Store at 4 °C.
4. Extraction buffer: 0.5 % Triton X-100, 4 % PEG in 1× PEM (*see* **Note 8**).

   To make 10 mL, combine 5 mL of 2× PEM, 1 mL of 10 % Triton X-100, 400 mg PEG, complete to 10 mL with dH_2O. Stir for 10 min until dissolved. Store at 4 °C and use within 1 week.
5. Prolong Gold anti-fade reagent (Invitrogen).
6. Superfrost glass slides.
7. Rectangular coverslips (thickness of category 1: 0.13–0.16 mm).

3 Methods

3.1 Native BM Invasion Assay

3.1.1 Preparation of Collagen I

1. Thaw rat tails at room temperature (RT).
2. Leave tails in 70 % ethanol for 30 min.
3. Remove tails from ethanol and air-dry (or with the help of a paper towel). From this point on, do everything in a hood to maintain sterility.
4. Remove the skin. Break the vertebrae.
5. Extract the tendons and place them in 70 % ethanol (use a 15 cm round plate). Separate thick strands of tendons into finer strands. Allow to air-dry under a hood.
6. Transfer the dried tendons to a recipient containing dilute acetic acid. Use 1 mL of dilute acetic acid for about 1–2 mg of tendons.
7. Close the recipient and leave for 5 days at 4 °C. Mix several times a day to ensure correct extraction.

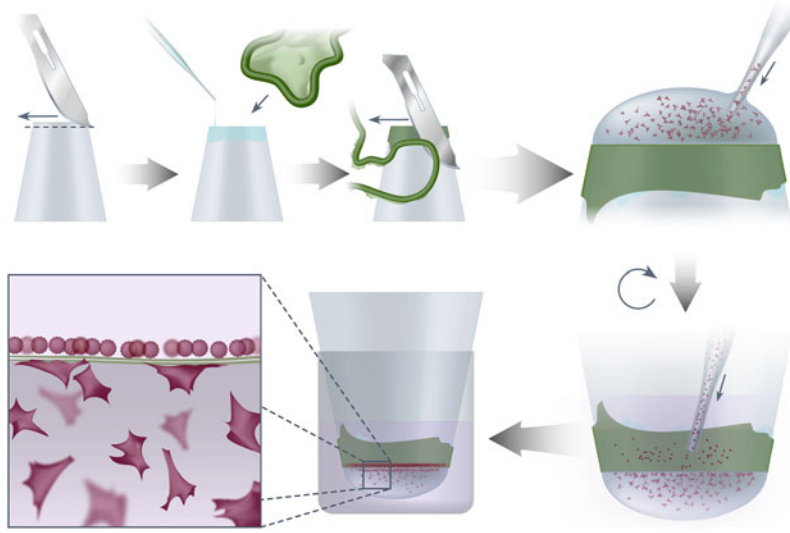

Fig. 3 Assembly of cocultures using the native basement membrane assay. Mesothelial basement membrane isolated from mouse or rat (intestine shown in *green*) (Color figure online)

8. Centrifuge the solution at 3,000 × *g* for 30 min at 4 °C. Collect the supernatant avoiding any solids and clumps of gelled collagen.
9. Transfer the supernatant into a 50 mL tube (approx. 20–30 mL/tube) and spin at 4,000 × *g* for 30 min at 4 °C.
10. Lyophilize the collagen and store it at −80 °C (*see* **Note 9**).
11. Prepare a stock solution of collagen at 2.2 mg/mL. Weigh the lyophilized collagen and dissolve it in cold dilute acetic acid overnight. Store at 4 °C.

3.1.2 Assay Assembly (Fig. 3)

1. Add antibiotic–antimycotic solution (1 % final) or gentamicin (100 μg/mL final) and amphotericin B (1 μg/mL final) to all buffers (PBS, HBSS) and media to avoid contamination.
2. Cut out the membrane from the non-coated cell culture insert using a scalpel and discard (*see* Fig. 3). Hold insert with forceps.
3. Euthanize rat or mouse.
4. Open the thoracic cage and keep it humid by placing PBS-soaked gaze around the opened thorax and filling the thorax with PBS.
5. Take out the intestine without cutting it (*see* **Note 10**).
6. If mouse tissue is used, apply Vetbond glue to the sides of the insert, stretch the mesentery around the insert (*see* **Note 11**) and press with forceps to ensure attachment. Cut the mesentery above glued area and remove intestine. If rat mesentery is used, stretch it around the insert. Cut the mesentery around the inset and sew it with silk thread above the plastic node (*see* **Note 12**).

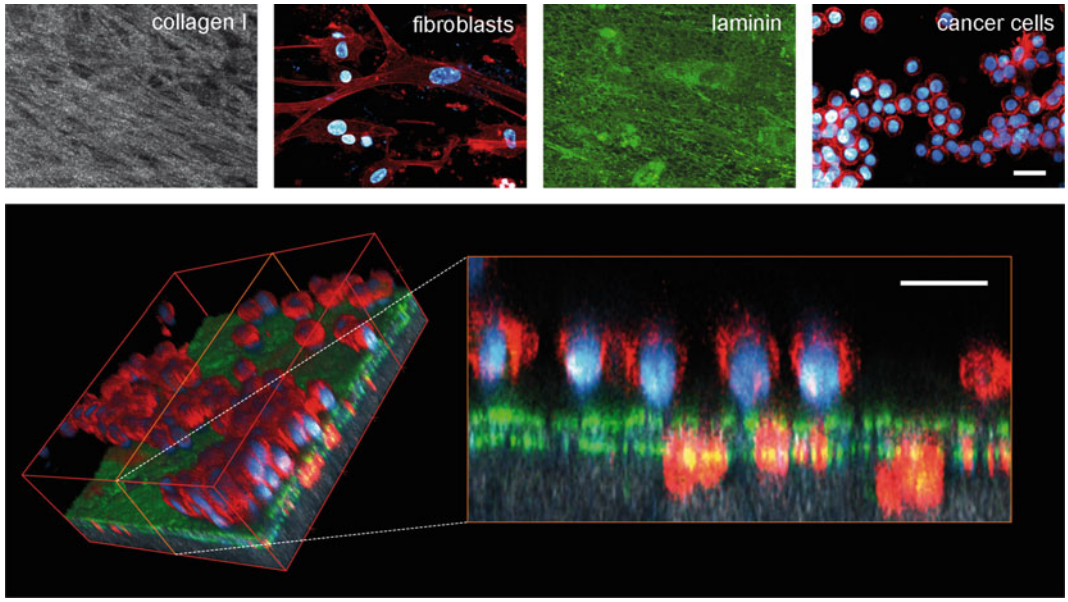

Fig. 4 Coculture of cancer cells and fibroblasts in the native basement membrane assay. Human colon carcinoma cells (HT29) cultured atop of a mesothelial basement membrane. *Top panels*: *x–y* projections of different focal planes. BM detected by laminin staining (*green*). Collagen I detected using reflectance (*white*). Cells visualized by staining the actin cytoskeleton using phalloidin-Cy3 (*red*) and the nucleus using DAPI (*cyan*). *Bottom panels*: *x–y–z* maximal projection projections. Grid pitch 50 μm. Scale bars 30 μm (Color figure online)

7. Place the insert in a 24-well plate filled with PBS.
8. Rinse 1× with PBS (*see* **Note 13**).
9. Add 1 N ammonium hydroxide. Incubate for 1 h at RT (*see* **Note 14**).
10. Wash 3× with PBS.
11. *Optional*: Wash 3× with HBSS.
12. To coat the bottom of the insert with collagen stock solution, aspirate the PBS. Turn the insert upside down. Place the insert on the cover plate of a 15 cm petri dish.
13. (a) For single cell type experiments: Add 50–100 μL of collagen stock solution on the top of the insert (i.e., bottom of the membrane when the insert is on the right orientation). Close the petri dish.
    (b) For coculture experiments (Fig. 4) (*see* **Note 15**): Prepare 1 mL of cell type 1 (for example fibroblasts) at a concentration of 10^5 cells/mL. Spin down cells at 100 × *g* using a top bench centrifuge, for 3 min and keep the pellet on ice. Add 500 μL of collagen stock solution on ice (*see* **Note 16**). Mix gently to avoid bubbles. Add a 100 μL drop of the collagen stock solution–cell mix on to the top of the insert.

14. Let the collagen–cell mixture polymerize for at least 30 min at RT (*see* **Note 17**). If the cells are not embedded in the collagen, polymerization could proceed at 37 °C (*see* **Note 18**).
15. Place the insert in a 24-well plate filled with 750 μL of complete medium (collagen drop pointing down) and add 500 μL of complete medium on top.
16. Prepare solution of cell type 2 (for example cancer cells) at a concentration of 2×10^5 cells/mL.
17. Aspirate the medium in the inserts. Add 500 μL of cell preparation in the upper side of the insert (final cell density 10^5).
18. Let the cells incubate at 37 °C for several days (*see* **Note 19**).

3.2 Chemoinvasion Assay

3.2.1 Laminin Labeling with Fluorescent Dyes

1. Thaw the laminin on ice or at 4 °C overnight.
2. Transfer the laminin solution into a Slide-A-Lyzer Dialysis Cassette. Dialyze against PBS overnight at 4 °C.
3. Label the laminin using the protein labeling kit. Follow instructions given by the manufacturer.
4. Select fractions that contain the labeled laminin: look at the collected fractions under a fluorescence microscope. Keep only the 2–3 fractions with the highest fluorescence intensity. Measure the concentration using the absorbance at 280 nm with a spectrophotometer (usually around 0.5 mg/mL) (*see* **Note 20**).

3.2.2 Assay Assembly

Work at 4 °C (in the cold room) unless specified.

1. Prepare the matrix. Thaw Matrigel and fluorescent laminin on ice. Make a 1:1 mix of Matrigel (stock solutions vary between batches but are usually around 9–10 mg/mL) with fluorescent laminin (*see* **Note 21**).
2. Add 80 μL of the Matrigel/laminin mix on top of the filter. Let it stand for 1 h at 4 °C.
3. Remove 75 μL of the matrix. Incubate the inserts at 37 °C for 30 min to allow matrix polymerization (*see* **Note 22**).
4. Rehydrate the matrix. Add 1.5 mL of complete medium in the well of the companion plate. Transfer the coated insert in the plate and cover with 1 mL of complete medium.
5. Let it stand at 37 °C while preparing cells.
6. Prepare cell solution at $4–5 \times 10^4$ cells/mL in serum-free medium (*see* **Note 23**). Add antibiotics to the medium to avoid contamination.
7. Prepare attraction medium: cell culture medium supplemented with 15 % FBS and 40 ng/mL HGF (*see* **Note 5**).
8. Aspirate the media from the inserts and the wells of the plate. Add 1.5 mL of the attraction medium to each well. Add 1 mL of cell preparation in the upper side of the insert.
9. Let the cells incubate at 37 °C overnight (*see* **Note 24**).

3.3 Immunofluorescence of Invading Cells and Imaging

All steps are carried out at RT. The buffers should be equilibrated to RT before use. During all the procedures, the reagents are added to both sides of the filter.

1. Aspirate the medium (bottom and top).
2. Wash 1× with PBS.
3. Fix the cells with 4 % PFA for 20 min.
4. (a) For the chemoinvasion assay: cut out the filter from the insert. Do all the following steps in 12-well or 24-well plates. Hold the membrane with thin forceps (*see* **Note 25**). (b) For native BM assay: keep mesentery on the insert until **step 12**.
5. Wash 2× briefly and 2× 5 min with PBS.
6. Permeabilize the cells with extraction buffer for 2–5 min (*see* **Note 26**).
7. Wash 2× 1 min each with 1 mL of PEM buffer.
8. Add primary antibodies. Prepare antibody solution in PBS. Add a 20 μL drop on a piece of parafilm. Place insert gently on top of the drop. Add 50 μL of antibody solution on top of the membrane. Incubate for 1 h at RT.
9. Wash 2× briefly and 2× 5 min with PBS.
10. Add secondary antibodies. Follow the same procedure as in **step 8**. Incubate for 1 h.
11. Wash 2× briefly and 2× 5 min with PBS.
12. To mount the cells: Add a drop of Prolong anti-fade reagent onto a glass slide. Place the insert on the drop of mounting media. Cut the mesentery from the insert and discard the insert (*see* **Note 27**). Add a drop of Prolong anti-fade reagent on the top of the BM. Slowly add a glass coverslip on top (*see* **Note 28**). Let dry overnight before imaging (*see* **Note 29**).
13. For imaging use a confocal microscope (for instance, Zeiss LSM 510 META) (*see* **Note 30**).
14. To visualize invasive structures, scan the sample by doing *z* sections of 0.2 μm using the 63× objective (*see* **Note 31**).
15. Process the images and *z* sections. We use ImageJ and Adobe Photoshop CS6 to work on the raw files.

4 Notes

1. In rats, the mesentery surface is bigger, thus more chambers could be assembled than when mouse mesentery is used. From one rat around six chambers for a 24-well plate could be assembled, while from one mouse, a maximum of two chambers could be assembled. Rat mesentery is also stronger and easier to handle.

2. Silk is better than nylon. Nylon is too rigid and can destroy the tissue when it is tied around the insert.
3. Use the culture medium appropriate for your cell line.
4. We have only used regular Matrigel and haven't tested the assay using growth factor reduced Matrigel.
5. Use the appropriate cytokine for your cell of interest. HGF works for a variety of cancer cell lines.
6. We used the Alexa488 fluorophore. We have tested Alexa350 but the signal intensity is too low for imaging. Red colors should work.
7. A diameter of 1 μm for the pores corresponds to the average diameter of an invadopodia [7]. We do not suggest using wider diameters since cells with small nuclei can penetrate through 3 μm-pores.
8. We routinely add high molecular weight polyethylene glycol (PEG) for general preservation of the cytoskeleton.
9. The centrifugation will pellet undissolved tendons. After lyophilization, the collagen looks like cotton.
10. Tissues should never be dried. Do not cut the intestine as this can result in contamination.
11. Choose the area of mesentery free of fat and vessels.
12. Vetbond is the best way to glue the membrane to the insert. Mouse mesentery has a smaller area and is more fragile than the rat one, making it hard to manipulate with the silk. Vetbond glues the membrane to the insert in seconds, providing a convenient way to proceed quickly to the washings.
13. All washes should be done by directly aspirating liquid from the insert. Be careful not to touch the membrane. Washes can be done at RT if you work fast enough. Otherwise, work on ice to avoid any degradation of the membrane by proteases.
14. Ammonium hydroxide is used to kill mesothelial cells.
15. Any cells, such as fibroblasts, can be embedded in collagen I, in the aim of creating an in vitro coculture system, in which the basement membrane will separate the cells in the collagen from the cells that will be added on top of the membrane.
16. While preparing the working solutions of collagen, the stock solution of collagen has to be kept on ice at all times to avoid its polymerization.
17. If cells are to be embedded in collagen, it is preferential to polymerize the collagen I at RT because it assembles into bundles that more closely resemble the organization of the extracellular matrix observed in vivo [12], thus providing a more physiological environment for the cells.

18. Polymerized collagen I is white, while unpolymerized collagen I is transparent. Stop the incubation at 37 °C when the collagen is fully polymerized (i.e., white). The required time for full polymerization may vary from 15 min to 1 h depending on the humidity of the incubator and of the membrane, as well as on how fresh the collagen solution is (freshly isolated collagen polymerizes faster).
19. Incubation time varies depending on the stage of invasion you are interested in. Typically, invasive cancer cells will fully cross the BM after 5–9 days. Before 5 days, earlier steps of invasion can be observed [7].
20. The dialysis dilutes the original solution. The final concentration of fluorescent laminin is approximately 0.5 mg/mL.
21. Use fluorescently labeled laminin to confirm that it penetrates the pores and when the matrix has to been imaged. Otherwise, the fluorescent laminin can be replaced by an unlabeled one.
22. 75 μL of the matrix is removed to leave only a thin layer on top of the filter.
23. The cell concentration depends on each cell type. The ideal cell density on the membrane is 70–80 %. A too low density may render it difficult to catch invasive structures, especially for cells with low invasive capacity.
24. Overnight incubation is optimal for many invasive cell types. Perform a time course experiment the first time a new cell type is used to determine the best time of incubation.
25. For easier handling and to reduce the amount of antibody used, the membrane from the chemoinvasion assay can be cut out of the insert after fixation. Cut the membrane carefully. Avoid cutting pieces of plastic from the insert. Remaining plastic pieces will favor bubble formation, thus preventing correct mounting.
26. Depending on the protein you wish to image, a pre-extraction step might be necessary, especially for proteins with a high cytoplasmic pool. Adjust the time of pre-extraction according to your protein of interest (usually from 15 s to 3 min). After fixation, continue with **step 6**.
27. For mouse mesentery, removal of the insert is extremely difficult without destroying the membrane. One solution is to place a whole insert on the drop of mounting media deposited on a glass-bottom dish. Imaging can then be performed using an inverted confocal microscope.
28. Mounting is performed cell side up, which will be the first side to be imaged.
29. The use of an anti-fade mounting medium is absolutely required to avoid bleaching during imaging.

30. In the chemoinvasion assay, the pore absorbs the fluorescent signal. Therefore, the laser power often needs to be gradually increased while imaging through the pores.

31. It is possible to image from the other side of the membrane if the membrane is mounted the other way around: "cells looking down." The first plane to be imaged will be the bottom of the membrane, which corresponds to the end of an invadopodia. It will be very bright, but the signal will decrease while reaching the other side (where the cells are sitting). The resolution is also lower and cells will be blurred. To overcome this issue and to be able to image both sides simultaneously, the membrane can be mounted between two thin coverslips, which are held on the sides by two glass rectangles cut out from a slide.

Acknowledgments

This work is supported by Association pour la Recherche sur le Cancer (ARC-SFI12111203862) and ANR-09-JCJC-0023-01.

References

1. Yurchenco PD (2011) Basement membranes: cell scaffoldings and signaling platforms. Cold Spring Harb Perspect Biol 3(2):1–27
2. Sherwood DR (2006) Cell invasion through basement membranes: an anchor of understanding. Trends Cell Biol 16(5):250–256
3. Carman CV, Sage PT, Sciuto TE, de la Fuente MA, Geha RS, Ochs HD, Dvorak HF, Dvorak AM, Springer TA (2007) Transcellular diapedesis is initiated by invasive podosomes. Immunity 26(6):784–797
4. Schoumacher M, Louvard D, Vignjevic D (2011) Cytoskeleton networks in basement membrane transmigration. Eur J Cell Biol 90(2–3):93–99
5. Rowe RG, Weiss SJ (2008) Breaching the basement membrane: who, when and how? Trends Cell Biol 18(11):560–574
6. Ihara S, Hagedorn EJ, Morrissey MA, Chi Q, Motegi F, Kramer JM, Sherwood DR (2011) Basement membrane sliding and targeted adhesion remodels tissue boundaries during uterine-vulval attachment in Caenorhabditis elegans. Nat Cell Biol 13(6):641–651
7. Schoumacher M, Goldman RD, Louvard D, Vignjevic DM (2010) Actin, microtubules, and vimentin intermediate filaments cooperate for elongation of invadopodia. J Cell Biol 189(3):541–556
8. Hotary K, Li XY, Allen E, Stevens SL, Weiss SJ (2006) A cancer cell metalloprotease triad regulates the basement membrane transmigration program. Genes Dev 20(19):2673–2686
9. Artym VV, Yamada KM, Mueller SC (2009) ECM degradation assays for analyzing local cell invasion. Methods Mol Biol 522: 211–219
10. Poincloux R, Lizarraga F, Chavrier P (2009) Matrix invasion by tumour cells: a focus on MT1-MMP trafficking to invadopodia. J Cell Sci 122(Pt 17):3015–3024
11. Lizarraga F, Poincloux R, Romao M, Montagnac G, Le Dez G, Bonne I, Rigaill G, Raposo G, Chavrier P (2009) Diaphanous-related formins are required for invadopodia formation and invasion of breast tumor cells. Cancer Res 69(7):2792–2800
12. Geraldo S, Simon A, Elkhatib N, Louvard D, Fetler L, Vignjevic DM (2012) Do cancer cells have distinct adhesions in 3D collagen matrices and in vivo? Eur J Cell Biol 91(11–12): 930–937

Chapter 9

Cytoplasmic Actin: Purification and Single Molecule Assembly Assays

Scott D. Hansen, J. Bradley Zuchero, and R. Dyche Mullins

Abstract

The actin cytoskeleton is essential to all eukaryotic cells. In addition to playing important structural roles, assembly of actin into filaments powers diverse cellular processes, including cell motility, cytokinesis, and endocytosis. Actin polymerization is tightly regulated by its numerous cofactors, which control spatial and temporal assembly of actin as well as the physical properties of these filaments. Development of an in vitro model of actin polymerization from purified components has allowed for great advances in determining the effects of these proteins on the actin cytoskeleton. Here we describe how to use the pyrene actin assembly assay to determine the effect of a protein on the kinetics of actin assembly, either directly or as mediated by proteins such as nucleation or capping factors. Secondly, we show how fluorescently labeled phalloidin can be used to visualize the filaments that are created in vitro to give insight into how proteins regulate actin filament structure. Finally, we describe a method for visualizing dynamic assembly and disassembly of single actin filaments and fluorescently labeled actin binding proteins using total internal reflection fluorescence (TIRF) microscopy.

Key words Actin polymerization assay, TIRF, Single molecule imaging, *Acanthamoeba*, Fluorimetry, Pyrene, Cytoskeleton, Phalloidin

1 Introduction

Over the past few decades dozens of actin binding proteins have been discovered, and there is a rapidly growing body of work focused on dissecting how each of these proteins regulates the kinetics and morphology of actin structures [1, 2]. Actin dynamics can be divided into three steps, each of which is specifically regulated. Polymerization is a nucleation-condensation reaction [3], which means that the first step (nucleation) is slow, and the second step (elongation) proceeds quickly once a stable nucleus is formed [4]. Nucleation refers to the assembly of actin monomers into a stable trimer, which is usually an extremely unfavorable reaction. As the filament elongates, incorporated actin monomers hydrolyze their ATP to ADP, making filaments more susceptible to

Amanda S. Coutts (ed.), *Adhesion Protein Protocols*, Methods in Molecular Biology, vol. 1046,
DOI 10.1007/978-1-62703-538-5_9,

depolymerization, the third step in the cycle. All steps of this cycle are regulated by actin binding proteins [1, 5]. The rate of nucleation is controlled by actin nucleation factors, including the Arp2/3 complex, formins, and WH2 family nucleation factors (e.g., Spire and JMY) [5–7]. Growth, maintenance and structural integrity of filaments are controlled by different classes of proteins that either elongate, cap, bundle, or sever actin filaments.

The primary in vitro assay used to study the effects of actin binding proteins on actin polymerization is the pyrene actin assembly assay, wherein the environmentally sensitive fluorophore pyrene indicates the polymerization state of actin [8]. Pyrene-labeled actin incorporated in a filament fluoresces significantly greater than a labeled monomer in solution [8]. In the absence of other proteins, a time dependent increase in pyrene fluorescence is directly proportional to the concentration of filamentous actin ([9]; protein binding to actin filaments can also increase pyrene fluorescence, so care must be taken with interpreting these data).

Actin polymerization assays are conducted using buffer conditions similar to those in vivo. Importantly, actin requires magnesium-ATP in its nucleotide pocket, and physiological concentrations of potassium for rapid polymerization at micromolar concentrations. Actin is stored in Buffer A—which contains calcium instead of magnesium, and lacks potassium—to prevent polymerization. Immediately before the assay, calcium is exchanged for magnesium by adding EGTA and magnesium. Polymerization is triggered by the addition of buffer containing potassium [10].

There are two standard sources of actin for biochemical studies: *Acanthamoeba castellani* and rabbit skeletal muscle. Actin from amoeba is cytoplasmic, and is a good model for cytoplasmic actins (beta-actin isoform) from other organisms [11]. Conversely, skeletal actin is predominantly the alpha-actin isoform, and does not necessarily interact the same with proteins that regulate cytoplasmic actin [12]. Furthermore, *Acanthamoeba* is an excellent source of actin binding proteins, such as the Arp2/3 complex [13, 14]. Although it is best to use actin and actin binding proteins from the same organism and tissue, actin is highly conserved, and in most cases amoeba actin can be used in conjunction with proteins from other organisms [10].

While the pyrene assay is very powerful for measuring kinetics of actin assembly, it does not reveal the structure of the actin filament networks it produces. In addition, pyrene assays are inherently difficult to interpret because the data output is based on an ensemble of protein interactions, and the binding of some proteins to actin filaments can affect pyrene fluorescence. There are two commonly used techniques which address this: fixing and staining polymerization reactions with fluorescently labeled phalloidin [6] and electron microscopy [9, 15]. Fixing actin with labeled phalloidin, detailed in Subheading 3.5, is a straightforward method that can be performed in parallel with pyrene actin experiments.

Recently, innovations in glass surface chemistry, synthesis of fluorescent dye conjugates, and improvements in microscope imaging technology have made it possible to image single dynamic cytoskeletal polymers in vitro using fluorescence microscopy [16–18]. These assays rely on visualizing single filaments adhered to polyethylene glycol (PEG) functionalized coverslips using total internal reflection fluorescence (TIRF) microscopy. Although more technically challenging than a pyrene assay, single filament TIRF assays offer unparalleled insight into actin filament dynamics and network architecture with single filament resolution. Using this method, several models for actin binding protein function based on pyrene actin polymerization assays have been recently challenged [19, 20]. Since pegylation reduces nonspecific protein absorption to coverslips, these glass surfaces can also be used for single molecule imaging of fluorescently labeled actin binding proteins [21]. These assays are detailed in Subheadings 3.6–3.9.

2 Materials

2.1 Culture of Acanthamoeba castellani

1. Amoeba medium: 7.5 g/L proteose peptone, 7.5 g/L yeast extract, 15 g/L glucose, 0.2 mM methionine, 3 mM KH_3PO_4, 10 μM $CaCl_2$, 1 μM $FeCl_3$, 0.1 mM $MgSO_4$, 1 mg/L thiamine, 0.2 mg/L biotin, 0.01 mg/L vitamin B12. Autoclave before use.
2. Wash buffer: 10 mM Tris–HCl, pH 8.0, 150 mM NaCl.

2.2 Actin Purification from Acanthamoeba castellani

1. Extraction buffer: 10 mM Tris–HCl, pH 8.0, 11.6 % (w/v) sucrose, 1 mM EGTA, 1 mM ATP, 5 mM dithiothreitol (DTT), 30 mg/L benzamidine, 5 mg/L pepstatin A, 10 mg/L leupeptin, 40 mg/L soybean trypsin inhibitor, 1 mM phenylmethylsulphonylfluoride (PMSF). The first three ingredients may be combined a day in advance and stored at 4 °C. Add the final ingredients fresh, pH to 8.0 and bring up to volume with cold water (*see* **Note 1**). Add PMSF immediately before use.
2. Pepstatin A (1,000×): 5 mg/mL pepstatin A in DMSO; store at −20 °C.
3. Protease cocktail (100×): 1 mg/mL leupeptin and 4 mg/mL soybean trypsin inhibitor in water; store at −20 °C.
4. PMSF: 200 mM in ethanol or methanol; store at −20 °C. Before use warm to 25 °C with rocking to resuspend. The half life of PMSF in aqueous solution is approximately 30 min, and so it is always added to buffers immediately before use.
5. 100 mM ATP, pH 7.0, dissolved in water.
6. Column buffer: 10 mM Tris–HCl, pH 8.0, 0.2 mM $CaCl_2$, 30 mg/L benzamidine, 0.5 mM ATP, 0.5 mM DTT. Add the

last three ingredients fresh and bring buffer up to volume with cold water. Adjust buffer to pH 8.0 while at 4 °C, just before use.

7. Diethylaminoethyl cellulose (DEAE) (DE52, Whatman): After use, cycle with 0.5 M NaOH and HCl to wash, and store in Tris base, pH 8.0, 0.2 % (v/v) benzalkonium chloride at 4 °C indefinitely (*see* **Note 2** for details on washing DEAE).
8. 1 M Tris base (Trizma).
9. High salt buffer: 600 mM KCl, 10 mM Tris–HCl, pH 8.0, 0.2 mM $CaCl_2$, 30 mg/L benzamidine, 0.5 mM ATP, 0.5 mM DTT. Prepare as in **step 1** (extraction buffer) above.
10. 200 mM $MgCl_2$.
11. Tris(2-carboxyethyl)phosphine hydrochloride (TCEP, Invitrogen): Prepare 0.5 M stock in cold water and pH to 7.0 with KOH.
12. Buffer A (1×): 2 mM Tris–HCl, pH 8.0, 0.2 mM ATP, 0.5 mM TCEP, 0.1 mM $CaCl_2$. pH to 8.0 with KOH and bring up to volume with cold water (*see* **Note 3**).
13. KMEI buffer (10×): 500 mM KCl, 10 mM $MgCl_2$, 10 mM EGTA, 100 mM Imidazole HCl, pH 7.0 (*see* **Note 4**).
14. Gel filtration column: Flex column (25 mm × 100 cm, Fisher Scientific) for packing resin manually. Alternatively, use a Superdex S-75 or S-200 column (GE Healthcare).
15. Sephacryl S-200 HR resin (GE Healthcare): Resin comes stored in 20 % (v/v) ethanol and will swell when fully hydrated. To avoid cracking the resin, equilibrate in buffer before decanting into gel filtration column. Pack the column by flowing 1–2 column volumes of Buffer A at a faster rate than will be used in gel filtration.
16. Parr Bomb (Parr Instrument Company).

2.3 Pyrene-Labeling of Actin

1. Actin: If actin is from *Acanthamoeba*, it must be gel filtered before labeling. Skeletal actin does not have this requirement.
2. KMEI buffer (10×): *see* Subheading 2.2, **item 13**.
3. Dialysis buffer: 50 mM KCl, 1 mM $MgCl_2$, 1 mM EGTA, 10 mM Imidazole HCl, pH 7.0, 0.2 mM ATP.
4. Pyrenyl iodoacetamide (Invitrogen): 10 mM stock solution in dimethylformamide (DMF), stored at −20 °C in the dark.
5. Buffer A (1×): *see* Subheading 2.2, **item 12**.
6. DTT: 1 M stock in water.

2.4 Pyrene Actin Assembly Assay

1. Buffer A (1×): *see* Subheading 2.2, **item 12**.
2. KMEI buffer (10×): *see* Subheading 2.2, **item 13**.
3. ME buffer (10×): 0.5 mM $MgCl_2$, 2 mM EGTA.

4. Ethanol, HPLC grade for washing cuvettes.
5. Vakuwash Cuvette washer (Fisher Scientific).

2.5 Microscopy of Stabilized, Labeled Actin Filaments

1. Reagents for pyrene actin assembly assay, as in Subheading 2.4.
2. Alexa Fluor 488 Phalloidin (Invitrogen): Make stocks in methanol, to be in molar excess to actin in reaction. For example, 5 μL of a 6.6 μM stock of phalloidin was used to stabilize an equal volume of 4 μM actin [6]. Store stocks at −20 °C for several months. TRITC phalloidin (Sigma) also works well.
3. Wide-bore pipette tips: Cut pipette tips with a sterile razor, and be consistent.
4. Poly-L-lysine: Prepare a 1 mg/mL stock in water.
5. Poly-L-lysine coated coverslips: Clean slides by sonication first in 1 M KOH, then in ethanol. Rinse in water, and air dry. Spot 1 mg/mL poly-L-lysine on parafilm, and float coverslips on drops (500 μL) for a few minutes, rinse with water, and use within a few days.
6. Clear nail polish.

2.6 Silanization and Pegylation of Glass Coverslips

1. Diamond pen (J&M Diamond Tool Inc., HS-110).
2. Glass weigh jars (Fisher, 03-420-5C).
3. Ceramic coverslip racks.
4. 18 mm × 18 mm coverslips, 1.5 mm thickness.
5. Bath sonicator.
6. Sodium hydroxide (Fisher, S318-1).
7. Sulfuric Acid (Fisher, A300-500).
8. Hydrogen peroxide (30 % solution, Fisher H325-500).
9. APTES (3-Aminopropyl)triethoxysilane (Sigma-Aldrich, A3648).
10. mPEG-5000-NHS (JenKem Technology USA, M-SCM-5000).
11. Biotin-PEG5000-NHS (JenKem Technology USA, Biotin-PEG-5000-NHS).
12. Dimethylformamide (anhydrous, Sigma-Aldrich 227056).
13. Isopropanol (Fisher, A451-4).
14. Ethanol (Fisher, A995-4).
15. Acetone (Fluka, 00561).
16. Ultrapure water (*see* **Note 1**).

2.7 Labeling A. castellani Actin with Maleimide Derivatives

1. Buffer A (1×): *see* Subheading 2.2, **item 12**.
2. Actin labeling buffer: 5 mM Tris–HCl, pH 8, 200 μM ATP, 100 μM $CaCl_2$.
3. KMEI buffer (10×): *see* Subheading 2.2, **item 13**.

4. Fluorescent dyes: Alexa Fluor 488 maleimide (Invitrogen, A-10254), Cy3 maleimide (GE Healthcare, PA13131), and Cy5 maleimide (GE Healthcare, PA15131).
5. Biotin-PEG2-Maleimide (Fisher Thermo Scientific/Pierce, #21901).
6. PD10 salt exchange column (G25 Sephadex resin, GE Healthcare 17-0851-01).
7. 500 mM TCEP-HCl, pH 7.0 with KOH (Pierce, 20491).
8. 1 M DTT dissolved in water (Roche, 100034).

2.8 Assembly of TIRF-M Flow Cells for Attachment of Filamentous Actin

1. 15 mm wide double sided tape (Tesa, 05338).
2. 25 mm × 75 mm × 1 mm Fisher Premium Microscope slides (Fisher, 12-544-7).
3. 3 mg/mL Poly-L-lysine PEG ((PLL-PEG) [22]; *see* ref. 18 for grafting protocol).
4. 500 mM TCEP-HCl, pH 7.0 with KOH (Pierce, 20491).
5. Streptavidin (Rockland Immunochemicals, S00-01): Resuspend lyophilized protein in 10 mM Tris–HCl, pH 8 to final concentration of 20–40 μM. Ultracentrifuge at 350,000 × *g* (80,000 rpm with a TLA100.4) for 20 min to remove aggregates. Freeze with liquid nitrogen. Store at −80 °C.
6. Heavy meromyosin (HMM; chymotrypsin cleaved rabbit skeletal muscle myosin, e.g., Cytoskeleton, Inc., MH01). Alternatively use NEM-inactivated myosin II (*see* refs. 19, 20).
7. Biotin-phalloidin (Sigma-Aldrich, P8716).
8. Biotin-PEG11-Maleimide (Fisher Thermo Scientific/Pierce, 21911) for labeling heavy meromyosin (HMM) (*see* Subheading 3.7, **step 19**).
9. 10 mg/mL kappa casein dissolved in 1× PBS, pH 7.2 (Sigma-Aldrich C0406; bovine milk): Ultracentrifuge at 350,000 × *g* (80,000 rpm with a TLA100.4) for 20 min to remove aggregates. Use within 3 days.
10. Pluronic F-127 (Sigma-Aldrich, P2443): Prepare 10 % (v/v) in water.
11. KMEI buffer (10×): *see* Subheading 2.2, **item 13**.
12. 1× PBS buffer: 2.9 mM NaH_2PO_4, 7.1 mM Na_2HPO_4, 137 mM NaCl, 2.7 mM KCl, pH 7.2 with NaOH.
13. Blocking buffer: 1 % Pluronic F127, 50 μg/mL kappa casein, 1× PBS, pH 7.2.
14. Wash buffer: 20 mM HEPES, pH 7.0, 200 mM KCl, 1 mM TCEP, 1 mg/mL BSA.

2.9 Visualization of Dynamic Actin Filament Assembly

1. Unlabeled monomeric actin stored in Buffer A.
2. Alexa Fluor 488, Cy3, or Cy5 labeled monomeric actin stored in Buffer A.
3. 100 mM ATP dissolved in water, pH 7.0 with KOH (Sigma-Aldrich, A26209-10G). Store aliquots at −20 °C.
4. 50 mg/mL BSA dissolved in water (Sigma-Aldrich, A0281-1G).
5. 1 M D-(+)-Glucose in water.
6. 14.3 M β-mercaptoethanol.
7. 2 % methylcellulose (w/v) (cP400, Sigma-Aldrich M0262): Suspend methylcellulose in 90–100 °C water by vortexing in a microfuge tube. Invert tube and chill on ice to solubilize. Microcentrifuge and resuspend methylcellulose to homogeneity.
8. 10 mg/mL glucose oxidase dissolved in OSS buffer (Biophoretics/Serva Electrophoresis, T#22778.01): Ultracentrifuge at 350,000 × *g* (80,000 rpm with a TLA100.4) for 20 min to remove aggregates. Use within 3 days.
9. 10 mg/mL catalase dissolved in OSS buffer (Sigma-Aldrich C40-100MG; bovine liver): Ultracentrifuge at 350,000 × *g* (80,000 rpm with a TLA100.4) for 20 min to remove aggregates. Use within 3 days.
10. Buffer A (1×): *see* Subheading 2.2, **item 12**.
11. ME Buffer (10×): *see* Subheading 2.4, **item 3**.
12. OSS buffer: 20 mM HEPES, pH 7.0, 150 mM NaCl.
13. 2× TIRF Buffer: 40 mM HEPES, pH 7.0, 50 mM KCl, 2 mM $MgCl_2$, 2 mM EGTA, 0.4 % methylcellulose (cP400), 40 mM glucose, 40 mM beta-mercaptoethanol, 2 mg/mL BSA, 2 mM ATP, 250 μg/mL glucose oxidase, 20 μg/mL catalase. Add oxygen scavenger enzymes (i.e., glucose oxidase and catalase) 5–10 min before combining with actin and imaging.
14. Protein dilution buffer: 20 mM HEPES, pH 7.0, 100 mM KCl, 1 mM TCEP, 1 mg/mL BSA.
15. VALAP (1:1:1 vasoline:lanoline:paraffin).
16. NIKON Eclipse TE2000-E microscope with Nikon Perfect Focus, or equivalent.
17. ANDOR iXon cooled EM CCD camera.
18. 100× Nikon Apo TIRF objective (NA 1.49).
19. 40 mW 488/514 nm Argon Ion laser or 40 mW 542 nm crystal laser.
20. Chroma/Shemrock multibandpass filter.
21. Micromanager 4.0 software (*recommended*; [23]).

3 Methods

3.1 Culture of Acanthamoeba castellani

1. Passage amoeba in 10 mL culture tubes with moderate bubbling of humidified air, at 25 °C [24, 25].
2. Fill beveled Fernbach flasks (3 L) with 1 L Amoeba medium and inoculate with cultures. Grow with moderate shaking at 25 °C, until growth plateaus (*see* **Note 5**). Use Fernbachs to inoculate 14 L carboys outfitted with bubblers. Practice sterile technique to avoid contaminating the cultures, which grow without any antibiotic.
3. When cultures plateau, harvest by centrifugation at 4,500 × *g* (4,000 rpm in a Sorvall RC-3B), 5 min. Refill tubes and centrifuge again until all amoeba have been pelleted.
4. Wash amoeba with wash buffer. Resuspend cell pellets in the smallest volume of buffer possible. Pool these, and centrifuge as above. In this way all amoeba are transferred into one or two tubes. During the pairing-down of tubes, weigh amoeba, to get approximately 500 g (enough for actin purification) into a single tube.

3.2 Purification of Actin from Acanthamoeba castellani

1. Resuspend pelleted amoeba in 1 mL of cold extraction buffer per gram of amoeba (example volumes given are for purification from 500 g amoeba. Buffer and resin volumes can be scaled linearly as needed). If amoeba are frozen, thaw in cold extraction buffer (*see* **Note 6**). After resuspension, conduct all subsequent steps at 4 °C (*see* **Note 7**).
2. Lyse cells by nitrogen decompression in a Parr Bomb. Rinse the Parr Bomb with water and cool on ice. Transfer cells into the Parr Bomb and pressurize with nitrogen gas at 400 psi for 5 min. To lyse, release cells from the Parr Bomb slowly, while maintaining constant pressure. Alternatively, amoeba can be lysed by rapid freezing with liquid nitrogen and then thawing into cold extraction buffer. This step can be immediately followed by centrifugation.
3. To remove cellular debris, centrifuge lysate at >5,000 × *g* (7,000 rpm in a GS-3 rotor), 10 min, 4 °C. Centrifuge supernatant from this spin at >100,000 × *g* (38,000 rpm in a Beckman Ti45 rotor), 2 h, 4 °C.
4. Equilibrate 500 g DEAE resin in 2 L column buffer. To equilibrate large volumes of resin; mix resin and buffer in beaker, then pour over a Buchner funnel fitted with a Whatman filter 541 (ashless) and pull vacuum until buffer has passed through but the resin is still damp. It is essential that the pH of the resin is 8.0 before use.

5. After the second spin, siphon off the lipid layer at the very top of each tube. Decant supernatants into a rinsed glass beaker, on ice. Mix supernatant with ~450 mL equilibrated DEAE resin, and stir for 30–60 min at 4 °C, to batch bind.
6. In the cold room, pour remaining ~50 mL equilibrated DEAE resin into a glass column (diameter 5 cm; height 60 cm) and let resin settle and excess liquid drip through. Gently pour DEAE slurry above this, and collect flow-through (*see* **Note 8**). Wash resin with 1 L column buffer, pumped at 6 mL/min.
7. To elute actin, use a gradient maker to run a linear gradient from 0 to 600 mM KCl using 1 L column buffer (low salt buffer) and 1 L high salt buffer, pumped at 3 mL/min. Actin normally elutes as a broad (~200 mL) peak between 300 and 400 mM KCl. Keep actin fractions in the cold room overnight, covered. (*See* **Note 2** regarding recycling of DEAE resin.)
8. The next day, move fractions to 25 °C to speed up polymerization. Actin will polymerize in a few hours. Detect polymerized actin fractions by tipping fraction tubes sideways; if there is sufficient polymerized actin, the fraction will be a gel.
9. Pool actin fractions into a beaker. Add $MgCl_2$ to 2 mM and ATP to 1 mM. Stir actin gently for 30 min at 25 °C to complete polymerization.
10. Centrifuge actin at 1,000 × *g* (3,000 rpm in a Sorvall GSA rotor), 5 min, 4 °C. Pour off supernatant, and wash with 1× KMEI buffer. Centrifuge at >100,000 × *g* (38,000 rpm in a Ti45 rotor), 2 h, 4 °C. Discard supernatant and rinse the pellet (polymerized actin) quickly with Buffer A. Scrape actin into a Dounce homogenizer. Homogenize 5–10 times with a "loose" pestle in Buffer A, to 40–80 mL final volume, without creating air bubbles.
11. Dialyze into Buffer A for 2–3 days at 4 °C to depolymerize actin. Change dialysis buffer daily. Actin can be stored in dialysis at 4 °C for several weeks.
12. Equilibrate an S-75 or S-200 gel filtration column with Buffer A. Centrifuge 15–20 mL depolymerized actin at >100,000 × *g* (38,000 rpm in a Ti45 rotor), 2 h, 4 °C. Load actin onto gel filtration column and gel filter in Buffer A, collecting ~3 mL fractions.
13. Determine the concentration of unlabeled actin by measuring absorbance at 290 nm, using an early fraction from the column to blank the spectrophotometer (*see* **Note 9**). The concentration of actin is 38.5 μM per absorbance unit at 290 nm (i.e., $A_{290} = 1.0$ when actin is at 38.5 μM), assuming a 10 mm pathlength.

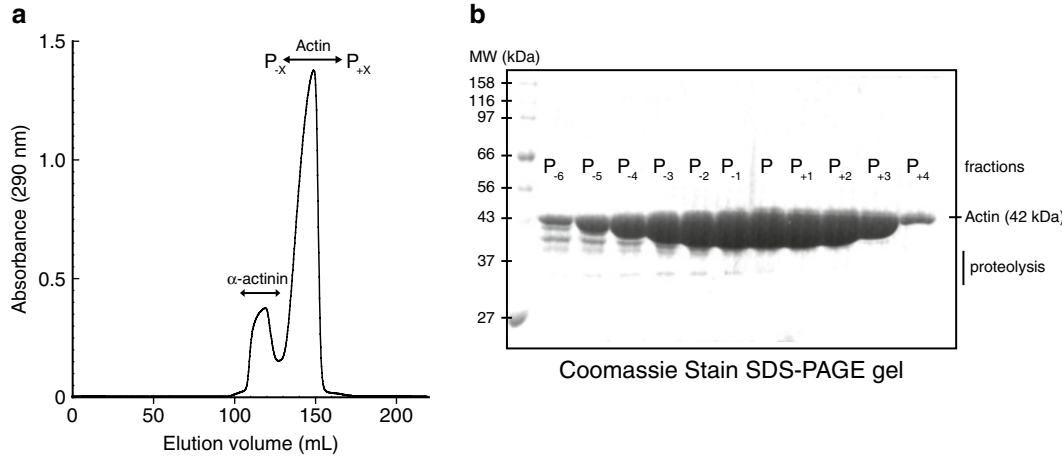

Fig. 1 Gel filtration of actin from *Acanthamoeba castellani*. (**a**) Depolymerized actin was gel filtered over a 323 mL Superdex 75 column (GE Healthcare) in Buffer A. Absorbance at 290 nm was measured, and concentration of actin plotted for each fraction. The *first peak* contains contaminants, including alpha-actinin. The *second* (major) *peak* is actin. It is important to test fractions for activity as early fractions may be contaminated with dimers, which will speed up assembly kinetics [29]. (**b**) Fractions of actin eluted from the Superdex 75 column (**a**) and visualized by SDS-PAGE. Peak fractions should contain less than 1 % proteolyzed actin

14. Gel filtered actin can now be pyrene labeled or used unlabeled in polymerization assays (Fig. 1a). For pyrene labeling, use the entire second (major) peak. Dark actin for fluorimetry is taken from the back end (later fractions) of this peak. The front end of the peak contains actin dimers, which will interfere with kinetic measurements [10].
15. Assay the purity of actin by SDS-PAGE and Coomassie staining. Actin is 42 kDa and should appear as a single band with little to no break-down (Fig. 1b).

3.3 Pyrene-Labeling of Actin

1. Pool 30–80 mg of actin and measure concentration. Dilute actin to 1.1 mg/mL (26.4 μM; due to the limited solubility of pyrene iodoacetamide, the final concentration of actin should be 1 mg/mL) in Buffer A.
2. Polymerize actin by adding one-tenth the final volume of 10× KMEI buffer and let stand at 25 °C. Actin will be completely polymerized within a few minutes; look for bubbles in the actin solution that do not move.
3. To remove reducing reagent for labeling, carefully transfer polymerized actin into dialysis tubing, and dialyze into dialysis buffer for a few hours at 4 °C.
4. Transfer actin to a beaker and measure the volume. Add 4–7 mol pyrenyl iodoacetamide per mol actin, while stirring. Cover the beaker to keep dark, and gently stir overnight at 4 °C.

5. Quench labeling reaction by adding DTT to 10 mM. (This immediately renders excess pyrene iodoacetamide unreactive, thus preventing it from reacting with the chromatography resin used in **step 11**.)
6. Centrifuge labeled actin at $2{,}000 \times g$ (5,000 rpm in a Beckman JA-20) rotor, 5 min, 4 °C, to pellet precipitated dye.
7. Centrifuge supernatant at $>100{,}000 \times g$ (38,000 rpm in a Ti45 rotor), 2 h, 4 °C, to pellet actin filaments.
8. Homogenize the pellet with a Dounce homogenizer as above, in Buffer A, into a final concentration of about 2–6 mg/mL (48–144 μM) (*see* **Note 10**).
9. Dialyze into Buffer A, at 4 °C, using at least two changes of buffer over at least 2 days, to depolymerize actin.
10. Centrifuge depolymerized pyrene actin at $>100{,}000 \times g$ (38,000 rpm in a Ti45 rotor), 2 h, 4 °C, to remove remaining actin filaments.
11. Gel filter supernatant over S-75 or S-200 gel filtration column equilibrated with Buffer A, as before.
12. Determine the concentration and percent labeling by measuring absorbance at 290 and 344 nm. To correct for pyrene absorption at 290 nm.

$$A_{290(\text{corrected})} = A_{290_{(\text{measured})}} - 0.127 \times A_{344} \quad (1)$$

The concentration of total actin is thus 38.5 μM per corrected A_{290}. The concentration of pyrene actin is 45.0 μM per A_{344}. To calculate percent labeling.

$$\text{percent labeled} = \frac{[\text{pyrene actin}]}{[\text{total actin}]} \quad (2)$$

13. Store pyrene actin fractions on ice, in the dark, in the cold room. Pyrene actin is more stable than unlabeled actin, and can be used for several months.

3.4 Pyrene Actin Assembly Assay

1. Mix unlabeled actin, pyrene actin and Buffer A to achieve a working stock that is 5–10 % labeled and 5–20 times the concentration to be used (*see* **Note 11**). Store on ice, in the dark.
2. Set up the fluorimeter. Set excitation wavelength to 365 nm, and emission wavelength to 407 nm.
3. Assemble reagents by the fluorimeter. (All volumes listed are based on a 100 μL total reaction volume.) Pre-aliquot buffers into labeled microfuge tubes to ensure that concentrations of each reagent are exactly the same for each experimental condition: (1) 10 μL aliquots of 10× KMEI buffer and (2) aliquots of 10× ME buffer (one tenth the volume of actin added to the

reaction). Make a dilution series of the protein to be tested in Buffer A and store on ice (*see* **Note 12**). Clean cuvettes extensively with water, ethanol, water, and wipe dry with lens paper.

4. Set a stop watch to 3 min and start time. Immediately, add actin to pre-aliquoted 10× ME buffer to exchange Ca^{2+} for Mg^{2+}. Exchange for 2 min exactly.
5. During this 2 min incubation, assemble the rest of the reagents: Add proteins to be tested to 10 μL pre-aliquoted 10× KMEI buffer (*see* **Note 13**). Add Buffer A to bring the total reaction volume (including actin and ME buffer) to 100 μL. Set a pipetteman to 110 μL and pipette up the KMEI/protein mixture.
6. After 2 min exchange, pipette KMEI/protein mixture into the actin. Triturate the reaction 1–3 times (be consistent) to mix thoroughly, then pipette into the cuvette, being careful to avoid bubbles. Load the cuvette into the fluorimeter, and activate data collection. Record dead time: the time from addition of the KMEI/protein mixture to actin until the second the first data point is collected. Always collect complete data sets, until pyrene fluorescence plateaus. Try the same condition at least three times to ensure reproducibility. (*See* **Note 14** for tips on improving data.)
7. Every time the fluorimeter is turned on, or a different concentration of actin is used, optimize settings to maximize signal while eliminating photobleaching (*see* **Note 15**). Polymerize actin as described, and monitor the plateau over the course of 1 h, maximizing the signal that causes no appreciable drop in plateau fluorescence over time. This is usually achieved by adjusting the diaphragm between the light source and the cuvette (*see* **Note 16**).
8. Figure 2 illustrates polymerization data and how they are analyzed. Plot fluorescence (arbitrary units) as a function of time (seconds). Add back dead time to *x*-axis data (time). Subtract baseline fluorescence from all *y*-axis data. Baseline fluorescence is fluorescence at time zero, assuming the reaction is slow enough to catch. If the conditions used do not alter the critical concentration of actin (i.e., protein being tested does not cap actin filaments or sequester monomers), normalize data by dividing all *y*-axis data by the fluorescence at plateau. *See* [10] for methods to determine critical concentration change.
9. Reaction half times are convenient metrics to measure (Fig. 2c inset). Replot the linear region of the curve surrounding half-maximal, and fit a linear equation to these points. Use this equation to solve for half time (the value of x where $y = 0.5$, if data are normalized).

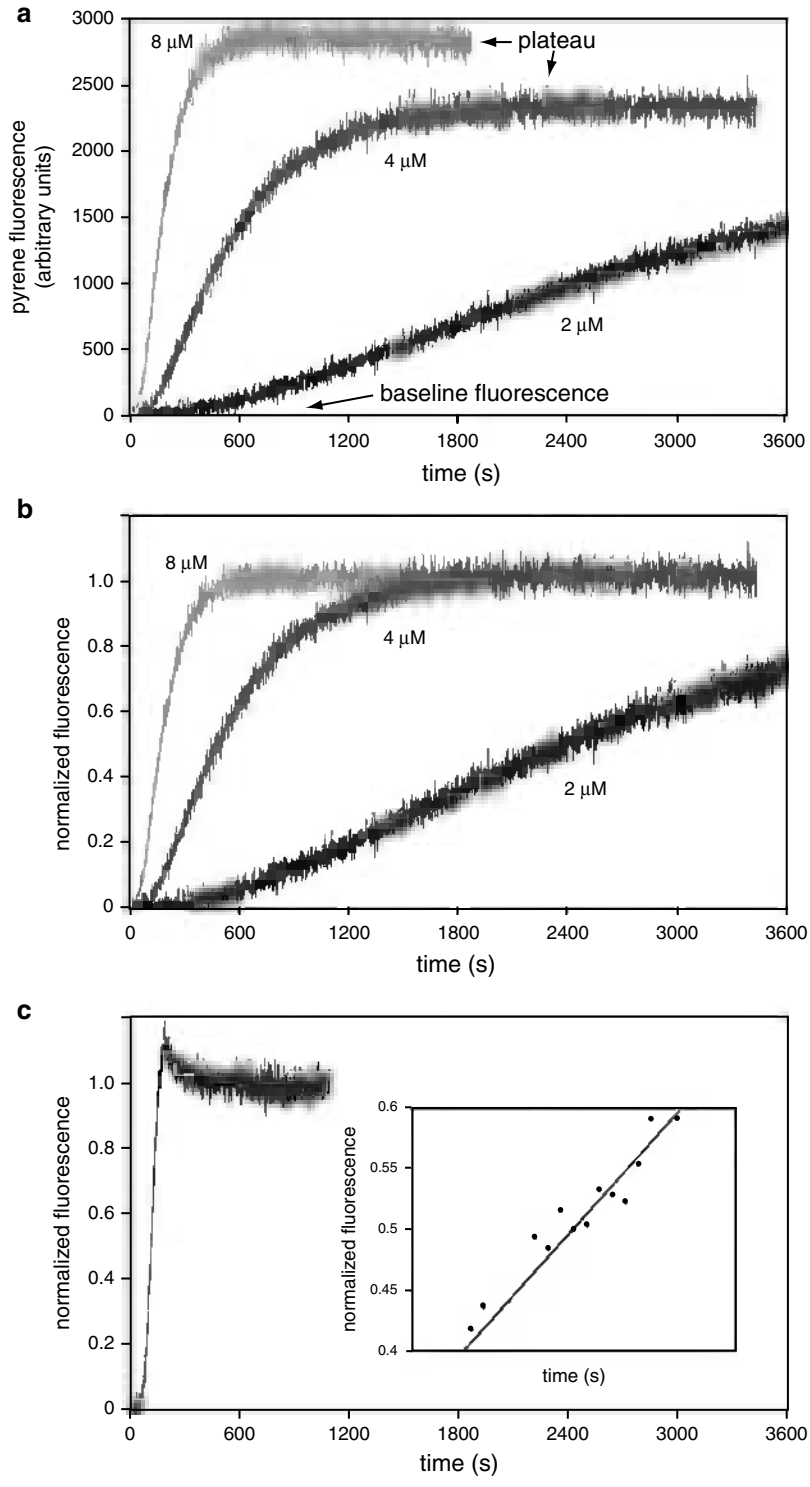

Fig. 2 Pyrene actin assembly assay. (**a**) Actin was polymerized as described; curves show spontaneous nucleation of 2 μM (*black*), 4 μM (*dark grey*) and 8 μM (*light grey*) actin. These data have been zeroed by subtracting baseline fluorescence from all fluorescence values. (**b**) Data from above were normalized by dividing all fluorescence values by average fluorescence at plateau. (**c**) 2 μM actin was polymerized in the presence of 10 nM Arp2/3 complex and 5 nM *Listeria* ActA. *Inset*: To calculate time to half-maximal fluorescence ($t½$), the linear region of the curve in (**c**) spanning 0.5 were replotted, and a linear trendline was fit to the data. Solving for time (x) where $y = 0.5$ yields $t½$

3.5 Microscopy of Stabilized, Labeled Actin Filaments

1. Polymerize unlabeled actin using conditions described above, in an eppendorf tube. Allow reaction to come to plateau (*see* **Note 17**).
2. In the meantime, desiccate Alexa Fluor 488 phalloidin in a speed vacuum, to remove all methanol. Labeled phalloidin should be superstoichiometric to actin.
3. Pipette 5 μL polymerized actin—using a wide-bore pipette tip—into the tube containing desiccated phalloidin to stabilize actin filaments.
4. Add 45 μL 1× KMEI buffer to dilute the reaction. Dilute to low nanomolar concentrations to resolve individual filaments.
5. Pipette 10 μL of the dilutions onto slides and cover with poly-L-lysine coverslips. Seal slides with clear nail polish.
6. Once nail polish dries, image filaments with an epifluorescence microscope.

3.6 Silanization and Pegylation of Glass Coverslips

1. Use a diamond pen to unambiguously mark individual 18 mm × 18 mm coverslips (e.g., mark the bottom right-hand corner of coverslip with an "e"). Decide which surface of the coverslips will be silanized and pegylated, and be consistent.
2. Place marked coverslips in a 1 L glass beaker containing 200 mL of 3 M NaOH (*see* **Note 18** for alternative cleaning strategies).
3. Sonicate in NaOH for 30–40 min. Swirl every 10 min. Save this base solution for washing glassware in later steps.
4. Decant NaOH and rinse coverslips with copious amounts of ultrapure water.
5. Add 200 mL of 100 % isopropanol and sonicate for 15 min.
6. Meanwhile, make 200 mL of 5 % APTES in isopropanol (containing 1 % water; *see* **Notes 19–21**). APTES is toxic and corrosive. Use glass pipets when alliquoting APTES.
7. Remove coverslips individually from isopropanol and transfer them to a new beaker containing the 5 % APTES solution. Swirl each coverslip in the solution before dropping into the beaker. Bath sonicate the coverslips for 20–30 min.
8. Pour silane solution into waste container. Dispose of waste following appropriate health and safety guidelines. Do not pour APTES and isopropanol down the drain.
9. Rinse coverslips 3× with 100 % isopropanol to remove excess silane.
10. Remove coverslips one-by-one. Dip into a series of three beakers containing isopropanol to wash off excess APTES. In

each beaker, move forceps back and forth in isopropanol to thoroughly remove excess silane from each coverslip. Rack coverslips in ceramic holders.

11. Bake for ≥2 h at 80–90 °C. The purpose of this step is to drive moisture off the glass surface which coordinates interactions between silane and water molecules. Dehydration of the coverslip surface causes the silane molecules to form a covalently linked monolayer on the glass surface. Excess APTES on the glass surface will form an insoluble white precipitate when the glass is heated above 70 °C. If this occurs, discard the coverslips; this is a sign that the silanized glass needs to be washed more thoroughly with isopropanol before baking.
12. After baking the APTES coated glass, bath sonicate the coverslips in 100 % ethanol for 15–30 min.
13. Using forceps, remove individual coverslips from the ethanol. Dip and waft coverslips in a beaker of ultrapure water. Slowly pull the coverslip out of the water. If the glass is properly silanized, water will bead-up and pull away from the coverslip. Oven dry to remove residual water.
14. Weigh 45 mg of mPEG-5000-NHS and 5 mg Biotin-PEG5000-NHS (*see* **Note 22**). The ratio can be varied depending on the desired % of biotin-PEG. Add anhydrous DMF to make a 50 mg/mL final concentration. If necessary, gently warm the solution to completely solubilize the PEG reagents. Be sure to use high quality/new DMF. Some solvents contain a large amount of fluorescent contamination which will bind to the glass. Scale up the amount of PEG-DMF solution as required.
15. Place six coverslips in each glass weigh jar with the diamond etched side up.
16. Spot 75 μL of solution onto each coverslip.
17. Place a second coverslip on top of first to make sandwich. Repeat, making 6 sandwiches/12 coverslips per weigh jar.
18. Incubate at 75 °C for 2 h.
19. Transfer weighing jars to a fume hood. Cool slightly before opening.
20. Separate coverslip sandwiches with forceps and place them in a large beaker of ultrapure water. Avoid touching the coverslips with hands or gloves. Wash coverslips with copious amounts ultrapure water.
21. Remove coverslips one-by-one with forceps and swirl in a large beaker of water. Dry and store coverslips in a covered container at 4–25 °C. Pegylated glass will last ≥2 months.

3.7 Labeling A. castellani Actin and Heavy Meromyosin with Maleimide Derivatives

1. Make actin labeling buffer.
2. Equilibrate PD10 column with 3 column volumes of actin labeling buffer.
3. Buffer exchange 2.5 mL of monomeric actin, 25–50 μM, using a PD10 column to remove the reducing agent (i.e., TCEP).
4. Determine the new actin concentration by measuring the absorbance at 290 nm. An A_{290} of 1.0 is equal to 38.5 μM amoeba actin.
5. Add 3–5 M excess Alexa Fluor 488, Cy3, or Cy5-maleimide. Maleimide dyes should be dissolved in DMSO to a concentration of 10–20 mM. These reagents should be stored in the −20 °C freezer and used within a year.
6. Incubate on ice for 5–10 min.
7. Quench the labeling reaction by adding DTT to 10 mM (1/100 dilution of 1 M stock). Incubate for 5 min on ice.
8. Ultracentrifuge the labeled monomeric actin at 350,000 × *g* (80,000 rpm with a TLA100.4) for 20 min. This will help remove aggregated proteins and insoluble fluorescent dye.
9. Transfer supernatant to a new tube. Add 10× KMEI to polymerize actin for 2–3 h at 20–25 °C. Final KMEI buffer concentrations should be 50 mM KCl, 1 mM $MgCl_2$, 1 mM EGTA, and 10 mM imidazole, pH 7.0. Add ATP to a final concentration of 1 mM.
10. Pellet labeled filamentous actin by ultracentrifugation at 195,000 × *g* (60,000 rpm with a TLA100.4) for 30 min.
11. Remove supernatant and gently wash the labeled actin pellet with 0.5 mL of Buffer A to remove free dye. *Note*: when labeling actin with tetramethyl-rhodamine, labeled actin will not polymerize. Monomeric TMR-labeled actin must be separated from free dye with a desalting or gel filtration column.
12. Gently resuspend the actin pellet in 250–500 μL of Buffer A. Pipet up and down to shear actin filaments. Transfer labeled actin to a microfuge tube. Allow actin filaments to depolymerize for 3–5 days at 4 °C.
13. After depolymerization, ultracentrifuge the labeled actin at 350,000 × *g* (80,000 rpm with a TLA100.4) for 20 min to remove aggregates and small actin filament seeds (*see* **Note 23**).
14. To remove the last trace of unconjugated fluorescent dye, buffer exchange the depolymerized actin into Buffer A using a NAP-5 (or PD10) desalting column. Determine the new actin concentration and labeling efficiency using a spectrophotometer.
15. Measure the A_{290} of labeled actin and absorbance at the dye excitation peak. Since fluorescent dyes contribute to the A_{290}

Table 1
Cysteine reactive maleimide fluorophores used for labeling actin

Fluorophore	Extinction coefficient (M^{-1} cm^{-1})	Absorbance peak (nm)	Contribution to A_{290} (%)
Alexa 488	71,000	494	13.2
Cy3	150,000	550	8
Cy5	230,000	649	3

signal, subtract this contribution from the A_{290} of the labeled actin to accurately calculate the concentration and labeling efficiency (Table 1).

16. To determine how much an unlisted dye contributes to the A_{280}, make a 1/1,000 dilution of the dye and perform a wave scan. Divide the A_{290} by the $A_{\text{ex peak}}$ of the dye; this is the A_{290} correction factor.
17. For actin labeled with Alexa488, A_{290} (actual) = A_{290} (labeled protein) – (A_{290} (labeled protein) × 0.132).
18. Labeling efficiency = $[\text{protein}]_{290}/[\text{protein label}]_{\text{ex peak}}$.
19. This protocol can also be used to biotinylate actin with maleimide-PEG2-Biotin or heavy meromyosin (HMM) labeling with maleimide-PEG11-Biotin. In the case of biotinylating HMM, buffer exchange reduced protein into 10 mM HEPES (pH 7.0) with 100 mM KCl. Add 5 M excess maleimide-PEG11-Biotin. Label for 15 min on ice. Quench with 10 mM DTT. Microcentrifuge to remove aggregates. Finally, remove free biotin-maleimide by gel filtration or desalting column. Freeze biotin-PEG11-HMM in buffer containing 10 mM HEPES (pH 7.0), 100 mM KCl, 1 mM TCEP, and 25 % glycerol.

3.8 Assembly of TIRF-M Flow Cells for Attachment of Filamentous Actin

1. Clean 25 mm × 75 mm × 1 mm glass slides with 3 M NaOH, 100 % ethanol, or oxygen plasma, as above (Subheading 3.6, **steps 2–4**).
2. Cut double sided tape and attach to glass slides (Fig. 3). Firmly rub across the tape with a capped Sharpie pen to form a tight seal with the slide. Although not essential for visualizing dynamic actin filaments, it's worth passivating the slides with poly-L-lysine PEG to minimize protein depletion effects (Fig. 3).
3. To passivate the slides, spread 5–10 μL of 3 mg/mL PLL-PEG on the space between the double sides tape. Allow the PLL-PEG to dry and then wash the glass under a stream of

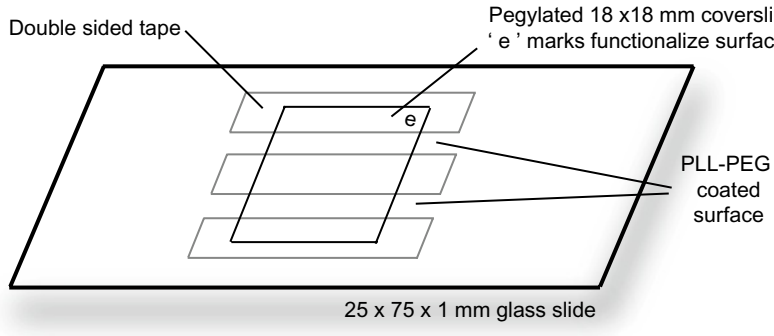

Fig. 3 Architecture of TIRF microscopy glass imaging chamber. Functionalized 18 mm × 18 mm coverslips are adhered to a glass slides using double sided tape with a spacing of ~5 mm per channel. Before attaching the PEG/biotin-PEG coverslips, coat the spaces between the double sided tape with PLL-PEG to reduce nonspecific absorption of proteins to the glass surface (*see* **Note 24**)

ultrapure water. Allow the slide and tape to dry before attaching the functionalized coverslip. After attaching a functionalized 18 mm × 18 mm coverslip to the double sided tape, gently press on the surface (e.g., using a capped Sharpie pen) to create a tight seal between the coverslip and tape.

4. Flow 40 μL blocking buffer into the flow chamber (*see* **Note 24**).
5. Incubate blocking solution for 1 min.
6. Wash with 40 μL wash buffer.
7. Flow 40 μL of 50 nM streptavidin diluted in wash buffer. Incubate for 30–60 s. Flush chamber with 40 μL wash buffer.
8. Flow 40 μL of 50 nM biotin-PEG11-HMM diluted in wash buffer. Incubate for 30–60 s. Flush chamber with 40 μL wash buffer. Alternatively, low concentration of biotin-phalloidin can be used to attach static or dynamic actin filaments. These methods of attachment may not be compatible with all actin binding proteins. Maleimide labeling of HMM can be performed as described in Subheading 3.7, **step 19**.
9. With myosin attached to the coverslip surface, phalloidin stabilized or dynamically elongating actin filaments can be attached to the functionalized glass surface (*see* Fig. 4 and **Note 25**).

3.9 Visualization of Dynamic Actin Filament Assembly

1. Combine the appropriate volumes of dark actin and fluorescently labeled actin in Buffer A to make a working stock of 4.44 μM (10–30 % Alexa488; *see* **Note 26**).
2. To exchange the Ca^{2+} for Mg^{2+}, combine 1 μL 10× ME and 9 μL of 4.44 μM actin. Incubate for 2 min.

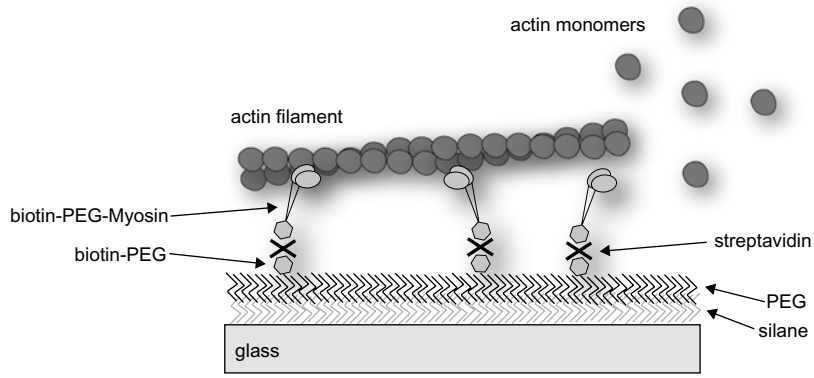

Fig. 4 Schematic for attachment of filamentous actin to biotin-PEG functionalized coverslips. Biotin-PEG functionalized glass can be coated with streptavidin and biotin-myosin. Pre-polymerized actin filaments can then be immobilized via the biotin-myosin linkage. Free actin monomers in solution can freely associate with the ends of actin filaments

3. Meanwhile combine 18 μL 2× TIRF buffer (lacking OSS) with 1 μL glucose oxidase (40×) and 1 μL catalase (40×) (*see* **Note 27**). Be sure to calculate buffer concentrations so that the addition of the OSS brings all of the TIRF buffer reagents/enzymes to 2× the desired final concentration.
4. Add 10 μL of protein dilution buffer to the 2× TIRF buffer (V_f = 30 μL). Typically this portion of the reaction mixture contains additional actin binding proteins (i.e., profilin, VASP, etc.).
5. To initiate the actin polymerization reaction, transfer the 30 μL TIRF buffer mix into the tube containing 10 μL of ME to exchange monomeric actin. Pipet up and down twice. Flow all 40 μL into the chamber using an aspirator and Whatman paper to wick the solution through the channel.
6. Seal the edges of the flow cells with VALAP, apply immersion oil, and mount on the TIRF microscope. In the presence of 1 μM actin, filaments will spontaneously nucleate and start elongating immediately. By the time the slide is mounted on the microscope and focused on the imaging surface (30–60 s), small actin filament seeds should be visible (Fig. 5a). Imaging with a frame rate of 5–10 s is sufficiently fast to capture the dynamics of actin filament assembly (Fig. 5b). Under these conditions, actin filament barbed ends should elongate at a rate of ~10 subunits/second (Fig. 5c).
7. For image analysis of microscopy data, we use ImageJ. By tracing the elongation path of a single actin filament, a kymograph can then be generated using the MultipleKymograph ImageJ plugin (J. Rietdorf, FMI Basel; A. Seitz, EMBL Heidelberg; http://rsbweb.nih.gov/ij/) available for free online. This will

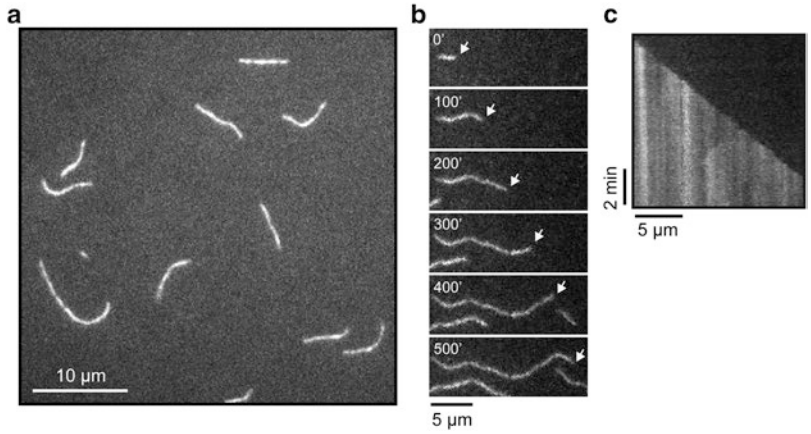

Fig. 5 Visualization of single actin filaments by TIRF microscopy. (**a**) Image showing a field of actin filaments generated by spontaneous nucleation of 1 μM actin (10 % Cy3 labeled) after about 1 min of mixing reactants. Actin filaments are attached to a biotin-myosin coated glass surface. (**b**) Montage of images showing a single actin filament elongating. The *white arrow* indicates the barbed end. (**c**) Kymograph showing the change in length as a function of time for a single elongating actin filament

create an image similar to the one shown in Fig. 5c. The *x*-axis corresponds to filament length (1 μm of actin filament contains 370 subunits; [26]) and the *y*-axis represents time (i.e., seconds). The slope of kymograph equals the change in filament length as a function of time. This value is typically expressed as subunits/second.

4 Notes

1. All solutions should be prepared in ultrapure water with resistivity of 18.2 Ω (e.g., Milli-Q water). Cold water refers to ultrapure water at 4 °C.
2. More complete protocol: Dry DEAE resin (vacuum resin until just damp; not white). Transfer to beaker and add water to 4 L. Add solid NaOH to 0.5 M and stir 5 min, 25 °C. Dry and wash with 4 L water. Repeat NaOH wash, this time stir for 30 min. Dry and wash with 8 L water. Resuspend in 2,870 mL water and add 130 mL concentrated HCl. Stir 30 min, 25 °C. Dry and wash with 8 L water. Resuspend in 3–4 L water and add 1 M Tris base until pH is 8.0. Add 0.2 % (v/v) benzalkonium chloride and store at 4 °C.
3. Make Buffer A as a 100× stock without $CaCl_2$—Calcium-ATP precipitates at this concentration—and freeze at −20 °C. Add $CaCl_2$ during dilution to 1×, and aliquot in 15 mL conical tubes and freeze at −20 °C. Once thawed, one aliquot may be used for up to 1 week.

4. Imidazole is best stored in the dark, at 4 °C, as a 1–2 M stock solution. Store 10× KMEI buffer for fluorimetry in the dark, at 4 °C. Discard when autofluorescence of the buffer becomes noticeable during fluorimetry. Alternatively, use HEPES buffer in place of imidazole in KMEI.
5. Assay growth by absorbance at 600 nm (A_{600}). A typical A_{600} of amoeba for purifying actin is 6. A_{600} values over 1.0 are out of the linear range in most cases, so dilute the amoeba before measuring. Amoeba settle out of solution, so mix before reading absorbance (amoeba that do not settle or media that remains turbid after ~10 min may indicate that the amoeba are dying in culture). Alternatively, amoeba can be grown in a fermenter.
6. We have noticed inconsistencies with actin purified from amoebae that have been frozen for longer than 6 months.
7. The first day of the actin purification protocol is significantly long, and is aided by making buffers and gathering equipment and reagents the day before. Once started, the entire purification takes 5–7 days, including 2–3 days for the actin to depolymerize.
8. To eliminate bubbles when decanting resin slurry into the column, pour it slowly down the outside of a Pasteur pipette or glass stir rod, onto the inside wall of the column. Do not let the resin drip directly into the column.
9. Actin requires ATP, which absorbs significantly less at 290 nm than at 280 nm. To limit the time that actin fractions are out of the cold room, it is practical to reuse pipettes and not wash the cuvette between each reading. To avoid contaminating monomeric actin with actin dimers, start at the highest fraction and take readings backwards.
10. The critical concentration of calcium-actin is 150 μM [10]. Actin will not fully depolymerize above this concentration.
11. Concentration of dark actin and pyrene actin stocks must both be measured. Because some proteins do not bind as tightly to pyrene actin as dark actin, the actin used in fluorimetry is normally only 5–10 % pyrene actin [10]. To calculate how much pyrene actin and dark actin to combine to yield a given percent labeling and a given concentration, use the equations:

    L_i = starting percent labeling of pyrene actin (100 % labeled = 100)

    C_p = starting concentration of pyrene actin (μM)

    C_d = starting concentration of dark actin (μM)

L_f = final percent labeled (i.e., 5–10)

C_f = Final concentration of actin (μM)

V_f = Final volume of actin (μL)

$$\text{volume pyrene actin}(\mu\text{L}) = \frac{L_f C_f V_f}{L_i C_p} \quad (3)$$

$$\text{volume dark actin}(\mu\text{L}) = \left(V_f - \frac{\text{volume pyrene actin } C_p}{C_f} \right) \frac{C_f}{C_d} \quad (4)$$

Bring up to volume (V_f) with Buffer A.

12. Because ATP absorbs significantly at 280 nm, proteins other than actin should not be in Buffer A for quantification by spectrophotometry.
13. It may be desirable to pre-mix proteins before starting actin exchange, to allow them to come to equilibrium. Although not recommended for detailed kinetic analysis, it is possible to add *E. coli* lysate containing expressed protein (or impure eluates from affinity chromatography) to pyrene actin assembly assays as a first-pass functional test. Uninduced (control) lysate should have no effect on actin polymerization.
14. There are many factors to consider for collecting meaningful and reproducible fluorimetry data. To list key points.
    (a) Always do an actin alone (control) reaction to test the actin first.
    (b) The assay is very sensitive to the concentration of monovalent salt (e.g., potassium in KMEI), so keep that constant in all reactions. In the event that a protein component is stored in a buffer containing salt, adjust the molarity of KCl in 10× KMEI buffer to keep the final concentration of monovalent salt in the reaction at 50 mM. If a higher salt concentration is required for protein stability, make sure that all reactions contain the same salt concentration.
    (c) Exchange in 10× ME buffer for exactly 2 min and be consistent.
    (d) Eliminate photobleaching.
    (e) Always collect complete data sets: until pyrene fluorescence plateaus.
    (f) Wash cuvettes extensively between each reaction, as polymerized actin remaining in the cuvette will nucleate new filaments in the next run.
    (g) Avoid bubbles, which both scatter light and cause oxidative damage to proteins.

(h) Store proteins on ice, but ensure all components are at 25 °C at the start of the reaction. Pre-incubating tubes in a water bath works well.

(i) When expressing Glutathione-S-Transferase (GST)-tagged recombinant proteins, it is critical to remove the GST, as GST will mediate the dimerization of the fusion protein. For example, Arp2/3 activators display faster kinetics when the GST remains uncleaved [27, 28].

(j) Pyrene is an environmentally sensitive fluorophore, and binding of proteins to the side of a labeled actin filament can affect fluorescence. Therefore pyrene fluorescence alone cannot be used to definitively conclude that a given actin binding protein increases or decreases actin assembly; visualization of actin filaments is an essential complementary approach to pyrene assembly assays.

15. Photobleaching is a complex phenomenon that cannot be corrected for mathematically [10]. If the overall signal is too low after eliminating photobleaching, try widening emission slits, increasing the voltage of the PMT, or increasing percentage of pyrene-labeled actin, and again measuring photobleaching after the change.
16. We polymerize the concentration of actin that will be used in the experiments in the presence of Arp2/3 and an activator (like *Listeria* ActA or Scar/WAVE VCA), which comes to plateau very quickly. It is also possible to polymerize a high concentration of actin, then dilute down to working concentration and measure in the fluorimeter.
17. First, to determine when a given condition will plateau, perform pyrene actin assembly assay as above. For microscopy, reaction volumes can be scaled down to less than 100 μL.
18. If the functionalized glass contains a high fluorescent background, Piranha etch the glass before silanizing. Piranha is a 3:1 mixture of sulfuric acid and hydrogen peroxide. Be sure to wear the proper protective gear. Alternative to 3 M NaOH or Piranha etching, 2 % Hellmanex (Fisher, 14-385-944), heated to ~60 °C, can be used to efficiently strip glass of fluorescence and organic matter.
19. The addition of a small amount of water is required for the amino-silane molecules to polymerize and form weak electrostatic interaction with each other. Most reagent grade alcohol will contain a sufficient trace amount of water.
20. Isopropanol is not the only solvent that can be used to dilute silanes. Although more expensive, ethanol and acetone are good alternatives. Depending on your source of solvents,

you may find that this is the source of most fluorescent contaminations on the final functionalized glass surface. If you plan to image single fluorescently labeled proteins, you might need to test multiple types of solvents to find the one with the least amount of fluorescent contamination.

21. Depending on the biochemical properties of actin binding proteins being characterized, the APTES silanization and NHS-PEG might not sufficiently passivate the glass. Instead, a more dense PEG functionalized glass surface may be required to efficiently reduce nonspecific protein absorption to the glass in the TIRF assay. Alternatively (3-Glycidyloxypropyl)-trimethoxysilane (GOPTS; Sigma-Aldrich 440167) and NH_2-PEG derivative can be used to silanize and pegylate coverslips, respectively. Note that GOPTS is destroyed by aqueous solvents. Therefore, it is necessary to wash the glass with anhydrous acetone after silanizing. After silanizing glass to GOPTS, Hydroxy-PEG-NH2 3000 Da (Rapp Polymere, 10-3000-20) and Biotin-CONH-PEG-NH2 3000 Da (Rapp Polymere, 13-5000-25-20) can be used to functionalize the coverslips. For more detail, refer to ref. 18.
22. PEG-NHS and biotin-PEG-NHS reagents are quickly destroyed by moisture. In aqueous buffer, water acts as a nucleophile and reacts irreversibly with the NHS (half-life ~15 min). NHS reagents should be store at –20 °C in a sealed desiccator. When using these reagents, allow the storage vial to warm to room temperature before opening the bottle. If the bottle is cold, water will condense on the lyophilized chemical and gradually reduce the activity. We recommend storing pre-weighed quantities of each NHS reagent in microfuge tubes that are sealed with parafilm and stored in a desiccator in the –20 °C freezer. This will minimize the number of times any particular reagent is exposed to moisture.
23. Without gel filtration, some actin dimers and trimers will be present. This is really only a problem if you want to measure nucleation rates (as in pyrene assembly assays, above). If you find that spontaneous nucleation is too rapid in the actin TIRF assay, centrifuge (350,000 × *g* or 80,000 rpm in a TLA100.4 for 20 min) or gel filter the labeled actin with a Superdex 75 column (as in Subheading 3.2, **step 12**). Alternatively, use profilin to suppress spontaneous actin nucleation. Note that equal molar concentrations of profilin relative to the actin monomer concentration will reduce the barbed end elongation rate of single actin filaments by ~50 %.
24. Passivating the slide surface with PLL-PEG will minimize protein depletion effects caused by nonspecific absorption of protein to the glass surfaces. Protein depletion can lead to

inconsistent results, especially when characterizing an actin binding protein that is present at a nanomolar concentration in the assay.

25. It is important to optimize conditions such that filaments are not so strongly adhered to the glass as to prevent them from polymerizing. Pauses in elongation/polymerization should be infrequent by kymograph analysis. If the filaments are pausing too much or growing slowly, use less streptavidin and Biotin-HMM. Alternatively, reduce the percentage of conjugated biotin-PEG.
26. For polymerization assays, it is best to use 10 % labeled actin. The higher the percentage labeled actin, the slower filaments will elongate. If more than 10 % labeled actin is required to visualize filaments, something could be wrong with your reagents. Check the quality of your actin by SDS-PAGE; actin that is partially proteolyzed will give the appearance of slower kinetics. In this event you can re-enrich for full-length actin by one cycle of polymerization and depolymerization: add 10× KMEI to polymerize, then centrifuge at 100,000 × *g* to pellet filaments, discard supernatant (containing non-polymerizable actin), depolymerize, and gel filter as in Subheading 3.2, **steps 10–12**. Alternatively, trouble-shoot actin polymerization by visualizing phalloidin-stabilized filaments as in Subheading 3.5. Other common sources of error include: lack of camera sensitivity, too low or high laser power coming through the objective, or improperly functionalized glass.
27. Make glucose oxidase and catalase stocks fresh and ultracentrifuge at 350,000 × *g* (80,000 rpm with a TLA100.4) for 20 min to remove aggregates. There is typically a large dark brown pellet after centrifuging catalase. Keep the supernatant and do not resuspend this pellet. Use within 3 days. If the glucose oxidase and catalase activity are not properly balanced in the TIRF assay buffer, the reaction can acidify. This may result in slower filament elongation rates and changes in photostability of the fluorophores. Be sure to use fresh lyophilized catalase that is not clumpy due to prolonged exposure to moisture.

Acknowledgments

The authors would like to thank their colleagues Orkun Akin, Margot Quinlan, and Peter Bieling for support and help in developing the techniques described. S.D.H was supported by a National Science Foundation predoctoral Fellowship. J.B.Z. was supported by an American Heart Association predoctoral fellowship, and is currently a Howard Hughes Medical Institute Fellow of the Life Sciences Research Foundation.

References

1. Pollard TD, Borisy GG (2003) Cellular motility driven by assembly and disassembly of actin filaments. Cell 112:453–465
2. Fletcher DA, Mullins RD (2010) Cell mechanics and the cytoskeleton. Nature 463: 485–492
3. Oosawa F, Kasai M (1962) A theory of linear and helical aggregations of macromolecules. J Mol Biol 4:10–21
4. Frieden C (1983) Polymerization of actin: mechanism of the Mg2+-induced process at pH 8 and 20 degrees C. Proc Natl Acad Sci USA 80:6513–6517
5. Welch MD, Mullins RD (2002) Cellular control of actin nucleation. Annu Rev Cell Dev Biol 18:247–288
6. Quinlan ME, Heuser JE, Kerkhoff E, Mullins RD (2005) Drosophila spire is an actin nucleation factor. Nature 433:382–388
7. Campellone KG, Welch MD (2010) A nucleator arms race: cellular control of actin assembly. Nat Rev Mol Cell Biol 11:237–251
8. Cooper JA, Walker SB, Pollard TD (1983) Pyrene actin: documentation of the validity of a sensitive assay for actin polymerization. J Muscle Res Cell Motil 4:253–262
9. Pollard TD (1983) Measurement of rate constants for actin filament elongation in solution. Anal Biochem 134:406–412
10. Mullins RD, Machesky LM (2000) Actin assembly mediated by Arp2/3 complex and WASP family proteins. Methods Enzymol 325:214–237
11. Gordon DJ, Eisenberg E, Korn ED (1976) Characterization of cytoplasmic actin isolated from *Acanthamoeba castellanii* by a new method. J Biol Chem 251:4778–4786
12. Blanchoin L, Pollard TD (1999) Mechanism of interaction of *Acanthamoeba* actophorin (ADF/Cofilin) with actin filaments. J Biol Chem 274:15538–15546
13. Kelleher JF, Mullins RD, Pollard TD (1998) Purification and assay of the Arp2/3 complex from *Acanthamoeba castellanii*. Methods Enzymol 298:42–51
14. Dayel MJ, Holleran EA, Mullins RD (2001) Arp2/3 complex requires hydrolyzable ATP for nucleation of new actin filaments. Proc Natl Acad Sci USA 98:14871–14876
15. Mullins RD, Heuser JA, Pollard TD (1998) The interaction of Arp2/3 complex with actin: nucleation, high affinity pointed end capping, and formation of branching networks of filaments. Proc Natl Acad Sci USA 95: 6181–6186
16. Kuhn JR, Pollard TD (2005) Real-time measurements of actin filament polymerization by total internal reflection fluorescence microscopy. Biophys J 88:1387–1402
17. Hermanson GT (1996) Bioconjugate techniques. Academic, San Diego, CA, pp 266–272 (Product # 20002T)
18. Bieling P, Telley IA, Hentrich C, Piehler J, Surrey T (2010) Fluorescence microscopy assays on chemically functionalized surfaces for quantitative imaging of microtubule, motor, and+TIP dynamics. Methods Cell Biol 95: 555–580
19. Kovar DR, Harris ES, Mahaffy R, Higgs HN, Pollard TD (2006) Control of the assembly of ATP- and ADP-actin by formins and profilin. Cell 124:423–435
20. Kuhn JR, Pollard TD (2007) Single molecule kinetic analysis of actin filament capping. J Biol Chem 282:28014–28024
21. Hansen SD, Mullins RD (2010) VASP is a processive actin polymerase that requires monomeric actin for barbed end association. J Cell Biol 191:571–584
22. Huang NP, Michel R, Voros J, Textor M, Hofer R, Rossi A, Elbert DL, Hubbell JA, Spencer ND (2000) Poly(l-lysine)-g-poly(ethylene glycol) layers on metal oxide surfaces: surface analytical characterization and resistance to serum and fibrinogen adsorption. Langmuir 17:489–498
23. Stuurman N, Amodaj N, Vale RD (2007) μManager: open source software for light microscope imaging. Microsc Today 15: 42–43
24. Neff RJ (1958) Mechanisms of purifying amoebae by migration on agar surfaces. J Protozool 5:226–231
25. Schuster FL (2002) Cultivation of pathogenic and opportunistic free-living amebas. Clin Microbiol Rev 15:342–354
26. Huxley HE, Brown W (1967) The low-angle x-ray diagram of vertebrate striated muscle and its behaviour during contraction and rigor. J Mol Biol 30:383–434
27. Higgs HN, Pollard TD (2000) Activation by Cdc42 and PIP(2) of Wiskott-Aldrich syndrome protein (WASp) stimulates actin nucleation by Arp2/3 complex. J Cell Biol 150: 1311–1320
28. Padrick SB, Cheng HC, Ismail AM, Panchal SC, Doolittle LK, Kim S, Skehan BM, Umetani J, Brautigam CA, Leong JM, Rosen MK (2008) Hierarchical regulation of WASP/WAVE proteins. Mol Cell 32:426–438
29. Selden LA, Kinosian HJ, Estes JE, Gershman LC (2000) Cross-linked dimers with nucleating activity in actin prepared from muscle acetone powder. Biochemistry 39:64–74

Chapter 10

Synthetic and Tissue-Derived Models for Studying Rigidity Effects on Invadopodia Activity

Alissa M. Weaver, Jonathan M. Page, Scott A. Guelcher, and Aron Parekh

Abstract

Invasion by cancer cells through the extracellular matrix (ECM) of tissues is a critical step in cancer progression and metastasis. Actin-rich subcellular protrusions known as invadopodia are thought to facilitate this process by localizing proteinases which degrade the ECM and allow for cancer cell penetration. We have shown in vitro that invadopodia activity is regulated by the rigidity of the ECM, which suggests that matrix remodeling in vivo may also be regulated by the mechanical properties of tissues. In order to study rigidity effects on invadopodia activity in a controlled manner, we have developed assays in which we have conjugated degradable fluorescent matrix molecules to tunable synthetic substrates. In addition, we have also utilized ex vivo tissue-derived substrates to corroborate our findings. In this chapter, we present detailed protocols describing the synthesis and preparation of our synthetic substrates, polyacrylamide gels and polyurethane elastomers, for use in these matrix degradation assays as well as the steps required to utilize our tissue-derived substrates.

Key words Invadopodia, Degradation, Rigidity, Polymer, Tissue

1 Introduction

During tumor development, cancer cells experience increasing environmental rigidity due to tumor cell packing, extracellular matrix (ECM) deposition and cross-linking, and higher fluid pressures [1]. In mouse models of breast cancer, changes in mammary tissue density have been shown to promote in vivo invasion and metastases [2]. Clinically, the increased tissue density of rigid tumor masses in breast tissue is frequently detected by physical evaluation (e.g., palpation), and mammographic density is now strongly correlated with increasing breast cancer risks [3–6]. Indeed, the rigidity of excised human pathological mammary tissue samples increases with their clinical grades [7]. This growing evidence suggests that tissue rigidity may play an integral role in driving cancer cell invasion and metastasis. Moreover, other tissues

Amanda S. Coutts (ed.), *Adhesion Protein Protocols*, Methods in Molecular Biology, vol. 1046,
DOI 10.1007/978-1-62703-538-5_10,

in the body have characteristic mechanical properties such as the Young's or elastic modulus (typically reported in Pascals—Pa) that span a wide range of rigidities [8], suggesting that the rigidities encountered by metastasizing cancer cells have the potential to significantly alter their malignant phenotype.

Penetration of ECM by invading cancer cells is generally regarded to involve proteolytic degradation given the existence of covalent cross-links in native tissues and may be particularly important for traversing dense basement membranes [9]. Actin-rich, subcellular protrusions known as invadopodia are thought to mediate this task due to their specialized function in degrading ECM [10]. Invadopodia are prototypically formed by invasive cells and have been implicated in tumor cell metastasis [11]. Evidence is building that these structures are required in 3-D environments and also exist in situations in vivo that are 2-D in nature [12]. Although the dynamics of invadopodia are not completely understood, they are regulated by numerous processes including growth factor signaling [13], the cytoskeletal contractile machinery [14], integrin adhesions [15, 16], ion transporters [17], signaling through reactive oxygen species [18], and fatty acid synthesis [19].

Several years ago, we developed a protocol to specifically examine the role of tissue rigidity on invadopodia activity [20, 21]. Although rigidity had been identified as an important component driving cancer progression in both animal [2, 22] and clinical studies [5, 23], it was unclear how changes in tissue mechanics influenced invasion at a cellular level, particularly in regards to invadopodia activity. Invadopodia are routinely detected in vitro by culturing cancer cells on glass coated with a fluorescent layer of ECM proteins and then colocalizing markers for invadopodia such as actin and cortactin with areas of ECM degradation, evident by loss of fluorescent signal [24]. Since a thin layer of cross-linked proteins is often used (approximately 1 μm in thickness from our observations), cells can easily detect the underlying rigidity of the glass surface, which has an elastic modulus similar to bone. Therefore, we developed an invadopodia assay in which the rigidity experienced by the cells can be varied by attaching the protein layer to polymer substrates of different rigidities cast in glass bottom dishes. This casting method is similar to methods developed for traction force microscopy substrates and for rigidity testing of other cellular phenotypes [25, 26]. We used this system to show that ECM rigidity promotes invadopodia activity [20] and that the activity modulation occurs over a wide range of rigidities [21]. Since polyacrylamide (PAA) gels and polyurethane (PUR) elastomers are optically clear, the fixed and stained samples are ideal for fluorescent imaging. Visualization of dual invadopodia markers (actin and cortactin) and fluorescent matrix degradation allows quantitative analyses of invadopodia activity. We also utilized tissue-derived basement membrane (BM) and stromal matrices as ex vivo models to validate our in vitro findings.

2 Materials

For all solutions use ultrapure water.

2.1 Glass Coverslip Materials

1. 35 mm glass bottom dishes with uncoated 14 mm coverslips (MatTek, catalog number P35G-0-14-C).
2. 12 mm coverslips.
3. 0.1 N NaOH: Dilute 1 N NaOH with water.
4. 10× PBS stock: 0.011 M KH_2PO_4, 1.54 M NaCl, 0.056 M Na_2HPO_4. Dilute with water to make a 1× PBS solution.
5. 3-Aminopropyltrimethoxysilane (Sigma-Aldrich).
6. 0.5 % Glutaraldehyde solution: Dilute 25 % glutaraldehyde (Polysciences) with 1× PBS solution.

2.2 Polyacrylamide Gel Materials

1. 40 % Acrylamide (Bio-Rad).
2. 2 % Bis solution (Bio-Rad).
3. Toluene (Sigma-Aldrich).
4. 2 % Acrylic acid *N*-hydroxysuccinimide ester solution in toluene: Prepare fresh in a fume hood (typically 5 mg in 250 μL of toluene).
5. 10 % (w/v) Ammonium persulfate solution: Prepare a fresh solution in 1× PBS each time.
6. *N,N,N′,N′*-tetramethylethylenediamine (TEMED).
7. 50 mM HEPES: Dilute 1 M HEPES with water to 50 mM and pH to 8.5 with 10 M NaOH.

2.3 Polyurethane Materials

1. 1 mg/mL Poly-D-lysine solution in water.
2. Methyl 2,6-diisocyanatohexane (lysine methyl ester diisocyanate, LDI, Adamas Reagent Co., Ltd., catalog number 13010).
3. Hexamethylene diisocyanate trimer (HDIt, Bayer Material Science, Desmodur N3300A).
4. ε-Caprolactone monomer (99 %, Acros Organics, catalog number AC17344-2500).
5. dl-Lactide (Polysciences, catalog number 17085).
6. Glycolide (Polysciences, catalog number 16640).
7. Stannous octoate (Nusil, catalog number 00002CAT0000AX).
8. Glycerol (99.5 %+).
9. Phthalic anhydride (99 %+, Sigma-Aldrich, catalog number 320064).
10. NaOH pellets (98 %).
11. Potassium hydrogen phthalate (99.9 %+, Sigma-Aldrich, catalog number P1088).

12. Pyridine, anhydrous (99.8 %, Sigma-Aldrich, catalog number 270970).
13. 1 N NaOH.
14. Dipropylene glycol (Sigma-Aldrich, catalog number D215554-500G).
15. 1,4 Diazabicyclo[2.2.2] octane (triethylene diamine (TEDA), Sigma-Aldrich, catalog number D27802-100G).
16. Polycaprolactone triol (300 Mn, Sigma-Aldrich, catalog number 200387-250G).
17. Magnesium sulfate, anhydrous (>99.5 %).
18. Di-*n*-butylamine (>99.5 %, Sigma-Aldrich, catalog number 471232).
19. Hydrochloric acid (37 %).
20. Potassium hydroxide in methanol (0.995–1.005 N, Fisher, catalog number SP220-1).
21. Methanol (99.9 %).
22. Hexanes (Fisher Scientific, catalog number H303-1).
23. Coscat 83 (Vertellus, catalog number CAT83).
24. 1,2 Dichloroethane, anhydrous (99.8 %, Sigma-Aldrich, 284505-1L).

2.4 Gelatin and Fibronectin Materials

1. Sucrose.
2. Gelatin (Polysciences, catalog number 00639). Prepare a stock of 1 % gelatin/1 % sucrose in 1× PBS solution (typically we make 10 mL at a time). Preheat PBS to aid in gelatin dissolution.
3. Sodium borohydride solution: 1 mg/mL sodium borohydride in 1× PBS solution. Prepare in a fume hood.
4. Fibronectin (Life Technologies, catalog number 33016-015).
5. 70 % Ethanol.

2.5 Experimental Assay Materials

1. Invadopodia medium: Equal parts of DMEM (Cellgro) and RPMI 1640 (Gibco), 5 % Nu-Serum (BD Biosciences, catalog number 355500), 10 % fetal bovine serum (Thermo Scientific), and 20 ng/mL of freshly added epidermal growth factor (Life Technologies, catalog number PHG0311).

2.6 Fluorescence Microscopy Materials

1. Sterile PBS (Cellgro).
2. 3.7 % Paraformaldehyde solution in 1× PBS: Weigh powdered paraformaldehyde in a closed container (or prepare in a fume hood). Solution should be placed in a 37 °C water bath to aid in dissolution. A few milliliters of 10 M NaOH can also be used to aid in dissolution. The final solution can be brought back to pH 7.4 with 10 M HCl.

3. 0.1 % Triton X-100 in 1× PBS solution.
4. Blocking solution: 3 % bovine serum albumin in 1× PBS solution.
5. Aqua Poly/Mount (Polysciences, catalog number 18606).
6. 22×22 mm Coverslips (Fisher, catalog number 12-541-B).
7. CellCrowns for 24-well plate (Scaffdex, catalog number C00001N).
8. 24-Well plates.
9. 12-Well plates.
10. Glass slides (Fisher, catalog number 12-545-C).
11. 10 mm Disposable tissue biopsy punches (Acuderm, catalog number P1050).
12. 22×40 mm Coverslips (Fisher, catalog number 12-545-C).
13. Alexa Fluor 546 phalloidin (Life Technologies, catalog number A22283).
14. Kimwipes, glass pipettes, pipette box lid, fine tip tweezers, surgical scissors, filter paper, Erlenmeyer flasks, funnels, magnetic stirrer, magnetic stir bars, overhead stirrer, 100 mL 3-neck flasks, heating sleeves for 3-neck flask, vacuum oven (with liquid nitrogen trap), oil bath, assorted glassware and standard polymer characterization equipment (gel permeation chromatography and automatic titrator).

3 Methods

3.1 Glass Coverslip Preparation for Polyacrylamide Gels

1. Dust off 12 mm coverslips with Kimwipes.
2. Pass coverslips of glass bottom dishes (inside surface) and 12 mm coverslips through a Bunsen burner flame.
3. Soak the glass bottom dish coverslips with 200 μL of 0.1 N NaOH for 5 min at room temperature.
4. Aspirate and air-dry for 20–30 min.
5. Soak the glass bottom dish coverslip with 50–100 μL of 3-aminopropyltrimethoxysilane for 10 min at room temperature in the fume hood. Use glass pipettes since it reacts with plastic (*see* **Note 1**).
6. Soak the glass bottom dish coverslips in water until clear (~5–10 min).
7. Rinse the glass bottom dish coverslips with water from a squeeze bottle twice.
8. Soak glass bottom dish coverslips with 2 mL of water at room temperature on a rocker at medium speed for 10 min.

9. Aspirate and air-dry for 20–30 min.
10. Soak the glass bottom dish coverslips with 2 mL of 0.5 % glutaraldehyde solution on a rocker at medium speed for 30 min at room temperature.
11. Wash the glass bottom dish coverslips with 2 mL of water three times, 10 min each, on rocker at medium speed.
12. Dry glass bottom dishes vertically (~60° angle or greater) for 20–30 min. Dishes can be stored up to 2 months in a desiccator.

3.2 Glass Coverslip Preparation for Polyurethanes

1. Dust off 35 mm MatTek dish with Kimwipes.
2. Soak 14 mm glass portion of the MatTek dish with 0.1 N NaOH for 5 min. Decant the solution and air-dry.
3. Coat the 14 mm glass portion of the MatTek dish with 3-aminopropyltrimethoxysilane for 15 min.
4. Wash with 10 mL of water. Repeat wash step five times. Allow the dishes to dry in air after final wash.
5. Coat the 14 mm glass portion of the MatTek dish with 0.5 % glutaraldehyde solution for 45 min.
6. Wash with 10 mL of water. Repeat wash step three times. Allow the dishes to dry in air after final wash.
7. Store treated dishes in a desiccator until use.

3.3 Polyacrylamide Gel Preparation

1. Make 5 mL of the polyacrylamide solutions (*see* **Note 2**). For soft polyacrylamide gels (8 % acrylamide/0.05 % bis solution; elastic modulus = 1,071 Pa); mix 3.875 mL of water, 1 mL of 40 % acrylamide, and 125 μL of 2 % bis solution. For hard polyacrylamide gels (8 % acrylamide/0.35 % bis solution; elastic modulus = 9,929 Pa); mix 3.125 mL of water, 1 mL of 40 % acrylamide, and 875 μL of 2 % bis solution. For rigid polyacrylamide gels (12 % acrylamide/0.6 % bis solution; elastic modulus = 28,283 Pa); mix 2 mL of water, 1.5 mL of 40 % acrylamide, and 1.5 mL of 2 % bis solution.
2. Make the 2 % acrylic acid *N*-hydroxysuccinimide ester solution in toluene in a fume hood.
3. Add 25 μL of a freshly made 10 % solution of ammonium persulfate and 2.5 μL of TEMED to each polyacrylamide solution. Mix by gentle pipetting or stirring to avoid creating bubbles.
4. In a fume hood, add 8.48 μL of polyacrylamide solution on to the center of each glass bottom dish coverslip (*see* **Note 3**).
5. Put 2 μL of the acrylic acid *N*-hydroxysuccinimide ester solution on top of the polyacrylamide solution (*see* **Note 4**).

6. Gently place the flamed side of the 12 mm coverslip on top of a glass bottom dish coverslip by lowering it parallel to the dish at one edge using fine tip tweezers.
7. Let the polyacrylamide solution polymerize for 60 min or until the leftover polyacrylamide has polymerized.
8. Add 2 mL of 50 mM HEPES.
9. Remove 12 mm coverslip with fine point tweezers.
10. Soak in 2 mL 50 mM HEPES for 1 h on a rocker at medium speed and change the solution every 15 min.

3.4 Polyurethane Precursor Preparation

3.4.1 Polyester Triol Preparation

The following describes steps to prepare a 100 g batch of 3,000 g/mol 70 % caprolactone, 20 % glycolide, 10 % lactide polyester; *see* **Note 5** for additional steps to prepare 900 g/mol triol.

1. Dry 5 g glycerol at 80 °C under vacuum (750 Torr) for 24 h. Store under desiccant until use.
2. Dry 75 g ε-caprolactone monomer with 1–5 g anhydrous magnesium sulfate (*see* **Note 6**), then pour through filter paper into a 100 mL beaker.
3. Add 0.1 g stannous octoate to a clean, dry 100 mL 3-neck flask.
4. Add 3.07 g of the dried glycerol to the 3-neck flask.
5. Add 9.69 g of dl-lactide to the 3-neck flask.
6. Add 19.39 g of glycolide to the 3-neck flask.
7. Add 67.85 g of the dry, filtered ε-caprolactone monomer to the 3-neck flask.
8. Place the 3-neck flask in a heating sleeve and stir with an overhead stirring apparatus at medium speed.
9. Flush the reactor with a constant stream of dry argon.
10. Slowly bring the temperature up to 140 °C and allow the reaction to occur for 48 h.
11. After 48 h of reaction time, the polymer should be a highly viscous, slightly milky white color liquid.
12. Pour polymer into a 250 mL beaker and add 100 mL of hexane. Stir with a magnetic stirrer and stir bar. If the polymer is too viscous to stir, apply heat up to 100 °C.
13. Carefully remove excess hexane and repeat the wash three times.
14. After the final wash, place the beaker on a hot plate at 100 °C for 8 h to remove excess solvent.
15. Dry the remaining polymer at 80 °C under vacuum (750 Torr) for 24 h. Store under desiccant until use.

*3.4.2 Characterization of Polyester Triol (OH# See **Note 7** for More Details)*

1. Dissolve 148.12 g of phthalic anhydride in 500 mL of anhydrous pyridine and bring the total volume to 1 L with excess anhydrous pyridine. Stir overnight in a dark bottle with closed cap. Prepare fresh daily as required.
2. Dissolve 40 g of NaOH pellets in 500 mL of water and bring the total volume to 1 L with water.
3. Weigh 2–3 g of potassium hydrogen phthalate into a beaker and add 150 mL of water with stirring until dissolved.
4. Titrate until end point with NaOH solution to calculate the solutions normality.
5. Weigh 1–5 g of polyester triol in a 125 mL Erlenmeyer flask and dissolve in 10 mL of phthalic anhydride/pyridine solution. Attach condenser and reflux at 170 °C for 30 min.
6. After cooling, rinse the condenser with 15 mL of anhydrous pyridine and 15 mL water.
7. Titrate to endpoint with 1 N NaOH solution.
8. Complete **steps 5**–7 without the addition of polyester for blank runs.
9. If the titrant volume required for the polyester samples is less than 75 % of the volume required for the blank, the sample was too large and **steps 5**–7 will need to be repeated with smaller samples of polyester.
10. The final OH# can be calculated from the following equation:

$$\mathrm{OH\#} = \frac{(B - A) \times N \times 56.11}{W},$$

where:

B = Average mL of NaOH solution consumed by the blanks.

A = NaOH solution consumed by the sample in mL.

N = Normality of the NaOH solution.

W = Grams of sample.

3.4.3 Isocyanate Prepolymer Preparation (50 g Batch of LDI Based Prepolymer)

1. Add 0.025 g of Coscat 83 to a dry, clean 100 mL 3-neck flask.
2. Add 44.07 g of lysine methyl ester diisocyanate (LDI) to the 3-neck flask.
3. Heat oil bath to 90 °C over a magnetic stir plate.
4. Place a 3-neck flask securely in the oil bath and apply medium stirring. Flush with a constant stream of dry argon.
5. Allow up to 1 h for temperature to equilibrate, then add 5.94 g of polycaprolactone triol (300 Mn) dropwise to the 3-neck flask.

6. Allow the reaction to proceed for 3 h.
7. After the reaction is complete, the prepolymer should be a low viscosity, light yellow color liquid.
8. Pour the prepolymer into a container for storage and keep under nitrogen at 4 °C until use.

*3.4.4 Characterization of the Prepolymer (NCO# See **Note 8** for More Details)*

1. Prepare 1 M solution of dibutylamine in toluene (for example 170 mL dibutylamine diluted up to 1 L with toluene).
2. Prepare a 1 M solution of HCl in methanol (for example 83.3 mL of 37 % HCl diluted up to 1 L with methanol).
3. Add 25 mL of 1 N KOH in methanol into a 100 mL beaker diluted with 50 mL water.
4. Titrate to end point with HCl in methanol and calculate HCl solution normality from the following equation:

$$N_{\mathrm{HCl}} = \frac{N_{\mathrm{KOH}} \times V_{\mathrm{KOH}}}{V_{\mathrm{HCl}}},$$

where:

N_{KOH} = Normality of KOH solution in methanol.

V_{KOH} = Volume of KOH in methanol (mL).

V_{HCl} = Titrant consumption (mL).

5. For sample analysis weight out 0.5–1 g of isocyanate prepolymer into a 125 mL Erlenmeyer flask.
6. Add 30 mL of toluene and stir until dissolution.
7. Add 20 mL of 1 M dibutylamine solution and stir for 10 min.
8. Add 30 mL methanol and titrate excess dibutylamine with 1 M HCl in methanol.
9. Repeat **steps 5–8** without the addition of samples to obtain the blank values.
10. Calculate the NCO# from the following equation:

$$\mathrm{NCO\,\#} = \frac{[(B - V) \times N \times 0.042]}{W},$$

where:

B = Volume of HCl for titration of the blank (mL).

V = Volume of HCl for titration of sample (mL).

N = Normality of HCl.

W = Weight of sample in grams.

3.5 Polyurethane Film Preparation (4 mL Batch Will Produce 50 Films, See Note 9)

1. Add 1 mg (0.2 wt %) of Coscat 83 to a 5-mL glass vial (#1).
2. Add 64 mg of LDI prepolymer to the glass vial (#1).
3. Add 435 mg of 3,000 g/mol polyester triol to a new glass vial (#2). *See* **Notes 10** and **11** for description of polyurethane reaction and additional comments on the use of different molecular weight triols or isocyanates with different NCO#'s.
4. Add 1.75 mL of anhydrous dichloroethane to each of the vials (#1 and #2).
5. Shake or vortex until dissolution of components.
6. Carefully transfer the solution in vial #2 to vial #1. The final concentration will be 10 wt % polymer.
7. Shake or vortex for 30 s to homogenize the solution.
8. Pipette 75 μL of solution to the glass portion of treated MatTek dishes (*see* **Note 12**).
9. Carefully transfer the dishes to an oven flushed with a steady stream of dry argon and cure overnight at room temperature.
10. Increase the temperature in the oven to 60 °C for an additional 24 h to ensure complete cure. MatTek dishes can be stored in a desiccator until use.
11. Incubate polyurethane films with 300 μL of poly-D-lysine solution for 1 h at 37 °C on a rack in a water bath such that the water makes contact with the bottom of the dishes.
12. Polyurethanes and polyesters have been known to autofluoresce causing some difficulty with sensitive fluorescent analysis. *See* **Note 13** for a discussion on reducing this phenomenon.

3.6 Tissue-Derived Scaffold Preparation

1. Sterilize 24-well CellCrowns by soaking in 70 % ethanol overnight and allowing to air-dry in a cell culture hood. Autoclave a small container such as a pipette box lid. Sterilize tweezers and scissors either with ethanol or by autoclaving.
2. Fill container in a cell culture hood with pre-warmed sterile 1× PBS solution so that the liquid height is just above the top of the CellCrowns (Fig. 1a).
3. Use the sterile scissors to cut ~2 cm × 2 cm pieces of tissue-derived scaffold such as urinary bladder matrix-basement membrane (UBM-BM, [27]) (in which case you will need to note which sides are basement membrane and stroma) and float them in the container.
4. Use the sterile tweezers to slide the body of the CellCrown under the floating piece of scaffold (Fig. 1b).
5. Use the sterile tweezers to put the CellCrown ring on top of the floating piece of scaffold and push down on the edges with tweezers to snugly anchor the ring on to the body of the

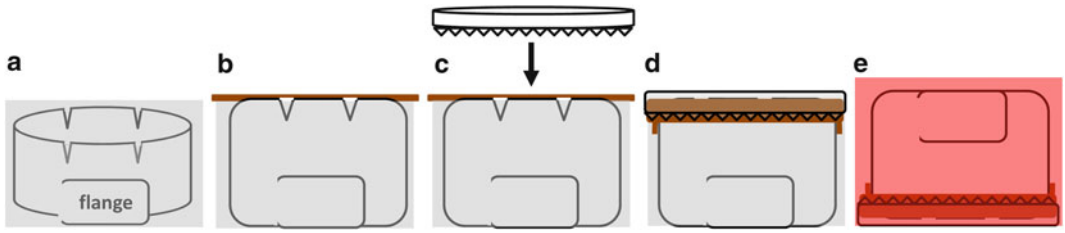

Fig. 1 Securing tissue-derived substrates in CellCrowns. (**a**) Place CellCrown insert upside down (*flanges* on bottom) into a sterile container and fill with sterile 1× PBS (*grey*) until level with the top of the insert. (**b**) Center insert underneath a floating piece of tissue-derived scaffold (*brown*). (**c**) Lower CellCrown ring (teeth down) gently on top of tissue-derived scaffold. (**d**) Center ring and secure by pushing it on to the insert until tight. (**e**) Flip CellCrown right side up and place in a well of a plate (flanges on top). Fill the inside of the CellCrown with cells and culture medium and the outside of the CellCrown with culture medium (*red*)

CellCrown with the piece of scaffold anchored between them (Figs. 1c, d).

6. Use the sterile scissors to trim away excess scaffold material sticking out from under the ring.
7. Inspect CellCrowns to ensure the ring is tight and that no tears or holes formed in the scaffold.
8. Keep CellCrowns hydrated in sterile 1× PBS solution prior to use.

3.7 Gelatin Conjugation and Fibronectin Adhesion

1. Preheat 1 % gelatin/1 % sucrose solution to 37 °C prior to use.
2. Place 150 μL of the gelation solution on to polyacrylamide and polyurethane surfaces in the glass bottom dishes and aspirate after 1 min.
3. Allow the remaining thin layer of gelatin to dry by placing dishes vertically (~60° angle or greater) for 60 min.
4. Add 2 mL of chilled 0.5 % glutaraldehyde solution and incubate on ice for 15 min then room temperature for 30 min.
5. Wash three times with 1× PBS solution with 5 min intervals.
6. Incubate in 2 mL of sodium borohydride solution for 1 min (*see* **Note 14**).
7. Aspirate and wash three times with 1× PBS solution with 5 min intervals.
8. Dilute the fluorescently labeled fibronectin solution (*see* **Note 15**) to 50 μg/mL with 1× PBS. 150 μL of this solution will be required for each dish. Centrifuge fluorescently labeled fibronectin solution at 175,000×*g* at 4 °C for 15 min to remove aggregates.
9. Place 150 μL of 50 μg/mL fluorescently labeled fibronectin solution in 1× PBS on top of the gelatin and incubate for 60 min at room temperature in the dark.

10. Aspirate fluorescently labeled fibronectin solution with great care in order not to damage the polymers (*see* **Note 14**).
11. Add 2 mL of a 70 % ethanol solution in a cell culture hood for 10 min to sterilize plates.
12. Incubate in invadopodia medium without serum for 1 h or wash three times in 5 min intervals with sterile 1× PBS solution. Dishes can be stored for approximately 1 week in sterile 1× PBS solution.

3.8 Preparation of Samples for Matrix Degradation Assays on Synthetic Substrates

1. Add cells at 25,000 cells per 2 mL of invadopodia medium and culture overnight (~18 h) in a cell culture incubator.
2. Fix cells in 2 mL of a 3.7 % paraformaldehyde solution for 20 min in the dark.
3. Wash two times with 1× PBS solution.
4. Permeabilize cells with 2 mL of a 0.1 % Triton X-100 solution for 5 min in the dark.
5. Wash with 1× PBS solution.
6. Incubate in 2 mL of blocking solution at room temperature for 60 min in the dark.
7. Incubate with a primary antibody for an additional marker of invadopodia (such as mouse anti-cortactin 4F11 at 1:750) in blocking solution for 1 h at room temperature in the dark (~200 μL per dish).
8. Wash with 1× PBS solution three times with 5 min intervals.
9. Incubate with a secondary antibody (such as goat anti-mouse Alexa Fluor 633 for cortactin at 1:500) and 546 phalloidin for F-actin at 1:750 in blocking solution at room temperature for 60 min in the dark (~200 μL per dish).
10. Wash with 1× PBS solution three times with 5 min intervals.
11. Mount with 5–6 drops of Aqua Poly/Mount mounting medium and 22 × 22 mm coverslips (*see* **Note 16**).
12. Cover with 22 × 22 mm coverslips and refrigerate for storage.

3.9 Preparation of Samples for Invadopodia Expression on Tissue-Derived Substrates

1. Fill wells of a 24-well plate with 1 mL of invadopodia medium.
2. Insert CellCrowns with sterile tweezers flush with the top of the wells so that the scaffold is on the bottom (the inside of the CellCrown will be the "top" surface since the cells will be placed inside the CellCrowns like an inverted drum) (Fig. 1e).
3. Seed 2,500 cells in 750 μL of invadopodia medium inside each CellCrown and culture overnight (~18 h) in a cell culture incubator (*see* **Note 17**).
4. Aspirate invadopodia medium both inside and outside the CellCrown.

5. Fix cells in 1 mL of 3.7 % paraformaldehyde solution for 20 min.
6. Wash two times with 1× PBS solution.
7. Permeabilize cells with 1 mL of a 0.1 % Triton X-100 solution for 5 min.
8. Wash with 1× PBS solution.
9. Remove CellCrowns and place each one in a well of a 12-well dish (*see* **Note 18**).
10. Incubate in 5 mL of blocking solution at room temperature for 60 min. Ensure that there is solution underneath the CellCrown as well as inside it to keep the scaffold hydrated.
11. Aspirate only the inside of the CellCrowns.
12. Incubate with a primary antibody for an additional marker of invadopodia (such as mouse anti-cortactin 4F11 at 1:500) in 300 μL of blocking solution for 1 h at room temperature.
13. Wash with 1× PBS solution three times with 5 min intervals and aspirate all liquid.
14. Replace the 5 mL of blocking solution on the inside and outside of CellCrown and aspirate just the inside.
15. Incubate with a secondary antibody (such as goat anti-mouse Alexa Fluor 633 for cortactin at 1:500) and 546 phalloidin for F-actin at 1:500 in 300 μL of blocking solution at room temperature for 60 min in the dark.
16. Wash with 1× PBS solution three times with 5 min intervals and aspirate all liquid after last wash.
17. Remove CellCrowns and place on glass slides.
18. Hold the rings down with tweezers against the glass slides and remove the bodies of the CellCrowns with another pair of tweezers.
19. Place a 10 mm tissue biopsy punch inside the ring and cut out a circular piece of UBM–BM sample. Remove the ring and excess sample still attached to the ring.
20. Mount with four drops of Aqua Poly/Mount.
21. Cover with 22×40 mm coverslips (*see* **Note 19**).
22. Allow to dry in the dark at bench or overnight then seal with nail polish and refrigerate for storage.

3.10 Fluorescence Microscopy of Invadopodia and/or Degradation

1. Typically, larger cells such as MCF10A CA1d breast carcinoma cells and/or degradation are visualized using an inverted microscope with a high NA objective such as a 40× Plan Fluor oil immersion lens for both the polymer substrates and scaffolds.
2. Smaller cells such as 804G bladder carcinoma cells may require visualization using a confocal microscope with a

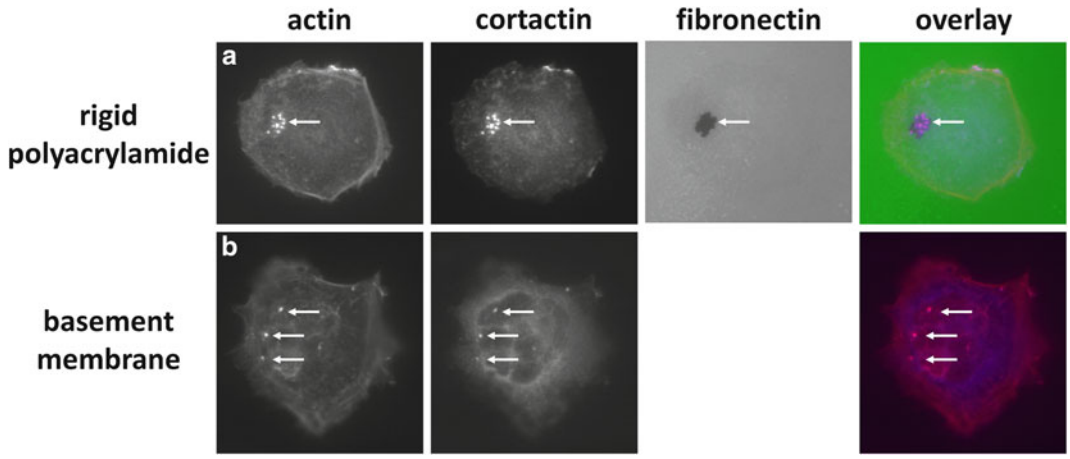

Fig. 2 Example wide-field fluorescence images of invadopodia in CA1d breast carcinoma cells on different substrates. Invadopodia can be identified by colocalization of actin (*red*) and cortactin (*blue*) puncta. (**a**) On a rigid polyacrylamide gel conjugated with 1 % gelatin and FITC-labeled fibronectin, invadopodia (*arrow*) can be colocalized with matrix degradation. (**b**) Invadopodia can also be identified on tissue-derived substrates such as the basement membrane side of UBM–BM

high NA objective such as a 63× Plan Apo oil immersion lens (*see* **Note 20**).

3. Excitation/emission at 632/647 nm allows for visualization of invadopodia markers such as cortactin, while excitation/emission at 556/570 nm allows for visualization of the actin cytoskeleton with 546 phalloidin (Fig. 2). Due to autofluorescence of the extracellular matrix in the scaffold, visualization of cells is limited to these fluorophores at these wavelengths (*see* **Note 21**). For the polymer substrates, excitation/emission at 492/518 nm allows for visualization of the fluorescently labeled fibronectin.

4 Notes

1. Since 3-aminopropyltrimethoxysilane reacts with plastic, great care must be taken when pipetting it on the glass bottom dish coverslip without letting it touch the plastic of the dish. Therefore, you will not be able to cover the entire coverslip. If it does touch, the plastic will turn white and the dish will not be usable (cells do not grow in these dishes).
2. Although our original protocol was based on 5 mL, these volumes (acrylamide, bis solution, and water) can be scaled down to 1 mL total in order not to waste materials. 25 and 2 μL of the 10 % ammonium persulfate solution and TEMED, respectively, can then be used to initiate polymerization which takes ~15 min (which may result in slightly different rigidities).

3. Although the thicknesses tend to vary, this volume of polyacrylamide solution should theoretically yield a gel with a thickness of 75 μm. Despite variability, the resulting gels are still quite thick (>40 μm) such that cells cannot detect the underlying glass surface. In addition, we have found it very difficult to adapt this system to larger areas since these coverslips are quite thin and often break when trying to remove the top coverslips.
4. In most cases, the pipetter will have to be squeezed to eject the 2 μL which will hang at the end of the tip. It can be gently brought into contact with the polyacrylamide solution. If done correctly, you will see the toluene solution coat the outside of the polyacrylamide solution.
5. For the synthesis of a 900 g/mol polyester triol the following changes need to be made to **steps 4–7** in Heading 3.4: (a) Add 10.23 g of dry glycerol. (b) Add 8.98 g of dl-lactide. (c) Add 17.95 g of glycolide. (d) Add 62.84 g of dry, filtered ε-caprolactone monomer. The remaining steps are kept the same. The final polyester triol is clear instead of milky white. The polycaprolactone triol (Sigma-Aldrich, catalog number 200387-250G) is utilized as the 300 g/mol precursor so no additional steps are required for synthesis.
6. The drying of ε-caprolactone monomer with $MgSO_4$ is convenient, but there is some loss upon filtration. Therefore it is required to add 10–15 g of additional ε-caprolactone monomer to ensure enough material for the reaction. Alternative drying procedures, such as vacuum drying, can be used.
7. Characterizations of OH# are required to obtain the exact amount of hydroxyls per mole of polyester triol. The OH# instructions were specified for a 789 MPT Titrino (Metrohm) although the instructions can be applied with most automated titration equipment. The procedure works by esterification of the hydroxyl with the phthalic anhydride. The excess phthalic anhydride is hydrolyzed with water to form phthalic acid. The acid is then titrated with the standard NaOH solution. The OH# is calculated from the difference in titration of the blank and sample solutions. For more information see ASTM D 4662-93. Additional characterization via GPC should show broad peaks (depending on the extent of washing) centered on the target molecular weight.
8. Characterization of the NCO# is required to accurately account for the isocyanate per mole of material. The NCO# instructions were specified for a 789 MPT Titrino (Metrohm) although the instructions can be applied with most automated titration equipment. The procedure works by the reaction of isocyanate with the dibutylamine. The excess dibutylamine is

titrated with standard HCl. For more information see ASTM D 4662-93.

9. The 4 mL batch is the smallest batch with which to easily measure out the catalyst. It should produce up to 50 films.
10. The polyurethane reaction is balanced by the amount of isocyanate and hydroxyl equivalents. The ratio of these equivalents multiplied by 100 is known as the index. For the films in this study an index of 105 is utilized. In order to keep this index value constant, the amount of triol and prepolymer is adjusted when a different molecular weight triol is utilized. Since the mechanical properties of the polyurethane film are directly related to the molecular weight of the polyester triol, it is essential to utilize the correct concentration of materials. More information can be found in the following publications [28, 29]. **Steps 2** and **3** in Subheading 3.5 need to be changed accordingly. For 900 g/mol polyester triol: (a) Add 164 mg of LDI prepolymer to vial #1. (b) Add 331 mg of 900 g/mol polyester triol to vial #2. For 300 g/mol polycaprolactone triol: (a) Add 297 mg of LDI prepolymer to vial #1. (b) Add 202 mg of 300 g/mol polycaprolactone triol to vial #2. The remaining steps are the same.
11. Similar to the OH#, the NCO# is a measure of the isocyanate per mole of material. This number varies for each isocyanate and new batch of the prepolymer. When accounting for different NCO#, generally, the higher the value the less isocyanate is required to keep the index constant. For instance, the NCO# for the LDI prepolymer is around 29.9 and HDI trimer has an NCO# of 21.8. To incorporate HDI trimer instead of the LDI prepolymer in the polyurethane films **steps 2** and **3** in Subheading 3.5 need to be changed accordingly. For a 3,000 g/mol polyester triol: (a) Add 84 mg of HDI trimer to vial #1. (b) Add 415 mg of 3,000 g/mol polyester triol to vial #2. For a 900 g/mol polyester triol: (a) Add 201 mg HDI trimer to vial #2. (b) Add 298 mg of 900 g/mol polyester triol to vial #2. Finally, for a 300 g/mol polycaprolactone triol: (a) Add 334 mg of HDI trimer to vial #2. (b) Add 165 mg of polycaprolactone triol to vial #2. The remaining steps are the same.
12. Dichloroethane is a good solvent for polystyrene, therefore care should be taken when applying the polyurethane solution to the MatTek dishes.
13. Autofluorescence is a common occurrence with many types of polymers. This can occur from conjugated bonds, cyclic moieties and hydrogen bonding [30, 31]. Due to the large amount of carbonyl moieties and hydrogen bonding that can be present in polyester based polyurethanes, it is not atypical to observe autofluorescence in red, green and blue channels. In

order to mitigate the effect, a method of quenching background autofluorescence in polyesters and polyurethanes using Sudan Black B (SB) was recently published [31]. The authors were able to show that SB does not interfere with immunofluorescent imaging of cells cultured on materials that autofluoresce. For our experiments, we ensure that we use bright fluorophores that are easily detectable so that we can observe them easily on the microscope without incurring significant background from the autofluorescence.

14. Bubbles will form in the sodium borohydride solution that is pipetted on to the coverslip. If they are not removed completely, they can leave deformities in the gelatin surface. You can tap the dishes on the bench to remove some of the bubbles. In addition, we have found that aspirating around the entire circumference of the coverslips when removing the solution helps remove these bubbles as well.
15. We typically do our own fluorescent labeling of fibronectin with FITC (Sigma-Aldrich, catalog number F7250). Briefly, we dissolve 5 mg of fibronectin in 10 mL of borate buffer composed of 170 mM sodium metaborate tetrahydrate (Sigma-Aldrich, catalog number S0251) and 40 mM NaCl and place it in a pre-equilibrated dialysis bag (Sigma-Aldrich, catalog number D9777). The bag is placed in 200 mL of borate buffer containing 6 mg of dissolved FITC and mixed at the slowest speed at room temperature for 1.5 h in the dark to label the fibronectin. The bag is then dialyzed extensively against 500 mL of 1× PBS solution for 2–3 days with two volume changes a day at 4 °C in the dark. Labeled protein concentration (in mg/mL) is determined by measuring the optical density (OD) of diluted aliquots (typically 1:200) at 280 and 493 nm and calculated as $[OD280-(0.36\times OD493)]/1.4$ times the dilution factor. The solution is then dialyzed overnight at 4 °C in a 50 % glycerol solution in 1× PBS which concentrates the solution so that the calculated fluorescently labeled fibronectin concentration must be multiplied by 2. Aliquots are stored at −20 °C.
16. Five-six drops ensure that the entire well of the glass bottom dish is filled with Aqua Poly/Mount so that no air gets trapped inside once the 22 × 22 mm coverslip is put in place.
17. This number of cells was chosen to yield approximately the same number of cells per area as the polymer substrates. However, we have found that in our experience smaller cells such as 804G bladder carcinoma cells should be seeded at higher values (~5,000 cells per CellCrown).
18. We have found that it is easier to manipulate and wash the samples when placed in the 12-well plates as opposed to keeping

them in the 24-well plates. In addition, the excess blocking solution on the outside acts to balance the volume that is placed inside the CellCrown and equilibrate all of the fluid at approximately the same height. Therefore, only the inside of the CellCrowns are aspirated in certain steps.

19. We have found that these larger coverslips are easier to use when mounting UBM–BM since the samples often float or slide during the process. In addition, the larger size ensures that the glass can be sealed properly to the slide. Smaller coverslips can be used; however, the thickness of the UBM–BM may make it difficult to properly seal the coverslips since they may be slightly raised at the edges.
20. In our experience, larger cells tend to spread and flatten more easily on the topography of the UBM–BM. However, smaller cells may fit inside areas of its architecture and appear more rounded. Therefore, they are difficult to visualize with widefield and require confocal z-stacks.
21. ECM molecules, particularly collagens, can autofluoresce at multiple wavelengths. We have found this to be the case with UBM–BM and have found that the listed excitations/emisssions work at wavelengths that minimize this autofluorescence.

Acknowledgments

AP is supported by the National Cancer Institute of the National Institutes of Health (NIH) under award number K25CA143412 with additional funding provided by the Department of Otolaryngology. JMP and SAG are supported by the NIH under award number U01CA143069 (Weaver). AMW is supported by the NIH under award numbers U01CA143069, R01GM075126, and U54CA113007 (Quaranta).

References

1. Paszek MJ, Weaver VM (2004) The tension mounts: mechanics meets morphogenesis and malignancy. J Mammary Gland Biol Neoplasia 9:325–342
2. Provenzano PP, Inman DR, Eliceiri KW, Knittel JG, Yan L, Rueden CT, White JG, Keely PJ (2008) Collagen density promotes mammary tumor initiation and progression. BMC Med 6:11
3. McCormack VA, dos Santos SI (2006) Breast density and parenchymal patterns as markers of breast cancer risk: a meta-analysis. Cancer Epidemiol Biomarkers Prev 15: 1159–1169
4. Maskarinec G, Pagano I, Lurie G, Wilkens LR, Kolonel LN (2005) Mammographic density and breast cancer risk: the multiethnic cohort study. Am J Epidemiol 162:743–752
5. Boyd NF, Rommens JM, Vogt K, Lee V, Hopper JL, Yaffe MJ, Paterson AD (2005) Mammographic breast density as an intermediate phenotype for breast cancer. Lancet Oncol 6:798–808
6. Boyd NF, Guo H, Martin LJ, Sun L, Stone J, Fishell E, Jong RA, Hislop G, Chiarelli A, Minkin S, Yaffe MJ (2007) Mammographic density and the risk and detection of breast cancer. N Engl J Med 356:227–236

7. Samani A, Zubovits J, Plewes D (2007) Elastic moduli of normal and pathological human breast tissues: an inversion-technique-based investigation of 169 samples. Phys Med Biol 52:1565–1576
8. Nemir S, West JL (2010) Synthetic materials in the study of cell response to substrate rigidity. Ann Biomed Eng 38:2–20
9. Sabeh F, Shimizu-Hirota R, Weiss SJ (2009) Protease-dependent versus -independent cancer cell invasion programs: three-dimensional amoeboid movement revisited. J Cell Biol 185:11–19
10. Weaver AM (2006) Invadopodia: specialized cell structures for cancer invasion. Clin Exp Metastasis 23:97–105
11. Weaver AM (2008) Invadopodia. Curr Biol 18:R362–R364
12. Linder S, Wiesner C, Himmel M (2011) Degrading devices: invadosomes in proteolytic cell invasion. Annu Rev Cell Dev Biol 27: 185–211
13. Yamaguchi H, Lorenz M, Kempiak S, Sarmiento C, Coniglio S, Symons M, Segall J, Eddy R, Miki H, Takenawa T, Condeelis J (2005) Molecular mechanisms of invadopodium formation: the role of the N-WASP-Arp2/3 complex pathway and cofilin. J Cell Biol 168:441–452
14. Vishnubhotla R, Sun S, Huq J, Bulic M, Ramesh A, Guzman G, Cho M, Glover SC (2007) ROCK-II mediates colon cancer invasion via regulation of MMP-2 and MMP-13 at the site of invadopodia as revealed by multiphoton imaging. Lab Invest 87:1149–1158
15. Nakahara H, Nomizu M, Akiyama SK, Yamada Y, Yeh Y, Chen WT (1996) A mechanism for regulation of melanoma invasion. Ligation of alpha6beta1 integrin by laminin G peptides. J Biol Chem 271:27221–27224
16. Nakahara H, Mueller SC, Nomizu M, Yamada Y, Yeh Y, Chen WT (1998) Activation of beta1 integrin signaling stimulates tyrosine phosphorylation of p190RhoGAP and membrane-protrusive activities at invadopodia. J Biol Chem 273:9–12
17. Magalhaes MA, Larson DR, Mader CC, Bravo-Cordero JJ, Gil-Henn H, Oser M, Chen X, Koleske AJ, Condeelis J (2012) Cortactin phosphorylation regulates cell invasion through a pH-dependent pathway. J Cell Biol 195:903–920
18. Diaz B, Courtneidge SA (2012) Redox signaling at invasive microdomains in cancer cells. Free Radic Biol Med 52:247–256
19. Scott KE, Wheeler FB, Davis AL, Thomas MJ, Ntambi JM, Seals DF, Kridel SJ (2012) Metabolic regulation of invadopodia and invasion by acetyl-CoA carboxylase 1 and de novo lipogenesis. PLoS One 7(1):e29761
20. Alexander NR, Branch KM, Parekh A, Clark ES, Iwueke IC, Guelcher SA, Weaver AM (2008) Extracellular matrix rigidity promotes invadopodia activity. Curr Biol 18:1295–1299
21. Parekh A, Ruppender NS, Branch KM, Sewell-Loftin MK, Lin J, Boyer PD, Candiello JE, Merryman WD, Guelcher SA, Weaver AM (2011) Sensing and modulation of invadopodia across a wide range of rigidities. Biophys J 100:573–582
22. Provenzano PP, Inman DR, Eliceiri KW, Keely PJ (2009) Matrix density-induced mechanoregulation of breast cell phenotype, signaling and gene expression through a FAK-ERK linkage. Oncogene 28:4326–4343
23. Vacek PM, Geller BM (2004) A prospective study of breast cancer risk using routine mammographic breast density measurements. Cancer Epidemiol Biomarkers Prev 13:715–722
24. Chen W-T, Yeh Y, Nakahara H (1994) An in vitro cell invasion assay: determination of cell surface proteolytic activity that degrades extracellular matrix. J Tissue Cult Methods 16: 177–181
25. Pelham RJ Jr, Wang Y (1997) Cell locomotion and focal adhesions are regulated by substrate flexibility. Proc Natl Acad Sci USA 94: 13661–13665
26. Kandow CE, Georges PC, Janmey PA, Beningo KA (2007) Polyacrylamide hydrogels for cell mechanics: steps toward optimization and alternative uses. Methods Cell Biol 83:29–46
27. Brown B, Lindberg K, Reing J, Stolz DB, Badylak SF (2006) The basement membrane component of biologic scaffolds derived from extracellular matrix. Tissue Eng 12:519–526
28. Guelcher SA, Srinivasan A, Dumas JE, Didier JE, McBride S, Hollinger JO (2008) Synthesis, mechanical properties, biocompatibility, and biodegradation of polyurethane networks from lysine polyisocyanates. Biomaterials 29:1762–1775
29. Ruppender NS, Merkel AR, Martin TJ, Mundy GR, Sterling JA, Guelcher SA (2010) Matrix rigidity induces osteolytic gene expression of metastatic breast cancer cells. PLoS One 5(11):e15451
30. Gachkovskii VF (1967) Universal fluorescence of polymers. J Struct Chem 8(2):318–320
31. Jaafar IH, LeBlon CE, Wei M-T, Ou-Yang D, Coulter JP, Jedlicka SS (2011) Improving fluorescence imaging of biological cells on biomedical polymers. Acta Biomater 7:1588–1598

Chapter 11

Determining Rho GTPase Activity by an Affinity-Precipitation Assay

Narendra Suryavanshi and Anne J. Ridley

Abstract

The Rho GTPases are members of the Ras superfamily of GTPases that are pivotal regulators of the actin cytoskeleton. They also contribute to other cellular processes such as gene transcription, cell polarity, microtubule dynamics, cell cycle progression and vesicle trafficking. Most Rho GTPases act as molecular switches cycling between an "active" GTP-bound form and an "inactive" GDP-bound form. Hence, to elucidate the mechanisms by which Rho GTPases regulate cellular responses, an important parameter to determine is the GTP-loading of each Rho family member in cells under different conditions. Here we describe a biochemical technique to assess this based on affinity-precipitation of the GTP-bound form from whole cell lysates.

Key words Rho GTPase, Cell signalling, Pull-down, Activity, Quantification, Immunoblot, Biochemical

1 Introduction

The Rho GTPases are signalling mediators that link extracellular stimuli to cytoskeletal remodelling. Since the discovery of the founding member Rho [1] and delineation of its role in cytoskeletal remodelling [2], these proteins have been found to be crucial regulators of the cytoskeleton. They also contribute to several other cellular processes such as control of gene transcription, vesicle trafficking, cell cycle progression and cell polarity. There are 20 known genes encoding Rho GTPases in the human genome [3]. Rho GTPases are highly conserved in evolution and have been found in all eukaryotic genomes sequenced so far, including plants and fungi [3].

Most Rho GTPases act as molecular switches and cycle between an "active" GTP-bound form and "inactive" GDP-bound form. This is regulated by three sets of proteins: guanine nucleotide exchange factors (GEFs), GTPase activating proteins (GAPs) and guanine nucleotide dissociation inhibitors (GDIs) [3]. GEFs promote the exchange of bound GDP for GTP while GAPs

Amanda S. Coutts (ed.), *Adhesion Protein Protocols*, Methods in Molecular Biology, vol. 1046,
DOI 10.1007/978-1-62703-538-5_11,

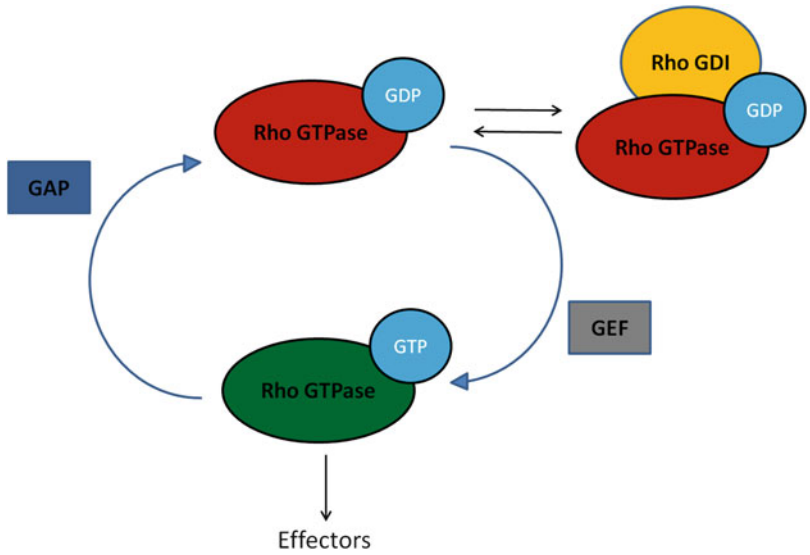

Fig. 1 Regulation of Rho GTPase activity. Schematic illustrating the regulation of Rho GTPase activity. Typical members of the Rho GTPase family cycle between an "active" GTP-bound form and an "inactive" GDP-bound form. GEFs facilitate the conversion of the GDP-bound form to the GTP-bound form. GAPs stimulate GTP hydrolysis and so downregulate Rho GTPase activity. Rho GDIs sequester several Rho proteins in the cytoplasm, preventing their association with membranes which is needed for their signalling

down-regulate Rho GTPase activity by stimulating GTP hydrolysis. Most Rho GTPases signal on membranes and to facilitate their localization to membranes, they are post-translationally modified at the C-terminus by the addition of a lipid group. This can be a geranylgeranyl or farnesyl lipid [4]. GDIs mask this C-terminal lipid group, preventing association of Rho GTPases with membranes and thus inhibiting their interaction with downstream effectors [5] (Fig. 1).

In contrast to other Rho GTPases, atypical members of the Rho family such as Rnd3 and RhoH are constitutively bound to GTP and their activity is thought to be regulated by protein stability and phosphorylation [6]. Rho proteins in their GTP-bound active form interact with an array of downstream signalling partners including protein kinases, adapter proteins and actin-regulatory proteins [7], and integrate information from a broad spectrum of upstream signals such as growth factors, chemokines and cell adhesion receptors [8].

The level of GTP loading for typical Rho GTPases indicates their activity and various techniques have been used to determine this. These can be classified into two classes: fluorescence based biosensors and biochemical affinity based methods. Fluorescence based probes primarily utilize FRET (Förster Resonance Energy Transfer) and have the advantage that they can be used to provide spatiotemporal information on GTP-loading in single, living cells.

This technique is described in detail by Hodgson et al. [9] and Nakamura et al. [10]. Biochemical affinity based approaches determine Rho GTP-loading in whole cell lysates and so have the disadvantage that they provide no spatial information and limited temporal resolution [11]. However, they have the advantage that they sample a whole cell population, and are relatively simple to perform and analyze.

In this chapter, we describe the "pull-down" approach to assess Rho GTPase activity biochemically, which was first described for Rac1 [12] and subsequently for RhoA and Cdc42 [13, 14]. This technique takes advantage of the fact that downstream effectors of the Rho proteins bind selectively to the GTP-bound form and hence can be used as a "bait" to "fish" out specifically the active form. Levels of the active, GTP-bound form are then compared to total protein levels by immunoblotting to determine relative activity of the Rho protein. We detail pull-down approaches to determine RhoA, RhoB, and RhoC activity using the Rho-binding domain (RBD) of Rhotekin (a Rho effector) and Rac and Cdc42 activity using the p21-binding domain (PBD) of PAK1 (p21-activated kinase, a Rac and Cdc42 effector). This approach can be extended to assay the activities of other Rho GTPases (e.g., using ELMO1 for RhoG activity [15, 16]).

2 Materials

2.1 Preparation of GST-RBD and GST-PBD Beads

1. BL21(DE3) strain of *Escherichia coli* (*see* **Note 1**) containing pGEX-2T plasmids to express GST-RBD or GST-PBD following IPTG (isopropyl-β-D-thiogalactopyranoside) induction.
2. Luria broth supplemented with 100 μg/mL ampicillin (LB-Amp): Use a stock solution of 100 mg/mL ampicillin in water (store aliquots at −20 °C) to prepare LB-Amp.
3. Isopropyl-β-D-thiogalactopyranoside (IPTG) (Sigma-Aldrich, I5502): 0.5 M stock solution in water (store aliquots at −20 °C).
4. STE (Sodium Tris-EDTA) buffer: 10 mM Tris–HCl pH 8.0, 150 mM NaCl, 1 mM EDTA, supplemented with protease inhibitor cocktail (Roche, 05056489001).
5. 19-gauge (19 G) needle with syringe.
6. Lysozyme (Sigma-Aldrich, L6876): Prepare fresh as a 1 mg/mL stock solution in STE buffer.
7. Dithiothreitol (DTT): 1 M stock solution in water (store aliquots at −20 °C).
8. Sodium dodecyl sulfate (SDS): 10 % (w/v) stock solution in water.
9. Tween-20.

10. Glutathione sepharose beads (GE Healthcare, 17-5132-01).
11. NuPAGE 4–12 % Bis–Tris pre-cast gels (Invitrogen).
12. Bovine serum albumin (BSA): 1 mg/mL stock solution in water.
13. Coomassie Blue staining solution: 0.25 % Coomassie Blue, 10 % acetic acid, 50 % methanol.
14. Destaining solution: 20 % methanol, 7 % acetic acid.

2.2 Cell Culture and Preparation of Cell Lysates

1. PC3 prostate cancer cells (ATCC).
2. RPMI: Roswell Park Memorial Institute 1640 medium (RPMI-1640) (Gibco) supplemented with 10 % fetal calf serum (FCS), 100 μg/mL streptomycin, 100 U/mL penicillin (Store at 4 °C).
3. Trypsin–EDTA (Store at 4 °C) (Gibco).
4. Phosphate buffered saline (PBS).
5. Pull-down lysis buffer: 50 mM Tris–HCl pH 7.5, 1 mM EDTA pH 8.0, 500 mM NaCl, 10 mM $MgCl_2$, 1 % (v/v) Triton X-100, 0.5 % sodium deoxycholate, 0.1 % SDS, 10 % (v/v) glycerol, 0.5 % (v/v) β-mercaptoethanol, supplemented with protease inhibitor cocktail (Roche, 05056489001), 25 mM NaF, 1 mM sodium orthovanadate, 1 mM phenylmethyl sulfonyl fluoride (PMSF).
6. Rubber policemen (Greiner Bio-One).
7. 0.5 M EDTA pH 8.0 stock solution in water (adjust pH with 5 M NaOH solution).
8. 1 M $MgCl_2$.
9. GTPγS (Cytoskeleton, BS01): Resuspend in water to yield a 20 mM stock solution. Store at −20 °C.
10. GDP sodium salt (Sigma-Aldrich, G7127): Prepare fresh as a 100 mM stock solution in water.

2.3 Western Blotting Components

1. 4× Sample buffer: 4 % SDS, 160 mM Tris–HCl pH 6.8, 20 % glycerol, 0.006 % Bromophenol blue, 10 mM DTT.
2. NuPAGE 4–12 % Bis-Tris pre-cast gels (Invitrogen).
3. MES SDS running buffer (Invitrogen).
4. PVDF membrane (Millipore, IPVH00010).
5. Western blot transfer buffer: 0.025 M Tris, 0.192 M glycine, 20 % methanol.
6. Tris buffered saline with Tween (TBST): 0.02 M Tris–HCl pH 7.6, 0.14 M NaCl, 0.1 % Tween-20.
7. Blocking solution: 5 % nonfat dried milk powder in TBST.
8. Primary antibodies: anti-RhoA (Santa Cruz, sc-418), anti-RhoB (Santa Cruz, sc-180), anti-RhoC (Santa Cruz, sc-26480),

anti-Rac1 (Millipore, 05-389), anti-Cdc42 (Cell Signaling, 2462).

9. Secondary antibodies: HRP-conjugated sheep anti-mouse (GE Healthcare, NA931V), donkey anti-rabbit (GE Healthcare, NA934V), and rabbit anti-goat (DAKO, P0449).
10. Enhanced chemiluminescence (ECL) reagent (GE Healthcare, RPN2209).
11. X-ray film (Fujifilm, 47410 19236).
12. ImageJ software: Available freely at http://rsbweb.nih.gov/ij/.

3 Methods

The Rho GTPase pull-down activity assay is described in this section using PC3 cells (a prostate cancer cell line) as an example. An example analysis is provided for RhoA, Rac1, and Cdc42 activity estimation. The method detailed here can be used similarly for other cell types, stimulations or treatments and for different Rho GTPases. Appropriate optimization of experimental conditions will have to be performed and guidelines as to how to achieve this are provided in Subheading 4.

3.1 Expression and Purification of GST-RBD and GST-PBD

1. Inoculate bacteria containing pGEX-2T plasmids encoding either GST-RBD or GST-PBD from glycerol stocks into 100 mL of LB-Amp. Incubate overnight at 37 °C with shaking.
2. Dilute the overnight culture 1:20 in fresh LB-Amp up to a total volume of 500 mL. Incubate at 37 °C until the culture reaches an OD of 1.0 (usually takes between 2.5 and 3 h) (*see* **Note 2**).
3. Induce protein expression by adding IPTG at a final concentration of 0.5 mM and incubate at 30 °C for another 2 h (*see* **Note 3**).
4. Centrifuge for 30 min at 1,000 × *g* and 4 °C to collect the cells. The bacterial pellet can be stored at −80 °C and the protocol resumed from this step at a later point.
5. Resuspend the bacterial pellet (with all cells containing the same pGEX-2T plasmid) in 10 mL of ice cold STE buffer. Homogenize the suspension with a 19 G needle. All procedures from this step onwards should be carried out on ice unless otherwise stated.
6. Add a final concentration of 100 μg/mL lysozyme in STE buffer to the bacterial suspension. Mix by inverting 6–7 times before incubating on ice for 15 min (*see* **Note 4**).
7. After the lysozyme incubation, the suspension should have a viscous consistency (*see* **Note 5**). At this stage add 5 mM DTT

and mix by gently inverting 6–7 times. Add Tween-20 and SDS to a final concentration of 1 and 0.03 % respectively and mix by inverting 8–10 times.

8. Transfer the lysed bacteria to multiple microfuge tubes as needed (the bacterial suspension will be very viscous at this stage and difficult to pipette). Clarify the bacterial lysate by centrifugation at 16,000 × *g* for 20 min at 4 °C. After centrifugation the lysate will still be very viscous and the best way to isolate the soluble protein fraction is to decant the supernatant quickly into a 15 mL tube (*see* **Note 6**). Combine supernatants (from bacteria containing the same plasmid) from all microfuge tubes into one tube.
9. Wash glutathione sepharose beads with STE buffer (250 μL of a 50 % slurry is used for 500 mL of starting culture from **step 2**). Add the washed beads to the 15 mL tube containing the soluble bacterial protein fraction (**step 8**) and place on a circular rotor for 1 h at 4 °C.
10. Centrifuge at 1,000 × *g* for 1 min at 4 °C to pellet the beads. Remove the supernatant, add 5 mL of ice cold STE buffer and repeat the centrifugation to pellet the beads. Repeat this wash step two more times. After the final wash, resuspend the beads with an equal volume of STE buffer.
11. Estimate the concentration of protein on the beads by boiling 10 μL of the beads and electrophoresing alongside BSA standards (1, 2, 5, 10 and 20 μg) on a polyacrylamide gel (*see* **Note 7**). Stain the gel for 30 min at room temperature with Coomassie Blue staining solution and destain with destaining solution. Change the destaining solution every hour until good contrast of the protein bands against background is achieved (approximately 2 h).
12. For long-term storage, beads can be snap frozen in liquid nitrogen with the addition of a final concentration of 10 % glycerol and stored at −80 °C (*see* **Note 8**). The ratio of bead volume to storage buffer volume should be 1:1.

3.2 PC3 Cell Culture

1. Thaw PC3 cells from frozen aliquots in a water bath at 37 °C, then seed into a 75 cm^2-flask containing 15 mL RPMI. Maintain cells at 37 °C and 5 % CO_2 and change the medium after 24 h. When cells reach 80 % confluency, passage the cells using trypsin–EDTA. First remove the medium from the flask and wash once with 1 mL PBS. Aspirate the PBS and add 1 mL of trypsin–EDTA for 3 min. Add 9 mL of RPMI to inactivate the trypsin–EDTA. Reseed into culture flasks to maintain the cells or for use in experiments. Split cells at between 1:2 and 1:10 and change the medium every 2–3 days (*see* **Note 9**).
2. For Rho GTPase pull-down experiments, seed 2×10^6 cells per 10 cm dish the day before the experiment (*see* **Note 10**).

Each 10 cm dish amounts to one "condition" in the assay. Reducing the serum concentration to 1 % FCS is recommended (*see* **Note 11**).

3.3 Preparation of Cell Lysates and Incubation with GST-RBD or GST-PBD Beads

1. Wash cells in 10 cm dishes twice with ice-cold PBS (*see* **Note 12**). Aspirate the PBS and lyse the cells in ice-cold pull-down lysis buffer (use 800 μL per 10 cm dish) (*see* **Note 13**). All steps detailed in this section should be carried out at 4 °C (*see* **Note 14**).
2. Immediately scrape each dish with a rubber policeman and collect the cell lysate in a microfuge tube. Clarify the lysate by centrifugation at 16,000 × *g* for 20 min at 4 °C. Transfer the supernatant to a new microfuge tube. Save a sample of the supernatant for "total protein" analysis by immunoblotting (usually a 40 μL sample is retained and boiled following addition of 4× sample buffer) (*see* **Note 15**).
3. It is recommended to include a positive control in each experiment. This also serves to verify the binding capacity of each batch of GST-RBD or GST-PBD beads (*see* **Note 16**). Load cell lysate from one 10 cm-dish with GTPγS. This converts and maintains all Rho GTPases in their active form, because GTPγS is very inefficiently hydrolyzed. Incubate the lysate with 100 μM GTPγS in the presence of 10 mM EDTA for 15 min at 30 °C. Terminate the reaction by adding $MgCl_2$ at a final concentration of 60 mM and placing the lysate on ice. A negative control can also be included by loading with GDP which converts all Rho GTPases to their inactive state. A final concentration of 1 mM GDP is used, following the same procedure for GTPγS loading.
4. Add the prepared glutathione beads bound to GST-RBD or GST-PBD (from Subheading 3.1) to the lysates (including the positive and negative controls from **step 3**) (*see* **Note 17**). Use 50 μg of GST-RBD and 10 μg of GST-PBD per condition (*see* **Note 18**). Incubate at 4 °C with gentle rotation for 1 h (*see* **Note 19**).
5. Centrifuge at 1,000 × *g* for 1 min to collect the beads. Remove the supernatant and add 500 μL of ice-cold pull-down lysis buffer. Pellet the beads by an additional centrifugation step and carry out a further two washes.
6. Add 4× sample buffer to the beads and boil to elute the bound proteins.

3.4 Immunoblotting for the Estimation of RhoA, Rac1, and Cdc42 Activity

1. Resolve the total lysates (from **step 2** of Subheading 3.3) and protein from boiled beads (from **step 6** of Subheading 3.3) on a SDS-polyacrylamide gel. Transfer the proteins onto PVDF membranes by Western blotting (pre-wet the membranes with 100 % methanol prior to this). After the Western transfer,

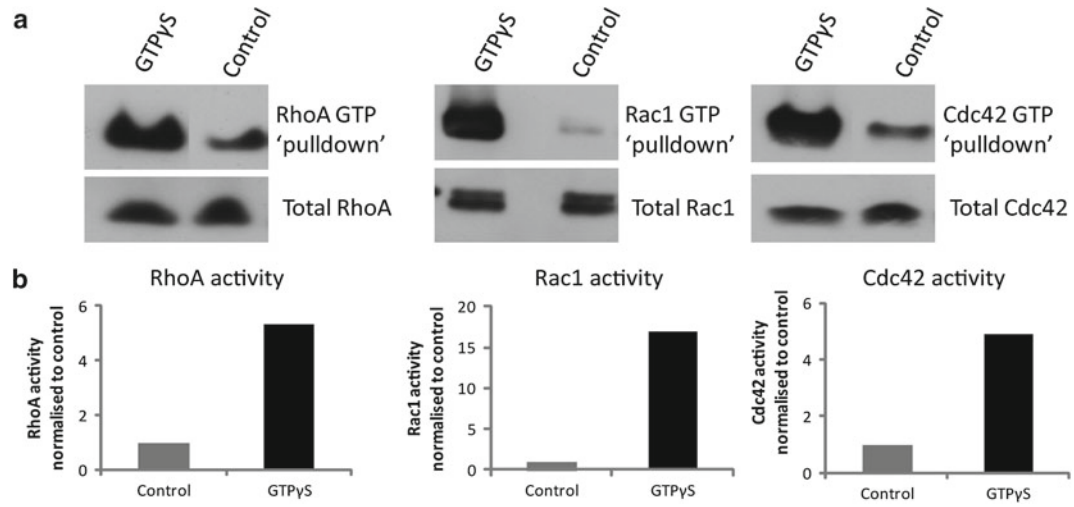

Fig. 2 Quantification of RhoA, Rac1, and Cdc42 activity. PC3 cell lysates were incubated with GTPγS (**step 3** of Subheading 3.3) to activate GTPases, or without GTPγS (Control). Activated RhoA-GTP was pulled down with GST-RBD, and Rac1-GTP and Cdc42-GTP were pulled down with GST-PBD on glutathione beads. (**a**) Immunoblots of samples from control lysates (no GTPγS) and GTPγS-loaded lysate conditions for each Rho GTPase. (**b**) Quantification of RhoA, Rac1, and Cdc42 activity was performed by normalizing the signal from the "pull-down" lane with that of the "total" lane. The graph represents this normalized signal for GTPγS-loaded lysates relative to control lysates (Control = 1)

block the membranes with blocking solution for 1 h at room temperature or overnight at 4 °C.

2. Incubate with appropriate primary antibodies overnight at 4 °C in blocking solution. Anti-RhoA, anti-RhoB, and anti-RhoC antibodies are used at a dilution of 1:500. RhoA, RhoB, and RhoC activity is assessed using pull-downs with GST-RBD. Anti-Rac1 and anti-Cdc42 antibodies are used at a dilution of 1:1,000 (*see* **Note 20**). Rac1 and Cdc42 activity is assessed using pull-downs with GST-PBD.
3. Wash the membranes three times for 10 min with TBST. After the final wash, incubate the membranes with the appropriate HRP-labelled secondary antibody for 2 h at room temperature. Secondary antibodies are used at a 1:5,000 dilution in blocking solution.
4. Wash the membrane three times for 10 min with TBST. The membrane is then treated with ECL reagents and developed by exposure to X-ray film.
5. Quantification of the protein activity is achieved by densitometry. The X-ray film is scanned and the intensity of the signal measured using ImageJ software. The signal from active GTP-bound Rho GTPase associated with GST-RBD or GST-PBD is normalized to the signal from the same Rho GTPase in total cell lysates. This value is then used to compare activity across samples (*see* **Note 21**) (Fig. 2).

4 Notes

1. The BL21(DE3) strain of *E. coli* is used as BL21 cells are deficient in proteases and therefore allow for high expression of the GST-RBD or GST-PBD proteins. DE3 indicates the strain allows for IPTG induction of gene expression.
2. Take care to prevent over-growth of the culture. This can reduce expression of GST-RBD or GST-PBD.
3. Reduction of the temperature from 37 to 30 °C prevents the formation of insoluble inclusion bodies and hence is an important step for obtaining optimal amounts of soluble GST-RBD or GST-PBD.
4. It is important that the bacterial pellet be completely resuspended before the addition of lysozyme.
5. If the suspension has not attained a viscous consistency even after 15 min of incubation, a longer incubation time of up to 30 min is recommended. If this does not resolve the problem, sonication of the lysate can be performed to improve lysis. Two rounds of 1 min sonication at an amplitude of 20 % (Sonics Vibra VC-130 sonicator) at 4 °C are used.
6. Take extra care in this step to ensure that the supernatant is decanted completely or the yield of protein obtained will be reduced.
7. We use 4–12 % polyacrylamide gradient NuPAGE gels but any polyacrylamide gel can be used. A 10 % polyacrylamide gel is suitable to resolve GST-RBD and GST-PBD.
8. We recommend preparing the beads on the day of the experiment and avoiding freezing if possible. This prevents protein denaturation that occurs due to the freeze–thaw cycle. If necessary, beads can be stored at 4 °C with the addition of 0.02 % sodium azide to prevent bacterial growth for a maximum of 1 month.
9. The health of the cells is an important determining factor for success with this technique. Ensure that your cells are free of any microbial contamination.
10. The amount of cells used will depend on your cell type and experimental conditions. An important parameter to determine is the lysate protein amount needed for the assay. A titration of different lysate protein amounts versus varying bead quantities is recommended to find the optimal conditions. This is detailed in **Note 18**.
11. We have found that reduction of the FCS concentration prior to performing the assay provides clearer differences in Rho-GTP levels across various samples. A high FCS concentration generally increases the basal activity (GTP-loading) of Rho

GTPases and hence can reduce the changes in activity across samples. The level of FCS will need to be optimized for different cell types.

12. Make sure all PBS is removed to prevent dilution of the lysis buffer.
13. Use a consistent amount of lysis buffer for all samples. If this is not done, protein concentration across samples will vary and this leads to unreliable results.
14. It is crucial that all steps be carried out at 4 °C. Endogenous GAP activity in cell lysates after lysis leads to a decrease in Rho-GTP levels, and this GAP activity is greatly reduced at 4 °C compared to working at room temperature. However, this still remains a problem at 4 °C, and thus steps should be carried out quickly to minimize the time from lysis to the addition of beads.
15. Ideally, the protein concentration should be measured for all samples to ensure equivalent amounts of protein are loaded on the polyacrylamide gels. However, it is usually sufficient to use the same number of cells and amount of lysis buffer used to obtain uniform loading.
16. A leading cause for the assay not working is a poor preparation of GST-RBD or GST-PBD, most likely due to denaturation of some of the protein. Hence, the Rho-GTP binding capacity of the beads should be confirmed by using a GTPγS positive control in all experiments.
17. Addition of GST-RBD or GST-PBD protects Rho GTPases against GAP activity. Hence, the time from cell lysis to incubation with beads should be minimized. If many samples are to be processed, consider performing the lysis of different cell samples in batches to minimize time to bead addition (a maximum of six conditions in one batch is advised).
18. To set up the optimal conditions for the assay, a titration of different cell lysate protein amounts (use varying volumes of cell lysate) versus varying bead amounts is recommended (for GST-RBD use a range of 25–100 μg and for GST-PBD use a range of 10–20 μg). Use the GTPγS positive control and GDP negative control for this standardization. Choose a pair of values for lysate protein concentration and bead amount such that an optimal difference between untreated, positive control and negative control samples is observed.
19. Incubation times of longer than 1 h are not necessary. Keep the incubation time consistent across all samples.
20. GST-RBD pulls down RhoA, RhoB, and RhoC. Hence, information on the activity of all three Rho proteins can be obtained in a single experiment. This can be achieved by sequential

incubation of the membrane with the three primary antibodies followed by secondary antibody incubation and development of the blot with ECL. Use the antibodies in the order anti-RhoC, anti-RhoB, and finally anti-RhoA. As the three antibodies are from different species, cross-reactivity is not a concern. This can be similarly done to determine Rac1 and Cdc42 activity from a single experiment. The signal can be quenched between successive primary/secondary antibody incubations by treatment of the membrane with 0.02 % sodium azide in TBST for 30 min. Ensure that complete quenching has occurred to prevent carryover of ECL signal. An alternative solution is to replace HRP-conjugated secondary antibodies with antibodies conjugated to fluorescent dyes. Different protein targets can then be detected in separate fluorescent channels of a fluorescence imaging system. This eliminates the need for sequential incubation with the different primary antibodies (for example, the LI-COR Odyssey system allows for detection of protein targets in two separate fluorescent channels). Alternatively, if your lysates contain sufficient protein, the GST-RBD or GST-PBD beads can be split at the end and each Rho GTPase analyzed on a separate Western blot.

21. Different treatments can change the total levels of the Rho GTPases and so signals from all the pull-down samples have to be normalized. Include a loading control to quantify any changes to total levels of protein (e.g., anti-GAPDH, Millipore MAB374 at a 1:10,000 dilution can be used).

Acknowledgments

This work was supported by Cancer Research UK (C6620/A8833) and King's College London British Heart Foundation Centre of Excellence (RE/08/003). N.S. was a recipient of King's College London graduate scholarships (ORS, K2K, KINGS, and KCS awards).

References

1. Madaule P, Axel R (1985) A novel ras-related gene family. Cell 41:31–40
2. Ridley AJ, Hall A (1992) The small GTP-binding protein rho regulates the assembly of focal adhesions and actin stress fibers in response to growth factors. Cell 70:389–399
3. Heasman SJ, Ridley AJ (2008) Mammalian Rho GTPases: new insights into their functions from in vivo studies. Nat Rev Mol Cell Biol 9:690–701
4. Bishop AL, Hall A (2000) Rho GTPases and their effector proteins. Biochem J 348(Pt 2): 241–255
5. Dovas A, Couchman JR (2005) RhoGDI: multiple functions in the regulation of Rho family GTPase activities. Biochem J 390:1–9
6. Aspenstrom P, Ruusala A, Pacholsky D (2007) Taking Rho GTPases to the next level: the cellular functions of atypical Rho GTPases. Exp Cell Res 313:3673–3679

7. Ridley AJ, Schwartz MA, Burridge K et al (2003) Cell migration: integrating signals from front to back. Science 302:1704–1709
8. Sahai E, Marshall CJ (2002) RHO-GTPases and cancer. Nat Rev Cancer 2:133–142
9. Hodgson L, Shen F, Hahn K (2010) Biosensors for characterizing the dynamics of rho family GTPases in living cells. Curr Protoc Cell Biol 14(11):1–26
10. Nakamura T, Kurokawa K, Kiyokawa E et al (2006) Analysis of the spatiotemporal activation of rho GTPases using Raichu probes. Methods Enzymol 406:315–332
11. Pertz O, Hahn K (2004) Designing biosensors for Rho family proteins-deciphering the dynamics of Rho family GTPase activation in living cells. J Cell Sci 117:1313–1318
12. Sander EE, van Delft S, ten Klooster JP et al (1998) Matrix-dependent Tiam1/Rac signaling in epithelial cells promotes either cell-cell adhesion or cell migration and is regulated by phosphatidylinositol 3-kinase. J Cell Biol 143: 1385–1398
13. Sander EE, ten Klooster JP, van Delft S et al (1999) Rac downregulates Rho activity: reciprocal balance between both GTPases determines cellular morphology and migratory behaviour. J Cell Biol 147:1009–1022
14. Ren X-D, Kiosses WB, Schwartz MA (1999) Regulation of the small GTP-binding protein Rho by cell adhesion and the cytoskeleton. EMBO J 18:578–585
15. Katoh HA, Negishi M (2003) RhoG activates Rac1 by direct interaction with the Dock180-binding protein Elmo. Nature 424:461–464
16. Ellerbroek SM, Wennerberg K, Arthur WT et al (2004) SGEF, a RhoG guanine nucleotide exchange factor that stimulates macropinocytosis. Mol Biol Cell 15:3309–3319

Chapter 12

Proteomic and Biochemical Methods to Study the Cytoskeletome

Richard L. Klemke, Xinning Jiang, Sunkyu Choi, and Jonathan A. Kelber

Abstract

The cytoskeleton is fundamental to many cellular functions including cell proliferation, differentiation, adhesion, and migration. It is composed of actin, microtubules, intermediate filaments, and integrin cell surface receptors, which form focal adhesions with the extracellular matrix. These elements are highly integrated in the cell providing a rigid network of interconnected cables and protein scaffolds, which generate force and mechanical support to maintain cell shape and movement. However, the cytoskeleton is not just a simple compilation of static filaments that dictate cell adhesion and morphology—it is highly plastic with the inherent ability to assemble and disassemble in response to diverse and complex cellular cues. Thus, biochemical and proteomic methods are needed to better understand the cytoskeleton network and its dynamic signal transduction functions in health and disease. This chapter describes methods for the biochemical enrichment and mass spectrometry-based proteomic analyses of the cytoskeletome. We also detail how these methods can be used to investigate the cytoskeletome of migrating cells and their purified pseudopodia membrane projections.

Key words Cytoskeletome, Proteomics, Pseudopodium dynamics, Cell migration

1 Introduction

The process of focal adhesion formation and maturation during cell migration illustrates the dynamic nature of the cytoskeleton to relay both force and signaling information to the cell in a temporal and spatial manner. The cytoskeleton is distinctly polarized in migrating cells to form a leading front and trailing rear compartment [1]. At the cell front, actin polymerization and assembly drive pseudopodia membrane protrusion and attachment to the underlying extracellular matrix (ECM) forming new focal complexes at the leading membrane edge. At the sides and rear of the cell, the cytoskeleton provides rigidity and contraction events that disengage focal adhesions to pull up the trailing tail from the underlying substratum [2]. The repeated cycle of pseudopodium extension at the front coupled with focal adhesion turnover and tail retraction

Amanda S. Coutts (ed.), *Adhesion Protein Protocols*, Methods in Molecular Biology, vol. 1046,
DOI 10.1007/978-1-62703-538-5_12,

at the back facilitates cell translocation. The direction of movement can be random or tightly regulated by gradients of ECM proteins and growth factors present in the extracellular environment. Cell migration is important for embryonic development, wound healing, and immune function, and can contribute to various pathologies including cancer cell metastasis and inflammatory diseases [3, 4].

While the signaling pathways that control cytoskeleton dynamics in migratory cells are being elucidated, little is known about how they are networked spatially within the cell to regulate cytoskeleton remodeling and front–rear cell polarity. This is largely because isolating the cytoskeleton for comprehensive proteomic profiling presents a significant technical challenge. The cell cytoskeleton is often insoluble under conventional cell lysis and detergent conditions making it incompatible with mass spectrometry-based protein detection methods [5, 6]. Confounding this issue, many signaling proteins that regulate the cytoskeleton bind with high affinity to the actin/tubulin scaffolds and focal adhesion complexes making them highly insoluble [7–10]. Also, current mass spectrometry techniques are limited by the inability to detect low-abundant cytoskeleton signaling proteins from complex whole cell protein extracts. While cytoskeleton enrichment methods have been described, they often do not maintain protein constituents in their native state and, thus, can disrupt important interactions with binding partners or alter critical posttranslational modifications. This makes it difficult to fully characterize the composition and activity state of the cytoskeletome, which is necessary for network analyses [11–14]. The need to characterize the cytoskeletome and its posttranslational modifications in migratory cells led us to develop a cytoskeleton purification method that enables the enrichment of cytoskeleton- and focal adhesion-associated proteins in their native state that is compatible with contemporary mass spectrometry methods. Using this technique, we examine the cytoskeleton proteomes from isolated pseudopodia. These technologies will facilitate a comprehensive understanding of how the cytoskeleton domain functions under a wide range of physiological and disease conditions.

2 Materials

2.1 Cell Culture

1. Cell lines: NIH3T3 or MEF (ATCC; *see* **Note 1**).
2. 150 mm tissue culture dishes.
3. Growth medium: Dulbecco's modified Eagle's medium (DMEM) supplemented with 10 % fetal bovine serum (FBS), 2 mM L-glutamine, 50 μg/mL gentamicin, and 1 mM sodium pyruvate.

4. Migration medium: Same as growth medium.
5. 0.25 % Trypsin–EDTA solution.
6. Phosphate-buffered saline (PBS) solution: One package of PBS powder (Gibco, 9.6 g per package) in 1 L of nano-pure water. Autoclave and store at 4 °C. Warm to 37 °C in a water bath before use.

2.2 Wound-Healing Migration and Cytoskeleton Enrichment

1. A Cell Comb™ (EMD Millipore, Catalogue No. 17-10191).
2. Cell scrapers.
3. Protease inhibitor cocktail (Roche).
4. Phosphatase inhibitor cocktail (1×): 5 mM NaF, 2 mM sodium vanadate, and 10 mM β-glycerophosphate.
5. Cell lysis buffer: 50 mM PIPES, 50 mM NaCl, 5 % glycerol, 0.1 % NP-40, 0.1 % Triton X-100, 0.1 % Tween 20, 1× protease inhibitor, and 1× phosphatase inhibitor.
6. TBS buffer: 50 mM Tris–HCl, pH 7.5.
7. TBS buffer with inhibitors: TBS buffer with 1× protease inhibitor and 1× phosphatase inhibitor.
8. Nuclease buffer: 10 U/mL benzoase nuclease (Sigma-Aldrich), 10 mM $MgCl_2$, and 2 mM $CaCl_2$ in TBS buffer, with 1× protease inhibitor and 1× phosphatase inhibitor.
9. Micro BCA protein assay kit (Pierce Biotechnology).
10. SDS solution, 1 % (w/v).

2.3 Pseudopodia Isolation and Cytoskeleton Enrichment

1. Transwell containing polycarbonate membrane with 3.0 μm pores in 6-well plate format (24 mm, Corning, # 3414).
2. Regular 6-well plate.
3. L-α-Lysophosphatidic acid (LPA), oleoyl, sodium (Sigma-Aldrich).
4. NuPAGE 4–12 % Bis-Tris gel.
5. Starvation medium: 500 mL DMEM, 1 mM sodium pyruvate, 2 mM L-glutamine, 50 μg/mL gentamicin.
6. Migration and adhesion medium: 500 mL DMEM, 1 mM sodium pyruvate, 2 mM L-glutamine, 50 μg/mL gentamicin, 1.25 g (0.25 %) BSA.
7. Migration and adhesion medium with chemoattractant: 500 mL DMEM, 1 mM sodium pyruvate, 2 mM L-glutamine, 50 μg/mL gentamicin, 1.25 g (0.25 %) BSA, and 0.1 μg/mL LPA.
8. Fibronectin solution (5 μg/mL): Dilute 0.1 % fibronectin stock solution (Sigma-Aldrich) with 200× water.
9. Cotton swab: Cotton-tipped swab, flatten the tip before use.

2.4 Protein Gel Separation and In-Gel Digestion

1. 50 % (vol/vol) Methanol in nano-pure water.
2. 100 mM Triethyl ammonium bicarbonate (TEAB) dissolved in nano-pure water.
3. 10 mM Dithiothreitol (DTT) dissolved in 100 mM TEAB.
4. 50 mM Iodoacetamide dissolved in 100 mM TEAB.
5. Trypsin solution: Trypsin (sequence grade) dissolved in 100 mM TEAB, protein ratio of 1:100 (w:w).
6. 50 % Acetonitrile (ACN), HPLC grade/1 % formic acid in nano-pure water.
7. NuPage 4–12 % Bis-Tris gel.
8. MOPS buffer (Invitrogen).
9. Power supply-Power-PAK300 (BIO-RAD).
10. Coomassie Brilliant Blue.
11. Destaining buffer: 40 % methanol/10 % acetic acid in nano-pure water.

2.5 Dimethyl Protein Labeling for Quantitative Proteomics

1. 100 mM TEAB dissolved in nano-pure water.
2. 4 % (vol/vol) Formaldehyde (CH_2O, Sigma-Aldrich) in nano-pure water.
3. 4 % (vol/vol) Formaldehyde ($^{13}CD_2O$, Isotec) in nano-pure water.
4. 0.6 mM sodium cyanoborohydride ($NaBH_3CN$, Fluka) dissolved in 100 mM TEAB.
5. 0.6 mM sodium cyanoborodeuteride ($NaBD_3CN$, Isotec) dissolved in 100 mM TEAB.
6. 1 % (vol/vol) ammonia solution (Merck) in nano-pure water.

2.6 Multidimensional Protein Identification Technology (MudPit)

1. Fused-silica capillary (I.D. 100 μm, O.D. 360 μm).
2. P-2000 laser puller (Sutter Instrument Co).
3. C18 (5 μm particle size).
4. SCX (strong cation exchange, 5 μm particle size).
5. Buffer A: 5 % ACN/0.02 % heptafluorobutyric acid (HFBA) in nano-pure water.
6. Buffer B: 80 % ACN/0.02 % HFBA in nano-pure water.
7. Buffer C: 250 mM Ammonium acetate/5 % ACN/0.02 % HFBA.
8. Buffer D: 500 mM Ammonium acetate/5 % ACN/0.02 % HFBA.

3 Methods

This section details two protocols for the biochemical enrichment of the cytoskeleton from wounded migrating cells and isolated pseudopodia. Procedures for inducing wound-healing cell migration [15, 16] and pseudopodia isolation have been previously described [17–20]. A flow diagram of our method for cytoskeleton extraction is shown in Fig. 1.

Western blot analysis (Fig. 2) illustrates the purification and enrichment of known cytoskeleton and adhesion proteins (actin, α-actinin, vinculin, Erk2, and Src) using this technique. Microscopy analysis of these domains within cells following this enrichment procedure also shows that the actin- and focal adhesion-associated proteins, α-actinin and paxillin, remain bound to the native, unperturbed, F-actin cytoskeleton and properly localize to their respective domains (Fig. 3).

3.1 Cytoskeleton Enrichment from Migrating Cells

We have coupled previously characterized methods for synchronously inducing directional cell migration [15, 16], with a commercially available tool for simultaneously wounding a large number of cells in confluent monolayers and our novel protocol for biochemical enrichment of the cytoskeletome. This has enabled proteomic analysis of this domain during directed cell migration while providing sufficient amount of material for mass spectrometry

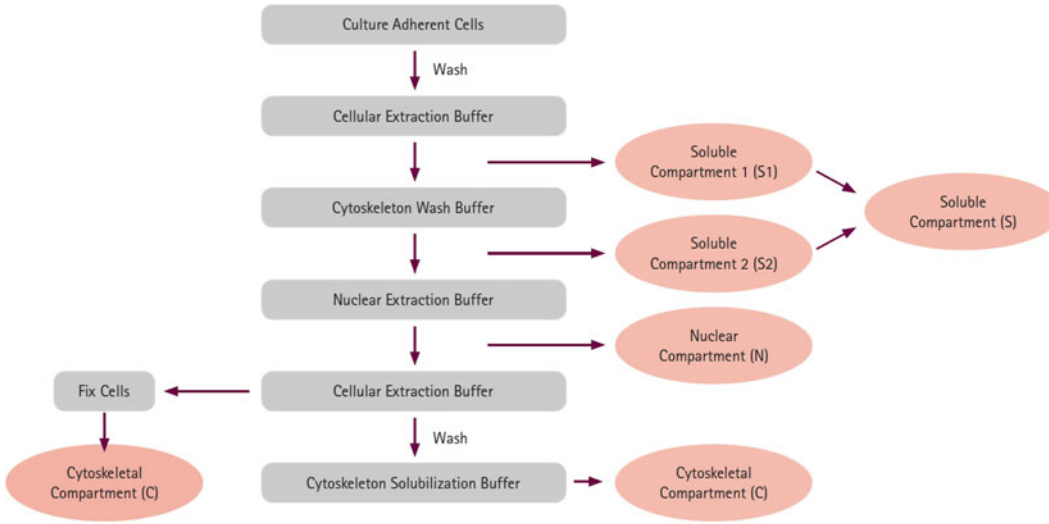

Fig. 1 Cytoskeleton enrichment procedure. The schematic demonstrates the flow diagram for our method of cytoskeleton enrichment

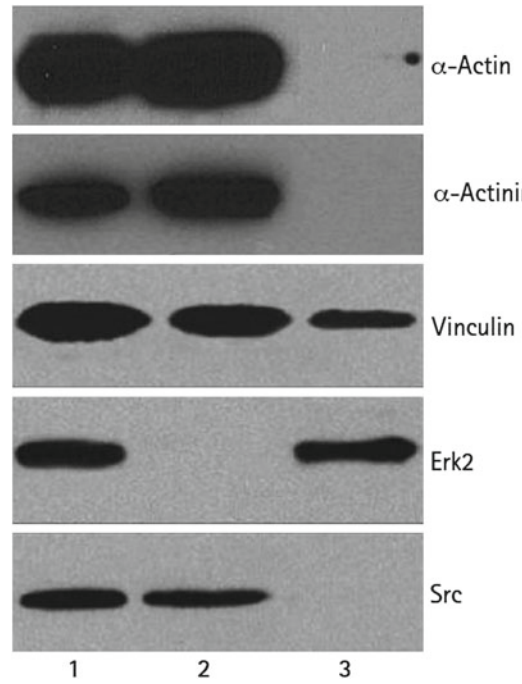

Fig. 2 Robust enrichment of known cytoskeletal proteins shown by Western blot. The soluble cytoplasmic proteins and insoluble fractions from embryonic fibroblast cells were separated and analyzed for the indicated proteins. For comparison, total cell protein was isolated using 1 % SDS. *Lane 1*. Total lysate. *Lane 2*. Cytoskeleton. *Lane 3*. Soluble proteins

(MS) analysis. As described below, confluent monolayers of fibroblast cells were scratched using the Cell Comb to induce wound-healing migration. This allowed us to visualize the closure of the wounds over time using phase-contrast microscopy (Fig. 4) in order to identify specific time points or an appropriate endpoint for subsequent enrichment and proteomic analysis of the insoluble protein fraction.

3.1.1 Cell Culture for Wound-Healing Migration Studies

1. Culture low-passage wild-type NIH3T3 or MEF cells in growth medium using 150 mm culture dishes and a humidified atmosphere with 5 % CO_2 at 37 °C. Change medium every 2 or 3 days.
2. When the cells are approximately 90 % confluent, split into four 150 mm dishes containing fresh growth medium. The cells will reach 90 % confluence within 4 days.

3.1.2 Cell Wounding and Migration

1. Remove cell culture medium.
2. Scratch surface of the four plates with a Cell Comb following the manufacturer's instructions (*see* **Note 2**).
3. Gently rinse the cells with PBS solution three times to remove detached cells and then add 15 mL of growth medium.

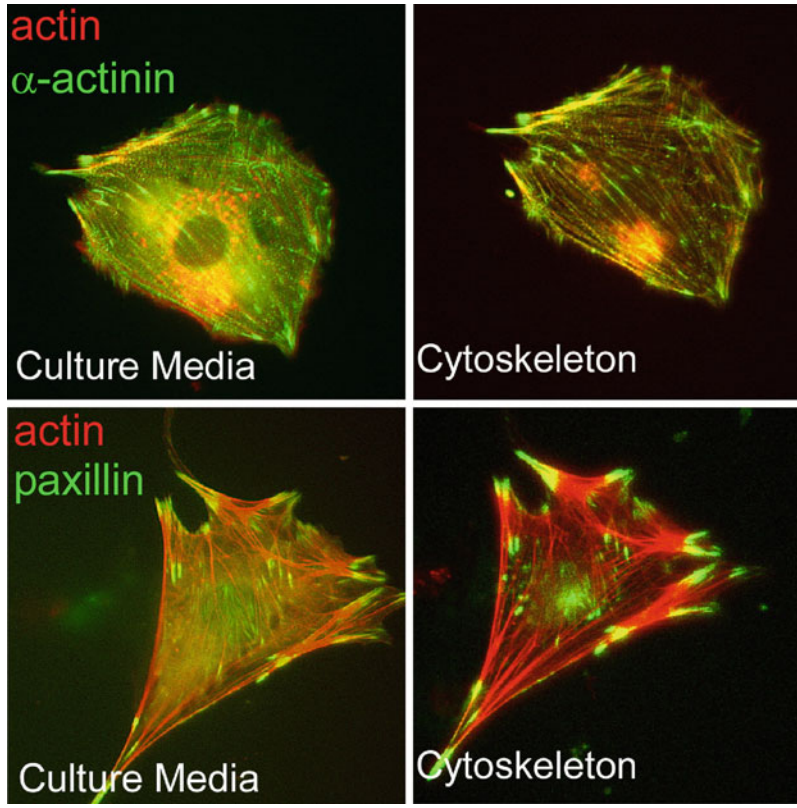

Fig. 3 α-Actinin (*top*) and paxillin (*bottom*) remain associated with the actin cytoskeleton after the cytoskeleton enrichment procedure and are more clearly visualized after removal of soluble background proteins. Fluorescent micrographs of MEFs co-expressing mCherry-tagged actin and GFP-tagged α-actinin (*top*) or paxillin (*bottom*). Images were captured from a live cell before and after extraction

4. Incubate the cells at 37 °C for 0, 6, 12, or 24 h (*see* **Note 3**).
5. Remove culture medium and rinse cells with 5 mL of cold PBS solution twice. Then, add 5 mL of cold cell lysis buffer on ice for 1.5 min (*see* **Note 4**).
6. Aspirate the soluble fraction gently and collect for further use.

3.1.3 DNA and RNA Extraction

Nuclease treatment provides the added advantage of removing background results due to nucleotide and nucleoprotein contamination.

1. Rinse the cell substrate with 5 mL of TBS buffer gently and then treat with 5 mL of nuclease buffer for 10 min at room temperature.
2. Remove the nuclease buffer and add the collected soluble fraction from Subheading 3.1.2 to solubilize the DNA- and RNA-binding proteins for another 30 s.
3. Rinse cytoskeleton proteins (insoluble fraction) remaining bound to the plates with 5 mL of TBS buffer three times.

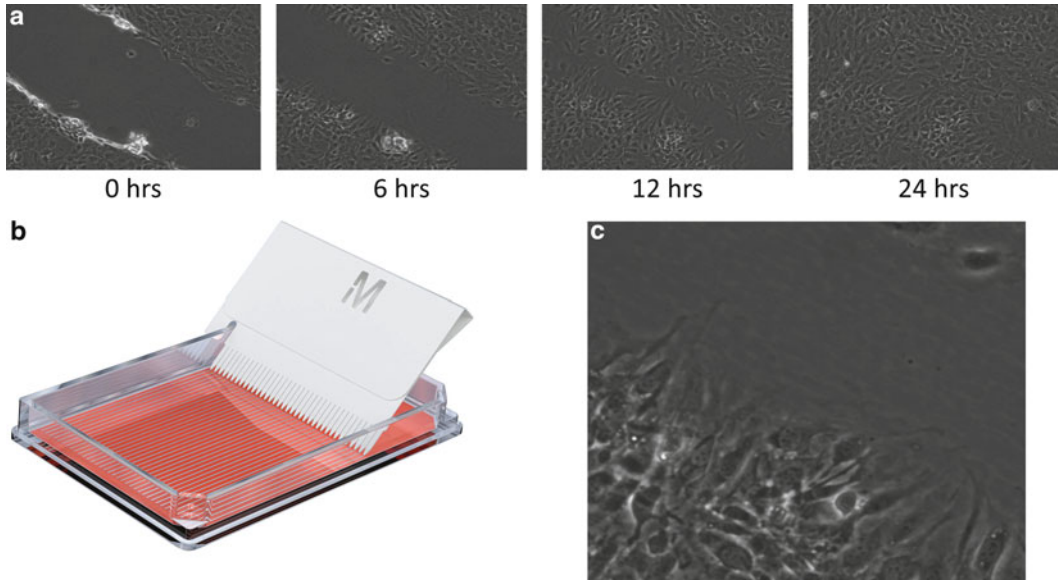

Fig. 4 A confluent monolayer of NIH3T3 mouse fibroblasts was wounded (**a**) using the Millipore Cell Comb (**b**). Wound closure was analyzed by time-lapse phase-contrast microscopy. (**c**) Enlarged region from wound showing cytoskeleton and adhesion structures

3.1.4 Extraction of Cytoskeleton and Adhesion Proteins for Proteomic Analysis

1. Collect the cytoskeleton fraction in 1 % SDS to completely solubilize and denature cytoskeleton proteins (*see* **Note 5**).
2. Transfer the insoluble fraction to a 1.5 mL microfuge tube and boil at 100 °C for 5 min. Freeze samples at –80 °C for further use.

3.2 Cytoskeleton Enrichment from Pseudopodia

Analysis of cell pseudopodia during directed migration has provided insight into the protein and phosphoprotein networks that control cell polarization and chemotaxis, leading to a system-wide understanding of how chemotactic cells organize signaling polarity to achieve directional movement. Our laboratory previously developed a method for the separation of pseudopodia and cell body for comparative proteomic and phosphoproteomic analyses [17–20]. To gain a deeper understanding of the cytoskeleton and adhesion complex regulation during pseudopodia formation, these previously published methods have been combined with our novel enrichment protocol (Fig. 1).

3.2.1 Cell Culture for Pseudopodial Assay

1. Split three 100 mm dishes of low-passage NIH3T3 (60–70 % confluent) into twelve 10 mm dishes containing 7 mL of growth media. Culture cells for 2–3 days at 5 % CO_2, 37 °C, until the cells are 70–80 % confluent.
2. The day before the pseudopodia assay, carefully remove the cell culture medium from the dishes, and add 7 mL of starvation medium to starve cells overnight at 5 % CO_2, 37 °C (*see* **Note 6**).

3.2.2 Stimulation of Pseudopodia Formation

1. Coat both the top and bottom sides of the polycarbonate membrane in a 6-well transwell plate with 5 μg/mL fibronectin solution. Incubate the 6-well plate at 37 °C for 2 h to allow the filters to be coated completely (*see* **Note 7**).
2. Add 2.5 mL of cell migration medium to each of the lower chambers in the transwell plate and put the microporous filters back into the plate.
3. Trypsinize and transfer the starved cells into the upper chamber on the microporous filter. Resuspend the cells with 4 mL migration medium to a final concentration of 1.5×10^6 cells per well.
4. Carefully place the plates in the cell culture incubator; allow the cells to attach and spread for 2–2.5 h at 37 °C, 5 % CO_2.
5. Add 2.5 mL migration and adhesion medium containing chemoattractant to the lower chamber of each well of a new 6-well dish (*see* **Note 8**). Carefully transfer the microporous filter to which the cells are attached to a well containing migration and adhesion medium containing chemoattractant (*see* **Note 9**). Gently place the 6-well plate into the cell culture incubator and allow pseudopodia to grow for ~60 min [21].

3.2.3 Extraction of Cytoskeleton for Proteomic Analysis

1. Thirty minutes before harvesting pseudopodia or cell bodies, add 5 mL of cell lysis buffer to each well of a clean used or new 6-well plate. Incubate the plate on ice.
2. Flatten out a piece of parafilm on the top of a glass plate and place a 200 μL drop of 1 % SDS on the parafilm to collect the protein.
3. Remove the filter to be processed for growth-phase pseudopodia or cell body isolation from the 6-well plate and quickly (but gently) dip into PBS solution to rinse the cells at room temperature.
4. Place the filter directly into ice-cold cell lysis buffer for 1.5 min.
5. Gently rinse the filter with TBS buffer and incubate the retained cytoskeleton proteins in nuclease buffer for 10 min at room temperature. Then rinse the filter with TBS buffer again.
6. With a cotton-tipped swab (with the tip flattened), remove the cell bodies from the rest of the filter paper and discard. Be gentle and careful as the filter paper is very fragile. Rinse with TBS buffer three times to remove cell debris. For cell body cytoskeleton enrichment, gently remove the cell pseudopodia from the bottom of the filter paper in a new well. Rinse three times before protein collection (*see* **Note 10**).
7. Carefully cut the filter along the outer edge of the chamber, using a sharp razor blade to generate a round piece of filter paper. Place the filters into the puddle of 1 % SDS on the

parafilm with the pseudopodia facing down and allow the proteins to solubilize for 30 s. Then with a cell scraper, scrape down the pseudopodia cytoskeleton from the filter into 1 % SDS.

8. Repeat **steps 3** through **7** for each of the pseudopodia filters of a 6-well dish. Transfer the lysate to a 1.5 mL microfuge tube. Boil at 100 °C for 5 min and freeze the sample at –80 °C for further use.

3.3 Gel Separation, In-Gel Digestion, Stable Isotope Dimethyl Labeling, and MudPIT

In-solution digestion and stable isotope labeling are also compatible with the above cytoskeleton enrichment protocols as well as the MudPIT procedures listed below. However, in our experience in-gel digestion of proteins isolated by gel electrophoresis gives better digestion efficiency and a wider dynamic range of protein identification.

1. Determine the protein concentration using the BCA protein assay, a microplate spectrophotometer, and a series of pre-diluted BSA protein standards.
2. Load protein samples onto a NuPage 4–12 % Bis-Tris gel.
3. Separate the proteins with 180 V constant voltage for 50 min.
4. Stain the gel with Coomassie Blue for 3 h.
5. Destain the gel with destaining buffer until bands are very clean.
6. Cut each lane of the gel into 14 bands and cut each band into small pieces separately.
7. Destain the gel cubes with 50 % MeOH.
8. Dehydrate the gel cubes with 100 % ACN and dry the cubes.
9. Add 10 mM DTT (enough to cover gel pieces) and incubate at 56 °C for 20 min.
10. Remove the DTT solution, dehydrate the gel cubes with 100 % ACN, and dry.
11. Add 50 mM iodoacetamide (enough to cover gel pieces) at room temperature and incubate in the dark for 20 min.
12. Remove the iodoacetamide solution, dehydrate the gel cubes with 100 % ACN, and dry.
13. Add enough trypsin solution to cover gel pieces and incubate at 37 °C overnight.
14. Extract peptides from the gel cubes with 50 % ACN/1 % formic acid.
15. Dry the samples in a centrifugal vacuum concentrator.
16. Dissolve the samples with 100 μL 100 mM of TEAB (*see* **Note 11**).
17. Add 4 μL of 4 % (vol/vol) CH_2O and $^{13}CD_2O$ to the sample to be labeled with light and heavy dimethyl, respectively (*see* **Note 12**).

18. Mix briefly and spin the solution down.
19. Add 4 μL of 0.6 M $NaBH_3CN$ to the samples to be light and add 4 μL of 0.6 M $NaBD_3CN$ to the samples to be heavy labeled.
20. Incubate in a fume hood for 1 h at room temperature.
21. Add 16 μL of 1 % (vol/vol) ammonia solution to quench.
22. Mix briefly and spin the solution down.
23. Add 8 μL of formic acid to further quench the reaction.
24. Mix briefly and spin the solution down.
25. Dry the samples in a centrifugal vacuum concentrator.
26. The peptide digests are now ready for mass spectrometry using MudPIT identification methods [22].
27. A fused-silica capillary column (100 μm i.d. × 365 μm o.d.) is pulled with laser puller.
28. The column is first packed with 10 cm of 5 μm C18 resin followed by 4 cm of 5 μm strong cation exchange resin and 4 cm of 5 μm C18 resin.
29. The column is placed in-line with the LC-MS system.
30. Four buffer solutions are used for the chromatography (buffers A–D).
31. A fully automated salt step chromatography run is carried out on each sample.
32. Protein identification and quantification are carried out using a search program such as MASCOT and SEQUEST.

3.4 Informatics

1. Data sets may be entered into freeware (e.g., FatiGO/Babelomics, http://babelomics.bioinfo.cipf.es/index.html) [23–26] or payware (e.g., IPA, http://www.ingenuity.com) bioinformatics packages. These platforms enable rapid comparison of large data sets against signaling pathway databases such as BioCarta (www.biocarta.com/genes/index.asp), KEGG (www.genome.jp/kegg), or EMBL-EBI (www.ebi.ac.uk/interpro/index.html) to find biological relationships among data sets in regard to known and/or predicted cellular and molecular functions. Importantly, the insoluble fraction quantified from the pseudopodia shows a significant enrichment for proteins that mediate cell assembly, morphology, and motility (Fig. 5a and Table 1).
2. In regard to the IPA analysis software, Ingenuity is a bioinformatics resource that facilitates the mapping of signaling networks and interactomes involving a range of biomolecules as they relate to normal physiological and pathophysiological functions [27, 28]. Using this comprehensive informatics

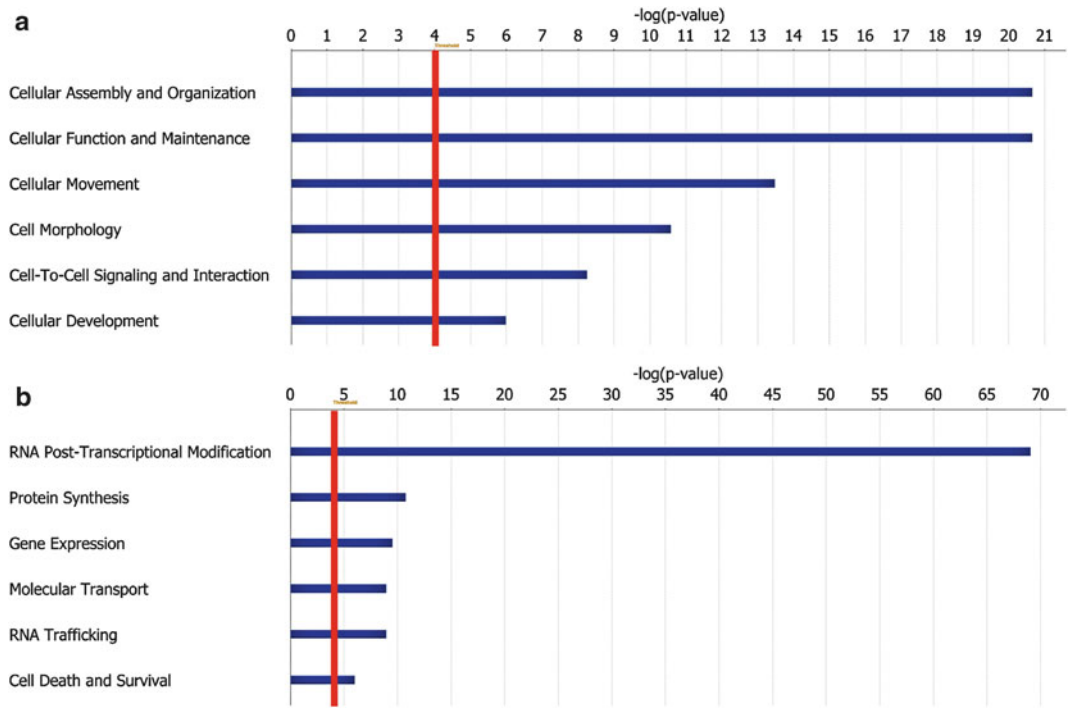

Fig. 5 Top 6 molecular and cellular functions annotated (using IPA software) for the pseudopodia cytoskeleton (**a**) and cell body cytoskeleton (**b**) fractions (*red line* represents a *p*-value threshold <0.0001)

program it is possible to model, analyze, and understand the complex integration of biological systems. IPA utilizes the Ingenuity Knowledge Base, a large repository of biological interactions and functional annotations created from millions of individually modeled relationships between proteins, genes, complexes, cells, tissues, drugs, and diseases. These modeled relationships include links to original articles and are manually reviewed biweekly for accuracy. It includes information from a wide range of published biomedical literature, textbooks, reviews, internally curated knowledge pathways, and a variety of established informatics sources and databases (e.g., EntrezGene, RefSeq, OMIM disease associations, KEGG, GWAS, LIGAND, and BIND).

4 Notes

1. In order to initially validate these methods, we began our studies in fibroblast cell lines. Importantly, these cell models have a well-defined cytoskeleton/adhesion complex network. Furthermore, these cells can be induced to migrate and extend numerous pseudopodia in response to chemical stimuli. In regard to mouse embryonic fibroblasts (MEF), there exists a large

Table 1
Top 20 proteins enriched in the pseudopodia cytoskeleton fraction

ID	Symbol	Entrez gene name
IPI00380436	ACTN1	Actinin, alpha 1
IPI00420172	AGFG1	ArfGAP with FG repeats 1
IPI00308852	DAB2	Disabled homolog 2, mitogen-responsive phosphoprotein (Drosophila)
IPI00378015	DBNL	Drebrin-like
IPI00115492	EPS8L2	EPS8-like 2
IPI00330862	EZR	Ezrin
IPI00353563	FSCN1 (includes EG:14086)	Fascin homolog 1, actin-bundling protein (*Strongylocentrotus purpuratus*)
IPI00311726	HIP1R	Huntingtin interacting protein 1 related
IPI00110588	MSN	Moesin
IPI00453692	NES	Nestin
IPI00309768	PDLIM1	PDZ and LIM domain 1
IPI00653381	PDLIM5	PDZ and LIM domain 5
IPI00264501	PICALM	Phosphatidylinositol-binding clathrin assembly protein
IPI00554989	PPIA	Peptidylprolyl isomerase A (cyclophilin A)
IPI00653921	RDX	Radixin
IPI00474602	RNF31	Ring finger protein 31
IPI00468418	STAM2	Signal transducing adaptor molecule (SH3 domain and ITAM motif) 2
IPI00125778	TAGLN2	Transgelin 2
IPI00314748	WDR1	WD repeat domain 1
IPI00387422	ZYX	Zyxin

pool of knockout line resources with which to immediately validate the roles of novel proteins in regulating cytoskeleton and adhesion domains. Nonetheless, these methods are also compatible with disease-relevant cell types such as fibroblasts harboring oncogenic mutations or primary cancer cells derived from patient tissues.

2. The Cell Comb gets wet easily from the medium. Do not reuse the Cell Comb when scratching other plates, as the wet comb is not able to sustain sharp edges when used repeatedly and it is difficult to wash away cell debris from previous scratching.

3. Based upon our cell imaging data (Fig. 4), we predict that a significant amount of cytoskeleton and adhesion complex remodeling will occur during this time frame. By analyzing the kinetic landscape, these experiments can provide important information about the dynamic nature of cell migration after wounding.
4. By keeping the cell lysis buffer cold, minimal protein and/or phosphoprotein degradation occurs. Based upon biochemical and microscopy analysis, this time point was determined to be the most efficient at extracting the soluble fraction while leaving behind the majority of proteins residing in the insoluble fraction (Figs. 2 and 3).
5. In order to avoid the need for SDS-PAGE separation of proteins and in-gel digestion methods, a urea-based buffer may be used. However, in our experience, the use of SDS significantly enhances protein extraction and solubility. Alternatively, the SDS can be removed prior to MS analysis by the FASP strategy as described previously by Wisniewski et al. [23].
6. Other cell lines that extend pseudopodia in response to ECM and growth factor gradients would be expected to work in this assay. We have utilized COS-7, NIH3T3, MEF, PANC-1, and MDA-MB-435 cell lines in this assay.
7. Before using the membrane filter, make sure that the filter's edge is completely sealed to avoid media leaking between upper and lower chambers. This prevents the exchange of chemoattractant between chambers and ensures efficient pseudopod extension through membrane pores.
8. LPA is known as a chemoattractant for NIH3T3 cells to induce directed cell migration [17]. Other chemoattractants may also be used at the appropriate concentrations, depending on the experiment and cell type.
9. To ensure the formation of the proper chemoattractant gradient, do not shake or bang the dish and remove any bubbles that may have been trapped underneath the filter by gently tilting the chamber to one side.
10. Before collecting the pseudopodia (or cell body) cytoskeleton, make sure that all the cell body (or pseudopodia) proteins have been removed completely. More than one cotton swab may be required.
11. Formaldehyde can react with amine, such as ammonium bicarbonate or Tris. The sample should be performed in amine-free solution, such as TEAB.
12. Formaldehyde solutions and formaldehyde vapors are toxic, so prepare solutions and perform in a fume hood.

Acknowledgments

This work was supported by the NIH-IRACDA (NIH—Institutional Research and Academic Career Development Award) Postdoctoral Fellowship GM06852 (J.A. Kelber) and NIH grants CA097022 and CA129231 (R.L. Klemke).

References

1. Petrie RJ, Doyle AD, Yamada KM (2009) Random versus directionally persistent cell migration. Nat Rev Mol Cell Biol 10(8): 538–549
2. Ridley AJ, Schwartz MA, Burridge K, Firtel RA, Ginsberg MH, Borisy G, Parsons JT, Horwitz AR (2003) Cell migration: integrating signals from front to back. Science 302(5651): 1704–1709
3. Richards TA, Cavalier-Smith T (2005) Myosin domain evolution and the primary divergence of eukaryotes. Nature 436(7054):1113–1118
4. Avraamides CJ, Garmy-Susini B, Varner JA (2008) Integrins in angiogenesis and lymphangiogenesis. Nat Rev Cancer 8(8):604–617
5. Borner A, Warnken U, Schnolzer M, Hagen J, Giese N, Bauer A, Hoheisel J (2009) Subcellular protein extraction from human pancreatic cancer tissues. Biotechniques 46(4):297–304
6. Ramsby ML, Makowski GS (1999) Differential detergent fractionation of eukaryotic cells. Analysis by two-dimensional gel electrophoresis. Methods Mol Biol 112:53–66
7. Luna EJ, Hitt AL (1992) Cytoskeleton plasmamembrane interactions. Science 258(5084): 955–963
8. Cowin P, Burke B (1996) Cytoskeleton-membrane interactions. Curr Opin Cell Biol 8(1):56–65
9. Chichili GR, Rodgers W (2009) Cytoskeleton-membrane interactions in membrane raft structure. Cell Mol Life Sci 66(14):2319–2328
10. Kuo JC, Han XM, Hsiao CT, Yates JR, Waterman CM (2011) Analysis of the myosin-II-responsive focal adhesion proteome reveals a role for beta-Pix in negative regulation of focal adhesion maturation. Nat Cell Biol 13(4):383–393
11. Nebl T, Pestonjamasp KN, Leszyk JD, Crowley JL, Oh SW, Luna EJ (2002) Proteomic analysis of a detergent-resistant membrane skeleton from neutrophil plasma membranes. J Biol Chem 277(45):43399–43409
12. Wang Q, He J, Meng L, Liu Y, Pu H, Ji J (2009) A proteomics analysis of rat liver membrane skeletons: the investigation of actin- and cytokeratin-based protein components. J Proteome Res 9(1):22–29
13. Tomazella GG, daSilva I, Thome CH, Greene LJ, Koehler CJ, Thiede B, Wiker HG, de Souza GA (2010) Analysis of detergent-insoluble and whole cell lysate fractions of resting neutrophils using high-resolution mass spectrometry. J Proteome Res 9(4):2030–2036
14. Xu P, Crawford M, Way M, Godovac-Zimmermann J, Segal AW, Radulovic M (2009) Subproteome analysis of the neutrophil cytoskeleton. Proteomics 9(7):2037–2049
15. Schneider L, Cammer M, Lehman J, Nielsen SK, Guerra CF, Veland IR, Stock C, Hoffmann EK, Yoder BK, Schwab A, Satir P, Christensen ST (2010) Directional cell migration and chemotaxis in wound healing response to PDGF-AA are coordinated by the primary cilium in fibroblasts. Cell Physiol Biochem 25(2–3):279–292
16. Nobes CD, Hall A (1999) Rho GTPases control polarity, protrusion, and adhesion during cell movement. J Cell Biol 144(6):1235–1244
17. Cho SY, Klemke RL (2002) Purification of pseudopodia from polarized cells reveals redistribution and activation of Rac through assembly of a CAS/Crk scaffold. J Cell Biol 156(4):725–736
18. Wang Y, Ding SJ, Wang W, Jacobs JM, Qian WJ, Moore RJ, Yang F, Camp DG II, Smith RD, Klemke RL (2007) Profiling signaling polarity in chemotactic cells. Proc Natl Acad Sci USA 104(20):8328–8333
19. Wang Y, Ding SJ, Wang W, Yang F, Jacobs JM, Camp D II, Smith RD, Klemke RL (2007) Methods for pseudopodia purification and proteomic analysis. Sci STKE 2007(400):pl4
20. Wang Y, Kelber JA, Tran Cao HS, Cantin GT, Lin R, Wang W, Kaushal S, Bristow JM, Edgington TS, Hoffman RM, Bouvet M, Yates JR III, Klemke RL (2010)

Pseudopodium-enriched atypical kinase 1 regulates the cytoskeleton and cancer progression [corrected]. Proc Natl Acad Sci USA 107(24):10920–10925

21. Wang Y, Klemke RL (2007) Biochemical purification of pseudopodia from migratory cells. Methods Mol Biol 370:55–66
22. Washburn MP, Wolters D, Yates JR (2001) Large-scale analysis of the yeast proteome by multidimensional protein identification technology. Nat Biotechnol 19(3):242–247
23. Wisniewski JR, Zougman A, Nagaraj N, Mann M (2009) Universal sample preparation method for proteome analysis. Nat Methods 6(5):359–362
24. Medina I, Carbonell J, Pulido L, Madeira SC, Goetz S, Conesa A, Tarraga J, Pascual-Montano A, Nogales-Cadenas R, Santoyo J, Garcia F, Marba M, Montaner D, Dopazo J (2010) Babelomics: an integrative platform for the analysis of transcriptomics, proteomics and genomic data with advanced functional profiling. Nucleic Acids Res 38 (Web Server issue):W210-213
25. O'Donoghue SI, Gavin AC, Gehlenborg N, Goodsell DS, Heriche JK, Nielsen CB, North C, Olson AJ, Procter JB, Shattuck DW, Walter T, Wong B (2010) Visualizing biological data-now and in the future. Nat Methods 7 (3 Suppl):S2-4
26. Gehlenborg N, O'Donoghue SI, Baliga NS, Goesmann A, Hibbs MA, Kitano H, Kohlbacher O, Neuweger H, Schneider R, Tenenbaum D, Gavin AC (2010) Visualization of omics data for systems biology. Nat Methods 7 (3 Suppl):S56-68

Chapter 13

Fabricating Surfaces with Distinct Geometries and Different Combinations of Cell Adhesion Proteins

Molly Lowndes and W. James Nelson

Abstract

A step-by-step procedure is described for functionalizing the surface of a glass coverslip so that a single cell contacts distinct patterns of extracellular matrix and cell–cell adhesion proteins. This dual-micropatterned substratum is accomplished through a two-step process. First, extracellular matrix (ECM) is microcontact-printed onto a silanized glass surface using electron beam lithography, etched resist-coated wafers, and Polydimethylsiloxane (PDMS) stamps of differing geometries. Then, non-ECM-coated surfaces are incubated sequentially with biotin, NeutrAvidin, and biotinylated Protein A to attach Fc-cadherin fusion proteins, Fc, or PEG. Cells are seeded at low density onto the functionalized surface for single-cell analysis of protein recruitment/turnover and cellular motility.

Key words Cadherin, Extracellular matrix (ECM), Micropatterning, Cross talk, Migration, Cell–cell adhesion

1 Introduction

Epithelia undergo dramatic morphogenetic changes during normal development, tissue regeneration, and cancer that range from cohesive sheet migration, cell position changes within cohesive tissues, to individual cell migration after dissociation from tissues. To maintain tissue integrity these cell movements require coordination between the cell migration machinery and intercellular adhesion complexes. Investigating how cells accomplish a dynamic balance between migration and cell–cell adhesion is complicated by the large number of adhesion proteins and their orientation in three-dimensions (3D; Fig. 1). Normal epithelial tissue contains several types of adhesion complexes. Extracellular matrix (ECM) adhesions vary depending on the ligand (collagen and laminin isoforms, for example) and the corresponding integrin adhesion proteins expressed [1]. In addition, epithelial tissues contain multiple cell–cell adhesion complexes including tight junctions, adherens junctions, and desmosomes [2]. The interrelationship

Amanda S. Coutts (ed.), *Adhesion Protein Protocols*, Methods in Molecular Biology, vol. 1046,
DOI 10.1007/978-1-62703-538-5_13,

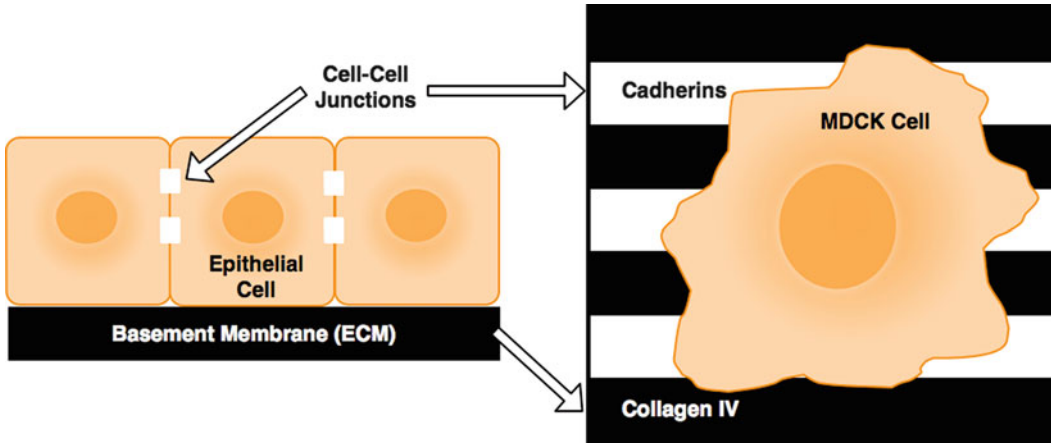

Fig. 1 Simplifying multicellular interactions from 3D organization of cell adhesion contacts, to a 2D representation. Cell–extracellular matrix (ECM) adhesions are normally localized on the basal side where cells contact the basement membrane, while cell–cell junctions are localized along the lateral membranes. To simplify this 3D geometry of adhesion complexes, collagen IV (ECM) stripes are printed onto a 2D surface for cell–ECM contacts and cadherins are functionalized between the collagen stripes for cell–cell adhesion complexes. A single cell (MDCK) plated onto the dual-patterned surface will come into contact with both types of cell adhesion proteins

between these different adhesion complexes in regulating cell migration and cell–cell adhesion remains unclear.

Pioneering studies by Abercrombie in the 1950s identified the potential importance of cross talk between cell–cell adhesion and cell migration. Abercrombie coined the term "contact inhibition" to describe how cell–cell interactions between fibroblasts initially inhibited, and then redirected their migration [3, 4]. It remains unclear, however, whether cell–cell contact inhibition of cell migration results from the spatial redistribution of the cell migration machinery upon cell–cell contact, or down-regulation of cell migration, or both.

Because of the spatial organization of cell–cell adhesion and cell–ECM adhesion complexes in 3D, it is difficult to examine changes in the dynamics and organization of both types of complexes at the same time. Therefore, we chose to dissect potential cross talk between adhesion complexes using a reductionist approach in which the 3D problem is reduced to 2D, in which both types of adhesion proteins are presented to the cell on the same surface. Such dual-patterning can test the effects of combinations of different adhesion proteins on membrane and cell dynamics, and cell motility at the single cell level (Fig. 1). Dual-patterning can be accomplished though a two step process in which ECM is first micro-contact printed onto a silanized glass surface that can be used for imaging, then, based on previously described techniques

[5, 6], non-ECM-coated surfaces are coated with cell–cell adhesion proteins [7].

Micro-patterns can be designed to test a variety of cellular behaviors. For example, single cell analysis using dual-patterning with collagen IV and E-cadherin stripes indicates that cross talk between these adhesion complexes regulates cell membrane dynamics and directed cell migration, but with little effect on average migration velocity [8]. This experimental approach provides an opportunity to understand the molecular regulation and cross talk between different adhesion complexes in the larger context of tissue regeneration, morphogenesis and cancer.

2 Materials

2.1 Micro-patterned Plate Components and Fabrication Equipment

1. Layout Editor (L-edit) Software (Tanner Research).
2. Chrome-coated quartz mask (Compugraphics, USA).
3. Silicon wafer (Silicon Valley Microelectronics (SVM)).
4. Hexamethyldisylazane (HMDS) (Sigma-Aldrich).
5. SPR 220-7.0 Positive Photoresist (Rohm and Haas Electronic Materials LLC).
6. Microposit developer LDD-26W (Shipley).
7. Nanofabrication Equipment: Electron beam lithographer (Raith 150 Ebeam Writer), Silicon Valley Group (SVG) Resist Coat Tracks, Electronic Visions System (620 aligner & 501 wafer bonder), Silicon Valley Group (SVG) Resist Develop Tracks. Maintain in a Class 100 cleanroom (*see* **Note 1**).
8. Polydimethylsiloxane (PDMS) (Sylgard 184, Dow Corning).

2.2 Glass Silanization Components

1. Borosilicate glass coverslips (VWR Scientific) or glass-bottomed imaging dishes (MatTek) (*see* **Note 2**).
2. UV-ozone plasma (Harrick plasma cleaner).
3. Silanization Solution: 2.5 % 3-aminopropyltriethoxysilane (APTES) (Pierce), 93 % methanol, 4 % deionized water, and 0.5 % glacial acetic acid (*see* **Note 3**).

2.3 Components for Preparing Purified Proteins

1. HEK 293 cells.
2. HEK 293 Cell Growth Medium: High-glucose Dulbecco's modified Eagle's medium (DMEM), 10 % FBS, 400 μM Geneticin (G418).
3. Pierce Chromatography Cartridges: Protein A Sepharose Column (1 mL).
4. Binding Buffer: 0.1 M Phosphate, 0.15 M NaCl, pH 7.2. Make buffer using a mix of monosodium phosphate and its

conjugate base, disodium phosphate (ratio of [Base]/[Acid] = 1.096). Adjust the pH to 7.2 by adding phosphoric acid or sodium hydroxide.

5. Elution Buffer: 0.1 M Glycine-HCl, pH 2.6. Store at 4 °C.
6. Neutralization Buffer: 1 M Tris–HCl, pH 9.
7. Storage Buffer: 10 mM Hepes, 184 mM NaCl, 7.2 mM KCl, pH 7.5. Store at 4 °C.
8. Amicon Ultra Centrifugal Filter (Millipore).
9. Collagen IV (Sigma-Aldrich).
10. Cy 3.5 or Cy 5.5 mono-reactive dye pack (Amersham—GE Healthcare Life Sciences).

2.4 Printing with Patterned Stamps Components

1. UV–ozone plasma (Harrick plasma cleaner).
2. Syringe (5 mL).
3. Sterile syringe filter (0.45 μm).
4. Steel Hex Nuts (5/8–11 callout size) (Hillman).
5. Phosphate Buffered Saline (PBS).

2.5 Cadherin Functionalization Components

1. Fc protein (Sigma-Aldrich).
2. Phosphate Buffered Saline (PBS).
3. EZ link sulfo-NHS-LC-LC-biotin (Pierce).
4. NeutrAvidin: 5 mg/mL in PBS (Pierce).
5. Biotinylated Protein A: 0.3 mg/mL in PBS (Pierce).
6. Biotin solution: 15 mM in DMSO (Pierce).
7. Succinimidyl PEG (mPEG-NHS): 50 mM in DMSO (Pierce).
8. DMSO.
9. DMEM/FBS: Low-glucose Dulbecco's modified Eagle's medium (DMEM), 10 % FBS.

2.6 Plating Single Cells

1. Madin-Darby Canine Kidney (MDCK) cells.
2. MDCK Growth Medium: Low-glucose Dulbecco's modified Eagle's medium (DMEM), 10 % FBS, 1 % penicillin/streptomycin.

2.7 Components for Cell Analysis

1. Live-cell imaging system.
2. Total Internal Reflection Florescence Microscopy (TIRF-M) system.
3. Fluorescence Recovery after Photobleaching (FRAP) system.
4. Image Processing tools (Image J, i.e., Manual Tracking plugin; http://rsb.info.nih.gov/ij/).

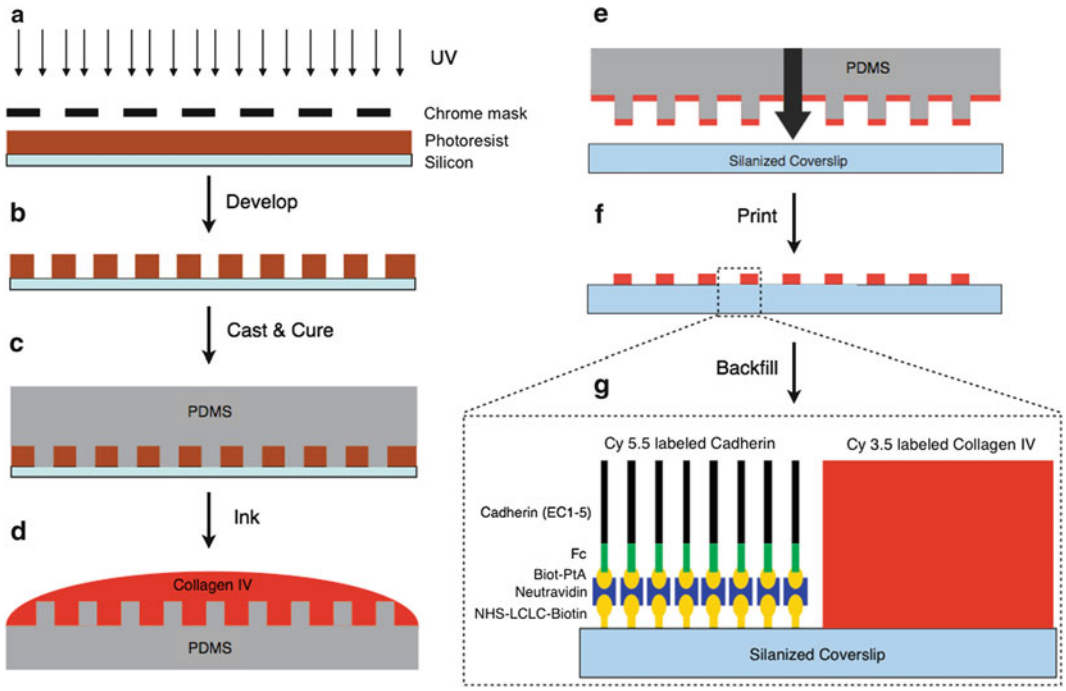

Fig. 2 Preparing dual-patterned surfaces. Micro-patterns are transferred onto a silicon wafer by first coating the wafer with photoresist and then exposing it to UV-radiation through a chrome mask (**a**). The photoresist is developed, and exposed photoresist becomes soluble and is removed leaving unexposed photoresist on the original pattern etched onto the chrome mask (**b**). PDMS can then be cast (poured) onto this surface and cured to create a PDMS stamp with grooves and ridges (**c**). The PDMS stamp is peeled off the silicon mask, and ECM (collagen IV) solution is added (inked) onto the patterned surface (**d**). Excess collagen IV is dried from the surface, and the stamp is printed onto a silanized glass surface (**e**, **f**). Non-collagen IV-coated surfaces can then be backfilled sequentially with biotin, NeutrAvidin, and biotinylated Protein A for binding of Fc-cadherin in its proper orientation (**g**)

3 Methods

3.1 Fabrication of Micro-patterned Plates

1. Pattern design is generated with L-edit software (*see* **Note 4**), such as stripes with a width of 10 μm (*see* **Note 5**).
2. Designed patterns are etched onto a chrome-coated quartz surface using electron beam lithography (Ebeam writer) (*see* **Note 6**).
3. Using an automated coater from Silicon Valley Group, silicon wafers are first vapor-primed with hexamethyldisylazane (HMDS) (*see* **Note 7**), then spin-coated with positive photoresist to a uniform thickness of 10 μm.
4. The Electronic Visions System exposes the wafers to UV radiation through the quartz mask (Fig. 2a).
5. Using an automated developer system, exposed/soluble photoresist (photosensitive layer) is removed upon addition of

microposit developer LDD-26W leaving transparent regions according to the pattern on the quartz mask (Fig. 2b).

6. Polydimethylsiloxane (PDMS) is cast onto the patterned resist-coated wafer (Fig. 2c) (*see* **Note 8**).
7. The PDMS coated wafer is cured for 2 h at 60 °C, and then peeled slowly off the wafer (*see* **Note 9**). The PDMS surface will display ridges and grooves according to the pattern design.

3.2 Glass Silanization

All steps involving methanol should be done in a fume hood and waste should be disposed of properly.

1. Borosilicate glass coverslips or glass-bottomed imaging dishes are cleaned in 100 % methanol for 1–2 h (*see* **Note 10**).
2. Glass coverslips should always be dried under filtered air/nitrogen (*see* **Note 11**).
3. Once the methanol is dried, coverslips are treated with UV-ozone plasma for 2 min (*see* **Note 12**).
4. Coverslips are incubated for 5 min in 1 mL of silanization solution per coverslip/dish (*see* **Note 13**).
5. After rinsing twice with 100 % methanol, coverslips are dried at 60 °C overnight.

3.3 Preparing Purified Cadherin Proteins

1. Cadherin fusion proteins, comprising the extracellular domain fused at the C-terminus to Fc (Fc-cadherin), were cloned into the expression vector CDM8FT (*see* **Note 14**).
2. HEK 293 cells stably transfected with the chimeric protein expression vector are maintained under selection with Geneticin and secrete the protein of interest into the growth media.
3. Before medium collection, cells are incubated in DMEM without FBS for 1 h to remove residual FBS (*see* **Note 15**).
4. Cells are grown in DMEM without FBS for 2 days.
5. The conditioned medium containing secreted Fc-cadherin is collected and centrifuged at 1,000 × *g* for 5 min at 4 °C to pellet cells and other debris, and the supernatant is stored at 4 °C until enough medium has been collected for affinity chromatography (usually 4–6 L).
6. Fc chimeric protein is purified from conditioned medium in one step by affinity chromatography over a Protein A Sepharose column (*see* **Note 16**).
7. Fractions containing protein are concentrated into storage buffer using a centrifugal filter.
8. Collagen IV and Fc-cadherin are labeled with Cy 3.5 or Cy 5.5 (*see* **Note 17**).

9. Protein aliquots are stored at −80 °C at stock concentrations of 500 μg/mL in water for collagen IV, and 1,600 μg/mL in storage buffer for Fc-cadherin.

3.4 Printing with Patterned Stamps

1. Cut out a section from the PDMS stamp (*see* **Note 18**).
2. The stamp is cleaned by sonication in water and then with 100 % ethanol for 5 min each.
3. The stamp is oxidized with UV-ozone plasma for 30 s to clean the surface.
4. Pipette 20 μL of collagen IV solution onto the PDMS surface, "inking" the stamp (at a working concentration of 160 μg/mL) (*see* **Note 19**) (Fig. 2d).
5. The "inked" stamp is incubated at room temperature for 20 min.
6. Excess collagen IV solution is aspirated off, and leftover droplets can then be dried under clean, low-pressure airflow (*see* **Note 20**).
7. During stamp/collagen incubation, remove the coverslips/glass-bottom dishes from the 60 °C oven and allow to cool to room temperature.
8. The "inked" stamp is applied gently to the silanized coverslip/glass-bottomed dish.
9. The stamp is put under load for 30 s by placing the coarse thread side of a hex nut onto the stamp and pressing with enough pressure to "stamp" the ECM but not crack the glass (*see* **Note 21**) (Fig. 2e).
10. After 2 min incubation, gently peel off the stamp from corner to corner (Fig. 2f).
11. Wash the coverslip with PBS twice before beginning cadherin functionalization (*see* Subheading 3.5).
12. Stamps can be stored at room temperature and reused after removing residual collagen IV by incubating with 0.5 % acetic acid solution overnight and re-sonicating the stamp in water and ethanol.

3.5 Cadherin Functionalization

1. Stamped coverslips are first incubated (*see* **Note 22**) with EZ link sulfo-NHS-LC-LC-biotin (50 mM in water; made fresh each time) for 1 h. All incubations and washes are done at room temperature in the dark (*see* **Note 23**).
2. Wash 3× with PBS.
3. Incubate with NeutrAvidin for 1 h.
4. Wash 3× with PBS.
5. Incubate with biotinylated-Protein A for 1 h (*see* **Note 24**).
6. Wash 3× with PBS.

7. Coverslips are blocked with biotin solution for 30 min (*see* **Note 25**). At this point coverslips can be stored at 4 °C overnight.
8. Immediately before cell seeding, incubate coverslips with Fc protein, Fc-cadherin (stock Fc-cadherin protein is diluted to 200 μg/mL) (Fig. 2g) (*see* **Note 26**), or succinimidyl PEG for 1 h.
9. Coverslips are washed 3× in PBS and once with DMEM/FBS.

3.6 Plating Single Cells

1. MDCK cells are cultured in MDCK growth medium. Before an experiment, cells are subcultured overnight at low density (~1.5×10^6 cells/10 cm diameter dish) (*see* **Note 27**).
2. Cells seeded onto dual-patterned surfaces should be a single-cell suspension (*see* **Note 28**) and plated at a density low enough to avoid individual cells contacting each other and aggregating (~2.5×10^5 cells/MatTek dish).
3. Cells should be allowed to adhere and spread for ~1 h (*see* **Note 29**).

3.7 Cell Analysis

Live cell imaging can be used to measure a variety of cell behaviors including, but not limited to, protein recruitment, protein turnover, membrane activity, directional cell movement and rates of cellular migration.

1. To assess protein recruitment and turnover on ECM versus cadherin surfaces, cells expressing fluorescently tagged proteins can be used including focal adhesion proteins (e.g., vinculin-GFP) or adherens junction proteins (e.g., E-cadherin-GFP).
2. Protein recruitment is best measured using total internal reflection fluorescence microscopy (TIRF-M) to visualize proteins on the plasma membrane contacting the patterned surface.
3. Fluorescence recovery after photobleaching (FRAP) can be used to measure protein turnover on the different functionalized surfaces.
4. Membrane-GFP (e.g., myristoylated-GFP) can also be used to measure lamellipodial/membrane activity on ECM versus cell–cell adhesion surfaces. These are typically short time-lapse movies of 5 min length with 10 s intervals. Analysis involves tracing the contour of the cell over time and comparing the number of protrusions and retractions on the different surfaces.
5. Cellular migration and directional movement of single cells on the dual-patterns can be assessed using longer time-lapse imaging (~8 h with 10 min intervals) and single molecule tracking (Manual Tracking plugin from Image J) of the nuclear centroid, visualized by differential interference contrast

microscopy (DIC). Migration rate is normalized to cells seeded on a control surface printed with ECM and functionalized with Fc.

6. Cells can also be processed for indirect immunofluorescence (i.e., fixation and permeabilization) following live cell imaging, for retrospective analysis of additional protein distributions as a function of cell behaviors.

4 Notes

1. Nanofabrication equipment is very expensive and requires extensive training. We performed our fabrications at the Stanford Nanofabrication Facility (SNF) with the help of their staff.
2. We used the standard 35 mm diameter MatTek dishes with a glass diameter of 20 mm, referred to as No. 0 thickness.
3. Solution should made fresh for each experiment with the addition of 3-aminopropyltriethoxysilane (APTES) last. Final solution volume will depend on the number of coverslip/dishes to be silanized.
4. When designing patterns one must consider the cell type used and the size of coverslip onto which the cells will be seeded. For example, we have used MDCK cells because they express both integrin-based ECM adhesion complexes and a range of cell–cell adhesion complexes including Adherens Junctions (E-cadherin) and Desmosomes (desmosomal cadherins—desmoglein, desmocolin); these cells spread to a diameter of 30–40 μm on ECM ligands or substrata with ECM proteins. Any other cell-type could be used, including fibroblasts that exogenously express different cell–cell adhesion proteins. However, it is important to test that each cell type expresses the correct repertoire of adhesion proteins for ligands that will be used to make the substrata.
5. Stripes with a width of 10 μm ensured that a single epithelial MDCK cell contacted multiple stripes, and overlapped at least two stripes that were functionalized with different adhesion ligands. Under this condition, cell behavior can be directly compared between membranes binding to adjacent adhesion ligands (*see* Subheading 3.7). However, any width of stripe can be fabricated, depending on the context of the experiment. For example, a wide stripe (>250 μm) functionalized with ECM ligand bordered by stripes functionalized with another adhesion ligand would allow cells to migrate (randomly) on the ECM surface, and then encounter a stripe functionalized with E-cadherin and change behavior.

6. Electrons are emitted across the chrome metal-absorbing film (resist) developing the exposed quartz areas and creating a "photomask."
7. HMDS promotes adhesion of the photoresist.
8. PDMS should be degassed and care should be taken not to introduce bubbles when pouring it over the wafer.
9. The patterned wafer can be used to make many PDMS stamps, although the patterns on the wafer may etch off over time.
10. If printing on another surface, such as PDMS, this step may be skipped due to cross-reaction with methanol.
11. We find this method of drying avoids residual spots of methanol, which would leave marks on the glass.
12. UV-ozone treatment removes any organic contaminants and creates an ultra-clean surface.
13. The inorganic and organic properties of APTES create an interface between the glass surface and the functionalized proteins (*see* Subheading 3.5). To reduce the evaporation of methanol from the solution, we use parafilm around the lid of the dishes, making sure that the parafilm does not contact the APTES solution since it will dissolve the parafilm.
14. This purification method has been described previously in detail (*see* ref. 7).
15. FBS contains antibodies that will interfere with the Protein A affinity chromatography purification.
16. The column is first equilibrated with 30 mL of binding buffer and then conditioned media is pumped through the column. The column is washed with 30 mL of binding buffer. Eluted buffer is added (10 mL), incubated for 10 min and collected into 1.5 mL eppendorf tubes containing 100 μL of neutralization buffer (1 mL fractions).
17. Protein labeling depends on experimental conditions required and was done according to the manufacturer's labeling kit directions.
18. Stamps should be cut into a shape that will fit completely onto the silanized glass surface. A square stamp will need to fit onto the round glass-bottomed portion of the MatTek dish, which comes in a variety of diameters (7–20 mm).
19. We find a solution with labeled/nonlabeled collagen IV (1:1 vol/vol) works best for imaging purposes.
20. Clean air can be generated by adding a syringe filter (0.45 μm) to a 5 mL syringe connected to tubing that connects to an air valve in a fume hood.
21. Finding the right amount of pressure may require some trial and error. MatTek dishes do not have an even base (the glass portion is slightly higher than the plastic) so another hex nut

should be placed under the glass portion before stamping to avoid cracking the glass.

22. We find the best way to cover the surface is to add a drop of solution (~20 μL for a 20 mm glass-diameter MatTek dish) and then place a piece of parafilm the size of the stamp onto the drop to spread it over the stamped glass.
23. Incubation is done in the dark to avoid photo-bleaching fluorescently tagged ECM protein.
24. The serial incubation with each protein ensures that Fc-cadherin binds in the proper orientation on the nonstamped surfaces (Fig. 2g).
25. Blocking with D-Biotin covers any non-functionalized surface, thereby reducing nonspecific binding of Fc-cadherin protein.
26. Fc-Cadherin can be mixed with Fc protein (200 μg/mL) to change the ratio of Fc-cadherin on the surface while keeping the total protein concentration constant.
27. Plating at low-density the night before allows for quick trypsinization (<5 min) into a single cell suspension prior to seeding on functionalized surfaces.
28. After resuspension, cells can be gently pipetted up and down to break up any residual cell aggregates before adding the cell suspension to patterned coverslips.
29. It is important to note that FBS contains ECM proteins and cells secrete ECM proteins, both of which may affect the purity of the functionalized surfaces over time.

Acknowledgments

We thank Dr. Nicolas Borghi for the design of dual-patterned substrata [5] and the Stanford Nanofabrication Facility (SNF) for their expertise. ML was supported by the Cancer Biology Program Training Grant (5T32 CA009151-34), and work in the Nelson laboratory was supported by the NIH (GM035527) and NSF (EFRI-MIKS).

References

1. Hynes RO, Naba A (2012) Overview of the matrisome—an inventory of extracellular matrix constituents and functions. Cold Spring Harb Perspect Biol 4(1):a004903
2. Franke WW (2009) Discovering the molecular components of intercellular junctions—a historical view. Cold Spring Harb Perspect Biol 1(3): a003061
3. Abercrombie M, Heaysman JE (1954) Observations on the social behaviour of cells in tissue culture. II. Monolayering of fibroblasts. Exp Cell Res 6:293–306

4. Abercrombie M, Heaysman JEM (1953) Observations on the social behaviour of cells in tissue culture. I. Speed of movement of chick heart fibroblasts in relation to their mutual contacts. Exp Cell Res 5:111–131
5. Nishizawa M, Takoh K, Matsue T (2002) Micropatterning of HeLa cells on glass substrates and evaluation of respiratory activity using microelectrodes. Langmuir 18:3645–3649
6. Cuvelier D, Rossier O, Bassereau P, Nassoy P (2003) Micropatterned "adherent/repellent" glass surfaces for studying the spreading kinetics of individual red blood cells onto protein-decorated substrates. Eur Biophys J 32: 342–354
7. Drees F, Reilein A, Nelson WJ (2005) Cell-adhesion assays: fabrication of an E-cadherin substratum and isolation of lateral and basal membrane patches. Methods Mol Biol 294: 303–320
8. Borghi N, Lowndes M, Maruthamuthu V, Gardel ML, Nelson WJ (2010) Regulation of cell motile behavior by crosstalk between cadherin- and integrin-mediated adhesions. Proc Natl Acad Sci U S A 107(30):13324–13329

Chapter 14

Purification of Native Arp2/3 Complex from Bovine Thymus

Lynda K. Doolittle, Michael K. Rosen, and Shae B. Padrick

Abstract

The Arp2/3 complex is an actin filament nucleator involved in cell motility and vesicle trafficking. Owing to the role the complex plays in important and fundamental cell biological processes, the purified complex is used in biochemical assays, reconstituted motility assays, and structural biology. As this is a eukaryotic complex assembled from seven polypeptides, the complex is purified from eukaryotic sources. Described here is a detailed method for purification of the complex from a mammalian tissue, bovine thymus.

Key words Actin nucleation factor, Arp2/3 complex, Biochemical purification, Endogenous source, Detailed protocol

1 Introduction

Dynamic rearrangements of the actin cytoskeleton are used by eukaryotic cells to generate protrusive and pinching forces, at specific places and times [1]. These rearrangements underlie aspects of cell motility [2], endocytosis [3, 4], cell division [5], and bacterial and viral pathogenesis [6, 7]. The nucleation of new actin filaments [8] is an essential component of each of these processes. Spontaneous nucleation of actin filaments is prevented in cells by a variety of factors including the proteins profilin and thymosin, but this can be overcome by the action of regulated actin nucleation factors [2]. One prominent nucleation factor is the Arp2/3 complex.

The Arp2/3 complex is formed from seven polypeptides, including two actin related proteins, Arp2 and Arp3 [9–11]. The Arp2/3 complex nucleates new filaments from the side of existing filaments, and anchors the nucleated filament in a branched structure [12–15]. In this process, Arp2, Arp3, and additional actin monomers serve as an actin nucleus, from which the new filament grows [15, 16]. Arp2/3 complex is basally inhibited, and can be stimulated to nucleate new filaments by the action of nucleation promoting factors, in particular those of the WASP family [8]. Together, nucleation promoting factors and Arp2/3 complex

Amanda S. Coutts (ed.), *Adhesion Protein Protocols*, Methods in Molecular Biology, vol. 1046,
DOI 10.1007/978-1-62703-538-5_14,

control the assembly of cellular structures such as lamellipodia [2] and the pinching off of nascent vesicles [4, 17]. Pathogens, such as *Listeria*, override the cellular control of Arp2/3 complex by providing their own highly potent activators of the complex [6, 18].

Purified Arp2/3 complex is used in two biochemical contexts. The first is the reconstitution of actin polymerization [19]. In this system, purified actin is present as a monomer that slowly polymerizes into filaments. Polymerization can be tracked through the use of a pyrene labeled actin, whose fluorescence intensity increases upon incorporation into an actin filament [20, 21]. Inclusion of Arp2/3 complex and an activator, such as the VCA domain of the WASP family member N-WASP, accelerates nucleation of new filaments and overall actin polymerization is much faster [8, 22, 23]. Alternatively, a variety of imaging based assays have been used to directly visualize Arp2/3 complex dependent branch formation using actin labeled with a variety of fluorophores [12, 13, 24]. A second context in which purified Arp2/3 complex is used is in reconstituted bead motility assays. In these assays, a mixture of purified proteins can trigger bacteria [25] or functionalized beads [26] to move through solution on a "comet tail" of polymerized actin. This reconstituted system has opened a window into how larger actin structures assemble and interact with surfaces [27–30].

For both of these assay systems, purified Arp2/3 complex is needed. Owing to the fact that this is an assembly of seven polypeptides, several of which are anticipated to need eukaryotic chaperones, overexpression in bacteria is not a viable option. Instead, purification from endogenous sources or recombinant expression in a eukaryotic host has been used. Purification of Arp2/3 complex from endogenous sources can be accomplished using one of two methods. A classical biochemical approach has been used to purify the complex from a variety of sources [18, 31–34], and we provide a time-tested version of one protocol here. Alternatively, engineered affinity columns can be used [10, 35–38] including columns derived from the VCA domain of N-WASP [36]. This approach has been adapted to the purification of Arp2/3 complex from a variety of sources [35–38]; purification of Arp2/3 complex from commercially available baker's yeast (*S. cerevisiae*) by this method is described in an accompanying chapter of this book [39]. Recombinant methods include the simultaneous overexpression of all the subunits of the human complex in insect cell lines [40], and the recombinant fusion of affinity tags to selected subunits in yeast [41–46], allowing purification by affinity methods. These two recombinant methods allow the production of mutant Arp2/3 complexes, and the use of readily available affinity chromatography methods. The primary difficulties of the recombinant systems are that eukaryotic expression systems are needed, and that the yields are low. These practical concerns have prevented the recombinant sources from displacing the endogenous sources for studies not requiring modified Arp2/3 complex.

Here we describe a method for purifying endogenous Arp2/3 complex from bovine thymus, derived from a method originally developed for purification from human leukocytes [31]. The method relies on classical biochemical methods including ammonium sulfate precipitation, ion exchange chromatography and gel filtration chromatography. The described protocol takes 3 days to perform, not including stock solution preparation. While a single person can perform the entire protocol, two people working as a team (particularly on the first day) simplify the procedure. Typical yields from the protocol range between 5 and 8 mg of highly purified complex. It should be noted that the protocol does not discriminate between the different subunit isoforms, for example ArpC1 runs as a multiplet on the final gel [47], owing to multiple isoforms. This has also been reported for ArpC1 of human origin [18]. It is also expected that there will be a degree of heterogeneity at the level of posttranslational modification. One characterized modification, phosphorylation of Arp2 at several sites [48], is expected to be present, but may not be uniformly present. The protocol can be scaled up and down. Given the columns described here, between one and four calf thymuses may be used.

2 Materials

All buffer and salt stocks are prepared using ultrapure water (>18 MΩ, using Millipore brand Milli-Q water purification system). Except where noted otherwise, all solutions are filtered through a 0.22 μm cellulose acetate membrane. Working buffers are prepared by dilution of buffer stocks into prechilled ultrapure water (except where noted). Where specific sources are recommended, the manufacturer and part numbers are indicated.

2.1 Stock Materials and Solutions

1. Bovine calf thymus: This protocol is described for two bovine calf thymuses, roughly 400 g total weight. Frozen thymus can be obtained from Pel-Freez Biologicals (Rogers, AR). Note the appearance of the thymus in a given lot, and track the lot number (*see* **Note 1**). Store thymus at −80 °C for less than 2 years.
2. Leupeptin hydrochloride (Bachem #N-1000.0100): 1 mg/mL stock, filtered and stored at −20 °C in 250 μL aliquots.
3. Calpain Inhibitor II 10 mM stock (ALLM, Calbiochem #208721): 25 mg in 6.2 mL 100 % ethanol and stored as a single volume at −20 °C until needed (use within 6 months).
4. Cathespin B Inhibitor I 10 mM stock (Caspase inhibitor, Calbiochem #342000): 5 mg in 1.3 mL 100 % ethanol and stored at −20 °C until needed (use within 6 months).
5. PMSF (Phenylmethanesulfonyl fluoride, Sigma-Aldrich #P7626): 100 mM stock in isopropanol, filtered and stored in 1 mL aliquots at −20 °C (*see* **Note 2**).

6. Benzamidine dihydrochloride (Sigma-Aldrich #B6506-100 g): 1 M stock, filtered and stored at −20 °C in 250 µL aliquots.
7. Antipain dihydrochloride (Sigma-Aldrich #A6191-100 mg): 1 mg/mL stock, filtered and stored at −20 °C in 250 µL aliquots.
8. Dithiothreitol (DTT): 1 mM stock, filtered and stored at −20 °C in 1 mL aliquots. Thaw in cool water until liquid then transfer to ice until needed. Once added to buffers, assume DTT is no longer functional after 48 h when stored at 4 °C.
9. 1 M Tris–HCl pH 8.0.
10. 0.5 M PIPES pH 6.8: Prepared using PIPES acid (piperazine-N,*N*′-bis(2-ethanesulfonic acid)), and titrated with sodium hydroxide to pH 6.8 at room temperature (*see* **Note 3**).
11. 1 M Imidazole pH 7.0: Solution is titrated with hydrochloric acid to pH 7.0 at room temperature.
12. 2 M KCl.
13. 5 M NaCl.
14. 0.5 M EGTA: Solution is titrated to pH 8.0 with sodium hydroxide. Initially, EGTA is insoluble, but comes into solution as the pH is adjusted.
15. 1 M $MgCl_2$.

2.2 Working Buffers

See **Note 4** for recommended buffer preparation schedule.

1. Buffer EB: 40 mM Tris–HCl pH 8, 10 mM EGTA, 1 mM $MgCl_2$, 1 mM DTT. Make with room temperature ultrapure water, not 4 °C water (*see* **Note 5**). Also, place 100 mL of EB on ice to be used for rinsing the blender jar.
2. Buffer QA: 20 mM Tris–HCl pH 8, 75 mM NaCl, 1 mM EGTA, 1 mM $MgCl_2$, 1 mM DTT, 10 µM Calpain Inhibitor II, 20 µg/mL leupeptin, 1 mM benzamidine, 2 µg/mL antipain.
3. Buffer DB: 2 mM Tris–HCl pH 8, 0.5 mM EGTA, 0.5 mM $MgCl_2$, 1 mM DTT.
4. Buffer QC: 20 mM Tris–HCl pH 8, 1 mM EGTA, 1 mM $MgCl_2$, 1 mM DTT.
5. Buffer QD: 20 mM Tris–HCl pH 8, 1 mM EGTA, 1 mM $MgCl_2$, 1 mM DTT, 1 M NaCl.
6. Buffer SA: 10 mM PIPES pH 6.8, 1 mM EGTA, 1 mM $MgCl_2$, 1 mM DTT.
7. Buffer SB: 10 mM PIPES pH 6.8, 1 mM EGTA, 1 mM $MgCl_2$, 1 mM DTT, 2 M NaCl.
8. Buffer KMEId: 50 mM KCl, 1 mM $MgCl_2$, 1 mM EGTA, 10 mM Imidazole pH 7, 1 mM DTT.

9. Buffer FB: 50 mM KCl, 10 mM Imidazole pH 7.0, 1 mM $MgCl_2$ 1 mM EGTA, 0.5 mM DTT, 100 μM ATP and 60 % (weight to volume) sucrose. This is prepared by adding appropriate volumes of salt and buffer stocks for 10 mL of buffer to 6 g of dry sucrose, and adding water to ~9 mL. The solution is mixed until most of the sucrose has come into solution, and the volume is corrected to 10 mL. The solution is then allowed to come completely into solution. At that point it is passed through a 0.22 μm PES filter. Prior to adding to the protein solution it is chilled on ice for ~10 min. This is enough time to reduce the temperature, but will not result in sucrose crystallizing out of solution. Use buffer FB the same day that it is prepared.
10. 5 M NaCl.
11. Q Cleaning buffer: 6 M guanidine hydrochloride, 200 mM acetic acid (*see* **Note 6**).

2.3 Chromatography Columns

Recommended flow rates and operating pressures are typical for a column in good condition. The operating pressures for the Q Sepharose FF column and SOURCE 15Q column refer to the pressure difference between the top of the column and the fractionation or waste outlet. If it is difficult to achieve the recommended flow rates without exceeding the operating pressure for the column, make sure that there is not a back pressure device after the column, that tubing bores are reasonable, and that you account for pressure build-up prior to the column.

1. 150 mL Q Sepharose FF: 150 mL Q Sepharose FF (GE #17-0510-01) is packed into an XK 26/40 (GE #28-9889-49) column. The maximum flow rate and pressure for the column are 26.5 mL/min and 0.5 MPa, respectively. We run this column at a flow rate of 8–15 mL/min at less than 0.5 MPa.
2. 50 mL SOURCE 15Q: Bulk SOURCE (GE #17-0947-05) is packed in an XK 26/20 column (GE #28-9889-48). The maximum flow rate is 26.5 mL/min and the maximum back-pressure is 0.6 MPa. We typically run this column at a flow rate of 6–10 mL/min at less than 0.6 MPa.
3. MonoS GL 10/100 column (GE #17-5169-01): The maximum pressure and flow rate for this column are 6 mL/min and 4 MPa, respectively. We run this column at 2.5–4 mL/min and at less than 4 MPa.
4. Superdex 200 pg column: This is a prepacked HiLoad 26/600 Superdex 200 pg column, with 320 mL of resin in an XK 26/600 column hardware (GE# 28-9893-36). The maximum flow rate is 4.25 mL/min with a maximum pressure of 0.5 MPa. We run this column run at 1–2.5 mL/min at less than 0.5 MPa back-pressure.

2.4 Hardware and Equipment

1. Liquid chromatography system(s) capable of delivering linear gradients and operating columns at the described flow rates and pressures. A system capable of applying linear gradients to columns at 1–5 mL/min and at 2–5 MPa is needed for the Mono S column. A system capable of applying the >500 mL of clarified lysate at low pressure is needed for the Q Sepharose column.
2. Three centrifuges are needed: (1) A low speed refrigerated centrifuge with swinging bucket rotor, capable of spinning 1 L bottles at 1,600 × *g*. (2) An ultracentrifuge (Beckman Optima or equivalent) with Type 45 Ti rotor. (3) A refrigerated high-speed centrifuge (Beckman Coulter Avanti Centrifuge), equipped with JA-10 and JA-25.50 rotors. Centrifuges equipped with a Beckman JA-20 or Sorvall SLA-3000 and SS-34 are equivalent for this purpose. All centrifugation steps are at 4 °C.
3. Warring blender for homogenization, with 1–2 L stainless steel jar.
4. Three each large stir plates, magnetic stir bars and 4 L beakers.
5. Cold room or cold box, with space for large stir-plates.
6. Conductivity meter.
7. Dialysis tubing (50 kDa cut-off dialysis membrane (Spectra/Por 6, #132544)) and clamps.
8. AmiconUltra-15 30 kDa cut-off (Fisher #UFC903024) centrifugal concentrator.

3 Methods

The overall protocol takes 3 days. A single person can complete the entire protocol, but working in a team of two greatly eases the process. We break each day up into a separate sub-protocol, but they are meant to occur on consecutive days.

3.1 Day 1: Lysis, Clarification and Ammonium Sulfate Cut

On the first day of the preparation, it is very helpful to have a second set of hands to keep up with the dishes that are generated during the process without needing to slow down other aspects of the preparation. Generally, assembly of materials and lysis can be completed within an hour and a half, clarification takes 3 h, the Q Sepharose column takes an hour, and the ammonium sulfate cut takes roughly three and a half hours, including setting up the dialysis afterwards. This timing doesn't account for cleanup, which can generally occur during subsequent steps. Thus, with two people, the protocol can be completed in about 9 h.

1. Chill the three centrifuges; 1 L capacity swinging bucket, JA-10 and Type 45 Ti rotors, and bottles (*see* **Note 7**).
2. Weigh the thymuses individually, aiming for a total weight of 200–450 g. Note their weight, and then place them on ice.

The scale limiting steps are the high-speed centrifugation step and the first two columns.

3. Use a lead brick to smash one frozen thymus (at –80 °C) into small pieces (*see* **Note 8**). Place the thymus pieces into the blender jar and add 2–3 mL of room temperature EB per gram of thymus (as weighed prior to breaking into pieces). Blend to homogenize, making sure that the thymus-buffer mix does not freeze. Add additional room temperature buffer if the homogenate appears slushy. After approximately 1 min of blending, stop the blender and add 10 μM calpain inhibitor II, 10 μM cathespin B Inhibitor I, 20 μg/mL leupeptin, 2 μg/mL antipain, 1 mM PMSF, and 1 mM benzamidine (according to volume of EB used). Then, continue blending until the final consistency and appearance is roughly that of a strawberry banana smoothie, typically after 3–5 min of total blending time (*see* **Note 9**). Split the homogenate across two 1 L bottles, rinse the blender with about 50 mL of EB and add to the homogenate in the 1 L bottles.
4. Repeat **step 3** for each thymus.
5. Centrifuge homogenate in 1 L bottles at ~1,600 × *g* (2,600 rpm in the Sorvall H6000A rotor) for 30 min.
6. Inspect the centrifuged homogenate, there should be a small pellet, and a whitish, fatty disk at the top (*see* **Note 1**). Scoop out the fatty disk and decant the supernatant through four layers of cheesecloth into a 2 L beaker.
7. Split the supernatant from **step 6** into 500 mL bottles and spin at ~4,000 × *g* (6,000 rpm in the Beckman JA-10 rotor) for 15 min.
8. Decant the supernatant through four layers of cheesecloth into a 2 L beaker.
9. Split the supernatant from **step 8** into multiple 70 mL polycarbonate bottle assemblies. Centrifuge the bottles at 138,000 × *g* for 1 h (42,000 rpm in the Type 45 Ti rotor). Note that the bottles must be full. If there is less than 65 mL of supernatant that does not fit into the bottles, discard the excess. It is common for the supernatant from **step 8** to fill more bottles than fit in a single Type 45 Ti rotor. If this is the case, keep the excess on ice until repeating the spin with additional bottles.
10. While the centrifuge for **step 9** is running, equilibrate the 150 mL Q Sepharose FF column with approximately 500 mL of buffer QA. Note the conductivity at the end of equilibration.
11. Decant the supernatant from **step 9** through four layers of cheesecloth into a 2 L beaker. Supernatant should be clear, but red in color.

12. Check the conductivity of QA using a conductivity meter. QA at 4 °C should be ~5–6 mS/cm. With the beaker containing the pooled supernatant on wet ice, adjust the conductivity of the supernatant to be 0.2–0.5 mS/cm greater than QA by adding 5 M NaCl. Note the initial, final and QA reference conductivities.
13. Inject the conductivity corrected, pooled supernatant from **step 12** onto the 150 mL Q Sepharose column equilibrated with QA and collect flow through. Rinse column with 1 column volume of QA and also collect flow through. To minimize volume, begin collection when the color of the flow through changes to red, and stop collecting flow through when the conductivity shifts back down to that seen for QA alone. Clean Q Sepharose column (*see* **Note 10**).
14. Measure volume of the combined flow through. Begin stirring the supernatant in a 4 °C cold room or packed into wet ice using a large magnetic stir plate and a large stir bar. Stirring should be aggressive enough to create a vortex with a depression which reaches at least halfway down the height of the liquid. The depression should not contact the stir bar, which would introduce air.
15. Weigh out enough solid ammonium sulfate to bring the solution to 35 % saturated (200 g of solid ammonium sulfate per liter). Very slowly add the ammonium sulfate (*see* **Note 11**) while stirring.
16. Let solution stir for 30 min at 4 °C.
17. Transfer the ammonium sulfate solution into 500 mL centrifuge bottles, filling the bottles approximately half full. Centrifuge at ~9,000×*g* for 30 min (9,000 rpm in the JA-10 rotor and bottles).
18. Carefully decant the supernatant into a glass beaker in wet ice. Discard the pellets.
19. Measure the volume of the supernatant with a cold graduated cylinder.
20. Weigh out enough ammonium sulfate to bring this 35 % saturated solution to 60 % saturated (an additional 150 g of ammonium sulfate solid per liter of supernatant). Very slowly add the ammonium sulfate (*see* **Note 11**) while stirring.
21. Let solution stir for 30 min at 4 °C.
22. Transfer the ammonium sulfate solution into 500 mL centrifuge bottles, filling the bottles approximately half full. Centrifuge at ~9,000×*g* for 30 min (9,000 rpm in the JA-10 rotor and bottles).
23. Carefully decant off the supernatant. Place the bottles at an angle in a large ice bucket with the pellets in contact with the ice,

but not at the lowest point. Let remaining liquid drain from the walls to the lowest point of the bottle for a few minutes, then use a pipette to remove it. Discard the supernatant.

24. Resuspend the pellet in 20–40 mL of buffer DB by pipetting up and down with a powered pipette aid, minimizing air introduction. If pellets do not resuspend quickly, they will "soften" somewhat as they are in contact with the DB.
25. Cut and rinse lengths of 50 kDa cut-off dialysis membrane with ultrapure water. Enough dialysis tubing should be prepared to hold roughly twice the resuspended volume. For this dialysis tubing cut a total of 50 cm per 60 mL, split across at least two pieces. Transfer the resuspended pellets into the dialysis tubing, leaving at least 30 % of the length as slack, after affixing dialysis clips to the ends. The resuspended pellets are of high salt content and thus will increase in volume during dialysis owing to osmotic effects. Dialyze the pellets against 8 L of DB overnight (greater than 6 h) at 4 °C, stirring slowly. It is usually necessary to use two medium or large dialysis clips at either end of the tubing to give the suspension/tubing sufficient buoyancy to prevent it from hitting the stir bar.

3.2 Day 2: SOURCE 15Q Column

The second day begins with the resuspended and dialyzed pellets from **step 25** of Subheading 3.1. Typically, this day can be performed by one person. Clarifying and correcting the salt concentration in the dialysate typically takes about an hour. The SOURCE 15Q column takes 2–5 h to run, depending on the volume to be loaded and the flow rate that is used. SDS-PAGE analysis takes roughly an hour. Setting up the dialysis and cleaning the SOURCE 15Q column typically takes about an hour. All told the second day typically can be completed in less than 8 h.

1. Transfer the dialysate from **step 25** of Subheading 3.1 to centrifuge tubes and spin at ~7,000 × *g* (9,000 rpm in a JA-25.50 rotor) for 30 min.
2. Decant the supernatant into a beaker. Dilute the supernatant with 2 mM Tris–HCl, pH 8.0, until the conductivity is lower than QC. Cold QC buffer has a conductivity of ~1 mS/cm. Note the initial, final and reference conductivities.
3. Filter the conductivity corrected dialysate through a 0.45 μm filter (*see* **Note 12**).
4. Purify the filtered, conductivity corrected dialysate using SOURCE 15Q ion exchange chromatography (*see* **Note 13**). Equilibrate the SOURCE 15Q column in buffer QC. Inject the filtered dialysate onto the column at 5 mL/min, wash out unbound proteins using 2 column volumes of QC. Elute proteins in 14 mL fractions, including Arp2/3 complex, from the column using a linear buffer gradient of 100 % QC to 90 %

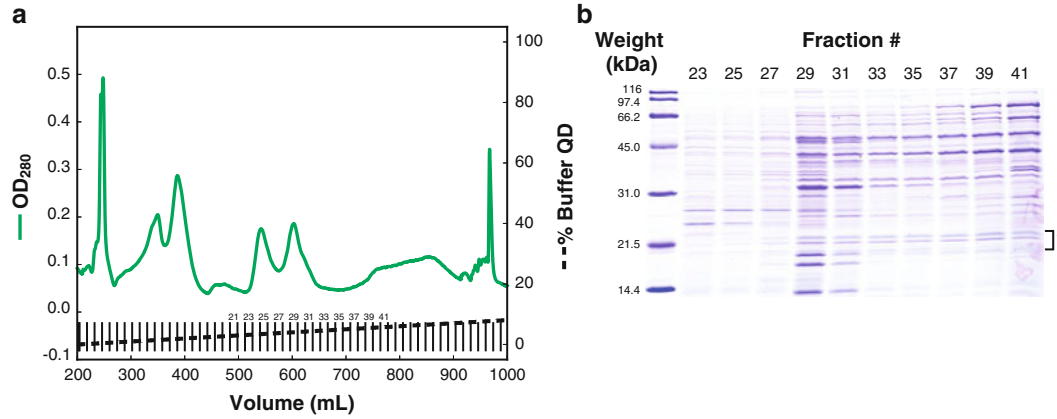

Fig. 1 Purification of bovine Arp2/3 complex using SOURCE 15Q ion exchange chromatography. (**a**) An example of the UV absorbance detected chromatogram for bovine Arp2/3 complex purification on a 50 mL SOURCE 15Q column. UV absorbance is shown with a *thick solid line*, fraction of QD (with buffer QC making up the remaining volume) is shown with a *dashed line*. Fractions collected are shown with *short vertical lines*. Relevant fraction numbers are shown. (**b**) SDS-PAGE analysis of relevant fractions was performed using a 15 % acrylamide gel, and stained using Coomassie Brilliant Blue dye. At this stage the complex is only marginally pure, and fraction assessment is accomplished by looking for ArpC3, ArpC4 and ArpC5, which run as a triplet between 19 and 23 kDa. This region of the gel is indicated with a *bracket* and an *asterisk*. Fraction numbers from the chromatogram are indicated at the *top* of the gel lanes, and molecular weights of standards are shown at the *left*. For this run fractions 28 through 35 were pooled and further purified (Color figure online)

QC/10 % QD developed over 20 column volumes (1 L of buffer volume).

5. Identify fractions to pool using SDS-PAGE (*see* **Note 14**). See example in Fig. 1.
6. Clean SOURCE 15Q column (*see* **Note 15**).
7. Place SOURCE 15Q pool into 50 kDa dialysis tubing, dialyze against 12 L of buffer SA overnight. Follow the protocol in **step 25** of Subheading 3.1, but allow less space for expansion as the osmotic differences will be lower in this case. Leaving 25 % of the tubing length as slack is sufficient.

3.3 Day 3: Mono S and Superdex 200 Columns

The third day begins with the dialyzed pool from **step 7** of Subheading 3.2, and typically requires only a single person to complete. Preparing and running the Mono S column typically takes 3–4 h. SDS-PAGE analysis takes about an hour, but may be performed while equilibrating the gel filtration column. Running the gel filtration column (once equilibrated) takes about 2 h. SDS-PAGE analysis takes about an hour, and is typically begun immediately after the primary peak elutes. Running the two columns can be completed in about 8 h, if the SDS-PAGE steps are performed when described. If fractions are pooled, concentrated, measured

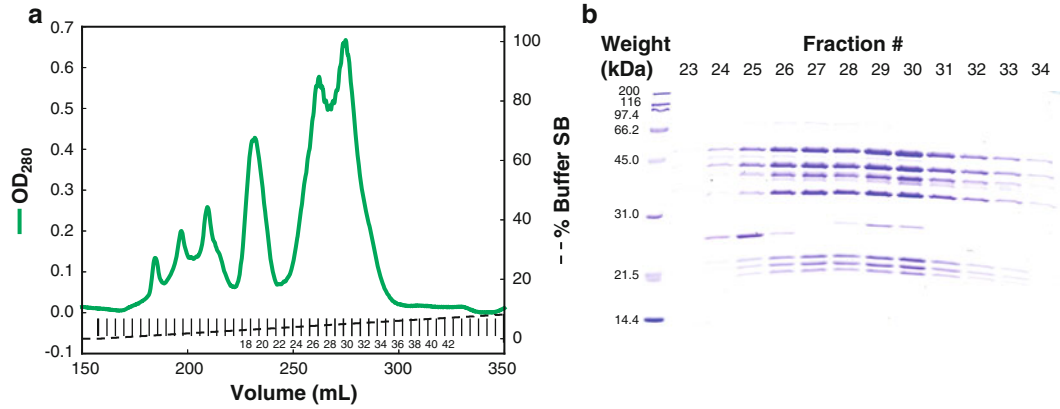

Fig. 2 Purification of bovine Arp2/3 complex using MonoS ion exchange chromatography. (**a**) An example of the UV absorbance detected chromatogram for bovine Arp2/3 complex purification on an 8 mL MonoS column. UV absorbance is shown with a *thick solid line*, fraction of SB (with buffer SA making up the remaining volume) is shown with a *dashed line*. Fractions collected are shown with *short vertical lines*. Relevant fraction numbers are shown. (**b**) SDS-PAGE analysis of relevant fractions was performed using a 15 % acrylamide gel, and stained using Coomassie Brilliant Blue dye. At this stage the complex is mostly pure, with contaminants at 26, 28 and 74 kDa. Fraction numbers from the chromatogram are indicated at the *top* of the gel lanes, and molecular weights of standards are shown at the *left*. For this run fractions 24 through 32 were pooled and further purified (Color figure online)

and frozen on the same day (this may be delayed until the next day), this adds an additional 2–3 h to day 3.

1. Collect the dialysate from **step 7** of Subheading 3.2. Filter through a 0.45 μm filter (*see* **Note 12**).
2. Measure the conductivity of the dialysate and dilute with 10 mM PIPES pH 6.8 until the conductivity is lower than buffer SA. Buffer SA has a conductivity of ~1 mS/cm. Note the initial, final and reference conductivity.
3. Purify Arp2/3 complex using MonoS cation exchange chromatography. Equilibrate the MonoS column with buffer SA. Inject onto the column at 2–4 mL/min. Wash unbound materials from the column with 3 column volumes of buffer SA. Elute proteins in 5 mL fractions, including the Arp2/3 complex, from the column with a linear buffer gradient from 100 % SA to 90 % SA/10 % SB, developed over 30 column volumes (240 mL of buffer volume).
4. Pool fractions containing Arp2/3 complex, as assessed by SDS PAGE (*see* Fig. 2 and **Note 16**).
5. Concentrate pooled fractions from **step 4** to roughly 11 mL using an AmiconUltra-15 30 kDa cut-off centrifugal concentrator. Spin at ~2,000 × *g* in a swinging bucket rotor (3,500 rpm in a Sorvall Legend with swinging bucket rotor). The concentrate should be mixed thoroughly and topped up after every

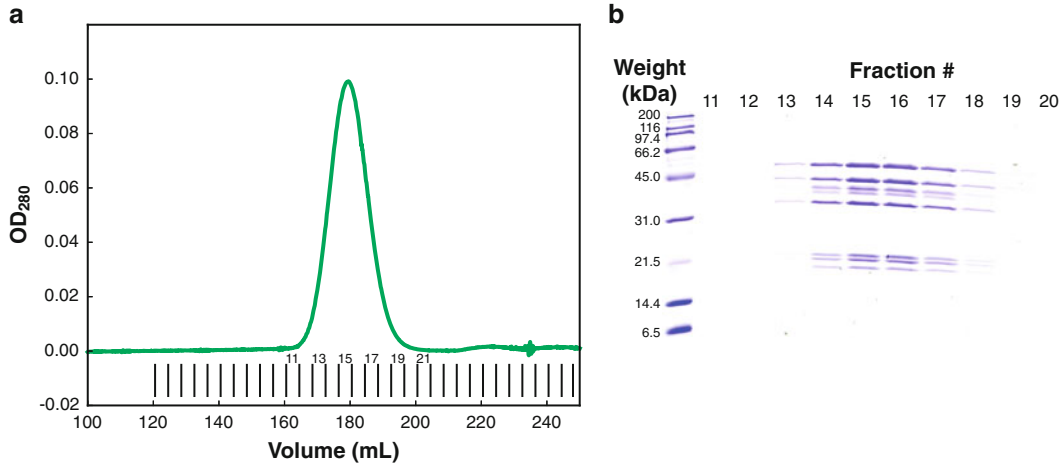

Fig. 3 Purification of bovine Arp2/3 complex using Superdex 200 gel filtration chromatography. (**a**) An example of the UV absorbance detected chromatogram for bovine Arp2/3 complex purification on a 320 mL Superdex 200 pg column. UV absorbance is shown with a *thick solid line*. Fractions collected are shown with *short vertical lines*. Relevant fraction numbers are shown. (**b**) SDS-PAGE analysis of relevant fractions was performed using a 15 % acrylamide gel, and stained using Coomassie Brilliant Blue dye. At this stage the complex is pure, with no contaminants observed. Multiple isoforms of ArpC1 are present, and appears as a multiplet. Fraction numbers from the chromatogram are indicated at the *top* of the gel lanes, and molecular weights of standards are shown at the *left*. Depending on intended use, Arp2/3 complex may be pooled (e.g., fractions 14–17) or kept separate (Color figure online)

3–5 min of centrifugation time. If any precipitate is observed, filter using a 0.22 μm syringe filter (not usually needed).

6. Purify Arp2/3 complex using Superdex 200 gel filtration chromatography. Equilibrate a 320 mL Superdex 200 pg column with at least 300 mL KMEId (*see* **Note 17**). Inject the concentrated Arp2/3 complex pool onto the column at 1 mL/min. Elute the Arp2/3 complex by flowing an additional column volume of buffer over the column, collecting 4–5 mL fractions beginning after 0.3 column volumes of buffer. Arp2/3 complex typically elutes as a single peak, with a maxima occurring when approximately 0.5–0.6 column volumes of buffer have been applied to the column.
7. Identify fractions to keep by SDS-PAGE analysis (*see* Fig. 3). Pool or keep fractions separate according to subsequent needs.
8. Quantify Arp2/3 complex concentration using ultraviolet absorption (*see* **Note 18**). If necessary, the complex may be concentrated as in **step 5**.
9. Either store fractions away from light at 4 °C for less than 4 weeks, or freeze the fractions (*see* **Note 19**). Beyond SDS-PAGE and gel filtration assessment of purity, typical quality control steps are to assay activity using pyrene actin polymerization assays [19]. 10 nM of the bovine Arp2/3 complex

should not show observable activity in the absence of nucleation promotion factor, and should trigger rapid actin nucleation in the presence of 250 nM monomeric N-WASP VCA.

4 Notes

1. Bovine thymus can be obtained in a few ways. Traditionally, they are obtained from a local slaughterhouse. This can work, but the relationship between the slaughterhouse and the laboratory is critical. Here, calf thymuses of approximately 200–300 g are necessary and they must be cooled promptly after collection. Larger thymus or those that have been allowed to sit at room temperature for an hour or more will yield Arp2/3 complex of poor purity and activity. Due to the variability in slaughterhouse events, and a lack of universal slaughterhouse availability, we recommend obtaining frozen calf thymus from Pel-Freez.

   This has improved our reliability substantially, with one exception. One lot arrived with particularly small thymuses, which were of somewhat different color. At the first centrifugation step it was noted that there was a general absence of the "fat-pad" normally observed at the top of the 1 L centrifugation bottles. This has correlated with low activity. The problem persisted through the entire lot of ten thymuses and cleared up once a new lot was obtained. If poor results are obtained and a fat pad was not observed at the first centrifugation step, consider obtaining a new lot of thymus.
2. PMSF is toxic. Care should be used when preparing this stock. In particular, use of gloves, lab coats, protective eye wear and dust masks will reduce inhalation and cross contamination. One effective strategy is to purchase <100 g bottles, and prepare the entire bottle at one time trusting the manufacturer's provided weight. The stock should be stored as 1 mL aliquots in 1.5 mL microfuge tubes at −20 °C. Once the stocks have been frozen PMSF will crystallize out of solution. Warming in a room temperature beaker of water for a few minutes is usually sufficient to bring the PMSF back into solution. Agitation by inversion may be needed. When adding PMSF to a buffer, avoid splashing the stock and buffers onto gloves, skin and eyes.
3. In the case of the PIPES buffer, you must use the free acid (Sigma-Aldrich #P6757), not the disodium salt. This is necessary to reduce overall ionic strength in later steps.
4. Recommended buffer preparation schedule and volumes for the provided protocol scale. On the first day you will need 1 L of EB, 1 L QA and 8 L of DB. The DB buffer can be prepared shortly before use, but make sure that you have a sufficient

quantity of cold water at hand. We accomplish this by keeping 12 L carboys of ultrapure water in the cold room for several hours. On the second day, you will need 1.5 L QC, 0.5 L QD, and 12 L of SA. As on day 1, ensure that you have sufficient cold water prepared to make 12 L of SA at the end of the day. On the third day you will need 1 L of SA, 0.5 L SB, and 1 L KMEId.

5. If you are using thymus stored at –80 °C, keep them as cold as possible until homogenizing. Since the thymuses are homogenized in a moderate excess of buffer, their heat capacity matters. While keeping the homogenate as cold as possible is desirable in general, when homogenizing thymus at near –80 °C with cold buffer, the entire homogenate can freeze solid and damage the blender. If you are using fresh (ice cold) thymus, cold buffer should be used.
6. Q Cleaning buffer is 6 M guanidine hydrochloride acidified with 200 mM acetic acid. This is generally useful for cleaning anion exchange columns. Technical or 98 % pure guanidine hydrochloride can be used for this buffer (analytic quality is prohibitively expensive). If some particulate matter remains insoluble, it can be removed by centrifugation at low speed (e.g., 3,000 × *g* for 20 min) prior to 0.22 μm filtration.
7. We use a Sorvall RC 3C plus centrifuge equipped with an H6000A rotor (swinging bucket rotor capable of holding six 1 L bottles), a Beckman Avanti J-26XPI centrifuge equipped with a JA-10 rotor and a Beckman Optima L-90X ultracentrifuge equipped with a Type 45 Ti rotor. The first two rotors are used with polypropylene copolymer bottles with threaded closures, and the Type 45 Ti rotor uses 70 mL thick wall polycarbonate bottles with two part aluminum closures. Check centrifuge availability and temperature. For the ultracentrifugation step, allow sufficient time for the centrifuge to cool to 4 °C. For most Beckman ultracentrifuges, the vacuum must be pulled for cooling to occur.
8. Here is a specific setup useable for breaking up and homogenizing calf thymus. A 38 quart, heavy-duty, stainless steel stock pot is placed against a cabinet on the floor, with eight layers of paper towels to protect the cabinet. A lead brick is wrapped with five to eight layers of clean heavy-duty aluminum foil. The “lead brick” is a piece of lead the size and shape of a construction brick. The purpose of the brick is that the mass is sufficient to shatter the thymus when hitting it.

   A frozen (–80 °C) thymus is placed, still in its packaging from Pel-Freez, into the pot. The thymus is then smashed into pieces with the lead brick. With a little practice one can break up a thymus in 3–5 min, which minimizes thawing. A good method is to first smash the thymus into three to six pieces, push them to

one side and remove the plastic bag. Then individual pieces can be smashed into smaller pieces that are less than 2 cm in their longest dimension. Once a large piece is completely broken down, use the brick to push the small pieces to one side. After one thymus is broken into pieces, it gets homogenized, and the homogenate goes on ice. Then the process is repeated for additional thymuses and the homogenates are combined.

9. Ideally, the blender jar will be sized such that one thymus plus buffer will fill it 40–80 % full. We use a 1 L blender jar to homogenize one thymus. A balance needs to be struck between blending to complete homogeneity and heating of the homogenate by the blender. A good working method is to blend in pulses of 5–10 s, counting the number of pulses. Initially, larger chunks can be heard hitting the bottom of the blender when a pulse is stopped. When this can no longer be heard, note how many pulses were used to reach this point, and continue with the same number of additional pulses. Total blending time will be 3–5 min. Once this point is reached, allow the blender to sit for ~20 s prior to opening to allow mists to condense and settle. Transfer to prechilled 1 L centrifuge bottles, rinse blender with cold EB and check for any large chunks remaining. These can be added to the next homogenization run or discarded after the final run.
10. Performance of the Q Sepharose column is substantially degraded during use. It is common for observable fat to accumulate at the top of the column during the run. This can be largely removed by cleaning the column on the same day that it is used. Cleaning is accomplished by flowing 3 column volumes (450 mL) of 5 M NaCl over the column, followed by 3 column volumes (450 mL) of 6 M guanidine hydrochloride/200 mM acetic acid and then 5 column volumes (750 mL) of water with 0.5 mM sodium azide. The column is stored in the latter buffer. Even with this cleaning procedure, we reserve this column for Arp2/3 complex purification only, and completely repack it with fresh media every third preparation.
11. A common mistake during the ammonium sulfate cut is to add the solid ammonium sulfate too quickly or all at once. This results in locally high concentrations of ammonium sulfate, which can cause undesired proteins to precipitate. A few precautions can minimize this problem.

    First, inspect the ammonium sulfate as it is weighed out. Often there are clumps of crystals present, some of which may be larger than 5 mm. If this is a problem, break them up by mashing them with a mortar and pestle. The goal is not to smash the crystals into powder (which does help, but not enough to warrant routinely doing) but just to break up any large crystals present.

Second, the addition of ammonium sulfate should occur over 20–25 min for the amounts described here (time can be scaled down somewhat for smaller volumes). The stirred solution should be checked periodically while the solid is added. Look at the bottom of the beaker, make sure solid ammonium sulfate is not accumulating. If it does, the ammonium sulfate is being added too quickly. Wait for a few minutes for the accumulated solid to disperse and then continue to add, but more slowly. A practical way to add the solid is to put half to one third of it in a plastic weigh boat, and to tap it with a spatula. By varying the frequency of tapping a reasonably controllable and uniform addition rate may be found.

12. For historical reasons we use a Whatman ZapCap-S 0.45 μm (VWR # 28152-182) with one Whatman #30 glass membrane on the top, pouring the dialysate through a portion of the membrane only. The supernatant typically still has some particulate remaining after centrifugation, and the addition of a glass prefilter speeds filtration.
13. Choice of SOURCE 15Q hardware and column size. The recommended linear flow rates for SOURCE 15 resins (>50 mL/min for a 26 mm wide column) produces column pressures well in excess of the tolerance of the XK26 hardware. Thus, flow rates are dictated by the column pressure tolerance, and flow rates may be a low as 5 mL/min. If the user scales down the preparation to one ~150 g thymus, then performance may be improved by packing 20 mL of SOURCE 15Q into HR16/10 hardware (which is designed for operation at higher pressures). Reduced flow rates (<8 mL/min) are still a good idea in this context, as our experience with SOURCE 15Q resins indicates that increased flow rate decreases resolution.
14. Pooling fractions at the SOURCE 15Q stage. Arp2/3 complex elutes roughly in the middle of the 0–10 % buffer QD gradient. At this stage, however, the mixture is still complex enough that the appearance of a well-defined peak cannot be reliably used to identify the fractions containing Arp2/3 complex. Further, each preparation is a little different, and the exact contaminants vary somewhat. Fractions containing Arp2/3 complex to pool are identified using SDS-PAGE analysis. 15 % acrylamide gels are run until the bromophenol blue loading dye runs off the gel. The gels are stained using Coomassie Brilliant Blue. Fractions to pool are identified by the presence of the ArpC3/ArpC4/ArpC5 triplet near the bottom of the gel (*see* Fig. 1). Typically, two 15-lane gels are run, analyzing every second 14 mL fraction through the middle of the gradient.
15. The SOURCE 15Q column should be cleaned the same day it is used. It is cleaned by passing 3 column volumes (150 mL) of 5 M NaCl over the column, followed by 3 column volumes

(150 mL) of 6 M guanidine hydrochloride/200 mM acetic acid. Finally, 5 column volumes (250 mL) of 0.5 mM sodium azide are passed over the column and the column is stored in the latter buffer. The entire SOURCE 15Q column is repacked with fresh resin after four Arp2/3 complex preparations, and the column is reserved for only Arp2/3 complex preparation. As SOURCE 15Q resin is quite expensive when purchased at the 10 mL lab pack scale, we reduce costs by purchasing Bioprocess scale packages (200 mL and larger).

16. Arp2/3 complex elutes from the MonoS column as two peaks, both of which are active [31]. All Arp2/3 complex containing fractions are customarily pooled at this point. Arp2/3 complex elutes between 3 and 6 % buffer SB. There should be pronounced peaks for the complex, guiding choice of fractions to analyze by SDS-PAGE. *See* Fig. 2 for an example of the chromatogram and gel. Fractions are chosen to contain Arp2/3 complex and to reject contaminants. At this point the complex should be pure enough that Arp3, Arp2, ArpC2 and a multiplet for ArpC1/ArpC1B can be easily seen. Contaminants at 26, 28 and 74 kDa are expected and tolerable, they are removed during gel filtration.
17. Typically we use the KMEId for the final gel filtration step, but this buffer is largely chosen for compatibility with our standard pyrene actin polymerization assay conditions. This buffer may be varied subtly at the user's discretion. Changes that we have not seen to affect the purification: substitution of 5 or 10 mM HEPES pH 7.0 for the imidazole, using pH 7.5 instead of pH 7.0, inclusion of 100 μM ATP, omission of the DTT. When experiments require substantially different buffers from this, we typically purify the complex under the standard conditions, then concentrate the complex and use a further gel filtration step to exchange into the desired buffer.
18. Our method of quantifying Arp2/3 complex is based on UV absorption. An extinction coefficient at 280 nm of 233,320 M^{-1} cm^{-1} was estimated from the number of tryptophan and tyrosine residues (24 and 68, respectively) in a complex composed of the reference sequences for Arp3, Arp2, ArpC1B, ArpC2, ArpC3, ArpC4 and ArpC5 (accession numbers: NP_776651.1, AAI51357.1, NP_001014844.1, NP_001029885.1, NP_001029443.1, NP_001069631.1, and NP_001030524.1). As the complex may bring an ATP or ADP nucleotide along with it during purification, we routinely measure absorption at 290 nm, and correct for any scatter by using the absorption at 314 nm. By measuring the relative absorbance of a sample judged to be devoid of nucleotide at 280 and 290 nm, we found the A_{290}/A_{280} ratio to be 0.6, and thus routinely measure the concentration using an extinction coefficient at 290 nm of 140,000 M^{-1} cm^{-1}.

19. Directly freezing small aliquots of Arp2/3 complex in KMEId in liquid nitrogen results in a slight degree of aggregation, and measurable loss of activity. This can be corrected for by including ATP and a cryoprotectant in the freezing buffer. For routine assay at 10 nM of Arp2/3 complex in pyrene actin polymerization assays, we now supplement 600 nM Arp2/3 complex in KMEId with one half of a part freezing buffer (i.e., 5 mL of buffer FB are added to 10 mL of Arp2/3 complex solution). While glycerol can also be used, our typical freezing buffer uses sucrose as a cryoprotectant (see recipe for buffer FB). The concentration of Arp2/3 complex should be measured prior to dilution, and some care should be used to carefully measure and dispense all of the viscous, sucrose-containing, buffer FB solution. At that point the concentration is inferred from the know dilution factor. Small volumes (e.g., 80 μL) can then be placed into small tubes (200 μL thin wall PCR tubes are convenient for this) and snap frozen in liquid nitrogen. Aliquots can then be stored at −80 °C until needed; complex maintains activity for at least 1 year under these conditions. Aliquots should be used soon after thawing.

    We have also had good results storing Arp2/3 complex at 4 °C, with DTT present for up to 4 weeks. More prolonged storage typically results in loss of activity, perhaps due to loss of phosphorylation at critical residues [48].

    For experiments that require a buffer incompatible with freezing, we routinely concentrate Arp2/3 complex to >5 mg/mL, quantify the concentration as in **Note 18**, supplement with freezing buffer as above and freeze in ~500 μL aliquots. These can be thawed, spun briefly and passed over a Superdex200 10/300 analytic gel filtration column into a desired buffer and quantified by UV absorption.

Acknowledgments

We thank Dr. Ayman Ismail for assembling early versions of this protocol.

References

1. Pollard TD, Cooper JA (2009) Actin, a central player in cell shape and movement. Science 326(5957):1208–1212
2. Pollard TD, Borisy GG (2003) Cellular motility driven by assembly and disassembly of actin filaments. Cell 112(4):453–465
3. Mooren OL, Galletta BJ, Cooper JA (2012) Roles for actin assembly in endocytosis. Annu Rev Biochem 81:661–686
4. Weinberg J, Drubin DG (2012) Clathrin-mediated endocytosis in budding yeast. Trends Cell Biol 22(1):1–13
5. Pollard TD (2010) Mechanics of cytokinesis in eukaryotes. Curr Opin Cell Biol 22(1):50–56
6. Haglund CM, Welch MD (2011) Pathogens and polymers: microbe-host interactions illuminate the cytoskeleton. J Cell Biol 195(1):7–17

7. Munter S, Way M, Frischknecht F (2006) Signaling during pathogen infection. Sci STKE 2006(335):re5
8. Pollard TD (2007) Regulation of actin filament assembly by Arp2/3 complex and formins. Annu Rev Biophys Biomol Struct 36:451–477
9. Goode BL, Rodal AA, Barnes G, Drubin DG (2001) Activation of the Arp2/3 complex by the actin filament binding protein Abp1p. J Cell Biol 153(3):627–634
10. Machesky LM, Atkinson SJ, Ampe C, Vandekerckhove J, Pollard TD (1994) Purification of a cortical complex containing two unconventional actins from Acanthamoeba by affinity chromatography on profilin-agarose. J Cell Biol 127(1):107–115
11. Mullins RD, Stafford WF, Pollard TD (1997) Structure, subunit topology, and actin-binding activity of the Arp2/3 complex from Acanthamoeba. J Cell Biol 136(2):331–343
12. Amann KJ, Pollard TD (2001) The Arp2/3 complex nucleates actin filament branches from the sides of pre-existing filaments. Nat Cell Biol 3(3):306–310
13. Blanchoin L, Amann KJ, Higgs HN, Marchand JB, Kaiser DA, Pollard TD (2000) Direct observation of dendritic actin filament networks nucleated by Arp2/3 complex and WASP/Scar proteins. Nature 404(6781):1007–1011
14. Mullins RD, Heuser JA, Pollard TD (1998) The interaction of Arp2/3 complex with actin: nucleation, high affinity pointed end capping, and formation of branching networks of filaments. Proc Natl Acad Sci U S A 95(11): 6181–6186
15. Rouiller I, Xu XP, Amann KJ, Egile C, Nickell S, Nicastro D, Li R, Pollard TD, Volkmann N, Hanein D (2008) The structural basis of actin filament branching by the Arp2/3 complex. J Cell Biol 180(5):887–895
16. Kelleher JF, Atkinson SJ, Pollard TD (1995) Sequences, structural models, and cellular localization of the actin-related proteins Arp2 and Arp3 from Acanthamoeba. J Cell Biol 131(2):385–397
17. Galletta BJ, Mooren OL, Cooper JA (2010) Actin dynamics and endocytosis in yeast and mammals. Curr Opin Biotechnol 21(5):604–610
18. Welch MD, Iwamatsu A, Mitchison TJ (1997) Actin polymerization is induced by Arp2/3 protein complex at the surface of Listeria monocytogenes. Nature 385(6613):265–269
19. Doolittle LK, Rosen MK, Padrick SB (2013) Measurement and analysis of in vitro actin polymerization. Methods Mol Biol 1046: 273–294
20. Cooper JA, Walker SB, Pollard TD (1983) Pyrene actin: documentation of the validity of a sensitive assay for actin polymerization. J Muscle Res Cell Motil 4(2):253–262
21. Kouyama T, Mihashi K (1981) Fluorimetry study of N-(1-pyrenyl)iodoacetamide-labelled F-actin. Local structural change of actin protomer both on polymerization and on binding of heavy meromyosin. Eur J Biochem 114(1):33–38
22. Machesky LM, Mullins RD, Higgs HN, Kaiser DA, Blanchoin L, May RC, Hall ME, Pollard TD (1999) Scar, a WASp-related protein, activates nucleation of actin filaments by the Arp2/3 complex. Proc Natl Acad Sci U S A 96(7):3739–3744
23. Welch MD, Rosenblatt J, Skoble J, Portnoy DA, Mitchison TJ (1998) Interaction of human Arp2/3 complex and the Listeria monocytogenes ActA protein in actin filament nucleation. Science 281(5373):105–108
24. Hansen SD, Zuchero JB, Mullins RD (2013) Cytoplasmic Actin: Purification and Single Molecule Assembly Assays. Methods Mol Biol 1046:145–170
25. Loisel TP, Boujemaa R, Pantaloni D, Carlier MF (1999) Reconstitution of actin-based motility of Listeria and Shigella using pure proteins. Nature 401(6753):613–616
26. Bernheim-Groswasser A, Wiesner S, Golsteyn RM, Carlier MF, Sykes C (2002) The dynamics of actin-based motility depend on surface parameters. Nature 417(6886):308–311
27. Achard V, Martiel JL, Michelot A, Guerin C, Reymann AC, Blanchoin L, Boujemaa-Paterski R (2010) A "primer"-based mechanism underlies branched actin filament network formation and motility. Curr Biol 20(5):423–428
28. Akin O, Mullins RD (2008) Capping protein increases the rate of actin-based motility by promoting filament nucleation by the Arp2/3 complex. Cell 133(5):841–851
29. Co C, Wong DT, Gierke S, Chang V, Taunton J (2007) Mechanism of actin network attachment to moving membranes: barbed end capture by N-WASP WH2 domains. Cell 128(5):901–913
30. Dayel MJ, Akin O, Landeryou M, Risca V, Mogilner A, Mullins RD (2009) In silico reconstitution of actin-based symmetry breaking and motility. PLoS Biol 7(9):e1000201
31. Higgs HN, Blanchoin L, Pollard TD (1999) Influence of the C terminus of Wiskott-Aldrich syndrome protein (WASp) and the Arp2/3 complex on actin polymerization. Biochemistry 38(46):15212–15222
32. Insall R, Muller-Taubenberger A, Machesky L, Kohler J, Simmeth E, Atkinson SJ, Weber I,

Gerisch G (2001) Dynamics of the Dictyostelium Arp2/3 complex in endocytosis, cytokinesis, and chemotaxis. Cell Motil Cytoskeleton 50(3):115–128

33. Welch MD, Mitchison TJ (1998) Purification and assay of the platelet Arp2/3 complex. Methods Enzymol 298:52–61
34. Ma L, Rohatgi R, Kirschner MW (1998) The Arp2/3 complex mediates actin polymerization induced by the small GTP-binding protein Cdc42. Proc Natl Acad Sci U S A 95(26): 15362–15367
35. Beltzner CC, Pollard TD (2008) Pathway of actin filament branch formation by Arp2/3 complex. J Biol Chem 283(11):7135–7144
36. Egile C, Loisel TP, Laurent V, Li R, Pantaloni D, Sansonetti PJ, Carlier MF (1999) Activation of the CDC42 effector N-WASP by the Shigella flexneri IcsA protein promotes actin nucleation by Arp2/3 complex and bacterial actin-based motility. J Cell Biol 146(6):1319–1332
37. Lechler T, Jonsdottir GA, Klee SK, Pellman D, Li R (2001) A two-tiered mechanism by which Cdc42 controls the localization and activation of an Arp2/3-activating motor complex in yeast. J Cell Biol 155(2):261–270
38. Zalevsky J, Lempert L, Kranitz H, Mullins RD (2001) Different WASP family proteins stimulate different Arp2/3 complex-dependent actin-nucleating activities. Curr Biol 11(24):1903–1913
39. Doolittle LK, Rosen MK, Padrick SB (2013) Purification of Arp2/3 complex from Saccharomyces cerevisiae. Methods Mol Biol 1046:251–272
40. Gournier H, Goley ED, Niederstrasser H, Trinh T, Welch MD (2001) Reconstitution of human Arp2/3 complex reveals critical roles of individual subunits in complex structure and activity. Mol Cell 8(5):1041–1052
41. Balcer HI, Daugherty-Clarke K, Goode BL (2010) The p40/ARPC1 subunit of Arp2/3 complex performs multiple essential roles in WASp-regulated actin nucleation. J Biol Chem 285(11):8481–8491
42. Daugherty KM, Goode BL (2008) Functional surfaces on the p35/ARPC2 subunit of Arp2/3 complex required for cell growth, actin nucleation, and endocytosis. J Biol Chem 283(24):16950–16959
43. Martin AC, Xu XP, Rouiller I, Kaksonen M, Sun Y, Belmont L, Volkmann N, Hanein D, Welch M, Drubin DG (2005) Effects of Arp2 and Arp3 nucleotide-binding pocket mutations on Arp2/3 complex function. J Cell Biol 168(2):315–328
44. Pan F, Egile C, Lipkin T, Li R (2004) ARPC1/Arc40 mediates the interaction of the actin-related protein 2 and 3 complex with Wiskott-Aldrich syndrome protein family activators. J Biol Chem 279(52):54629–54636
45. Rodal AA, Sokolova O, Robins DB, Daugherty KM, Hippenmeyer S, Riezman H, Grigorieff N, Goode BL (2005) Conformational changes in the Arp2/3 complex leading to actin nucleation. Nat Struct Mol Biol 12(1):26–31
46. Winter DC, Choe EY, Li R (1999) Genetic dissection of the budding yeast Arp2/3 complex: a comparison of the in vivo and structural roles of individual subunits. Proc Natl Acad Sci U S A 96(13):7288–7293
47. Padrick SB, Doolittle LK, Brautigam CA, King DS, Rosen MK (2011) Arp2/3 complex is bound and activated by two WASP proteins. Proc Natl Acad Sci USA 108(33): E472–E479
48. LeClaire LL III, Baumgartner M, Iwasa JH, Mullins RD, Barber DL (2008) Phosphorylation of the Arp2/3 complex is necessary to nucleate actin filaments. J Cell Biol 182(4):647–654

Chapter 15

Purification of Arp2/3 Complex from *Saccharomyces cerevisiae*

Lynda K. Doolittle, Michael K. Rosen, and Shae B. Padrick

Abstract

Much of the cellular control over actin dynamics comes through regulation of actin filament initiation. At the molecular level, this is accomplished through a collection of cellular protein machines, called actin nucleation factors, which position actin monomers to initiate a new actin filament. The Arp2/3 complex is a principal actin nucleation factor used throughout the eukaryotic family tree. The budding yeast *Saccharomyces cerevisiae* has proven to be not only an excellent genetic platform for the study of the Arp2/3 complex, but also an excellent source for the purification of endogenous Arp2/3 complex. Here we describe a protocol for the preparation of endogenous Arp2/3 complex from wild type *Saccharomyces cerevisiae*. This protocol produces material suitable for biochemical study and yields milligram quantities of purified Arp2/3 complex.

Key words Actin nucleation factor, Arp2/3 complex, Biochemical purification, Endogenous source, *Saccharomyces cerevisiae*, Detailed protocol

1 Introduction

Plant, animal and fungal cells all make use of dynamic rearrangements of actin filaments to move and reshape themselves [1]. In yeasts such as *Saccharomyces cerevisiae* and *Schizosaccharomyces pombe*, these rearrangements have been intensely studied in both vesicle trafficking [2, 3] and in cell division [4]. Force generation needed during yeast clathrin dependent endocytosis requires precise control of the initiation of actin filaments by the Arp2/3 complex [2, 3].

The Arp2/3 complex is composed of one copy each of seven polypeptides [5–7], all of which are needed for function [8, 9]. Two of these polypeptides are the actin related proteins Arp2 and Arp3, from which the complex derives its name. There are five additional subunits, with no homology to actin, known as ArpC1, ArpC2, ArpC3, ArpC4, and ArpC5. The complex is basally inhibited, but can be activated by a collection of ligands known as nucleation promoting factors [7, 10]. Nucleation promoting factors are

Amanda S. Coutts (ed.), *Adhesion Protein Protocols*, Methods in Molecular Biology, vol. 1046,
DOI 10.1007/978-1-62703-538-5_15,

able to integrate a broad range of cellular signals to activate Arp2/3 complex at specific places and times [11]. These ligands must both trigger an activating conformational change in the complex [12–14], and deliver the actin monomers that become the first subunits in the nucleated filament [15–17]. The activity of the *Saccharomyces cerevisiae* Arp2/3 complex may be assayed in vitro through the increase in fluorescence of pyrene labeled actin upon polymerization [18] or through the microscopic observation of fluorescent actin filaments assembling on beads [19].

Given the complexity of this multi-protein complex, it is most typically purified from endogenous sources. In addition to purification schemes that use only standard chromatography [20–25], endogenous Arp2/3 complex can be purified through the use of an affinity column with an immobilized ligand. Immobilized ligand columns were used to originally identify the complex [5]. More recently, the use of affinity beads bearing the VCA domain of the nucleation promotion factor N-WASP has proven of broad utility. This method was first described for the purification of Arp2/3 complex from bovine brain [26], but the general strategy has since been adapted to the purification of Arp2/3 complex from *Saccharomyces cerevisiae* [27], from *Acanthamoeba castellanii* [28], and from *Schizosaccharomyces pombe* [29].

We describe here our version of a protocol to purify Arp2/3 complex from commercially available baker's yeast (*Saccharomyces cerevisiae*). The described protocol is derived from published work [27], but has several added purification steps that improve the final purity of the complex when isolated from commercial baker's yeast. We describe the Arp2/3 complex purification at a scale where milligram quantities may be prepared. We hope that others may use this protocol to purify Arp2/3 complex from *Saccharomyces cerevisiae*, and as a template to develop new protocols for the purification of the complex from additional sources. The purification protocol typically requires 4 days of work, after completion of the two additional protocols. We recommend that two people be involved during the first 2 days of the purification, and a single person complete the third and fourth days of work.

2 Materials

All buffer and salt stocks are prepared using ultrapure water (>18 MΩ, using Millipore brand Milli-Q water purification system). Except where noted, all solutions are filtered through a 0.22 μm cellulose acetate membrane. Working buffers are prepared by dilution of buffer stocks into prechilled ultrapure water. Where specific sources are recommended, the manufacturer and part numbers are indicated.

2.1 Stock Materials and Solutions

1. Baker's yeast (*Saccharomyces cerevisiae*) (*see* **Note 1**).
2. Leupeptin hydrochloride (Bachem #N-1000.0100): 1 mg/mL stock, filtered and stored at −20 °C in 250 μL aliquots.

3. Antipain dihydrochloride (Sigma-Aldrich #A6191): 1 mg/mL stock, filtered and stored at –20 °C in 250 µL aliquots.
4. Phenylmethanesulfonyl fluoride (PMSF; Sigma-Aldrich #P7626): 100 mM stock in isopropanol, filtered and stored in 1 mL aliquots at –20 °C until needed (*see* **Note 2**).
5. Dithiothreitol (DTT): 1 mM, filtered and stored at –20 °C in 1 mL aliquots. When thawing, place tube in cool water until solution is liquid then transfer to ice until needed. Once added to buffers, assume DTT is no longer functional after 48 h when stored at 4 °C.
6. Adenosine 5′ triphosphate disodium salt (ATP; Sigma-Aldrich #A7699): 100 mM stock in 100 mM Tris–HCl pH 8.0, and titrated to pH 7.4–7.5 with sodium hydroxide. The solution is filtered and stored at –20 °C in 1 mL aliquots.
7. 1 M HEPES pH 7.5 and 1 M HEPES pH 7.0: Prepared from HEPES acid, and titrated with sodium hydroxide to pH 7.5 or pH 7.0 at room temperature.
8. 0.5 M EGTA: Prepared using ethylene glycol tetraacetic acid powder and titrated to pH 8.0 with sodium hydroxide. Initially, EGTA is insoluble, but comes into solution as the pH is adjusted.
9. 1 M $MgCl_2$.
10. 2 M KCl.
11. 5 M NaCl.
12. 1 M Tris–HCl pH 8.0: Prepared using Tris–base, and titrated to pH 8.0 at room temperature with concentrated hydrochloric acid.
13. 0.5 M EDTA: Prepared using ethylenediaminetetraacetic acid powder and titrated to pH 8.0 with sodium hydroxide. Like EGTA, EDTA is initially insoluble, but comes into solution as the pH is adjusted to 8.0.
14. 1 M Imidazole pH 7.0: Titrated with hydrochloric acid to pH 7.0 at room temperature.
15. Isopropyl β-D-1-thiogalactopyranoside (IPTG) stock solution: 1 M stock, filtered and stored at –20 °C in 1 mL aliquots.
16. Construct for the expression of GST N-WASP VCA in *E. coli* (*see* **Note 3**).
17. Chemically competent BL21(DE3) $T1^R$ cells.
18. Ampicillin stock: 100 mg/mL, filtered and stored at –20 °C in 1 mL aliquots.
19. LB agar plates supplemented with 100 µg/mL of ampicillin.
20. Luria (LB) broth.
21. Ammonium sulfate.

2.2 Working Buffers

1. Buffer IBS: 150 mM NaCl, 10 mM imidazole pH 7.0.
2. UB: 50 mM HEPES pH 7.5, 100 mM KCl, 1 mM EGTA, 3 mM $MgCl_2$, 1 mM DTT.
3. UBpi: UB with 2 μg/mL antipain, 20 μg/mL leupeptin, and 1 mM PMSF. Add antipain and leupeptin directly to the buffer, add PMSF once buffer is added to cells, but prior to resuspending the cells.
4. Buffer QA1: 20 mM Tris–HCl pH 8, 2 mM EDTA, 1 mM DTT.
5. Buffer QB1: 20 mM Tris–HCl pH 8, 2 mM EDTA, 1 mM DTT, 1 M NaCl.
6. Buffer QLB: 20 mM Tris–HCl pH 8, 2 mM EDTA, 1 mM DTT, 70 mM NaCl.
7. Buffer GSH–WB1: 20 mM HEPES pH 7, 2 mM EDTA, 1 mM DTT, 100 mM NaCl.
8. Buffer GSH-WB2: 20 mM HEPES pH 7, 2 mM EDTA, 1 mM DTT, 700 mM NaCl.
9. Buffer A: 20 mM HEPES pH 7.5, 25 mM KCl, 1 mM $MgCl_2$, 1 mM DTT, 0.5 mM EGTA, 100 μM ATP.
10. Buffer B: 20 mM HEPES pH 7.5, 200 mM KCl, 1 mM $MgCl_2$, 1 mM DTT, 0.5 mM EGTA, 100 μM ATP.
11. Buffer C: 20 mM HEPES pH 7.5, 200 mM $MgCl_2$, 25 mM KCl, 1 mM DTT, 0.5 mM EGTA, 100 μM ATP.
12. Buffer QC: 20 mM Tris–HCl pH 8, 1 mM DTT, 10 mM EGTA, 2 mM $MgCl_2$.
13. Buffer QD: 20 mM Tris–HCl pH 8, 1 mM DTT, 10 mM EGTA, 2 mM $MgCl_2$, 1 M NaCl.
14. Buffer KMEHd-A: 100 mM KCl, 10 mM HEPES pH 7.5, 1 mM $MgCl_2$ 1 mM EGTA, 0.5 mM DTT, 100 μM ATP.
15. Buffer F: 100 mM KCl, 10 mM HEPES pH 7.5, 1 mM $MgCl_2$, 1 mM EGTA, 0.5 mM DTT, 100 μM ATP and 60 % sucrose. This is prepared by adding appropriate volumes of salt stocks for 10 mL of buffer to 6 g of dry sucrose, and adding water to ~9 mL. The solution is mixed until most of the sucrose has come into solution, and the volume is corrected to 10 mL. The solution is then allowed to come completely into solution. At that point it is passed through a 0.22 μm PES filter. Prior to adding to the protein solution it is chilled on ice for ~10 min. This is enough time to reduce the temperature, but will not result in sucrose crystallizing out of solution. Use buffer F the same day that it is prepared.

2.3 Chromatography Columns

Recommended flow rates and operating pressures are typical for a column in good condition.

1. DEAE Sepharose FF: 40 mL of DEAE Sepharose FF (GE #17-0709-01) is packed into a 26 mm wide medium pressure column such as an XK26/20 (GE #28-9889-48). The maximum flow rate and pressure for this column are 26.5 mL/min and 0.5 MPa, respectively. We run this column at a flow rate of 8–15 mL/min at less than 0.5 MPa.
2. GSH Sepharose column: Bulk Glutathione Sepharose 4B (GE #17-0756-05) is either handled as a batch suspension, or drained through a 2.5 cm low-pressure column (e.g., Bio-Rad Econo-Column #737-2512). To achieve reasonable flow rates, the column has a 2-position stopcock and approximately 8 cm of 1.6 mm inner diameter tubing (Bio-Rad silicone tubing #731-8211) attached via a Luer fitting.
3. 50 mL G-25 desalting column: Dry G-25 Medium Sephadex resin (GE# 17-0033-01) was hydrated according to manufacturer's instructions and packed into an XK 26/20 hardware (GE #28-9889-48). The maximum pressure is 0.5 MPa. We typical run at flow rates of 8–18 mL/min at less than 0.3 MPa. Prepacked HiPrep Desalting column (GE# 17-5087-01) can also be used, but with reduced flow rates. The maximum pressure for prepacked columns is 0.15 mPa.
4. 4 mL SOURCE 15Q column: Bulk SOURCE 15Q (GE# 17-0947-05) was packed into an empty Tricorn 10/50 GL column (GE #8-1163-14). The maximum flow rate is 23.5 mL/min at less than 4 MPa. We use this column at flow rates of 4 mL/min operated at <1.0 MPa.
5. Superdex 200 pg column: This is a prepacked HiLoad 26/600 Superdex 200 pg column, with 320 mL of resin in XK26/600 column hardware (GE# 28-9893-36). The maximum flow rate is 4.25 mL/min with a maximum pressure of 0.5 MPa. We run this column run at 1–2.5 mL/min at less than 0.4 MPa back pressure.

2.4 Hardware and Equipment

1. A liquid chromatography system capable of delivering linear gradients and operating columns at the described flow rates and pressures.
2. Three centrifuges are needed: (1) A low speed refrigerated centrifuge with swinging bucket rotor, capable of spinning 1 L bottles at 1,600 × *g*. (2) An ultracentrifuge (Beckman Optima or equivalent) with Type 45 Ti rotor. (3) A refrigerated high-speed centrifuge (Beckman Coulter Avanti Centrifuge), equipped with JA-10 and JA-25.50 rotors. Centrifuges equipped with a Beckman JA-20 or Sorvall SLA-3000 and

SS-34 are equivalent for this purpose. All centrifugation is performed at 4 °C.

3. Three each: large stir plates, magnetic stir bars, and 4 L beakers.
4. Cold room or cold box with space to plug in and run stir plates.
5. 50 kDa MWCO dialysis tubing (Spectra/Por 6 #132544) and clamps.
6. Cell extruder(s). A system capable of lysing bacteria is needed as is a system capable of lysing yeast cells. These may comprise the same system. We use an Avestin EmulsiFlex-C5 microfluidizer for lysing bacteria, and a Microfluidics M-110P microfluidizer with an H10Z 180μ Diamond homogenizing chamber for lysing yeast cells. The latter is capable of achieving the high pressures (>22,000 psi) needed to lyse yeast cells (*see* **Note 7**).
7. Liquid nitrogen and suitable vessels for freezing cell suspension.

3 Methods

This is a time intensive protocol and greatly benefits from having two people working together. Using commercially sourced yeast, one person can perform Subheading 3.1 (Preparing Yeast Suspension) with two 1 lb/454 g blocks of yeast in less than a day. Typically, we repeat the procedure several times over 1–2 days, producing enough frozen prepared yeast suspension for several preparations. Subheading 3.2 (Expression of GST N-WASP VCA in *E. coli*) can be performed by one person, and may be performed while the yeast suspension is being prepared. The described protocol prepares enough GST N-WASP VCA for multiple Arp2/3 complex preparations. Both Subheadings 3.1 and 3.2 must be completed before the Arp2/3 complex can be purified. The protocol for Arp2/3 complex purification takes 4 full days, which we break into four Subheadings here (3.3–3.6). Two people working in a team are needed during the first 2 days (Subheadings 3.3 and 3.4). Typically, these 2 days require 12-14 h workdays at the scale of prep described here. Working as a team keeps the process manageable. The third and fourth days (Subheadings 3.5 and 3.6) can be completed by a single person.

3.1 Preparing Yeast Suspension

The preparation described here removes any preservatives and stabilizers from the suspension, or any remaining media components if produced in house. Subheadings 3.3–3.6 yield approximately 1 mg of purified Arp2/3 from 150 g of yeast cells. The described preparation begins with ~300 g of yeast cells, but we typically prepare more than one preparations worth of cell suspension at a time. Two 1 lb/454 g blocks can be washed at one time using a centrifuge equipped with a six position, 1 L swinging bucket rotor. This protocol generates roughly >2 L of resuspended cells;

ensure that sufficient liquid nitrogen and freezer space are available to complete the protocol.

1. Obtain wild type *Saccharomyces cerevisiae* through fermentation or by purchase (*see* **Note 1**).
2. Resuspend in 5 mL of IBS per gram of wet cell weight in a large beaker. Commercial blocks can be crumbled by hand, and then stirred, and finally pipetted until homogeneous. Allow any dried out yeast to settle briefly before decanting homogenous suspension into 1 L centrifuge bottles. Any yeast that does not resuspend is discarded.
3. Centrifuge for 20 min at ~4,700 × *g* in 1 L bottles (4,000 rpm in Sorvall H6000A rotor).
4. Decant supernatant and retain cell pellet.
5. Repeat **steps 2** through **4** for a total of three washes.
6. Resuspend the final cell pellet with 2 mL of fresh UBpi per gram of wet cell weight. Appreciable loss of cell weight relative to starting weight is common.
7. Flash freeze the cell suspension by slowly dripping it directly into liquid nitrogen in a clean vessel, such that it freezes as individual pellets. Collect the cell suspension and store in a tightly sealed plastic container at –80 °C.

3.2 Expression of GST N-WASP VCA in E. Coli

1. Obtain a construct for the expression of GST N-WASP VCA in *E. coli* (*see* **Note 3**).
2. Transform vector into chemically competent BL21(DE3) $T1^R$ cells. Plate on LB agar supplemented with 100 μg/mL of ampicillin. Incubate at 37 °C overnight.
3. The following day prepare 1.5 L LB broth in 4-L flasks and autoclave. We typically prepare six of these flasks, but this is sufficient for many Arp2/3 complex purifications (*see* **Note 4**). In the evening, use the center of a single colony to inoculate a 7 mL LB culture (supplemented with 100 μg/mL ampicillin). Repeat such that two 7 mL cultures are prepared for each 1.5 L culture planned. Place tubes at an angle in a shaking incubator and grow with shaking (200–250 rpm for a 1 in. orbit) overnight at 37 °C.
4. The following morning, spin down overnight cultures at ~2,000 × *g* (3,500 rpm in a Sorvall Legend centrifuge with swinging bucket rotor) for 10 min at 4 °C. Decant the supernatant and resuspend all cultures in fresh LB with 100 μg/mL ampicillin, using a volume easily divided among the 1.5 L cultures (e.g., 12 mL for six flasks). Reserve a small volume of fresh media for blanking optical density measurements. Inoculate large-scale growths with the resuspended cultures.

5. Place the large cultures in a 37 °C shaking incubator, shaking at 225–250 rpm for 1 in. orbit. Begin checking optical density after approximately 2 h. When optical density at 600 nm reaches between 0.6 and 0.9 for a 1 cm path-length, induce the culture with 1 mL of a 1 M IPTG stock per L of culture volume. Save a small volume of the culture for pre-induction gel sample (*see* **Note 5**).
6. Return the induced culture to 37 °C with shaking for 3 h.
7. Collect post induction gel sample (*see* **Note 5**).
8. Harvest the culture by centrifugation at ~6,000 × *g* (4,500 rpm in a Sorvall H6000A rotor) for 25 min at 4 °C.
9. Decant spent media and resuspend with 25 mL of QLB per L of culture volume. Add 250 μL of 1 M PMSF stock per 25 mL of QLB near the end of resuspension. Cells should be completely resuspended prior to freezing. Check resuspension by watching as the suspension is pipetted against the bottom of the centrifuge bottle, there should be no visible cell clusters. Place resuspended cells into 50 mL plastic conical tubes and freeze at −80 °C.

3.3 Arp2/3 Complex Purification, Day 1

On the first day of the protocol, yeast cell suspension is lysed using a cell extruder and clarified by high-speed centrifugation. These are the principle limiting steps in the entire protocol and available hardware will greatly influence the overall preparation scale. If the preparation changes in scale, use the given VCA column and SOURCE 15Q column sizes to guide rescaling of the column sizes. Finally, if the prep is scaled up substantially, it may be impractical to increase the volume of dialysis buffer. In that case, additional buffer change steps may be used. As described, this protocol takes approximately 14 h to complete, with a second person needed through the first 8–10 h.

1. Weigh out the desired quantity of frozen yeast cell suspension. The protocol is designed for roughly 900 g of cell suspension, equivalent to 300 g of wet cell weight (*see* Subheading 3.1, **step 6**). Place frozen cell suspension into a glass beaker and thaw (*see* **Note 6).**
2. Lyse the yeast by extrusion at high pressure (*see* **Note 7**). Use three passes operated at 24,000–30,000 psi. Verify lysis by placing 250 μL of cell suspension before extrusion, and after each pass, into 1.5 mL centrifuge tubes, and spinning in a microfuge to clarify for 10 min at 16,000 × *g*. (This spin can be performed at room temperature.) Compare sample before extrusion and after each pass for changes in pellet size and supernatant color. The pellet should reduce in size and the supernatant should become more turbid and golden brown with each pass through the extruder. Lysis is deemed complete

when the centrifuged samples from the final and penultimate passes through the extruder are roughly the same. Microscopic inspection or release of protein to the supernatant could also be used to follow lysis. If the cell disruptor is operated at the lower end of the pressure range, an additional 1–2 passes may be needed. In this case, lysis efficiency may be assessed after only a portion of the lysate has been processed.

3. Clarify lysed yeast suspension by centrifugation at 138,000 × *g* for 1 h at 4 °C (42,000 rpm using Type 45 Ti rotor and compatible 70 mL polycarbonate bottle assemblies). As the volume of lysate produced exceeds the capacity of the rotor, the lysate is split across multiple cycles of centrifugation. To save time, a portion of the lysate is centrifuged while additional cell suspension is lysed. The volume processed here, 900 g of cell suspension, will need to be divided across three centrifugation cycles.
4. Inspect the clarified lysate. Four layers should be visible: a solid tan pellet at the bottom of the tube, a jelly-like darker brown layer on top of the pellet, a golden brown liquid layer on top of the jelly layer, and a thin stark white layer at the very top (which may not completely cover the surface). The golden brown liquid layer contains the soluble Arp2/3 complex. Decant clarified liquid supernatant through four layers of cheesecloth (to catch most of the white top layer and any of the jelly layer that comes loose as the supernatant is poured off) into a glass beaker packed into wet ice.
5. Measure the combined supernatant volume, while keeping it at 4 °C (or on wet ice). Return the measured lysate to the beaker from **step 4** and add a clean magnetic stir bar.
6. Place the beaker on a magnetic stir plate and begin stirring. Stirring should be aggressive enough to create a vortex with a depression which reaches at least halfway down the height of the liquid. The depression should not contact the stir bar, which would introduce air. Weigh out enough solid ammonium sulfate to bring the solution to 25 % saturated (134 g/L dry ammonium sulfate powder). Add ammonium sulfate slowly while stirring in cold room (*see* **Note 8**).
7. Continue to stir for an additional 30 min.
8. Spin down pellet at ~9,000 × *g* (9,000 rpm in a JA-10 or equivalent) for 15 min. Use half full 500 mL centrifuge bottles, splitting into two spins if necessary. Pool, measure, and retain the supernatant.
9. While supernatant from **step 8** is held at 4 °C in a cold room, weigh out enough ammonium sulfate to bring this 25 % saturated solution to 55 % saturated (an additional 179 g of ammonium sulfate solid per L of supernatant). Slowly add the ammonium sulfate powder while stirring (*see* **Note 8**).

10. Continue to stir for an additional 30 min.
11. Spin down pellet at ~9,000 × *g* (9,000 rpm in a JA-10 or equivalent) for 15 min. Use half full 500 mL centrifuge bottles, splitting into two spins if necessary.
12. Decant and discard supernatant from **step 11** and place bottles on ice at an angle such that the pellet is away from the ice and excess liquid can collect at the lowest part of the bottle. Let sit for 3 min and remove any accumulated liquid with a pipette.
13. Resuspend ammonium sulfate cut pellet in 40 mL of buffer A per 300 g of cell suspension (*see* **Note 9**).
14. Place resuspended pellet into 50 kDa MWCO dialysis tubing and dialyze against ~4 L of buffer A per 300 g of cell suspension (*see* **Note 9**) overnight at 4 °C, with gentle stirring (*see* **Note 10**).

3.4 Arp2/3 Complex Purification, Day 2

The second day of the protocol begins with the dialyzing samples from the first day. This day prepares the GST-VCA column while dialysis continues, and then performs the affinity column step twice. If the prep has been scaled up substantially, it may be necessary to add an additional dialysis buffer change step. As described, this protocol takes approximately 14 h to complete, with a second person needed through the first 8–10 h.

1. Change the dialysis buffer once with an equal volume of buffer A. Continue to dialyze during the GST N-WASP VCA purification.
2. Thaw the cell pellets from 2 to 3 L of *E. coli* expressing GST N-WASP VCA (prepared in Subheading 3.2) in cool water. Lyse using 2–3 passes through an Avestin Emulsiflex C5 cell disruptor/homogenizer, cooling the lysate as it passes out of the aperture. The system should be operated at >8,000 psi (*see* **Note 11**).
3. Load lysate into 50 mL round-bottom centrifuge tubes and clarify by spinning for 40 min at 30,000 × *g* (19,000 rpm using a JA-25.50 rotor).
4. Equilibrate a clean DEAE column (*see* **Note 12**) in 92 % QA1/8 % QB1.
5. Pool the supernatant from **step 3** and load onto the DEAE column at 5–10 mL/min. Wash with 2 column volumes of 92 % QA1/8 % QB1, then with 3 column volumes of 85 % QA1/15 % QB1. Elute GST N-WASP VCA with 3 column volumes of 50 % QA1/50 % QB1, collecting and saving the eluate. Save 20 μL samples from the supernatant, column flow-through, column wash (combine 8 % QB1 and 15 % QB1 washes), and elution fractions for SDS-PAGE analysis.

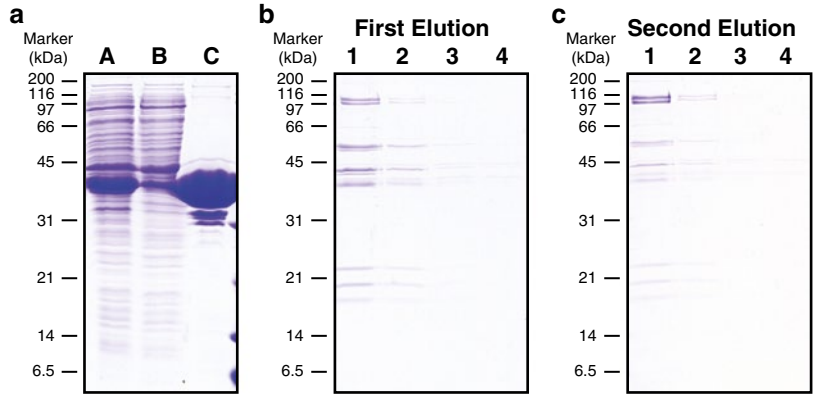

Fig. 1 Preparation and use of GST-VCA column. (**a**) Preparation of the GST-N-WASP VCA column using over-expressed protein. GST N-WASP VCA is bound and eluted from DEAE sepharose (elution shown in *Lane A*). The DEAE Sepharose elution is passed over glutathione sepharose beads, with the flow-through (*Lane B*) and final washed beads (*Lane C*) shown. (**b**) Dialysate from Subheading 3.4, **step 1** is passed over the GST-VCA beads, washed extensively and eluted with Buffer C. Elution fractions #1–4 are shown. (**c**) Flow-through from the first application onto GST-VCA beads is reapplied to the column, washed extensively, and eluted with Buffer C. Elution fractions #1–4 are shown. Position and mass of molecular weight standards are indicated to the *left* of each panel. Elution fraction #1–3 were pooled for both the first and second binding passes

6. Load 6 mL of Glutathione Sepharose 4B (*see* **Note 13**) into a 2.5 cm low-pressure column and equilibrate by passing 60 mL of buffer GSH-WB1 over the beads (*see* **Note 14**).
7. Resuspend GSH Sepharose beads using 10 mL of GSH-WB1 and add to the eluate from **step 5**. Distribute eluate/bead suspension into 50 mL conical tubes, filling the tubes to >90 % of capacity and topping off with additional buffer GSH-WB1 as necessary. Allow proteins to bind to the beads in batch mode for 30 min, with gentle rotation at 4 °C.
8. Separate the beads from the liquid by passing the suspension through the low-pressure column used in **step 6**. Retain the beads and collect the flow-through.
9. Wash the beads five times with 2.5 column volumes of buffer GSH-WB1, pooling and retaining the wash. Clean the beads further by washing five times with 2.5 column volumes of buffer GSH-WB2. Finally, wash the beads an additional five times with 2.5 column volumes of buffer GSH-WB1. Save 20 µL samples of flow-through, pooled wash and a small quantity of the washed beads for SDS-PAGE analysis (*see* Fig. 1).
10. Clarify the yeast dialysate from **step 1** by centrifugation at 30,000×*g* for 30 min (19,000 rpm in JA-25.50 rotor, or equivalent). The volume will have increased and this may fill more than eight tubes. Decant the supernatant through four layers of cheesecloth, into a 600 mL glass beaker on ice.

Supernatant will not appear completely clear following centrifugation.

11. Equilibrate the affinity column from **step 9** with 30 mL of buffer A. Once the column has drained, apply another 30 mL of buffer A to the column and allow it to flow through.
12. Stop liquid flow through the column and resuspend the resin with a small amount of buffer A. Mix resuspended resin with the clarified dialysate from **step 10**. Distribute into 50 mL conical tubes, filling nearly full and topping off with buffer A as necessary. Incubate with gentle mixing for 25 min at 4 °C.
13. Drain bead suspension through the 2.5 cm low-pressure column, collecting the flow-through.
14. Wash the beads 5 times with 4 column volumes of buffer A, collecting the wash. Then wash the beads 10 times with 5 column volumes of buffer B, collecting this wash separately. Finally, pass 2.5 column volumes of buffer C over the resin collecting the eluted proteins. Repeat the buffer C wash a total of five times, collecting each elution as a separate fraction.
15. Re-equilibrate the resin in buffer A as in **step 11**. Repeat **steps 12–14** substituting the flow-through from **step 13** for the clarified dialysate in **step 12**. This second pass captures about half the Arp2/3 complex captured on the first pass over the beads (*see* **Note 4**).
16. Determine buffer C elution fractions to pool by SDS-PAGE analysis. Arp2/3 complex should be visible by Coomassie staining at this step (*see* Fig. 1 and **Note 15**).
17. Once fractions are pooled, they can be held overnight at 4 °C (*see* **Note 16**).

3.5 Arp2/3 Complex Purification, Day 3

The third day of the protocol begins with the pooled GST-VCA elution fractions. The buffer is exchanged and Arp2/3 complex is further purified using SOURCE 15Q ion exchange chromatography. A preparative gel filtration column is then run as an overnight step. A single person can perform desalting, ion exchange, SDS-PAGE analysis, and beginning the gel filtration column in 8–10 h.

1. Exchange pooled buffer C elution into buffer QC using the 50 mL G-25 desalting column. Equilibrate the column in 1.5 column volumes of QC and inject 13–18 mL of sample onto the column. Continue to pass QC over the column and collect the peak containing the eluted protein.
2. Repeat **step 1** until the entire sample has been buffer exchanged. For the combined pool of two passes of the yeast cell lysate over the VCA column, roughly ten injections onto the desalting column will be needed. Pool all desalted eluate.
3. Equilibrate the 4 mL SOURCE 15Q column in 100 % QC. Inject desalted pool onto the column. Bind and run at

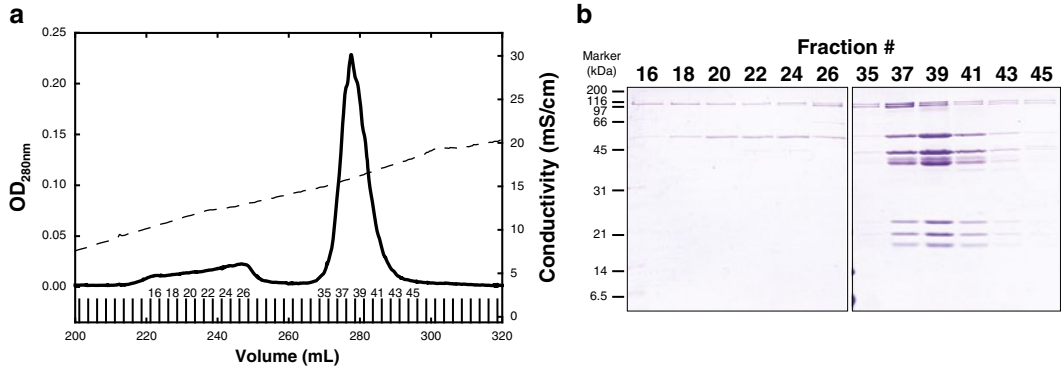

Fig. 2 Purification of Arp2/3 complex using SOURCE 15Q anion exchange chromatography. (**a**) Chromatogram for the resolving portion of the protocol, showing one dominant peak in the UV signal, occurring near a conductivity of 17 mS/cm. *Spaces* between *long vertical lines* beneath the UV trace represent the collected fractions, with relevant fraction numbers labeled. (**b**) SDS-PAGE analysis of fractions from the SOURCE 15Q column. Bands at 48, 42, 40, 35, 19, 18, and 15 kDa are Arp2/3 complex. Fractions containing substantial quantities of Arp2/3 complex and avoiding the contaminant at ~33 kDa (fractions #36–40) were pooled. Position and mass of molecular weight standards are indicated to the *left* of the panel

1–2.5 mL/min. Wash out unbound sample with 2 column volumes of QC. Quickly shift to 96 % QC/4 % QD, then run a linear gradient from 96 % QC/4 % QD to 71 % QC/29 % QD over 50 column volumes, collecting 2.5 mL fractions. Assess purity by SDS-PAGE, pool relevant samples (*see* Fig. 2).

4. Purify Arp2/3 complex using Superdex 200 gel filtration chromatography. Equilibrate a 320 mL Superdex 200 pg column with at least 300 mL KMEHd–A. If necessary, concentrate the SOURCE 15Q pool to ~10 mL using an Amicon Ultra-15, 30,000 MWCO centrifugal concentrator unit. Inject the concentrated Arp2/3 complex pool onto the column at 1 mL/min. Elute the Arp2/3 complex by flowing an additional column volume of buffer over the column at 1.5–2.5 mL/min, collecting 5 mL fractions beginning after 0.3 column volumes of buffer. Arp2/3 complex typically elutes as the dominant peak, with its maxima occurring when ~0.6 column volumes of buffer have been applied to the column. This is typically begun as an automated overnight step and allowed to run unattended. If possible arrange to have the column run somewhat slower than usual such that the Arp2/3 complex containing fractions elute in the early morning.

3.6 Arp2/3 Complex Purification, Day 4

The fourth day of the protocol begins by assessing the overnight gel filtration results by SDS-PAGE. If necessary a second pass over gel filtration is used to complete the purification. Otherwise, the complex is concentrated, quantified and frozen. A single person can complete the fourth day in about 5 h if the additional gel filtration step is not needed, and in about 10 h if the additional gel

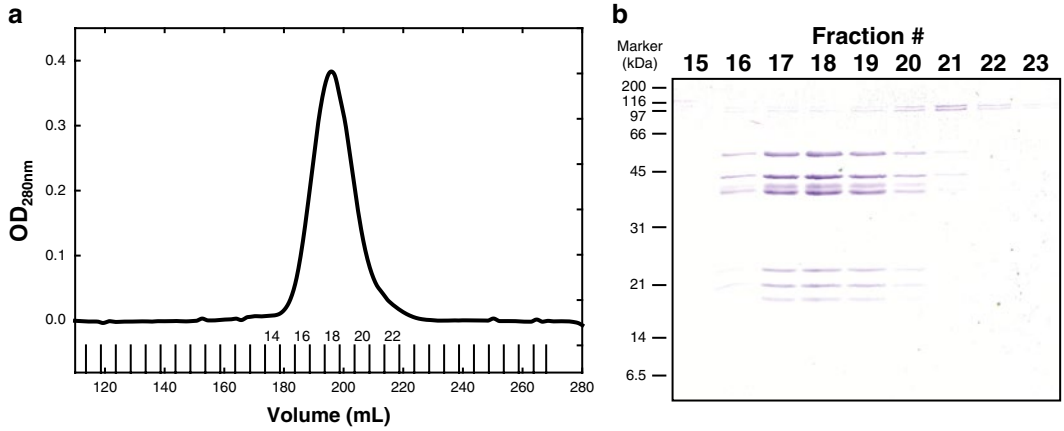

Fig. 3 Purification of Arp2/3 complex using Superdex 200 pg gel filtration chromatography. (**a**) Chromatogram for the included volume portion of the protocol, showing one dominant, slightly trailing, peak in the UV signal, eluting with a maximum near 195 mL. *Spaces* between *long vertical lines* beneath the UV trace represent the collected fractions, with relevant fraction numbers labeled. (**b**) SDS-PAGE analysis of fractions from the Superdex 200 pg gel filtration column. Bands at 48, 42, 40, 35, 19, 18, and 15 kDa are Arp2/3 complex. Fractions containing substantial quantities of Arp2/3 complex and avoiding the contaminating doublet near 100 kDa (fractions #16–19) were pooled. Position and mass of molecular weight standards are indicated to the *left* of the panel

filtration step is needed. Concentrating and freezing of the complex can be delayed until the fifth day.

1. Assess purity using SDS-PAGE analysis, pool relevant fractions (*see* Fig. 3).
2. If contaminating proteins are observed, typically a doublet at ~100 kDa, inject the pool back onto the Superdex 200 pg column as described in **step 4** of Subheading 3.5, dividing it into two injections. Assess purity by SDS-PAGE, pool relevant fractions (*see* Fig. 4).
3. Measure concentration (*see* **Note 17**); concentrate using an Amicon Ultra-15 30,000 MWCO centrifugal concentrator if desired.
4. Pooled materials can be diluted to 1.5-fold the desired working concentration, mixed with buffer F, aliquoted, and frozen (*see* **Note 18**).

4 Notes

1. The wild type budding yeast (*Saccharomyces cerevisiae*) used in this protocol can be grown in the lab or acquired from commercial sources. We have had good success with both routes. This protocol can be performed using in house grown yeast from either shaker flasks (yeast grown to roughly OD_{600} of 1–2 in 18 L YPD is a good starting point for this protocol), or

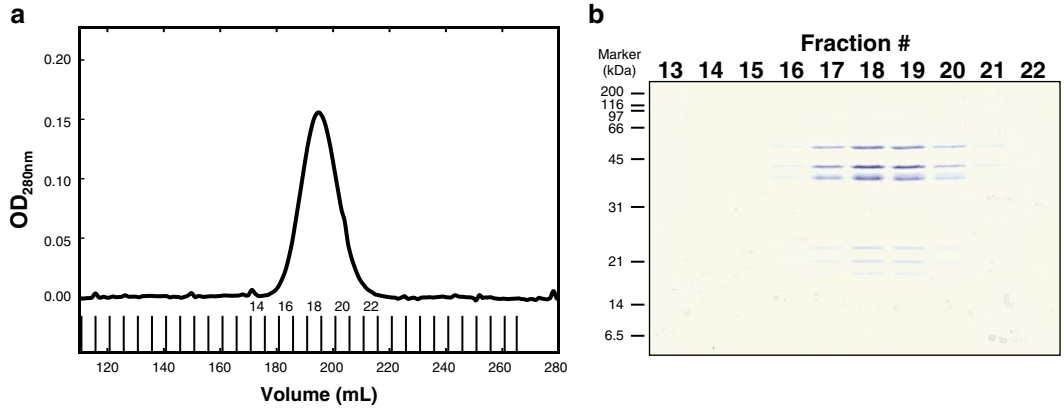

Fig. 4 Further purification of Arp2/3 complex using Superdex 200 pg gel filtration chromatography. (**a**) Chromatogram for the included volume portion of the first injection of the protocol, showing one dominant peak in the UV signal, eluting with a maximum near 195 mL. The second injection is indistinguishable from the first. *Spaces* between *long vertical lines* beneath the UV trace represent the collected fractions, with relevant fraction numbers labeled. (**b**) SDS-PAGE analysis of fractions from the Superdex 200 pg gel filtration column. Bands at 48, 42, 40, 35, 19, 18, and 15 kDa are Arp2/3 complex. Fractions containing substantial quantities of Arp2/3 complex and avoiding the contaminating doublet near 100 kDa (fractions #16–19) were pooled. Position and mass of molecular weight standards are indicated to the *left* of the panel

produced at high density using a fermentation system. Given the cost and time needed to produce this quantity of yeast, we recommend purchasing yeast from a commercial source. Dry yeast should not be used. One pound cakes of fresh yeast are commonly used in small commercial bakeries. The yeast has a shelf life of about 1 month, and thus most bakeries receive frequent shipments and are willing to part with one or two cakes at a price that is much less than the cost of media used to grow the yeast in house. Alternatively, one may be able to acquire a very fresh case of cakes directly from a distributor. This protocol has had good results with Red Star #05020 cake yeast, although washing, resuspending, freezing, and storing at −80 °C an entire 20 lb case is impractical.

2. PMSF is toxic. Care should be used when preparing this stock. In particular, use of gloves, lab coats, protective eye wear and dust masks will reduce inhalation and cross contamination. One effective strategy is to purchase <100 g bottles, and prepare the entire bottle at one time trusting the manufacturer's provided weight. The working concentrations are high enough that small errors due to variability in the manufacturer's weight will not have a significant effect. The stock should be stored as 1 mL aliquots in 1.5 mL microfuge tubes at −20 °C. Once the stocks have been frozen PMSF will crystallize out of solution. Warming in a room temperature beaker of water for a few minutes is usually sufficient to bring the PMSF back into solution. Agitation by inversion may be needed. When adding PMSF to a buffer, avoid splashing the stock and buffers onto gloves, skin and eyes.

3. For this protocol, we use N-WASP VCA to capture Arp2/3 complex because it was used in the first reported version of this protocol. N-WASP VCA binds Arp2/3 complex more tightly than most VCAs. Also of note, the GST fusion to N-WASP VCA means that, in addition to binding to the target affinity column, the VCA will be a dimer. VCA dimers are important here as they increase the affinity towards Arp2/3 complex appreciably, and the protocol may not work with lower affinity VCA monomers. It is not clear whether VCA constructs will perform better than CA constructs, but we have used a VCA construct composed of amino acid residues 393–504. This is expressed from a modified pGEX 2T (GE) vector such that VCA has an N-terminal GST fusion, with a short linker and a thrombin cleavage site separating them.
4. The quantity of GST N-WASP VCA used to prepare the affinity column is not a critical element. As the binding of Arp2/3 complex from solution is fairly inefficient, there should be an excess of GST-VCA present. Using our bacterial expression system, we use cells from 0.5 to 1 L of LB culture for each 100 g of yeast cells lysed or 300 g of cell suspension lysed (as prepared in Subheading 3.1). The DEAE column will bind nearly all of the VCA dimers from solution, and the glutathione sepharose should be overloaded with VCA dimer. By overloading this column, we minimize contaminants at the cost of yield. This saves additional purification steps, and thus greatly shortens the VCA purification.

   We have found that Arp2/3 complex is never completely captured when working with beads suspended in batch. Thus, we save the flow-through following separation of beads from lysate after a binding step. The flow-through is then reapplied to the beads a second time, and the purification repeated. We have found that additional Arp2/3 complex can be purified by additional cycles of capture from the lysate, but that the purity and amount captured decreases with each cycle. Typically, the second pass has only 30–80 % of the Arp2/3 complex captured in the first pass, but shows only an incremental increase in contaminants. The third pass typically shows a similar decrease in quantity captured, but a substantial increase in contaminants. Thus, two cycles seems to be the best compromise in terms of yield, purity, and time involved.
5. The induction of proteins can be best seen in SDS-PAGE analysis if the samples are well matched. We have good results by collecting ~1.5 mL of culture and measuring its optical density at 600 nm (OD_{600}). Calculate how much of this sample is needed to prepare a matched expression sample using the formula: volume = $0.15 / OD_{600}$ mL. Place that volume of culture in a 1.5 mL tube, and pellet the cells by spinning at

~10,000 × *g* for 2 min. Remove the medium, and resuspend the cells completely in 50 µL of water or neutral buffer by pipetting up and down. Add an additional 50 µL of 2× concentrated SDS sample buffer and mix. After induction, repeat the process, adjusting the volume for the increase in optical density. Heat the samples for 5 min immediately before loading 6–8 µL onto a denaturing SDS-PAGE gel. We routinely use continuous 15 % acrylamide PAGE gels for the analysis of GST N-WASP VCA expression.

6. Thawing the yeast cell suspension can be performed more than one way. For any method, it is important to remember to keep the yeast cell suspension cool, to thaw it as evenly as possible and to use it soon after thawing. One suggestion is to place the weighed frozen cell suspension in a 1 L glass beaker with a clean stir bar. Cover the 1 L beaker with aluminum foil and place it in a plastic 4 L beaker with cool water. Hold the 1 L beaker down with a lead ring and place the nested beakers on a stir plate. Once the yeast begins to thaw begin stirring. As the water in the lower beaker is chilled by the thawing cell suspension, replace it with fresh cool (but not cold) water. Alternatively, once the cell suspension is sufficiently thawed, it can be stirred with a serological pipette.
7. Lysis of yeast cells requires more aggressive physical methods than does lysis of bacteria. Common ways to lyse yeast cells include grinding in liquid nitrogen, agitation with glass beads, and extrusion at high pressure. The latter can be achieved using the same type of equipment used for bacterial lysis, but efficient lysis requires substantially higher pressures. We lyse yeast cells by passing the cell suspension through a Microfluidics M-110P microfluidizer operated at ~25,000 psi, then repeating for a total of three passes. To address the heat generated, particular care is used to cool the system and lysate. Cooling is achieved by packing much of the system in wet ice, and by stopping the flow each time 90 mL had been homogenized to allow several minutes for the system to cool.
8. A common mistake during the ammonium sulfate cut is to add the solid ammonium sulfate too quickly or all at once. This results in locally high concentrations of ammonium sulfate, which can cause undesired proteins to precipitate in a nonequilibrium fashion. A few precautions can minimize this problem.

   First, inspect the ammonium sulfate as it is weighed out. Often there are clumps of crystals present, some of which may be larger than 5 mm. If this is a problem, break them up by mashing them with a mortar and pestle. The goal is not to smash the crystals into powder (which does help, but not enough to warrant routinely doing) but just to break up any large clumps of crystals that may be present.

Second, for the amounts described here the addition of ammonium sulfate should occur over 20–25 min. Time can be scaled down somewhat for smaller volumes. The stirred solution should be checked periodically while the solid is added. Look at the bottom of the beaker, make sure that solid ammonium sulfate is not accumulating. If it does, the ammonium sulfate is being added too quickly. Wait for a few minutes for the accumulated solid to disperse, then continue to add, but more slowly. A practical way to add the solid is to put half to one third of it in a plastic weigh boat, and to tap it with a spatula. By varying the frequency of tapping a reasonably controllable and uniform addition rate may be found.

9. Here, cell suspension weight refers to cells resuspended as in Subheading 3.1 **step 6**, where one third of the suspension weight is wet cell mass. If cells are resuspended at a different cell density, the protocol should be scaled according to the wet cell weight lysed, not according to the cell suspension weight.
10. Cut and rinse lengths of 50 kDa cut-off dialysis membrane (Spectra/Por 6, #132544) with ultrapure water. Enough dialysis tubing should be prepared to hold the resuspended volume, plus a 70 % increase in volume due to the difference in osmotic strength between the resuspended pellets and buffer A. For the indicated dialysis tubing cut a total of 50 cm per 60 mL, split across at least two pieces. Affix dialysis clips onto one end of the tubing and transfer the resuspended pellets into the dialysis tubing, leaving at least 50 % of the length as slack. Close off the other end with additional dialysis tubing clips. Dialyze the pellets against 12 L of buffer A overnight (greater than 6 h) at 4 °C, stirring slowly. It is usually necessary to use two medium or large dialysis clips at either end of the tubing to give the suspension/tubing sufficient buoyancy to prevent it from hitting the stir bar. Alternatively, hang the dialysis tubing from a rod arranged over the dialysis vessel.
11. *E. coli* expressing GST N-WASP VCA can be lysed by a number of common methods. We have used sonication and extrusion using an Avestin EmulsiFlex-C5 cell disruptor. In either case, some care should be used to minimize heating of the sample. When using sonication, use a series of sonication pulses (about 10 s total sonication time) and place the solution on ice for 1–2 min between pulse series. For extrusion, the cell disruptor has a heat exchanger mounted immediately following the lysis aperture, and chilled water is flowed through this during lysis.
12. The DEAE column should be sized according to how much culture is lysed. At least 10 mL of DEAE Sepharose FF should be used per L of LB VCA culture. When lysing volumes larger than 4 L it is usually more practical to repeat the DEAE step and pool the results than to use a larger column.

The DEAE Sepharose column can be reused many times. The principle reason the column should be repacked is accidental introduction of air. Between uses, the column should be thoroughly cleaned. The final high salt wash (in 100 % QB1) does a reasonable job removing most protein contaminants, but leaves behind a significant amount of nucleic acid. This can be depleted with washes at different percentages of QB1 (with QA1 making up the balance). Wash the DEAE column with ~1 column volume at 5 % QB1, followed by 35, 65, 100, 5, 35, 65, and 5 % QB1. If there is still substantial absorbance at 254 nm eluted during the 35 % QB1 step, add an additional 1–2 cycles of 35, 65, and 5% QB1.

13. To save costs, we routinely regenerate Glutathione Sepharose 4B after use in purifying bacterially expressed proteins. The resin is regenerated with 3 column volumes of 6 M guanidine hydrochloride (98 % purity), and then washed extensively with water. The resin can be further washed with 2 % SDS, although extensive washes with water are necessary between the guanidine and SDS washes. After the initial use, capacity of the resin drops by roughly half, and then is more or less stable for subsequent uses. Regenerated resin can be used here, but adjust the total column volume for the twofold decrease in capacity. Given the different possible contaminants, once used with yeast lysate glutathione resin is not regenerated but is instead discarded.
14. A smaller column such as a 1.5 cm diameter disposable column (e.g., Bio-Rad Econ-Pac #732-1010) is needed when scaling down the prep (~100 g of cells) and less than 2.5 mL of Glutathione Sepharose 4B resin is used. These smaller columns can also be used in the prep described here as an alternative to the 2.5 cm glass Econo-Column. If using for this prep, split the 6 mL of resin into three 1.5 cm columns. In either case, a stopcock and a piece of tubing attached to the bottom of the column will help to keep the solution flowing (due to the increased height between the top of the liquid and the column outlet) and will allow stopping the flow to recover the resin.
15. The *Saccharomyces cerevisiae* Arp2/3 complex ArpC1 subunit (ARC40) has been reported to have an odd mobility on SDS-PAGE gels [30]. We have routinely noted this as well. The protein may not appear on the gel at all when samples are prepared in a standard fashion (mixed with 2× reducing SDS loading buffer and heated at 95 °C for 3–5 min). This seems to be specific to ARC40 at moderate to high concentrations, and is dependent on heating of the SDS-PAGE samples. If it is necessary that ARC40 completely enter the gel, dilute the sample to ~40 nM or less prior to the addition of SDS and reducing agent, and omit the heating of the sample. In many

cases, this drops the concentration out of standard Coomassie gel staining sensitivity, necessitating silver staining or Western blotting methods.

16. Given the length of the second day of the preparation (Subheading 3.4), once Arp2/3 complex is eluted from the GST-VCA column it is held at 4 °C overnight and then exchanged into buffer QC the following day. A desalting column is employed to save time (Subheading 3.5**, steps 1** and **2**). If necessary, this allows delaying of SDS-PAGE assessment and pooling until the morning of the third day. Alternatively, dialysis could be set up against 4 L of buffer QC at the end of the second day and **steps 1** and **2** of Subheading 3.5 skipped.
17. Our method of quantifying Arp2/3 complex is based on tryptophan UV absorption. An extinction coefficient at 280 nm of 245,240 M^{-1} cm^{-1} was estimated from the number of tryptophan and tyrosine residues (24 and 76, respectively) in a complex. As the complex may bring an ATP or ADP nucleotide along with it during purification, we routinely measure absorption at 290 nm, and correct for any scatter by using the absorption at 314 nm. By measuring the relative absorbance of a sample judged to be devoid of nucleotide at 280 and 290 nm, we found the A_{290}/A_{280} ratio to be 0.6. Thus, we routinely measure the concentration using an extinction coefficient at 290 nm of 147,000 M^{-1} cm^{-1}. Our experience using laser interference to quantify the complex during analytical ultracentrifugation experiments shows this extinction coefficient to be within 10 % of the correct value.
18. Directly freezing small aliquots of Arp2/3 complex in liquid nitrogen results in a slight degree of aggregation, and measurable loss of activity. For routine assay at 10 nM of Arp2/3 complex in pyrene actin polymerization assays, we supplement 600 nM Arp2/3 complex in KMEHd-A with one half of a part buffer F (i.e., 5 mL of buffer F is added to 10 mL of 600 nM Arp2/3 complex solution). Small volumes (e.g., 80 μL) can then be placed into small tubes (200 μL thin wall PCR tubes are convenient for this) and snap frozen in liquid nitrogen. For additional commentary, see the bovine Arp2/3 complex purification notes [23].

References

1. Pollard TD, Cooper JA (2009) Actin, a central player in cell shape and movement. Science 326 (5957):1208–1212
2. Galletta BJ, Mooren OL, Cooper JA (2010) Actin dynamics and endocytosis in yeast and mammals. Curr Opin Biotechnol 21(5):604–610
3. Weinberg J, Drubin DG (2012) Clathrin-mediated endocytosis in budding yeast. Trends Cell Biol 22(1):1–13
4. Pollard TD, Wu JQ (2010) Understanding cytokinesis: lessons from fission yeast. Nat Rev Mol Cell Biol 11(2):149–155
5. Machesky LM, Atkinson SJ, Ampe C, Vandekerckhove J, Pollard TD (1994) Purification of a cortical complex containing two unconventional actins from Acanthamoeba by affinity chromatography on profilin–agarose. J Cell Biol 127(1):107–115

6. Mullins RD, Stafford WF, Pollard TD (1997) Structure, subunit topology, and actin-binding activity of the Arp2/3 complex from Acanthamoeba. J Cell Biol 136(2):331–343
7. Pollard TD (2007) Regulation of actin filament assembly by Arp2/3 complex and formins. Annu Rev Biophys Biomol Struct 36:451–477
8. Winter DC, Choe EY, Li R (1999) Genetic dissection of the budding yeast Arp2/3 complex: a comparison of the in vivo and structural roles of individual subunits. Proc Natl Acad Sci USA 96(13):7288–7293
9. Gournier H, Goley ED, Niederstrasser H, Trinh T, Welch MD (2001) Reconstitution of human Arp2/3 complex reveals critical roles of individual subunits in complex structure and activity. Mol Cell 8(5):1041–1052
10. Machesky LM, Mullins RD, Higgs HN, Kaiser DA, Blanchoin L, May RC, Hall ME, Pollard TD (1999) Scar, a WASp-related protein, activates nucleation of actin filaments by the Arp2/3 complex. Proc Natl Acad Sci USA 96(7):3739–3744
11. Padrick SB, Rosen MK (2010) Physical mechanisms of signal integration by WASP family proteins. Annu Rev Biochem 79:707–735
12. Xu XP, Rouiller I, Slaughter BD, Egile C, Kim E, Unruh JR, Fan X, Pollard TD, Li R, Hanein D, Volkmann N (2012) Three-dimensional reconstructions of Arp2/3 complex with bound nucleation promoting factors. EMBO J 31(1):236–247
13. Robinson RC, Turbedsky K, Kaiser DA, Marchand JB, Higgs HN, Choe S, Pollard TD (2001) Crystal structure of Arp2/3 complex. Science 294(5547):1679–1684
14. Goley ED, Rodenbusch SE, Martin AC, Welch MD (2004) Critical conformational changes in the Arp2/3 complex are induced by nucleotide and nucleation promoting factor. Mol Cell 16(2):269–279
15. Marchand JB, Kaiser DA, Pollard TD, Higgs HN (2001) Interaction of WASP/Scar proteins with actin and vertebrate Arp2/3 complex. Nat Cell Biol 3(1):76–82
16. Hufner K, Higgs HN, Pollard TD, Jacobi C, Aepfelbacher M, Linder S (2001) The verprolin-like central (vc) region of Wiskott–Aldrich syndrome protein induces Arp2/3 complex-dependent actin nucleation. J Biol Chem 276(38):35761–35767
17. Boczkowska M, Rebowski G, Petoukhov MV, Hayes DB, Svergun DI, Dominguez R (2008) X-ray scattering study of activated Arp2/3 complex with bound actin-WCA. Structure 16(5):695–704
18. Doolittle LK, Rosen MK, Padrick SB (2013) Measurement and analysis of in vitro actin polymerization. Methods Mol Biol 1046: 273–294
19. Hansen SD, Zuchero JB, Mullins RD (2013) Cytoplasmic Actin: Purification and Single Molecule Assembly Assays. Methods Mol Biol 1046:145–170
20. Insall R, Muller-Taubenberger A, Machesky L, Kohler J, Simmeth E, Atkinson SJ, Weber I, Gerisch G (2001) Dynamics of the Dictyostelium Arp2/3 complex in endocytosis, cytokinesis, and chemotaxis. Cell Motil Cytoskeleton 50(3):115–128
21. Higgs HN, Blanchoin L, Pollard TD (1999) Influence of the C terminus of Wiskott–Aldrich syndrome protein (WASp) and the Arp2/3 complex on actin polymerization. Biochemistry 38(46):15212–15222
22. Ma L, Rohatgi R, Kirschner MW (1998) The Arp2/3 complex mediates actin polymerization induced by the small GTP-binding protein Cdc42. Proc Natl Acad Sci USA 95(26): 15362–15367
23. Doolittle LK, Rosen MK, Padrick SB (2013) Purification of native Arp2/3 complex from bovine thymus. Methods Mol Biol 1046: 231–250
24. Welch MD, Iwamatsu A, Mitchison TJ (1997) Actin polymerization is induced by Arp2/3 protein complex at the surface of Listeria monocytogenes. Nature 385(6613):265–269
25. Goode BL, Rodal AA, Barnes G, Drubin DG (2001) Activation of the Arp2/3 complex by the actin filament binding protein Abp1p. J Cell Biol 153(3):627–634
26. Egile C, Loisel TP, Laurent V, Li R, Pantaloni D, Sansonetti PJ, Carlier MF (1999) Activation of the CDC42 effector N-WASP by the Shigella flexneri IcsA protein promotes actin nucleation by Arp2/3 complex and bacterial actin-based motility. J Cell Biol 146(6):1319–1332
27. Lechler T, Jonsdottir GA, Klee SK, Pellman D, Li R (2001) A two-tiered mechanism by which Cdc42 controls the localization and activation of an Arp2/3-activating motor complex in yeast. J Cell Biol 155(2):261–270
28. Zalevsky J, Lempert L, Kranitz H, Mullins RD (2001) Different WASP family proteins stimulate different Arp2/3 complex-dependent actin-nucleating activities. Curr Biol 11(24): 1903–1913
29. Beltzner CC, Pollard TD (2008) Pathway of actin filament branch formation by Arp2/3 complex. J Biol Chem 283(11):7135–7144
30. Pan F, Egile C, Lipkin T, Li R (2004) ARPC1/Arc40 mediates the interaction of the actin-related protein 2 and 3 complex with Wiskott–Aldrich syndrome protein family activators. J Biol Chem 279(52):54629–54636

Chapter 16

Measurement and Analysis of In Vitro Actin Polymerization

Lynda K. Doolittle, Michael K. Rosen, and Shae B. Padrick

Abstract

The polymerization of actin underlies force generation in numerous cellular processes. While actin polymerization can occur spontaneously, cells maintain control over this important process by preventing actin filament nucleation and then allowing stimulated polymerization and elongation by several regulated factors. Actin polymerization, regulated nucleation, and controlled elongation activities can be reconstituted in vitro, and used to probe the signaling cascades cells use to control when and where actin polymerization occurs. Introducing a pyrene fluorophore allows detection of filament formation by an increase in pyrene fluorescence. This method has been used for many years and continues to be broadly used, owing to its simplicity and flexibility. Here we describe how to perform and analyze these in vitro actin polymerization assays, with an emphasis on extracting useful descriptive parameters from kinetic data.

Key words Actin polymerization, In vitro reconstitution, Biochemical assay, Quantitative analysis

1 Introduction

Dynamic rearrangements of the actin cytoskeleton underlie key aspects of many cellular functions, including aspects of cell motility, vesicle trafficking, and cytokinesis [1–3]. Many of these rearrangements rely on control of when and where actin polymerization occurs. This is regulated at the level of nucleation of new filaments [4–6], elongation of these filaments [5, 6], cross-linking of filaments into higher order structures, arrest of filament growth, and disassembly of filaments [2]. Given the broad cellular importance of these processes, great effort has been put into studying the mechanisms of how these processes are regulated at the biochemical level.

Here we describe a widely used biochemical assay for actin polymerization [7, 8] that can be used to answer many important biochemical questions. Although more complex assays are possible [9–12], for questions regarding the activity of actin filament nucleation factors [13–16], often the most direct way to analyze activity is through the use of a bulk kinetic assay. Further, in order to

Amanda S. Coutts (ed.), *Adhesion Protein Protocols*, Methods in Molecular Biology, vol. 1046,
DOI 10.1007/978-1-62703-538-5_16,

interpret the results from filament mesh reconstitution and bead motility assays, an understanding of the underlying biochemistry is of great utility.

Actin will polymerize into filaments whenever its concentration is greater than its critical concentration. The critical concentration of actin can be modified by type of actin, bound nucleotides [17] and numerous solution conditions [18, 19]. Thus, purified actin can be maintained as monomers by removing almost all salts present, storing it under mildly alkaline conditions and by including calcium ions rather than magnesium ions [20]. This solution can then be induced to form filaments by adding a concentrated buffer mix that alters pH, switches divalent cations, and increases salt concentrations into the physiological range. The polymerization of actin can be tracked in bulk solution by following a variety of observables, including tracking the increase in light scatter or solution viscosity as the polymers grow. Owing to greater flexibility, it is far more common to introduce the environmentally sensitive fluorophore, pyrene, onto an existing cysteine in actin, and follow the increase in fluorescence intensity as the polymers form [7, 8].

Part of the great power of the pyrene detected method is that the changes in fluorescence intensity for an actin solution can be measured in real-time with high signal to noise, and thus is well suited to kinetic assays, which are generally of the most interest for this system. We describe this assay in detail, with particular attention paid to constructing quantitative assays.

Analysis of the resulting kinetic profiles is somewhat complicated. The difficulty stems from the fact that polymerization kinetics are a combination of processes: elongation of filaments at both their fast growing "barbed" end and their slow growing "pointed" end, nucleation of new filaments from bulk solution, and nucleation of filaments in a filament dependent manner. These processes all have distinct kinetic effects. There is no general analytic solution for actin polymerization kinetics in the presence of nucleation factors, and thus descriptive metrics for the kinetics are typically used for quantification instead of parameters determined by fitting to the entire dataset (*see* **Note 1**). Here we describe the calculation of several simple metrics (*see* **Note 2**): the time at which half of the actin has polymerized ($t_{1/2}$), the actin polymerization rate at $t_{1/2}$, the number of barbed ends present at $t_{1/2}$ (*see* **Note 3**), and the initial nucleation rate.

2 Materials

All buffer and salt stocks are prepared using ultrapure water (>18 MΩ, using a Millipore brand Milli-Q water purification system). Except where noted, all solutions are filtered through a

0.22 μm cellulose acetate membrane. Working buffers are prepared by dilution of buffer stocks into prechilled ultrapure water. Where specific sources are recommended, the manufacturer and part numbers are indicated.

2.1 Stock Materials and Solutions

1. Rabbit muscle acetone powder (Pel-Freez #41995-2).
2. *N*-(1-pyrene) iodoacetamide (Invitrogen #P-29): 10 mM stock in anhydrous dimethylformamide (DMF). The solution is stored at −20 °C in 1 mL aliquots.
3. Dithiothreitol (DTT): 1 mM stock in ultrapure water, filtered, and stored at −20 °C in 1 mL aliquots. When thawing, place in cool water until solution is liquid, then transfer to ice until needed. Once added to buffers, assume DTT is no longer functional after 48 h when stored at 4 °C.
4. Adenosine 5′ triphosphate disodium salt (ATP; Sigma-Aldrich #A7699): 100 mM stock in 100 mM Tris–HCl pH 8.0, and titrated to pH 7.4–7.5 with sodium hydroxide. The solution is filtered and stored at −20 °C in 1 mL aliquots.
5. 0.5 M EGTA: Prepared using ethylene glycol tetraacetic acid powder and titrated to pH 8.0 with sodium hydroxide. Initially, EGTA is insoluble, but comes into solution as the pH is adjusted.
6. 1 M Tris–HCl pH 8.0: Prepared using tris base, and titrated to pH 8.0 at room temperature with concentrated hydrochloric acid.
7. 1 M Imidazole pH 7.0: Titrated with hydrochloric acid to pH 7.0 at room temperature.
8. 2 M KCl.
9. 5 M NaCl.
10. 1 M $MgCl_2$.
11. 1 M $CaCl_2$.
12. 1 M Sodium Azide.

2.2 Working Buffers

1. KMEI: 50 mM KCl, 10 mM imidazole pH 7.0, 1 mM $MgCl_2$, 1 mM EGTA.
2. 10× KMEI: 500 mM KCl, 100 mM imidazole pH 7.0, 10 mM $MgCl_2$, 10 mM EGTA.
3. Buffer G: 2 mM Tris–HCl pH 8, 200 μM ATP, 0.5 mM DTT, 0.1 mM $CaCl_2$, 1 mM sodium azide.
4. Buffer G-Mg: 2 mM Tris–HCl pH 8, 200 μM ATP, 0.5 mM DTT, 0.1 mM $MgCl_2$.
5. 10E/1 M: 10 mM EGTA, pH 8, 1 mM $MgCl_2$.

2.3 Chromatography Columns

1. Superdex 200 pg column: This is a prepacked HiLoad 26/600 Superdex 200 pg column, with 320 mL of resin in XK26/600 column hardware (GE# 28-9893-36). The maximum flow rate is 4.25 mL/min with a maximum pressure of 0.5 MPa. We run this column run at 1–2.5 mL/min at less than 0.4 MPa back pressure.

2.4 Hardware and Equipment

1. Two centrifuges are needed: (1) An ultracentrifuge (Beckman Optima or equivalent) equipped with Type 45 Ti, Type 70 Ti and SW 41 Ti or other appropriate rotors (*see* **Note 4**). (2) A refrigerated centrifuge (Beckman Coulter Avanti Centrifuge), equipped with JA-25.50 rotors. Any refrigerated centrifuge capable of spinning 50 mL tubes at ~2,000 × *g* is equivalent for this purpose.
2. A liquid chromatography system capable of delivering linear gradients and operating columns at the described flow rates and pressures.
3. A 40 mL and 15 mL Dounce homogenizer.
4. 14 kDa dialysis tubing and clamps.
5. A large stir plate and a magnetic stir bar.
6. Cold room or cold box with space for the stir plate.
7. Fluorometer: We recommend a system with monochromator based excitation and emission wavelength selection, and some degree of band-pass control. Fluorescence light source must be capable of illuminating at 365 nm.
8. Fluorescence cuvettes: Many styles of cuvette may be used for this assay, but we use a 3 mm × 3 mm microvolume cuvette. This cuvette ends up being a good compromise between sample volume (200 μL), cost and ease of complete cleaning.
9. Microvolume pipettes: P-200, P-20, P-10, or equivalent.

3 Methods

3.1 Purify and Pyrene Label Actin

1. Ensure that centrifuges and rotors are cold.
2. Weigh out 4–5 g rabbit muscle acetone powder.
3. Place 20 mL of cold buffer G per gram of rabbit muscle acetone powder in a beaker and add muscle acetone powder. Stir at 4 °C for 30 min.
4. Filter solution through four layers of cheesecloth. Recover and resuspend the muscle acetone powder residue in 20 mL of cold buffer G per gram of starting weight (*see* **step 2**). Stir at 4 °C for 30 min.
5. Filter solution through four layers of cheesecloth and combine with the filtrate from **step 4**.

6. Centrifuge the filtrate for 30 min at 20,000×*g* (16,000 rpm) at 4 °C in a JA-25.50 rotor or equivalent.
7. Carefully decant the supernatant into a graduated cylinder (pellet is soft) and measure the volume.
8. Begin stirring and slowly add 2 M KCl to a final concentration of 50 mM. Slowly add 1 M $MgCl_2$ to a final concentration of 2 mM. Continue to stir for 2 h at 4 °C.
9. After 2 h has passed, slowly add solid KCl to a final concentration of 800 mM (add 5.6 g per 100 mL of solution volume). Stir for 30 min at 4 °C.
10. Collect actin filaments from **step 9** by centrifugation. Centrifuge at >100,000×*g* for 2 h at 4 °C (35,000 rpm in a Type 70 Ti or Type 45 Ti rotor) (*see* **Note 4**).
11. Discard supernatant. Rinse pellet (containing filamentous actin) with ~500 μL of buffer G.
12. Transfer the pellet into a Dounce homogenizer. Place 8 mL/g of starting rabbit muscle acetone powder weight into the body of a 40 mL Dounce homogenizer. Lightly scrape the pellets from the centrifuge tube using a curved spatula and transfer to the homogenizer. The pellet will stick to the spatula and can be transferred by scraping it onto the pestle, and then dislodging from the pestle into the buffer in the homogenizer. Gently passage the homogenizer pestle up and down about 50 times to resuspend the pellet, trying not to incorporate air. If the solution remains highly viscous as it is processed, dilute it slightly with buffer G.
13. Rinse 12–15 cm lengths of 14 kDa MWCO dialysis tubing in water and equilibrate a few minutes in buffer G.
14. Place resuspended actin from **step 12** into 14 kDa MWCO dialysis tubing. Dialyze against 2 L buffer G overnight.
15. Change the buffer on the second and third nights, using buffer G made without DTT.
16. On the morning following the third night of dialysis, collect the solution in the dialysis bags. Retain a small amount of dialysis buffer. Remove actin filaments from the dialyzed solution by centrifugation at >100,000×*g* for 2 h, at 4 °C (using a Type 70 Ti rotor at 35,000 rpm or a SW 41 Ti rotor at 40,000 rpm) (*see* **Note 4**).
17. Equilibrate a Superdex 200 pg gel filtration column with buffer G.
18. Carefully remove the centrifuge tubes from the rotor, minimizing jostling. Collect the upper 1/2 of the supernatant and inject onto the equilibrated Superdex 200 pg gel filtration column, collecting in 5 mL fractions. Decant the remaining supernatant solution into a small glass beaker and reserve at 4 °C.

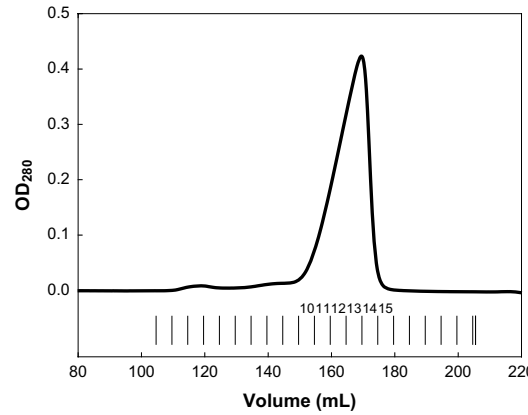

Fig. 1 Gel filtration chromatogram for pyrene labeled actin. An example of the UV absorbance detected chromatogram for pyrene labeled actin purification using a 320 mL Superdex 200 pg column. UV absorbance is shown with a *thick black line*. Fractions collected are shown with *short vertical lines*. Relevant fraction numbers are shown. The shape of the chromatographic peak is characteristic for actin purified using Superdex 200, and running the column in buffer G. For this purification, fractions 12, 13, and 14 were retained, and fractions 13 and 14 were used preferentially

19. Choose gel filtration fractions to save (*see* Fig. 1 and **Note 5**). Measure the concentration of actin in each fraction by UV absorbance (*see* **Note 6**). Transfer fractions into separate small pieces of equilibrated 14 kDa MWCO dialysis tubing (*see* **Note 7**), and store in buffer G. Store actin in a large stirred beaker at 4 °C, in 2 L of buffer G; change the buffer twice per week. Seal the top of the beaker with plastic wrap and aluminum foil. Stored in this fashion, actin can typically be kept for 2 months.
20. Add a clean magnetic stir bar to the glass beaker with the actin supernatant in it (*see* **step 18**), and begin stirring the solution slowly at 4 °C. Note the volume of supernatant. Measure the concentration of actin by UV absorbance (*see* **Note 6**), using the dialysis buffer reserved in **step 16** as the absorbance blank.
21. Slowly add 2 M KCl to a final concentration of 50 mM. Slowly add 1 M $MgCl_2$ to a final concentration of 2 mM. Continue to stir for 2 h.
22. From the concentration and volume measured in **step 20**, calculate the total actin present. Add a five- to ten-fold molar excess of *N*-(1-pyrene) iodoacetamide. Close off the top of the beaker with parafilm or saran wrap. Then wrap the entire beaker with aluminum foil to protect it from light (*see* **Note 8**). Stir over night at 4 °C.
23. The next morning, centrifuge the labeling reaction at 4 °C, at ~2,000 × *g* (5,000 rpm the Beckman Avanti JA-25.50 rotor)

for 5 min to remove excess dye. Remove the supernatant with a pipette (the pellet is very soft).

24. Collect actin filaments from the supernatant from **step 23** by centrifugation. Centrifuge at >100,000 × *g* for 2 h at 4 °C (using a Type 70 Ti rotor at 35,000 rpm or a SW 41 Ti rotor at 40,000 rpm) (*see* **Note 4**).
25. Collect centrifuge tubes and discard supernatant. Rinse pellets (containing pyrene labeled filamentous actin) with ~500 μL of buffer G.
26. Transfer the pellet into a Dounce homogenizer. To do this, place 8–12 mL of buffer G into the homogenizer body. Lightly scrape the pellets from the centrifuge tube using a 3–7 mm wide, slightly curved spatula. The pellet will stick to the spatula, and can be transferred by scraping it onto the pestle, and then dislodging from the pestle into the buffer in the homogenizer. The pellet will typically be somewhat opaque with residual pyrene iodoacetamide. Gently passage the homogenizer pestle up and down about 50 times to resuspend the pellet, trying not to incorporate air. Once resuspended the solution will appear slightly turbid. If the solution remains highly viscous as it is processed, dilute it slightly with buffer G.
27. Rinse 12–15 cm lengths of 14 kDa MWCO dialysis tubing in water and equilibrate a few minutes in buffer G.
28. Place resuspended actin from **step 26** into 14 kDa MWCO dialysis tubing. Dialyze against 2 L buffer G for 3 nights, changing the buffer on the second and third nights.
29. On the morning following the third night of dialysis, collect the solution in the dialysis bags. Remove actin filaments from the dialyzed solution by centrifugation at >100,000 × *g* for 2 h at 4 °C (using a Type 70 Ti rotor at 35,000 rpm or a SW 41 Ti rotor at 40,000 rpm) (*see* **Note 4**).
30. Equilibrate a Superdex 200 pg gel filtration column with buffer G.
31. Carefully remove the centrifuge tubes from the rotor, minimizing jostling. Collect the upper 2/3 of the supernatant. Inject supernatant onto equilibrated Superdex 200 pg gel filtration column.
32. Choose gel filtration fractions to save (*see* Fig. 1 and **Note 5**). Measure the concentration of actin and degree of pyrene labeling in each fraction (*see* **Note 9**). Transfer fractions into separate small pieces of equilibrated 14 kDa MWCO dialysis tubing (*see* **Note 7**), and store in buffer G. Store pyrene labeled actin in a large stirred beaker at 4 °C, in 2 L of buffer G; change the buffer twice per week. Seal the top of the beaker with plastic wrap and cover the whole beaker with aluminum foil to prevent

light from reaching the labeled actin, which will photobleach the pyrene. Stored in this fashion, pyrene actin can typically be kept for 2 months.

3.2 Pyrene Actin Polymerization Assays

Below is our protocol for preparing actin polymerization assays. The exact timing and addition order is not necessarily critical, but for best data reproducibility a specific order and timing should be planned. For clarity we also include an example of the process (*see* **Note 10**).

1. Turn on fluorometer, ignite the lamp and start the software (*see* **Note 11**).
2. Optionally remeasure the concentrations of actin and pyrene labeled actin by UV absorbance (*see* **Notes 6** and **9**).
3. Prepare actin stock. Calculate the number of reactions needed, including controls (*see* **Note 12**). Calculate the volume of actin and pyrene labeled actin needed for the entire "actin stock" at the desired actin concentration and labeling (*see* **Note 13**). Check that the concentration of actin in the planned actin stock is at least 2.2-fold greater than the desired assay concentration. Following this check, mix the calculated volumes of actin and pyrene labeled actin. Store the actin stock in a light-proof tube on ice.
4. Calculate the volumes of all materials needed in the assay. The assay solution is divided into two parts. The first is an actin containing mixture (Mix A) and the second contains all additional proteins in a salt containing solution (Mix P). For our assay, Mix A and Mix P are both 100 μL in volume. The components of Mix A are typically kept constant throughout the experiment; Mix P is usually different for each reaction, as the experiment dictates. Before starting to mix the components for a reaction, calculate all the volumes needed in both Mix A and Mix P. Mix A contains the actin stock prepared above, 10E/1 M buffer and buffer G-Mg (*see* **steps 6–10** below). Mix P components include buffer KMEI, nucleation factors, additional proteins, 10× KMEI and additional KCl, if needed (*see* **steps 11–14** and **Note 14**).
5. Initialize the fluorometer for data acquisition. On most fluorometer systems, positioning monochromators, setting slit widths, and initializing the data set can be performed prior to starting data collection. This helps to minimize the delay between combining Mix A and P and beginning data collection. Pyrene-actin fluorescence is excited at 365 nm and emission is detected around 407 nm. The overall excitation and emission of pyrene is actually rather broad, but the enhancement used to detect filament formation occurs only in narrow bands. We use 1 nm band pass for excitation, and 5 nm band

pass for emission when using a PTI QuantaMaster fluorometer with monochromator based wavelength selection for both excitation and emission (*see* **Note 11**).

6. Begin preparing Mix A by pipetting the volume of actin stock needed to give a 4 μM final concentration in 200 μL into a 1.5 mL tube.
7. One tenth of the volume (of the actin stock) of 10E/1 M is added to Mix A to exchange the Ca^{2+} for Mg^{2+}.
8. Finally, add the volume of buffer G-Mg needed to give a final volume of 100 μL.
9. Mix by pipetting up and down three times and start a timer counting up.
10. Mix A is incubated at room temperature (~22 °C) for 2 min. Two minutes is enough time for the exchange of calcium and magnesium bound to actin to come to completion. Any time between 2 min and 1 h of exchange time will be fine, but the timing should be consistent between samples. If a different exchange time is desired, adjust the timing in **steps 14** and **15** accordingly.
11. Begin preparing Mix P by pipetting the volume of KMEI needed into a new 1.5 mL tube.
12. Add the appropriate volumes of the nucleation factors and additional proteins (*see* **step 4**), beginning with the nucleation factor (if used). For improved assay reproducibility, add proteins and additives in the same order and with the same timing and pipetting operations.
13. Add 10× KMEI to Mix P. The 10× KMEI accounts for the different buffer conditions in Mix A. Add enough 10× KMEI to bring the final salt concentration (after Mix A and P are combined) to 50 mM KCl, while maintaining the final imidazole, magnesium and EGTA concentrations at those of KMEI. If different salt conditions are used, it may also be necessary to add 2 M KCl and or KMEI lacking KCl to correct the salt while keeping the other buffer components constant. In that case, correct the 10× KMEI addition to account for the volume of 2 M KCl, which lacks imidazole, magnesium and EGTA (*see* **Note 14**).
14. With P-200 pipette set on 200 μL pipette Mix P up and down three times being careful not to blow bubbles into the liquid. When the timer shows 1 min 50 s, pull all of Mix P into the pipette tip.
15. At exactly 2 min (*see* **Note 15**) add all of Mix P (100 μL) to the tube containing Mix A. Pipet up and down one time to mix, and then transfer total volume to a clean cuvette (*see* **Note 16**).

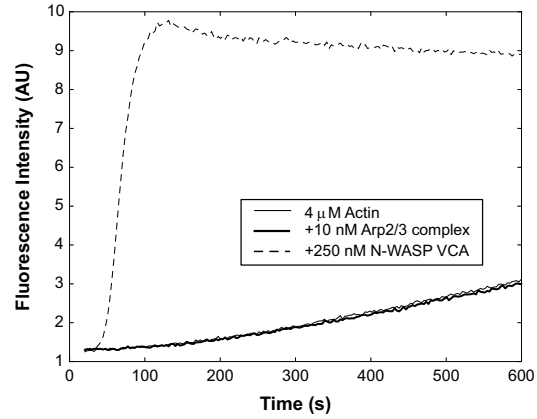

Fig. 2 Pyrene actin polymerization assay example. Four micromolar actin, 5 % pyrene labeled is brought from buffer G-Mg conditions to KMEI conditions to trigger polymerization of actin. Pyrene fluorescence intensity (*Y*-axis) as a function of time (*X*-axis) are shown for actin alone (*thin line*), actin in the presence of 10 nM bovine Arp2/3 complex (*thick line*) and actin in the presence of 10 nM bovine Arp2/3 complex and 250 nM N-WASP VCA (*dashed line*). These three curves are the controls for the basic behavior of actin and Arp2/3 complex

16. Place the cuvette into the fluorometer and start data collection. Record the time elapsed between addition of Mix P to Mix A and the time data collection begins (*see* **Note 15**).
17. Record the time course for pyrene intensity (*see* **Note 11** and Fig. 2) until a maximum intensity is reached and begins to descend again. Depending on the reaction conditions, this may take less than 100 s (expected for our example) or longer than 10,000 s (e.g., 1 μM actin alone). For reactions with such different time scales, it may be necessary to alter the illumination method to reduce photobleaching. While short kinetic reactions can be illuminated continuously, longer time courses may benefit from illumination in 0.1–0.5 s intervals, separated by as long 10 s (*see* **Note 11**).
18. Repeat **steps 4** through **17** for each reaction desired.

3.3 Analysis of Pyrene Actin Polymerization Assays

Here we describe the calculation of several simple metrics: the time at which half of the fluorescence intensity change has occurred ($t_{1/2}$) (*see* **steps 1–6**), the actin polymerization rate at $t_{1/2}$ (*see* **steps 1–8**), the number of barbed ends present at $t_{1/2}$ (*see* **steps 1–10**), and the initial filament nucleation rate (*see* **steps 1–5**, **7**, and **11**). The calculation of $t_{1/2}$ is the most resilient with noisy data, and does not require knowledge of actin critical concentration or growth rate constants. The other three metrics inform more directly on the underlying biochemical activities, but require additional knowledge about actin biochemistry. Typically, only one of these metrics will be presented for a dataset. To simplify

automation of the analysis process, our method emphasizes a work-flow that reduces human intervention (*see* **Note 2**).

1. Import the data into a spreadsheet or other computational environment (*see* **Note 2**).
2. Correct the time values for any known delay between the mixing of Mix A and Mix P and the first time point. This is the recorded time elapsed in Subheading 3.2, **step 16**. Time corrected fluorescence intensity data will be referred to as $f(t)$ below.
3. Plot the intensity data as a function of time, ideally comparing it to a series of control datasets to ensure that the data appears sensible, and does not show any obvious pathologies (excessive noise, spurious peaks, etc.) (*see* **Note 17**).
4. Find the minimum intensity, $I_{\min}$, for the data set (*see* Fig. 3). In cases of slow kinetics, short dead-times, and high sampling rates, choose ten points that are near the minimum and average them. For faster kinetics and hand mixed samples with dead-times of greater than 30 s, any group of points will overestimate the minimum. Instead we use the minimum intensity data point. Alternatively, we make use of the fact that the minimum intensity should agree between datasets collected in the same session (Fig. 2). This allows us to use the slowest dataset in a group (typically actin alone) to estimate the minimum intensity for all datasets collected in a given session.
5. Find the maximum intensity, $I_{\max}$, for the data set (*see* Fig. 3). Find the ten highest intensity data points and record the associated times. Take the average of these times to estimate the time when the maximum intensity occurs (this reduces the cases where a single anomalous data point leads to incorrect identification of the maximum), retain this time at $t_{\max}$. Find the ten datapoints closest to $t_{\max}$, and take the average of their intensity. This average intensity is used as the maximum intensity, $I_{\max}$.
6. Calculate $t_{1/2}$ for the data set (*see* Fig. 3). First, exclude all datapoints at times greater than $t_{\max}$. Choose the fraction of the intensity change used to find $t_{1/2}$, which we term δ. δ is typically between 0.04 and 0.2. Collect the data points with intensities between $(0.5-\delta/2)\times(I_{\max}-I_{\min})+I_{\min}$ and $(0.5+\delta/2)\times(I_{\max}-I_{\min})+I_{\min}$. Using linear least squares, fit a line to these data points. Record the slope, $m_{t1/2}$, and intercept, $b_{t1/2}$, of the line. Visually inspect where these points fall in the dataset, and how the line fits to the considered points. $t_{1/2}$ is then found using:

$$t_{1/2}=\left(0.5\times(I_{\max}-I_{\min})+I_{\min})+b_{t1/2}\right)/m_{t1/2}. \quad (1)$$

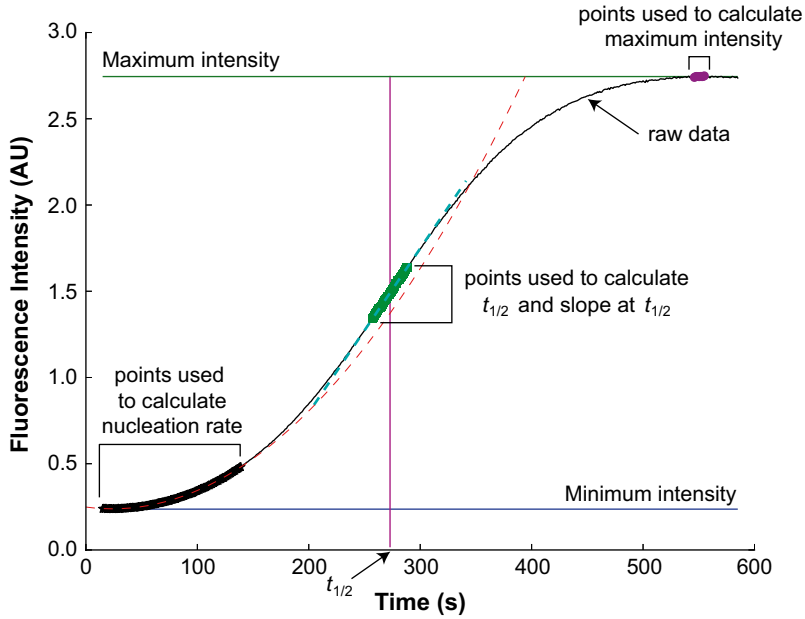

Fig. 3 Graphical representation of the analysis of pyrene actin polymerization data. 4 μM rabbit muscle actin (5 % pyrene labeled) is induced to polymerize by shifting to KMEI conditions (*see* Subheading 3.2) and adding 10 nM bovine Arp2/3 complex and 40 nM of N-terminally modified WASP VCA. This results in nucleation of actin filaments. Raw data is shown as a *thin black line*. Shown are the aspects of the data used to calculate $t_{1/2}$, actin polymerization rate at $t_{1/2}$, barbed ends at $t_{1/2}$ and the initial nucleation rate. The minimum and maximum intensities are shown as *horizontal lines*. *Enlarged purple points* were averaged to determine the maximum intensity, these are also bracketed for clarity. *Enlarged green points* were used to find $t_{1/2}$ and to find the slope at $t_{1/2}$, these are also bracketed for clarity. *Enlarged black points* were used to find the initial nucleation rate, these are also bracketed for clarity. The determined value for $t_{1/2}$ is shown with a *vertical line*. The line fit to find $t_{1/2}$ and the slope at $t_{1/2}$ is shown as a *thick*, *dashed*, *cyan line*. The parabola fit to find the initial nucleation rate is shown as a *thin*, *dashed*, *red line*. Note that the parabola has a slight negative slope at $t=0$, and undershoots the raw data at later time points, both are indications that a single nucleation rate is not a good metric for this type of data

7. Rescale the deadtime corrected data from fluorescence intensity values into units of filament concentration. First, find the fluorescence intensity to actin filament concentration scaling factor, SF, for the data set. For this, one needs knowledge of the initial actin concentration, [Actin](0) and the critical concentration, c_0. c_0 can be calculated from the on-rate constant, k_+, and off rate constant, k_-, for filament assembly using:

$$c_0 = k_- / k_+. \quad (2)$$

In KMEI at room temperature, the barbed ends of rabbit muscle actin elongate and shrink with values of 11.6 $\mu M^{-1}s^{-1}$ and 1.4 S^{-1} for k_+ and k_-, respectively [17]. These rate

constants are highly sensitive to solution conditions, particularly to the presence of salt and changes in viscosity [19]. This allows calculation of the SF:

$$\mathrm{SF} = \left([\mathrm{Actin}](0) - c_0\right) / \left(I_{\max} - I_{\min}\right). \quad (3)$$

8. Calculate $AP_{t1/2}$, the rate of actin polymerization at $t_{1/2}$. Use $m_{t1/2}$, the slope of the line used to find $t_{1/2}$ in **step 6** (*see* **Note 3**), and SF, to calculate $AP_{t1/2}$:

$$\mathrm{AP}_{t1/2} = \mathrm{SF} \times m_{t1/2} \quad (4)$$

9. Find [Actin]($t_{1/2}$), the remaining free actin at $t_{1/2}$. This can be determined from values already calculated:

$$[\mathrm{Actin}]\left(t_{1/2}\right) = [\mathrm{Actin}](0) - \mathrm{SF} \times \left(\left(m_{t1/2} \times t_{1/2} - b_{t1/2}\right) - I_{\min}\right). \quad (5)$$

10. Find $BE_{t1/2}$, the number of filament barbed ends at $t_{1/2}$. This calculation recognizes that actin filaments grow at their ends and the rate constants for these processes are known in certain cases (e.g., rabbit skeletal muscle actin polymerizing in KMEI buffer). The calculation ignores growth at the pointed end, as the barbed end grows much faster than the pointed end, and for Arp2/3 complex nucleated reactions, many pointed ends are capped by Arp2/3 complex. Thus, barbed end growth dominates the kinetics, and the rate law for actin polymerization reduces to:

$$\mathrm{d}[\mathrm{Filament}](t) / \mathrm{d}t = k_+ \times [\mathrm{Actin}](t) \times [\mathrm{Barbed\ Ends}](t) - k_- \times [\mathrm{Barbed\ Ends}](t). \quad (6)$$

Considering the rate law at $t_{1/2}$ we can solve for $BE_{t1/2}$ and substitute in the known values of actin polymerization and actin concentration, we then find $BE_{t1/2}$ using

$$\mathrm{BE}_{t1/2} = \mathrm{AP}_{t1/2} / \left(k_+ \times [\mathrm{Actin}]\left(t_{1/2}\right) - k_-\right). \quad (7)$$

11. Find NR_0, the initial nucleation rate. If there is a constant rate of nucleation of actin filaments through the initial portion of the reaction, then filament end concentration will grow linearly with time. This is true in some systems, and may be more directly related to the nucleation factor activity than the other metrics (*see* **Note 18**). By limiting our analysis to times where the concentration of free actin has not changed much from the initial concentration, we can directly fit the data with an approximate solution to the time dependence of the system (*see* **Note 19**).

Choose a fraction of the intensity change to use in determining the nucleation rate, which we refer to as γ. From the

time corrected dataset (*see* **step 2**), select those data points that have intensity values between $I_{\min}$ and $\gamma \times (I_{\min} - I_{\min}) + I_{\min}$, where γ is between 0.05 and 0.2 (typically 0.1 is used). Using linear least squares fitting, fit the selected data to:

$$f(t) = A \times t^2 + B \times t + C. \tag{8}$$

Visually inspect the quality of the fit to the data (*see* Fig. 3). B should be near zero and C should be near $I_{\min}$ (*see* **Notes 18** and **19**). Repeating the fit with slightly different values of γ (e.g., 0.06, 0.08, 0.1 and 0.12) should not result in substantially different values of A, B or C. The nucleation rate is then calculated as:

$$\mathrm{NR}_0 = (2 \times A \times \mathrm{SF}) / \left(k_+ \times [\mathrm{Actin}](0) - k_-\right). \tag{9}$$

4 Notes

1. In a few cases, the system can be set up such that pseudo-first order conditions can be achieved. For example, if the reaction is set up with a known quantity of seed, which is sufficient to overwhelm any nucleation, the system will elongate in a fashion consistent with a first order reaction. This can be fit using analytic equations. Further, if one has a known kinetic model with only a few varied parameters, one could in principle use numeric approaches to solve the rate laws for the model and fit pyrene actin polymerization data directly [15, 21, 22]. Owing to the complexity of the kinetic models for nucleation pathways, this is not a widely used approach. The initial nucleation rate method described in Subheading 3.3/**Note 19** is an example of this approach.
2. We have found that automating the analysis of the kinetics through the use of an in house developed computer script improves the consistency, reliability and practicality of such analyses. Despite this, we still find it helpful for a human to visually examine the data and extracted numbers (*see* Fig. 3).
3. In our experience, the determination of the maximum slope, or maximum barbed ends introduces a fair bit of noise. Examining the polymerization rate or barbed ends as a function of time, a maximum can typically be seen, and the rough center identified by eye. Unfortunately, automatically identifying this maximum in an unbiased fashion, in the context of noisy data, is challenging. Instead, we recommend that the barbed ends or actin polymerization rate be tracked at some easily identified characteristic time, such as $t_{1/2}$. Moreover, for

Arp2/3 complex dependent nucleation assays, the time at which barbed ends reach their maximum and $t_{1/2}$ are typically very similar. Thus, the actual numbers found by the two methods tend to be quite similar, but determining the value at $t_{1/2}$ removes the noise and bias associated with finding the maximum.

4. Fill tubes according to manufacturer's instructions. Generally, at the speeds used here, tubes should be very nearly full. In scaling the preparation up and down, try to anticipate the changes in volume that will result and change the rotor and tube choices accordingly.
5. The actin and pyrene-actin gel filtration peaks have a characteristic asymmetric shape, with a leading tail (*see* Fig. 1). This may stem from the low salt conditions under which the column is run, or may be related to oligomerization. For the 320 mL Superdex 200 column, we collect 5 mL fractions. We keep only the three most concentrated fractions, which should be greater than 10 μM actin and, for the pyrene labeled actin, be greater than 35 % labeled, and discard fractions from the leading edge of the peak.
6. To calculate the actin concentration, measure the absorbance at 290 nm to reduce the interference from ATP. Use of absorbance at 290 nm instead of 280 nm reduces the interference from nucleotide. Actin has an extinction coefficient at 290 nm of 26,600 $M^{-1}cm^{-1}$.
7. Conventional dialysis tubing is recommended for the actin preparation because our experience shows that it is the least prone to actin losses during the prolonged dialysis steps.
8. To reduce photobleaching of pyrene actin we take several steps to minimize light exposure. We wrap columns in aluminum foil to prevent light penetration while the column is running. Similarly, we shield fractions with another piece of aluminum foil during and after collection. We turn off lights in the cold box containing the chromatography system.
9. To calculate the concentration and labeling efficiency of pyrene actin we measure the absorbance at 290 and 344 nm. Pyrene concentration is determined by absorbance at 344 nm, using an extinction coefficient of 22,000 $M^{-1}cm^{-1}$. To calculate the actin concentration we first account for the contribution from pyrene at 290 nm, which is found by multiplying the absorbance at 344 nm by 0.127. The remaining absorbance at 290 nm comes from actin. The fraction of pyrene labeling is found by dividing the concentration of pyrene by the concentration of actin. The fractional pyrene labeling should be relatively consistent across the different fractions, but different preparations may vary between 35 and 100 % labeled.

10. For clarity, we provide an example of the calculations used to run a hypothetical assay (analogous to the Actin + Arp2/3 complex + VCA sample in Fig. 2).

    First we make an actin stock for twenty five 200 μL reactions with 4 μM of 5 % pyrene labeled actin. We will make these from a 30 μM actin stock and a 20 μM 50 % labeled pyrene actin stock. The stock needs a total of 1 nmol of pyrene and 20 nmol of actin. Thus, we find that 100 μL of the pyrene labeled actin is needed (1×10^{-9} mol/1×10^{-5} M pyrene). As the actin is 50 % labeled, this introduces 2 nmol of actin, and the remaining 18 nmol of actin is provided with 600 μL of the 30 μM actin stock. We want at least an 8.8 μM actin concentration (4 μM × 2.2) in the actin stock, and our stock is ~28.6 μM.

    Next we plan out an actual reaction. Our reaction will contain 4 μM actin (5 % pyrene labeled), 10 nM Arp2/3 complex and 250 nM VCA. We assume stock concentrations of 400 nM Arp2/3 complex in KMEI and 10 μM VCA in KMEI. We plan Mix A as 28 μL from the above prepared actin stock, and 2.8 μL of 10E/1 M. The remaining volume is made up with 69.2 μL of buffer G-Mg. Mix P will need 5 μL each of the Arp2/3 complex stock and the VCA stock. As Arp2/3 complex and VCA are in KMEI, we only need to add 10× KMEI to account for the volume of Mix A (which we treat as not contributing to either total salt or the "MEI" concentration) and the volume of 10× KMEI added. This is 11.1 μL of 10× KMEI, and 78.9 μL of KMEI to bring the Mix P volume to 100 μL.

    With the calculations complete, we prepare the actual reaction. We setup the fluorometer to acquire one data point every other second, illuminating only during the 0.5 s time that data is acquired. The system is initialized and left waiting to start the kinetic acquisition. We prepare Mix A by placing 28 μL of the actin stock in a fresh tube and adding 2.8 μL of 10E/1 M. Shortly after, we add 69.2 μL of buffer G-Mg, mix by pipetting and begin our timer counting up. We prepare Mix P by placing 78.9 μL of KMEI in a separate fresh tube. We add 5 μL of the 400 nM Arp2/3 complex stock, then we add 5 μL of the 10 μM VCA stock. When the timer reads 1 min 50 s, 11.1 μL of 10× KMEI is added to Mix P. Then all of Mix P is picked up with a P-200. When the timer reads 2 min exactly, Mix P is added to Mix A. The contents are mixed, transferred to a cuvette and data acquisition is started when the timer reads 2 min 20 s. The dead time is recorded as 20 s.

11. We have also adapted the assay to a plate reader (Thermo Scientific Varioskan Flash) with good results. In this case, the instrument uses monochromators for wavelength selection, but allows very little control over the width of the excitation and emission band pass, with only 5 and 12 nm options. As a

result we found that the overall change in signal was only six- to eightfold. While the resulting dynamic range is not as large as is theoretically possible, the plate-reader based assay is still very useful. In principal, filter based excitation and emission methods are also possible, but the filters will need to be selected carefully.

Pyrene-actin fluorescence intensity is prone to photobleaching. Photobleaching can be reduced to acceptable levels by either attenuating illumination intensity through decreased band pass or with neutral density filters, or decreasing the time of illumination. In using a narrow band pass (1 nm), we have strongly attenuated our excitation intensity, which partly improves photobleaching. For longer kinetics, we further decrease photobleaching by illuminating and measuring for 0.5 s and then closing an excitation shutter for 2.5 s. This is then repeated for as many as 1,000 cycles, depending on the timing of the reaction.

Pyrene emission intensity is slightly sensitive to events in addition to polymerization. In faster kinetics, a slight "overshoot" is frequently observed. This is not due to photobleaching, but instead is commonly ascribed to events of ATP hydrolysis and/or phosphate release [23]. For slower kinetics the overshoot is not observed at all, as the later step will occur as filament is formed. We have also observed a few cases where the proteins added to a polymerization reaction have changed the intensity of pyrene fluorescence, presumably by binding filament and changing the environment of the pyrene. The exact solution to such a problem will depend on the system (increasing salt concentrations has helped for our systems), but it is worth paying attention to any anomalous pyrene fluorescence intensity that is observed.

12. Actin polymerization is very sensitive to small differences in concentration, and to very small quantities of seed fibers that may be present. Thus, we run a set of controls each day that detects any problems in the actin stock, or in the nucleation factors. The controls run for a series of actin nucleation assays in the presence of Arp2/3 complex are: actin in the absence of Arp2/3 complex, actin with Arp2/3 complex, and actin with Arp2/3 complex in the presence of saturating N-WASP VCA (*see* Fig. 2). Together, comparison of these data to analogous data acquired on other days will detect problems with buffers, actin, or Arp2/3 complex. For the best results, compare kinetics collected on the same day using a single actin mix. We have generally had good results comparing between actin mixes, but this eliminates all variability concerns.
13. Up to 10 % pyrene labeling of actin is routinely used. For actin polymerization assays in the absence of profilin, total actin concentrations between 1 and 4 μM are routinely used.

For single reactions, we generally use 4 μM actin (5 % pyrene labeled) in a 200 μL reaction. When working in a multi-well plate, we generally use 2 μM actin (10 % pyrene labeled) in a 200 μL reaction. We generally make a single actin mix sufficient for a day's worth of assays, accounting for controls and including ~10 % extra. The mix is stored, protected from light, on ice. Typically, we use a mix within 16 h of preparation, but have not seen evidence of changes in behavior up to about 36 h.

14. The protocol presented here is for assay of actin polymerization in KMEI, a buffer with 50 mM KCl. Different pHs, concentrations of salts, or osmolytes can be used, but will result in substantial differences in actin polymerization kinetics. Thus, particular attention should be paid to normalizing the buffer across a given set of assays, and comparisons should typically only be made between samples under identical buffer conditions.

    Despite this, some proteins may need to be prepared under different buffer conditions, and then corrected back to a standard condition in the assay. We address this problem by tracking the total concentrations of KCl, and of $MgCl_2$, EGTA and imidazole pH 7.0. Do not account for differences in salt concentrations just by changing the volume of 10× KMEI added. Doing so will usually result in higher or lower concentrations of the rest of the KMEI components, and will perturb the kinetics. Instead we prepare all proteins in buffers with different concentrations of KCl, but matched concentrations of all other components. Then the final protein mixes are supplemented with 2 M KCl, or a KMEI buffer lacking any KCl, such that the final salt and other component concentrations are matched. Where necessary, a similar procedure is used for matching glycerol concentrations.

15. As mentioned in Subheading 3.2, **steps 9**, **10**, **14**, and **15**, we perform actin polymerization assay pipetting events at exact times. This is not due to a 2 min incubation timing being essential (although we have found having a carefully planned pipetting schedule does improve reproducibility), but because it facilitates tracking the delay between combining Mix A and P and beginning the data collection without requiring additional equipment. With the timer counting up, combine Mix P with Mix A when it reads 2 min (after preparation of Mix A), and record the delay time as the time shown on the timer when monitoring of the kinetics begins, minus the 2 min delay.

16. A clean cuvette is essential for high quality data. Before performing actin polymerization assays, clean the cuvette by filling it with concentrated nitric acid and allowing it to sit

for at least 10 min. Discard the nitric and wash the cuvette thoroughly (7–10 times) with ultrapure water. Rinse the cuvette with ethanol and rapidly dry inside and outside the cuvette with compressed gas. After each reaction we rinse the cuvette seven times with ultrapure water and the three times with ethanol before drying. Every second or third assay we also find it useful to treat with 30 % bleach before the water wash. We recommend using just one cuvette for a set of assays, as different cuvettes will have different background scattering.

17. Random noise in these assays is on the order of 5 % or less of total signal. Noise of this order is easily addressed using the methods described. Nonrandom, systematic noise will be poorly handled.

18. If B is not near zero and C is different from $I_{\min}$, examine the fit. If it is of poor quality a fixed nucleation rate may be a poor metric for analysis. If the fit is of good quality, check the results for an actin alone control dataset from the same day; ensure that there is not extensive evidence of seed filament.

    We note that this approximation is not expected to hold once a significant portion of actin monomer has been consumed to form filaments, nucleation should slow as actin monomers are depleted from solution. Thus, only a small fraction of the signal change should be fit in this way. The fraction used will depend somewhat on the signal to noise in the data. When analyzing Arp2/3 complex dependent actin polymerization reactions, we also note that Arp2/3 complex requires binding to an existing filament in order to nucleate a new filament. Thus, depending on the affinity of Arp2/3 complex for filament, the nucleation rate may accelerate as filament accumulates. The latter effect is noticeable in Fig. 3, the curve extrapolated through the data underestimates the intensity at longer times.

19. Assuming that growth is dominated by growth at the barbed ends, we have the rate law for the increase of actin polymerization from Subheading 3.3, **step 10**:

$$\begin{aligned} \mathrm{d}[\text{Filament}](t) / \mathrm{d}t = k_{+} \times [\text{Actin}](t) \times [\text{Barbed Ends}](t) \\ - k_{-} \times [\text{Barbed Ends}](t). \end{aligned}$$

    We limit our analysis to the region of the portion of the data where little of the actin has been consumed. Thus:

$$[\text{Actin}](t) \sim [\text{Actin}](0). \tag{10}$$

    Interpreting the data in terms of a single nucleation rate means that the concentration of barbed ends grows linearly with time, with the rate of nucleation being NR_0.

$$[\text{Barbed Ends}](t) = \mathrm{NR}_0 \times t + [\text{Barbed Ends}](0). \tag{11}$$

By substituting this growth of barbed ends (11), and the actin concentration approximation (10) into the rate law for filament growth (6) we find:

$$\mathrm{d}[\mathrm{Filament}](t)/\mathrm{d}t = \left(k_{+} \times [\mathrm{Actin}](0) - k_{-}\right) \left(\mathrm{NR}_0 \times t + [\mathrm{Barbed\ Ends}](0)\right). \quad (12)$$

To simplify, we substitute:

$$\kappa = \left(k_{+} \times [\mathrm{Actin}](0) - k_{-}\right). \quad (13)$$

into (12) and find:

$$\mathrm{d}[\mathrm{Filament}](t)/\mathrm{d}t = \kappa \times \left(\mathrm{NR}_0 \times t + [\mathrm{Barbed\ Ends}](0)\right). \quad (14)$$

Integrating (14) with respect to time we find that filament concentration (in monomer actin units incorporated) over time is:

$$[\mathrm{Filament}](t) = 1/2 \times \kappa \times \mathrm{NR}_0 \times t^2 + \kappa \times [\mathrm{Barbed\ Ends}](0) \times t + [\mathrm{Filament}](\mathbf{0}). \quad (15)$$

Assuming the fluorescence intensity reports directly on the total concentration of monomers incorporated into filament, the data will follow:

$$f(t) = [\mathrm{Filament}](t)/\mathrm{SF} + I_{\min}. \quad (16)$$

We have fit the data (*see* Subheading 3.3, **step 11**) where the actin concentration is near the initial concentration to:

$$f(t) = A \times t^2 + B \times t + C.$$

We substitute (16) into (8), removing $f(t)$:

$$[\mathrm{Filament}](t)/\mathrm{SF} + I_{\min} = A \times t^2 + B \times t + C. \quad (17)$$

Substituting the expression for $[\mathrm{Filament}](t)$ in (15) into (17) and find:

$$\left(1/2 \times \kappa \times \mathrm{NR}_0 \times t^2 + \kappa \times [\mathrm{Barbed\ Ends}](0) \times t + [\mathrm{Filament}](0)\right)/\mathrm{SF} + I_{\min} = A \times t^2 + B \times t + C. \quad (18)$$

By subtracting the right hand side from the left hand side of (18), then grouping the constant, t, and t^2 terms, and solving for A, B, and C we find:

$$A = 1/2 \times \kappa \times \mathrm{NR}_0/\mathrm{SF}. \quad (19)$$

$$B = \kappa \times [\mathrm{Barbed\ Ends}](0)/\mathrm{SF}. \quad (20)$$

$$C = [\mathrm{Filament}](0)/\mathrm{SF} + I_{\min}. \quad (21)$$

If we assume that upon dilution of actin into salt, there are no barbed ends or filament initially (that [Barbed Ends](0) = [Filament](0) = 0) we find that B should be 0 and C should be $I_{\min}$.

Substituting for κ (using (13)) in (19), and solving for NR_0, we find:

$$NR_0 = (2 \times A \times SF) / \left(k_+ \times [\text{Actin}](0) - k_-\right).$$

References

1. Weinberg J, Drubin DG (2012) Clathrin-mediated endocytosis in budding yeast. Trends Cell Biol 22(1):1–13
2. Pollard TD, Cooper JA (2009) Actin, a central player in cell shape and movement. Science 326(5957):1208–1212
3. Pollard TD (2010) Mechanics of cytokinesis in eukaryotes. Curr Opin Cell Biol 22(1):50–56
4. Campellone KG, Welch MD (2010) A nucleator arms race: cellular control of actin assembly. Nat Rev Mol Cell Biol 11(4):237–251
5. Dominguez R (2009) Actin filament nucleation and elongation factors–structure–function relationships. Crit Rev Biochem Mol Biol 44(6): 351–366
6. Chesarone MA, DuPage AG, Goode BL (2010) Unleashing formins to remodel the actin and microtubule cytoskeletons. Nat Rev Mol Cell Biol 11(1):62–74
7. Kouyama T, Mihashi K (1981) Fluorimetry study of N-(1-pyrenyl)iodoacetamide-labelled F-actin. Local structural change of actin protomer both on polymerization and on binding of heavy meromyosin. Eur J Biochem 114(1):33–38
8. Cooper JA, Walker SB, Pollard TD (1983) Pyrene actin: documentation of the validity of a sensitive assay for actin polymerization. J Muscle Res Cell Motil 4(2):253–262
9. Reymann AC, Boujemaa-Paterski R, Martiel JL, Guerin C, Cao W, Chin HF, De La Cruz EM, Thery M, Blanchoin L (2012) Actin network architecture can determine myosin motor activity. Science 336(6086):1310–1314
10. Pollard TD, Mooseker MS (1981) Direct measurement of actin polymerization rate constants by electron microscopy of actin filaments nucleated by isolated microvillus cores. J Cell Biol 88(3):654–659
11. Blanchoin L, Amann KJ, Higgs HN, Marchand JB, Kaiser DA, Pollard TD (2000) Direct observation of dendritic actin filament networks nucleated by Arp2/3 complex and WASP/Scar proteins. Nature 404(6781):1007–1011
12. Akin O, Mullins RD (2008) Capping protein increases the rate of actin-based motility by promoting filament nucleation by the Arp2/3 complex. Cell 133(5):841–851
13. Yu B, Cheng HC, Brautigam CA, Tomchick DR, Rosen MK (2011) Mechanism of actin filament nucleation by the bacterial effector VopL. Nat Struct Mol Biol 18(9):1068–1074
14. Padrick SB, Doolittle LK, Brautigam CA, King DS, Rosen MK (2011) Arp2/3 complex is bound and activated by two WASP proteins. Proc Natl Acad Sci U S A 108(33):E472–E479
15. Padrick SB, Cheng HC, Ismail AM, Panchal SC, Doolittle LK, Kim S, Skehan BM, Umetani J, Brautigam CA, Leong JM, Rosen MK (2008) Hierarchical regulation of WASP/WAVE proteins. Mol Cell 32(3):426–438
16. Otomo T, Tomchick DR, Otomo C, Panchal SC, Machius M, Rosen MK (2005) Structural basis of actin filament nucleation and processive capping by a formin homology 2 domain. Nature 433(7025):488–494
17. Fujiwara I, Vavylonis D, Pollard TD (2007) Polymerization kinetics of ADP- and ADP-Pi-actin determined by fluorescence microscopy. Proc Natl Acad Sci U S A 104(21): 8827–8832
18. Cooper JA, Buhle EL Jr, Walker SB, Tsong TY, Pollard TD (1983) Kinetic evidence for a monomer activation step in actin polymerization. Biochemistry 22(9):2193–2202
19. Drenckhahn D, Pollard TD (1986) Elongation of actin filaments is a diffusion-limited reaction at the barbed end and is accelerated by inert macromolecules. J Biol Chem 261(27):12754–12758
20. Spudich JA, Watt S (1971) The regulation of rabbit skeletal muscle contractionI. Biochemical studies of the interaction of the tropomyosin-troponin complex with actin and the proteolytic fragments of myosin. J Biol Chem 246(15):4866–4871
21. Beltzner CC, Pollard TD (2008) Pathway of actin filament branch formation by Arp2/3 complex. J Biol Chem 283(11):7135–7144
22. Zalevsky J, Lempert L, Kranitz H, Mullins RD (2001) Different WASP family proteins stimulate different Arp2/3 complex-dependent actin-nucleating activities. Curr Biol 11(24):1903–1913
23. Brooks FJ, Carlsson AE (2008) Actin polymerization overshoots and ATP hydrolysis as assayed by pyrene fluorescence. Biophys J 95(3):1050–1062

Chapter 17

Use of the xCELLigence System for Real-Time Analysis of Changes in Cellular Motility and Adhesion in Physiological Conditions

Simon Scrace, Eric O'Neill, Ester M. Hammond, and Isabel M. Pires

Abstract

Investigation of the mechanisms behind the regulation of cellular motility and adhesion is key to understanding metastasis and the biology of tumor spreading. There are many technologies available for these studies, but the majority of them are either dependent on the use of labels or limited to endpoint analysis. The xCELLigence RTCA (real-time cell analysis) provides a platform for label free and operator independent investigation of the migration, invasion and adhesion proprieties of cells in physiologically relevant conditions. The real-time kinetic data acquisition also allows for a more accurate characterization of short-lived cellular events. In this chapter we describe the use of the xCELLigence Real-Time Cell Analyzer to investigate changes in cellular adhesion and motility in real time.

Key words xCELLigence, RTCA DP Analyzer, Real-time, Motility, Invasion, Adhesion

1 Introduction

Modulation in cellular adhesion and interaction with the extracellular basement matrix (ECM) is key for the regulation of cellular migration, invasion, and, subsequently, the metastatic process. Cellular migration is essential for normal development and homeostasis, but also an important contributor to pathologies such as vascular disease, chronic inflammatory disease, and metastatic cancer spread [1].

In vitro methodologies for studying cellular adhesion and/or migration have been established for many years. The majority depend on the use of ECM-like matrices, which are used to coat conventional 2D (2-dimensional) vessels [2, 3].

For protocols investigating cell adhesion, cells are labelled with either fluorescent tags or more conventional stains, such as crystal violet. The cells are then scored and quantified in regards to their

Amanda S. Coutts (ed.), *Adhesion Protein Protocols*, Methods in Molecular Biology, vol. 1046,
DOI 10.1007/978-1-62703-538-5_17,

ability to adhere to the ECM substrate, or imaged and analyzed regarding changes in morphology due to interactions with the ECM.

In vitro assays focused on studying cellular migration comprise of mainly two types. Scratch or wound healing of confluent cellular monolayers which correspond to endpoint assays that allow both the quantification of the ability of cells to migrate into the scratch wound and the imaging of motility-associated factors in the cells at the wound/scratch edge [4]. Boyden-type transwell assays, also an endpoint measurement approach, use chamber inserts lined with membranes containing micrometer-size pores (Boyden chambers) separating the cells from medium containing chemoattractant, which induces migration through the pores [5]. Again, the number of cells that migrate through the membrane can be quantified. A variation of this assay uses reconstituted basement matrices (Matrigel) to coat the Boyden chamber porous membrane to evaluate the ability of the cells to invade through ECM and basement membranes [6].

Although these assays allow morphological assessment and endpoint quantification of cellular migration and adhesion, this corresponds to only a snapshot of these processes. Furthermore, most of these techniques involve fixing and labelling of the cells, and so do not allow live-cell analysis. Finally, the scoring involved in many of these assays is operator-dependent.

In this chapter we describe the use of real-time analysis of cellular events using the xCELLigence RTCA (Real-Time Cell Analyzer), a label-free, dynamic system which is nonintrusive. This uses changes in electric impedance as a measure of cellular status such as number and shape [7–9]. Due to its real-time feature it also allows a kinetic analysis without recurring time points and multiple sample taking. Therefore the same cell population is followed and analyzed throughout the experiment. Finally, due to the nature of the experimental setup, the studies can also be performed in tumor relevant physiological conditions, such as hypoxia, by placing the instrument in a specialized incubator or chamber [10]. This system was initially developed by ACEA Biosciences and subsequently in a partnership initially with Roche Applied Science and more recently with Cambridge Biosciences, to investigate cell proliferation and viability [11]. Subsequently, it has been adapted to study cellular adhesion, spread, motility, and invasion [10, 12–15]. In this chapter we present a clear and detailed methodology for these different applications.

2 Materials

2.1 Cell Culture Reagents

All solutions should be prepared using ultrapure water (deionized water purified to attain a sensitivity of 18 MΩ cm at 25 °C). Check

the sterility of all reagents before use. All cell culture reagents should be prepared and handled in aseptic conditions in a laminar flow hood to minimize risk of contamination.

1. Cancer cell lines: HT-29 colorectal cancer cell line (used for the adhesion protocol) and MDA-MB-231 breast cancer cell line (used for the motility and invasion protocols) were obtained from the ATCC and maintained at 37 °C with a humid atmosphere containing 5 % CO_2 (*see* **Note 1**).
2. DMEM medium: DMEM supplemented with 10 % Fetal Bovine Serum (FBS) (*see* **Note 2**), 1 % Penicillin/Streptomycin (P/S) (*see* **Note 3**). All medium should be kept at 4 °C for storage and equilibrated at 37 °C before use.
3. Serum-free medium: DMEM with no FBS. All medium should be kept at 4 °C for storage and equilibrated at 37 °C before use.
4. 1× PBS (phosphate buffered saline).
5. Trypsin–Ethylenediaminetetraacetic acid (Trypsin-EDTA): Used for routine cell culturing, should be kept at 4 °C for short-term storage and equilibrated at 37 °C before use.
6. Fibronectin solution: Fibronectin (Sigma) diluted to 10 μg/mL in sterile 1× PBS.
7. Matrigel (BD Biosciences) (*see* **Note 4**).

2.2 xCELLigence RTCA DP Instrument and Components

1. RTCA DP Analyzer and control unit (ACEA Biosciences/Cambridge Biosciences Cat. No 00380601050 *see* **Note 5**): Used for the detection of changes of electronic impedance of sensor electrodes via connection between contact pins in the instrument and conductive pads in the plates. It can connect up to three different E-Plates 16 or CIM-Plates 16. Plates can be read in groups of 2 or 3 or individually.
2. RTCA Software 1.2: Specialized software for the RTCA DP Analyzer that mediates signal generation, processing, and analysis, alongside rapid scanning and measurements (*see* **Note 6**). The software is installed in a control unit and this is connected to the RTCA DP unit via an USB cable (Fig. 1).
3. E-plate 16 (Roche Applied Science, Cat. No. 05469830001, Fig. 2). Single use and sterile. Used specifically for cell proliferation, viability and adhesion assays (*see* **Note 7**).
4. CIM-plate 16 (Roche Applied Science, Cat. No 05665817001, Fig. 3). Single use and sterile. Used for migration and invasion assays (*see* **Note 8**).

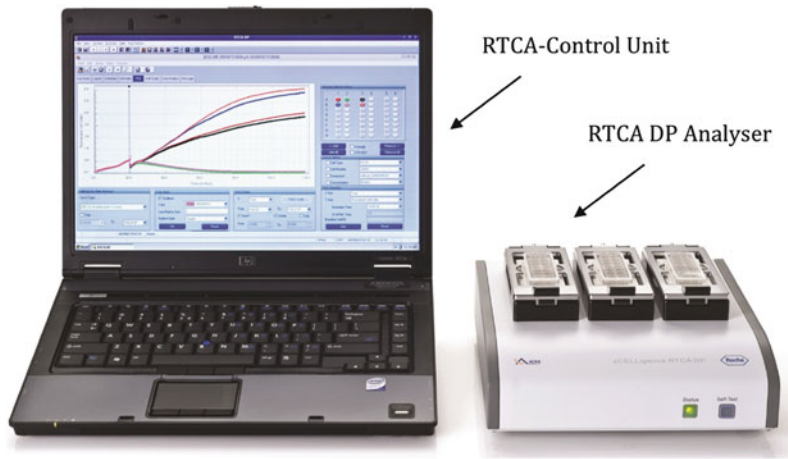

Fig. 1 RTCA DP Analyzer instrument and control unit. The RTCA DP Analyzer contains three cradle pockets, which allows three experiments to be set up independently. The RTCA Software 2.1 is installed on the control unit. Image provided by ACEA Biosciences

Fig. 2 The E-Plate 16. The microelectrodes at the bottom of the wells are visible (*golden structures*). Image provided by ACEA Biosciences

3 Methods

3.1 Culturing Cancer Cell Lines

All cell culture work should be performed in a laminar flow hood dedicated to tissue culture work.

1. Before starting, the hood surface should be cleaned with 70 % ethanol, as well as after use and whenever spills occur. All equipment, disposable plastic bottles, reagents and other items should be kept clean by spraying and wiping with 70 % ethanol solution before taking into the hood.
2. In order to subculture (passage) cells (*see* **Note 9**) first remove medium.

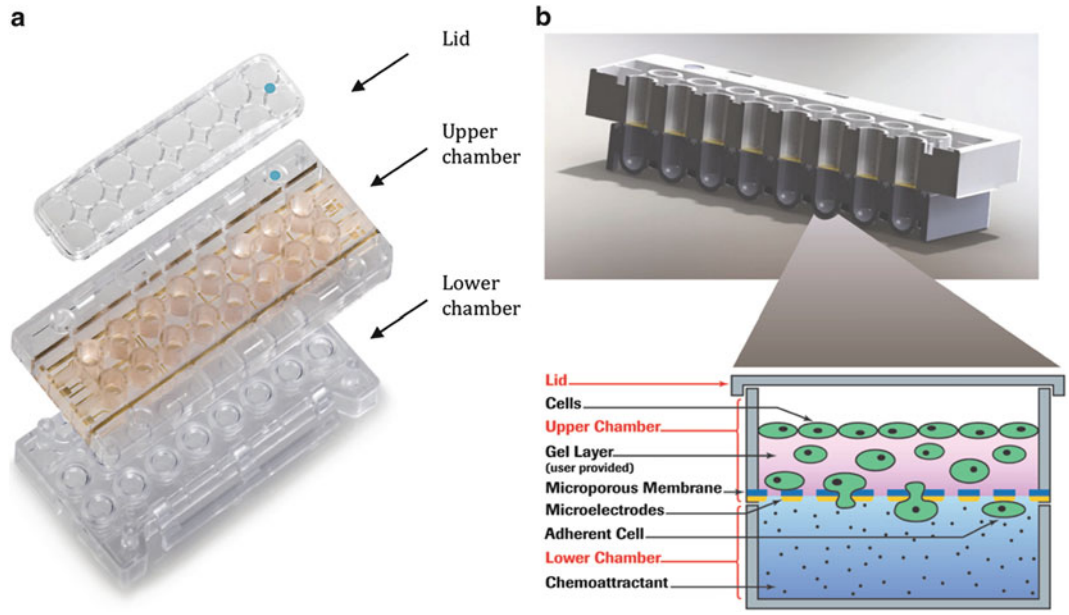

Fig. 3 The CIM-Plate 16. (**a**) CIM-Plate 16 components. (**b**) The CIM-Plate 16 is functionally an adaptation of a Boyden chamber transwell assay. Image provided by ACEA Biosciences

3. Wash the cells with equilibrated 1× PBS to remove any traces of medium (*see* **Note 10**).
4. Add Trypsin-EDTA and incubate at 37 °C until cells are completely detached.
5. Resuspend cells in fresh DMEM medium. If setting up an experiment, count cells using a hemocytometer and dilute in fresh medium accordingly (see later sections for specific cell numbers for each experiment).

3.2 Setting Up of the xCELLigence RTCA DP Analyzer

1. Place the RTCA DP Analyzer in a humidified incubator maintained at 37 °C with 5 % CO_2. The RTCA DP Analyzer needs to equilibrate in the incubator for at least 2 h to allow condensation-free performance (*see* **Note 11**).
2. Connect the RTCA DP Analyzer to the control unit via the USB cable.
3. Perform resistor plate verification as described in the manual. This is an important step to verify both installation and functionality of the instrument. This process must be performed every time the instrument is moved, and before and after the RTCA DP Analyzer is placed inside the incubator (*see* **Note 12**).

3.3 Real-Time Measurement of Cellular Adhesion and Spreading Using the RTCA DP Analyzer and the E-Plate 16

1. Prepare the plates in a laminar flow hood and open the E-Plate 16 packaging carefully. Do not touch the contact pads on the bottom of the plate (*see* **Note 13**).
2. Add 50 μL fibronectin solution by pipetting gently into each of the 16 wells of the E-plate 16 (*see* **Note 14**).
3. Incubate the plate for 1 h at room temperature inside the laminar flow hood in order for the fibronectin to coat the well.
4. Remove any excess fibronectin from the wells by washing twice with 100 μL 1× PBS.
5. Add 50 μL of DMEM medium to each well (*see* **Note 15**). Leave the E-Plate 16 in the hood at room temperature to ensure the culture medium and the E-Plate 16 coated surface achieve equilibrium.
6. Before adding cells to the well perform a background measurement in the machine.
   (a) Insert the E-Plate 16 front end into the cradle pocket of the RTCA DP Analyzer. Make sure that the E-Plate 16 is properly aligned (use the corner on the top right), without any tilting. Release the thumb from the press button and the fingers from the cradle's grip; the clamp plate will lock the E-Plate 16 in the horizontal position.
   (b) Close the door of the cell culture incubator. An automatic Scan Plate is performed to check for proper contact after the E-Plate 16 has been inserted and the lock handle locked. Open the Message tab of the RTCA Software to check whether Scan Plate was successful. The following message should be displayed: Plate scanned. Connections ok.
   (c) Perform Background Measurement. Select all the wells in the Layout tab. Select the Schedule tab on the software and click Start a Step icon to begin the experiment. The conditions are pre-set and should not be changed. Background impedance of each well is measured during this step. After completion of the measurement the bottom-left of the main program window displays the message Ready for Next Step. Please Click Next Step to start (see detailed protocol for setting up).
7. Prepare a single cell suspension of HT-29 cells as described in Subheading 3.1. Dilute cells to 8×10^5 cells/mL.
8. Add 50 μL of cells (4×10^4 cells) to each well of the E-Plate 16 and allow cells to equilibrate at room temperature for 20 min. Set up a minimum of triplicate wells per condition.
9. Load E-Plate 16 into the RTCA DP Analyzer as described in **step 6** above.
10. Set up the experimental conditions using the software. In the Layout tab label all wells with condition and cell number. In

Fig. 4 Example of an experiment visualized using RTCA Software 2.1. This image is a representative plot viewed on the Plot tab on the RTCA Software 2.1. It represents a cellular motility experiment. Wells are highlighted in color and data has been shown as an average of all four wells, with *error bars* representing the SDEV. These can be chosen by ticking the boxes below the wells (*arrow*). (**a**) MDA-MB-231 cells untransfected. (**b**) MDA-MB-231 transfected with non-targeting siRNA. (**c**) MDA-MB-231 transfected with siRNA against PTK6. (**d**) Media only

the Schedule tab add a second step to the Schedule setup to take measurements every 3 min for 3 h.

11. Start experiment by clicking Start Step on the Schedule tab.
12. In order to observe the measurements plotted in real time select all wells in the Plot tab. Wells can be individually selected, and average and standard deviations of well groups for same condition can be grouped (*see* Fig. 4).
13. The signal increases as cells spread on the plate before reaching a plateau. An example is shown in Fig. 5a. The Cell Index (CI) values correspond to a measure of relative changes in electric impedance and represents cell status (number, shape, etc.). In the case of the cell spreading experiment, it relates to the changes of space occupied in the wells.

3.4 Real-Time Measurement of Cellular Motility Using the RTCA DP Analyzer and the CIM-Plate 16

1. Plate preparation must be performed in a laminar flow hood. Open the CIM-Plate upper and lower chamber carefully and do not touch the contact pads on the bottom of the plates.
2. Place the CIM-Plate assembly tool in the laminar flow hood. Load the lower chamber onto the assembly tool making sure to align the blue spots in both items.

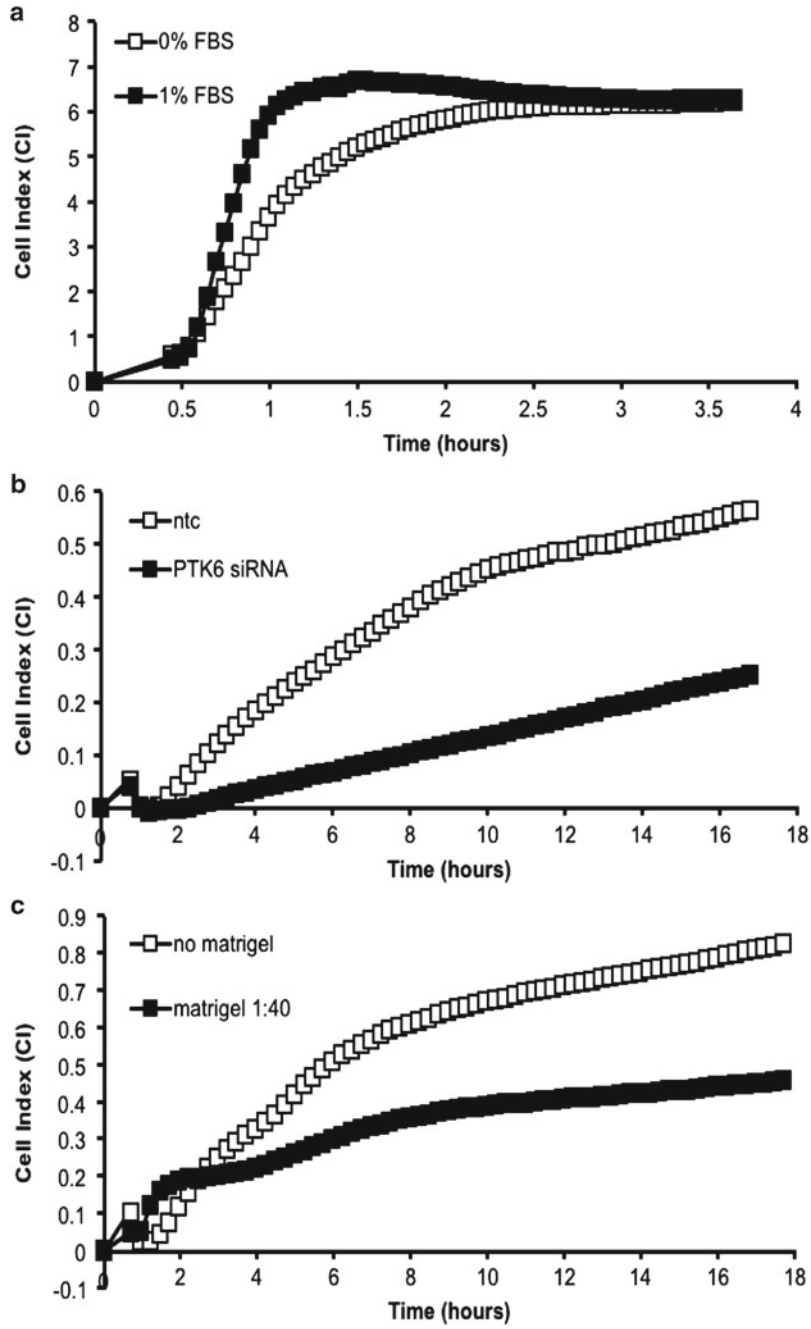

Fig. 5 Representative examples of experiments performed using the RTCA DP Analyzer. (**a**) The presence of serum increases the ability of HT-29 cells to adhere. HT-29 (4×10^4 cells) were seeded in each well of an E-Plate 16 (in duplicate wells), in either serum-free (0 % FBS) or serum-containing (1 % FBS) media. Impedance measurements were taken every 3 min for 4 h. (**b**) Knockdown of the non-receptor tyrosine kinase PTK6 decreases cellular motility. MDA-MB-231 were transfected with non-targeting siRNA (ntc) or PTK6 siRNA (4×10^4 cells) for 48 h. Cells were then seeded in each well in the upper chamber of a CIM-Plate 16 (in triplicate wells), in serum-free media. Media containing 10 % FBS was used as chemoattractant in the lower chamber. Impedance measurements were taken every 15 min for 18 h. (**c**) Matrigel coating delays the invasion kinetics of MDA-MB-231 cells. MDA-MB-231 cells were seeded in per well in the upper chamber of a CIM-Plate 16 (in triplicate wells), in serum-free media. The wells were either left uncoated (no Matrigel) or coated in Matrigel diluted 1:40 in serum-free media (Matrigel 1:40). Media containing 10 % FBS was used as chemoattractant in the lower chamber. Impedance measurements were taken every 15 min for 18 h

3. Fill the lower chamber wells with 160 µL of media containing chemoattractant (e.g., 10 % FBS). For a negative control, add serum-free medium.

   It is of uttermost importance that a clearly defined meniscus is formed on each medium-filled well (*see* **Note 16**).

4. Turn the assembly tool 90° clockwise. Place the upper chamber onto the lower chamber, again making sure the blue dots are aligned. Push the upper chamber down to lock the connection between the two (*see* **Note 17**).

5. Add 25–50 µL of serum-free medium to each upper chamber well. This will cover the surface of the membrane (*see* **Note 18**).

6. Leave the assembled CIM-Plate 16 to equilibrate by placing it in a 37 °C incubator for 1 h.

7. Place the assembled CIM-Plate 16 in the cradle pocket in the RTCA DP Analyzer and perform a background measurement as described in Subheading 3.3, **step 6**.

8. Prepare a single cell suspension of MDA-MB-231 cells as described in Subheading 3.1. Dilute cells in serum-free media to 4×10^5 cells/mL.

9. Add 100 µL of cells (4×10^4 cells) to each well of the upper chamber of the CIM-Plate 16 and allow cells to equilibrate at room temperature for 20 min. Set up a minimum of triplicate wells per condition.

10. Load the assembled CIM-Plate 16 into the RTCA DP Analyzer as described in Subheading 3.3, **step 6**.

11. Set up the experimental conditions using the software. In the Layout tab label all wells with condition and cell number. In the Schedule tab add a second step to the Schedule setup to make measurements every 15 min for 24 h.

12. The signal increases as cells move through the pores of the upper chamber lower membrane. Cellular migration occurs between 0 and 10 h. Beyond this time cellular proliferation starts to impact in the Cell Index. An example of a migration assay is shown in Fig. 5b.

3.5 Real-Time Measurement of Cellular Invasion Using the RTCA DP Analyzer and the CIM-Plate 16

This is a modification of the migration assay described in Subheading 3.4. In order to examine cellular invasion specifically, an extracellular matrix is added to the upper chamber wells prior to addition of medium and cells (*see* **Note 19**). All the other steps of the protocol are the same as described in Subheading 3.4.

1. Thaw Matrigel overnight at 4 °C on ice (*see* **Note 20**). All pipettes, media, and plastics used to handle the Matrigel need to be chilled overnight.

2. Prepare the Matrigel using ice-cold serum-free medium. Dilute as required (1:10, 1:20, and 1:40 are good starting points).
3. Add 50 μL of Matrigel solution per well of the CIM-Plate. Place the CIM-Plate at 37 °C to allow Matrigel to set.
4. The presence of the Matrigel will delay the ability of the cells to migrate through the membrane at the bottom of the lower chamber (Fig. 5c).
5. Continue the protocol from **step 5** of Subheading 3.4 (preparation of cells) and proceed as described for motility assay.

4 Notes

1. Other adherent cancer cell lines can be used for this protocol, as well as primary cell lines. All cells should be tested regularly for mycoplasma contamination and should be replaced if found to be positive for this bacterium. Infection with mycoplasma can lead to alteration of cellular growth and changes in other morphological and phenotypical characteristics.
2. FBS or Fetal Calf Serum (FCS) should be heat inactivated by incubating in a water bath at 56 °C for 30 min if not purchased heat inactivated already. Heat inactivation was originally performed to inactivate the complement system for immunoassays. Its absolute requirement for day-to-day cell culture is undocumented but remains a standard in most laboratories.
3. Cells should not be grown in penicillin/streptomycin continuously since antibiotics can mask bacterial and fungal infections that affect cell growth.
4. Extracellular matrix (BD Matrigel™ Basement Membrane Matrix) is a solubilized basement membrane preparation. It is extracted from a tumor rich in extracellular matrix, the Engelbreth-Holm-Swarm (EHS) mouse sarcoma. It contains, amongst other components, laminin (predominant component), collagen IV, proteoglycans, and entactins. It also contains in smaller proportions TGF-β, epidermal growth factor (EGF), insulin-like growth factor (IGF), and fibroblast growth factor (FGF).
5. The xCELLigence RTCA DP Analyzer was developed by ACEA Biosciences Inc. (San Diego, CA, US) in partnership with Roche Applied Science (Roche Diagnostics Ltd, West Sussex, UK). It is now distributed by Cambridge Biosciences Ltd (Cambridge, UK).
6. The RTCA Software 1.2 is only available for Windows operating systems.
7. The RTCA DP E-Plate 16 is used to perform cellular proliferation, viability and adhesion assays in the RTCA DP

Analyzer. It contains 16 wells and a low evaporation lid. Each of the wells has sensor electrode arrays incorporated, which allow for the real-time monitoring of the assays.

8. The CIM-Plate 16 (Fig. 3) is specifically designed for cellular migration and invasion assays. It is composed of two individually packaged parts: an upper chamber (which contains a low evaporation lid) and a lower chamber. The bottom of the upper plate is sealed by a microporous polyethylene terephthalate (PET) membrane with a median pore size of 8 μm. These plates are similar to conventional transwells with additional micro-electrodes located on the underside of the membrane of the upper chamber. The wells in the lower chamber are designed to contain the chemoattractant for the cells in the upper chamber. Both parts are assembled using the CIM-Plate 16 Assembly Tool.
9. Cell lines should be fed or subcultured in order to maintain exponential growth (as often as necessary, once to four times a week or even more frequently). Maintenance (feeding) of cell cultures corresponds to the complete replacement of exhausted media. Subculturing of cells should be performed just before the culture reaches confluency. In order to accurately determine the exact timings for maintenance and subculture of cells a growth curve should be performed for each cell line. Maintenance should be performed during the exponential growth phase and subculture should be performed just before reaching confluency, before a plateau growth phase is reached.
10. Any traces of serum-containing media need to be removed before trypsinization by washing with equilibrated 1× PBS. This is due to the fact that serum has anti-trypsin properties.
11. The incubator should be opened and closed carefully whilst the RTCA DP instrument is inside since vibrations can affect the measurements.
12. Whilst the RTCA DP instrument requires 2 h before any experiments are initiated, resistor plate verification can be performed immediately.
13. Always wear powder-free gloves since the system is dependent on a dust-free clean environment.
14. It is not advised by the manufacturer to use only part of the wells on an E-Plate 16. If the whole plate is not used then it is advised to fill the remaining unused wells with buffer (e.g., 1× PBS). This is also applicable to the CIM-Plate 16.
15. The maximum experimental volume of each well must be below 200 μL.
16. The presence of the meniscus guarantees that when the upper chamber is clicked into placed there is no air trapped underneath

the membranes at the bottom of the upper chamber wells. Careful pipetting should ensure also that no bubbles are present in the media inside the lower chamber wells.

17. Two clicking sounds should be heard as the chambers lock properly.
18. The exact volume here is not crucial. The role of the media is to cover the surface of the membrane on the bottom of each upper chamber well. As for the lower chamber, avoid bubble formation during pipetting.
19. For the invasion assay the only suitable chemoattractant placed in the lower chamber wells is serum-containing medium. This is due to the ECM proteins and factors contained in the Matrigel.
20. If the Matrigel is thawed at 4 °C but not incubated in ice it might not completely liquefy which makes it harder to pipette and prone to bubble generation.

References

1. Vicente-Manzanares M, Webb DJ, Horwitz AR (2005) Cell migration at a glance. J Cell Sci 118(Pt 21):4917–4919
2. Benton G et al (2009) Advancing science and technology via 3D culture on basement membrane matrix. J Cell Physiol 221(1):18–25
3. Even-Ram S, Yamada KM (2005) Cell migration in 3D matrix. Curr Opin Cell Biol 17(5): 524–532
4. Wong MK, Gotlieb AI (1988) The reorganization of microfilaments, centrosomes, and microtubules during in vitro small wound reendothelialization. J Cell Biol 107(5): 1777–1783
5. Kleinman HK, Jacob K (2001) Invasion assays. Curr Protoc Cell Biol. Chapter 12:Unit 12.2
6. Simon N, Noel A, Foidart JM (1992) Evaluation of in vitro reconstituted basement membrane assay to assess the invasiveness of tumor cells. Invasion Metastasis 12(3–4): 156–167
7. Kirstein SL et al (2006) Live cell quality control and utility of real-time cell electronic sensing for assay development. Assay Drug Dev Technol 4(5):545–553
8. Irelan JT et al (2011) Rapid and quantitative assessment of cell quality, identity, and functionality for cell-based assays using real-time cellular analysis. J Biomol Screen 16(3): 313–322
9. Atienza JM et al (2006) Dynamic and label-free cell-based assays using the real-time cell electronic sensing system. Assay Drug Dev Technol 4(5):597–607
10. Coutts AS et al (2011) Hypoxia-driven cell motility reflects the interplay between JMY and HIF-1alpha. Oncogene 30(48): 4835–4842
11. Ke N et al (2011) The xCELLigence system for real-time and label-free monitoring of cell viability. Methods Mol Biol 740:33–43
12. Rahim S, Uren A (2011) A real-time electrical impedance based technique to measure invasion of endothelial cell monolayer by cancer cells. J Vis Exp (50)
13. Rahim S et al (2011) YK-4-279 inhibits ERG and ETV1 mediated prostate cancer cell invasion. PLoS One 6(4):e19343
14. Chung H et al (2011) Keratinocyte-derived laminin-332 promotes adhesion and migration in melanocytes and melanoma. J Biol Chem 286(15):13438–13447
15. Atienza JM et al (2005) Dynamic monitoring of cell adhesion and spreading on microelectronic sensor arrays. J Biomol Screen 10(8): 795–805

Chapter 18

Measuring Chemotaxis Using Direct Visualization Microscope Chambers

Andrew J. Muinonen-Martin, David A. Knecht, Douwe M. Veltman, Peter A. Thomason, Gabriela Kalna, and Robert H. Insall

Abstract

Direct visualization chambers are considered the gold standard for measuring and analyzing chemotactic responses, because they allow detailed analysis of cellular behavior during the process of chemotaxis. We have previously described the Insall chamber, an improved chamber for measuring cancer cell chemotaxis. Here, we describe in detail how this system can be used to perform two key assays for both fast- and slow-moving mammalian and nonmammalian cell types. This allows for the detailed analysis of chemotactic responses in linear gradients at the levels of both overall cell behavior and subcellular dynamics.

Key words Chemotaxis chamber, *Dictyostelium* chemotaxis, Hemopoietic cell chemotaxis, Cancer cell chemotaxis, Melanoma chemotaxis

1 Introduction

Chemotaxis—the ability of cells to navigate using gradients of soluble molecules—plays a central part in normal cell physiology [1]. Particularly conspicuous examples include immune cells homing on pathogens and inflammatory mediators [1] and the spread of cancer cells [2], but chemotaxis is an evolutionarily ancient process that has roles in every aspect of biology. It is also a popular subfield—more than 6,000 papers related to chemotaxis have been published in the last 5 years, and the field is served by its own Gordon conference, among other meetings.

Despite its importance, chemotaxis is difficult to study. Cell movement is a complex process with great variability and a strong stochastic component [3, 4]. A huge variety of biological variables affect both cell movement and orientation. One approach to managing the complexity of chemotaxis has been to use simplified assays. For example, transwell assays in which chemoattractant gradients are set up on either side of a filter membrane in a 96-well

Amanda S. Coutts (ed.), *Adhesion Protein Protocols*, Methods in Molecular Biology, vol. 1046,
DOI 10.1007/978-1-62703-538-5_18,

plate can be quantified by staining the membrane and examining the up-gradient and down-gradient sides. However, such assays are subject to a wide range of artifacts [5]. Also, because this assay cannot directly visualize the process of cell motility, it misses large amounts of information that helps form a mechanistic understanding of chemotaxis. Examples include cell speed, cell polarity, pseudopod generation, and turning rate [6, 7].

Laboratories with an interest in the processes underlying chemotaxis therefore favor assays in which the cells can be directly visualized as they move. This generates far more data, which are laborious to process, but in doing so offers greater insight. Direct visualization chemotaxis chambers—which apply a consistent and measured gradient to visible cells and allow live observation of their responses—are the gold standard and should be used as widely as possible. The original direct visualization chamber, the Zigmond chamber [1], was first used to observe the details of chemotaxis in human neutrophils. The eponymous chamber allowed Sally Zigmond to obtain unparalleled insight into the basis of chemotaxis. In the Zigmond chamber, two medium-filled reservoirs are connected by a narrow (1 mm wide), shallow (20 μm deep), optically clear bridge [1]. The bridge is too shallow to allow medium to flow, so adding a chemoattractant to one well sets up a linear gradient across the bridge by diffusion. These chambers are appropriate for viewing neutrophils and other rapidly moving cells (which are usually hemopoietic cells such as macrophages and dendritic cells, which move at speeds of up to 10 μm/min). However, their ends are left open, and the relatively large length of bridge compared to the volume of buffer means that gradients are not long-lived. Thus they are not appropriate for studying slower cells which require long periods of observation to allow movement to occur.

The next technological step was the Dunn chamber [8], which allows the investigation of slower-moving cells such as fibroblasts (in addition to faster-moving cells). Dunn chambers are circular, allowing the coverslip to be sealed onto the chamber, and have proportionately less bridge compared to the volume of the wells. Consequently, once assembled they can maintain a roughly constant linear gradient for 12 h and a significant gradient for 48 h. This allows fibroblastic and cancer cells, which usually move at speeds substantially below 1 μm/min, to be assayed [8]. Disadvantages include the need for great care in processing data, as the circular bridge means that the direction of the gradient is variable. Another problem, shared with the Zigmond chamber, is that thicker glass coverslips are needed to maintain the chamber's shape—the thin ones normally used for microscopy are not well enough supported and bend [6]. This diminishes the optical quality of all images, and in particular means that most high numerical aperture microscope objectives cannot be used.

In 2010, we described the Insall chamber, as an improved tool for measuring cancer cell chemotaxis [6]. This was a further

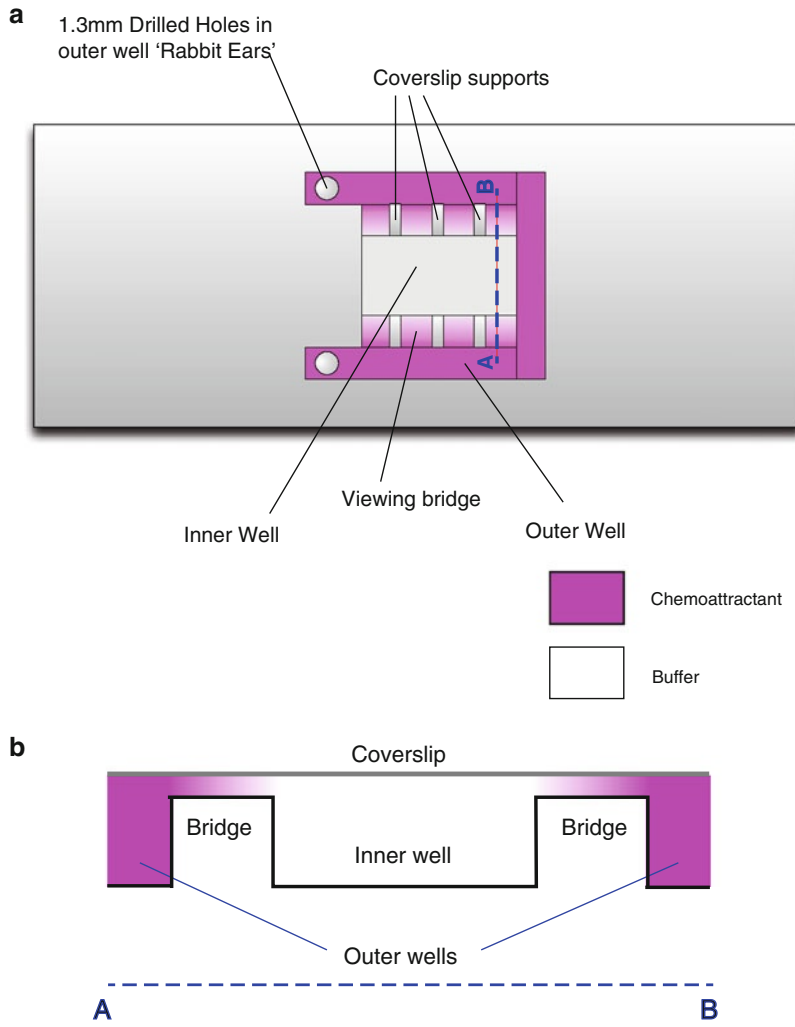

Fig. 1 Insall Chamber features and Gradient. (**a**) Schematic of an Insall Chamber from above highlighting the key features. Drilled holes in the "rabbit ears" necessary for >1 h experiments to allow reverse side filling in order to seal the chamber and prevent evaporation. The inner buffer well and outer chemoattractant wells along with the viewing bridges are also emphasized. *Magenta* highlights the location and gradient of the chemoattractant. (**b**) A cross section along the *blue dashed line* in (**a**) highlights the chamber shape and the resultant linear chemoattractant gradient (again in *magenta*) produced across the bridge

refinement of the Zigmond and Dunn chambers. It is microfabricated out of stress-free Perspex, with supports for the coverslip engineered at intervals along the bridge. This allows consistently oriented gradients and the use of standard thickness coverslips (Fig. 1), allowing aberration free microscopy and short working distance objectives. The design also makes changing medium more straightforward. Using this improved chamber we can now outline two key assays for investigating chemotaxis responses in linear gradients for both fast-moving cells in unsealed chambers and

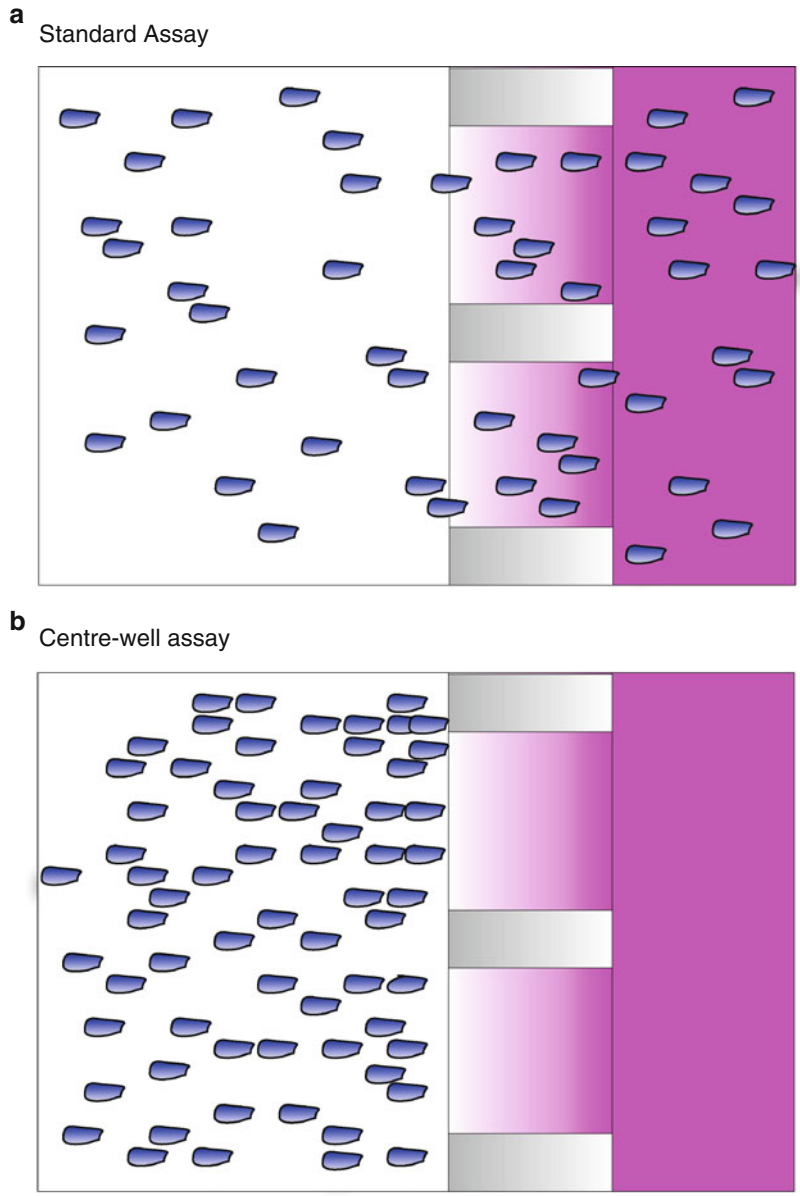

Fig. 2 Two Insall chamber assays for investigating chemotaxis. (**a**) The standard assay starts with cells spread evenly across a coverslip and therefore throughout the chemotactic gradient on the bridges. (**b**) The center-well assay is set up with all the cells originating in the center-well from which they can emerge into an undisrupted gradient onto the viewing bridges

slow-moving cells in sealed chambers. The standard assay is comparable with typical Zigmond or Dunn assays, with cells spread throughout the chemoattractant gradient. The second is the "center-well assay", in which the cells are introduced into one buffer well and the chemoattractant into the other. This makes it possible to see cells' initial response to the gradient in the absence of other cells or conditioned medium (Fig. 2). These two assay

formats offer contrasting views of cell behavior, the first under homogenous conditions of cells and attractant gradient, and the center-well assay of cells responding to a gradient as it forms.

2 Materials

Prepare and store all reagents at room temperature (unless indicated otherwise). Diligently follow all disposal regulations when disposing of waste materials.

2.1 Cell Culture Reagents: Cancer Cells

1. Complete growth medium: Appropriate medium e.g., RPMI, supplemented with 10 % Fetal Bovine Serum (FBS; PAA Labs) and 2 mM L-Glutamine (Gibco) and stored at 4 °C.
2. Trypsin-EDTA (Sigma-Aldrich) stored at 4 °C.
3. Phosphate Buffered Saline (PBS).

2.2 Cell Culture Reagents: Dictyostelium Cells

1. Cells are cultured in Petri dishes in HL5 medium (Formedium Ltd.) at 21 °C in a cooled incubator.
2. Development buffer (DB): 10 mM Na_2–K phosphate buffer pH 6.5 containing 2 mM $MgCl_2$ and 0.1 mM $CaCl_2$.
3. DB-agarose: Dissolve the required amount of agarose in DB (1.5 % w/v for plates). Bring the DB-agarose to boiling in a microwave. Swirl to ensure that all agarose has dissolved. Cool off the DB-agarose under running tap water until hand-warm and pour into a Petri dish (15 mL per 10 cm dish). The $MgCl_2$ and $CaCl_2$ should be added after the agarose is cooled or the magnesium and calcium phosphates will precipitate out.

2.3 Chambers and Related Materials

1. Insall chambers (*see* **Note 1**) are manufactured from polymethyl methacrylate by Epigem Ltd. as described [6].
2. VALAP sealant (Vaseline, Lanolin and Paraffin): Combine the three components together in a weight ratio 1:1:1 and mix by melting to 100 °C on a heat block.
3. A micropipette with P200 pipette tips and ultrafine pipette tips e.g., Microloader (Eppendorf) for exchanging medium in the *Dictyostelium* assay.
4. 22 mm × 22 mm No 1.5 coverslips (VWR International).
5. 1 M HCl.
6. Absolute ethanol.
7. 18 G needle and coverslip forceps.
8. Blu-tack® (Bostick Inc.) and chamber holder cassette.
9. Fine artists paint brush.
10. Cotton or plastic swab.

2.4 Chamber Reagents

1. Human Fibronectin (BD Biosciences): Prepared according to the manufacturer's instructions by dissolving in distilled water to make a 1 mg/mL stock solution and stored aliquoted at −20 °C.
2. 0.5 % w/v BSA solution in PBS: Use cell culture grade Bovine Serum Albumin (BSA; Sigma-Aldrich). Heat to 85 °C for 13 min and allow to cool to room temperature. Pass through a 0.45 μm sterile filter (Minisart, Sigma-Aldrich) and then store it for a maximum of 1 week at 4 °C.
3. For cancer cells, the medium comprises the appropriate Serum Free Medium (SFM) e.g., RPMI. Chemoattractant (e.g., 10 % FBS) is added to the buffer as required. A 1 M HEPES solution (PAA Labs) is added to both buffer (SFM-H) and chemoattractant solution (FBS-H) to a final working concentration of 5–15 mM. The solutions can then be adjusted to pH 7.2 before filter sterilizing.
4. For *Dictyostelium*, the chemoattractant cAMP (Sigma-Aldrich) is made up as a 1 mM stock solution in DB. Aliquots (20 μL per tube) are stored at −20 °C.

2.5 Time-Lapse Microscopy

1. We use a Nikon TE2000-E inverted time-lapse microscope equipped with a motorized stage (Prior) and Perfect Focus System (PFS) or equivalent system to prevent focal drift due to thermal fluctuations. The entire microscope is enclosed in a plexiglass box which is maintained at 37 °C.
2. Our microscope system is driven by Metamorph software; many other packages are equally effective.

2.6 Quantification of Migration and Chemotaxis

1. ImageJ: http://rsb.info.nih.gov/ij/.
2. LOCI plugin: http://rsbweb.nih.gov/ij/plugins/index.html.
3. MTrackJ plugin: http://www.imagescience.org/meijering/software/mtrackj/.

3 Methods

3.1 Cell Culture

Carry out all procedures at room temperature unless otherwise specified.

1. Cancer cells are cultured in complete growth medium at 37 °C in a 5 % CO_2 incubator until 50–80 % confluent.
2. *Dictyostelium cells* are most often used in their developed state, chemotaxing in response to cyclic AMP (cAMP). Cells are grown to confluence in Petri dishes in HL5 medium. This usually yields 2×10^7 cells per 10 cm dish. The cells are then washed in DB and starved for 6 h, either by shaking in DB or by plating

on a DB-agarose surface. Alternatively growing cells may be used, chemotaxing towards folic acid (used at a concentration of 100 μM), but less effectively.

3.2 Pre-assay Coverslip Preparation

1. Acid wash coverslips. Etch up to 20 coverslips with 1 M HCl for 15 min in a 300 mL glass beaker and rinse extensively for at least 15 min in a constant stream of water. Store coverslips in ethanol until use.
2. Coat with fibronectin. Air dry coverslips and dilute 1 mg/mL fibronectin stock to 20 μg/mL working solution with PBS. Then submerge each coverslip with 1.5 mL of the fibronectin working solution (*see* **Note 2**) in a 6-well dish for 30 min at room temperature or overnight at 4 °C.
3. Block with BSA. Aspirate fibronectin solution from the coverslips and wash three times with distilled water. Coat coverslips with 2 mL 0.5 % BSA solution in each well for 1 h.

3.3 Insall Chamber Setup for Standard Cancer Cell Chemotaxis Assay

1. Prepare chambers. The chambers need to be drilled in advance with a 1.3 mm drill bit using an overhead drill press. During drilling, the chamber is secured in a small machine vice sitting inside a V-block at 45° and a hole is drilled into each "rabbit ear" of the outer well to allow reverse filling.
2. Seed cells T-minus 24 h. Aspirate BSA solution from coverslips and wash thrice with PBS. Trypsinize cells after washing with PBS and count. Seed 2 mL of a 4.5×10^4 cells/mL suspension in complete medium. Place cells on a shock absorbent base (to prevent vibration induced patterns of cell accumulation) in a CO_2 incubator at 37 °C.
3. Starve cells T-minus 14 h. Aspirate complete medium and wash thrice with PBS. Add 2 mL SFM and continue to incubate at 37 °C (*see* **Note 3**).
4. Prepare reagents T-minus 1 h. Pre-warm reagents in 1.5 mL centrifuge tubes to 37 °C in a heating block. Place microscope chamber holder cassette on 37 °C heating block. Wash chambers thoroughly under a stream of water to remove debris and then immerse in ethanol before blotting with a lint free cloth and leave to air-dry. Melt VALAP mixture at 100 °C for 10 min.
5. Assemble chamber T-minus 30 min. Add 45 μL SFM-H to center well (*see* **Note 4**). Carefully pick up a cell-coated coverslip from a 6-well dish using the 18 G needle (*see* **Note 5**) and/or a set of coverslip forceps. Hold the coverslip vertically and gently blot the accumulated medium at the edge. Place one edge down on the chamber and using this as the pivot point, steadily lower the coverslip onto the chamber, being careful to ensure that it does not slip. Whilst holding the outer

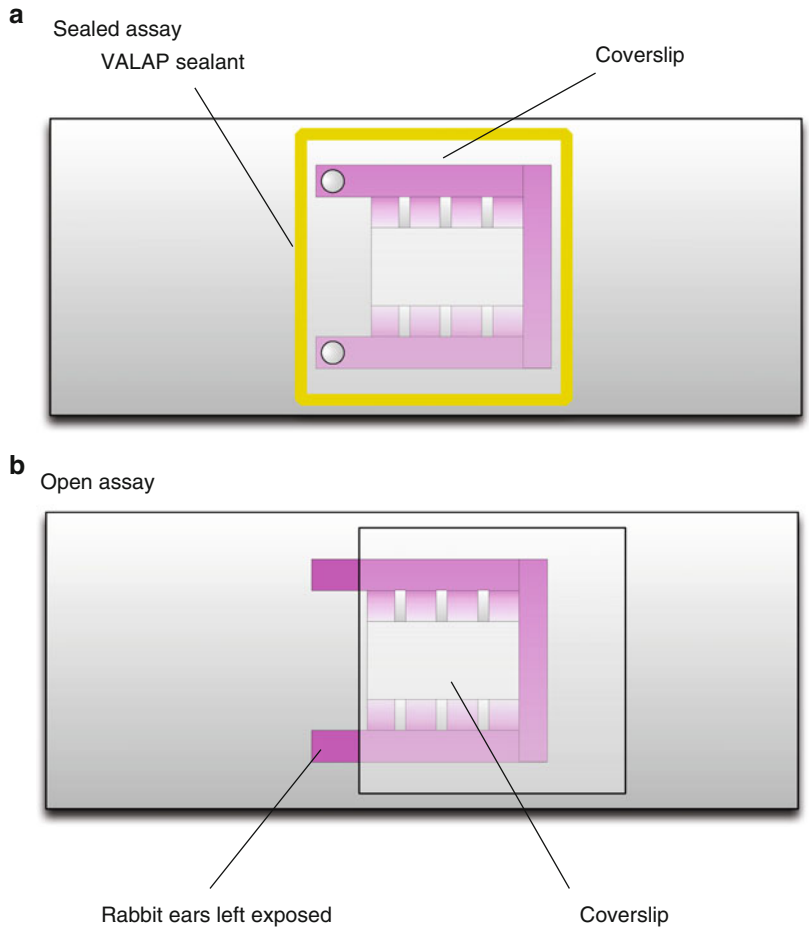

Fig. 3 Sealed and open chamber assay comparison. (**a**) Chambers are sealed with VALAP in 1–24 h assays for slow-moving cells to prevent evaporation from disrupting the experiment. (**b**) Assays using fast-moving cells that require imaging for 30 min–1 h are left open and unsealed for ease of filling when evaporation is unlikely to cause an issue during this relatively brief time-frame

edges of the coverslip, wipe and blot the other two edges dry and paint the VALAP mixture along the edges with a fine paint brush to seal. Release and blot the remaining two edges before sealing them with VALAP (Fig. 3). Wipe residue off the coverslip from the center with a cotton or plastic swab using increasing concentric circles to reduce risk of smearing. Draw up 160 μL of chemoattractant solution e.g., FBS-H (*see* Subheading 2.4, **step 3**), using a micropipette with a 200 μL tip and slowly fill the outer well from the reverse side (*see* **Note 6**). As the outer well fills, gently move the chamber to allow air bubbles to rise towards the outlet hole as the solution passes each corner. Once the solution passes through the outlet, continue to add a further 40 μL to ensure that any buffer that has leaked from the center well is washed out of the chamber.

Carefully blot the excess solution from the outlet hole and then seal both drilled holes with a strip of electrical tape. Label the chamber on the tape and secure to the microscope cassette with Blu-tack® before incubating at 37 °C until up to four chambers are assembled and secured in the cassette.

3.4 Insall Chamber Setup for Center-Well Cancer Cell Chemotaxis Assay

1. Prepare coverslips (*see* Subheading 3.2) and chambers (*see* Subheading 3.3, **step 1**).
2. Cell Culture and seeding. Grow cells in a Petri dish in complete medium until 50–80 % confluent. Aspirate medium, wash once with SFM and then incubate overnight in SFM. The cells will round up slightly and be less adherent to the dish. Detach the cells by triturating them with a 1,000 µL micropipette and then harvest them into a 15 mL centrifuge tube. Remove a portion of cells to count (*see* **Note 7**) and pellet the rest at $180 \times g$ for 5 min at room temperature. Resuspend cell pellet to 5×10^5/mL in SFM-H (*see* Subheading 2.4).
3. Assemble chamber. Add 40 µL of cells to the center well of an Insall chamber. Remove as much buffer as possible from an acid washed/fibronectin coated coverslip (*see* **Note 8**) and place the coverslip onto the chamber. Allow a few seconds for the medium to spread so capillary action is holding it to the coverslip and then gently (so as not to allow the coverslip to move) flip the chamber over and place it in the microscope cassette. Place chambers in the 37 °C incubator for 10–15 min to allow cells to settle and attach to the coverslip. After incubation, the cells will still be round, but will be loosely attached to the surface. Remove the cassette from the incubator and proceed to seal each chamber individually. Gently flip it to over and coat the edges with VALAP with a fine paint brush. After all four sides are sealed, clean the coverslip and proceed (*see* Subheading 3.3, **step 5**) to fill the outer chemoattractant well with e.g., FBS-H (*see* Subheading 2.4, **step 3**) before returning it to the cassette and securing with Blu-tack®.

3.5 Insall Chamber Setup for Dictyostelium or Rapidly Moving Mammalian Cell Chemotaxis Assay

This protocol is suitable for assays up to about 90 min or less; beyond this time it is limited by evaporation of the buffer. All protocols are for *Dictyostelium*, but cells such as neutrophils (*see* **Note 9**) can be treated similarly.

1. Starve cells T-minus 5 h. Cells are harvested by trituration, centrifuged at $360 \times g$ for 3 min, and washed three times with DB. Cells are resuspended at 10^7/mL in DB and shaken at 120 rpm for 1 h to starve, then pulsed with 60 nM cAMP every 6 min for 4 h. A sample of pulse-developed cells can if needed be taken and diluted 50-fold in buffer to give the working cell concentration. Cells should be vortexed vigorously when diluting to ensure that they are not clumped.

2. Prepare chambers and reagents. Carefully wipe the surface of the chamber clean with a cotton swab drenched in ethanol. Confirm that the chamber is free of debris by viewing on a microscope. Rinse the cleaned chamber with distilled water to remove all traces of ethanol. Blot excess water with a lint free cloth and allow to air dry. Prepare the chemoattractant by diluting 1 μL of the 1 mM cAMP stock solution in 1 mL DB.
3. Prepare cells. Harvest and count the chemotactically competent *Dictyostelium* cells. Wash the cells once in DB and resuspend in DB to a density of 5×10^4 cells/mL.
4. Assemble chamber. Dispense 100 μL of the cell suspension on a 22 mm × 22 mm No 1.5 coverslip (*see* **Note 10**) and allow the cells to adhere for 15 min. Check the cell density on a microscope. Optimally, the cells should be far enough below confluence that they rarely collide—we often use about 2–5 % confluent cells. If required, adjust the cell density and seed the cells on a new coverslip. To assemble the chamber, put the coverslip with cells on a paper towel on a level surface. Take the chamber, bridge side down, and place one edge down next to the coverslip. Gently lower the chamber over the coverslip and adjust the position of the chamber so that the bridge is exactly over the droplet with cells. The rabbit ears of the outer chemoattractant well will need to remain clear of the coverslip. When ready, let go of the other edge of the chamber to drop it onto the coverslip. Gently press the chamber on the coverslip to expel any excess liquid between the chamber and the coverslip. Invert the chamber and drain the buffer from the outer chemoattractant well using a P200 micropipette fitted with a microloader tip. Finally, fill the outer chemoattractant well with a solution of 1 μM cAMP in DB (*see* **Note 11**).

3.6 Image Cells Using Phase, DIC or Fluorescence Microscopy

1. Image the inverted chambers secured in the cassette (Fig. 4) using an appropriate objective, having focused the condenser and minimized the shutter aperture (*see* **Note 12**). A 10× objective will allow the entire width of the bridge to be imaged as well as a few cell widths either side into the wells (*see* **Note 13**). Note the direction of the gradient for each imaging position.
2. Use perfect focus—or equivalent if fitted—to correct for any chamber movement or Z-position differences between chambers (*see* **Note 14**).
3. For cell tracking, frame rates and imaging duration will depend on the cell speed, but generally frame rates between 15 min to 1 h are adequate for cancer cell chemotaxis for a total duration of 24–36 h (*see* **Note 15**). For pseudopod analysis or *Dictyostelium* chemotaxis, images should be captured every 10 s for about 30 min–1 h total.

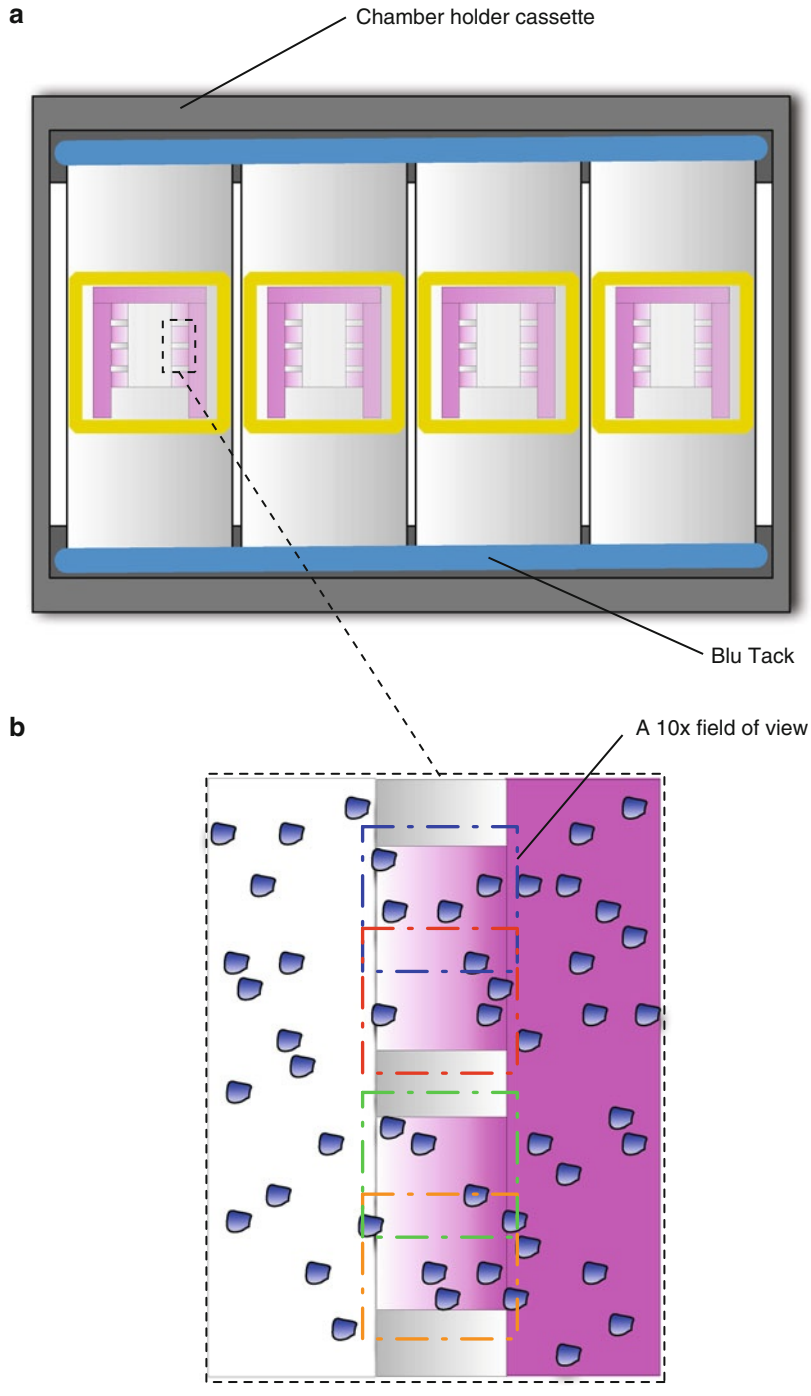

Fig. 4 Insall chamber imaging setup. (**a**) Up to four chambers can be positioned inverted on a purpose built aluminum cassette that fits into the motorized stage. The chambers are secured in place with Blu-tack® or tape. The rectangular area over the viewing bridges in (**a**) is exploded in (**b**). The *colored dashed squares* represent the field of view for a 10× objective showing that the entire width of the bridge can be viewed. Two overlapping images can be stitched together to provide images of the entire bridge between the coverslip supports

3.7 Quantification of Migration and Chemotaxis Parameters

1. Image processing and cell tracking. Import the TIFF sequence into ImageJ (http://rsb.info.nih.gov/ij/) using the Bio-formats importer found within the LOCI plugin (http://rsbweb.nih.gov/ij/plugins/index.html). To visualize all the cells on both bridges, we usually stitch two 10× images from each bridge (using a macro which can be obtained from us). The images are then calibrated with time and distance before commencing cell tracking with the ImageJ plugin MTrackJ (http://www.imagescience.org/meijering/software/mtrackj/) (*see* **Note 16**).
2. Chemotaxis analysis. The tabulated cell tracking data from MTrackJ produced are then exported to an excel spreadsheet (written by Drs. DM Veltman and AJ Muinonen-Martin) for processing (*see* **Note 17**). This spreadsheet automatically produces spider plots, speed and chemotaxis index data. A time window is then selected (e.g., 6–12 h for melanoma cells) and values zeroed to produce rose or polar plots with 95 % confidence intervals. Circstat toolbox for MATLAB [9] is used to perform a Rayleigh test to determine whether there is statistical support for unimodal cell movement (*see* **Note 18**).

4 Notes

1. Insall chambers are currently only made to order, but we hope to arrange a commercial supplier (contact RI for details—r.insall@beatson.gla.ac.uk). Following an open assay, chambers can easily be reused—wash with distilled water and Haemo-sol if necessary, and remove debris with a cotton bud. Strong solvents should not be used as they can attack Perspex or disrupt the bond between the slide and the coverslip props.
2. We describe the use of fibronectin as an ideal extracellular matrix (ECM) for cancer cell and melanoma cell chemotaxis in particular but other ECMs can be used. The optimal concentration should be determined after performing a serial dilution of the ECM and testing which concentration enables the fastest random motility of cells in a 6-well dish.
3. The optimal timing for seeding cells in the standard cancer cell assay will depend on the rate of cell adhesion and spreading. Likewise, the optimal duration of starvation is experiment and cell type-specific and should be experimentally calculated to optimize chemotaxis. Failure to wash cells adequately prior to starvation will result in diminished chemotaxis in the standard assay.
4. The volumes used to fill the Insall chamber will vary depending on the version of chamber used. All calculations here are

based on the use of the Mark IV chamber. As the chambers are made to order, their dimensions evolve and may also be changed for particular experiments.

5. A handy tool for picking up a coverslip from a 6-well dish can be made by pushing the bevelled tip of a hypodermic needle against a hard surface (e.g., a glass slide) to generate a 90° kink which can be used to catch the edge of the coverslip to lift it. To mount the coverslip on the chamber, use your fingers to both fix one edge of the coverslip and check that it is centrally placed. This ensures that when it is lowered it is parallel to the edges and the chamber is situated as centrally as possible.

   Sliding the coverslip once it has been lowered onto the chambers is to be avoided—shear stresses from the movement frequently damage cells, and the supports may also crush them.

6. In order to reverse fill the Insall chamber, the tip can be either: (1) placed just inside the drilled hole allowing the outer well to fill by capillary action, or (2) inserted slightly further to form a seal between the hole and the pipette tip before gently pushing the solution through. Either way, care should be taken not to insert the tip too far and push on the inner surface of the coverslip, which will result in fluid flowing between the coverslip and the chamber thereby disturbing the integrity of the chamber and the quality of the linear gradients.

7. For the center-well assay, rather than harvest cells by treating them with Trypsin-EDTA, it is simpler to remove them from the dish surface by trituration. Withdraw the medium into a pipette or P1000 tip and discharge repeatedly while moving the pipette over the surface of the dish to gently blow the cells off the surface.

8. In assays with *Dictyostelium*, neutrophils, or melanoma cells, it is not necessary to use an ECM. Other cell types may be more fastidious, particularly if they are susceptible to anoikis.

   Migration speeds are significantly faster with an ECM, but chemotactic movement is similar for coated and uncoated coverslips. When attaching the coverslip in the center-well assay, dry acid washed coverslips without an ECM work best. This is because the coverslip has no extra liquid on it so the spread of medium/cells from the center-well is contained and there is no need to blot the edges before applying VALAP. But with ECM coated coverslips, blot excess liquid from the coverslip before placing on the chamber, and then use a tissue or paper to blot away excess fluid from between the coverslip and the chamber. In all assays it is essential not to move the coverslip once it is positioned flat on the chamber otherwise the cells will shear against supports or they will become positioned over the bridge of the center-well assay.

9. Fast-moving mammalian cells include, in particular, hemopoietic lineage cells. These cells require their own specific culture conditions. Although this is beyond the scope of this review, the chamber methods can easily be adapted using the principles laid out here.
10. Acid washing of coverslips is not usually necessary for *Dictyostelium* cells. However, if the cells do not adhere well, the coverslips can be washed in 35 % nitric acid for 5 min. Rinse well with distilled water. Use immediately or store in absolute ethanol.
11. Chemotaxis of *Dictyostelium* cells starts while the gradient is still forming. Solution from the outer chemoattractant well will slowly evaporate. Therefore cells must be imaged within 90 min at the most, and less if evaporation is rapid.
12. Minimizing the illuminated field is of particular importance for fluorescence imaging. This will reduce fluorescence contamination on neighboring fields, which will otherwise result in premature cell death.
13. When using oil immersion objectives it should be remembered that it is only possible to image one coverslip otherwise the oil dissipates during a long time-lapse or the objective will become smeared in the VALAP mixture due to the proximity of coverslip and objective.
14. Chambers do have a tendency to move slightly during imaging and so if PFS is not available, then a z-stack can be taken and at the point of processing the focussed images can be selected in series from the Z-stack
15. Chemotaxis can be seen for up to 36 h in the standard cancer cell assay although it should be noted that for analysis in a linear gradient then tracking should be limited to 24 h and similarly for the center-well assay.
16. After stitching, each bridge is rotated if necessary so that the edge of the bridge is perpendicular to the direction of the gradient running from left (buffer) to right (chemoattractant) for consistency. If there is any chamber drift, this can often be corrected by running the image sequence through the image stabilizer plugin (http://www.kangli.org/code/Image_Stabilizer.html).
17. For chemotaxis analysis, the authors can be contacted for a copy of the Excel spreadsheet or alternatively data can be imported into the freely available ImageJ chemotaxis tool plugin (Ibidi Inc.) http://ibidi.com/software/chemotaxis_and_migration_tool/.
18. There are many possible criteria for whether cells are chemotaxing or not. We prefer them to fulfil two criteria: (a) there must be a significant Rayleigh test, and (b) the cells must be

moving in the direction of the chemoattractant gradient (i.e., the actual direction of the attractant gradient must fall within the 95 % confidence interval for the direction of the cell migration).

Acknowledgments

We thank Epigem (http://epigem.co.uk) for manufacturing the Insall chambers, Don MacBean for manufacturing the chamber holder cassettes and drilling the chambers, and Michael Carnell for writing the stitching plugin.

This work has been supported by a Wellcome Trust and a CRUK core grant.

References

1. Zigmond SH (1974) Mechanisms of sensing chemical gradients by polymorphonuclear leukocytes. Nature 249:450–452
2. Roussos ET, Condeelis JS, Patsialou A (2011) Chemotaxis in cancer. Nat Rev Cancer 11: 573–587
3. Insall RH, Machesky LM (2009) Actin dynamics at the leading edge: from simple machinery to complex networks. Dev Cell 17:310–322
4. Insall RH (2010) Understanding eukaryotic chemotaxis: a pseudopod-centred view. Nat Rev Mol Cell Biol 11:453–458
5. Zigmond SH, Hirsch JG (1973) Leukocyte locomotion and chemotaxis. New methods for evaluation, and demonstration of a cell-derived chemotactic factor. J Exp Med 137:387–410
6. Muinonen-Martin AJ, Veltman DM, Kalna G, Insall RH (2010) An improved chamber for direct visualisation of chemotaxis. PLoS One 5:e15309
7. Soll DR (1995) The use of computers in understanding how animal cells crawl. Int Rev Cytol 163:43–104
8. Zicha D, Dunn GA, Brown AF (1991) A new direct-viewing chemotaxis chamber. J Cell Sci 99:769–775
9. Berens P (2009) CircStat: a MATLAB toolbox for circular statistics. J Stat Software 31:1–21

Chapter 19

In Vitro Microtubule Severing Assays

Natasza E. Ziółkowska and Antonina Roll-Mecak

Abstract

Microtubules are rigid and highly dynamic cellular polymers essential for intracellular transport, cell division and differentiation. Their stability is tightly regulated by a vast array of cellular factors. In vitro microtubule assays have proven to be powerful tools for deciphering the mechanism of microtubule dynamics regulators such as molecular motors and microtubule associated proteins. In this chapter we focus on microtubule severing enzymes that use the energy of ATP hydrolysis to introduce internal breaks in the microtubule lattice. We present a detailed protocol for a light microscopy based in vitro microtubule severing assay that was instrumental in the identification and characterization of these enzymes.

Key words Cytoskeleton, Microtubule, Tubulin, Severing, Depolymerization, Spastin, Katanin, AAA ATPase

1 Introduction

The microtubule cytoskeleton is a highly dynamic structure that undergoes constant restructuring in response to environmental and developmental cues. Microtubules display a polymerization characteristic called "dynamic instability," i.e., they undergo growth (rescue) and shrinkage (catastrophe) of their polymer ends and can switch rapidly between these two states in a stochastic manner [1]. In addition to their intrinsic dynamic properties, microtubule stability is regulated by a vast array of molecular motors and microtubule associated proteins (MAPs). Microtubules can be destabilized by cellular factors *via* depolymerization from their ends (reviewed in [2]) or severing along their length (reviewed in [3, 4]). Microtubule severing was first observed in metaphase-like *Xenopus* egg extracts [5]. The protein responsible for this activity was later purified and named katanin after the Japanese for sword "katana" [6]. Since this initial discovery, several other enzymes that can sever microtubules have been identified: spastin [7, 8], fidgetin [9, 10], and the katanin-like proteins [9, 11]. These

Amanda S. Coutts (ed.), *Adhesion Protein Protocols*, Methods in Molecular Biology, vol. 1046,
DOI 10.1007/978-1-62703-538-5_19,

enzymes belong to the large family of AAA ATPases (ATPases associated with various cellular activities) and use the energy of ATP hydrolysis to destabilize the microtubule lattice. Microtubule severing enzymes are involved in basic cellular processes ranging from cell division [9–15] and cilia biogenesis [16, 17] to neurogenesis [18–21], axonal maintenance and regeneration [22, 23]. Even though katanin was discovered more than 25 years ago, the mechanism of action of microtubule severing proteins is still poorly understood. In vitro microtubule severing assays are powerful tools for deciphering the biophysical mechanism of microtubule severing enzymes as well as for the identification and characterization of cellular factors that regulate their activity.

Here we describe the recombinant expression and purification of the microtubule severing enzyme spastin and illustrate in detail a fluorescence microscopy based in vitro microtubule severing assay. This assay is an adaptation of earlier microtubule severing assays that were used to identify katanin and spastin as microtubule severing enzymes [7, 24]. Direct observation by light microscopy was key to being able to establish that these proteins were indeed severing microtubules along their length and not depolymerizing them from their ends [5].

2 Materials

2.1 Expression and Purification of Recombinant Spastin

2.1.1 Materials and Equipment

1. pDEST15 Gateway destination vector expressing *Drosophila melanogaster* spastin (residues 220—C-terminus [25]).
2. *Escherichia coli* Rosetta 2(DE3)pLysS competent cells (Novagen #71403-4).
3. LB Broth, Miller.
4. Ampicillin sodium salt: 200 mg/mL stock solution in water. Store at −20 °C.
5. Chloramphenicol: 34 mg/mL stock solution in ethanol. Store at −20 °C.
6. Isopropylthiogalactoside (IPTG): 1 M stock solution in water. Store at −20 °C.
7. Dithiothreitol (DTT): 1 M stock solution in water. Store at −20 °C.
8. Phenylmethylsulfonyl fluoride (PMSF): 1 M stock solution in DMSO. Store at −20 °C.
9. 5 M NaCl.
10. DNase I (Roche Applied Science #10104159001).
11. PreScission protease (GE Healthcare # 27-0843-01). Store at −80 °C.
12. Bottle-top filters, 500 mL, pore size 0.22 μm.

13. Glutathione Sepharose 4 Fast Flow (GE Healthcare).
14. Econo-Column Chromatography Columns (Bio-Rad #737-2512).
15. HiTrap Capto S column: 5 mL (GE Healthcare #17-5441-23) or Mono S 10/100 GL, 8 mL (GE Healthcare #17-5169-01) for higher resolution separation.
16. Millex—GV Syringe Driven Filter Units, PVDF, low protein binding, pore size 0.22 μm (Millipore #SLGV033NB).
17. Amicon Ultra Centrifugal Filters, 10K MWCO (Millipore).
18. Dialysis tubing with 10K MWCO or Slide-A-Lyzer Dialysis Cassettes, 10K MWCO, 12 mL (Thermo Scientific).
19. EmulsiFlex C5 homogenizer (Avestin).
20. FPLC system (AKTA, GE Healthcare).

2.1.2 Solutions and Buffers

Prepare all buffer solutions with ultrapure water (>18 MΩ cm at 25 °C) and filter using 0.22 μm bottle-top filters.

1. Lysis buffer: Phosphate buffered saline (PBS) supplemented with 10 mM $MgCl_2$, 1 mM PMSF, protease inhibitor cocktail (0.001 mg/mL aprotinin, 0.002 mg/mL leupeptin, 0.001 mg/mL pepstatin). The EDTA free inhibitor cocktail tablets from Roche Applied Science can also be used.
2. Wash buffer: 20 mM Tris–HCl pH 7.5, 500 mM NaCl, 10 mM $MgCl_2$, 5 mM DTT.
3. Elution buffer: 50 mM Tris–HCl pH 8.8, 300 mM NaCl, 10 mM $MgCl_2$, 5 mM DTT, 20 mM reduced glutathione. Glutathione lowers the pH of the solution, thus the use of Tris–HCl pH 8.8. The final pH of the elution buffer is 8.0.
4. Ion exchange buffer A: 50 mM MES pH 6.5, 10 mM $MgCl_2$, 5 mM DTT, 10 % glycerol.
5. Ion exchange buffer B: 50 mM MES pH 6.5, 10 mM $MgCl_2$, 2 M NaCl, 5 mM DTT, 10 % glycerol.
6. Dialysis buffer: 20 mM HEPES pH 7.0, 300 mM KCl, 10 mM $MgCl_2$, 5 mM DTT, 15 % glycerol.

2.2 Microtubule Severing Assay

2.2.1 Microscope

This assay requires a fluorescence microscope equipped with filters to detect rhodamine and suitable for time lapse image capturing. For example in our lab we use the following:

1. Motorized inverted microscope (e.g., Nikon Ti-E 2000 with perfect focus).
2. TIRF objective (e.g., CFI Apochromat TIRF 100× Oil, NA 1.49, Nikon). A high NA TIRF objective is not essential.
3. 532 nm solid-state laser (Sapphire, Coherent). Microtubules can also be imaged in epifluorescence using a Xe-Hg lamp.

4. Appropriate single-band filters and dichroic mirrors for TMR fluorescence imaging.
5. Cooled charged-coupled device (CCD) camera (e.g., iXON 897, Andor).
6. Controller software: μManager (100× Imaging).

2.2.2 Flow Chamber Preparation

1. Frosted microslides (3 × 1 in.).
2. Cover glass (22 × 40 mm).
3. Polytetrafluoroethylene racks for holding cover glass and slides (custom made in our workshop). Polytetrafluoroethylene (also known as Teflon®) is resistant to the highly corrosive Piranha solution (see below).
4. 500 mL glass beakers to hold the racks.
5. Hot plate.
6. Sonicating water bath.
7. Scotch permanent double-sided tape.
8. Parafilm.
9. Chemical fume hood.
10. Lab coat and safety glasses.

2.2.3 Solutions and Buffers for Slide and Cover Glass Preparation

1. Mucasol: 2 % solution (dilute in water).
2. Sulfuric acid.
3. Hydrogen peroxide (30 %).
4. 0.1 M KOH.
5. Trichloroethylene (TCE) (≥99.5 %).
6. Dichlorodimethylsilane (DDS) (≥99.5 %). Store DDS in a desiccator at 4 °C.
7. Methanol.
8. Ethanol, 200 proof.

2.2.4 Equipment, Solutions and Buffers for Flow Chamber Assembly and Severing Assays

1. TLA 100 rotor (Beckman).
2. 0.1 μm low protein binding filters (Millipore # UFC30VV00).
3. Anti-Tetramethylrhodamine (TMR) antibody (Life Technologies #A-6397).
4. Casein: 32 mg/mL stock solution in 20 mM Tris–HCl, pH 8.0.
5. Guanosine 5′-triphosphate (GTP): 100 mM stock solution in water. Store at −80 °C.
6. Adenosine 5′-triphosphate disodium salt (ATP): 100 mM stock in water and adjusted to pH 7.0 with 5 M NaOH. Store at −80 °C.

7. Dimethyl sulfoxide (DMSO) (≥99.7 %).
8. DTT: 1 M stock solution in water. Store at −20 °C.
9. Taxol, commercially available under the trade name "Paclitaxel" (Acros Organics #328420050): 10 mM stock solution in DMSO. Store at −20 °C.
10. BRB80: 80 mM PIPES pH 6.8, 1 mM EGTA, 1 mM $MgCl_2$ (*see* **Note 1**).
11. BRB80-D: 80 mM PIPES pH 6.8, 1 mM EGTA, 1 mM $MgCl_2$, 5 mM DTT.
12. BRB80-DT: 80 mM PIPES pH 6.8, 1 mM EGTA, 1 mM $MgCl_2$, 5 mM DTT, 20 μM taxol.
13. 2× Polymix: 80 mM PIPES pH 6.8, 1 mM EGTA, 1 mM $MgCl_2$, 2 mM GTP, 20 % DMSO. Store at −80 °C.
14. D-(+)-Glucose: 2 M stock solution in water. Store at −80 °C.
15. Glucose oxidase (Sigma-Aldrich #G-7016). Store as powder at −20 °C.
16. Catalase (Roche Applied Science #106810). Store at 4 °C.
17. Oxygen scavenger mix (100× stock solution): mix 200 μL of BRB80, 50 μL catalase (65,000 units), and 30 mg glucose oxidase (~6,000 units). Mix gently and incubate for 5 min at 4 °C. The solution will be cloudy. Spin at 20,000 × *g* in a tabletop centrifuge and retain the supernatant. Filter the supernatant using a 0.1 μm filter (Millipore). Prepare 10 μL aliquots, snap-freeze in liquid nitrogen, and store at −80 °C.

2.2.5 Tubulin

1. Unlabeled tubulin purified from porcine brain (Cytoskeleton, Inc. #T240).
2. TMR-labeled tubulin (Cytoskeleton, Inc. #TL447M). Resuspend the lyophilized pellet in BRB80, aliquot and freeze immediately in liquid nitrogen. Use one aliquot *per* experiment and discard any unused material (*see* **Note 2**).

2.3 Data Analysis

ImageJ (NIH) for basic image processing. http://rsb.info.nih.gov/ij/

3 Methods

3.1 Spastin Purification

1. Transform N-terminal glutathione S-transferase (GST) fusion spastin (residues 220—C-terminus) expression vector into *E. coli* strain Rosetta2(DE3)pLysS. Grow cells to an OD_{600} of 0.8 in LB broth containing 0.2 mg/mL ampicillin and 0.034 mg/mL chloramphenicol at 37 °C. Use beveled culture flasks for maximal aeration. Induce expression with 0.5 mM IPTG and harvest cells after 16 h of induction at 16 °C.

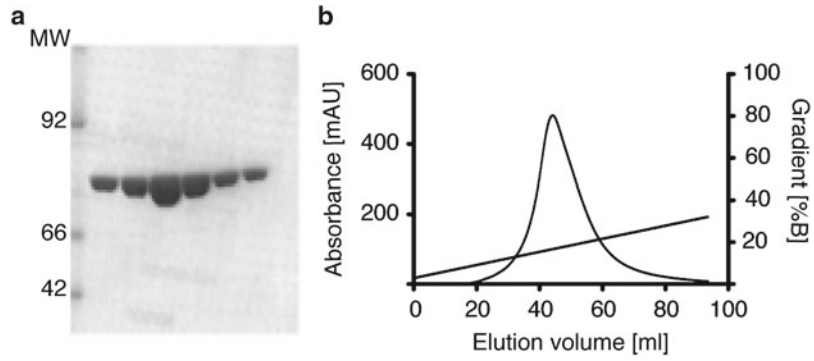

Fig. 1 (**a**) SDS-PAGE gel showing spastin purity after the ion exchange chromatography step. (**b**) Elution profile of spastin from a HiTrap Capto S ion exchange chromatography column

2. Resuspend cells in lysis buffer and disrupt using the EmulsiFlex C5 (three passes at 10–12 Kpsi while making sure that the sample is kept constantly chilled on ice).
3. Supplement the lysate with 0.02 mg/mL DNAse I and incubate on ice for 15 min while mixing gently. Add 400 mM NaCl and incubate on ice for an additional 15 min.
4. Pack a GST-affinity column using the glutathione sepharose 4 fast flow resin (10 mL of resin are sufficient for 15 g of wet cell pellet).
5. Collect supernatant after centrifugation in SS-34 rotor at 30,000 × *g* for 50 min. Supplement supernatant with 5 mM DTT and load on the GST-affinity column equilibrated in wash buffer.
6. Wash the GST-affinity column with 20 column volumes (CV) of wash buffer and elute the fusion protein with the elution buffer. Run a SDS-PAGE gel to estimate the purity of the fusion protein.
7. Cleave the GST fusion tag by incubating with PreScission protease (1 unit will cleave >90 % of 100 μg of a GST-fusion protein) at 4 °C overnight.
8. Run SDS-PAGE gel the next morning to examine whether cleavage is complete (*see* **Note 3**).
9. If cleavage is successful, dilute the protein sample 1:2 in ion exchange buffer A. Filter sample through a PVDF low protein binding filter with pore size 0.22 μm and load on a HiTrap Capto S column equilibrated in 5 % ion exchange buffer B. Wash the column with 20 CV of 5 % ion exchange buffer B. Elute the protein using a continuous gradient of 5–50 % ion exchange buffer B over 20 CV.
10. Collect peak fractions and run a SDS-PAGE gel to determine the purity of the eluted sample (Fig. 1).

11. Dialyze overnight against dialysis buffer using Slide-A-Lyzer Dialysis Cassettes 10K MWCO.
12. Prepare 20 μL aliquots of the purified protein, snap-freeze in liquid nitrogen, and store at −80 °C (*see* **Note 4**).

3.2 Light Microscopy Based Microtubule Severing Assay

3.2.1 Cover Glass and Slide Preparation

Proteins adsorb nonspecifically to untreated glass. Thus, preparation of clean, silanized cover glass that can be efficiently passivated by a blocking agent is essential for these assays. In the absence of this treatment, most of the spastin protein adsorbs to the glass and is rendered inactive. This results either in failure to see robust activity or the need to use large concentrations of the severing enzyme in these assays. We detail below a procedure we adapted from [26] and use in our laboratory to prepare slides and cover glass for microtubule severing assays.

1. Sonicate cover glass and slides for ~1 h in 2 % mucasol.
2. Rinse cover glass and slides five times with ultrapure water.
3. Prepare "Piranha" solution by mixing sulfuric acid and hydrogen peroxide in a 2:1 ratio. Make sure to add the peroxide to the acid and not the other way around! The reaction is exothermic. Having an excess of hydrogen peroxide to sulfuric acid can cause an explosion (*see* **Note 5**). Prepare the Piranha solution just before use as it loses its efficacy after ~1 h.
4. Place polytetrafluoroethylene racks with the cover glass and slides in a beaker with Piranha solution for 1 h. Make sure that the slides and cover glass are completely submerged in the solution. Maintain the temperature at ~60 °C by placing the beaker on a hot plate.
5. Rinse cover glass four times with ultrapure water.
6. Transfer the rack to a beaker with 0.1 M KOH solution and incubate at room temperature for 15 min.
7. Rinse glass three times with ultrapure water.
8. Place glass in ethanol for ~1 min and air dry.
9. Prepare silanizing solution just before usage by mixing 150 mL TCE with 75 μL DDS. Withdraw the appropriate volume of DDS using a syringe with a long needle. Seal the bottle well with parafilm when finished and store in a desiccator.
10. Submerge racks with the cover glass in silanizing solution at room temperature for 1 h.
11. Transfer the rack to a beaker with methanol and sonicate for 5 min. Exchange the methanol and sonicate again for 10 min.
12. Transfer to ethanol.
13. Dry cover glass and slides. Store in sealed containers. Cleaned cover glass and slides can also be stored for longer periods of time in ethanol and dried before use.

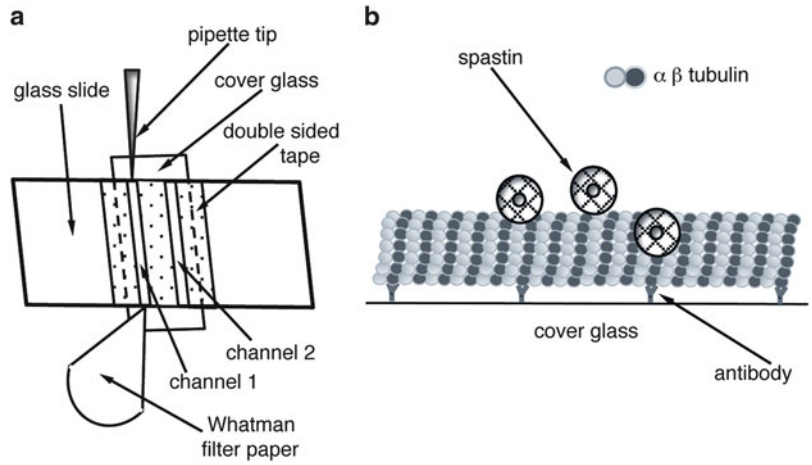

Fig. 2 (**a**) Schematic of the flow chamber used in microtubule severing assays. (**b**) Cartoon of the microtubule severing assay. A TMR-labeled microtubule is immobilized on the glass surface using anti-TMR antibodies. The microtubule severing enzyme is perfused into the chamber in the presence of ATP and oxygen scavengers

3.2.2 Preparation of TMR Labeled Taxol Stabilized Microtubules

1. Mix 2 μL of 2 mg/mL TMR-tubulin with 3 μL of 10 mg/mL unlabeled tubulin and incubate on ice for 2 min. This results in microtubules that have ~11 % of tubulin fluorescently labeled.
2. Add 5 μL of 2× Polymix and incubate in a water bath at 37 °C for 40 min.
3. Add 10 μL of BRB80-DT (prewarmed to 37 °C) and continue to incubate in the water bath at 37 °C for another 10 min.
4. Spin down in TLA 100 rotor (prewarmed to 30 °C) for 7 min at 109,000 × *g* (50,000 rpm) to remove unpolymerized tubulin.
5. Discard supernatant and resuspend pelleted microtubules in 50 μL of BRB80-DT. Because microtubules shear easily, use a cut pipette tip to resuspend the microtubule pellet. Store the TMR-labeled microtubules on your bench covered with aluminum foil (*see* **Note 6**). They are suitable for assays for several days.

3.2.3 Flow Chamber Assembly and Severing Assay

1. Attach pieces of double-sided tape to a slide forming two 2-mm wide chambers and cover with a cover glass. This creates a thin "channel" between the strips of tape and the two pieces of glass with a volume of ~5 μL (Fig. 2a).
2. Perfuse the flow chamber by adding 10 μL of 50 μg/mL anti-TMR antibody to one end of the chamber while fluid is wicked on the other end with a filter paper strip. Incubate at room temperature for 20 min (*see* **Note 7**).
3. Wash the flow chamber with 20 μL of BRB80-D supplemented with 2 mg/mL casein. In order to exchange the solution in the

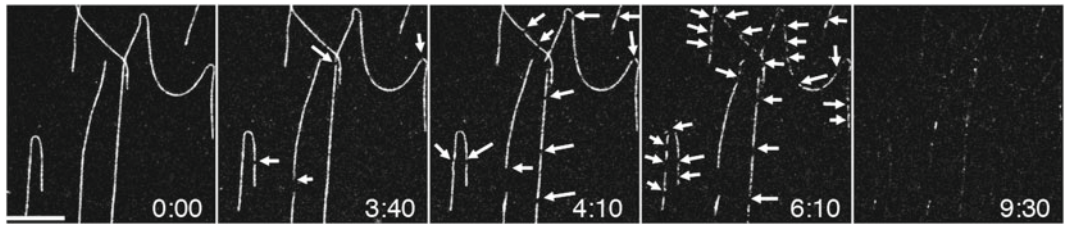

Fig. 3 TMR-labeled microtubules severed by spastin. Severing sites along the microtubules are indicated by *arrows*. The last time point shows the almost complete disassembly of the microtubules. Time is in minutes. Scale bar is 10 μm

channel completely, it is necessary to flow at least two channel volumes of solution.

4. Dilute TMR-labeled microtubule stock (typically a 25× dilution gives a suitable microtubule density) in BRB80-DT supplemented with 2 mg/mL casein. Perfuse 20 μL into the flow chamber and incubate at room temperature for 10 min. Microtubules are attached to the silanized cover glass surface by the anti-TMR antibodies that adsorbed nonspecifically to the glass (Fig. 2b; *see* **Note 8**). It might be necessary to adjust the dilution of the microtubule stock depending on the preparation. For a new microtubule stock we quickly test a series of dilutions by assembling slides with multiple channels (Fig. 2a). A typical chamber with an optimal density of microtubules is shown in Fig. 3. The antibodies act as spacers between the glass and the microtubule and prevent a collapse of the microtubule structure through strong nonspecific interactions with the glass surface. This configuration also allows better access to the microtubule of the severing enzyme.
5. Wash the flow chamber with 30 μL of BRB80-DT supplemented with 2 mg/mL casein, oxygen scavenger mix (1:100 dilution of stock), 20 mM glucose.
6. Prepare 20 μL of a solution containing 50 nM spastin, 2 mg/mL casein, 1 mM ATP, oxygen scavenger mix, 20 mM glucose in BRB80-DT and perfuse in the flow chamber while trying to maintain the focal plane unperturbed. Start imaging shortly before perfusion. After data acquisition is completed, move to a different field of view that was not illuminated and examine the integrity of the microtubules in that area (*see* **Note 9**).

3.3 Data Analysis

Microtubule severing activity can be quantified using two basic methods: (a) counting the number of severing events observed *per* unit time *per* total microtubule length or (b) by measuring the rate of tubulin removal, i.e., the extension rate of the microtubule gap after the initial severing event (*see* **Notes 10** and **11**). These analyses can be performed using basic functions available in ImageJ (NIH).

3.4 Conclusions

The microtubule severing assay described here can be very powerful as it allows the severing reaction to be reconstituted entirely from purified components and thus can be used to investigate the basic biophysical mechanism of severing enzymes (*see* **Note 12**) as well as to test the effects of cellular factors on severing activity. These can influence severing activity by directly binding and/or post-translationally modifying the microtubule severing enzyme itself [15, 24] or indirectly by binding or post-translationally modifying the microtubule track [27–30]. Through the gradual addition of purified components this basic assay can be used to investigate mechanisms of microtubule severing enzyme regulation and identify novel cellular cofactors that regulate microtubule severing enzyme activity.

4 Notes

1. This buffer is commonly used in microtubule assays.
2. Tubulin denatures easily and needs to be stored at −80 °C in single use aliquots flash frozen in liquid nitrogen. When thawing a new aliquot, spin it in a precooled rotor in the ultracentrifuge at 440,000 × *g* (100,000 rpm in a TLA 100 rotor) at 4 °C to remove any aggregates formed during the freezing and thawing process.
3. The cleavage is usually 80 % complete after overnight incubation. The two fragment sizes expected (spastin and GST) are 54 and 26 kDa, respectively.
4. Spastin activity decreases if the protein is stored for more than a day at 4 °C. Discard any unused protein at the end of the day and start with a fresh aliquot for a new set of assays. When thawing a new aliquot, spin it in a precooled rotor in the ultracentrifuge at 440,000 × *g* (100,000 rpm in a TLA 100 rotor) at 4 °C to remove any aggregates formed during the freezing and thawing process.
5. Cover glass cleaning and silanization must be performed in a chemical fume hood with caution and using protective equipment. Familiarize yourself with the appropriate protocols for chemical spill handling.
6. Unpolymerized tubulin should be kept on ice. Microtubules should not be placed on ice as they will immediately depolymerize.
7. The anti-TMR antibody denatures and loses its activity over time if stored at 4 °C. It can be flash frozen in liquid nitrogen in single use aliquots without loss of activity.
8. An anti-tubulin antibody (clone TUB 2.1) (Sigma-Aldrich #T4026) [31] or a rigor kinesin construct [7, 32] can also be used to immobilize microtubules on the cover glass.

9. TMR-labeled microtubules can break if photodamaged [33]. To minimize photodamage, decrease light exposure as much as possible and use fresh oxygen scavengers. Always perform your controls judiciously.
10. Severing rates measured in these assays vary as a function of the density of anti-TMR antibodies used to immobilize the microtubules on the glass. Thus, when comparing severing activities between samples it is important that the same antibody concentration and glass treatment be used.
11. The microtubule severing reaction is dependent on the electrostatic interaction between the enzyme and the negatively charged C-terminal tubulin tails [7, 8, 24]. Thus, the ionic strength of the buffer used in severing assays is important and should be kept as low as protein stability allows in order to observe maximal activity.
12. The assay described here can be adapted to also observe the dynamics of spastin molecules on the microtubule by using a fluorescently labeled variant of the enzyme and total internal reflection fluorescence microscopy.

Acknowledgments

A. Roll-Mecak is supported by the National Institutes of Health Intramural Program. N. E. Ziółkowska is supported by a Searle Scholar Award to A. Roll-Mecak.

References

1. Mitchison T, Kirschner M (1984) Dynamic instability of microtubule growth. Nature 312:237–242
2. Howard J, Hyman AA (2007) Microtubule polymerases and depolymerases. Curr Opin Cell Biol 19:31–35
3. Roll-Mecak A, McNally FJ (2010) Microtubule-severing enzymes. Curr Opin Cell Biol 22:96–103
4. Sharp DJ, Ross JL (2012) Microtubule-severing enzymes at the cutting edge. J Cell Sci 125:2561–2569
5. Vale RD (1991) Severing of stable microtubules by a mitotically activated protein in Xenopus egg extracts. Cell 64:827–839
6. McNally FJ, Vale RD (1993) Identification of katanin, an ATPase that severs and disassembles stable microtubules. Cell 75:419–429
7. Roll-Mecak A, Vale RD (2005) The Drosophila homologue of the hereditary spastic paraplegia protein, spastin, severs and disassembles microtubules. Curr Biol 15:650–655
8. Evans KJ, Gomes ER, Reisenweber SM, Gundersen GG, Lauring BP (2005) Linking axonal degeneration to microtubule remodeling by Spastin-mediated microtubule severing. J Cell Biol 168:599–606
9. Zhang D, Rogers GC, Buster DW, Sharp DJ (2007) Three microtubule severing enzymes contribute to the "Pacman-flux" machinery that moves chromosomes. J Cell Biol 177:231–242
10. Mukherjee S, Diaz Valencia JD, Stewman S, Metz J, Monnier S, Rath U, Asenjo AB, Charafeddine RA, Sosa HJ, Ross JL, Ma A, Sharp DJ (2012) Human Fidgetin is a microtubule severing the enzyme and minus-end depolymerase that regulates mitosis. Cell Cycle 11:2359–2366
11. Sonbuchner TM, Rath U, Sharp DJ (2010) KL1 is a novel microtubule severing enzyme that regulates mitotic spindle architecture. Cell Cycle 9:2403–2411
12. Mains PE, Kemphues KJ, Sprunger SA, Sulston IA, Wood WB (1990) Mutations affecting the meiotic and mitotic divisions of

the early Caenorhabditis elegans embryo. Genetics 126:593–605
13. Clark-Maguire S, Mains PE (1994) mei-1, a gene required for meiotic spindle formation in Caenorhabditis elegans, is a member of a family of ATPases. Genetics 136:533–546
14. McNally K, Audhya A, Oegema K, McNally FJ (2006) Katanin controls mitotic and meiotic spindle length. J Cell Biol 175:881–891
15. Loughlin R, Wilbur JD, McNally FJ, Nedelec FJ, Heald R (2011) Katanin contributes to interspecies spindle length scaling in Xenopus. Cell 147:1397–1407
16. Sharma N, Bryant J, Wloga D, Donaldson R, Davis R, Jerka-Dziadosz M, Gaertig J (2007) Katanin regulates dynamics of microtubules and biogenesis of motile cilia. J Cell Biol 178:1065–1079
17. Dymek EE, Smith EF (2012) PF19 encodes the p60 catalytic subunit of katanin and is required for assembly of the flagellar central apparatus in Chlamydomonas. J Cell Sci 125:3357–3366
18. Ahmad FJ, Yu W, McNally FJ, Baas PW (1999) An essential role for katanin in severing microtubules in the neuron. J Cell Biol 145: 305–315
19. Lee HH, Jan LY, Jan YN (2009) Drosophila IKK-related kinase Ik2 and Katanin p60-like 1 regulate dendrite pruning of sensory neuron during metamorphosis. Proc Natl Acad Sci U S A 106:6363–6368
20. Stewart A, Tsubouchi A, Rolls MM, Tracey WD, Tang Sherwood N (2012) Katanin p60-like1 promotes microtubule growth and terminal dendrite stability in the larval class IV sensory neurons of Drosophila. J Neurosci 32:11631–11642
21. Wood JD, Landers JA, Bingley M, McDermott CJ, Thomas-McArthur V, Gleadall LJ, Shaw PJ, Cunliffe VT (2006) The microtubule-severing protein Spastin is essential for axon outgrowth in the zebrafish embryo. Hum Mol Genet 15:2763–2771
22. Sherwood N, Sun Q, Xue M, Zhang B, Zinn K (2004) Drosophila Spastin regulates synaptic microtubule networks and is required for normal motor function. PLoS Biol 2:e429
23. Stone MC, Rao K, Gheres KW, Kim S, Tao J, La Rochelle C, Folker CT, Sherwood NT, Rolls MM (2012) Normal Spastin gene dosage is specifically required for axon regeneration. Cell Rep 2:1340–1350
24. Hartman JJ, Mahr J, McNally K, Okawa K, Iwamatsu A, Thomas S, Cheesman S, Heuser J, Vale RD, McNally FJ (1998) Katanin, a microtubule-severing protein, is a novel AAA ATPase that targets to the centrosome using a WD40-containing subunit. Cell 93:277–287
25. Roll-Mecak A, Vale RD (2008) Structural basis of microtubule severing by the hereditary spastic paraplegia protein spastin. Nature 451:363–367
26. Gell C, Bormuth V, Brouhard GJ, Cohen DN, Diez S, Friel CT, Helenius J, Nitzsche B, Petzold H, Ribbe J, Schaffer E, Stear JH, Trushko A, Varga V, Widlund PO, Zanic M, Howard J (2010) Microtubule dynamics reconstituted in vitro and imaged by single-molecule fluorescence microscopy. Methods Cell Biol 95:221–245
27. McNally KP, Buster D, McNally FJ (2002) Katanin-mediated microtubule severing can be regulated by multiple mechanisms. Cell Motil Cytoskeleton 53:337–349
28. Yu W, Qiang L, Solowska JM, Karabay A, Korulu S, Baas PW (2008) The microtubule-severing proteins spastin and katanin participate differently in the formation of axonal branches. Mol Biol Cell 19:1485–1498
29. Sudo H, Baas PW (2011) Strategies for diminishing katanin-based loss of microtubules in tauopathic neurodegenerative diseases. Hum Mol Genet 20:763–778
30. Lacroix B, van Dijk J, Gold ND, Guizetti J, Aldrian-Herrada G, Rogowski K, Gerlich DW, Janke C (2010) Tubulin polyglutamylation stimulates spastin-mediated microtubule severing. J Cell Biol 189:945–954
31. Diaz-Valencia JD, Morelli MM, Bailey M, Zhang D, Sharp DJ, Ross JL (2011) Drosophila katanin-60 depolymerizes and severs at microtubule defects. Biophys J 100:2440–2449
32. McNally FJ, Thomas S (1998) Katanin is responsible for the M-phase microtubule-severing activity in Xenopus eggs. Mol Biol Cell 9:1847–1861
33. Vigers GP, Coue M, McIntosh JR (1988) Fluorescent microtubules break up under illumination. J Cell Biol 107:1011–1024

Chapter 20

VE-Cadherin Status as an Indicator of Microvascular Permeability

Elizabeth Monaghan-Benson and Keith Burridge

Abstract

VE-cadherin phosphorylation and binding partner status are important indicators of endothelial permeability. Here we describe several techniques aimed at discerning total tyrosine phosphorylation levels of VE-cadherin, VE-cadherin phosphorylation on specific tyrosine residues, and the ability of VE-cadherin to bind its binding partner beta-catenin. Taken together, these approaches to studying VE-cadherin status on microvascular endothelial cells are excellent complements to traditional permeability assays.

Key words Microvascular endothelial cells, Endothelial permeability, VE-cadherin, Immunoprecipitation, Co-immunoprecipitation

1 Introduction

Adherens junctions are composed of cadherins bound together to link adjacent endothelial cells [1]. Cadherins interact through their cytoplasmic tails with the catenin family, which in turn provide anchorage to the actin cytoskeleton [2]. The interaction of VE-cadherin with the cytoskeleton is important for junction stability and for the dynamic opening and closing of the junctions. In endothelial cells, adherens junctions are largely composed of VE-cadherin, an endothelial specific cadherin that binds to multiple protein partners, including p120 and beta-catenin. While the barrier function of the endothelium is supported by multiple cell–cell adhesion systems (adherens and tight junctions) disruption of VE-cadherin is sufficient to disrupt intercellular junctions [3–5]. Previous data has demonstrated increased permeability both in vitro and in vivo after treatment with VE-cadherin blocking antibodies [3, 6]. Additionally, VE-cadherin is required to prevent disassembly of blood vessel walls [5, 7] and to coordinate the passage of macromolecules through the endothelium [8]. The phosphorylation of VE-cadherin at Tyr (tyrosine)-658 and Tyr-731 prevents the binding of p120 and

Amanda S. Coutts (ed.), *Adhesion Protein Protocols*, Methods in Molecular Biology, vol. 1046,
DOI 10.1007/978-1-62703-538-5_20,

beta-catenin, respectively [9]. Tyrosine phosphorylation provides a regulatory link, as increased phosphorylation of VE-cadherin and partial dissociation of the catenin/cadherin complex results in deceased cell-cell adhesion and increased permeability [9].

Here we describe several methods to examine VE-cadherin status, as it pertains to vascular permeability, in microvascular endothelial cells. We describe the immunoprecipitation of VE-cadherin and the determination of both total tyrosine phosphorylation and beta-catenin binding partner status. We also describe a method for determining the site specific phosphorylation of VE-cadherin at tyrosines 658 and 731.

2 Materials

2.1 Cell Culture

1. Pooled Human Microvascular Endothelial Cells (HMVEC) (Lonza CC-2516). HMVECs were routinely used between passage 4 and 7.
2. EGM-2MV: EBM-2 basal medium plus the included SingleQuots of supplements: hEGF, hydrocortisone, GA-1000, FBS, VEGF, hFGF-B, R3-IGF-1, ascorbic acid, heparin.
3. Tissue Culture Incubator: 37 °C, 5 % CO_2.
4. PureCol (Advanced BioMatrix 5005-B).
5. Trypsin/EDTA: (0.05 %, Gibco 25300-054).

2.2 Preparation of Cell Lysates

1. 1× PBS.
2. IP (Immunoprecipitation) lysis buffer: 10 mM Tris–HCl pH 7.4, 150 mM NaCl, 1 mM sodium vanadate, 0.2 mM PMSF, 1 % Triton-X 100, 0.5 % NP-40, and a cocktail of protease inhibitors (leupeptin, aprotinin, PMSF).
3. 1.5 mL microfuge tubes.
4. Tabletop microcentrifuge that can be cooled or placed in a cold room.
5. VEGF: 10 ng/mL (R&D Biosystems).

2.3 VE-Cadherin Immunoprecipitation

1. 2× sample buffer: 0.125 M Tris–HCl pH 6.8, 20 % glycerol, 4 % SDS, 10 % 2-mercaptoethanol, 0.02 % bromophenol blue.
2. VE-cadherin monoclonal antibody (Santa Cruz sc-9989).
3. Protein A/G plus sepharose beads.

2.4 Analysis of Immunoprecipitates for Total Tyrosine Phosphorylation Levels

1. 10 % SDS-PAGE gels.
2. Nitrocellulose.
3. 5 % BSA/TBST: 5 g BSA into 100 mL TBST.
4. TBST: 100 mM Tris–HCl, 150 mM NaCl, 0.1 % Tween-20.

5. Anti-phosphotyrosine antibody (recommended 4G10 Millipore 05-321).
6. Total VE-cadherin antibody (Santa Cruz sc-9989).
7. Goat anti-mouse HRP conjugated secondary antibody.
8. ECL.

2.5 Analysis of VE-Cadherin Immunoprecipitates for Beta-Catenin

1. 10 % SDS-PAGE gels.
2. Nitrocellulose.
3. 5 % BSA/TBST.
4. TBST.
5. Anti-beta-catenin antibody.
6. Total VE-cadherin antibody (Santa Cruz sc-9989).
7. Goat anti-mouse HRP conjugated secondary antibody.
8. ECL.

2.6 Lysate Preparation for Analysis of Site Specific Phosphorylation of VE-Cadherin

1. EBM: Lonza CC-3156.
2. 2× Sample Buffer.
3. VEGF (10 ng/mL).

2.7 Analysis of Lysates for Site Specific Phosphorylation of VE-Cadherin

1. Three 10 % SDS-PAGE gels.
2. Nitrocellulose.
3. TBST.
4. 5 % BSA/TBST.
5. VE-cadherin PY731 antibody (Millipore 44-1145G).
6. VE-cadherin PY658 antibody (Millipore 44-1144G).
7. Total VE-cadherin antibody (Santa Cruz sc-9989).
8. Goat anti-rabbit HRP secondary antibody.
9. Goat anti-mouse secondary antibody.
10. ECL.

3 Methods

3.1 Endothelial Cell Cultures

1. HMVEC are grown and maintained in EGM-2MV on 100 mm tissue culture dishes coated with PureCol (20 μg/mL) at 37 °C and 5 % CO_2 (*see* **Note 1**).
2. Cells are passaged at 90 % confluence with 0.05 % trypsin/EDTA.

3. Cells are fed fresh medium every second day and are typically used for experiments between passages 4–7.
4. To ensure the health of the cells, never subculture at a dilution ratio of greater than 1:3.

3.2 Preparation of the Cell Lysates for VE-Cadherin Immunoprecipitation

1. HMVEC are grown to confluence in 100 mm dishes.
2. Treat cells with desired compounds (*see* **Notes 2** and **3**).
3. Place dishes of cells on ice. Wash cells 1× with 1 mL ice-cold PBS (*see* **Note 4**).
4. Add 500 μL IP lysis buffer to each dish of cells. Scrape cells and place lysates into 1.5 mL microfuge tubes on ice. Leave on ice for 15 min.
5. Remove the insoluble material by centrifuging lysates for 20 min at 4 °C and 25,000 × *g* in a tabletop microcentrifuge.
6. Transfer supernatants to new tubes and place on ice. Discard the pellets.

3.3 VE-Cadherin Immunoprecipitation

1. Remove 50 μL of lysate from each tube and place in new tubes. This will serve as the input for loading when blotting. Add 50 μL of 2× sample buffer to each tube (*see* **Note 5**).
2. To each of the original tubes of lysate add 2 μg of the VE-cadherin monoclonal antibody.
3. Place tubes at 4 °C and rotate overnight.
4. Add 100 μL of Protein A/G plus sepharose beads to each tube and rotate for 1 h at 4 °C (*see* **Note 6**).
5. Centrifuge the tubes at 4 °C and 5,000 × *g* for 1 min to pellet the beads. Aspirate the supernatant (*see* **Note 7**).
6. Add 500 μL IP lysis buffer to the beads to wash and centrifuge again. Repeat this process two more times.
7. After the IP lysis buffer from the last wash has been aspirated add 100 μL 2× sample buffer to each tube. Boil samples for 10 min.

3.4 Analysis of VE-Cadherin Immunoprecipitates for Total Tyrosine Phosphorylation

1. Pour two 10 % SDS-PAGE gels.
2. Load 50 μL of IP sample to each well of one gel.
3. Add 50 μL of input sample taken before the immunoprecipitation to the second gel (*see* **Note 8**).
4. Run gels until dye front reaches the bottom of the gel.
5. Transfer proteins to nitrocellulose for 1 h at 100 V.
6. Block membranes with 5 % BSA/TBST for 1 h with gentle shaking.
7. Incubate the immunoprecipitation blot with anti-phosphotyrosine antibody overnight at 4 °C. Incubate input blot with VE-cadherin antibody overnight at 4 °C.

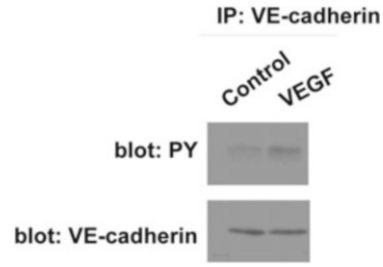

Fig. 1 VE-cadherin phosphorylation. Monolayers of HMVECs were treated with 10 ng/mL VEGF. VE-cadherin was immunoprecipitated from cell lysates using a mouse anti-VE-cadherin antibody and the resulting immunoprecipitates were analyzed for phosphotyrosine by immunoblotting (PY: 4G10, *top*) or total VE-cadherin (*bottom*)

8. Wash both blots with TBST for 1 h changing buffer every 15 min.
9. Incubate both blots with goat anti-mouse HRP conjugated secondary antibody (1/10,000) for 1 h.
10. Wash both blots with TBST for 2 h changing buffer every 15 min.
11. Develop with ECL according to manufacturer's instructions.

An example of a typical experiment is shown in Fig. 1 where MVCEs have been treated with VEGF prior to immunoprecipitation with VE-cadherin antibody. Immunoprecipitates were then analyzed for total levels of phosphor-tyrosine.

3.5 Analysis of VE-Cadherin Immunoprecipitates for Beta-Catenin

1. Pour two 10 % SDS-PAGE gels.
2. Load 50 μL of IP sample onto each gel (*see* **Note 8**).
3. Run gels until dye front reaches bottom of gel.
4. Transfer proteins to nitrocellulose for 1 h at 100 V.
5. Block blots in 5 % BSA/TBST for 1 h at room temperature.
6. Incubate one blot with beta-catenin antibody (1/1,000) and one blot with the VE-cadherin antibody (1/1,000) overnight at 4 °C with gentle rocking.
7. Wash blots for 1 h with TBST changing buffer every 15 min.
8. Add appropriate HRP-conjugated secondary antibodies (1/10,000) (goat anti-rabbit HRP for beta-catenin and goat anti-mouse HRP for VE-cadherin) to blots for 1 h at room temperature.
9. Wash blots with TBST for 2 h at room temperature changing the buffer every 15 min.
10. Develop with ECL according to manufacturer's instructions.

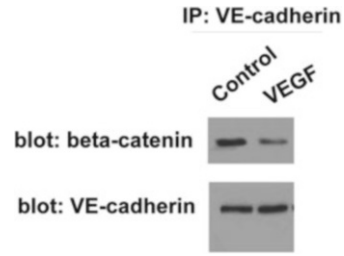

Fig. 2 VE-cadherin/beta-catenin co-immunoprecipitation. HMVECS were treated with 10 ng/mL VEGF for 5 min. VE-cadherin was immunoprecipitated from cell lysates and immunoprecipitates were blotted for the presence of beta-catenin (*top panel*) or VE-cadherin (*bottom panel*)

An example of a typical experiment is shown in Fig. 2 where HMVECs have been treated with VEGF prior to immunoprecipitation with VE-cadherin antibody. Immunoprecipitates were then analyzed for levels of bound beta-catenin.

3.6 Preparing Lysates for Analysis of Site Specific Phosphorylation of VE-Cadherin

1. HMVEC are grown to confluence in 6-well dishes as described in Subheading 3.1.
2. Cells are serum starved overnight (*see* **Note 9**).
3. Cells are treated with desired compounds (*see* **Notes 2** and **3**).
4. Cells are lysed with 100 μL/well 2× sample buffer.
5. Lysates are boiled for 10 min (*see* **Note 10**).

3.7 Analysis of Site Specific VE-Cadherin Phosphorylation

1. Pour three 10 % SDS-PAGE gels.
2. Load 30 μL per sample of prepared lysate onto each gel.
3. Run gels until dye front reaches bottom of gel.
4. Transfer proteins to nitrocellulose for 1 h at 100 V.
5. Block blots in 5 % BSA/TBST for 1 h at room temperature.
6. Incubate one blot with VE-cadherin PY731 antibody (1/1,000), the second blot with the VE-cadherin PY658 antibody (1/1,000) and the third blot with the total VE-cadherin antibody (1/1,000) overnight at 4 °C with gentle rocking.
7. Wash blots for 1 h with TBST changing buffer every 15 min.
8. Add appropriate HRP-conjugated secondary antibodies (1/10,000) to blots for 1 h at room temperature (goat anti-rabbit HRP for the VE-cadherin PY731 and PY658 antibodies and goat anti-mouse HRP for the total VE-cadherin antibody).
9. Wash blots with TBST for 2 h at room temperature changing the buffer every 15 min.

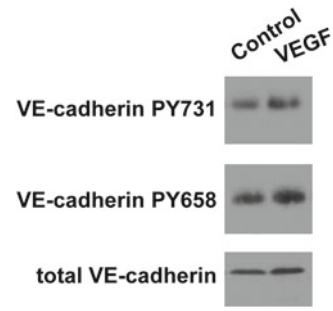

Fig. 3 Phosphorylation of VE-cadherin at Y658 and Y731. HMVECs were treated with 10 ng/mL VEGF for 5 min. Cell layers were lysed in sample buffer. Lysates were electrophoresed, immunoblotted, and analyzed for phosphorylated forms of VE-cadherin using antibodies which specifically recognize VE-cadherin phosphorylated at tyrosines 658 and 731. Total VE-cadherin was used as a loading control

10. Develop with ECL according to manufacturer's instructions.

An example of a typical experiment is shown in Fig. 3 where HMVECs have been treated with VEGF prior to lysis. Lysates were then analyzed for the phosphorylation of VE-cadhering at tyrosines 658 and 731.

4 Notes

1. Keep the collagen at 4 °C until immediately before use. Do not allow collagen to warm to room temperature or it will begin to gel.
2. For some treatments it is desirable to serum-starve the cells first. To serum-starve the cells before experimental treatment remove the EGM medium and replace it with EBM medium. Leave the cells in EBM medium for a minimum of 2 h and a maximum of overnight.
3. An excellent positive control for VE-cadherin phosphorylation is the treatment of endothelial cells with 10 ng/mL VEGF for 5 min.
4. Prechill both the 1× PBS and the IP lysis buffer for at least 30 min on ice before beginning the experiment.
5. As multiple sets of tubes are needed for this experiment it is best to prelabel the needed tubes. Also be sure to denote that the tube with lysate that has not undergone an immunoprecipitation is labeled as such.
6. Vortex the tube of Protein A/G plus sepharose beads to resuspend the beads evenly before pipetting.

7. Aspirate with a gel loading tip hooked up to a vacuum flask. The opening of the gel loading tip is small enough to prevent the beads from being accidentally aspirated.
8. Load the first gel and the second gel with the samples in the same order.
9. To serum starve the cells aspirate growth medium from wells. Replace with 2 mL/well EBM medium.
10. Lysates may be used immediately or frozen at –20 °C.

References

1. Kemler R (1992) Classical cadherins. Semin Cell Biol 3:149–155
2. Aberle H, Schwartz H, Kemler R (1996) Cadherin-catenin complex: protein interactions and their implications for cadherin function. J Cell Biochem 61:514–523
3. Corada M, Mariotti M, Thurston G et al (1999) Vascular endothelial-cadherin is an important determinant of microvascular integrity in vivo. Proc Natl Acad Sci USA 96: 9815–9820
4. Carmeliet P, Lampugnani MG, Moons L et al (1999) Targeted deficiency or cytosolic truncation of the VE-cadherin gene in mice impairs VEGF-mediated endothelial survival and angiogenesis. Cell 98:147–157
5. May C, Doody JF, Abdullah R et al (2005) Identification of a transiently exposed VE-cadherin epitope that allows for specific targeting of an antibody to the tumor neovasculature. Blood 105:4337–4344
6. Hordijk PL, Anthony E, Mul FP et al (1999) Vascular-endothelial-cadherin modulates endothelial monolayer permeability. J Cell Sci 112:1915–1923
7. Crosby CV, Fleming PA, Argraves WS et al (2005) VE-cadherin is not required for the formation of nascent blood vessels but acts to prevent their disassembly. Blood 105:2771–2776
8. Kooistra MR, Corada M, Dejana E et al (2005) Epac1 regulates integrity of endothelial cell junctions through VE-cadherin. FEBS Lett 579:4966–4972
9. Potter MD, Barbero S, Cheresh DA (2005) Tyrosine phosphorylation of VE-cadherin prevents binding of p120- and beta-catenin and maintains the cellular mesenchymal state. J Biol Chem 280:31906–31912

Chapter 21

High-Resolution Live-Cell Imaging and Time-Lapse Microscopy of Invadopodium Dynamics and Tracking Analysis

Ved P. Sharma, David Entenberg, and John Condeelis

Abstract

Invadopodia are specialized structures of cancer cells which aid in cancer cell invasion and metastasis. Therefore, studying the early steps of invadopodium assembly and its life cycle at the subcellular level by using high spatiotemporal resolution imaging provides an opportunity for understanding the signaling mechanisms involved in this very important process. In this chapter, we describe the design of a custom-built high-resolution fluorescence microscope which makes this challenging imaging possible. We also describe an ImageJ plugin that we have developed for tracking of invadopodia and lifetime analysis.

Key words Live-cell imaging, Time-lapse microscopy, Autofocus, Invadopodia, Breast carcinoma cells, Gelatin degradation, Particle tracking

1 Introduction

Metastasis is the leading cause of death in most cancer patients, as opposed to the growth of the primary tumor, which can be managed clinically to a large extent by surgery and chemotherapy. Invadopodia are specialized protrusive structures found in cancer cells, with a diameter around 0.5–1 μm and length of a couple of microns [1]. These structures are proteolytically active and degrade extracellular matrix (ECM) which aids in cancer cell invasion into the surrounding tissue and blood vessels leading to metastasis [2–4]. Since their first discovery in src-transformed fibroblasts [5], invadopodia have been found in many types of cancer cells including: breast [3, 6–8], melanoma [9, 10], head and neck [11], glioma [12], colon [13], pancreatic [14], and prostate [15].

By utilizing a 2D model in which cancer cells are plated on ECM coated surfaces, the mechanism of invadopodium formation and regulation has been studied in great detail. Although many

Amanda S. Coutts (ed.), *Adhesion Protein Protocols*, Methods in Molecular Biology, vol. 1046,
DOI 10.1007/978-1-62703-538-5_21,

invadopodium-associated proteins (e.g., cortactin, N-WASp, Tks5, Cofilin, Nck1, p190RhoGAP [7, 16–18]) have been identified, the molecular interaction(s) during invadopodium initiation is not well understood. We were interested in imaging various invadopodium proteins during invadopodium precursor assembly at high spatial and temporal resolution (on the order of seconds). To achieve these challenging imaging requirements, we have developed a robust custom-built wide-field fluorescence microscope. In this chapter, we provide technical details on the microscope design and data acquisition. To analyze the arrival of different invadopodium proteins, invadopodia lifetimes and trajectories, we have also developed an ImageJ plugin called "Invadopodia tracker." This plugin tracks multiple invadopodia in a cell throughout the whole time-lapse sequence. A step-by-step invadopodia tracking analysis procedure is also described.

2 Materials

2.1 Microscope Design

1. Excitation, emission, and ND filters (*see* Table 1).
2. Mercury arc lamp and controller (Chiu Technical Corporation, Mercury-100 W).
3. Dual filter wheel with six positions each for Excitation and ND filters (Ludl Electronics, Dual Filter Wheel).
4. 8-position filter wheel for emission filters (Applied Scientific Instrumentation, FW1000).
5. Continuous Reflective-Interface Feedback Focus unit (Applied Scientific Instrumentation, CRIFF).
6. Z-focus Stepper Motor (Applied Scientific Instrumentation, MFC2000 Z Axis Drive).
7. Fast piezo controlled Z-focus drive (Physik Instrumente, PIFoc).
8. Linear encoded XY Stage (Applied Scientific Instrumentation, MFC2000).
9. Glass reflector, 6 % reflection/94 % transmission (Chroma, 6/94bs).
10. 60× 1.42 NA oil, Plan Apo N objective (Olympus, part# 1-U2B933).
11. Two channel image splitter (Optical Insights, Dual-View).
12. High Performance 12 bit CCD camera (Cooke, SensiCamQE).

2.2 Labeling Gelatin with Alexa 405 Dye

1. Bio-Gel P-30 Gel (Bio-Rad cat#150-4154).
2. PBS with 2 mM sodium azide: Add 65 mg sodium azide in 500 mL PBS. Use this PBS for all the steps described in Subheadings 2.2 and 3.2.

Table 1
List of excitation, emission, ND, Turret, and Dual-View filters

Location	Use	Filter	Vendor
Filter Turret Pos. A	Dichroic Emission	FF01-444/520/590 FF01-465/537/623	Semrock Semrock
Filter Turret Pos. B	Dichroic Emission	FF493/574-Di01 FF01-512/630-25	Semrock Semrock
Filter Turret Pos. C	Dichroic Emission	FF660-Di01 FF01-685/40-25	Semrock Semrock
Filter Turret Pos. D	6 % Reflector	6/94bs	Chroma
Excitation Wheel Pos. 1	CFP Excitation	FF01-434/17-25	Semrock
Excitation Wheel Pos. 2	GFP Excitation	FF01-472/30-25	Semrock
Excitation Wheel Pos. 3	YFP Excitation	FF01-500/24-25	Semrock
Excitation Wheel Pos. 4	RFP Excitation	FF01-550/32-25	Semrock
Excitation Wheel Pos. 5	RFP Excitation	FF01-575/25-25	Semrock
Excitation Wheel Pos. 6	Cy5 Excitation	FF01-617/73-25	Semrock
Emission Wheel Pos. 1	Dual View Emission	Open	-
Emission Wheel Pos. 2	CFP Emission	FF01-475/50-25	Semrock
Emission Wheel Pos. 3	GFP Emission	FF01-514/30-25	Semrock
Emission Wheel Pos. 4	YFP Emission	FF01-519-LP	Semrock
Emission Wheel Pos. 5	RFP Emission	FF01-607/36-25	Semrock
Emission Wheel Pos. 6	Cy5 Emission	FF01-685/40-25	Semrock
CFP-YFP DualView Cube	Dichroic Short Pass Long Pass	t505lpxr FF01-475/50-25 FF01-500LP-25	Chroma Semrock Semrock
GFP-RFP DualView Cube	Dichroic Short Pass Long Pass	t540lpxr FF01-514/30-25 BLP01-532R-25	Chroma Semrock Semrock
ND Filter Wheel	0.1, 0.2, 0.3, 0.5, 0.6, 1.0, 2.0	nd filter set	Chroma

3. Glass column (Bio-Rad, cat# 737-1021).
4. Alexa Fluor 405 dye (Life Technologies, cat#A30000).
5. 0.2 % gelatin solution: Add 50 mg gelatin from porcine skin (Sigma-Aldrich, cat# G2500) into 25 mL PBS. Vortex briefly to mix and leave in the 37 °C water bath for ½–1 h. During the incubation period, take the tube out two times and vortex briefly.

6. 1 M sodium bicarbonate solution: 840.1 mg sodium bicarbonate powder in 10 mL ddH_2O; prepare fresh every time.
7. DMSO.
8. UV lamp.

2.3 Preparation of Gelatin-Coated MatTek Dishes

1. MatTek dish (MatTek corporation, cat# P35G-1.5-14-C).
2. 1 N HCl.
3. 2 mg/mL Poly-L-lysine solution: Add 12.5 mL ddH_2O to 25 mg poly-L-lysine powder (Sigma-Aldrich, cat# P1399). The solution can be stored at 4 °C for up to 1 year.
4. Prepare 0.2 % gelatin solution as described in Subheading 2.2, **item 5**.
5. 0.2 % glutaraldehyde solution: Add 160 μL of 25 % glutaraldehyde stock (Sigma-Aldrich, cat#G5882) into 20 mL PBS, leave on ice.
6. Sodium borohydride (Sigma-Aldrich, cat#452882).
7. 70 % ethanol solution.
8. 10× penicillin/streptomycin solution: Add 2 mL, 100× penicillin/streptomycin stock (Life Technologies, cat# 15140-122) into 18 mL PBS.

2.4 Transfection of MTLn3 Cells and Preparing Cells for Live Imaging

1. MTLn3 cells [19].
2. Culture medium: MEM Alpha (Life Technologies, cat#12561-056), 5 % fetal bovine serum (FBS) (Gemini Bio-products, cat#100106) and 1× penicillin/streptomycin.
3. 0.05 % trypsin–EDTA (Life Technologies).
4. Lipofectamine 2000 (Life Technologies).
5. Opti-MEM medium (Life Technologies).
6. DNA constructs (e.g., TagRFP-cortactin and GFP-Cofilin [17, 20]).
7. Serum starvation medium: Dissolve 0.345 g bovine serum albumin (BSA; Fisher Scientific, cat# BP1600-100) in 5 mL ddH_2O. Syringe filter through a 0.2 μm size filter. Add 2.5 mL of this solution into 47.5 mL L-15 medium (Life Technologies, cat# 21083). Place at 37 °C before use.
8. Steady state imaging medium: L-15 + 5 % FBS.

2.5 Live Imaging of Invadopodia

1. 10 nM EGF: Dilute 5 μL EGF stock (50 μM, Life Technologies, cat# 53003-018) into 245 μL serum starvation medium. Add 25 μL of this solution into 2 mL serum starvation medium.

3 Methods

3.1 Microscope Design

The microscope system (Fig. 1a) is built upon an Olympus IX-70 microscope stand with the following custom modifications:

1. The use of a glass reflector in place of a dichroic mirror in the filter turret of the microscope enables complete flexibility in the choice of fluorophores and efficient collection of emitted photons (Fig. 1b). However, as only 6 % of the excitation light makes it to the sample, a bright light source is required. For this purpose we have chosen a mercury arc lamp over other options (e.g., xenon or LED source). In cases where the fluorophores chosen were not bright enough for use with the glass reflector, other filter turret positions were loaded with multiband dichroics specific for particular applications (e.g., CFP-YFP-RFP, GFP-RFP and Cy5 imaging).
2. Control of the excitation intensity is accomplished with ND filters in one wheel of a dual filter wheel system. The second wheel of this system is used to house excitation filters which allow separate and individual control of excitation wavelengths.
3. Emission wavelengths were individually controlled with a separate filter wheel mounted in front of the CCD camera. The sensitivity of the measurements to drifts in focus necessitates an active autofocus module. For this purpose, a CRIFF unit utilizing a stepper motor z-focus drive was employed. To accommodate both the emission filter wheel and the CRIFF unit in the emission path of the microscope, a custom mount was designed and machined (Fig. 1c, d, *see* **Note 1**).
4. Additional fast z-scanning capabilities are attained by use of a piezo controlled focus mount. Mosaicing and multiple sample position acquisition are facilitated by a motorized xy stage equipped with linear encoders for accurate stage repositioning.
5. In some experiments, performing sequential imaging would be too slow to capture the rapid dynamics of the biological process of interest. In these cases, the emission filter wheel is put into an "open" position and an image splitter device (DualView) is placed in the emission path. This device splits the image into two halves, passing one through a long pass filter and the other through a short pass filter, and then projects the two images onto each half of the CCD chip.
6. The microscope utilizes a high numerical aperture objective lens (60×, 1.42 NA) for high resolution imaging.

For a list of fluorophores (and dyes) which can be imaged sequentially or simultaneously on the microscope, *see* Table 2.

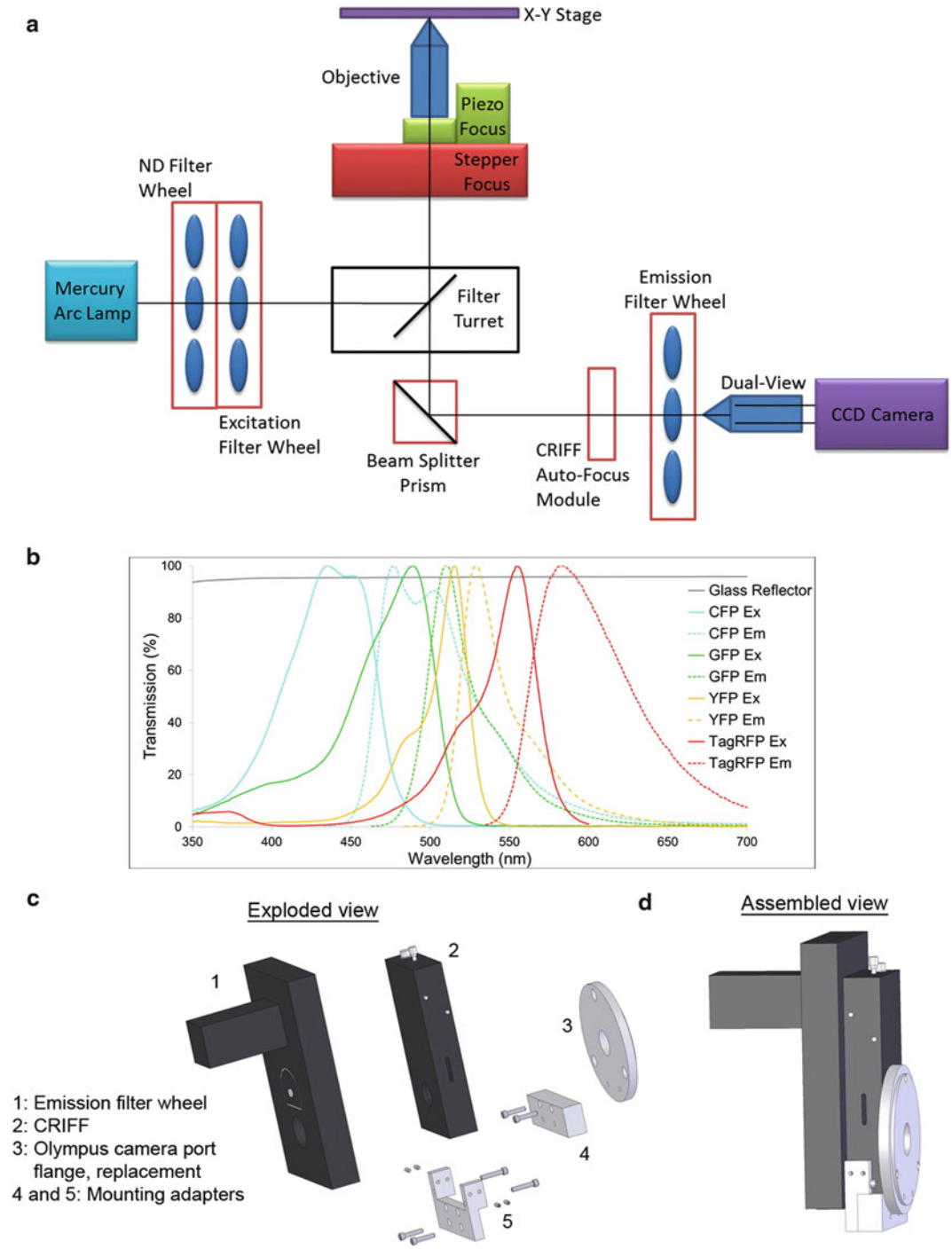

Fig. 1 Design of custom-built high-resolution wide-field fluorescence microscope. (**a**) Optical layout showing different parts of the microscope. For clarity, the environmental heat chamber, which surrounds the microscope, is not shown. (**b**) Transmission properties of the glass reflector (6 % reflection/94 % transmission) and excitation and emission spectra of commonly used fluorophores in live cell imaging. (**c**) Exploded view of CRIFF, emission filter wheel, flange and the mounting adapters. (**d**) Assembled view of the microscope parts shown in (**c**)

Table 2
Microscope imaging modes

Use #	Turret position	Dual-view	Usage
1	A, B, C, D	OFF	Trans-illumination
2	A	OFF	CFP, Cerulean
3	A	OFF	YFP, Venus
4	A	OFF	RFP, mCherry, TRITC, Alexa 555
5	A	OFF	CFP-YFP FRET, Cerulean-Venus FRET
6	B	OFF	GFP, FITC, Alexa 488
7	B	OFF	RFP, mCherry, TRITC, Alexa 555
8	B	OFF	GFP-RFP FRET
9	C	OFF	Cy5, Alexa 647
10	D	OFF	CFP, Cerulean
11	D	OFF	YFP, Venus
12	D	OFF	CFP-YFP FRET, Cerulean-Venus FRET
13	D	OFF	GFP, FITC, Alexa 488
14	D	OFF	RFP, mCherry, TRITC, Alexa 555
15	D	OFF	GFP-RFP FRET
16	D	OFF	Cy5, Alexa 647
17	D	CFP-YFP DualView cube	CFP (Left half) + YFP-FRET (right half)
18	D	CFP-YFP DualView cube	Blank (Left half) + YFP (right half)
19	D	CFP-YFP DualView cube	Blank (Left half) + RFP (right half)
20	D	CFP-YFP DualView cube	Blank (Left half) + Cy5 (right half)
21	D	GFP-RFP DualView cube	GFP (Left half) + RFP-FRET (right half)
22	D	GFP-RFP DualView cube	Blank (Left half) + RFP (right half)
23	D	GFP-RFP DualView cube	Blank (Left half) + Cy5 (right half)

3.2 Labeling Gelatin with Alexa 405 Dye

1. A day before labeling the gelatin, take 2 g Bio-Gel P-30 powder and add 36 mL PBS, mix by gently inverting the tube 5–6 times and leave at room temperature (RT). Hold the glass column vertical by clamping on a stand. Mix Bio-Gel slurry from the previous day by pipetting up and down and transfer it to the column until it is full. The column will start draining PBS from the bottom. As the top level of packed column drops, add mixed Bio-Gel slurry to the column. Leave approximately a 3 cm space with PBS above the packed column. The column can be stored at 4 °C for up to 1 week (*see* **Notes 2** and **3**).

2. While the column is draining in **step 1** above, bring 0.2 % gelatin solution to RT. Transfer 2 mL gelatin solution into a 15 mL conical tube. Add 200 μL 1 M sodium bicarbonate solution.
3. Briefly centrifuge Alexa 405 dye containing tube to dislodge any dye stuck in the cap. Add 100 μL DMSO to 1 mg Alexa 405 dye, mix by pipetting up and down 3–4 times. Add the dye/DMSO solution into 2.2 mL gelatin solution from **step 2**. Cover the conical tube with aluminum foil and rotate at RT for 1 h.
4. After the column in **step 1** has stopped draining, transfer the dye–gelatin solution from **step 3** to the top of the column. After all the dye–gelatin solution enters the column, add PBS gently to the top.
5. After 15 min, check the dye–gelatin solution in the column with a UV lamp. It should look like a bright blue smear through the column. As the dye–gelatin solution reaches the bottom of the column, start collecting the dye labeled gelatin solution into eppendorf tubes. Collect about 2–2.5 mL (*see* **Note 4**). This solution can be stored at 4 °C for up to 2 months.

3.3 Preparation of Gelatin-Coated MatTek Dishes (For Ten Dishes)

1. Add 300 μL 1 N HCl into the well of each MatTek dish. Incubate for 10 min at RT. Wash three times with PBS in 5 min intervals.
2. Dilute poly-L-lysine solution to 50 μg/mL (75 μL stock solution in 3 mL PBS). Put 300 μL into each well and incubate for 20 min at RT. Wash three times with PBS in 5 min intervals.
3. Take out 50 μL of Alexa 405 dye-labeled gelatin (prepared above in Subheading 3.2) into an eppendorf tube, cover it with aluminum foil and leave it on the bench for it to reach RT.
4. Once gelatin is completely dissolved, take it out of the water bath and leave it at RT to cool. Add 50 μL of Alexa 405 dye-labeled gelatin from **step 3** into 2 mL 0.2 % gelatin solution (final concentration 1:40). Mix by pipetting 3–4 times and leave the mixture in a 37 °C water bath for 5–10 min. Take the tube out and let it cool at RT for 5 min before placing 200 μL of the solution into each well of the MatTek dish. Leave for 10 min at RT (*see* **Note 5**).
5. For making unlabeled gelatin dishes, skip **steps 3** and **4** above. Place 200 μL of 0.2 % RT gelatin solution into each well of the MatTek dish and leave for 10 min at RT.
6. Wash three times with PBS in 5 min intervals. Transfer dishes on a tray filled with ice. Add 2 mL cold 0.2 % glutaraldehyde solution into each dish and incubate on ice for 15 min. Remove the dishes from ice and wash three times with PBS in 5 min intervals.

7. Prepare 5 mg/mL sodium borohydride solution (100 mg powder in 20 mL PBS) and immediately add 2 mL of this solution into each dish. Incubate for 15 min at RT. Wash three times with PBS in 5 min intervals.
8. Add 2 mL 70 % ethanol into each dish and incubate at RT for 15 min. Wash three times with PBS in 5 min intervals.
9. Add 2 mL 10× penicillin/streptomycin solution into each dish. Store dishes at 4 °C for up to 10 days.

3.4 Transfection of MTLn3 Cells and Preparing Cells for Live Imaging

1. The day before the transfection plate MTLn3 cells in 35 mm dishes at 1.2×10^5 cells/dish in 2 mL culture medium.
2. For each dish take two eppendorf tubes. Add 250 μL Opti-MEM into each tube. In the first tube add 0.5–1 μg of DNA and mix. In the second tube, add 4 μL of Lipofectamine 2000 and mix. Leave both tubes in the culture hood for 5 min.
3. Mix DNA and Lipofectamine 2000 solutions together and leave in the hood for 20 min.
4. Wash MTLn3 cells with pre-warmed Opti-MEM solution two times and leave 500 μL Opti-MEM. Add 500 μL DNA–Lipofectamine mixture from **step 3** into each dish. Transfer cells into the cell culture incubator for 45 min.
5. Wash cells two times with cell culture medium and leave 2 mL culture media on cells. Transfer cells to the cell culture incubator and let the gene(s) of interest express for 6–8 h.
6. Wash gelatin coated MatTek dishes two times with the culture medium and leave 1 mL culture medium each dish. Transfer dishes in the incubator for at least 30 min. Trypsinize transfected cells and plate cells from each 35 mm dish into two gelatin coated MatTek dishes. Leave cells in the incubator overnight.

3.5 Live Imaging of Invadopodia

1. For EGF stimulation experiments: Wash cells two times with serum starvation medium, leave 2 mL serum starvation medium on cells. Incubate cells for 3–4 h in a 37 °C incubator (no CO_2). Transfer cells from the incubator to the microscope stage and take the cover off the MatTek dish. Depending on the number of fluorophores you want to image, set the imaging parameters. For two fluorophores (e.g., GFP and RFP), we typically image every 3 s for up to 5 min (Fig. 2a, b). After capturing 1–2 frames in each channel, pause imaging, add 2 mL 10 nM EGF (final concentration 5 nM) in the dish and resume imaging.
2. For steady state imaging: Wash cells two times with steady state imaging medium, leave 2 mL steady state imaging medium on cells. Transfer cells to the microscope stage, start imaging.
3. For both EGF stimulation and steady state imaging, using the autofocus unit helps in maintaining focus throughout the

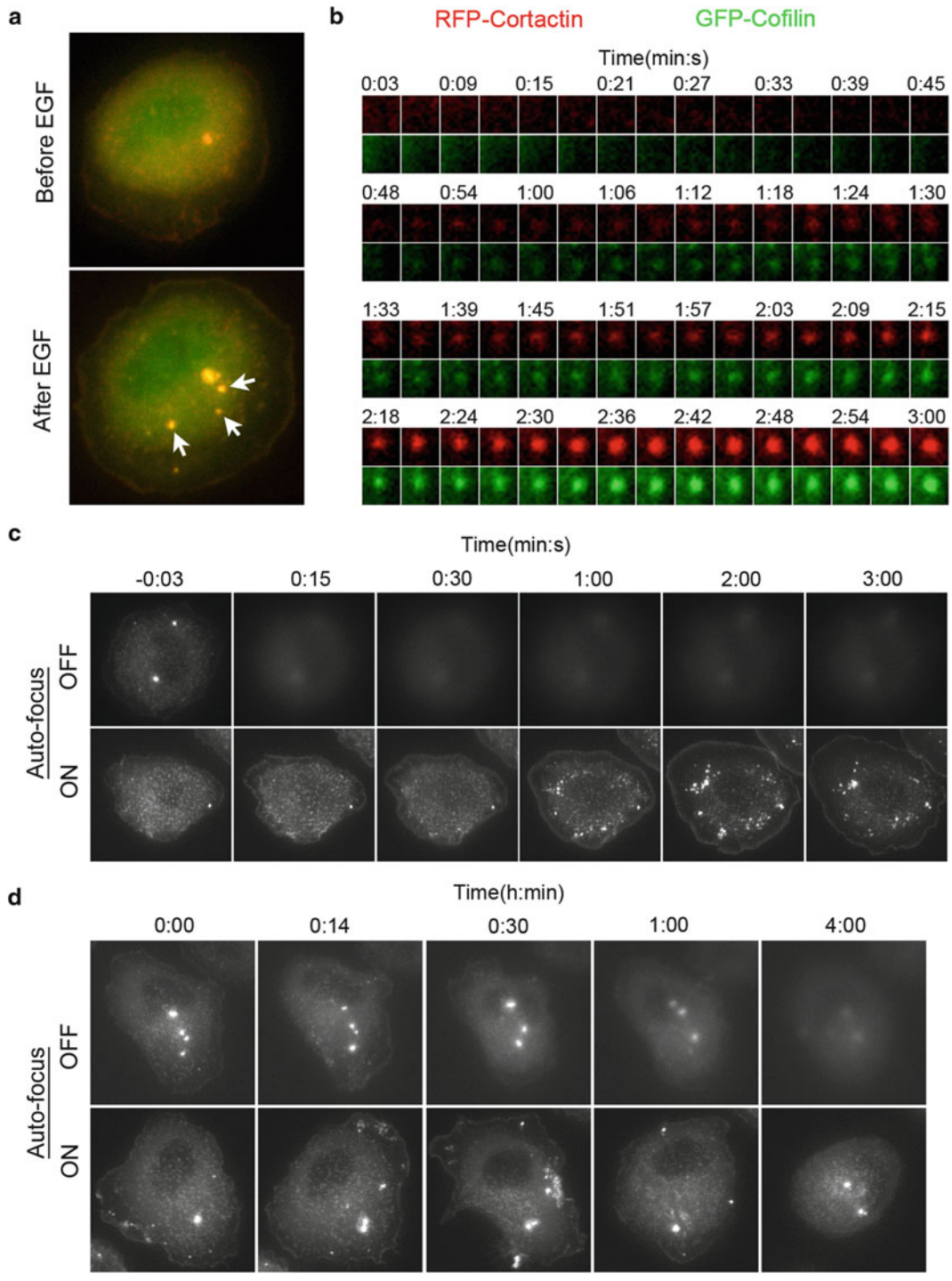

Fig. 2 Live-cell image acquisition. (**a**) TagRFP-Cortactin and GFP-Cofilin transfected MTLn3 cells were stimulated with EGF and imaged every 3 s for up to 5 min. Images show an MTLn3 cell before and after EGF stimulation. *White arrows* indicate newly forming invadopodium precursors after EGF stimulation. (**b**) Time-lapse sequence of a single invadopodium precursor in GFP and RFP channels is depicted as montage. Time is in min:s. (**c**) Demonstration of the advantage of using autofocus (with CRIFF unit) in maintaining focus during EGF

imaging period (Fig. 2c, d). To use the autofocus unit, before starting imaging, turn the CRIFF laser ON and calibrate the focus by following the vendor's protocol.

3.6 Invadopodia Tracking with "Invadopodia Tracker" Plugin

1. Put the plugin file Invadopodia_tracker.java (available upon request) under the plugins folder in ImageJ. Run "Plugins ->Compile and Run…," select Invadopodia_tracker.java file from the plugins folder. Ignore any error(s). Check to see that there is a new file named "Invadopodia_tracker.class" in the plugins folder. Restart ImageJ, "Invadopodia tracker" command should appear under Plugins menu in ImageJ.
2. Open the 16-bit time-lapse stack of a single fluorescence channel (Fig. 3a).
3. Go through the whole stack and choose the frame where invadopodia are clearly visible (typically after 1–2 min in EGF stimulation experiments). Using multi-point tool, select invadopodia-of-interest (Fig. 3b). Alternatively, invadopodia-of-interest can be automatically selected by "Process ->Find Maxima…" command and adjusting the noise tolerance.
4. Run "Invadopodia tracker" from the Plugins menu. A GUI will open asking for maximum invadopodium displacement from one frame to the next (a typical value is 3–5 pixels) and estimates of minimum and maximum number of particles considered to be invadopodia in the whole field per frame (Fig. 3c). A typical range for minimum and maximum number of invadopodia is 25–50 and 100–300, respectively. The user needs to optimize these numbers for correct invadopodia tracking (*see* **Notes 6** and **7**). For the next three parameters—Noise tolerance, Delta noise tolerance and maximum iterations, the user should start with default values—500, 20, 200 respectively (*see* **Note 8**).
5. After tracking is over, tracked invadopodia are marked in red circles and added as overlays (Fig. 3d, f; *see* **Note 9**). A log file, containing invadopodia centroids in each frame, is also generated (Fig. 3e).
6. Copy and paste invadopodia centroids into Excel. It will show up as three columns—first column is the frame number,

Fig. 2 (continued) stimulation experiment. Cells expressing TagRFP-Cortactin were imaged with (*lower panel*) or without (*upper panel*) autofocus every 3 s for up to 5 min. Only selected time points are shown. Time is in min:s and time 0:00 corresponds to EGF addition. (**d**) Demonstration of the advantage of using autofocus (with CRIFF unit) in maintaining focus during steady state long time-lapse imaging. Cells expressing TagRFP-Cortactin were imaged with (*lower panel*) or without (*upper panel*) autofocus every 2 min for up to 4 h. Only selected time points are shown. Time is in h:min. (**a**–**d**) In all experiments, an environmental heat chamber enclosing the microscope was preheated to 37 °C for > 3 h, before the start of imaging

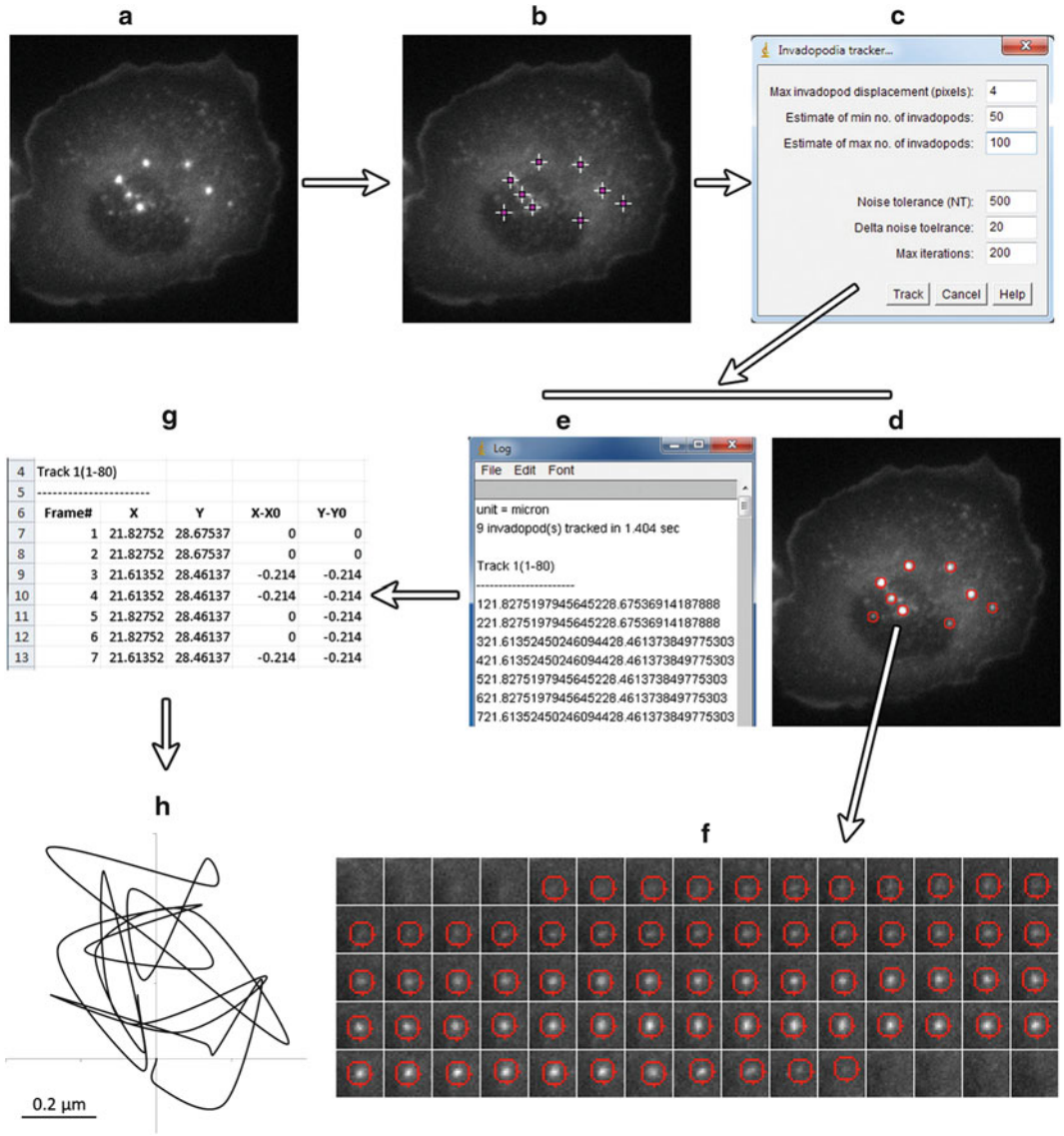

Fig. 3 Flow diagram of invadopodia tracking with the "Invadopodia tracker" plugin in ImageJ. Step-by-step analysis procedure is described in Subheading 3.6.

second and third columns are the *x* and *y* coordinates of invadopodium centroid (Fig. 3g).

7. From the centroid data, invadopodium trajectories can be easily plotted in Excel (Fig. 3h).

4 Notes

1. The use of CRIFF unit requires a high numerical aperture objective e.g., 60×, 1.42 NA, because it works on the total internal reflection (TIR) principle.

2. While packing the column make sure that the top of the packed column does not dry up. As soon as the PBS level falls off, replenish the top with more PBS.
3. If the column is packed properly then it will flow approximately 2–3 drops per min. If not, then transfer the column packing into a tube, add some PBS, mix, and transfer it to a thoroughly cleaned column.
4. The Alexa 405 dye–gelatin solution runs as a bright blue smear in the column. As the leading front reaches the bottom of the column, a slightly gray zone separating the Alexa 405 dye labeled gelatin (fast running fraction) with the Alexa 405 dye alone (slower running fraction) will become visible.
5. If you start seeing many aggregated bright Alexa 405 dye particles in your Alexa 405 labeled gelatin MatTek dishes (which might interfere with imaging and affect degradation area calculation), then the pre-warmed dye–gelatin solution in Subheading 3.3 **step 4** can be centrifuged at 10,000 × *g* for 5 min before adding it to the wells of the MatTek dish.
6. In the case that "Invadopodia tracker" plugin does track invadopodia through only some frames but misses others, the sensitivity of the invadopodia detection can be enhanced by increasing the values for the estimates of minimum and maximum number of invadopodia. Conversely, if the tracker identifies faint particles (i.e., background noise) as invadopodia, the sensitivity of the invadopodia detection can be decreased by lowering the values for the estimates of minimum and maximum number of invadopodia.
7. If the "Invadopodia tracker" fails to track invadopodia due to a narrow range between the estimates of minimum and maximum number of invadopodia, then either the value for estimate of minimum number of invadopodia should be decreased or the value for estimate of maximum number of invadopodia should be increased, or both.
8. The last three parameters in the "Invadopodia tracker" plugin are automatically adjusted according to user-selected values for maximum invadopodium displacement and the estimates of minimum and maximum number of invadopodia. In the case where plugin is not tracking invadopodia properly after adjusting the parameters described in **Notes 6** and **7**, the last three parameters may be changed to help converge on a solution.
9. After running the "Invadopodia tracker" plugin, tracked invadopodia are shown in red circles as overlays. In the case a user wants to run the plugin again with different parameters, these overlays can be removed by selecting "Image ->Overlay ->Remove Overlay" command in ImageJ.

Acknowledgments

We thank Dr. Louis Hodgson, and members of the Analytical Imaging Facility and Gruss-Lipper Biophotonics Center for helping in the microscope design. We also thank people from Condeelis, Segall, and Cox laboratories for helpful discussions. This work was supported by a postdoctoral fellowship to Ved Sharma from Susan G. Komen for the Cure© (KG111405), the Integrated Imaging Program and CA150344.

References

1. Murphy DA, Courtneidge SA (2011) The 'ins' and 'outs' of podosomes and invadopodia: characteristics, formation and function. Nat Rev Mol Cell Biol 12:413–426
2. Bravo-Cordero JJ, Hodgson L, Condeelis J (2012) Directed cell invasion and migration during metastasis. Curr Opin Cell Biol 24:277–283
3. Eckert MA, Yang J (2011) Targeting invadopodia to block breast cancer metastasis. Oncotarget 2:562–568
4. Stylli SS, Kaye AH, Lock P (2008) Invadopodia: at the cutting edge of tumour invasion. J Clin Neurosci 15:725–737
5. Chen WT, Chen JM, Parsons SJ, Parsons JT (1985) Local degradation of fibronectin at sites of expression of the transforming gene product pp60src. Nature 316:156–158
6. Artym VV, Zhang Y, Seillier-Moiseiwitsch F, Yamada KM, Mueller SC (2006) Dynamic interactions of cortactin and membrane type 1 matrix metalloproteinase at invadopodia: defining the stages of invadopodia formation and function. Cancer Res 66:3034–3043
7. Yamaguchi H, Lorenz M, Kempiak S, Sarmiento C, Coniglio S, Symons M, Segall J, Eddy R, Miki H, Takenawa T, Condeelis J (2005) Molecular mechanisms of invadopodium formation: the role of the N-WASP-Arp2/3 complex pathway and cofilin. J Cell Biol 168:441–452
8. Yamaguchi H, Takeo Y, Yoshida S, Kouchi Z, Nakamura Y, Fukami K (2009) Lipid rafts and caveolin-1 are required for invadopodia formation and extracellular matrix degradation by human breast cancer cells. Cancer Res 69:8594–8602
9. Baldassarre M, Ayala I, Beznoussenko G, Giacchetti G, Machesky LM, Luini A, Buccione R (2006) Actin dynamics at sites of extracellular matrix degradation. Eur J Cell Biol 85:1217–1231
10. Monsky WL, Lin CY, Aoyama A, Kelly T, Akiyama SK, Mueller SC, Chen WT (1994) A potential marker protease of invasiveness, seprase, is localized on invadopodia of human malignant melanoma cells. Cancer Res 54: 5702–5710
11. Ammer AG, Kelley LC, Hayes KE, Evans JV, Lopez-Skinner LA, Martin KH, Frederick B, Rothschild BL, Raben D, Elvin P, Green TP, Weed SA (2009) Saracatinib impairs head and neck squamous cell carcinoma invasion by disrupting invadopodia function. J Cancer Sci Ther 1:52–61
12. Chuang YY, Tran NL, Rusk N, Nakada M, Berens ME, Symons M (2004) Role of synaptojanin 2 in glioma cell migration and invasion. Cancer Res 64:8271–8275
13. Gianni D, Taulet N, DerMardirossian C, Bokoch GM (2010) c-Src-mediated phosphorylation of NoxA1 and Tks4 induces the reactive oxygen species (ROS)-dependent formation of functional invadopodia in human colon cancer cells. Mol Biol Cell 21:4287–4298
14. Neel NF, Rossman KL, Martin TD, Hayes TK, Yeh JJ, Der CJ (2012) The RalB small GTPase mediates formation of invadopodia through a GTPase-activating protein-independent function of the RalBP1/RLIP76 effector. Mol Cell Biol 32:1374–1386
15. Desai B, Ma T, Chellaiah MA (2008) Invadopodia and matrix degradation, a new property of prostate cancer cells during migration and invasion. J Biol Chem 283: 13856–13866
16. Bravo-Cordero JJ, Oser M, Chen X, Eddy R, Hodgson L, Condeelis J (2011) A novel spatiotemporal RhoC activation pathway locally regulates cofilin activity at invadopodia. Curr Biol 21:635–644
17. Oser M, Yamaguchi H, Mader CC, Bravo-Cordero JJ, Arias M, Chen X, Desmarais V, van Rheenen J, Koleske AJ, Condeelis J (2009) Cortactin regulates cofilin and N-WASp activities to control the stages of invadopodium assembly and maturation. J Cell Biol 186: 571–587

18. Stylli SS, Stacey TT, Verhagen AM, Xu SS, Pass I, Courtneidge SA, Lock P (2009) Nck adaptor proteins link Tks5 to invadopodia actin regulation and ECM degradation. J Cell Sci 122:2727–2740
19. Segall JE, Tyerech S, Boselli L, Masseling S, Helft J, Chan A, Jones J, Condeelis J (1996) EGF stimulates lamellipod extension in metastatic mammary adenocarcinoma cells by an actin-dependent mechanism. Clin Exp Metastasis 14:61–72
20. Sharma VP, Beaty BT, Patsialou A, Liu H, Clarke M, Cox D, Condeelis JS, Eddy RJ (2012) Reconstitution of in vivo macrophage-tumor cell pairing and streaming motility on one-dimensional micro-patterned substrates. IntraVital 1:77–85

Chapter 22

Live Cell Imaging of RhoGTPase Biosensors in Tumor Cells

Jose Javier Bravo-Cordero, Yasmin Moshfegh, John Condeelis, and Louis Hodgson

Abstract

Tumor cell motility and invasion rely on actin cytoskeleton rearrangements mediated by the activation of RhoGTPase signaling pathways. Invadopodia are membrane-degrading protrusions that mediate extracellular matrix degradation. Here, we provide procedures for imaging RhoGTPase biosensors in tumor cells during the formation of invadopodia and matrix degradation.

Key words RhoGTPase, FRET, Biosensors, Invadopodia

1 Introduction

The use of fluorescent biosensors in systems that are highly significant to understanding disease processes including breast adenocarcinomas [1] has opened new avenues to address signal transduction studies in contexts that were not possible before. One such process recently described is how the Rho family of GTPases regulates tumor invasive protrusions [1]. When plated on two-dimensional matrices, tumor cells form actin-rich membrane degrading protrusions on their ventral surfaces called invadopodia [2]. In transverse section, invadopodia display a dot-like shape and are rich in actin and actin binding proteins such as cofilin, cortactin, and Arp2/3, which mediate actin polymerization.

Invadopodia formation is a multistep process that begins with the formation of an invadopodium precursor structure that matures into a matrix degrading invadopodia [3]. Invasive tumor cells including the rat adenocarcinoma cell line MTLn3 or the human MDA-MB-231 cell line have been used as model systems to study the different stages of invadopodia formation [3, 4]. RhoGTPases have been shown to be directly involved and regulate the formation of invadopodia [1], and thus are ideal targets to elucidate the regulatory mechanisms and dynamics of tumor cell invasion.

Amanda S. Coutts (ed.), *Adhesion Protein Protocols*, Methods in Molecular Biology, vol. 1046,
DOI 10.1007/978-1-62703-538-5_22,

As such, the use of the FRET (Forster Resonance Energy Transfer)-based biosensors in these systems requires careful considerations of the methods in order to ascertain that the biosensor readout is physiologically relevant. Here we provide methods to image RhoGTPase activation by using FRET based biosensors [1, 5] during invadopodia formation in tumor cells.

2 Materials

All stock solutions and buffers should be prepared in distilled water unless otherwise mentioned.

1. Cell lines: MTLn3 [6], MDA-MB-231, LinXE 293T and LinXA 293T cells (www.bioxys.com).
2. α-MEM: Supplemented with 5 % Fetal Bovine Serum (FBS) and 0.5 % penicillin/streptomycin.
3. D-MEM: Supplemented with 10 % FBS and 0.5 % penicillin/streptomycin.
4. L-15 media (Gibco): Store at 4 °C, protected from light.
5. Opti-MEM: Store at 4 °C, protected from light.
6. Ham's F-12K without phenol-red.
7. Trypsin.
8. Lipofectamine 2000 reagent (Invitrogen).
9. Lipofectamine and Plus reagents (Invitrogen).
10. Nucleofection Kit V (Lonza).
11. PBS.
12. Gelatin from Porcine skin, Type A (Sigma-Aldrich).
13. Glutaraldehyde solution: Grade I, 25 % in distilled water (Sigma-Aldrich).
14. Poly-L-lysine: 5 mg/mL stock in distilled water. Prepare a 1:10 dilution in PBS.
15. Hexadimethrine bromide (Polybrene; Sigma-Aldrich): 8 μg/μL stock.
16. Oxyfluor reagent (Oxyrase).
17. Mouse EGF (Gibco) and human EGF (Invitrogen): 50 μM stock. Store mouse EGF at −80 °C in 5 μL aliquots and human EGF at −20 °C in 5 μL aliquots.
18. $NaBH_4$ (Sodium Borohydrate): Store in a desiccated environment.
19. Paraformaldehyde (PFA) 16 % stock in distilled water.
20. Bovine serum albumin (BSA): Store at 4 °C.

21. DL-Lactate.
22. Triton X-100: 0.1 % stock in PBS.
23. Blocking solution: 1 % BSA, 1 % FBS in PBS.
24. 1 % BSA in PBS.
25. MatTek dishes: 14 mm microwell (MatTek corporation).
26. G-418/neomycin: 100 μg/μL stock.
27. Puromycin: 10 μg/μL stock.
28. Doxycycline (Dox): 10 μg/mL stock.
29. Penicillin/streptomycin: 10,000 units of penicillin and 10,000 μg of streptomycin per mL. Use 0.5 % of this stock for cell culture.
30. Alexa 568 carboxylic acid, succinimidyl ester (Molecular Probes).
31. TagRFP-Cortactin plasmid [3].
32. pREV-tet-OFF advanced (Clontech), p-Babe-sin-puro-tet-CMV-RhoA biosensor [5] (https://www.addgene.org), pCL-ECO and pCL-AMPHO (www.imgenex.com).
33. Antibodies: Cortactin (ab81208, Abcam), Tks5 (Santa Cruz Biotechnology, sc-30122).
34. Beckman Coulter MoFlo XDP FACS System.
35. Microscope Filters: The filter sets used for ratiometric imaging were (excitation, emission, respectively): ECFP/mCerulean: ET436/20X, ET480/40M (Chroma Technology, Rockingham, VT); FRET: ET436/20X, ET535/30M (Chroma Technology); and TagRFP: FF585/29, FF628/32 (Semrock, Rochester, NY). The main fluorescence turret utilized a 10/90 (Reflection/Transmittance) mirror (Olympus, Center Valley, PA) that provided compatibility with all of the band pass filters used. Additionally, a 575DCXR dichroic mirror (Chroma Technology, Rockingham, VT) was installed to replace the internal prism of the microscope, enabling beam-splitting of CFP-YFP FRET emissions to the left port of the microscope and all the longer wavelengths to the bottom port of the microscope. 505DCXRU dichroic mirror (Chroma Technology, Rockingham, VT) was used to split the CFP and YFP-FRET emissions in the external beamsplitter attached to the left side port of the microscope. A 94:6 mirror from Olympus.
36. Microscope Lens: Olympus 60× Plan Apo N 1.45 NA UIS2 DIC lens.

3 Methods

3.1 Preparation of Gelatin Matrices

1. Place 25 mm round coverslips in a 6 well plate (*see* **Note 1**).
2. Treat 25 mm round coverslips or MatTek dish glass wells with 50 μg/mL of poly-L-lysine in PBS. Add 400 μL of poly-L-lysine to the inner MatTek dish glass well or 2 mL to completely cover the 25 mm coverslips (*see* **Note 2**).
3. Leave the coverslips/MatTek dishes at room temperature for 20 min.
4. Wash three times with 2 mL PBS.
5. Dissolve the gelatin powder in PBS to 0.2 %. Adjust the volume needed depending on the number of coverslips/MatTek dishes to prepare.
6. Preheat the PBS with the gelatin in a microwave for 2–3 min. Make sure all the gelatin is dissolved. Let it cool at 37 °C in a water bath.
7. Add 500 μL of 0.2 % gelatin (*see* Subheading 3.1.1 for different labeling options) to the MatTek dishes or 2 mL to the coverslips in the 6 well dishes. Incubate for 10 min at room temperature.
8. Wash three times with 2 mL PBS.
9. Treat MatTek dishes with 300 μL (or coverslips with 2 mL) of 0.5 % glutaraldehyde diluted in PBS for 15 min at room temperature. Glutaraldehyde cross-links the gelatin.
10. Wash three times with 2 mL PBS.
11. Dissolve $NaBH_4$ in PBS to make a 5 mg/mL solution. Bubbles will form after adding the powder. Add the solution immediately to the dishes. Treat dishes/coverslips with 2 mL of $NaBH_4$ for 15 min at room temperature (*see* **Note 3**). This treatment will quench autofluorescence.
12. Wash three times with 2 mL PBS.
13. Prepare PBS with 5 % penicillin/streptomycin. Add 2 mL per dish/coverslip to sterilize and keep at 4 °C in a humidified chamber (*see* **Note 4**).
14. Before plating cells wash with 2 mL PBS three times and add 2 mL of appropriate media (depending on the cell type). Leave at 37 °C for 15 min.

3.1.1 Preparing Labeled Gelatin

Gelatin can be prepared in two different ways: un-labeled or fluorescently labeled, depending on the requirements of the experiment. Un-labeled gelatin can be mixed with labeled gelatin in order to produce a fluorescent matrix to study the processes of matrix degradation by invadopodia as follows:

1. Conjugate gelatin with Alexa dyes following manufacturer's instructions (Invitrogen). Alexa 568 can be used for these assays.
2. Prepare 0.2 % gelatin stock solution in PBS.
3. After heating the gelatin, let it cool at room temperature. Mix 0.2 % gelatin with Alexa-conjugated gelatin in a 40:1 dilution ratio.
4. After this step follow the protocol in Subheading 3.1 starting from **step 8**.
5. Place the dishes in a humidified chamber, covered with aluminum foil (*see* **Note 4**).

3.2 EGF Preparation for Tumor Cell Stimulation

1. Prepare 1 μM EGF by diluting the mouse/human EGF 50 μM stock in 245 μL of starvation medium (*see* Subheading 3.7). Keep at 4 °C on ice during the experiment.
2. Prepare 5 nM (MTLn3 cells) or 10 nM (MDA-MD-231 cells) EGF by diluting 1 μM solution in starvation imaging medium (*see* Subheading 3.8).
3. Keep at 37 °C.

3.3 Viral Production and Stable tet-OFF Cell Lines

1. Coat 10 cm dishes with poly-L-lysine by adding 5 mL of diluted poly-L-lysine (diluted 1:10 in PBS from 5 mg/mL stock) for 20 min and aspirate prior to plating cells.
2. Wash with PBS three times.
3. Plate 6×10^6 LinXE 293 or LinXA 293 cells overnight in a 10 cm dish coated with poly-L-lysine (*see* **Note 5**).
4. The following day prepare the transfection mixture.

   Eppendorf tube 1: 10 μg pREV tet-OFF, 6 μg of pCL-ECO, 120 μL of Lipofectamine Plus reagent; all mixed in 800 μL of Opti-MEM. For MDA-MB-231 use 6 μg pCL-Ampho instead of pCL-ECO (*see* **Note 5**).

   Eppendorf tube 2: 100 μL of Lipofectamine diluted in 800 μL of Opti-MEM.

   Incubate both tubes for 15 min at room temperature.
5. Combine the solutions of the two eppendorf tubes into one tube and incubate for 15 min at room temperature.
6. Replace the growth media in the LinXE or LinXA plates with 5 mL of Opti-MEM during the DNA–Lipofectamine incubation time. Add the transfection mixture to the cells following the 15 min incubation.
7. After 6 h stop the transfection by changing the media to α-MEM for MTLn3 or DMEM for MDA-MB-231.
8. Transfer the plates to a 32 °C incubator. At this temperature virus production is more efficient [7].

9. Collect the viral supernatant 48 h after transfection. Centrifuge for 5 min at 660 × *g* to remove any debris. Add polybrene at 8 μg/mL.
10. The day before infection plate 2–5 × 10^5 MTln3 or MDA-MB-231 cells on a 10 cm dish (*see* **Note 6**).
11. Add the supernatant from LinXE or LinXA cells containing the virus to the MTLn3 or MDA-MD-231 cells. We usually infect four times, once every 12 h before starting the selection.
12. Select for stable incorporation of the tet-OFF tetracycline trans-activator using G418 at 1 mg/mL.

3.4 Viral Production and Stable Biosensor Cell Line

1. Virus production can be performed as described in Subheading 3.3 by using the viral carrier construct under the tet-CMV promoter, such as p-Babe-sin-puro-tet-CMV-RhoA biosensor [5] containing the biosensor expression cassette, instead of pREV tet-OFF.
2. Transduction of MTLn3 or MDA-MB-231 cells expressing pREV tet-OFF plasmid can be performed as described in Subheading 3.3, **steps 9–11**. The transductions should be performed in the presence of 1 μg/mL Dox in order to suppress the biosensor expression during infection.
3. The selection of stably transduced cells is performed by adding gradually the selection reagent (puromycin) starting at 1 μg/mL, and eventually reaching the concentration of 10 μg/mL (*see* **Note 7**).
4. Once stable populations of biosensor expressing cells are obtained, induce the biosensor expression by removing the Dox for 72 h. At this point, cells should be FACS sorted to obtain uniform expression levels (*see* **Note 8**).
5. For routine imaging experiments, biosensor expression through Dox removal should follow the following steps.
   (a) Wash cells with PBS and briefly trypsinize to lift cells.
   (b) Resuspend in growth medium without Dox, and centrifuge at 300 × *g* for 5 min to pellet the cells.
   (c) Suction out as much of the medium as possible following the centrifugation, then resuspend in fresh growth medium without Dox.
   (d) Plate cells at sparse density, routinely 1–2 × 10^5 cells per 10 cm dish (*see* **Note 9**).

3.5 Transfection of Tumor Cells with Invadopodia Markers

3.5.1 MTLn3

1. Plate 2 × 10^5 MTLn3 cells in a 6 well plate the day before transfection.
2. Prepare transfection mixture in two eppendorf tubes (the volumes are for a single transfection in one well of a 6 well plate; for multiple transfections scale up the volumes).

Eppendorf 1: 4 μL of Lipofectamine 2000 reagent in 250 μL of Opti-MEM.

Eppendorf 2: 0.5–1 μg of DNA (invadopodium marker such as TagRFP-cortactin (red-shifted fluorescence proteins can be used in combination with a CFP/YFP biosensor)) in 250 μL of Opti-MEM.

Incubate for 5 min at room temperature.

3. Mix the two solutions and incubate for 20 min at room temperature.
4. During the incubation, wash the cells with Opti-MEM and add 500 μL of Opti-MEM.
5. Add the transfection mixture to the cells and leave for 45 min (*see* **Note 10**).
6. After the transfection wash three times with growth medium.
7. 8 h following the transfection, wash cells with PBS and trypsinize. Plate 2×10^5 cells per gelatin coated coverslip/MatTek dish.

3.5.2 MDA-MB-231

For MDA-MB-231 we recommend using Lonza Nucleofection Kit V.

1. Use the kit following manufacturer's instructions by using 1 μg of DNA per 1×10^6 cells.
2. Plate 2×10^5 cells per gelatin coated coverslips/MatTek dish.

3.6 Biosensor Induction and Transfection for Invadopodium Precursor Imaging

1. Induce biosensor expression in MTLn3 or MDA-MB-231 cells 72 h before the start of imaging (*see* **Note 11**). Wash the cells two times with PBS. Trypsinize and centrifuge for 5 min at 300 × *g*. Make sure to remove all media containing the Dox.
2. 24 h before the experiment perform transfection with the invadopodium marker Cortactin-RFP [3] as described in Subheading 3.5.
3. Plate 2×10^5 cells on un-labeled gelatin coverslips.

3.7 Tumor Cell Starvation

3.7.1 MTLn3 Cells

1. Prepare starvation medium: L-15 containing 0.35 % BSA. Filter it to sterilize.
2. Wash cells two times with L-15 medium.
3. Wash cells once with the starvation medium and keep them in starvation medium.
4. Place cells for 3 h at 37 °C in a CO_2-free incubator in starvation medium (*see* **Note 12**).

3.7.2 MDA-MB-231 Cells

1. MDA-MB-231 cells should be starved overnight with starvation medium: DMEM, 0.5 % FBS, 0.8 % BSA.

2. Wash cells two times with L-15 medium the next day. 10 min before the experiment, change the medium to L-15 with 0.35 %BSA.
3. Proceed with the EGF stimulation as in Subheading 3.9.

3.8 Starvation Imaging Medium

1. 6 mL of Ham's F-12K without phenol-red [8, 9] is warmed to 37 °C to release any dissolved gases. Ham's F-12K reduces the background autofluorescence in the channels used for CFP/YFP FRET.
2. Bubble argon gas into the medium for 1 min to displace the oxygen.
3. BSA is added at 0.35 % and the medium is aliquoted into 2 mL tubes together with Oxyfluor reagent (Oxyrase) at 1:100 dilution along with 5 mM DL-lactate (*see* **Note 13**).
4. The mixture is then incubated at 37 °C for 1 h and spun for 1 min at 24 °C, 20,000 × *g* to remove any debris from the Oxyfluor treatment prior to imaging. Filter it to sterilize.

3.9 EGF Stimulation and Image Acquisition

1. Mount the coverslips onto an imaging chamber as previously described [9] (Fig. 1) by using silicone vacuum grease. Add 400 μL of starvation imaging medium to the coverslips and place onto the microscope heating stage.
2. Start the imaging following the diagram in Fig. 2. For sequential acquisition mode of four channels (CFP, FRET, RFP, DIC) we used a microscope set up [9] with a side port with two cameras for simultaneous acquisition of CFP/FRET and a bottom port for Red/DIC images (Fig. 3).
   (a) First acquire CFP and FRET images simultaneously for 500–700 ms exposure time with binning 2 × 2 (*see* **Note 14**).
   (b) Acquire TagRFP-Cortactin image by exposing for 200–400 ms at 2 × 2 binning.
   (c) Acquire DIC image.
3. After 1–2 min add 400 μL of EGF at 10 nM for MTLn3 cells or 5 nM for MDA-MB-231 cells (the final concentration of EGF on the coverslips is 5 nM for MTLn3 and 2.5 nM for MDA-MB-231). Mix the volumes gently.
4. Continue imaging for 10–15 min.

3.10 Fixed Cell Imaging of RhoGTPase Biosensors

Alternatively, tumor cells expressing Rho GTPase biosensors can be fixed after EGF stimulation or in steady state conditions and immunofluorescence can be performed to localize endogenous proteins at invadopodia and visualize matrix degradation.

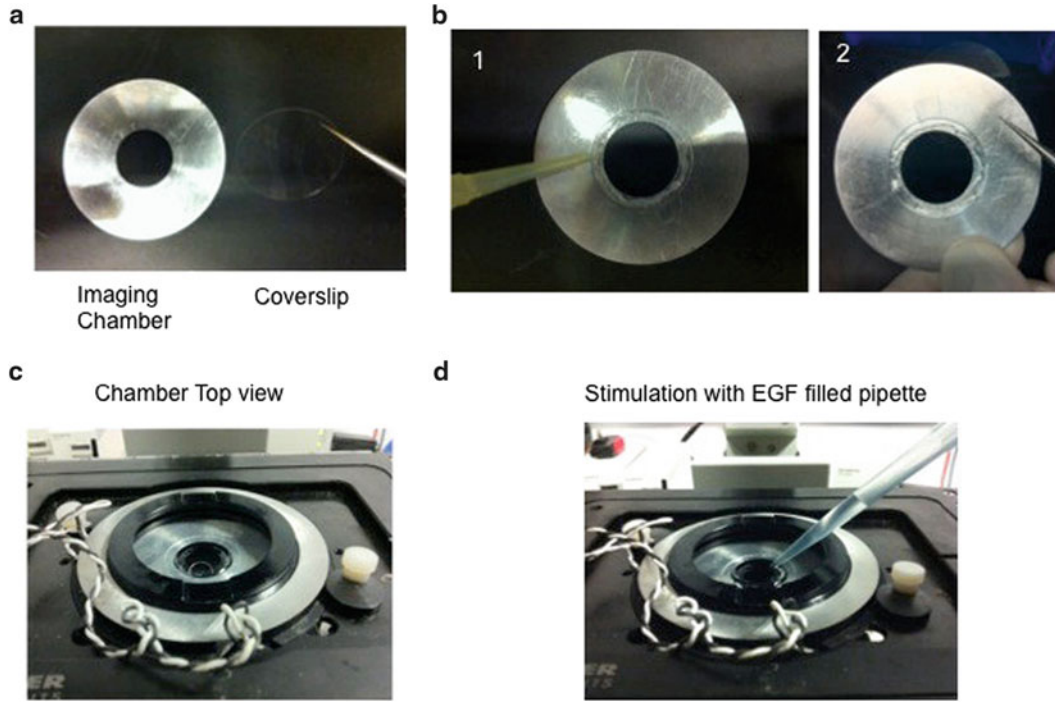

Fig. 1 Mounting the imaging chamber. (**a**) Front view of the metal chamber and the coverslip. (**b**) Add grease to the inner part of the metal chamber (*1*) and place the coverslip on top of the greased area with the cell facing the grease (*2*). (**c**) Cover the coverslips with media. (**d**) Example of EGF stimulation. Approximately 800 μL can be added to the imaging chamber without spilling the imaging solution

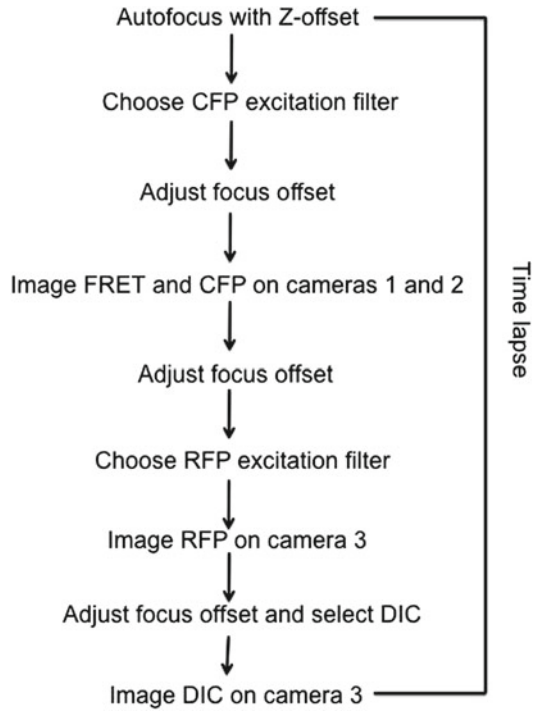

Fig. 2 Flow diagram for the dual-camera for single-chain biosensor imaging. The red fluorescence acquisition and DIC acquisition using a third camera is also shown. The autofocus is achieved by an Olympus ZDC system [9]

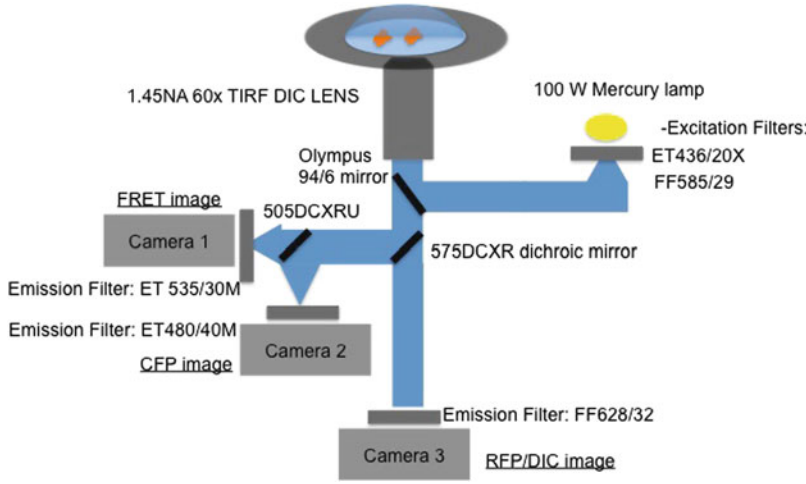

Fig. 3 The light path diagram for the dual-camera, single-biosensor mode imaging. The third camera will enable acquisitions of red and DIC images

1. The day before the experiment plate 2×10^5 MTLn3 or MDA-MB-231 cells on Alexa 568 gelatin matrices.
2. Prepare 3.7 % PFA in PBS by diluting the 16 % stock.
3. After tumor cell stimulation or under steady state conditions, remove the media and add 2 mL of 3.7 % PFA and fix for 20 min at room temperature.
4. Wash two times with PBS for 5 min each.
5. Permeabilize the cells with 0.1 % Triton X-100 for 5 min.
6. Wash three times with PBS for 5 min each.
7. Incubate in blocking solution for 1 h.
8. Incubate with the primary antibody (anti-cortactin at 1:400 dilution or anti-TKs5 at 1:100 dilution) in blocking solution for 1 h at room temperature.
9. Wash three times with 1 % BSA in PBS.
10. Incubate with secondary antibody (use a far-red labeled secondary antibody) at room temperature for 1 h.
11. Wash two times with PBS and store at room temperature before imaging (*see* **Note 15**).

4 Notes

1. 25 mm coverslips need to be washed in ethanol to sterilize before starting the poly-L-lysine treatment. We recommend keeping the coverslips in 100 % ethanol and flame sterilize before starting the coating.

2. We recommended using 25 mm coverslips for live cell imaging. When incorporated in the imaging chamber (*see* Subheading 3.9) grease sealing provides for better stability when doing EGF stimulations. For immunofluorescence we recommend using MatTek dishes since the volumes of antibodies can be minimized by adding 100 μL to the inside well.
3. $NaBH_4$ should be kept in a desiccated environment with no air. Use the Desi-vac system (Fisher).
4. Gelatin-coated coverslips and MatTek dishes can be stored at 4 °C for 1–2 weeks.
5. MDA-MB-231 cells have to be transduced by using virus generated in cells expressing pCL-Ampho (LinXA) to allow infection of human cell lines and MTLn3 cells have to be transduced with virus generated in cells expressing pCL-ECO (LinXE).
6. When growing MTLn3 cells, it is very important to use very low passage (between 19 and 25) and not let them grow beyond 30–50 % confluence. MDA-MB-231 cells should not be kept for more than a month in culture.
7. Suggested increments; 1, 2, 4, 8, and 10 μg/mL. Add the puromycin at the time of cell splitting and allow cells to reach the correct subconfluency.
8. It is useful to obtain several differently gated populations in FACS sorting, representing low, medium and high biosensor expressors. Also, maintain frozen cell aliquots of unsorted cells for later analysis of effects of various expression levels of the biosensor, as necessary.
9. Here, sparse plating is important for induction. In order to enhance the levels of biosensor expression, trypsinization and direct replating at 24 and 48 h time points during induction can enhance biosensor expression.
10. In order to express transiently fluorescent proteins in MTLn3 cells, Lipofectamine 2000 transfection gives the best transfection efficiency. Do not leave the transfection mixture more than 45 min as this causes significant cell death.
11. Induction times may vary depending on the biosensor used and the cell line in which the biosensor is being expressed. For Rho biosensors we usually get the best expression levels 72 h after induction.
12. L-15 media must be used in CO_2-free conditions.
13. Treatment of the medium with argon gas and Oxyfluor/Lactate will control the production of oxygen radicals during imaging.
14. Imaging conditions must be controlled to minimize photodamage [8]. Furthermore, signal to noise ratio of 2:1–3:1

should be targeted between the cell fluorescence and the background at the dimmest part of the cell to achieve optimal results [8].

15. Gelatin coated dishes with stained cells can be stored at 4 °C for a week.

Acknowledgments

We thank the Condeelis, Cox, Hodgson, and Segall laboratories for helpful discussions. This work was funded by GM093121 (J.J.B-C, Y.M., L.H.), T32 GM007491 (Y.M.), and CA150344 (J.C, J.J.B-C).

References

1. Bravo-Cordero JJ et al (2011) A novel spatiotemporal RhoC activation pathway locally regulates cofilin activity at invadopodia. Curr Biol 21:635–644
2. Bravo-Cordero JJ, Hodgson L, Condeelis J (2012) Directed cell invasion and migration during metastasis. Curr Opin Cell Biol 24:277–283
3. Oser M et al (2009) Cortactin regulates cofilin and N-WASp activities to control the stages of invadopodium assembly and maturation. J Cell Biol 186:571–587
4. Oser M et al (2010) Specific tyrosine phosphorylation sites on cortactin regulate Nck1-dependent actin polymerization in invadopodia. J Cell Sci 123:3662–3673
5. Pertz O, Hodgson L, Klemke RL, Hahn KM (2006) Spatiotemporal dynamics of RhoA activity in migrating cells. Nature 440:1069–1072
6. Segall JE et al (1996) EGF stimulates lamellipod extension in metastatic mammary adenocarcinoma cells by an actin-dependent mechanism. Clin Exp Metastasis 14:61–72
7. Kaptein LC, Greijer AE, Valerio D, van Beusechem VW (1997) Optimized conditions for the production of recombinant amphotropic retroviral vector preparations. Gene Ther 4:172–176
8. Hodgson L, Shen F, Hahn K (2010) Biosensors for characterizing the dynamics of rho family GTPases in living cells. Curr Protoc Cell Biol Chapter 14(Unit 14.11):11–26, Editorial board, Juan S. Bonifacino … [et al.]
9. Spiering D, Hodgson L (2012) Multiplex imaging of Rho family GTPase activities in living cells. Methods Mol Biol 827:215–234

Chapter 23

Electrospun Nanofiber Scaffolds for Investigating Cell–Matrix Adhesion

Joshua S. McLane, Nicholas J. Schaub, Ryan J. Gilbert, and Lee A. Ligon

Abstract

It has become increasingly clear that the cellular microenvironment, in particular the extracellular matrix, plays an important role in regulating cell function. However, the extracellular matrix is extraordinarily complex in both its makeup and its physical properties. Therefore, there is a need to develop model systems to independently evaluate the effect of specific extracellular matrix features upon cells. Here we describe a model system to evaluate one aspect of the extracellular matrix, its fibrous topology. We describe how to generate bio-mimetic nanofibers by electrospinning, how to grow cells on these fibers, and also some methods for fixing and visualizing cells grown on these fibers. These methods can be used to investigate a wide range of biological questions, including, but not limited to, cell–extracellular matrix adhesion and cell motility on extracellular matrix.

Key words Electrospinning, Extracellular matrix, Cell adhesion, Topography, Fibers

1 Introduction

Traditionally, cells have been studied in two dimensional planar cultures without much consideration to the topographical features of the noncellular extracellular matrix (ECM). More recently, however, it has become clear that the topography [1], physical properties [2, 3], and the makeup of the ECM [4] are fundamental factors in determining cell function and fate. Therefore, numerous methods have been developed to mimic aspects of the in vivo ECM including, but not limited to, electrospun fibers [5], hydrogels composed of collagen-I [6] and/or other biological and nonbiological materials [7, 8], microfabricated substrates [9], and even decellularized organs [10]. Each of these models provides a system to study interactions between cells and the ECM, and to investigate

Joshua S. McLane and Nicholas J. Schaub have equally contributed to this chapter.

Amanda S. Coutts (ed.), *Adhesion Protein Protocols*, Methods in Molecular Biology, vol. 1046,
DOI 10.1007/978-1-62703-538-5_23,

the effect of the organization, makeup, and physical parameters of the ECM on cell function and fate.

Electrospun fibers are a powerful tool for investigating cell–ECM interactions. Although a number of studies have presented their findings of cell behavior on electrospun fibers, there are many inconsistencies in the results. For example, one study reported that dorsal root ganglion explants grown on large diameter fibers (diameter >750 nm) show greater neurite guidance and extension [11], while another study showed that smaller fiber diameters (diameter <500 nm) promote better neurite extension [12], but no mechanism to explain this discrepancy was presented. Studies of this sort typically consist of a description of the generation and characterization of the electrospun fiber material, followed by the quantification of various aspects of cell morphology, proliferation, or migration. Very rarely do these studies go beyond a superficial cellular analysis. Exceptions include a study in which it was shown by immunofluorescence that fiber diameter influences the expression of neural stem cell differentiation markers [13], and another study in which cytokine production by cells grown on scaffolds with different fiber alignment and diameters was analyzed [14]. Even in these cases, however, an investigation into the mechanism behind the cell response was absent.

1.1 Nanofibers In Vivo

Nanofibers comprised of proteins such as collagen, elastin, and fibronectin are found in vivo throughout healthy, healing, and diseased tissues [15]. These fibers have been shown to function as structural components to provide support and strength [15]. They appear in healing wounds [16] and atypical fibrotic tissue [16], and have also been shown to function in cellular guidance [17, 18]. The abundance of these fibers in vivo emphasizes their importance, but raises the question as to whether cells sense the ligand composition of the fibers or the structural topography, or both.

Multiple cell types interact with, and even migrate along, nanofibers in vitro and in vivo including neurons [19], lymphocytes [20], and epithelial cells [21]. Neither the purpose of, nor the effects of these interactions upon cells are yet wholly understood, and the differences between physical and biological interactions between cells and nanofibers cannot be elucidated in vivo. Consequently, in vitro modeling of these extracellular fibers is essential to determine their precise roles.

1.2 Electrospun Nanofibers

Electrospinning was first described in the early 1900s as a means of generating nonwoven textiles. This technique was extensively used in research in polymer physics, but in the last decade and a half, electrospinning is increasingly used in biological investigations [22, 23]. Electrospun fibers are useful in biological models for a variety of reasons. They are long, continuous fibers, similar to their physiological counterparts. They can be made with diameters varying from tens of nanometers (smaller than a cellular adhesion) to tens of microns (larger than a single cell). Not only is it possible to create fibers with

diameters spanning several orders of magnitude, but varying the diameter of fibers requires just a simple adjustment of a few parameters. Since electrospun fibers are fabricated from a wide variety of polymers and proteins (such as collagen), it is possible to make fibers with different surface chemistries. Additionally, electrospun fibers can be used for local drug delivery, and the inclusion of drug occurs simply by adding the drug to the electrospinning solution.

Here we will describe the basic procedures used to generate electrospun fibers, how to culture cells on these fibers, and techniques for fixation and visualization of cells grown on electrospun fibers. While we do discuss the basics of electrospinning, it is important to note that there are a large number of electrospinning apparatus configurations and parameters. Changing a single parameter can drastically alter a number of fiber characteristics including fiber diameter, alignment, surface structure, and mechanical properties. For simplicity, we have described the system we use to generate electrospun fibers, and include information on how changing particular parameters can alter the results as reported by previous studies, theories, and personal experience. We highly recommend reading through all of the electrospinning notes as they contain valuable information on how fiber properties change.

2 Materials

2.1 Electrospinning

1. High voltage power supply (Gamma High Voltage Research, ES50P-10W).
2. Syringe pump (Razel Scientific Instruments, R99-E) (*see* **Note 1**).
3. Electric motor for collecting disk (IKA, 2482000).
4. Aluminum collection disk (15 cm diameter, 1 cm width).
5. Stainless steel shaft (1 cm diameter, 20 cm length).
6. Methylene chloride.
7. Chloroform.
8. Poly-L-lactic acid (PLLA) (Nature Works, 6201D).
9. 4 % PLLA: 0.24 g PLLA into 3 g of chloroform, 3 g methylene chloride (wt polymer:wt solvent).
10. 8 % PLLA: 0.24 g PLLA into 1.5 g of chloroform, 1.5 g of methylene chloride.
11. Coverslip (circular, 15 mm diameter, 0.13–0.17 mm thickness).
12. 5 mL syringe.
13. 21 G needle, 1.5″ long with a short bevel.
14. Tubing for needle insulation.
15. Double sided tape.
16. Razor blade.

17. Wooden dowel.
18. Aluminum foil.

2.2 Cell Culture

1. 6- or 12-well cell culture plate.
2. Appropriate cell culture medium.
3. ECM ligand protein or peptide (i.e., Fibronectin or RGD peptide) (*see* **Note 2**).
4. Electrospun scaffolds (made as in Subheading 3.1).
5. Cloning cylinders (6 mm × 8 mm open ended, such as Corning, 3166-6).
6. CellTracker Green (Invitrogen, C2925).

2.3 Fixation

1. 6- or 12-well cell culture plate.
2. Cell Blocking Solution (CBS): 5 % goat serum, 1 % bovine serum albumin (BSA), 0.05 % NaN_3 in PBS.
3. PBS/NaN_3: 140 mM NaCl, 2.8 mM NaH_2PO_4 (monobasic), 12.3 mM Na_2HPO_4 (dibasic), 0.05 % NaN_3.
4. Methanol fix: 99.8 % MeOH, 1 mM EGTA, pH 8.0.
5. 1 mM EGTA: 1 mM EGTA in water, pH 8.0 with NaOH.
6. Paraformaldehyde fix: 4 % paraformaldehyde in PBS, pH 7.3 (*see* Subheading 3.3.2).
7. 10× PBS: 1.4 M NaCl, 28 mM NaH_2PO_4 (monobasic), 123 mM Na_2HPO_4 (dibasic).
8. Sodium hydroxide (NaOH).
9. 0.25 % Triton X-100: 0.25 % (v/v) Triton X-100 in PBS.

2.4 Visualization

1. Large coverslip (66 mm × 24 mm).
2. Dental wax or parafilm.
3. Fluorescent microscope (*see* **Note 3**).
4. Mounting reagent such as Prolong Gold.
5. PBS/NaN_3.
6. Primary and secondary antibodies and/or dyes.
7. Sealable container.

3 Methods

3.1 Electrospinning Aligned Fibers

3.1.1 Casting Polymer Films

Electrospun fibers are typically collected onto coverslip slides. One issue with electrospinning fibers in this manner is that the fibers tend to detach from the coverslip when immersed in culture medium. To overcome this issue, we cast a film onto the surface of the coverslip before electrospinning. This causes the fibers that still

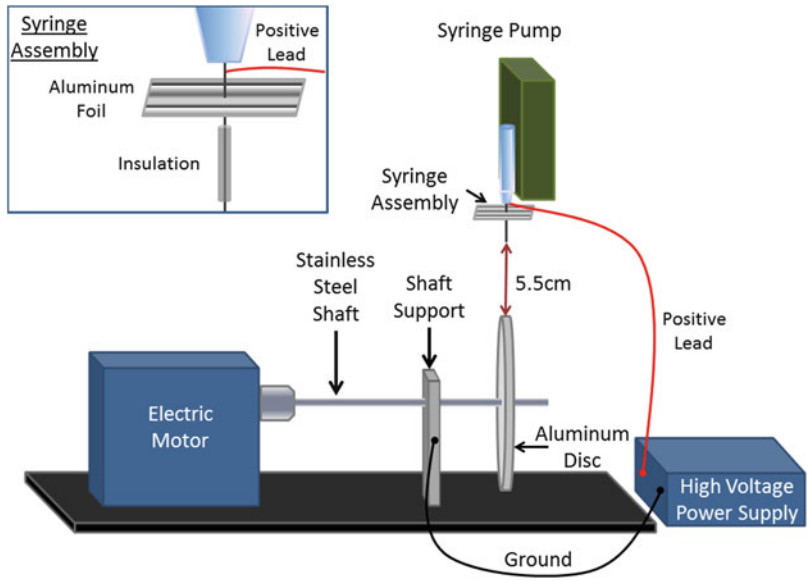

Fig. 1 Electrospinning apparatus setup

contain a small amount of solvent to attach to the film, preventing detachment. For an alternative method, *see* **Note 4**.

1. Prepare 4 % poly-L-lactic acid (PLLA) solution by mixing PLLA into chloroform/methylene chloride solvent. Stir with a magnetic stir bar in a capped glass vial sealed with parafilm to prevent solvent evaporation until completely dissolved. Dissolution of the PLLA should take approximately 2 h.
2. Place 4 % PLLA solution into a 5 mL syringe, making sure there are few bubbles in the solution. In a dry room (relative humidity <50 %, *see* **Note 5**), spread a thin layer of the solution onto the coverslips. There should be sufficient solution for ~90 coverslip slides. This should take less than 30 min.

3.1.2 Electrospinning Aligned Fibers

1. Set up the electrospinning apparatus using electrospinning materials 1–5 (*see* Subheading 2.1), according to Fig. 1 (*see* **Note 6** for alternative configurations, *see* **Note 7** for collecting random fibers). Be sure to ground the collection disk. Otherwise, the fibers will not be drawn to the disk.
2. Prepare 8 % PLLA solution by mixing PLLA into chloroform/methylene chloride solvent (*see* **Note 8**). Stir with a magnetic stir bar in a capped glass vial sealed with parafilm to prevent evaporation until completely dissolved. This should take approximately 2–3 h (*see* **Note 9**).
3. Before continuing, be sure that the electrospinning apparatus is in an environment where the relative humidity is between 30 and 40 % (*see* **Note 10**).

4. Cut the double sided tape into 15 small squares (~0.25 cm × 0.25 cm, *see* **Note 11**). Place the double sided tape onto the collection wheel with even spacing. Remove the back side of the tape.
5. Place one 4 % PLLA coated coverslip (prepared in Subheading 3.1.1) onto each piece of tape, making sure the film is facing up.
6. Place the 8 % PLLA solution into a 5 mL syringe, minimizing bubbles, then attach the needle to the syringe. After attaching the needle, remove any air that may remain in the syringe by inverting the syringe (needle pointing up) and push the plunger until solution begins to come out of the needle.
7. Fold a piece of aluminum foil in half several times until it is approximately a square with 3 cm sides. Push the needle through the center of the aluminum foil square. Add ~2 cm of needle insulating tubing to the needle (Fig. 1). There should be enough room at the base of the needle to attach the high voltage power supply lead to the needle.
8. Attach the positive lead of the high voltage power supply to the base of the needle. Push the insulation on the needle so that the aluminum foil is close to or touching the lead of the power supply.
9. Place the syringe in the syringe pump and set the syringe pump to 2 mL/h (*see* **Note 12**). Make sure the distance from the needle to the collection disk is 5.5 cm (*see* **Note 13**). Turn on the pump and wait until a steady flow of solution is coming from the needle, wiping away any excess with the wooden dowel or a paper towel.
10. Once the flow rate appears to be constant, turn on the motor for the rotating disk and set the speed to 1,000 rotations per minute (rpm) (*see* **Note 14**).
11. After the motor has reached 1,000 rpm, turn the high voltage supply on and set it to 10 kV (*see* **Notes 15** and **16** for safety recommendations). Be sure to keep hands at least 6 in. away from the needle after the voltage is turned on. Once the voltage is turned on, a thin jet of solution should be seen coming from the tip of the needle.
12. Allow the machine to run for 20 min. Periodically wipe the tip of the needle with the wooden dowel to remove dried polymer (about once every 10 s). Remember to keep hands away from the needle tip while the voltage is on.
13. After 20 min of electrospinning, turn off the power supply, followed by the syringe pump, and then the disk motor. Ensure that the polymer solution from the needle tip does not drop onto the rotating disk during the shutdown process.

14. Once the disk is finished spinning, a layer of electrospun fibers should be on the surface of the disk. Because the fibers are continuous, the fibers on the glass need to be cut. Place a razor gently on the edge of the coverslip, steady the coverslip with one hand by grabbing two sides of the coverslip (do not touch the fibers), and cut the fibers as close to the underside of the coverslip as possible. It is important to use a sharp razor to do this since a dull razor will displace the fibers.
15. Pull the coverslip off the wheel by grabbing the tape beneath the coverslip with a pair of forceps and pulling the tape and coverslip off at the same time. Then grab the sides of the coverslip and remove the tape. It is easiest to pinch the sides of the tape and twist the forceps so that the tape is rolled off the coverslip. This helps to prevent the coverslip from breaking.

3.2 Cell Culture

3.2.1 Monolayer Culture

Perform all cell culture in a sterile laminar flow hood observing sterile technique. If no ECM ligand has been incorporated during electrospinning, treat PLLA substrates with ligand solution to adsorb ligand to substrate (*see* **Notes 17** and **18**).

1. Place coverslip coated with PLLA fibers in a 12-well culture plate and add 1 mL culture medium or enough to submerge the coverslip. It may be necessary to push the sample under the surface of the medium with a micropipette tip (*see* **Note 18**).
2. Prepare cells to be seeded onto the PLLA substrates by trypsinization of a stock culture. Resuspend cells in 0.5–1.0 mL culture medium at the desired seeding concentration. We have seeded as few as 10,000 cells per coverslip successfully and generally seed 150,000 cells per coverslip.
3. Add cell suspension dropwise to the submerged substrate.
4. Do not move plate for 5–10 min to allow for initial adhesion to the substrate. This helps ensure that most cells will adhere to the desired surface and not the well.
5. Cells can be grown on PLLA substrates for various durations, depending on experimental needs. We have grown cells for as little as 2 h, and as long as 2 weeks.

3.2.2 Migration Assay

As traditional migration assays, such as a Boyden chamber assay, are not feasible for observing migration upon fibrous substrates, we developed this assay to investigate the direction and/or rate of cell migration upon these substrates.

1. Place PLLA coated coverslip in a well of a clean 12-well culture plate.
2. Place a dry, sterile cloning cylinder onto the sample substrate (*see* **Note 18**).

3. Collect cells via trypsinization of stock culture and resuspend in 75 μL culture medium at the desired seeding concentration.
4. It is preferable to have a monolayer of cells to begin the migration experiment, so calculate the number of cells needed to cover the internal area of the cloning cylinder (28 mm^2). More cells may be necessary, though, due to the increased surface area available with fibrous substrates.
5. Carefully pipette the 75 μL of cell suspension into the cloning cylinder. The solution may not immediately flow to the bottom of the cylinder; this is not typically a problem. Do not add additional culture medium at this time.
6. Replace dish cover and carefully move well plate into the culture incubator.
7. Allow cells to attach. We generally culture cells overnight to achieve this.
8. After cells have attached to the substrate, carefully remove the cloning cylinder.
9. Add culture medium to sample wells.
10. If tracking of migration over time is desired, treat cells with CellTracker per manufacturer's instructions. For this assay, we image the entire cell island using a fluorescent dissecting microscope, but composite images can be taken with a low magnification objective on a standard fluorescent microscope as well.
11. Cells can be cultured for varying times on PLLA substrates, depending on the experimental design.

3.3 Fixation

The selection of fixation method is vital when considering which features of the cell are to be examined (*see* **Note 19**).

3.3.1 Methanol Fixation

1. Prechill an empty 6- or 12-well plate with approximately 2.5 or 1 mL, respectively, per well of cold fixing methanol in a –20 °C freezer for 30 min.
2. Immerse samples (i.e., cells on PLLA coated coverslips) in the methanol, working quickly. We typically leave the plate in the –20 °C freezer during this process (*see* **Note 20**).
3. Fix for 8–12 min at –20 °C. Ten minutes is optimal, therefore if a large number of samples are to be fixed, fix in batches.
4. Remove the plate from the freezer and remove samples from the methanol using forceps. Allow samples to air dry at room temperature. Lean samples on the edge of the well plate cover to ensure that both sides of the coverslip dry.
5. When dry, rinse in PBS/NaN_3 for 5 min. Remove the PBS by aspiration to minimize fluid flow across the surface of the coverslip. Repeat for three PBS rinses.

6. Incubate samples in CBS overnight at 4 °C to block nonspecific binding. Results are best when blocked overnight but this may be shortened to 2–4 h at room temperature if necessary.

3.3.2 Paraformaldehyde Fixation

Paraformaldehyde can either be purchased as a powder or presuspended liquid under inert gas. If using liquid, dilute to 4 % with PBS and skip to **step 6**.

1. Heat 25 mL ddH_2O to 60 °C. This is easiest by adding ddH_2O to a 50 mL tube and placing it in a 60 °C water bath.
2. Transfer ddH_2O to a beaker with a stir bar and add 2 g paraformaldehyde powder and approximately 0.15 g NaOH.
3. Stir covered until dissolved. It may be necessary to add ddH_2O to approximately 40 mL to ensure complete dissolution.
4. Add 5 mL 10× PBS.
5. Bring to 50 mL with ddH_2O and pH to 7.3 with HCl. 4 % paraformaldehyde is good for approximately 3–5 days if stored at 4 °C.
6. When ready to fix samples, warm paraformaldehyde to 37 °C.
7. Aspirate media from sample wells and add 1–2 mL 4 % paraformaldehyde solution.
8. Fix for 20 min at room temperature.
9. Aspirate paraformaldehyde and permeabilize with 0.25 % Triton X-100 in PBS for 10 min, then aspirate.
10. Rinse with PBS/NaN_3 for 5 min, then aspirate. Repeat for three rinses.
11. Incubate samples with CBS overnight at 4 °C to block nonspecific binding. Results are best when blocked overnight but this may be shortened to 2–4 h at room temperature if necessary.

3.4 Visualization

1. Prepare a humid chamber by placing paper towels in the bottom of a sealable container such as those used for household food storage. Add PBS/NaN_3 to moisten the paper towels and place a hydrophobic barrier such as dental wax or parafilm on top of the moist paper towels.
2. Make primary antibody dilution in PBS/NaN_3. Approximately 75 μL will be necessary for a sample on a 15 mm coverslip. Dilution factor will vary by antibody.
3. Centrifuge diluted antibody in 4 °C centrifuge at 12,000 × *g* for 5 min to pellet any aggregated antibody.
4. Remove samples from blocking solution and place in humid chamber (with cells facing up).
5. Carefully pipette primary antibody onto surface of samples. Seal humid chamber.

6. Incubate at room temperature for 1–1.5 h or at 4 °C overnight.
7. Remove samples from humid chamber and place them in wells of an empty 6- or 12-well plate.
8. Add PBS/NaN_3 to rinse for 5 min. Aspirate and repeat for three rinses.
9. Make secondary fluorescent antibody dilution in PBS/NaN_3. Approximately 75 μL will be necessary for each sample.
10. Centrifuge diluted antibody in 4 °C centrifuge at 12,000 × *g* for 5 min.
11. Remove samples from PBS/NaN_3 and place in humid chamber, cells facing up.
12. Add secondary antibody to surface of samples. Seal humid chamber.
13. Incubate, covered to protect fluorophores from light, at room temperature for 1–1.5 h or at 4 °C overnight.
14. Rinse with PBS/NaN_3 for 5 min. Aspirate, and repeat for three rinses.
15. If desired, incubate with nuclear dye such as DAPI, followed by an additional three rinses with dH_2O for 5 min each.
16. Place a drop of mounting reagent onto a "mounting" coverslip. We use 66 mm × 24 mm coverslips (*see* **Note 21**).
17. Invert sample and place it onto the mounting coverslip.
18. Remove excess mounting reagent by aspiration.
19. Let dry in the dark, at room temperature, for approximately 1 h or overnight at 4 °C.
20. Set coverslips with nail polish and store at 4 °C until visualization (*see* **Note 22**).
21. Visualize samples with a fluorescent microscope by imaging through the larger, "mounting" coverslip, not through the fibrous substrate.

4 Notes

1. It is important that the syringe pump comes with an internal power supply. The current version sold by Razel comes with a power cord and external power supply. The older version of this model came with an internal power supply, and when we contacted Razel they were able to send us the model with an internal power supply. The outer casing of this syringe pump is stainless steel. Because the needle and positive lead of the high voltage power supply are close to the outer casing, we have

found that the external power supply is instantly shorted when using higher voltages (>15 kV) and shorts out after ~6 months when using lower voltages. An internal power supply is protected by the outer casing acting as a Faraday cage, and we have used this model with an internal power supply for a few years without issue.

2. Choose your adhesion ligand based upon the cell type being cultured or the environment you wish to create. We cultured epithelial cells and fibroblasts by adsorbing fibronectin or RGD peptide to the electrospun fibers. There are many other ligands and peptide sequences, however, that may be used, such as collagen-I, collagen-IV, laminin, or peptide sequences such as IKVAV and GKKQRFRHRNRKG (laminin and vitronectin derived).
3. We use a DMI 4000B Inverted Microscope by LEICA but any fluorescent microscope can be utilized based upon the requirements of your experimental design.
4. Instead of collecting on the 4 % PLLA coated coverslip, fibers can be collected directly onto the glass coverslip. To prevent fibers detaching during culture, take some of the 4 % PLLA solution used to make the films and place a small amount of this solution along the edges of the coverslip. It is important to use the 4 % PLLA solution rather than the solvent alone since the solvent alone will travel up the fibers and dissolve a considerable amount of the scaffold.
5. The humidity is important when allowing the fibers to dry, because if the humidity is too high the films will become opaque. This is likely due to water condensing onto the surface of the fibers during the drying process, and probably creates a different surface structure compared to when the films are allowed to form in a dry environment.
6. The electrospinning platform mentioned here is very common, although many groups use a system where the syringe pump is placed on its side and the long-axis of the syringe is parallel to the floor. Models of electrospinning typically neglect the effects of gravity and appear to be reasonably accurate at modeling the jet bending instability and time it takes for a fiber to reach the collector [24, 25]. Typically groups that use the horizontal placement of the syringe pump use large collection distances (>15 cm).

   One modification to the above setup is worth mentioning because of its simple implementation. Instead of mechanically orienting the fibers on a rotating disk, it is possible to align the fibers between two grounded plates or wires (gap orientation method) [26, 27]. While the gap orientation method does produce aligned fibers, it also causes considerable alignment of

the polymer chains within the fiber compared to mechanical orientation on a rotating disk [28]. While mechanical orientation of fibers does create some degree of polymer chain orientation in the fibers over random collection [29], the increase in chain alignment for gap orientation over mechanical orientation is great enough to cause a noticeable change in cell morphology [30].

7. Collecting random fibers using this setup can be achieved a number of ways. Some groups use the same setup described here, but they turn the collection disk speed down to its lowest setting. This ensures a similar number of fibers are collected on each coverslip in a reproducible way. However, we have found fibers collected on a slow rotating disk are somewhat aligned. We are unsure if cells are able to respond to this very small degree of alignment compared to random fibers collected on an aluminum plate. We typically place the PLLA coated coverslip on an aluminum plate or cardboard wrapped in aluminum foil. If the plate is used, it is important to periodically move the plate around to ensure an even fiber density.
8. Electrospun fibers using a particular polymer change drastically when the solvent is changed. Fiber formation and fiber diameter are dependent on the number of polymer chain entanglements [31]. When there are insufficient chain entanglements, electrospraying of micro or nanoparticles occurs. If electrospraying occurs, using a higher molecular weight or increasing the concentration of polymer in the solution should allow for the formation of fibers [32]. It is important to note that some solvents are better for electrospinning a particular polymer because they are more likely to form a fiber without defects or electrospraying, and the ability of a polymer-solvent system to form a fiber is referred to as the "spinnability" of the solution. A method of selecting the proper solvent for a particular polymer has been suggested [33].

   One additional factor to consider when selecting a solvent is the volatility of the solvent, or how quickly the solvent evaporates. Typically this is characterized by the boiling point or vapor pressure of the solvent, with lower boiling point and higher vapor pressure indicating more rapid evaporation. Since the solvent is the predominant charge carrier [24, 25], the use of solvents that evaporate rapidly (such as methylene chloride) typically results in fewer fibers when collected on a rotating disk, likely because the fibers do not have sufficient charged solvent to be attracted to the disk. Because our setup uses a shorter collection distance than is often utilized, this is usually not a significant issue. However, some groups use large collection distances (>15 cm) and typically require an additional "drawing" agent, or solvent that has low volatility and high polarity. The

shorter distance we use may present a problem if a less volatile solvent is used since the fiber may be too "wet" to keep its form when it reaches the collector.

It is important to be aware of other issues when comparing fibers created using different solvents or combinations of solvents. It is possible to use different solvents to create fibers of different diameters, but an analysis of superficial properties (such as fiber alignment and diameter) is typically insufficient in determining the effects of the solvent on fiber characteristics. The polarity of the solvent plays a role in fiber formation, as fiber diameter generally decreases with increasing solvent polarity (as measured by dielectric constant) [34]. However, the solvent also dictates how crystalline the fibers are [35], and this changes the mechanical properties (elastic modulus, brittleness) of the fibers [36]. Additionally, solvent volatility plays a role in the surface structure of individual fibers [37], and this altered surface structure can alter protein adsorption, cell viability, and cell behavior [38].

Instead of changing solvents to alter diameter, we recommend changing the polymer concentration because it is less likely to change the mechanical properties. The diameter of fibers generated from electrospinning is directly proportional to the concentration of the polymer in solution [31, 35–39], with highly polar solvents generating smaller diameter fibers and solvents with less polarity generating larger diameter fibers for solutions that contain the same polymer concentration [31, 40]. We mention solvent polarity because this can be a barrier to achieving the desired fiber diameters when one solvent is used and polymer concentration is varied. While there is generally a linear relationship between fiber diameter and polymer concentration, there is a minimum polymer concentration under which fibers are not formed [29] and it seems as though there is a concentration above which there is little diameter increase [36]. Another option to help control fiber diameter is to increase or decrease the molecular weight to increase or decrease the fiber diameter [41].

9. We typically use one electrospinning solution per electrospinning run. Because the solvents used to electrospin are volatile (high vapor pressure), evaporation over time causes the polymer concentration to increase. Because of this, we recommend making up a fresh solution for every electrospinning trial (do not make a stock solution) and make sure to use the solution within 24 h.
10. Controlling the relative humidity in the electrospinning environment is critical. From personal experience, high humidity for some solvents can be the difference between electrospraying and electrospinning, or an intermediate between these two

states where the electrospray particles are attached with a thin fiber (giving rise to a "beads on a string" morphology). Additionally, changing the relative humidity even a few percentage points critically changes the number of fibers collected. It is well known that humidity alters fiber surface morphology [33, 42, 43]. We have performed experiments using chloroform alone as the solvent and found that 30 % relative humidity produces fibers with a smooth surface while 40 % relative humidity produces fibers with a porous or rough surface. This demonstrates that within a relatively small range of values, surface morphology can change significantly. For the chloroform and methylene chloride solvent we recommend here, there is little significant change between 30 and 40 % humidity.

11. The tape we use can act as an insulator and reduce fiber collection if too large a piece is used. However, if too small a piece is used, the tape will not hold the coverslip to the wheel. We have tried a few alternatives, the best of which was carbon tape used for scanning electron microscopy because it is conductive and actually helps with fiber collection. However, it is difficult to remove the carbon tape from the bottom of the coverslip so we typically do not use this for cell work.
12. Syringe pump flow rate can be adjusted to alter fiber diameter with increasing flow rate leading to an increase in fiber diameter [13, 33, 35, 39, 44]. However, it should be noted that if the polymer concentration is too low, lowering the syringe pump flow rate may result in fiber defects while increasing the flow rate at low polymer concentration only results in marginal increases in fiber diameter [35]. *See* **Note 8** for information on polymer concentration.
13. Collection distance is known to alter fiber diameter with increasing distance decreasing fiber diameter as expected according to elongation due to the whipping action of the polymer jet [24, 25]. However, the changes do not appear to be significant when the distance is changed from 5 to 25 cm [35]. The main concern with altering the collection distance has to do with solvent volatility and fiber deposition. As discussed in **Note 8**, solvent volatility is important because the solvent is the charge carrier and rapid evaporation causes the fiber to have less draw to the rotating collector. Although an additional agent may be added to help draw the fiber to the collector, modifying the composition of the solvent modifies the structure of the fiber. While we rarely modify our collection distance because it typically has little effect on fiber morphology, we do typically use much shorter collection distances compared to other groups in order to avoid having to use drawing agents. If fibers are melting into the polymer film, increase the collection distance to allow more solvent to evapo-

rate. If fiber collection is poor, decrease the collection distance. The poor collection rate typically is not an issue for random fibers since it is likely the laminar airflow around the collection disk blows away the thin fibers.

14. When the fibers are mechanically aligned by collecting on a rotating plate, the fiber diameters are smaller than random collection if all other parameters are kept constant, and there is a trend of decreasing fiber alignment with increasing rotation speed [14, 37, 45]. Also, in order to achieve high degrees of alignment it is necessary to try several rotation speeds since spinning the collector too fast or slow may cause fiber defects and lower degrees of alignment [27, 40].
15. Voltage does play a role in the electrospinning process, but it is not entirely intuitive. There is a minimum voltage needed to overcome the surface tension of the polymer solution. Once this minimum voltage is reached, increasing the voltage further decreases the fiber diameter. When a critical voltage is reached, the fiber diameter increases [35], and while the mean fiber diameter increases, the fiber population consists of both large and small diameter fibers. Because of this, we find the use of higher voltages ambiguous when performing cell work since it is unclear if cells are responding to the large or small diameter fibers or some combination of both.
16. Because high voltage is used, it is necessary to use some precaution when the voltage is turned on. The particular high voltage supply used in this protocol only allows a maximum of 200 μA of current, meaning the power output is low, so if you do get shocked, there is little risk of any significant danger. Of course, there is always the chance of an unfortunate situation developing from getting shocked, so it is important to not touch the needle with anything metal or detach the positive voltage lead while the power is on. We typically keep hands at least 6 in. away and only touch the tip of the needle with the wooden dowel. When we use higher levels of humidity, absorbed water in the dowel can cause the charge to travel up the dowel so we also have insulating gloves rated for high voltages. However, there is the potential of a more serious problem since some voltages and fiber types have shown the ability to produce high energy x-rays [46]. The risk is minimal, being limited to higher voltages (30 kV and larger) and it seems as though it is necessary for the fibers to be ~100 nm and smaller. We do not use high enough voltages for this to be an issue, because using a voltage much higher than what we use in our design has little advantage (*see* **Note 15**).
17. Cells typically require an ECM ligand in order to adhere to a surface. We adsorb ligand by submerging the coated coverslip in 1.5 mL ligand solution (i.e., RGD peptide or fibronectin

at 10 μg/mL) in a well of a 12-well culture plate. As the PLLA substrates are very hydrophobic, you may need to press the coverslip into the liquid with a micropipette tip. Place plates in a 37 °C incubator for 6 h, then remove the ligand solution by aspiration. Ligand solution can be reused 3–4 times. In the absence of ligand, cells may still adhere by secreting their own matrix proteins or by the adsorption of serum proteins (from the culture medium) onto the fibers, but for experiments using low cell seeding density or short incubation periods, it is highly recommended that the fibers be pretreated with ligand.

18. PLLA substrates are highly hydrophobic. This hydrophobicity is largely overcome by adsorption of an ECM ligand. We have also found that plasma treating the substrates completely abolishes the hydrophobicity, but can lead to media leakage during the initial phase of the migration assay.
19. All fixation methods have both positive and negative aspects. A review of fixation theory and methods such as those listed here can be found in the Handbook of Biological Confocal Microscopy [47] and may be helpful in determining a fixation protocol suitable for a specific situation.
20. We find that we achieve the best preservation of cell morphology with methanol fixation when the methanol is kept very cold (best at least −20 °C) during fixation. We use a small, dedicated freezer, for fixation, so that the internal air temperature can be tightly controlled.
21. When examining cells grown on electrospun fibers, it is difficult to image through the scaffold at low magnification and essentially impossible to image through the scaffold at high magnification, due to optical interference by the substrate. Mounting on a coverslip allows for high quality imaging from the top down.
22. Different mounting reagents have different requirements for how they are "cured." Prolong Gold should not be completely sealed and only the corners of the coverslip should be set with nail polish. Other mounting reagents may require complete sealing of the perimeter of the coverslip.

Acknowledgments

This work has been supported by the American Cancer Society Research Scholar Grant (RSG-10-245-01-CSM) to LAL and National Science Foundation, Biomaterials Program CAREER Award (1150125) to RJG.

References

1. Kim D-H, Provenzano PP, Smith CL et al (2012) Matrix nanotopography as a regulator of cell function. J Cell Biol 197:351–360
2. Leight JL, Wozniak MA, Chen S et al (2012) Matrix rigidity regulates a switch between TGF-β1-induced apoptosis and epithelial-mesenchymal transition. Mol Biol Cell 23:781–791
3. Huebsch N, Arany PR, Mao AS et al (2010) Harnessing traction-mediated manipulation of the cell/matrix interface to control stem-cell fate. Nat Mater 9:518–526
4. Swamydas M, Eddy JM, Burg KJL et al (2010) Matrix compositions and the development of breast acini and ducts in 3D cultures. In vitro cellular and developmental biology. Animal 46:673–684
5. Lim SH, Mao H-Q (2009) Electrospun scaffolds for stem cell engineering. Adv Drug Deliv Rev 61:1084–1096
6. Richards J, Larson L, Yang J et al (1983) Method for culturing mammary epithelial cells in a rat tail collagen gel matrix. J Tissue Culture Methods 8:31–36
7. Tan H, Marra KG (2010) Injectable, biodegradable hydrogels for tissue engineering applications. Materials 3:1746–1767
8. Santos E, Hernández RM, Pedraz JL et al (2012) Novel advances in the design of three-dimensional bio-scaffolds to control cell fate: translation from 2D to 3D. Trends Biotechnol 30:331–341
9. Tan JL, Tien J, Pirone DM et al (2003) Cells lying on a bed of microneedles: an approach to isolate mechanical force. Proc Natl Acad Sci USA 100:1484–1489
10. Nakayama KH, Batchelder CA, Lee CI et al (2010) Decellularized rhesus monkey kidney as a three-dimensional scaffold for renal tissue engineering. Tissue Eng Part A 16: 2207–2216
11. Wang HB, Mullins ME, Cregg JM et al (2010) Varying the diameter of aligned electrospun fibers alters neurite outgrowth and Schwann cell migration. Acta Biomater 6:2970–2978
12. He L, Liao S, Quan D et al (2010) Synergistic effects of electrospun PLLA fiber dimension and pattern on neonatal mouse cerebellum C17.2 stem cells. Acta Biomater 6:2960–2969
13. Christopherson GT, Song H, Mao H-Q (2009) The influence of fiber diameter of electrospun substrates on neural stem cell differentiation and proliferation. Biomaterials 30:556–564
14. Saino E, Focarete ML, Gualandi C et al (2011) Effect of electrospun fiber diameter and alignment on macrophage activation and secretion of proinflammatory cytokines and chemokines. Biomacromolecules 12:1900–1911
15. Frantz C, Stewart KM, Weaver VM (2010) The extracellular matrix at a glance. J Cell Sci 123:4195–4200
16. Micallef L, Vedrenne N, Billet F et al (2012) The myofibroblast, multiple origins for major roles in normal and pathological tissue repair. Fibrogenesis Tissue Repair 5:S5
17. Provenzano PP, Inman DR, Eliceiri KW et al (2008) Contact guidance mediated three-dimensional cell migration is regulated by Rho/ROCK-dependent matrix reorganization. Biophys J 95:5374–5384
18. Zhou F, Yuan L, Huang H et al (2009) Phenomenon of "contact guidance" on the surface with nano-micro-groove-like pattern and cell physiological effects. Chin Sci Bull 54:3200–3205
19. Fueshko S, Wray S (1994) LHRH cells migrate on peripherin fibers in embryonic olfactory explant cultures: an in vitro model for neurophilic neuronal migration. Dev Biol 166: 331–348
20. Friedl P, Entschladen F, Conrad C et al (1998) CD4+ T lymphocytes migrating in three-dimensional collagen lattices lack focal adhesions and utilize beta1 integrin-independent strategies for polarization, interaction with collagen fibers and locomotion. Eur J Immunol 28:2331–2343
21. Provenzano PP, Eliceiri KW, Campbell JM et al (2006) Collagen reorganization at the tumor-stromal interface facilitates local invasion. BMC Med 4:38
22. Sill TJ, von Recum HA (2008) Electrospinning: applications in drug delivery and tissue engineering. Biomaterials 29:1989–2006
23. Lee Y-S, Livingston Arinzeh T (2011) Electrospun nanofibrous materials for neural tissue engineering. Polymers 3:413–426
24. Reneker DH, Yarin AL, Fong H et al (2000) Bending instability of electrically charged liquid jets of polymer solutions in electrospinning. J Appl Phys 87:4531
25. Yarin AL, Koombhongse S, Reneker DH (2001) Bending instability in electrospinning of nanofibers. J Appl Phys 89:3018
26. Kakade MV, Givens S, Gardner K et al (2007) Electric field induced orientation of polymer chains in macroscopically aligned electrospun polymer nanofibers. J Am Chem Soc 129: 2777–2782
27. Chaurey V, Block F, Su Y-H et al (2012) Nanofiber size-dependent sensitivity of fibroblast directionality to the methodology for scaffold alignment. Acta Biomater 8:3982–3990
28. Fennessey SF, Farris RJ (2004) Fabrication of aligned and molecularly oriented electrospun polyacrylonitrile nanofibers and the mechanical

behavior of their twisted yarns. Polymer 45: 4217–4225
29. Shenoy S, Bates W, Frisch H et al (2005) Role of chain entanglements on fiber formation during electrospinning of polymer solutions: good solvent, non-specific polymer–polymer interaction limit. Polymer 46:3372–3384
30. Luo CJ, Nangrejo M, Edirisinghe M (2010) A novel method of selecting solvents for polymer electrospinning. Polymer 51:1654–1662
31. Guarino V, Cirillo V, Taddei P et al (2011) Tuning size scale and crystallinity of PCL electrospun fibres via solvent permittivity to address hMSC response. Macromol Biosci 11:1694–1705
32. Asran AS, Salama M, Popescu C et al (2010) Solvent influences the morphology and mechanical properties of electrospun poly(L-lactic acid) scaffold for tissue engineering applications. Macromol Symp 294:153–161
33. Megelski S, Stephens JS, Chase DB et al (2002) Micro- and nanostructured surface morphology on electrospun polymer fibers. Macromolecules 35:8456–8466
34. Leong MF, Chian KS, Mhaisalkar PS et al (2009) Effect of electrospun poly(D, L-lactide) fibrous scaffold with nanoporous surface on attachment of porcine esophageal epithelial cells and protein adsorption. J Biomed Mater Res A 89:1040–1048
35. Baker SC, Atkin N, Gunning PA et al (2006) Characterisation of electrospun polystyrene scaffolds for three-dimensional in vitro biological studies. Biomaterials 27:3136–3146
36. Meechaisue C, Dubin R, Supaphol P et al (2006) Electrospun mat of tyrosine-derived polycarbonate fibers for potential use as tissue scaffolding material. J Biomater Sci Polym Ed 17:1039–1056
37. Yang F, Murugan R, Ramakrishna S et al (2004) Fabrication of nano-structured porous PLLA scaffold intended for nerve tissue engineering. Biomaterials 25:1891–1900
38. Deitzel J, Kleinmeyer J, Harris D et al (2001) The effect of processing variables on the morphology of electrospun nanofibers and textiles. Polymer 42:261–272
39. Fridrikh S, Yu J, Brenner M et al (2003) Controlling the fiber diameter during electrospinning. Phys Rev Lett 90:144502
40. Wang HB, Mullins ME, Cregg JM et al (2009) Creation of highly aligned electrospun poly-L-lactic acid fibers for nerve regeneration applications. J Neural Eng 6:016001
41. Koski A, Yim K, Shivkumar S (2004) Effect of molecular weight on fibrous PVA produced by electrospinning. Mater Lett 58: 493–497
42. Casper CL, Stephens JS, Tassi NG et al (2004) Controlling surface morphology of electrospun polystyrene fibers: effect of humidity and molecular weight in the electrospinning process. Macromolecules 37: 573–578
43. Bognitzki M, Czado W, Frese T et al (2001) Nanostructured fibers via electrospinning. Adv Mater 13:70–72
44. Yao L, O'Brien N, Windebank A et al (2009) Orienting neurite growth in electrospun fibrous neural conduits. J Biomed Mater Res B Appl Biomater 90:483–491
45. Bashur CA, Shaffer RD, Dahlgren LA et al (2009) Effect of fiber diameter and alignment of electrospun polyurethane meshes on mesenchymal progenitor cells. Tissue Eng Part A 15:2435–2445
46. Pokorný P, Mikeš P, Lukáš D (2010) Electrospinning jets as X-ray sources at atmospheric conditions. Europhys Lett EPL 92:47002
47. Bacallao R, Sohrab S, Phillips C (2006) Guiding Principles of Specimen Preservation for Confocal Fluorescence Microscopy. In: Pawley JB (ed) Handbook of biological confocal microscopy, 3rd edn. Plenum Press, New York, pp 368–380

Chapter 24

Method for Measuring Single-Molecule Adhesion Forces and Attachment Lifetimes of Protein–Membrane Interactions

Serapion Pyrpassopoulos, Henry Shuman, and E. Michael Ostap

Abstract

Many proteins that reside in the cytoplasm bind directly to cell membranes and play roles in signaling, adhesion, metabolism, cell structure, and cell motility. Several of these membrane-binding proteins, especially cytoskeletal proteins, have mechanical functions that result in the transmission of forces to the plasma membrane and organelle-membranes. Despite the importance of these interactions, remarkably little is known about the mechanical properties of the bonds between membranes and proteins. In this chapter, we describe a single-molecule, optical-trapping method for the measurement of protein–membrane adhesion forces and force-dependent attachment-lifetimes.

Key words Optical tweezers, Adhesion force, Single molecule, Myosin-I, Phosphoinositide, Supported lipid bilayer, Membrane

1 Introduction

Many proteins that reside in the cytoplasm bind directly and dynamically to cell membranes and play roles in signaling, adhesion, metabolism, cell structure, and cell motility. Many of these interactions are mediated by well-defined protein domains or by post-translational modifications that insert into the hydrophobic core of the membrane bilayer [1, 2]. Some proteins bind via stereospecific interactions allowing recognition of various lipids, while others bind without substantial specificity through a combination of delocalized electrostatic interactions of charge clusters and/or hydrophobic interactions [3].

In many cases, the binding of proteins to the membrane is simply a means for concentrating the proteins at the membrane for polarization and targeting of cell signals. However, an important subset of peripheral membrane-binding proteins has mechanical functions that impart forces on the membrane [4–6]. For example

Amanda S. Coutts (ed.), *Adhesion Protein Protocols*, Methods in Molecular Biology, vol. 1046,
DOI 10.1007/978-1-62703-538-5_24,

many membrane-binding proteins deform the lipid directly by their binding (e.g., bar domains), while others are (a) cytoskeletal components that actively generate force, (b) anchoring proteins that attach force-generating motors to membrane-encapsulated cargos, or (c) force-bearing elements that bind to cytoskeletal filaments to confer a specific morphology to the membrane.

Very little is known about the mechanical properties of membrane-binding proteins, which is problematic when one is interested in determining the mechanisms of protein action. Mechanical parameters that need to be determined include adhesion forces and force-dependent attachment lifetimes. These properties are particularly important in the context of cytoskeletal proteins, since the job of these proteins is to power motility or cell shape changes, in part by moving and deforming membranes.

Myosin-I proteins are a class of molecule motors that bind directly to cell membranes and provide an active link to the underlying actin cytoskeleton [7–9]. Myosin-I isoforms are thought to transport membrane-bound organelles through the cytoplasm, as well as to affect membrane morphology by generating force relative to actin filaments. Indeed, in vitro experiments have shown that myosin-I isoforms can power actin gliding while bound to supported fluid bilayers [10, 11]. While much progress has been made determining the cellular functions of myosin-I, the molecular roles are largely unknown. Our goal was to (a) develop an assay to measure the adhesion forces of the bonds between a membrane and a peripheral-membrane protein that are in the piconewton range, and (b) determine the adhesion strength and force-dependent attachment lifetimes of myosin-I–membrane interactions with the goal of understanding how myosins generate force and perform mechanical work relative to fluid bilayers. The experimental protocol outlined below has been optimized for the study of the interaction between the tail domain of Myosin-1C (Myo1c) and PtdIns(4,5)P_2-containing membranes [12]. However, the procedure can be applied to the investigation of a variety of protein–membrane interactions.

2 Materials

Prepare all solutions using ultrapure water (18 MΩ) and analytical grade reagents. Follow local regulations when using and disposing of volatile and organic reagents. Wear gloves and eye protection. Work in fume hood as necessary. We store all aqueous buffers at 4 °C.

2.1 Assay Components, Materials, and Equipment

1. Clear glass vials (8 mL) with Teflon caps (Fisher B7800) for preparation of lipid solutions.
2. Teflon tape for sealing threads of vials.
3. Probe sonicator with 2–3 mm tip.

4. Bath sonicator.
5. Ultracentrifuge polycarbonate tubes.
6. Rotary evaporator for removing organic solvents from lipid mixtures.
7. Capillary glass tubes for Drummond positive displacement pipettes.
8. Glass coverslips, 22 mm × 40 mm × 1.5 mm (Fisher cat# 12 544 B).
9. Double-stick tape.
10. Silicon vacuum grease.
11. Filter paper.
12. Silica (Polysciences cat# 24326–15) and hydroxylated-polystyrene beads (Polysciences cat# 17142–15).
13. Optical tweezers microscope.
14. Optional: Lipid extruder for creating unilamellar vesicles from vesicle suspensions (Avant Polar Lipids).

2.2 Buffers, Solutions, and Reagents

1. HNa100 buffer: 1 M HEPES (pH 7.0), 100 mM NaCl, 1 mM EGTA, 1 mM DTT.
2. Myo1c$^{IQ\text{-}tail}$: A protein construct that contains the tail and regulatory domains of mouse Myo1c (residues 690–1,028) and N-terminal poly-His and Avitag sequences co-expressed with calmodulin in Sf9 cells using a Baculovirus expression system and purified as described [13, 14].
3. NeutrAvidin solution: NeutrAvidin (Sigma-Aldrich) suspended to 5 mg/mL in HNa100.
4. Glutathione-S-transferase (GST) blocking solution: 2 mg/mL in HNa100. A screen of various proteins showed that GST was the best blocking protein for our needs; however, other suitable proteins can be used for blocking.
5. Silica-bead solution: Silica beads in amyl acetate to final concentration of 2 mg/mL [15] (*see* **Note 1**).
6. Casein blocking solution: Dissolve 0.4 g casein in 40 mL of HNa100 and incubate for 1 h at 37 °C. After vortexing, filter (0.22 μm bottle-top filter) the solution to remove aggregates. The casein solution can be stored at −20 °C in small aliquots.
7. Lipids: 1,2-Dioleoyl-sn-glycero-3-phosphocholine (DOPC), L-α-phosphatidylinositol-4,5-bisphosphate (PtdIns(4,5)P_2), 1,2-dioleoyl-sn-glycero-3-phosphoethanolamine-n-(lissamine rhodamine B sulfonyl) (18:1 LRPE) (Avanti Polar Lipids).
8. Nitrocellulose (Collodion) solution: EM grade solution of 2 % nitrocellulose in amyl acetate (Electron Microscopy Sciences cat# RT 12620–55).
9. Amyl acetate (Electron Microscopy Sciences cat# RT 10816).

3 Methods

All procedures are performed at 20–22 °C, unless indicated otherwise.

3.1 Preparation of Lipid-Coated Beads

1. Remove lipids from −20 °C storage and allow vials to thermally equilibrate to room temperature in a desiccator (*see* **Note 2**).
2. Prepare a lipid mixture of 97.9 % DOPC and 2 % PtdIns(4,5)P_2, 0.1 % LRPE mix (in the fume hood) in a round bottom 50 mL glass flask. Usual volumes and stock concentrations are as follows: 77 μL DOPC (12.7 mM), 22 μL PtdIns(4,5)P_2 (0.9 mM) and 13 μL LRPE (0.077 mM) (*see* **Note 3**).
3. Bring the temperature of the rotatory-evaporator water bath to 37 °C. Attach the flask, start rotation, and immerse the flask in the water bath. After thermal equilibration (~5 min), gradually apply vacuum so as not to boil the sample (*see* **Note 4**). Dry lipid film under hard vacuum overnight (*see* **Note 5**).
4. Switch off the vacuum and remove the flask. Add 1–2 mL of HNa100 and bring the lipid film into suspension by vortexing for 2 min (*see* **Note 6**).
5. Form a suspension of small unilamellar vesicles (SUVs) by placing the lipid suspension in a 2 mL thin transparent microcentrifuge tube on a float in an ice-water bath. Sonicate in cycles of 10 s on and 30 s off for 10 min (*see* **Note 7**). Ultracentrifuge at 25 °C in polycarbonate tubes for 30 min at 100,000 × *g*. Remove and keep the upper two thirds of the supernatant that contain the SUVs (*see* **Note 8**).
6. Wash 50 μL of hydroxylated-polystyrene beads (~2×10^{10} beads/mL) in 1 mL of H_2O and spin at 13,000 rpm (15,700 × *g*) for 15 min at room temperature in a benchtop centrifuge (*see* **Note 9**). Remove and discard supernatant, resuspend beads in 50 μL of H_2O, and bath sonicate for 5 min to disperse beads.
7. Mix 500 μL of SUVs with 6 μL of freshly washed hydroxylated polystyrene beads in microcentrifuge tube. Vortex briefly to enhance mixing and let sit for 4 h to overnight (*see* **Note 10**). Wash beads with 1 mL HNa100 3 times using a benchtop centrifuge at 13,000 rpm (15,700 × *g*) for 5 min each. After the final wash, resuspend the beads in 200–250 μL of HNa100. The lipid-coated beads are now ready for use. Store the beads for <2 days on ice or 4 °C.
8. Coating of lipids can be verified by fluorescence microscopy (Fig. 1a; *see* **Note 11**).

3.2 Preparation of Assay Chamber

1. Mix 92 μL amyl acetate with 5 μL 2 % nitrocellulose and 2 μL of the silica-bead solution. Vortex briefly (2–3 s). Spread 4 μL of the bead solution on a glass coverslip using the tip of the

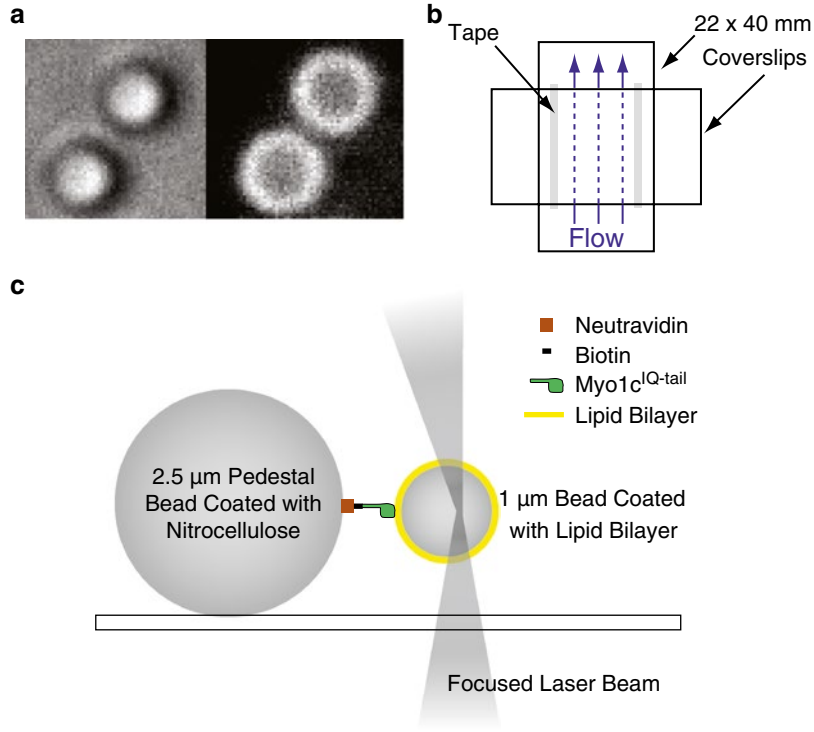

Fig. 1 (**a**) Transmitted and fluorescence micrographs showing 1 µm diameter beads coated with 2 % PtdIns(4,5)P_2, 97.5 % DOPC, and 0.5 % LRPE. (**b**) Flow chamber made using double-stick tape, vacuum grease and two glass coverslips 22 × 40 mm. (**c**) Diagram of experimental set-up used to measure the interaction of pedestal-attached Myo1c$^{IQ\text{-}tail}$ with membrane-coated beads held in an optical trap. The trap position was oscillated, resulting in the compression of the trapped beads against Myo1c$^{IQ\text{-}tail}$-coated pedestals, followed by retraction. Adhesions forces displace the bead from the trap center during retraction, which is measured as a beam deflection at the back focal plane with a quadrant detector. Formation and subsequent rupture of bonds appeared as negative peaks in the data traces (Fig. 2). Myo1c$^{IQ\text{-}tail}$ molecules were site-specifically attached to pedestals via NeutrAvidin–biotin linkages. Beads and protein molecules are not drawn to scale

pipette and let it dry covered in a Petri dish or under a hood for 20 min (*see* **Note 12**). Use double-stick tape and vacuum grease to assemble a flow cell as shown in Fig. 1b (*see* **Note 13**). The chamber volume is ~20 µL.

2. Use a pipette to inject 20 µL of the following solutions into one side of the assay chamber while holding a strip of absorbent filter paper to the opposite side of the chamber to facilitate flow. (1) 0.01 mg/mL NeutrAvidin and incubate 5 min, (2) 2 mg/ML GST and incubate for 5 min, (3) 0.2–2.5 nM biotinylated Myo1c$^{IQ\text{-}tail}$ in the presence of blocking protein 2 mg/mL GST and 5 µM calmodulin for 5 min. Wash the chamber three times with 5 mg/mL casein, 5 µM calmodulin (*see* **Note 14**). Dilute the lipid coated beads 100-fold in HNa100, 5 mg/mL casein, 5 µM calmodulin flow into assay chamber (*see* **Note 15**). Seal the flow cell with vacuum grease to avoid evaporation and place on stage of optical trapping microscope.

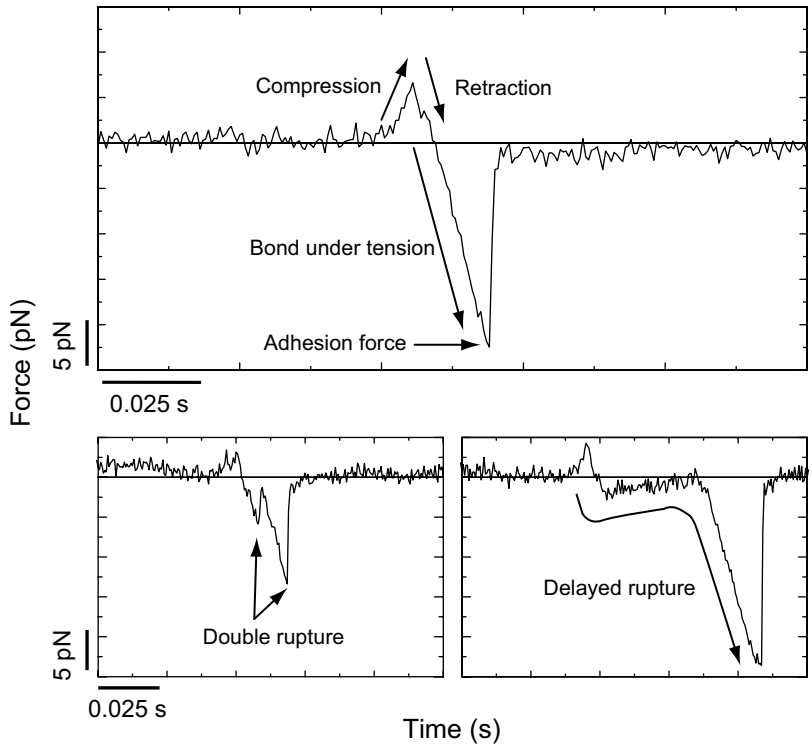

Fig. 2 Representative examples of ramp-load rupture events. (*Top*) The three characteristic regions are: compression of the bead on the pedestal, retraction of the bead in the opposite direction until the compressive force reaches zero and bond under linearly increasing tension until rupture. (*Bottom left*) Double rupture and (*bottom right*) delayed rupture events made up <10 % of interactions and were excluded from the analysis

3.3 Measurement of Adhesion Forces (Ramp Force Measurement)

Detailed descriptions of optical trapping practice and theory are beyond the scope of the current chapter. We refer the reader to refs. 16, 17. For details regarding our experimental setup, *see* refs. 12, 18, 19.

1. After trapping a lipid-coated bead, the stiffness of the trap and the force calibration coefficient must be determined by analysis of the power spectrum of the thermal motion of the trapped bead (*see* **Note 16**).
2. Move the trapped bead close to a silica-bead pedestal (Fig. 1c), and move the trapping laser using a triangular oscillation. Move the pedestal towards the oscillating bead using a piezo-stage until the trapped bead and the pedestal touch each other, yielding a compression peak (positive force) (Fig. 2; *see* **Note 17**).
3. Formation and subsequent rupture of an interaction upon retraction of the bead will appear as a negative peak (Fig. 2; *see* **Note 18**). The height of the negative peak is proportional to the adhesion force (*see* **Note 19**).

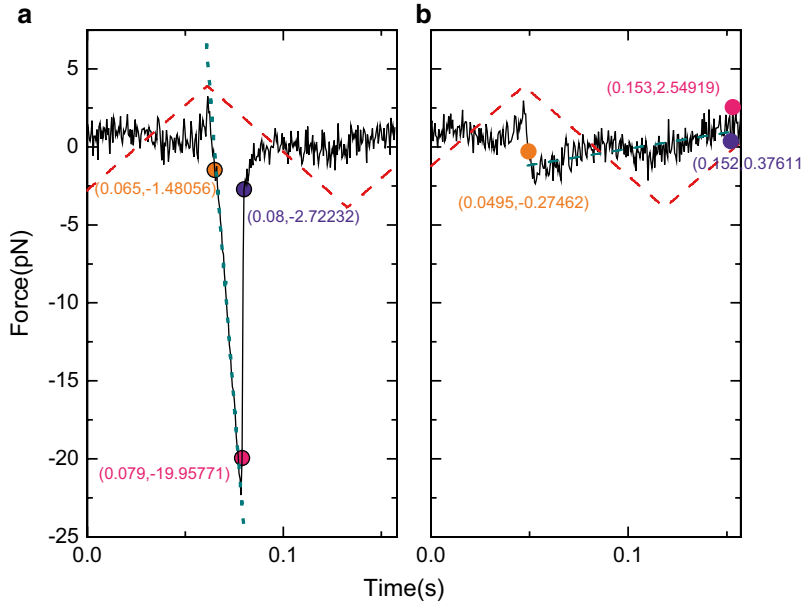

Fig. 3 A triangular pulse (*red dashed trace*) is the command signal that drives retraction of the membrane-coated bead. At an acquisition rate of 2,000 Hz, rupture peaks are recognized as sharp transitions that take place within three data points, equivalent to 1.0 ms (compare time coordinate between *purple* and *pink* points in the plots). (**a**) A rupture peak (*black trace*) with slope of −1,630 pN/s as calculated by linear fit of the data between the orange and pink points (*cyan dark dashed line*). The nominal value of loading rate was −1,900 pN/s. Rupture peaks that have loading rates that fall within 10 or 20 % of the expected loading rate are reported. (**b**) A rupture peak with slope of 20 pN/s, which was excluded using the aforementioned selection rule

4. Control experiments should be performed in the absence of Myo1c$^{IQ\text{-}tail}$, in the absence of PtdIns(4,5)P_2 (i.e., 100 % DOPC) (*see* **Note 20**) and in the presence of soluble IP6 which competitively inhibits the interaction between Myo1c$^{IQ\text{-}tail}$ and PtdIns(4,5)P_2.
5. Measure the rupture force as the largest negative peak in each oscillation cycle by selecting rupture peaks with slope within 10 or 20 % of the expected loading rate (Fig. 3; *see* **Note 21**). Calculate the frequency distributions of rupture events for the experimental and control data sets (Insets Fig. 4; *see* **Note 22**).
6. After subtraction of the contribution of nonspecific interactions, normalize the remaining distribution with respect to the size of the selected force bin and the total number of events to get the probability density distribution (rupture probability/pN) such that

$$\sum_i h_i \Delta b = 1, \tag{1}$$

where, h_i is the probability density (pN^{-1}) and Δb is the size of the bin (Fig. 4).

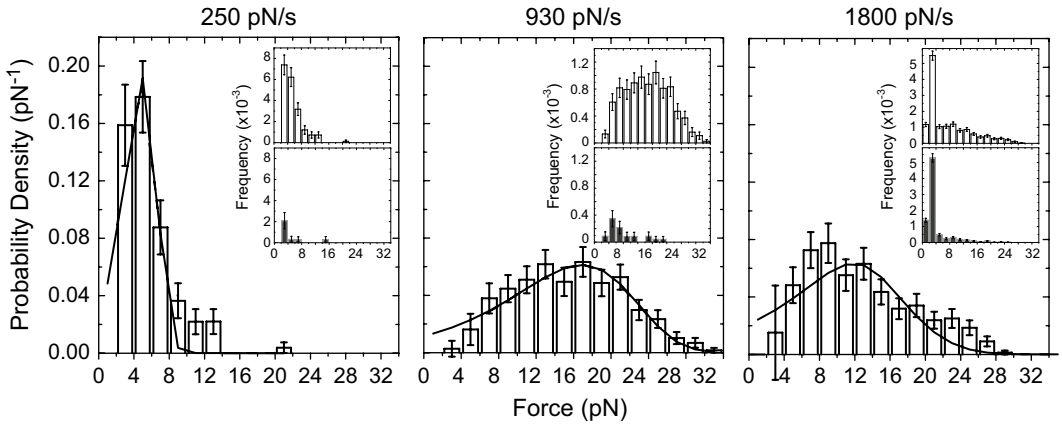

Fig. 4 Probability density distributions of forces required to dissociate Myo1c$^{IQ\text{-}tail}$ from supported lipid membranes containing 2 % PtdIns(4,5)P_2 at loading rates of 250 ± 29, 930 ± 120 and 1,800 ± 230 pN/s (the loading rates are given in absolute values and the error is the standard deviation). The corrected distributions in the main panels were obtained by subtracting (*inset, bottom*) frequency distributions (per contact cycle) obtained in the absence of Myo1c$^{IQ\text{-}tail}$ from (*inset, top*) uncorrected frequency distributions. Best fits of the distributions to Bell–Evans model (*see* **Note 23**)

7. The probability distribution can be fitted to the Bell–Evans model [20, 21] to obtain values for the unloaded dissociation rate (k_0) and the distance to the transition state (d_{tr}, *see* **Note 23**).
8. Since the most probable rupture-force depends on the loading rate [21], data should be collected for at least three different oscillation frequencies (*see* **Note 24**) to see if the mechanical rupture is indeed described by the Bell–Evans model.

3.4 Measurement of the Force-Dependence of Adhesion Lifetime (Constant Force Measurement)

1. Oscillate the trapped bead using a square wave (Fig. 5a). Move the pedestal towards the oscillating bead using a piezo-stage, and set the square-wave amplitude to attain the desired compressive and separating forces (Fig. 5a). Use a force-clamp to ensure a constant tension during the separation phase (*see* **Note 25**).
2. Double bond events can be recognized by double-peaks of the error signal (Fig. 5b) and should be excluded from data analysis (*see* **Note 26**).
3. Perform control experiments using the conditions outlined above (*see* Subheading 3.3, **step 4**).
4. Determine the attachment duration for each interaction (Fig. 5a; *see* **Note 27**).
5. Calculate the frequency distribution of the attachment durations for the experimental and control data sets (Fig. 6a), and subtract the contribution of the nonspecific interactions (*see* **Note 28**). Normalize the resultant distributions similarly to Subheading 3.3, **step 6** to get probability density distributions.

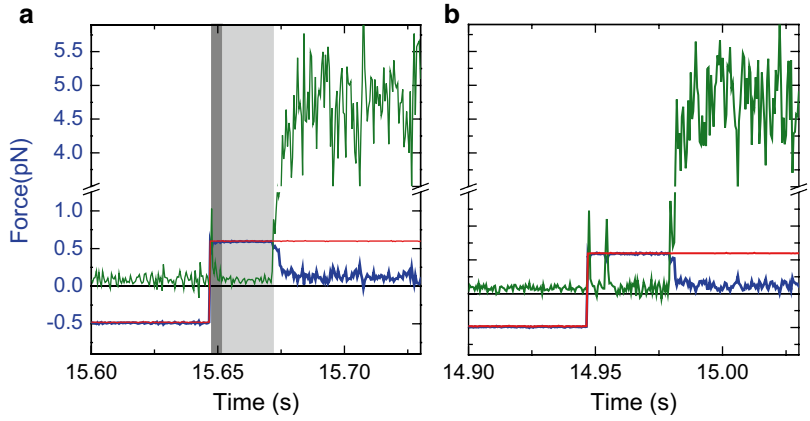

Fig. 5 (**a**) Example of attachment duration of a single attachment under 0.6 pN of load. A square pulse (*red trace*) is the command signal to drive compression and retraction of the membrane coated bead. Positive forces on the bond (*blue trace*) and the 10× amplified error signal (*green trace*) are recorded during attachments. When a bond is formed between the membrane-coated bead and the Myo1c$^{IQ\text{-}tail}$ a constant force is maintained via a feedback loop until the bond ruptures and the force trace (*blue*) drops back to zero. The time period that it takes to develop a constant load and the error signal to become ~0 is indicated by the dark gray shaded area. The actual duration of the attachment under constant load is indicated by the light gray shaded area. (**b**) Example of a double bond event, which is indicated by the two peaks in the 10× amplified error signal

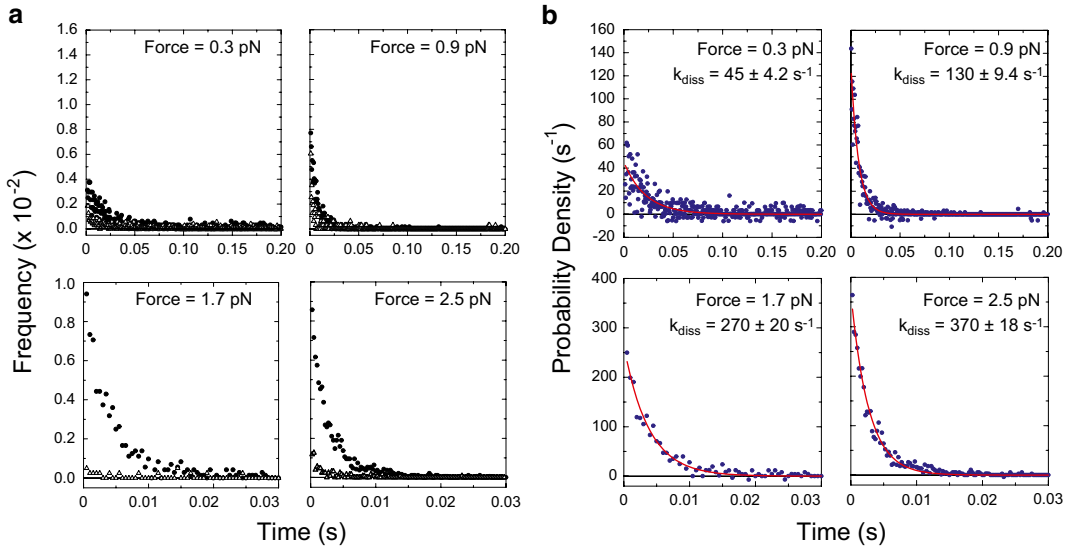

Fig. 6 (**a**) Frequency distributions (per cycle) of attachment-durations acquired under constant forces between beads coated with 2 % PtdIns(4,5)P_2 and 98 % DOPC and pedestals decorated with (*filled circle*) Myo1c$^{IQ\text{-}tail}$ or (*triangle*) in the absence of Myo1c$^{IQ\text{-}tail}$. Frequencies were calculated over the total number of contacts between the trapped bead and the pedestals. The constant pulling force is indicated in each plot. (**b**) After subtracting the control (*triangle*) from the experimental (*filled circle*) data in (**a**) and normalizing with respect to the total number of interactions and the size of the time-bin one gets the survival probability density of the bond as a function of attachment duration under constant tension is plotted. (*Solid lines*) Fitting curves of survival probability densities to Eq. 2

Assuming a single-step dissociation reaction, determine the dissociation rate constant (k_{dis}) by fitting the probability density distributions to the exponential distribution (Fig. 6b):

$$k_{dis} e^{(-k_{dis} t)}. \quad (2)$$

3.5 Comparison of Ramp Force and Constant Force Measurements

One can extract the force dependence of the dissociation rate (k_{dis}) from the probability density distribution of adhesion forces as described in Dudko et al. [22] and Pyrpassopoulos et al. [12]. However, as pointed out by Dudko et al., the experimenter should be careful as this transformation is valid only after constant force experiments are done and the dissociation rate is found to be a single exponential.

4 Notes

1. It may take more than 15 min to resuspend dry silica beads in amyl acetate. Use a glass pipette (e.g., Pasteur pipette) to resuspend the beads, rather than using a digital pipette (e.g., Pipetman). With prolonged exposure, the amyl acetate vapors may damage the seals within the Pipeman and dissolve the disposable tips. The final solution can be stored at 4 °C.
2. Wear lab coat and Nitrile gloves to avoid accidental skin contact with chloroform solutions. Transfer lipid solutions to vials (8 mL) with Teflon cap. Briefly flow Nitrogen over the top to remove oxygen before sealing. One can also use Teflon tape to seal the caps to prevent evaporation of chloroform. Store stock solutions −20 °C.
3. Use either glass Hamilton syringes or Drummond positive displacement pipettes with Teflon plunger and capillary glass tubes. Take care to minimize evaporation of chloroform, or else evaporation will change the stock concentration.
4. Minimize boiling to ensure that the lipids dry in a confined region that will allow for easy resuspension.
5. The application of hard vacuum for extended period (at least 4 h) is required. Slight traces of chloroform can damage lipids during tip sonication in Subheading 3.1, step 5 [23]. In general the time period that is required to remove traces of chloroform depends on the volume of the sample. If a rotary evaporator is not available, the lipid solution can be dried under gentle flow of nitrogen gas while continuously swirling the flask or a glass vial under a fume hood. The dried lipid can then be placed under hard vacuum.
6. The lipid concentration is 0.5–1 mM. If using a buffer other than HNa100, ensure it is compatible with the efficient coating of the beads (see ref. 24). When resuspended, there should be no visible trace of the fluorescent lipid bound to the glass.

7. Some lipids are sensitive to heat and sonication (e.g., [23]). Perform sonication in pulse mode with a duty ratio low enough to prevent sample heating. The total tip sonication time may have to be increased up to 15 or 20 min when negatively charged lipid is not included in the lipid mixture e.g., 99.9 % DOPC–0.1 % LPRE.
8. Ultracentrifugation is required to remove multilamellar vesicles and possible metal contaminants from the tip-sonication probe. SUVs can also be formed by extrusion through polycarbonate filters with 30 nm nanopores; however, we have not verified this procedure.
9. Wash beads in water (not buffer). Washing in HNa100 will result in the beads sticking to the walls of the plastic tube, rather than pelleting. It should be noted that polystyrene beads, and not silica beads, were selected for our experiments. The higher refractive index of polystyrene allows us to achieve higher trap stiffness at a lower laser power. However silica beads can be used and should be cleaned as in ref. 23 prior to mixing with SUVs.
10. The number of lipid molecules to coat a 1 μm bead with a lipid bilayer is ~9.0×10^6, assuming that the area of a lipid head group is ~70 Å2 [25]. Since the number of beads in 6 μL of 2×10^{10} beads/mL solution is 1.2×10^5, the number of lipids required to fully coat the beads is 1.1×10^{12}. 1 mL of lipid solution with a concentration of 1 mM corresponds to 6.023×10^{17} lipid molecules. This 10^5-fold lipid excess ensures that it is not the lipid concentration that is the limiting factor in the efficient coating of the beads.
11. If fluorescent lipid is used in laser trap experiments, oxygen scavenger reagents should be added in the last wash of the flow cell in Subheading 3.2, step 2.
12. Amyl acetate, nitrocellulose and beads can be mixed in a microcentrifuge tube and spread on the coverslip using a plastic tip. Contamination of the solution from the plastic does not appear to be a problem for this rapid step. In our experience, prepared coverslips should be used within 48 h.
13. Silicon vacuum grease is required to avoid any possible contamination of the solution in the flow cell from the double-side tape.
14. Casein may contain biotin (see datasheet from Sigma-Aldrich for Casein blocking buffer cat# C7594); therefore, we avoid using it as a blocker in the steps before the attachment of the biotinylated Myo1c$^{IQ\text{-}tail}$. We do not use bovine serum albumin (BSA) as a blocker since it is known to interact with lipids. Calmodulin is necessary only for the structural rigidity of the IQ motifs of the Myo1c$^{IQ\text{-}tail}$ construct.

15. This 100-fold dilution will produce a very dilute solution of lipid coated beads in the flow cell. Instead of injecting a very dilute solution, one can inject 2–4 μL of the concentrated lipid-coated bead solution on the one side of the chamber. The assay chamber can be positioned to trap a bead and then moved to a bead-free region.
16. When recording the thermal motion (Brownian motion) of the lipid-coated bead, the trapped bead should be away from immobilized spherical pedestals and ~5 μm above the bottom surface of assay chamber to minimize hydrodynamic coupling with the coverslip.
17. After succeeding in creating a compressive force between the immobilized pedestal and the trapped bead (positive peak in Fig. 2), release the bead from the trap. Oscillate the trap in the absence of the trapped bead to ensure there are no detection artifacts.
18. The concentration of biotinylated Myo1c$^{IQ\text{-}tail}$ (0.2–2.5 nM) was selected so that fewer than 10 % of the total number of contacts between the bead and the pedestal resulted in specific interactions. This frequency increased the probability of observing single-molecule interactions. Data traces that deviated from simple rupture peaks (e.g., double peaks and delayed peaks (Fig. 2)) were excluded.
19. It is important that the amplitude of the oscillation does not exceed 1/2 of the trapped bead's radius ($r/2$). At distances greater than $r/2$ from the center of the trapped bead the laser trap doesn't behave as a Hookean spring. Therefore the maximum force that one can accurately measure is given by the product of the trap stiffness (pN/nm) with $r/2$. In order to increase the maximum measurable force, if necessary, either the trap stiffness should be increased (by increasing the laser power or using beads with higher refractive index) or the radius of the trapped bead.
20. Depending on the pH and the charge of the lipid surface, streptavidin may be more appropriate instead of NeutrAvidin to minimize nonspecific interactions between the pedestal and the lipid coated bead in the absence of Myo1c$^{IQ\text{-}tail}$. This should be checked experimentally.
21. A value for an adhesion force is reported at every cycle in this analysis, even if a specific interaction does not occur. The reported forces are due to specific interactions or a nonspecific interaction between the pedestal and the trapped bead or due to thermal noise. To select against false interactions due to thermal noise or delayed rupture peaks as in Fig. 2, one can select only those peaks with a slope (pN/s) that is within 10 % or 20 % of the expected loading rate (Fig. 3). The expected loading rate

can be calculated from the product of the trap stiffness (pN/nm) times the amplitude (nm) times the oscillation frequency (Hz) multiplied by 4.

22. The bin size should be selected based on the range between the minimum and maximum measured force and be such that half or twice the selected bin size doesn't significantly change the shape of the distribution. The errors in the estimation of the number of events in each bin should be determined using bootstrap technique [26].

23. The probability density distribution of rupture events, $p(F)$, for a single transition state according to the Bell–Evans model:

$$p(F) = k(F)S(F) / r(F) \tag{3}$$

where the dissociation rate as a function of force (k(F)) is given by Bell's model:

$$k(F) = k_o \mathrm{e}^{\frac{F \times \mathrm{d}_{tr}}{k_B \times T}} \tag{4}$$

k_o is the dissociation rate in the absence of force (F), d_{tr} is the distance to the transition state, k_B is Boltzmann's constant, and T is the temperature in Kelvin. The survival probability ($S(F)$) is:

$$S(F) = \mathrm{e}^{\left\{\frac{k_o \times k_B \times T}{r \times \mathrm{d}_{tr}} \times \left(1 - \mathrm{e}^{\frac{F \times \mathrm{d}_{tr}}{k_B \times T}}\right)\right\}} \tag{5}$$

and the loading rate (r) is:

$$r(F) = \frac{\mathrm{d}F}{\mathrm{d}t} \tag{6}$$

where t is time.

24. At different loading rates, the concentration of Myo1c$^{\text{IQ-tail}}$ may have to be adjusted to ensure single-molecule interactions.

25. A square pulse is used to change from compression to separating tension as fast as possible, while keeping the separating tension between the trapped bead and the pedestal constant. To keep a constant separating tension during the interaction, a force-clamp is used [18]. Briefly a command square-wave signal (Fig. 5a) is applied to a summing junction with the trap force signal, such that the output of the junction is the difference between the command and the trap force signal. This difference ("error signal") is fed as input to a feedback amplifier whose output is fed in the acousto-optic deflector that moves the trap towards the appropriate direction to minimize the error signal. When the bead is in mechanical equilibrium (under compression or upon separating tension if a bond has been formed), the feedback loop settles. Therefore the error

signal is minimized ~0 (Fig. 5a) and the beam is displaced relative to the center of the bead to produce the appropriate compressive or separating constant force (Fig. 5a).

26. A square pulse that is the same frequency as the triangular oscillation in the previous ramp-force measurements should give the same frequency of interactions.
27. The part of the data trace that corresponds to the lifetime of the attachment is contained in the light gray area in Fig. 5a. The part in the dark area corresponds to the time that is required to develop a constant force, which is the "dead time." This time depends on the combined compliance of the laser trap and the attachment between the trapped bead and the lipid membrane. To adequately sample very short lived attachments, the stiffness of the trap should be increased by increasing the laser power. However increasing the laser power may increase the partial interaction between the laser beam and the immobilized pedestal (as mentioned earlier in **Note 17**) which may lead to an effective attraction between the bead and the pedestal and obscure the measurement.
28. The measurement accuracy of attachment duration is limited by the rate of data acquisition. If data are recorded at a rate of 2,000/s, then the time resolution is 0.5 ms. When binning the attachment durations to get the frequency distribution, the upper and lower bounds of each bin should correspond to values that are fractional and not integer multiples of 0.5 ms. This way there will be no events with durations right on the boundary of successive bins.

Acknowledgment

This work was supported by a grant from the NIH (GM057247) to E.M.O.

References

1. Lemmon MA (2008) Membrane recognition by phospholipid-binding domains. Nat Rev Mol Cell Biol 9(2):99–111
2. Levental I, Grzybek M, Simons K (2010) Greasing their way: lipid modifications determine protein association with membrane rafts. Biochemistry 49(30):6305–6316
3. McLaughlin S, Murray D (2005) Plasma membrane phosphoinositide organization by protein electrostatics. Nature 438(7068):605–611
4. Sheetz MP, Sable JE, Dobereiner HG (2006) Continuous membrane-cytoskeleton adhesion requires continuous accommodation to lipid and cytoskeleton dynamics. Annu Rev Biophys Biomol Struct 35:417–434
5. Hokanson DE, Laakso JM, Lin T, Sept D, Ostap EM (2006) Myo1c binds phosphoinositides through a putative pleckstrin homology domain. Mol Biol Cell 17(11):4856–4865
6. Dippold HC et al (2009) GOLPH3 bridges phosphatidylinositol-4- phosphate and actomyosin to stretch and shape the Golgi to promote budding. Cell 139(2):337–351
7. McConnell RE, Tyska MJ (2010) Leveraging the membrane-cytoskeleton interface with myosin-1. Trends Cell Biol 20(7):418–426

8. Greenberg MJ, Ostap EM (2013) Regulation and control of myosin-I by the motor and light chain-binding domains. Trends Cell Biol 23:81–89
9. Feeser EA, Ignacio CM, Krendel M, Ostap EM (2010) Myo1e binds anionic phospholipids with high affinity. Biochemistry 49:9353–9360
10. Pyrpassopoulos S, Feeser EA, Mazerik JN, Tyska MJ, Ostap EM (2012) Membrane-bound Myo1c powers asymmetric motility of actin filaments. Curr Biol 22(18):1688–1692
11. Zot HG, Doberstein SK, Pollard TD (1992) Myosin-I moves actin filaments on a phospholipid substrate: implications for membrane targeting. J Cell Biol 116(2):367–376
12. Pyrpassopoulos S, Shuman H, Ostap EM (2010) Single-molecule adhesion forces and attachment lifetimes of myosin-I phosphoinositide interactions. Biophys J 99(12): 3916–3922
13. McKenna JM, Ostap EM (2009) Kinetics of the interaction of Myo1c with phosphoinositides. J Biol Chem 284(42):28650–28659
14. Tang N, Lin T, Ostap EM (2002) Dynamics of Myo1c (myosin-ibeta) lipid binding and dissociation. J Biol Chem 277(45):42763–42768
15. Veigel C, Bartoo ML, White DC, Sparrow JC, Molloy JE (1998) The stiffness of rabbit skeletal actomyosin cross-bridges determined with an optical tweezers transducer. Biophys J 75(3): 1424–1438
16. Neuman KC, Block SM (2004) Optical trapping. Rev Sci Instrum 75(9):2787–2809
17. Batters C, Veigel C (2011) Using optical tweezers to study the fine details of myosin ATPase mechanochemical cycle. Methods Mol Biol 778:97–109
18. Takagi Y, Homsher EE, Goldman YE, Shuman H (2006) Force generation in single conventional actomyosin complexes under high dynamic load. Biophys J 90(4):1295–1307
19. Litvinov RI, Bennett JS, Weisel JW, Shuman H (2005) Multi-step fibrinogen binding to the integrin (alpha)IIb(beta)3 detected using force spectroscopy. Biophys J 89(4):2824–2834
20. Bell GI (1978) Models for the specific adhesion of cells to cells. Science 200(4342):618–627
21. Evans E (2001) Probing the relation between force-lifetime-and chemistry in single molecular bonds. Annu Rev Biophys Biomol Struct 30: 105–128
22. Dudko OK, Hummer G, Szabo A (2008) Theory, analysis, and interpretation of single-molecule force spectroscopy experiments. Proc Natl Acad Sci USA 105(41):15755–15760
23. Galneder R et al (2001) Microelectrophoresis of a bilayer-coated silica bead in an optical trap: application to enzymology. Biophys J 80(5): 2298–2309
24. Pucadyil TJ, Schmid SL (2010) Supported bilayers with excess membrane reservoir: a template for reconstituting membrane budding and fission. Biophys J 99(2):517–525
25. Huang C, Mason JT (1978) Geometric packing constraints in egg phosphatidylcholine vesicles. Proc Natl Acad Sci USA 75(1): 308–310
26. Press WH, Teukolsky SA, Vetterling WT, Flannery BP (2002) Numerical revipes in C++. Cambridge University Press, New York

INDEX

Amanda S. Coutts (ed.), *Adhesion Protein Protocols*, Methods in Molecular Biology, vol. 1046,
DOI 10.1007/978-1-62703-538-5, © Springer Science+Business Media, LLC 2013

F

G

I

L

M

N

P

R

S

T

V

W

X